SYNTHESIS AND COMPLEXATION PROPERTIES OF NAPHTHALENE RING-BASED RECEPTORS

HUU-ANH TRAN

SYNTHESIS AND COMPLEXATION PROPERTIES OF NAPHTHALENE RING-BASED RECEPTORS

by

Huu-Anh Tran

(B.Sc., M.Sc.) University of Natural Sciences,
National University of Hochiminh City, Vietnam

A thesis submitted to the School of Graduate Studies
in partial fulfillment of the requirements for
the degree of Doctor of Philosophy

Department of Chemistry
Memorial University of Newfoundland
St. John's, Newfoundland and Labrador, Canada
August 2006

Your file Votre référence
ISBN: 978-0-494-31332-9
Our file Notre référence
ISBN: 978-0-494-31332-9

Dedication

To the memory of my late Father Trần Quý Thuyết

To my Mom Nguyễn Thị Minh Nguyệt

To my Wife Đặng Thị Anh Thư

And to the other members of my family

Abstract

The work described in this thesis deals mainly with the synthesis of new molecular receptors containing naphthalene-ring units ("calixnaphthalenes"), and their solution complexation properties with neutral guests such as fullerene (C_{60} and C_{70}) and/or cationic guests, *e.g.* tetramethylammonium chloride and/or several metal ions (alkali metal and silver ions).

In order to develop practical methodology for the solution complexation studies using ^{1}H NMR spectroscopy, thiocorannulene derivatives synthesized by the L.T. Scott group were employed as model hosts with fullerenes (C_{60} and C_{70}) in CS_2. The results of this work are described in Chapter 2. The study revealed that pentakis(1,4-benzodithiino)corannulene (**53**) formed the strongest 1:1 complexes of any corannulene derivative with C_{60} and C_{70} reported to date.

In Chapter 3, the syntheses of calix[4]naphthalenes and the attempted modification of the narrow-rim of *tert*-butylcalix[4]naphthalene **18** via alkylation, or via the Sonogashira coupling reaction are reported. In addition, a recent reinvestigation of the complexation properties of calix[4]naphthalenes such as **17** and **18** with C_{60} and C_{70} in toluene (toluene-d_8) and CS_2 was conducted using ^{1}H NMR and/or UV-vis absorption spectroscopy. Under the conditions studied, only **18** was revealed to be a good host for C_{60} and also for C_{70} in toluene-d_8.

In Chapter 4 the syntheses of ethoxycarbonylmethoxy ethers ("hexaester" **123** and "octaester" **124**) of homocalix[*n*]naphthalenes are described. These new compounds were employed as alkali ionic receptors using

a two-phase extraction ($CHCl_3$-H_2O) system and compound **123** was shown to be a highly selective receptor for potassium ion under the conditions studied.

The work described in the remaining Chapters concerns the synthesis and/or complexation properties of the homohetero-bridged calixnaphthalenes, including homooaxa- **159a-d**, **160a** and **160d**, homothia- **205**–**208**, and homoaza analogues **264a**-**d**. While octahomotetraoxacalix[4]naphthalenes **159a** and **159b** were shown to be good hosts for TMACl in $CDCl_3$ with 1:1 binding ratio, no complexes were observed to be formed between these new homothia receptors with TMACl. In contrast, the transition-metal ion Ag^+, formed 1:1 host-guest complexes with octahomotetrathiaisocalix[4]naphthalenes **205a** and **205b**.

Acknowledgements

I would like to thank Dr. Paris E. Georghiou, my supervisor, for his countless guidance, encouragement and support over the past years, and I owe much to him.

I would also like to thank Dr. Graham J. Bodwell and Dr. Peter Pickup, members of my supervisory committee, for their helpful discussions and for their diligent review of this thesis.

The following individuals are also acknowledged with thanks: Dr. L. T. Scott, Boston College, for providing samples for the work described in Chapter 2; Dr. D. W. Thompson, M.U.N. for his valuable insights and contribution to the work described in Chapter 3; Drs. M. Ashram, Mu'tah University, and S. Mizyed, Yarmouk University, are also acknowledged for their contribution to the collaborative studies described in Chapter 4.

I am also grateful to Drs. Sunil V. Pansare, Yuming Zhao, Tran Gien and Lan Gien for their encouragement; Mr. David Miller and Ms. Julie Collins for the X-ray crystallography and to Ms. Linda Winsor for mass spectral analyses. As well, all of the Faculty and Staff of the Chemistry Department are acknowledged for creating a great place to work.

I am deeply grateful to my family, my relatives and my wife for their encouragement and love in reaching this milestone.

I would also like to thank Janette Georghiou, Mervyn and Judith Mc. Intyre, and also my Vietnamese friends for their encouragement and support during my study. All members of the Georghiou group, as well as my fellow graduate students are acknowledged for their cooperation and friendship.

Financial support from the School of Graduate Studies (including the Albert George Hatcher Memorial and J. Beryl Truscott Graduate Scholarships), and the Department of Chemistry, Memorial University of Newfoundland and NSERC is gratefully acknowledged.

Table of contents

List of Figures

List of Schemes

List of Tables

List of Symbols, Abbreviations and Acronyms

Å	angstrom units
(+)-APCI	Atmospheric Pressure Chemical Ionization in positive mode
(–)-APCI	Atmospheric Pressure Chemical Ionization in negative mode
aq.	aqueous
B–H	Benesi–Hildebrand
br	broad (in NMR)
Bu	butyl
t-BuLi	*tert*-butyllithium
n-BuLi	*n*-butyllithium
Bn	benzyl
ca	circa
calcd.	calculated
cat.	catalytic
conc.	concentrated
CPK	Corey-Pauling-Koltum
CT	charge-transfer
δ	chemical shift in ppm downfield from tetramethylsilane
DCM	dichloromethane
ES	electron spray
Δ	heat
$\Delta\delta$	difference in chemical shift values (in ppm)
ΔH	enthalpy change

ΔS	entropy change
dec.	decomposed
DMF	*N,N*-dimethylformamide
equiv.	equivalent(s)
Et	ethyl
F–F	Foster–Fyfe
h	hour(s)
Hz	hertz
J	coupling constant (Hz)
K	Kelvin (degree)
K_{assoc}	association constant
χ	mole fraction
LC	liquid chromatography
lit.	literature
m	multiplet (in NMR)
M^+	molecular ion
MALDI-TOF	Matrix-Assisted Laser Desorption Ionization-Time of Flight
Me	methyl
MHz	megahertz
min	minute(s)
mp	melting point
MS	mass spectrometry
NMR	nuclear magnetic resonance

NLO	non-linear optical
nr	no reaction
p	*Para*
PCC	pyridinium chlorocromate
Ph	phenyl
PLC	preparative thin layer chromatography
ppm	parts per million
PPTS	pyridinium *p*-toluenesulfonate
Pr	propyl
Phth	*N*-phthalimido
PTSA	*p*-toluenesulfonic acid
q	quartet (in NMR)
R	gas constant
R^2	Correlation coefficient on chart
rt	room temperature
s	singlet (in NMR)
t	triplet (in NMR)
tert	tertiary
THF	tetrahydrofuran
TPE	tetraphenylethylene
TLC	thin-layer chromatoghaphy
TMACl	tetramethylammonium chloride
TMEDA	*N*,*N*,*N*,*N*-tetramethylethylenediamine

TMS	tetramethylsilane (in NMR)
TsCl	*p*-toluenesulfonyl chloride
USA	United State of America
UV	ultraviolet
vis	visible
vs	*versus*
VT	variable temperature

Chapter 1

Introduction

1.1 The calixarenes: background

1.1.1 Early history

Although Adolph von Baeyer noted the formation of a resinous tar[1] from the reaction of *p-tert*-butylphenol and formaldehyde in 1872, it took almost 70 years for Zinke and Ziegler to propose a structure for this product.[2] Without the benefit of modern high-resolution analytical equipment in 1949, they insightfully assigned the cyclic tetrameric structure **1** to an oligomeric product formed from the base-induced condensation of *para*-substituted *tert*-butylphenol with formaldehyde. Upon reinvestigating this condensation reaction in the early 1950's, Cornforth *et al.* found that the "resinous tar" was a mixture of such cyclic oligomers.[3]

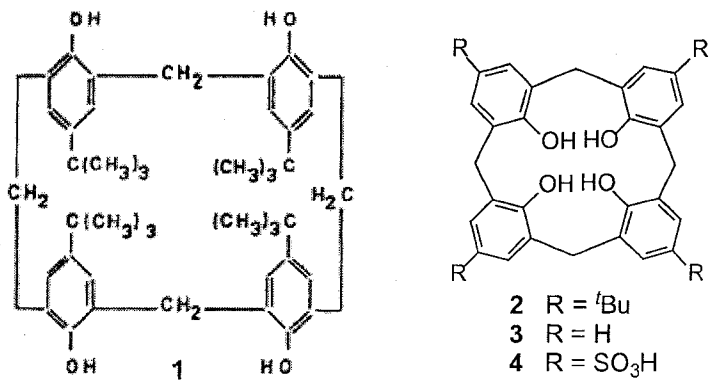

Figure 1.1 Zinke and Ziegler's structure (**1**) (*left*) as depicted in Reference 2, and a modern structural representation (**2**) (*right*).[4]

In the early 1970's, while looking for molecular structures that could be employed as biomimetic receptors, Gutsche became interested in Zinke's compounds, since they resemble molecular "baskets". The Gutsche group later successfully developed the most efficient methods to specifically synthesize cyclic compounds **2**, **5** and **6** (Scheme 1.1) using single-step, base-induced cyclocondensation reactions of *p-tert*-butylphenol and formaldehyde in multigram scale reactions.[5] The products containing an odd number of *p-tert*-butylphenol units (n = 5,[6] 7[7]) have also been prepared but the yields were much lower (15-20%).

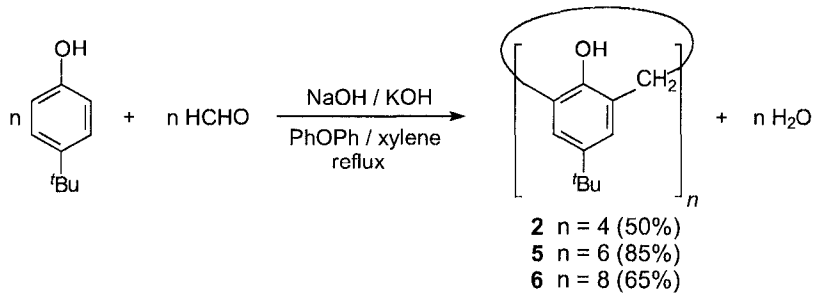

Scheme 1.1 Synthesis of calixarenes (n = 4, 6, 8).

1.1.2 Nomenclature of calixarenes

According to the nomenclature system invented by Cram and Steinberg[8] in 1951, compounds such as **2**–**6** are classified as [1$_n$] metacyclophanes. However, the resulting systematic names are very long and are not convenient for writing and communication. For example, *Chemical Abstracts*[9] named the basic ring structure of the cyclic tetramer **2** as: "[19.3.1.1^{3,7}1^{9,13}1^{15,19}]octacosa-1(25),3,5,7(28),9,11,13(27),15,17,19(26)21,23-dodecaene". Therefore, it was desirable to have another shorter nomenclature for these cyclic compounds.

In 1975, Gutsche noticed the resemblance in shape between a Greek vase called a "calix" krater and one of the space-filling molecular models corresponding to Zinke's cyclic tetramer, in which all four aryl groups are oriented in the same direction (Figure 1.2). He coined the name "calixarene" for this compound, and the word "calixarene" first appeared in print in 1978.[5a]

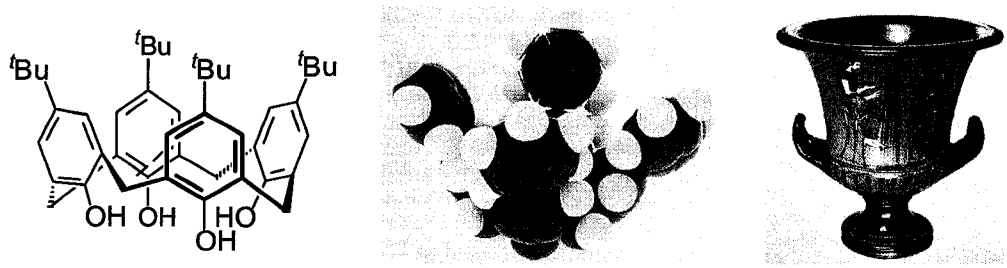

Figure 1.2 *Cone* conformer of **2** (*left*), CPK model of a cyclic tetramer (*middle*) and a calix krater (*right*).[10]

The annulus containing the hydroxyl groups in **2** (Fig 1.3) forms the narrow rim (also referred to in calixarene parlance as the "lower rim") of the basket, as a result of hydrogen bonding between these hydroxy groups. In contrast, the opposite end comprising the aromatic rings and their alkyl substituent groups, forms the wide rim ("upper rim") of the basket.

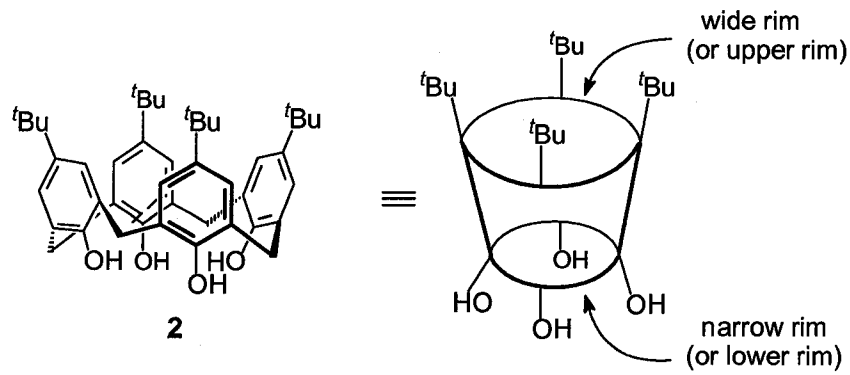

Figure 1.3 Rims defined in calixarenes.[10]

The various calixarenes can be distinguished by the value of "[*n*]" which is placed between "calix" and "arenes" to become "calix[*n*]arenes", which indicates the number of the aromatic units (Figure 1.4). More commonly, authors prefer to use the short names in the text of their publications, and/or the short names, or the more systematic ones in the experimental sections.

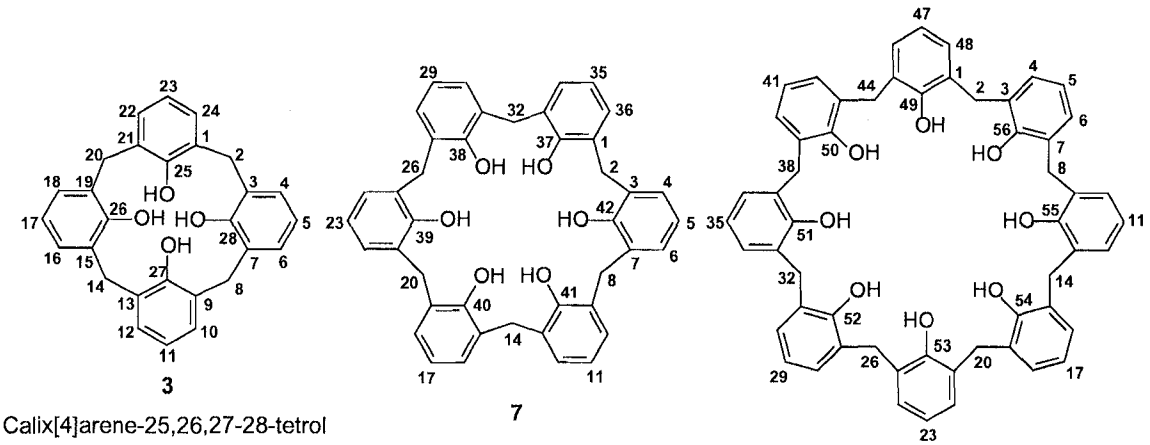

Figure 1.4 Nomenclature system used for calixarenes.[10]

The nomenclature of calixarenes has also been extended to another class of cyclic tetramer, *e.g.* **9**, which is derived from the acid-catalyzed reaction between resorcinol and aldehydes (Scheme 1.2). Although these compounds do not have exactly the same shapes as **2**, they have also been given the prefix "calix" by many authors, and have been referred to as "calix[*n*]resorcinarenes", and also as "resorcinarenes" and/or "resorcarenes". Forty years after Niederl and Vogel[11] investigated the chemistry of **9** in 1940, Högberg[12] proposed the structure of **9** in which all of the hydroxy groups are situated *exo* to the annulus.

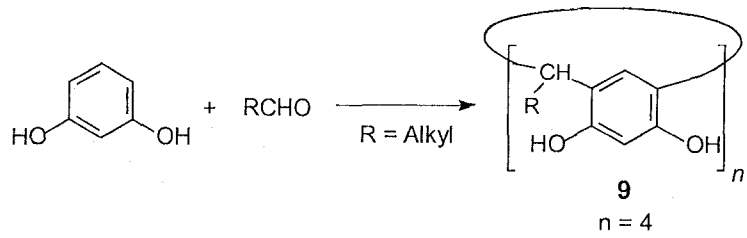

Scheme 1.2 Calix[*n*]resorcarenes.

1.1.3 Conformational properties of calixarenes

Due to the flexibility of the bridges between the arene units, calix[4]arenes such as *p-tert*-butylcalix[4]arene (**2**) can adopt four main conformers, in which the aryl groups orient upward ("u") or downward ("d") relative to an average plane defined by the methylene bridges. These conformers are named as the *cone* or *crown* (u,u,u,u); *partial-cone* or *partial-crown* or "*paco*" (u,u,u,d); *1,2-alternate* (u,u,d,d); and *1,3-alternate* (u,d,u,d) conformers, respectively by Gutsche[13] and Cornforth[3] (Figure 1.5). Advantageously, these four conformers can, in most cases, be easily distinguished by employment of the "de Mendoza rule" for correlation of both the ^{1}H and ^{13}C NMR spectra of calix[4]arenes.[14,15]

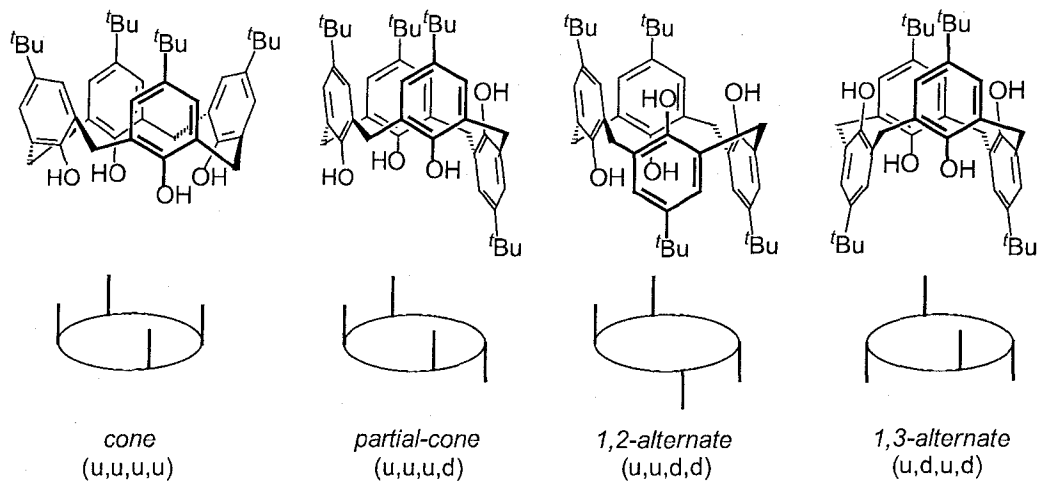

Figure 1.5 Four possible conformers of calixarenes **2**.

Specifically, while the *cone* or the *1,3-alternate* conformations exhibit only a pair of doublets or only a singlet, respectively, in their ^{1}H NMR spectra (Figure 1.6) for the methylene bridge groups, both the *partial-cone* and the less common *1,2-altenate* conformations each show a pair of doublets and a singlet.

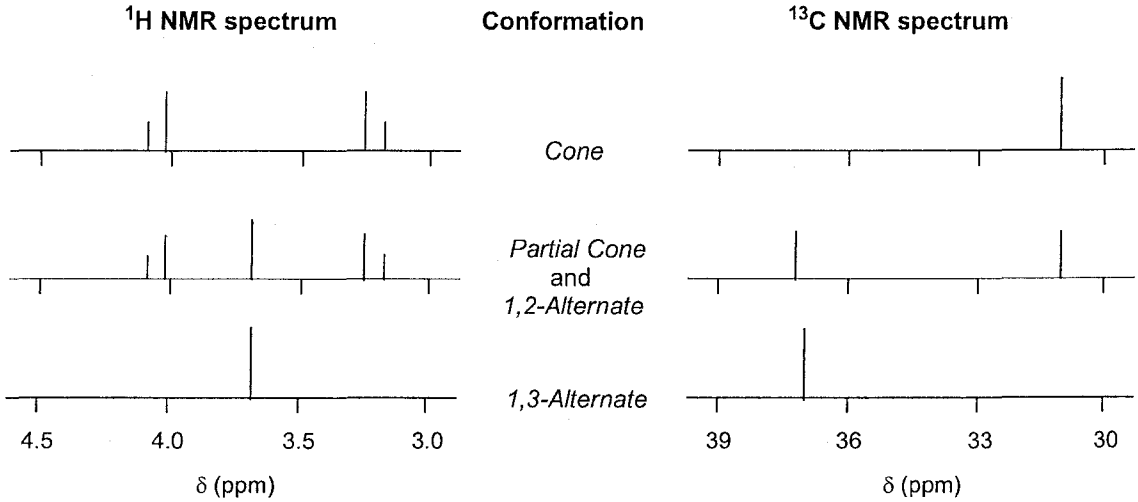

Figure 1.6 NMR spectral patterns of the methylene groups in the four calix[4]arene-conformational isomers.[14,15]

Similarly, in the ^{13}C NMR spectra for the methylene groups (Figure 1.6), the *cone* conformation, having all *syn* adjacent aryl groups, shows only a single signal near δ 31 ppm; the 1,3-alternate conformation with all *anti* adjacent aryl groups also possesses only a single chemical shift near δ 37 ppm, while both the *partial-cone* and *1,2-altenate* conformations each show a pair of signals having chemical shifts at δ 31 and 37 ppm for their *syn* and *anti* adjacent aryl groups, respectively. The "de Mendoza rule" has been also successfully extended to identify the conformational behavior in solution of some calix[5]arenes,[16] and also calix[6]arenes.[17]

In brief, since the pioneering work by Gutsche in the late 1970s, calix[*n*]arenes have been the subject of many studies which to date have been reported in more than 6000 publications. These studies involve developing synthetic methodology, molecular modeling and the design of new structures, and also investigations of their physicochemical and supramolecular properties.[16,18]

1.2 Discovery of and development of the chemistry of calixnaphthalenes

In 1993, Georghiou and Li[3,19] serendipitously discovered three new naphthalene ring-based cyclic regioisomers, *i.e.* **10**–**12** (Figure 1.7), which were formed as a mixture, from the base-mediated cyclocondensation of 1-naphthol with formaldehyde. Molecular models suggested that these new naphthalene-based cyclic compounds could adopt conformations similar to the calix[4]arenes, but would form deeper and/or wider molecular baskets than those of the calixarenes. As a result, it was hypothesized that these compounds could have potentially significant supramolecular complexation properties with neutral or charged guest species. Therefore, these new cyclic compounds were named "calix[4]naphthalenes".[4,20]

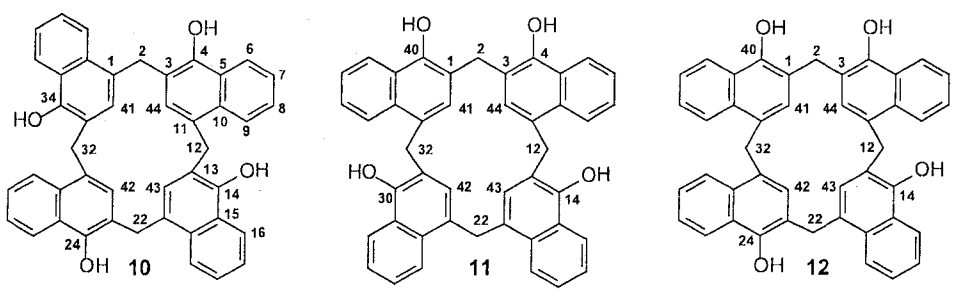

Figure 1.7 Calix[4]naphthalenes and the numbering system used.

There are only a few reports concerning macrocyclic naphthalene ring-containing compounds to date. Poh's group first reported in 1989 the formation of methylene-bridged macrocyclic compound **14**, cyclotetrachromotropylene, from the cyclocondensation of chromotropic acid disodium salt (**13**), with an excess amount of formaldehyde (Scheme 1.3).[21] Since then, his group has reported on several supramolecular complexation studies in aqueous solution involving this highly water-soluble compound.[22]

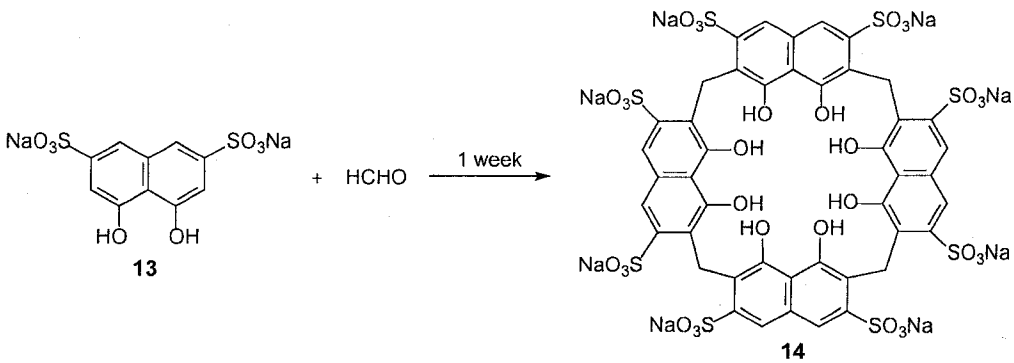

Scheme 1.3 Synthesis of **14** derived from chromotropic acid, disodium salt **13**.

In 1993, Böhmer *et al.* reported the synthesis of the naphthalene ring-containing macrocycle **17** (5%) from 3-hydroxymethyl-2-naphthol (**15**) via a $TiCl_4$-mediated cyclocondensation in dioxane (Scheme 1.4).[23] *tert*-Butyl-substituted calix[4]naphthalene **18** was later synthesized from the *tert*-butyl intermediate **16** by Georghiou *et al.* (Scheme 1.4). The structures of **17** and **18** were also fully elucidated by this group.[24]

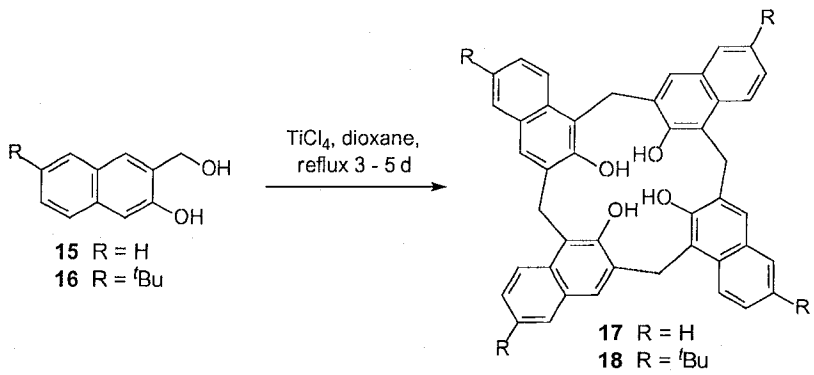

Scheme 1.4 Synthesis of calix[4]naphthalenes **17** and **18.**

In 1996, Shinkai *et al.* reported the conversion of an aromatic unit in calixarene **19** to a naphthalene ring in **20** via a sequential acetalization-pyrolysis procedure (Scheme 1.5).[25]

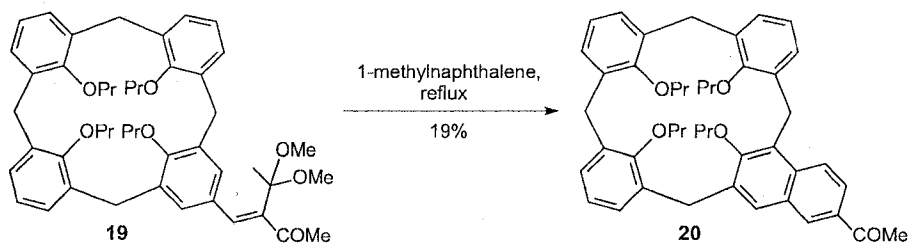

Scheme 1.5 Synthesis of the calixarene **20** containing a naphthalene unit.

Glass *et al.* recently synthesized the expanded "3,5-linked" calix[3]naphthalene[26] **22** derived from **21,** whereas from **23**, the expanded "3,6-linked" calix[*n*]naphthalene (n = 3–6) oligomers **24** were obtained via an acidic-catalyzed cyclocondensation of hydroxymethyl derivatives (Scheme 1.6).

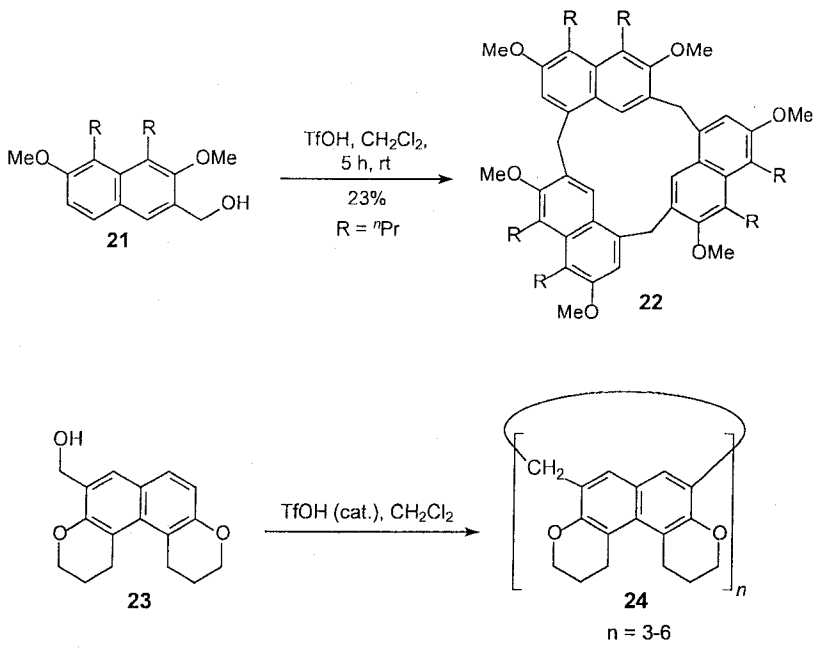

Scheme 1.6 Synthesis of "3,5- and 3,6-linked" calix[*n*]naphthalenes **22** and **24**.

They also produced a mixture of *cis*/*trans* isomers of the 3,6-linked-calix[4]naphthalene **27** from the cyclocondensation–cyclodimerization of **26** with hexanal / $SnCl_4$ (Scheme 1.7).

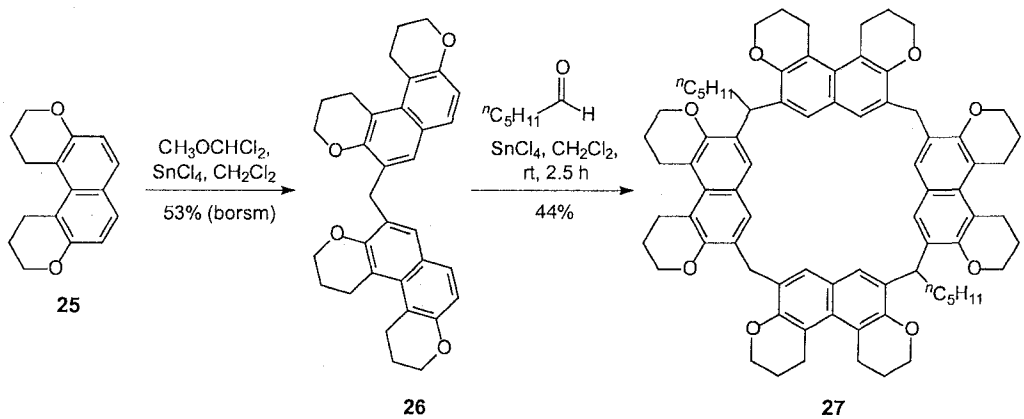

Scheme 1.7 Synthesis of "3,6-linked" calix[4]naphthalenes **27**.

The chemistry and study of properties of the naphthalene-based calixarenes have been the subject of ongoing research here at Memorial University of Newfoundland.[27] The Georghiou group has produced several different types of calixnaphthalenes[13,28,29,30] from various subunits such as 1-naphthol,[23,31] 2-naphthol,[32] 1,8-naphthalene sultone,[33] 3-hydroxy-2-naphthoic acid,[34] and 2,3-dihydroxynaphthalene[13c,35] and these have been recently reviewed elsewhere.[4]

1.3 Supramolecular chemistry of calixarenes and calixnaphthalenes

1.3.1 Supramolecular chemistry

Supramolecular chemistry continues to attract much attention from chemists, biochemists, physicists, material scientists and computational modelers. In 1987, Jean-Marie Lehn[36] defined "supramolecular chemistry" as being "chemistry beyond the molecule", which deals with weak intermolecular interactions and the molecular assemblies between two or more chemical species that are based upon them. These larger species can be formed with a high degree of control and efficiency.[37,38] If the binding occurs between units of different size, the larger (and usually cyclic) species, containing binding sites (cavities) are considered to be the "hosts". The "guests" are the smaller species, commonly ions, or neutral molecules ranging from solvent molecules to fullerenes or hormones or pheromones.[39]

The strength of host-guest binding to form complexes is mainly determined by the nature of the non-covalent interactions between host and

guest units. The non-covalent interaction can operate individually or in a combination of the following ways:[40] ion-ion (bond energy 100–350 kJ mol^{-1}); ion-dipole (50–200 kJ mol^{-1}); dipole-dipole (5–50 kJ mol^{-1}); hydrogen bonding (4–120 kJ mol^{-1}); cation-π (5–80 kJ mol^{-1}); π-π stacking (< 50 kJ mol^{-1}); methyl-π;[41] dispersion and induction forces, *i.e.* van der Waals forces, (<5 kJ mol^{-1}; variable); close packing in the solid state; hydrophobic or solvophobic effects; and charge-transfer.[42] The stability of a host-guest complex is evaluated via its binding constant or association constant, which can be measured by several physical chemical and /or spectroscopic methods such as IR, UV-vis, NMR, ESR, Scanning Probe Microscopy (SPM), Atomic Force Microscopy (AFM), and/or electrochemical techniques.[43]

1.3.2 Supramolecular chemistry of calixarenes and calixnaphthalenes

Calixarenes and their derivatives, having basket-like structures, have been shown to be very useful hosts in host-guest recognition studies both in solution and in the solid state. Several different guests such as cations (*e.g.* alkali, alkali-earth, transition metal and ammonium ions); anions (*e.g.* halides, nitrate, carboxylate, biphosphate and bisulfate), amino acid derivatives and neutral small molecules (*e.g.* solvent molecules, amines, phenols, arenes, sugars and terpenes[44]) and larger molecules (*e.g.* C_{60}, C_{70}, peptides[45]) have been employed. [15,18,32-39]

Endo-type calix[4]naphthalenes, in which all their hydroxy groups are inside the annulus, such as **17** and **18** are closely analogous to calix[4]arenes derived from *p-tert*-butylphenol. CPK models and computer-aided molecular mechanics modeling indicate that the former have deeper cavities than the latter. A computer-assisted molecular modeling study[46] revealed that the distance from the intraannular oxygen atom in the *cone* conformer of **17** to the most distant hydrogen atom on the same naphthalene ring, is around 7.7 Å. By comparison, the analogous distance in the corresponding calix[4]arene is 5.3 Å. In addition, electrostatic potential calculations of their *cone* conformations indicate that **17** has greater regions of electron density within its cavity than that found within the corresponding shallower calix[4]arene **3** (Figure 1.8). As a result, it is anticipated that calixnaphthalenes would be efficient hosts for electron-deficient guests. Accordingly, the research described in this thesis focuses only on metal cation, ammonium cation and fullerene guests.

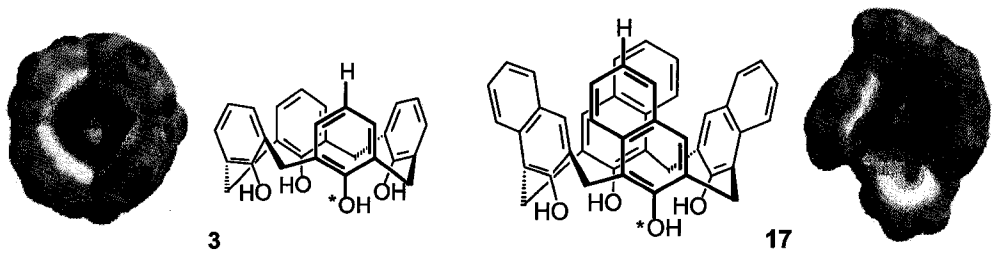

Figure 1.8 Electrostatic potential maps of the surfaces of calix[4]arene **3** (*left*) and calix[4]napththalene **17** (*right*).[4,47]

1.3.2.1 Cations as the guests

Complexation between calixarenes and metal cation guests could occur both at the wide rim or narrow rim depending on the nature of the cations. For example, the "harder" cations, such as Li^+ and Na^+,[47] have a tendency to bind with the narrow rim oxygen atoms in both *cone* and *partial-cone* conformations of calixarene tetramethyl ether **28** (Figure 1.9) while the "softer" cations, *e.g.* K^+ Ag^+,[48] or alkylammonium cations bind with two opposite aromatic units, or three or four of them in calixarene tetra-*n*-propyl ether **29**, respectively, in their *1,3-alternate*, *partial-cone* or *cone* conformations, (Figure 1.10). This may result from a favorable, weak cation-π interaction with the aromatic rings.[49] These binding tendencies were confirmed by ^{1}H NMR study, and X-ray crystallography in some cases.[36,49]

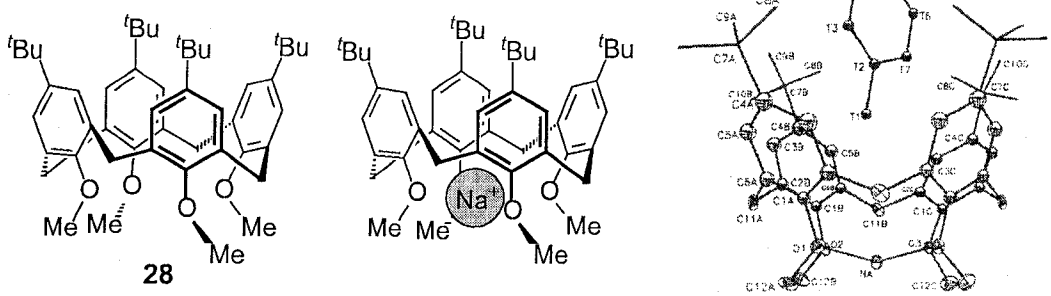

Figure 1.9 *Cone* conformation of *p-tert*-butylcalix[4]arene tetramethyl ether **28** (*left*); binding mode of **28** and Na^+ (*middle*); X-ray structure of **28**:PhMe:Na^+ complex (*right*).[46b]

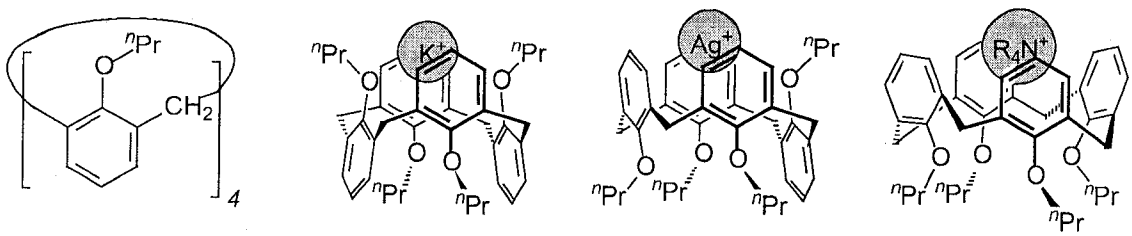

29 *1,3-alternate* *partial cone* *cone*

Figure 1.10 Binding modes of calix[4]arene tetra-*n*-propyl ether **29** with K^+; Ag^+,[48] and alkylammonium ions.[48]

So far, there are only two publications on metal cation recognition with calixnaphthalenes, both of which came from the Georghiou group. Upon treatment with $AgNO_3$ in THF, both tetrahomodithiacalix[4]naphthalenes **30** and **31** (Figure 1.11) formed 1:1 complexes with Ag^+.[27,28] However, their complexation properties have not been fully investigated yet. The tris(ethoxycarbonylmethoxy) ethers of hexahomotrioxacalix[3]naphthalene[50] such as **32** and **33** (in both *cone* and *partial-cone* conformations) (Figure 1.11) have been employed to extract alkali metal (Li^+, Na^+, K^+, Rb^+ and Cs^+) and silver picrates from aqueous solution. The *cone* conformer of triester **33** is selective towards K^+, while the *partial-cone* conformer extracted Rb^+. However, these compounds were not very efficient receptors under the conditions used. The efficiencies of the extractions were less than 10% in all cases.

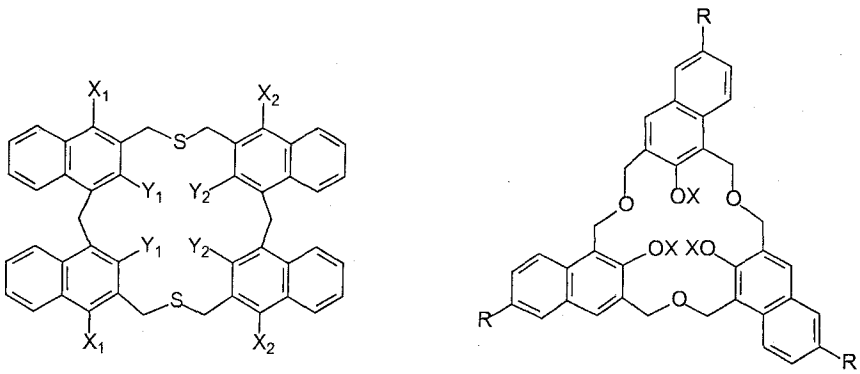

30 X_1, X_2 = OMe, Y_1, Y_2 = H
31 X_1, Y_2 = OMe, X_2, Y_1 = H

32 X = CH_2CO_2Et; R = H
33 X = CH_2CO_2Et; R = ^tBu

Figure 1.11 Tetrahomdithiacalix[4]naphthalenes **30**, **31** (*left*) and tris(ethoxycarbonylmethoxy) esters **32**, **33** of hexahomotrioxacalix[3]naphthalenes (*right*)

1.3.2.2 Fullerenes (C_{60} and C_{70}) as the guests

Since the discovery of fullerenes in 1985,[51,52] the supramolecular complexation properties of these carbon allotropes have been the subjects of much interest.[32-36] Atwood,[53] Shinkai,[54] Haino[55] and their co-workers independently showed that some calix[*n*]arenes (n = 5, 6, 8) were effective C_{60} and/or C_{70} hosts.[10,15,18] The complexes between calixarenes and fullerenes most likely result from the π-π^* interactions between the cavities of the calixarenes and the electron-deficient surface of the fullerene. In contrast, the cavities of calix[4]arenes are not large enough to be occupied by fullerene molecules, *e.g.* C_{60} or C_{70}. This was confirmed by the X-ray structures of co-crystals of *p*-halocalix[4]arene ethers and C_{60}.[56]

Homooxacalixarenes such as **34**–**42**, in which each of the bridging methylene groups has been expanded by $-OCH_2-$ units, have also demonstrated complexing abilities with C_{60} (Figure 1.12).[57,58] This is probably due to their larger cavity diameters, or due to the extra electron-donating abilities of the oxygen atoms in the $-CH_2OCH_2-$ bridges. Interestingly, *p*-halohexahomotrioxacalix[3]arenes **39**–**42** favorably formed precipitates with C_{70} over C_{60} from mixtures of fullerenes in toluene solution.[55]

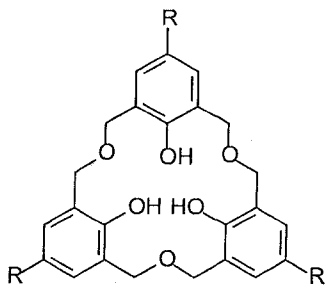

34 R = *p*-$CMe_2C_6H_4OMOM$
35 R = ^{t}Bu
36 R = OMe
37 R = Bn
38 R = H
39 R = F
40 R = Cl
41 R = Br
42 R = I

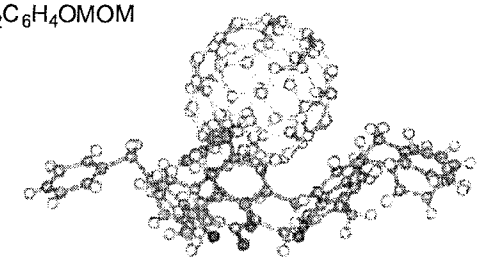

Figure 1.12 Hexahomtrioxacalix[3]arenes (*left*); X-ray crystal structure of **37**:C_{60} complex (*right*).[59]

This success prompted the development of other such calixarenes, as well as calixnaphthalene hosts for fullerenes. It can be shown that the *endo* hydroxyl calixnaphthalenes, such as **18** (Figure 1.13), possess cavities approximately 30% deeper than those of the corresponding calixarenes.[30] It was predicted that such cavities in calix[4]naphthalene would be deep and large enough to be filled by C_{60} or C_{70} which have outer diameters of 10.18 Å[60,61] and 7.12–7.96 Å,[61] respectively, from the upper rim. Indeed, unlike *p-tert*-butylcalix[4]arenes, *tert*-butylcalix[4]-naphthalene **18** did show significant complexation properties with

the neutral, electron-deficient molecule C_{60} guest in toluene.[62] In addition, Georghiou and co-workers also found that, similar to homoxacalixarenes, a crystalline supramolecular complex could be formed between C_{60} and hexahomotrioxacalix[3]naphthalene **43** (Figure 1.13). These crystals afforded an X-ray structure[63] showing 2:1 complexion between **43** and C_{60}. A solution complexation study of **43** and C_{60} using ^{1}H NMR spectrometry revealed that **43** was also a good host for C_{60} having the values of K_{assoc} 296 ± 9 and 441 ± 23 in benzene-d_6 and toluene-d_8, respectively.[62]

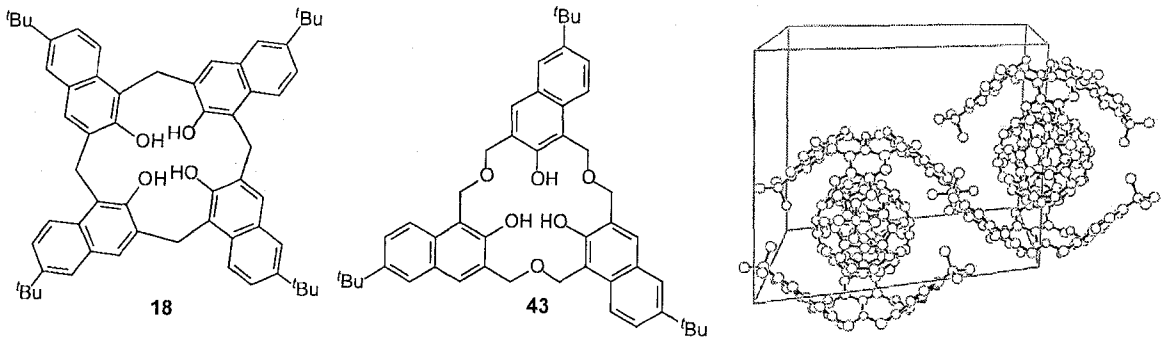

Figure 1.13 *tert*-Butylcalix[4]naphthalene **18** (*left*), hexahomotrioxacalix[3]-naphthalene **43** (*middle*), partial packing diagram of the 2:1 complex of **43** and C_{60}.

1.4 Objectives and results

Part of the objective of the work described in this thesis was to synthesize new calixnaphthalenes, which could serve as larger, wider and deeper molecular receptors for neutral guest molecules such as fullerenes C_{60} and C_{70} as well as for cationic guests, *e.g.* organic and metal cations. At first, CPK models and

computer-aided molecular modeling studies were employed to design the target structures, including examining and evaluating their potential for formation of supramolecular complexes. The binding abilities of these new hosts in solution were then determined subsequently via complexation study experiments. A variety of techniques including UV-vis and NMR spectroscopy were employed. The results from this research are useful for evaluating the accuracy of the modeling predictions. In addition to investigation of their complexation behaviour with fullerenes, the newly synthesized calixnaphthalenes, in some cases, were also tested for their binding abilities with some transition metal cations or their potentially selective extraction of specific alkali metal cation guest from aqueous solution.

To expand the cavities of calixnaphthalenes, the methylene bridges can be replaced by $-CH_2XCH_2-$ groups (X = O, S and NTs) in order to produce homooxa-, homothia- and homoaza*iso*calixnaphthalenes, respectively. On the other hand, the numbers of naphthalene-based units can also be increased to create 6- or 8-naphthyl ring containing calixnaphthalenes having even larger cavities. Another factor considered was that most of the newly synthesized calixnaphthalenes have the potential to be easily functionalized at both the wide and narrow rims, thereby having potentially more applications. Some of the results obtained to date are described in the the following chapters.

To gain expertise with complexation experiments involving fullerenes, a practical binding study between fullerenes (C_{60} and C_{70}) and some bowl-shaped

corannulene derivatives synthesized by the Scott group[64] was conducted in CS_2. The binding was monitored by ^1H NMR spectroscopy as a model study. The results from this collaborative study with Prof. L. T. Scott, at Boston College, U.S.A. are reported in Chapter 2.

The syntheses of calix[4]naphthalenes and the attempted modification of the narrow rim of *tert*-butylcalix[4]naphthalene **17** via alkylation and via the Sonogashira coupling reaction are reported in Chapter 3. Recent results from a reinvestigation of the complexation properties of calix[4]naphthalenes such as **17** and **18** with C_{60} using both ^1H NMR and UV-vis absorption spectroscopy are also included in this chapter.

The synthesis of new macrocyclic homocalix[*n*]naphthalene *O*-esters as new cationic receptors and their recognition behavior towards alkali cations in aqueous solution are reported in Chapter 4. These results were obtained as part of a collaboration with M. Ashram, Mutah University, Jordan and S. Mizyed, Yarmouk University, Jordan both of whom are graduates of the Georghiou group, Memorial University.

The synthesis of "Zorbarene", a member of a new group of homooxa*iso*calixnaphthalenes having $-CH_2OCH_2-$ bridges, and their complexation behaviour towards neutral hosts such as C_{60}, C_{70} and the tetramethyl ammonium cation (TMA) are described and discussed in Chapter 5.

An attempted synthesis of a "double-handled" homooxa*iso*calix[4]-naphthalene, expected to be a more rigid naphthalene-based receptor as compared with homooxa*iso*calixnaphthalenes is reported in Chapter.6.

The syntheses of new homothio*iso*calixnaphthalenes having $-CH_2SCH_2-$ bridges and four or six naphthyl-ring units are reported in Chapter 7. The binding abilities of some of them with C_{60} or C_{70} and cationic guests (*e.g.* TMA and Ag^+) are also included in this chapter.

The syntheses of azacyclophanes which resulted from an attempted synthesis of homoaza*iso*calixnaphthalenes are reported in Chapter 8. The X-ray structure and computer-aided molecular mechanics modeling of *O*-methyl or *O*-*n*-propyl azacyclophanes revealed that these new aza-cyclic compounds have calixarene-like structures.

Finally, the findings from this research will hopefully contribute to the further development of the chemistry of calixnaphthalenes with respect to their synthetic methodology, as well as their physicochemical studies.

1.5 References

1. Baeyer, A. *Ber. Dtsch. Chem. Ges.* **1872**, 5, 25, 280, 1904.

2. Zinke, A; Ziegler, E. *Ber. Dtsch. Chem. Ges.* **1944**, *77,* 264-272.

3. (a) Cornforth, J. W.; D'Arcy Hart, P.; Nicholls, G. A.; Rees, R. J. W.; Stock, J. A. *Br. J. Pharmacol.* **1955**, *10*, 73-86. (b) Cornforth, J. W.; Morgan, E. D.; Potts, K. T.; Rees, R. J. W. *Tetrahedron* **1973**, *29*, 1659-1667.

4. Main reference for Chapter 1: Georghiou, P. E.; Li, Z.; Ashram, M.; Chowdhury, S.; Mizyed, S.; Tran, H. A.; Al-Saraierh, H.; Miller, D. O. *Synlett* **2005**, 879-891.

5. (a) Gutsche, C. D.; Muthukrishnan, R. *J. Org. Chem.* **1978**, *43*, 4905-4906. (b) Muthukrishnan, R.; Gutsche, C. D. *J. Org. Chem.* **1979**, *44*, 3962-3964. (c) Gutsche, C. D.; Dhawan, B.; No, K. H.; Muthukrishnan, R. *J. Am. Chem. Soc.* **1981**, *103*, 3782-3792. (d) Gutsche, C. D.; Iqbal, M., Stewart, D.*J. Org. Chem.* **1986**, *51*, 742-745. (e) Gutsche, C. D.; Iqbal, M. *Org. Synth.* **1990**, *68*, 234-237. (f) Gutsche, C. D.; Dhawan, B.; Leonis, M.; Stewart, D. *Org. Synth.* **1990**, *68*, 238-242. (g) Munch, J. H.; Gutsche, C. D. *Org. Synth.***1990**, *68*, 243-246.

6. (a) Stewart, D.; Gutsche, C. D. *Org. Prep. Proced. Int.* **1993**, *25*, 137-139. (b) Iwamot, K.; Araki, K.; Shinkai, S. *Bull. Chem. Soc. Jpn.* **1994**, *67*, 1499-1502. X ray structures of *p-tert*-butylcalix[5]arenes: (c) Coruzzi, M.; Andreetti, G. D.; Bocchi, V.; Pochini, A.; Ungaro, R. *J. Chem. Soc., Perkin Trans. 2*, **1982**, 1133-1138. (d) Juneja, R. K.; Robinson, K. D.; Orr, G. W.; Dubois, R. H.; Belmore, K. A.; Atwood, J. L. *J. Incl. Phenom. Mol. Recognit. Chem.* **1992**, *13*, 93-96. (e) Atwood, J. L.; Juneja, R. K.;Junk, P. C.; Robinson, K. D. *J. Chem. Crystallogr.* **1994**, *24*, 573-576. (f) Gallagher, J. F.; Ferguson, G.; Böhmer, V.; Kraft, D. *Acta Crystallogr.* **1994**, *C50*, 73-77.

7. Vocanson, F.; Lamartine, R.; Lanteri, P.; Longeray, R.; Gauvrit, J. Y. *New. J. Chem.* **1995**, *19*, 825-829.

8. (a) Cram, D. J.; Steinberg, H. *J. Am. Chem. Soc.* **1951**, *73,* 5691-5704. (b) IUPAC Tentative Rules for Nomencalture of Organic Chemistry, Section E. Fundamental Stereochemistry; *J. Org. Chem.* **1970**, *35*, 284.

9. Patterson, A. M.; Capell, L. T.; Walker, D. F. *The Ring Index*, 2nd ed., American Chemical Society, Washington D.C., **1960**, Ring Index No. 6485.

10. Gutsche, C. D. *Calixarenes, Monographs in Supramolecular Chemistry*; Stoddart, J. F., Ed.; The Royal Society of Chemistry 1989 and references cited therein.

11. Niederl, J. B.; Vogel, H. J. *J. Am. Chem. Soc.* **1940**, *62*, 2512-2514.

12. (a) Högberg, A. G. S. *J. Am. Chem. Soc.* **1980**, *102*, 6046-6050. (b) Högberg, A. G. S. *J. Org. Chem.* **1980**, *45*, 4498-4500.

13. Gutsche, C. D.; Dhawan, B.; Levine, J. A.; No, K. H.; Bauer, L. J. *Tetrahedron* **1983**, *39*, 409-426.

14. Jaime, C.; de Mendoza, J.; Prados, P.; Nieto, P. M.; Sanchez, C. *J. Org. Chem.* **1991**, *56*, 3372-3376.

15. Mandolini, L.; Ungaro, R. *Calixarenes in Action*, Imperial College Press, London, 2000.

16. Stewart, D.; Krawiec, M.; Kashyap, R. P.; Watson, W. H.; Gutsche, C. D. *J. Am. Chem. Soc.* **1995**, *117*, 586-601.

17. Kanamathareddy, S.; Gutsche, C. D. *J. Org. Chem.* **1994**, *59*, 3871-3879.

18. (a) Vicens, J.; Böhmer, V., Eds., *Calixarenes A Versatile Class of Macrocyclic Compounds*, Kluwer Acadamic Publishers, Dordrecht, The Netherlands, 1991. (b) Gustshe, C. D. *Calixarenes revisited, Monographs in Supramolecular Chemistry*; Stoddart, J. F., Ed.; The Royal Society of Chemistry, 1998. (c) Afari, Z.; Böhmer, V.; Harrowfield, J.; Vicens, J., Eds., *Calixarenes 2001*, Kluwer Acadamic Publishers, Dordrecht, The Netherlands, 2001 and references cited therein.

19. (a) Georghiou, P. E.; Li, Z. *Tetrahedron Lett.* **1993**, *34*, 2887-2890; (b) Georghiou, P. E.; Li, Z. *J. Incl. Phenom. Mol. Recogni. Chem.* **1994**, *19*, 55-66. (c) Li, Z. *Ph.D. Dissertation,* Memorial University of Newfoundland, 1996.

20. The Chemical Abstract named for compounds **6-8** respectively, are: 6*H*,14*H*,22*H*,30*H*-5,31:7,13:15,21:23,29-tetramethenotetrabenzo[*a*,*g*,*m*,*s*]-cyclo-tetracosene-8,16,24,32-tetrol;7*H*,15*H*,23*H*,31*H*-6,32:8,14:16,22:24,30-tetramethenotetrabenzo[*a*,*f*,*l*,*s*]cyclo-tetracosene-5,13,17,25-tetrol; and 6*H*,14*H*,22*H*,30*H*-5,31:7,13:15,21:23,29-tetramethenotetrabenzo[*a*,*f*,*l*,*r*]-cyclotetracosene-12,20,28,32-tetrol.

21. (a) Poh, B.-L.; Lim, C. S.; Khoo, K. S. *Tetrahedron Lett.* **1989**, *30,* 1005-

1008. (b) For a different interpretation of the structures of products obtained from the reaction of formaldehyde with chromotropic acid (4,5-dihydroxy-2,7-naphthalenedisulfonic acid) under similar conditions, see: Georghiou, P. E.; Ho, C. K. *Can. J. Chem.* **1989**, *67,* 871-876; and references cited therein.

22. (a) Poh, B-L.; Team, C. M. *Tetrahedron* **2005**, *61*, 5123-5129. (b) Poh, B-L.; Tan, C-M. *J. Incl. Phenom. Macro. Chem.* **2000**, *38*, 69-74. (c) Poh, B-L.; Tan, C-M. *Tetrahedron* **1995**, *51*, 953-8. (d) Poh, B-L.; Tan, C. M. *Tetrahedron* **1994**, *50*, 3453-3462. (e) Poh, B-L.; Tan, C. M. *Tetrahedron* **1993**, *49*, 9581-9592. (f) Poh, B-L.; Lim, C. H.; Tan, C. M.; Wong, W. M. *Tetrahedron* **1993**, *49*, 7259-7266. (g) Poh, B-L.; Tan, C. M.; Loh, C. L. *Tetrahedron* **1993**, *49*, 3849-3856. (h) Poh, B-L; Lim, C. S.; Koay, L. S. *Tetrahedron* **1990**, *46*, 6155-6160. (i) Poh, B-L; Lim, C. S.; Koay, L. S. *Tetrahedron* **1990**, *46*, 3651-3658. (j) Poh, B-L.; Seah, L. H.; Lim, C. S. *Tetrahedron* **1990**, *46*, 4379-4386. (k) Poh, B-L.; Koay, L. S. *Tetrahedron Lett.* **1990**, *31*, 1911-1914.

23. Andreetti, G. D.; Böhmer, V.; Jordon, J. G.; Tabatabai, M.; Ugozzoli, F.; Vogt, W.; Wolff, W. *J. Org. Chem.* **1993**, *58,* 4023-4032.

24. Georghiou, P. E.; Ashram, M.; Clase, H. J.; Bridson, J. N. *J. Org. Chem.* **1998**, *63*, 1819-1826.

25. Ikeda, A.; Yoshimura, M.; Lhotak, P.; Shinkai, S. *J. Chem. Soc., Perkin Trans. 1,* **1996**, 1945-1950.

26. (a) Shorthill, B. J.; Granucci, R. G.; Powell, D. R.; Glass, T. *E. J. Org. Chem.* **2002**, *67,* 904-909. (b) Shorthill, B. J.; Glass, T. E. *Org. Lett.* **2001**, *3*, 577-579.

27. For a recent review on calixnaphthalenes: see reference 4.

28. Ashram, M. *Ph.D. Dissertation,* Memorial University of Newfoundland, 1997.

29. Chowdhury, S. *Ph.D. Dissertation,* Memorial University of Newfoundland, 2001.

30. Mizyed, S. *Ph.D. Dissertation,* Memorial University of Newfoundland, 2002.

31. Georghiou, P. E.; Li, Z.; Ashram, M.; Miller, D. O. *J. Org. Chem.* **1996**, *61*, 3865-3869.

32. Ashram, M.; Miller, D. O.; Georghiou, P. E. *J. Chem. Soc., Perkin Trans. 1*, **2002**, 1470-1476.

33. Georghiou, P. E; Li, Z.; Ashram, M. *J. Org. Chem.* **1998**, *63*, 3748-3752.

34. (a) Ashram, M.; Mizyed, S.; Georghiou, P. E. *J. Org. Chem.* **2001**, *66*, 1473-1479. (b) Chowdhury, S.; Georghiou, P. E. *J. Org. Chem.* **2002**, 67, 6808-6811.

35. Tran, A. H.; Miller, D. O.; Georghiou, P. E. *J. Org. Chem.* **2005**, *70*, 1115-1121.

36. Donald J. Cram, Jean-Marie Lehn and Charles J. Pedersen shared the 1987 Nobel Prize in Chemistry for their "development and use of molecules with structure-specific interaction of high selectivity".

37. Lehn, J. M. *Supramolecular Chemistry: Concepts and Perspectives,* VCH, Weinheim, 1995.

38. (a) Schneider, H. J.; Yatsimirsky, A. K. *Principles and Methods in Supramolecular Chemistry*, Wiley, Chichester, 2000. (b) Beer, P. D.; Gale, P. A.; Smith, D. K. *Supramolecular Chemistry*, Oxford, 1999.

39. Cram, D. J.; Cram, J. M. *Container Molecules and their Guests, Monographs in Supramolecular Chemistry*; Stoddart, J. F., Ed.; The Royal Society of Chemistry, 1994.

40. Steed, J. W., Atwood, J. L. *Supramolecular Chemistry*, John Wiley & Sons, 2000.

41. (a) Ungaro, R.; Pochini, A.; Andreetti, G. D.; Domiano, P.; *J. Chem. Soc., Perkins Trans. 2* **1983**, 1773-1779. (b) Andreetti, G.D.; Ori, O.; Ugozzoli, F.; Alfieri, C.; Pochini, A.; Ungaro, R. *J. Inclusion Pheom.* **1988**, *6*, 523-536. (c) Zanotti-Gerosa, A.; Solari, E.; Giannini, L.; Floriani, C.; Re, N.; Chiesi-Villa, A.; Rizzoli C. *Inorg. Chim. Acta* **1988**, *270*, 298-311. (d) Zanotti-Gerosa, A; Solari, E.; Giannini, L.; Floriani, C.; Chiesi-Villa, A.; Rizzoli, C. *J. Chem. Soc., Chem. Commun.* **1996**, 119-120.

42. Foster, R. *Organic Charge-Transfer Complexes*, Academic Press, Elsevier. New York, 1950.

43. Dodziuk, H. *Introduction to Supramolecular Chemistry*, Kluwer Academic Publishers, Dordrecht, The Netherlands 2002 and references cited therein.

44. Ramon, G.; Coleman, A. W.; Nassimbeni, L. R. *Cryst. Growth Des.* **2006**, *6*, 132-136.

45. Kubo, M.; Nashimoto, E.; Tokiyo, T.; Morisaki, Y.; Kodama, M.; Hioki, H. *Tetrahedron Lett.* **2006**, *47*, 1927-1931.

46. Computer-assisted molecular modeling studies were conducted using Spartan'04, V1.0.3 or Spartan Pro V1.1 from Wavefunction, Inc., Irvine, CA, USA. Molecular mechanics (MMFF94) calculations were conducted on the optimized geometry of the hosts and guests and their respective complexes.

47. (a) Iwamoto, K.; Ikeda, A.; Araki, K.; Harada, T.; Shinkai, S. *Tetrahedron* **1993**, *49*, 9937-9946 (b) Bott, S. G.; Coleman, A. W.; Atwood, J. L. *J. Am. Chem. Soc.* **1986**, *108*, 1709-1710.

48. (a) Ikeda, A.; Tsuzuki, H.; Shinkai, S. *J. Chem. Soc., Perkin Trans. 2*, **1994**, 2073-2080. (b) Ikeda, A.; Shinkai, S. *J. Am. Chem. Soc.* **1994**, *116*, 3102-3110.

49. (a) Ikeda, A.; Shinkai, S. *Chem. Rev.* **1997**, *97*, 1713-1734. (b) Araki, K.; Shimizu, H.; Shinkai, S. *Chem. Lett.* **1993**, 205-208. (c) Harrowfield, J. M.; Richmond, W. R.; Sobolev, A. N.; White, A. H. *J. Chem. Soc., Perkin Trans. 2*, **1994**, 5-9. (d) Arduini, A.; McGregor, W. M.; Paganuzzi, D.; Pochini, A.; Secchi, A.; Ugozzoli, F.; Ungaro, R. *J. Chem. Soc., Perkin Trans. 2*, **1996**, 839-846.

50. Ashram, M.; Mizyed, S.; Georghiou, P. E. *Org. Biomol. Chem.* **2003**,*1*, 599-603

51. Robert F. Curl Jr., Richard E. Smalley, and Harold W. Kroto shared the 1996 Nobel Prize in Chemistry for their "for their discovery of fullerenes".

52. (a) Kroto, H. W.; Heath, J. R.; O'Brien, S. C.; Smalley, R. F. *Nature* **1985**, *318*, 162-163. (b) Krätschmer, W.; Lamb, L. D.; Fostiropoulos, K.; Huffmann, D. R. *Nature* **1990**, *347*, 354-358.

53. Atwood, J. L.; Koutsoantonis, G. A.; Raston, C. L. *Nature* **1994**, *368*, 229-231.

54. Suzuki, S.; Nakashima, K.; Shinkai, S. *Chem. Lett.* **1994**, 699-702.

55. (a) Haino, T.; Yanase, M.; Fukazawa, Y. *Angew. Chem. Int. Ed. Engl.* **1997**, *36*, 259-260. (b) Haino, T.; Yanase, M.; Fukazawa, Y. *Tetrahedron Lett.*

1997, *38*, 3739-3743. (c) Haino, T.; Yanase, M.; Fukazawa, Y. *Angew. Chem. Int. Ed.* **1998**, *37*, 997-998.

56. (a) Barbour, L. J.; Orr, G. W.; Atwood, J. L. *Chem. Commun.* **1998**, 1901-1902. (b) Barbour, L. J.; Orr, G. W.; Atwood, J. L. *Chem. Commun.* **1997**, 1939-1940.

57. (a) Ikeda, A.; Suzuki, Y.; Yoshimura, M.; Shinkai, S. *Tetrahedron*, **1998**, *54*, 2497-2504. (b) Ikeda, A.; Suzuki, Y.; Yoshimura, M.; Shinkai, S. *Tetrahedron Lett.*, **1997**, *38*, 2107-2110. (c) Ikeda, A.; Yoshimura, M.; Udzu, H.; Fukuhara, C.; Shinkai, S. *Chem. Lett.* **1994**, 587-588. (d) Ikeda, A.; Udzu, H.; Yoshimura, M.; Shinkai, S. *Tetrahedron*, **2000**, *56*, 1825-1832.(e) (f) Ikeda, A.; Yoshimura,M.; Udzu, H.; Fukuhara, C.; Shinkai, S. *J. Am. Chem. Soc.* **1999**, *121*, 4296-4297. (g) Tsubaki, K.; Tanaka, K.; Kinoshita, T.; Fuji, K. *Chem. Commun.* **1998**, 895-896. (h) Shokova, E. A.; Kovalev, V. V. *Russ. J. Org. Chem.* **2004**, *40*, 1547-1571.

58. (a) Komatsu, N. *Tetrahedron Lett.* **2001**, *42*, 1733-1736. (b) Komatsu, N. *Org. Biomol. Chem.* **2003**, *1*, 204-209.

59. Atwood, J. L.; Barbour, L. J.; Nichols, P. J.; Raston, C. L.; Sandoval, C.A. *Chem. Commun.* **1998**, 1901-1902.

60. http://www.sesres.com/PhysicalProperties.asp

61. (a) Nikolaev, A. V.; Dennis, T. J. S.; Prassides, K.; Soper, A. K.; *Chem. Phys. Lett.* **1994**, *223*, 143-148. (b) Hirsch, A.; Brettreich, M. *Fullerenes, Chemistry and Reactions*, Wiley-VCH, Strauus GmbH, Morlenbach, 2005.

62. (a) Georghiou, P. E.; Mizyed, S.; Chowdhury, S. *Tetrahedron Lett.* **1999**, *40*, 611-614. (b) Mizyed, S.; Georghiou, P. E.; Ashram, M. *J. Chem. Soc., Perkin Trans. 2*, **2000**, 277-280. (c) Mizyed, S.; Tremaine, P. R.; Georghiou, P. E. *J. Chem. Soc., Perkin Trans. 2*, **2001**, 3-6.

63. Mizyed, S.; Ashram, M.; Miller, D. O.; Georghiou, P. E. *J. Chem. Soc., Perkin Trans. 2*, **2001**, 1916-1919.

64. Bancu, M.; Rai, A. K.; Cheng, P.-C.; Gilardi, R. D.; Scott, L. T. *Synlett* **2004**, 173-176.

Chapter 2

A complexation study with fullerenes using corannulene derivatives as model compounds

2.1 Introduction

In the field of supramolecular chemistry, host-guest recognition has become a very important multidisciplinary research area. The complexes can form from various hosts and guests, such as crown ethers and cations; spherands or calixarenes and alkyl ammonium cations; and/or organic cyclodextrins or calixarenes and organic molecules.[1]

The strength of host-guest binding is dependent on electrostatic interactions, which are mainly controlled by host-guest topological features, solvophobic effects and temperature. Conventionally, the stability of resulting complexes is evaluated via their binding or association constants K_{assoc}. Although there are many different types of host-guest systems in supramolecular chemistry, the methodology employed to determine the binding constants and stoichiometry is similar in both basic principles and in their experimental practicality. In this thesis, thiocorannulene derivatives synthesized by the Scott group[2] were employed as model compounds for a practical complexation investigation with fullerenes (C_{60} and C_{70}). The protocol and experience which resulted from this study was later employed in the study of calixnaphthalene inclusions.

In this chapter, the methodology employed in the complexation studies is presented first, followed by a brief introduction to the corannulene derivatives examined, and finally their complexation properties with fullerene guests in carbon disulfide solutions. The results from the complexation studies described in this chapter have been published recently.[3]

2.2 Complexation study methodology[4,5,6]

Commonly, a host-guest complexation study commences with determination of the complex stoichiometry using the Job plot (or continuous variation) method[7] or the mole ratio method.[4] The host-guest binding constant K_{assoc} for a 1:1 complexation, is subsequently obtained from a treatment of the titration experimental data with suitable methods such as the Benesi-Hildebrand treatment,[8] the Foster-Fyfe (Statchard) method,[9] the Rose-Drago method,[10] or a simple linear regression method.[11]

Practically, if binding occurs upon addition of aliquots of guests (in solution or solid state) into a host solution, or *vice versa*, there will be observable changes in the appearance and/or absorption spectrum of the resulting mixtures. The experimental data can then be collected by monitoring these changes with conventional analytical techniques, including IR, UV-vis, NMR, ESR, or even by novel techniques, such as Scanning Probe Microscopy (SPM), Atomic Force Microscopy (AFM), and electrochemical techniques.[12]

In this section, the basic principles of host-guest binding studies using ^{1}H NMR and/or UV-visible spectroscopy will be described as these two simple and convenient methods were employed throughout this study.

2.2.1 Determination of host – guest stoichiometry

2.2.1.1 Job plot method[6]

The Job plot method, also called Job's method or the method of continuous variations, is widely used to determine host-guest complex stoichiometry. In this method, the measurements are conducted on a series of samples with varying host:guest mole fractions (χ). The sum of the initial concentrations of host and guest is kept such that $[H]_o = [H]_i + [G]_i = [G]_o$, where $[H]_o$ and $[G]_o$ are the concentrations of pure host and guest solutions, respectively, $[H]_i$ and $[G]_i$ are the initial concentrations of host and guest in a host-guest mixture sample and $\chi_H = [H]_i/([H]_i + [G]_i)$ or $\chi_G = [G]_i/([H]_i + [G]_i)$.

^{1}H NMR spectroscopic method

In an ^{1}H NMR spectroscopic study, the observable change resulting from host-guest complex formation can be monitored following the host signal shifts ($\Delta\delta_H = \delta_{complex} - \delta_{free\ host}$) and/or the guest signal shifts ($\Delta\delta_G = \delta_{complex} - \delta_{free\ guest}$). The Job plot here is a plot of the observed change multiplied by mole fraction ($\Delta\delta_H \cdot \chi_H$ or $\Delta\delta_G \cdot \chi_G$) *vs* mole fraction ($\chi_H$ or χ_G), respectively. If a 1:1 host-guest binding occurs, the Job plot will show a maximum at $\chi = 0.5$ (*e.g.* see Figure 2.1).

In the case of 2:1 or 1:2 complexation, the plot will have a maximum at $\chi = 0.33$ or 0.67, respectively.

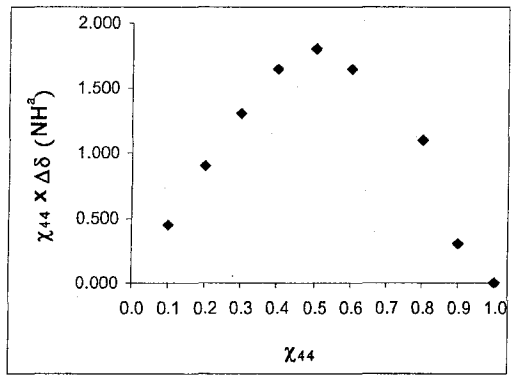

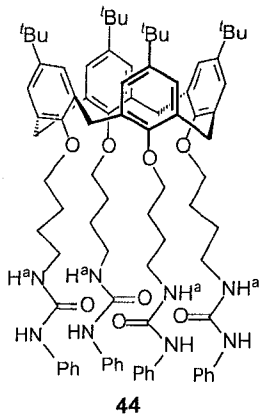

44

Figure 2.1 Job plot (*left*) for 1:1 complexation of tetraphenyl urea calix[4]arene **44** (*right*) with tetrabutylammonium chloride (TBACl) in $CDCl_3$ ([**44**] = [TBACl] = 5 x 10^{-3} M).[13]

UV-vis spectroscopic method

Similarly, host-guest stoichiometry can also be determined by UV-vis absorption spectroscopy by plotting the absorbance change (ΔA) at a particular wavelength *vs* the mole fraction.[14]

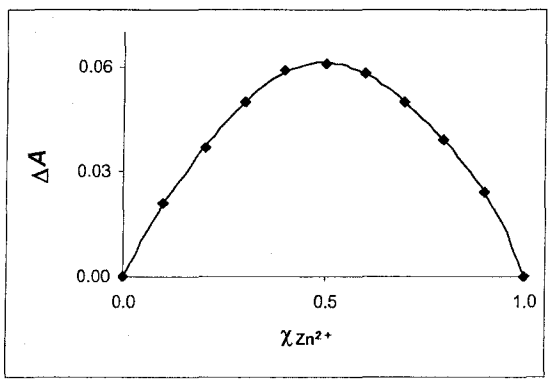

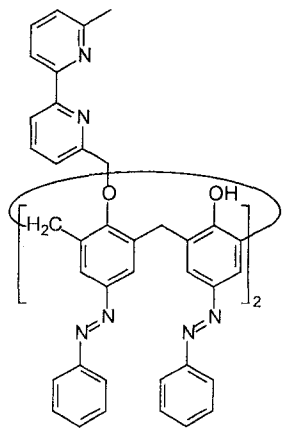

45

Figure 2.2 Job plot (*left*) for 1:1 complexation of azocalix[4]arene **45** (5 x 10^{-5} M) (*right*) and $Zn(CF_3SO_3)_2$ (5 x 10^{-5} M) in DCM at 25 °C and λ = 222 nm.[14]

2.2.1.2 Mole ratio method

In the mole ratio method, the concentration of the host or guest is kept constant, or almost constant, while the concentration of guest or host is gradually increased. In a plot of the chemical shift $\Delta\delta$ (using ^{1}H NMR)[4] or ΔA (using UV-vis)[15] *vs* the [G]/[H] ratios, a discontinuity or abrupt change of the slope indicates the binding stoichiometry (Figure 2.3). In addition, the K_{assoc} can be derived from the mole ratio plot.[3]

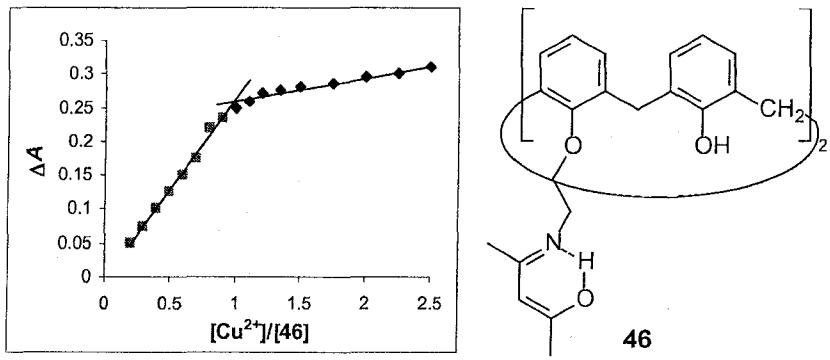

Figure 2.3 Mole ratio plot (*left*) for 1:1 complexation of *β*-ketoimine calix[4]arenes **46** (5 x 10^{-4} M) (*right*) with Cu^{2+} in MeCN at λ = 431.5 nm.[16]

2.2.2 Determination of association constants (binding constants)[2–16]

It is generally assumed that upon addition of aliquots of guest to the host solution, that the monitored signals are those of the host and host-guest complex. The concentration being plotted will be that of the guest concentration, [G].

2.2.2.1 ^{1}H NMR spectroscopic method

When a 1:1 association occurs, the formation of the H:G complex can simply be represented by equation 2.1, and the corresponding binding constant K_{assoc} can be defined by equation 2.2.

$$H + G \rightleftharpoons H:G \quad \text{(Eq 2.1)}$$

$$K_{assoc} = \frac{[H:G]}{[H] \cdot [G]} \quad \text{(Eq 2.2)}$$

$$[H] = [H]_o - [H:G] \quad \text{(Eq 2.3)}$$

$$[G] = [G]_o - [H:G] \quad \text{(Eq 2.4)}$$

For these equations, $[H]_o$ and $[G]_o$ are the initial molar concentrations of host and guest, respectively, and [H:G], [H] and [G] are the molar concentrations of host-guest complex, host and guest at equilibrium, respectively.

When there is a rapid exchange between host and H:G complex, the observable chemical shift is only contributed fractionally by host and complex, as expressed by equations 2.5–2.8. The mole fraction of host χ_H and of H:G complex $\chi_{H:G}$ are now defined as described in equation 2.7 and 2.8.

$$\delta_{obs} = \chi_H.\delta_H + \chi_{H:G}.\delta_{H:G} \quad \text{(Eq 2.5)} \quad \text{and} \quad \chi_H = 1 - \chi_{H:G} \quad \text{(Eq 2.6)}$$

$$\text{Where } \chi_H = \frac{[H]}{[H]+[H:G]} \quad \text{(Eq 2.7)} \quad \text{and} \quad \chi_{H:G} = \frac{[H:G]}{[H]+[H:G]} \quad \text{(Eq 2.8)}$$

Combining equations 2.5–2.8, δ_{obs} can be now expressed by equation 2.9:

$$\delta_{obs} = (1 - \frac{[H:G]}{[H]+[H:G]}) \cdot \delta_H + \frac{[H:G]}{[H]+[H:G]} \cdot \delta_{H:G} = \delta_H + \frac{[H:G]}{[H]+[H:G]} \cdot (\delta_{H:G} - \delta_H) \quad \text{(Eq 2.9)}$$

Combining equation 2.3 and equation 2.9 gives equation 2.10:

$$\frac{\Delta\delta_o}{\Delta\delta} = \frac{\delta_{H:G} - \delta_H}{\delta_{obs} - \delta_H} = \frac{[H]_o}{[H:G]} \quad \text{(Eq 2.10)}$$

where $\Delta\delta = \delta_{obs} - \delta_H$ and $\Delta\delta_o = \delta_{H:G} - \delta_H$

Combining equation 2.3 and equation 2.2 gives equation 2.11:

$$K_{assoc} = \frac{[H:G]}{([H]_o - [H:G]) \bullet [G]} \quad \text{therefore} \quad \frac{[H]_o}{[H:G]} = \frac{1}{K_{assoc} \bullet [G]} + 1 \quad \text{(Eq 2.11)}$$

The **Benesi-Hildebrand (B–H) equation** 2.12 in double-reciprocal plotting form results from a combination of equations 2.10 and 2.11. The binding constant K_{assoc} (K_{B-H}) value is the ratio of intercept/slope derived from the straight line plot of $1/\Delta\delta$ *vs* 1/[G] (Figure 2.4).

$$\frac{1}{\Delta\delta} = \frac{1}{K_{assoc} \bullet \Delta\delta_o \bullet [G]} + \frac{1}{\Delta\delta_o} \quad \text{(Eq 2.12)}$$

The **Foster-Fyfe (F–F) equation** (a form of the Scatchard equation) is obtained in a single reciprocal plotting form by multiplying equation 2.12 with $\Delta\delta_o.\Delta\delta.K_{assoc}$ and rearranging to give equation 2.13. The K_{assoc} (K_{F-F}) is obtained from the slope of the plot of $\Delta\delta/[G]$ *vs* $\Delta\delta$ (Figure 2.4).

$$\frac{\Delta\delta}{[G]} = -K_{assoc} \bullet \Delta\delta + K_{assoc} \bullet \Delta\delta_o \quad \text{(Eq 2.13)}$$

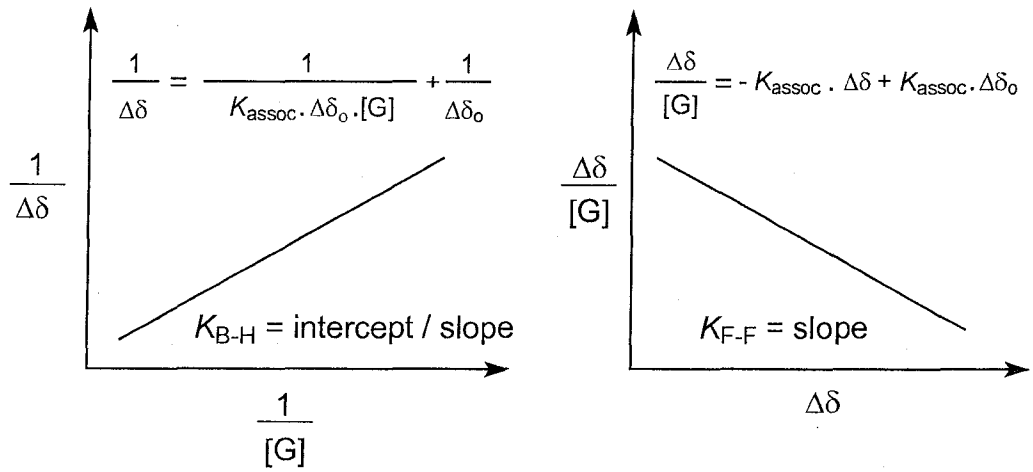

Figure 2.4 Benesi-Hildebrand plot (*left*) and Foster-Fyfe plot (*right*).

2.2.2.2 UV-vis spectroscopic method

It is assumed in this case, that the host-guest association is also a 1:1 binding, and that the absorptions of the host and the complex are significantly different, follow Beer's law, and are measured using 1 cm light path cuvettes.

The initial absorbance A_o of the host solution is expressed as

$$A_o = \varepsilon_H . [H]_o \qquad \text{(Eq 2.14)}$$

where ε_H is the molar absorptivity of the host, and $[H]_o$ is the initial molar concentration of host.

Upon addition of aliquots of guests to the host solution, the absorbance A_H of the resulting mixture is written as

$$A_H = \varepsilon_H . [H] + \varepsilon_G . [G] + \varepsilon_{H:G} . [H:G] \qquad \text{(Eq 2.14)}$$

where ε_G is the molar absorptivity of the guest, and $\varepsilon_{H:G}$ is the molar absorptivity of the H:G complex.

Substituting [H] and [G] from equations 2.3 and 2.4 into equation 2.14 gives equation 2.15, in which the difference in the molar extinction coefficient between the H:G complex and that of uncomplexed host and guest is $\Delta\varepsilon_c = \varepsilon_{H:G} - \varepsilon_H - \varepsilon_G$.

$$A_H = \varepsilon_H.([H]_o - [H:G]) + \varepsilon_G.([G]_o - [H:G]) + \varepsilon_{H:G}.[H:G]$$

$$A_H = \varepsilon_H.[H]_o + \varepsilon_G.[G]_o + (\varepsilon_{H:G} - \varepsilon_H - \varepsilon_G)[H:G]$$

$$A_H = \varepsilon_H.[H]_o + \varepsilon_G.[G]_o + \Delta\varepsilon_c.[H:G] \qquad \text{(Eq 2.15)}$$

By subtracting the initial absorbance of the guest solution ($\varepsilon_G.[G]_o$) used as the reference, the measured absorbance becomes:

$$A_H = \varepsilon_H.[H]_o + \Delta\varepsilon_c.[H:G] \qquad \text{(Eq 2.16)}$$

Substituting [H:G] from equation 2.2 into equation 2.16 gives

$$A_H = \varepsilon_H.[H]_o + \Delta\varepsilon_c.K_{assoc}.[H].[G] \qquad \text{(Eq. 2.17)}$$

and rearranging equation 2.17 gives the absorption of the solutions (measured against the blank) ΔA as:

$$\Delta A = A_H - \varepsilon_H.[H]_o = K_{assoc}.\Delta\varepsilon_c.[H].[G] \qquad \text{(Eq 2.18)}$$

From equations 2.2 and 2.3

$$[H] = \frac{[H]_o}{1 + K_{assoc} \cdot [G]} \qquad \text{(Eq 2.19)}$$

Combining equations 2.18 and 2.19 gives

$$\Delta A = K_{assoc} \cdot \Delta\varepsilon_c \cdot \frac{[H]_o}{1 + K_{assoc} \cdot [G]} \cdot [G] \qquad \text{(Eq 2.20)}$$

The **Benesi-Hildebrand equation**, equation 2.21, is obtained by taking the reciprocal of equation 2.20:

$$\frac{[H]_o}{\Delta A} = \frac{1}{K_{assoc} \bullet \Delta\varepsilon_c \bullet [G]} + \frac{1}{\Delta\varepsilon_c} \quad \text{(Eq 2.21)}$$

A plot of $1/[G]$ *vs* $1/\Delta A$ (or $[H]_o/\Delta A$), known as a double-reciprocal plot, gives a straight line, for which the y-intercept divided by the slope gives K_{assoc} (K_{B-H}). Extrapolation, using least-squares linear regression analysis gives the value for the intercept.

The **Foster-Fyfe equation** is obtained by multiplying the Benesi-Hildebrand equation 2.21 with $K_{assoc} \cdot \Delta\varepsilon_c \cdot \Delta A$ and rearranging to give equation 2.22:

$$\frac{\Delta A}{[G]} = -K_{assoc} \bullet \Delta A + [H]_o \bullet K_{assoc} \bullet \Delta\varepsilon_c \quad \text{(Eq 2.22)}$$

The K_{assoc} (K_{F-F}) is obtained from the slope of the straight line obtained by plotting $\Delta A/[G]$ *vs* ΔA.

2.3 Corannulene derivative hosts[3]

With its bowl-shaped geometry, corannulene (**47**) and its substituted derivatives appear to be ideal hosts for a "contact lens" style of supramolecular associations with fullerenes (Figure 2.5). Specifically, the concave surface of corannulene (**47**) has almost exactly the right degree of curvature to bring all 20 carbon atoms of the polynuclear aromatic bowl into contact with the more steeply

curved convex surface of C_{60}, when allowance is made for the van der Waals thickness of the two π-systems.[17]

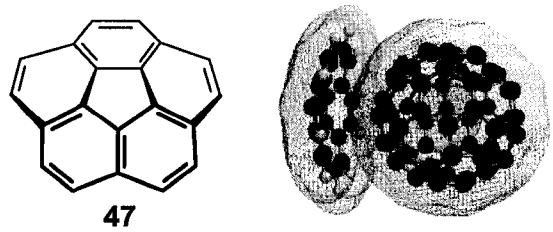

47

Figure 2.5 Structure of corannulene (**47**) ($C_{20}H_{10}$) (*left*); computer-generated model of van der Waals contact between **47** and C_{60} (*right*).[3]

In addition, the electron-deficient nature of the convex C_{60} surface (a good π–acceptor) has been amply demonstrated by the ease with which nucleophiles were (*e.g.* cyanide ion) added, by the ability of C_{60} to serve as a dienophile toward electron-rich dienes (*e.g.* anthracene), and by the propensity of C_{60} to form complexes with electron-rich metals (*e.g.* $Pt(PEt_3)_2$). The concave π–surface of **47**, by contrast, is calculated to exhibit an electrostatic potential that is even more negative (good π–donor) than that of its planar counterparts.[18]

As a result, a significant binding constant value would be expected to be found for the complexation of corannulene (**47**) and C_{60} if their two surfaces exert some level of electronic attraction toward one another via a π–donor/π–acceptor interaction. Indeed, a previous study[19] revealed that thiocorannulene derivatives **48**–**50** (Figure 2.6) all form supramolecular complexes with C_{60} in toluene-d_8 with K_{assoc} values about 2.8–4.5 $\times$ 10^2 M^{-1} for solutions in the 0.96–1.25 x 10^{-3} M concentration range. For the strongest of these complexes, **49**:C_{60}, a downfield

shift in the ^{1}H NMR signal for the *para*-methoxy groups at the termini of the five appendages suggests that the arms swing up and embrace the C_{60} thereby becoming deshielded either all at once (Figure 2.7) or in combinations that rapidly equilibrate.

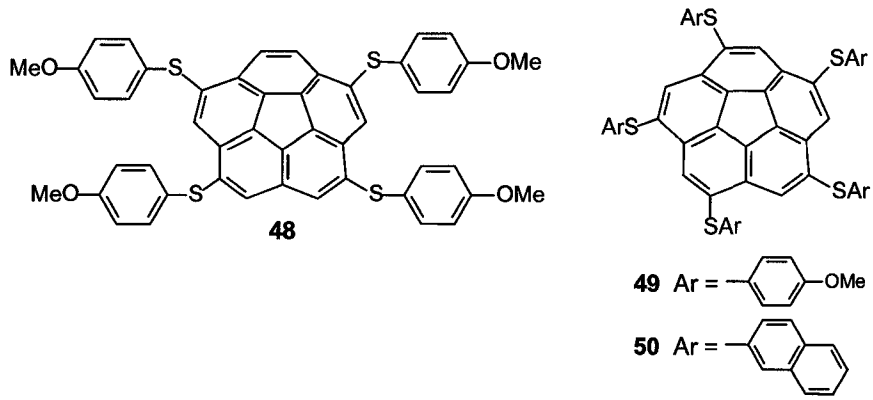

Figure 2.6 Thiocorannulene derivatives **48**–**50**.

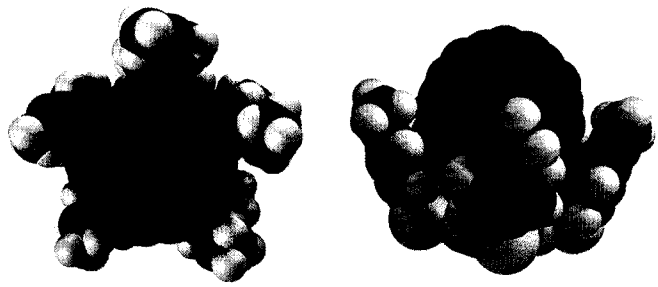

Figure 2.7 Top view (*left*) and side view (*right*) of the computer-generated[20] model of **49** embracing C_{60} with maximal contact.[3]

The new studies described here and which were recently published[3] were designed to probe: (*a*) whether or not the aryl groups on the arms actually play a critical role in the binding; (*b*) to what extent the number of sulfur atoms attached to the corannulene core affects the strength of the binding; and (*c*) whether C_{70}

will be attracted with a greater or a lesser affinity than C_{60} to such corannulene hosts.

Therefore, the thiocorannulene derivatives **50**–**53**, which were synthesized in reasonable yields by the Scott group from penta- and deca-chlorocorannulenes **54** and **55**[2,21] and sodium alkanethiolates or sodium 2-arylthiolate (NaSAr) or disodium 1,2-benzenedithiolate, respectively (Scheme 2.1), were employed as model hosts for a practical complexation study with fullerene (C_{60} and C_{70}) guests.

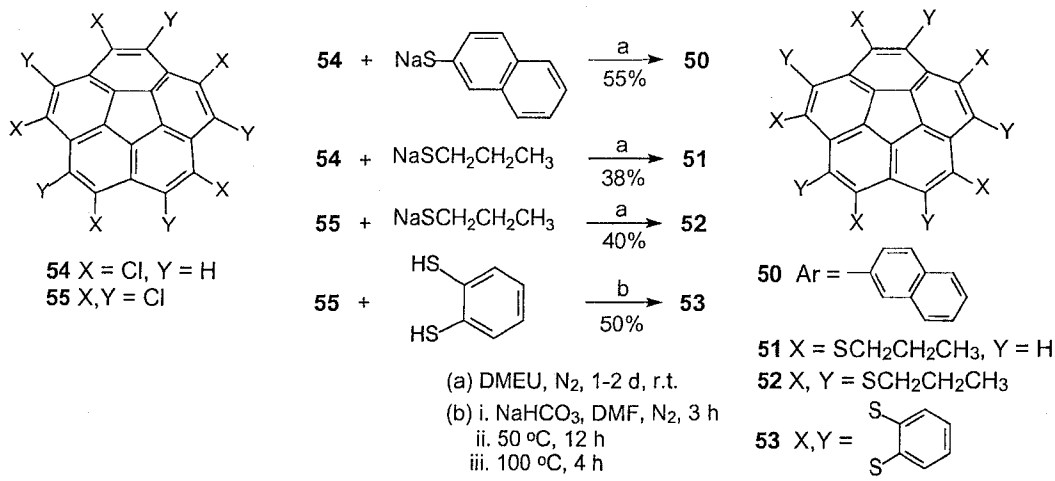

Scheme 2.1 Synthesis of thiocorannulene derivatives **50**–**53**.

2.4 Results of solution complexation studies, discussion and conclusions

2.4.1 Choice of corannulene hosts, experimental solvent and lock solvent

To learn whether the pendant aryl groups are required for complexation of C_{60} by the corannulene derivatives **48**–**50**, the 1,3,5,7,9-pentakis($SCH_2CH_2CH_3$) derivative (**51**),[2] which lacks electron-rich π-systems on the arms but retains the

geodesic polyarene core and the five attached sulfur atoms, was tested. Decakis(1-propylthio)corannulene **52**,[2] a poly(alkylthio) derivative with twice the number of sulfur atoms attached to the corannulene core, was also tested. Preliminary attempts to synthesize the corresponding pentakis- and decakis(methylthio)corannulenes (like **51** and **52**, but X = SMe) by the Scott group gave products that were too insoluble to use in the subsequent ^{1}H NMR titration experiments, but the 1-propylthio chains were found to impart acceptable levels of solubility. The pentakis- and decakis(alkylthio)corannulenes with *n*-hexyl and *n*-dodecyl chains[2] show even greater solubility in organic solvents, but **51** and **52** were the only poly(alkylthio) derivatives used for these complexation studies.

The conformational motions that are available to the five flexible flaps on the poly(arylthio)- host with 10 sulfur atoms on the corannulene core, pentakis(1,4-benzodithiino)corannulene (**53**),[2] resemble those of a Venus fly trap,[22] and this compound emerged as the best host for fullerenes among all the corannulene derivatives we have studied to date. Per(arylthio)aromatic compounds have previously been observed to complex guests in the solid state.[6] However, the complexes reported here are the first of their kind to be studied in solution.

The solubilities of pentakis(propylthio)- (**51**), "fly trap"-corannulene (**53**), and of C_{60} and C_{70} (2.99–4.44 x 10^{-3} and 1.27–1.70 x 10^{-3} M, respectively)[23] were too low in toluene-d_8 to allow for the unambiguous determinations of K_{assoc} values

on the basis of ^{1}H NMR complexation-induced chemical shifts. Preliminary ^{1}H NMR titration experiments[4] in toluene-d_8 at the low concentrations imposed by these solubility limitations revealed only very small chemical shift differences ($\Delta\delta$). Attempts to determine either the complexation stoichiometries or association constants (K_{assoc}) by UV-vis spectroscopic titration experiments at these low concentrations in toluene were also equivocal, since both host and guest molecules are coloured, making the unambiguous assignment of any charge-transfer bands difficult. In CS_2, however, the solubilities of both the host molecules and the fullerenes employed in this study are higher than in toluene-d_8. For example, the solubilities of C_{60} and C_{70} in CS_2 are reported to be in the range of 7.2–16.4 x 10^{-3} and 11.8–18.2 x 10^{-3} M, respectively.[19] Carbon disulfide, therefore, became the solvent of choice. The concentrations of **51** and **53** in CS_2 used in the ^{1}H NMR studies reported herein were both approximately 7.9 x 10^{-4} M.

Since CS_2 has no proton, a deuterated solvent is needed to provide a lock for the ^{1}H NMR experiments. The use of $CDCl_3$ as an external lock[24] was not suitable, as it did not provide a sufficiently stable lock and required long instrument time usage in order to obtain the best precision for determining the chemical shift changes. When used as an internal lock,[25] up to 20% v/v of $CDCl_3$ in the CS_2 was needed to achieve a stable lock and observe chemical shifts with an acceptable level of precision of (0.001 ppm from repeat measurements. At these elevated concentrations of $CDCl_3$, however, the solubilities of both C_{60} and

C_{70} were compromised (*e.g.*, the solubility of C_{60} fullerene in chloroform is reported to be only in the range 0.22–0.71 x 10^{-3} M). In addition, compound **53** was also partly precipitated in this solvent mixture. A far superior external lock was achieved with DMSO-d_6, which contains a higher percentage of deuterium per mole (14.4%) than does $CDCl_3$ (1.67%). All of the experimental results in this Chapter were therefore conducted in CS_2 solution using DMSO-d_6 as the external lock.

2.4.2 Complexation studies of 53 with C_{60} and C_{70}

The ^{1}H NMR spectrum of **53** (Figure 2.8) consists of only the orthophenylene ring hydrogen atoms, which appear as a pair of AA'BB' half spectra with four main overlapping signals each, one set having chemical shifts at δ = 7.393, 7.384, 7.382, and 7.374 ppm and the other at δ = 7.045, 7.139, 7.034, and 7.027 ppm. Upon addition of C_{60} and C_{70}, the host-guest solution turned to brown and dark brown, respectively. In addition, the signal shifts to lower field were both clearly observed (Figure 2.8). These indicated that complexes are formed between **53** and the fullerenes studied.

2.4.2.1 C_{60} as the guest

A Job plot determination of the complexation stoichiometry between **53** and C_{60} indicated the formation of a 1:1 host-guest complex (Figure 2.9). As well, a subsequent mole ratio plot of $\Delta\delta$ *vs* guest-to-host molar ratios confirmed this stoichiometry (Figure 2.9; Appendix 2.1). Preliminary experiments were

conducted next to determine the optimum solution concentration ranges on the basis of the Job plot and mole ratio plot observations. The most consistent data were obtained when C_{60} or C_{70} was added as a solid to solutions of **53** in NMR tubes followed by sonication to ensure complete dissolution.

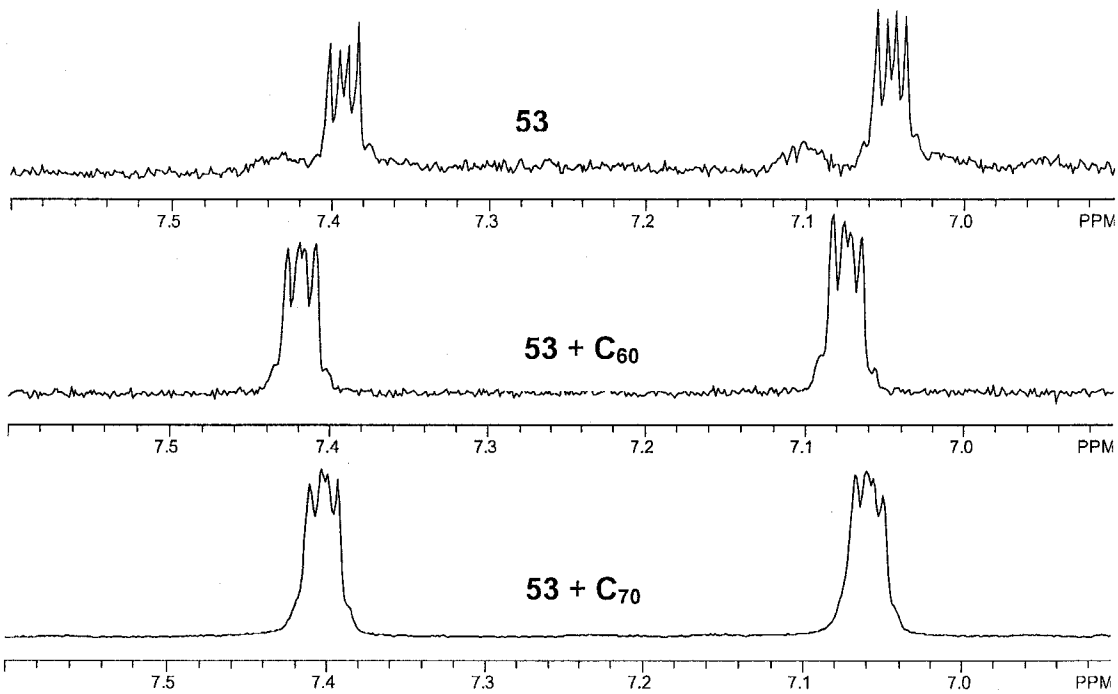

Figure 2.8 ^{1}H NMR spectra of **53** (*top*); mixture of **53** and C_{60} (*middle*); and mixture of **53** and C_{70} (*bottom*) in CS_2 (measured with a DMSO-d_6 external lock) at room temperature.

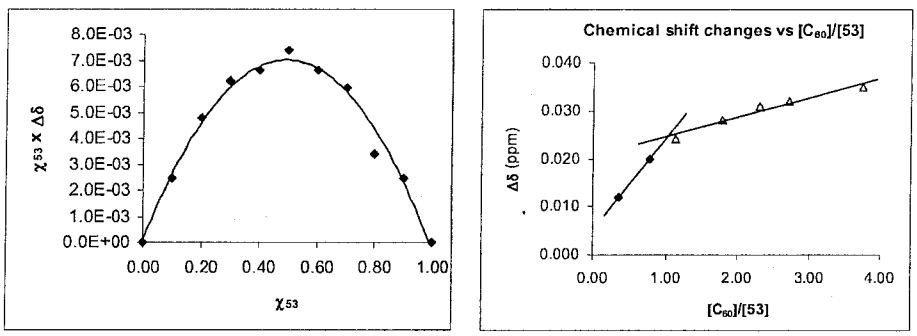

Figure 2.9 Job plot (*left*) and mole ratio plot (*right*) both showing the 1:1 stoichiometry of **53** and C_{60}. (Appendix 2.1).[3]

Two final determinations were then conducted to determine K_{assoc} of this complexation, one in which the mole ratios of C_{60} to **53** ranged from 0.36 to 3.74 ("low ratios" in which [**53**] is *ca.*7.86 x 10^{-4} M) and another in which the mole ratios of C_{60} to **53** ranged from 9.9 to 29.8 ("high ratios" in which [**53**] is *ca.* 1.05 x 10^{-4} M). These experiments yielded similar K_{assoc} values, which when averaged were 1420 ± 64 and 1420 ± 54 M^{-1}, respectively (Table 2.1, Entries 1 and 2; Figure 2.10; Appendix 2.2), as determined by the Benesi-Hildebrand[13] and Foster-Fyfe data treatments, respectively.[3a,14]

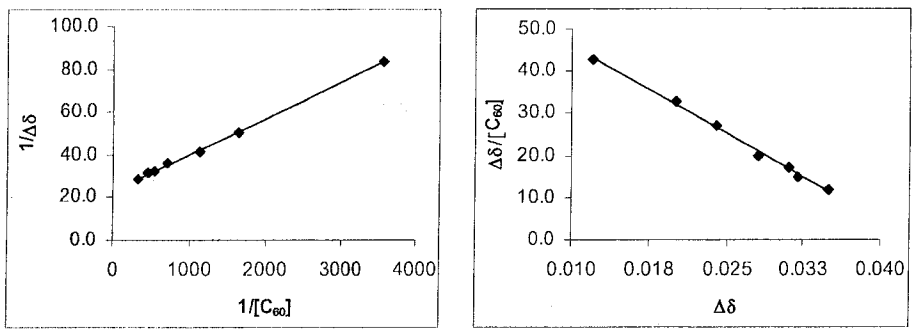

Figure 2.10 Benesi-Hildebrand plot (*left*) and Foster-Fyfe plot (*right*) for the complexation of **53** and C_{60} (*Note: chemical shifts changes are to lower fields*).[3]

2.4.2.2 C_{70} as the guest

With C_{70} and **53,** the 1:1 stoichiometry was established via mole ratio plots, and the K_{assoc} values for this system were 1101 ± 92 and 1059 ± 24 M^{-1}, determined in a manner similar to that used with C_{60} (Table 2.1, Entries 3 and 4; Figure 2.11; Appendix 2.3).

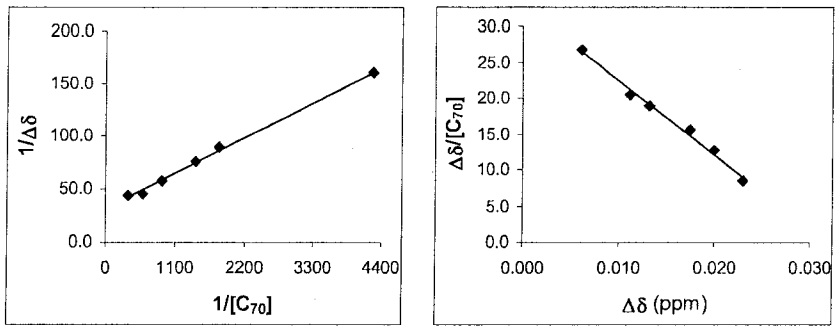

Figure 2.11 Benesi-Hildebrand plot (*left*) and Foster-Fyfe plot (*right*) for the complexation of **53** and C_{70} (*Note: chemical shifts changes are to lower fields*).[3]

2.4.3 Complexation studies of 51 with C_{60} and C_{70}

2.4.3.1 C_{60} as the guest

The stoichiometry of the complexation between pentakis(propylthio)-corannulene (**51**) and C_{60} or C_{70} in both cases was found also to be 1:1. Their K_{assoc} values, however, were significantly lower than those observed with **53**. Average values of only 62 ± 23 and 53 ± 6 M^{-1} (Table 2.1, Entries 5 and 6; Figure 2.12; Appendix 2.4) were obtained from the double (B–H) and single reciprocal (F–F) treatments, respectively, for the **51**:C_{60} complexation.

Slightly higher K_{assoc} values were obtained from the determinations conducted using the low [C_{60}]:[**51**] mole ratios (*i.e.* 0.70–3.51). As is well known, the B–H treatment gave the higher correlation coefficient and K_{assoc} values for the linear plot since it tends to overemphasize smaller chemical shift changes. With the higher [C_{60}]:[**51**] mole ratios (*i.e.* 10.4–35.6), the agreement between the K_{assoc} values obtained from the B–H and F–F treatments was closer (45 ± 4 and

49 ± 4 M^{-1}, respectively), as compared with 69 ± 12 and 58 ± 9 M^{-1}, as obtained using the lower [C_{60}]:[**51**] mole ratios.

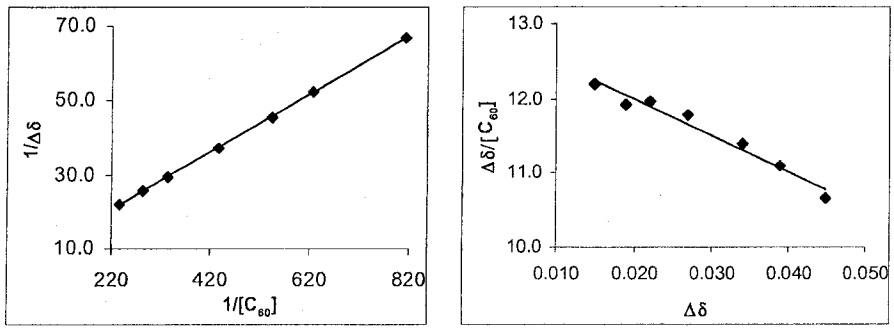

Figure 2.12 Benesi-Hildebrand plot (*left*) and Foster-Fyfe plot (*right*) for the complexation of **51** and C_{60} (*Note: chemical shifts changes were to higher fields*).[3]

2.4.3.2 C_{70} as the guest

The K_{assoc} values for the **51**:C_{70} complexation determined by the B–H and F–F treatments gave K_{assoc} average values of 90 ± 16 and 94 ± 19 M^{-1} (Table 2.1, Entries 7 and 8; Appendix 2.5). Slightly higher K_{assoc} values were obtained for the complexation between **51** and C_{70} as compared with C_{60}, which is just the reverse of what was seen with **53**. Figure 2.13 shows the chemical shift changes ($\Delta\delta$) of the protons of the **51** host as functions of added C_{60} and C_{70} guests, respectively. The chemical shifts for the corannulene protons (Ar–H) in both cases were also shifted to higher fields, whereas all other shifts were shifted to lower fields.

The largest (absolute) $\Delta\delta$ changes are observed for the protons on the corannulene ring, followed by those on the propyl methylene group β to the sulfur

atom, then by the protons on the propyl methyl group, and finally by the protons on the propyl methylene group α to the sulfur atom. All of the association constants reported herein were determined using the values obtained from the largest chemical shift changes.

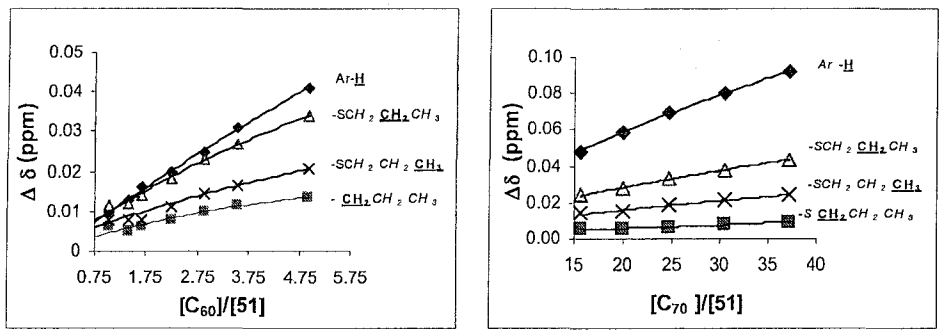

Figure 2.13 Plots showing absolute values of chemical shift changes (Δδ) of the various protons on **51** as a function of added C_{60} (*left*); and as a function of added C_{70} (*right*).[3]

2.4.4 Complexation studies of 47, 50 and 52 with C_{60} and C_{70}

When similar complexation studies were conducted using C_{60} and C_{70} with unsubstituted corannulene (**47**) and with decakis(propylthio)corannulene (**52**) in CS_2, no indication for complexation could be seen in these cases. However, in a study using CS_2 as the solvent, values of 320 ± 25 and 296 ± 21 M^{-1} for the complexation of **50** and C_{60}, were obtained using the B–H and F–F methods, respectively (Table 2.1, Entries 9 and 10; Appendix 2.6). Similarly, for complexation of **50** and C_{70}, the K_{assoc} values were 99 ± 20 and 97 ± 11 M^{-1} using the B–H and F–F methods, respectively (Table 2.1, Entries 11 and 12; Appendix 2.7).

2.4.5 Discussion of results and conclusions

The earlier study of the complexation of substituted corannulenes **48**–**50**, and of corannulene **47** itself, with C_{60} and C_{70} had been conducted in toluene-d_8.[19] It is well-known that the solvent used in complexation studies may have a significant effect on the binding constants.[26] It was therefore decided to conduct an additional complexation study of **50** in CS_2 with C_{60} and C_{70} in order to make some comparisons with the earlier study. This compound is representative of the compounds previously reported since it had K_{assoc} values of approximately 360 M^{-1} for binding with C_{60} in toluene-d_8.[19] In this study using CS_2 as the solvent, values of 320 ± 25 and 296 ± 21 M^{-1} for the complexation of **50** and C_{60} were obtained from the B–H and F–F treatment, respectively. Within experimental error, these values cannot be considered to be significantly different from those found in toluene-d_8. The K_{assoc} values for **50**:C_{70} in CS_2 are also listed in Table 2.1, but these had not previously been measured in toluene-d_8.

For **51,** the complexation-induced chemical shift changes for the protons on the corannulene ring were to higher (upfield) fields, as they also were for the corannulene protons on **48**–**50**.[3] A similar shielding effect by the respective fullerene on these protons upon complexation of **51** with C_{60} and C_{70} could therefore also account for the observations made in the present study. This would indicate that an inclusion analogous to that depicted in Figure 2.7 for C_{60} with **49** occurs for C_{60} (or C_{70}) with **51**, in which the corannulene protons are

those which have the closest contact with the fullerenes that have been embraced by the propylthio pendants.

The trends in chemical shift changes for the propylthio group protons in **51** with either C_{60} or C_{70} were very similar, as can be seen in Figures 2.13. It is somewhat puzzling; however, that with both C_{60} and C_{70}, it is the protons on the $-CH_2-$ groups that are β to the sulfur atoms that experience the largest downfield shifts and not those α to the sulfur atoms. This could be due to two opposing effects. The protons on the $-CH_2-$ groups α to the sulfur atoms would be expected to be shielded due to the proximity of these protons to the embedded or embraced fullerene, but they might also experience a deshielding effect due to an enhanced electron-withdrawing effect of the sulfur atoms interacting with the complexed electron deficient fullerenes. The methyl groups are situated more remotely from the guest and behave in a manner similar to what was previously observed in the cases of **48** and **49**.

The higher average K_{assoc} values obtained for the 1:1 complexation of **51** with C_{70} *vs* C_{60} in the present study (Table 2.1, Entries 7 *vs* 5 and 8 *vs* 6) suggest that the propylthio appendages can more effectively embrace the more cylindrically shaped C_{70} molecule than they are able to with C_{60}. The relatively larger chemical shift differences in the corannulene ring protons in the case of the **51**:C_{70} complex *vs* those seen with the **51**:C_{60} complex further support the contention that C_{70} forms the more deeply embedded complex of the two.

As indicated above, no evidence for complexation was found between either fullerenes studied with unsubstituted corannulene (**47**) or with the decakispropylthio compound **52**. Apparently, the bare face of the parent hydrocarbon (**47**) without any sulfur atoms attached is not a strong enough π-donor to complex neutral fullerenes. In the case of decakis(propylthio)corannulene (**52**), on the other hand, a doubling of the electron-rich sulfur atoms from 5 to 10 might have been expected to enhance the binding capability toward the electron-deficient C_{60} and C_{70} fullerenes. A binding enhancement toward C_{60} had been observed in our previous study[19] with **49**, which has five arylthio appendages, over **48**, which has only four. However, the long side chains on **52** probably crowd the concave face in order to avoid each other and thereby block access of the fullerenes (Figure 2.14).

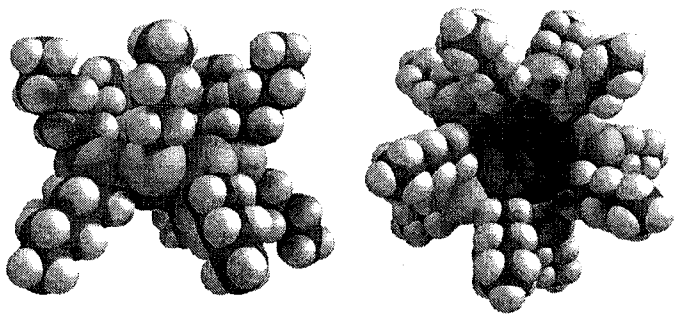

Figure 2.14 Side view (*left*) and top view/concave face (*right*) of a computer-generated model of decakis(propylthio)corannulene (**52**).[3]

As well, a larger entropic cost would result from the greater number of degrees of freedom possible in the 10 propylthioether appendages. Both of these factors could inhibit complexation with the fullerenes used under the conditions

examined. A similar entropic effect was noted by Masci[27] in his complexation studies with homooxacalixarenes and was also proposed by us with "Zorbarene", a new naphthalene-ring-based receptor that we recently reported and which is the subject of Chapter 5 in this thesis.[28]

The "fly trap" molecule **53**, on the other hand, shows much higher binding affinities than **51** for both C_{60} and C_{70}. In contrast to **51**, however, the larger K_{assoc} values were observed for the **53** complexation with C_{60} than with C_{70}. Possible explanations for both phenomena will be considered. First, a solvophobic effect[29] due to the higher solubility of C_{70} *vs* C_{60} in CS_2 could account for the higher K_{assoc} values observed for the complexation of **53** with C_{60}. Second, even though there are multiple sulfur atoms in both **51** and **53**, the latter has twice as many and does not have its sulfur atoms encumbered with tetrahedral carbon atoms. In the fly trap, the sulfur atoms are connected via orthophenylene rings, which are planar and thus reduce the steric impedance that occurs with the propylthio appendages. Since there are also fewer degrees of freedom of motion in these groups in **53**, there is a considerably smaller entropic cost to overcome in order to bring the sulfur atoms into contact with the surfaces of the respective fullerenes. Finally, the relatively electron-rich orthophenylene rings also can augment binding of the fullerenes within the corannulene bowl through favorable embracing π-π interactions with the surfaces of the fullerene guests. A crystal structure of a clathrate formed between two molecules of **53** embracing a single molecule of benzene[30] obtained by the Scott group[2] (Figure 2.15) shows the

ability of the host to wrap three of the flaps around the entrapped benzene. In this research, on the basis of both the X-ray data from the above clathrate and computer-assisted molecular modeling studies, it was hypothesized that three out of five flaps could flex to accommodate a spherical guest. The results from the study reported herein would appear to be consistent with this hypothesis.

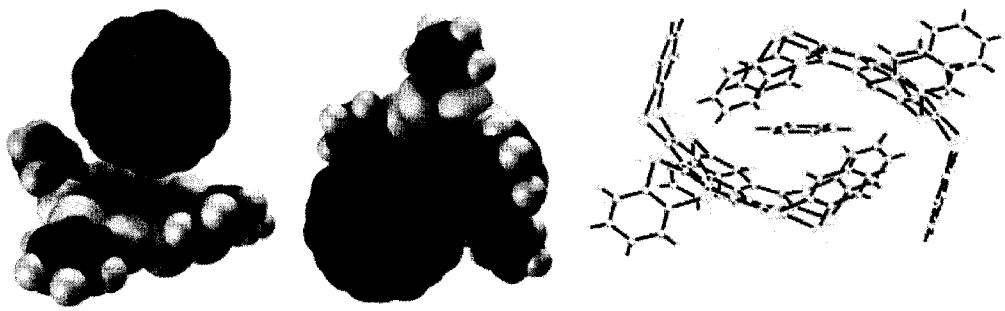

Figure 2.15 Side view (*left*) and top view (*middle*) of a computer-generated structure of **53** (resembling a Venus fly trap) embracing C_{60} and X-ray crystal structure (*right*) showing two molecules of **53** wrapped around a molecule of benzene.[3]

In brief, new insights into the steric requirements for these convex-concave supramolecular associations of corannulene and fullerenes were also brought to light. Specifically, the thioether appendages are necessary to enhance the encapsulation of fullerenes by corannulene derivatives to some extent of entropic cost.

Table 2.1 K_{assoc} (M^{-1}) for **50**, **51** and **53** complexes with C_{60} and C_{70} in CS_2 at 298 K.

Entry	Complex	Method ([G]/[H])	K_{assoc} (R^2)	Method ([G]/[H])	K_{assoc} (R^2)	Averages
1	**53**:C_{60}	B–H (0.36–3.74)	1373 ± 17 (0.999)	B–H (9.90–29.8)	1462 ± 27 (0.991)	1420 ± 64
2	**53**:C_{60}	F–F (9.92–29.78)	1384 ± 38 (0.996)	F–F (9.90–29.8)	1460 ± 94 (0.980)	1420 ± 54
3	**53**:C_{70}	B–H (0.29–3.43)	1040 ± 48 (0.996)	B–H (0.37–3.29)	1170 ± 46 (0.998)	1101 ± 92
4	**53**:C_{70}	F–F (0.29–3.43)	1042 ± 52 (0.990)	F–F (0.37–3.29)	1076 ± 60 (0.985)	1059 ± 24
5	**51**:C_{60}	B–H (0.70–3.51)	69 ± 12 (0.999)	B–H (10.4–35.6)	45 ± 4 (1.000)	62 ± 23
6	**51**:C_{60}	F–F (10.40–35.6)	58 ± 9 (0.999)	F–F (10.4–35.6)	49 ± 4 (0.968)	53 ± 6
7	**51**:C_{70}	B–H (0.53–3.96)	78 ± 5 (1.000)	B–H (10.7–37.1)	101 ± 6 (0.999)	90 ± 16
8	**51**:C_{70}	F–F (0.53–3.96)	80 ± 3 (0.991)	F–F (10.7–37.1)	107 ± 6 (0.986)	94 ± 19
9	**50**:C_{60}	B–H (0.35–3.13)	302 ± 13 (1.000)	B–H (0.34–3.90)	338 ± 19 (0.999)	320 ± 25
10	**50**:C_{60}	F–F (0.35–3.13)	281 ± 19 (0.983)	F–F (0.35–3.90)	311 ± 13 (0.976)	296 ± 21
11	**50**:C_{70}	B–H (0.71–3.91)	84 ± 9 (1.000)	B–H (1.07–4.71)	113 ± 12 (0.999)	99 ± 20
12	**50**:C_{70}	F–F (0.71–3.91)	89 ± 10 (0.956)	F–F (1.07–4.71)	105 ± 10 (0.971)	97 ± 11

2.5 Experimental section

2.5.1 General methods

Carbon disulfide (redistilled, industrial hygiene analysis grade) and buckminsterfullerenes C_{60} (99.5%) were purchased from Aldrich. C_{70} (>98%) were purchased from *BuckyUSA*. All chemicals were used without further purification. All mass determinations were conducted on a CAHN 27 microbalance. Unless otherwise indicated, ^{1}H NMR spectra were conducted in CS_2 with TMS as internal standard and a DMSO-d_6 external lock and recorded in pulse mode at 298 K at 500 MHz, using a 16 K data table for a 10.0 ppm sweep width having a digital resolution of 0.321 Hz. Chemical shifts in the ^{1}H NMR spectra are reported relative to TMS shifts (0.000 ppm). The chemical shifts used for plotting and data analysis were the mean values of the multiplet signals that were observed. The DMSO-d_6 external lock was made by injecting a sample of DMSO-d_6 with 5% TMS into a closed-end capillary tube and sealing the open end. For each measurement, the same capillary tube containing the DMSO-d_6 was inserted into the NMR tube using a specially designed Teflon® insert.

2.5.2 Determination of host-guest stoichiometry

Job plot determinations were conducted by varying the mole fractions of the host compound and C_{60}, using solutions which were approximately 7.86×10^{-4} M in CS_2 solution. After mixing, each of the respective solutions (total combined final volumes = 1.00 mL) in a series of nine NMR tubes which was sonicated for approximately 10 min, and in some cases were then allowed to

stand overnight. Job plots were produced by plotting the mole fractions of the host compound against the mole fractions of C_{60}, multiplied by the $\Delta\delta$ values determined for each set of chemical shifts present for both the host and guest molecules. With other samples for which quantities were limited, mole ratio plots of $\Delta\delta$ against [host]/[guest] ratios were determined and in all cases examined either confirmed or indicated the formation of 1:1 complexes.

2.5.3 Determination of association constant (K_{assoc}).

The association (stability) constants K_{assoc} were determined by ^{1}H NMR spectroscopy.[4] Changes in the chemical shift ($1/\Delta\delta$) of the aromatic signal of the host as a function of $1/[C_{60}]$ or $1/[C_{70}]$ were determined, and K_{assoc} values were determined using the double reciprocal or Benesi-Hildebrand data treatment or by using the Foster-Fyfe treatment by plotting $\Delta\delta/[C_{60}]$ or $\Delta\delta\ /[C_{70}]$ *vs* $\Delta\delta$. In a typical experiment, aliquots of a stock solution of the host (for the C_{60} experiment, approximately 600 μL, 7.86×10^{-4} M; for C_{70} experiment, approximately 600 μL, 7.73×10^{-4} M) were added to NMR tubes; the DMSO-d_6 external lock was inserted into the sample, and the reference signals of pure host were recorded. The calculated amounts of solid C_{60} or C_{70} were then added in small portions to the host solutions in the NMR tubes. After each addition, the solutions were sonicated for approximately 10 min. ^{1}H NMR measurements were recorded at 298 K at 500 MHz, as above. Data were analyzed by least-squares regression analyses using Excel and validated according to criteria described by Hirose[5] and Fielding.[4]

2.6 References

1. (a) Steed, J. W., Atwood, J. L. *Supramolecular Chemistry*, John Wiley & Sons **2000**. (b) Dodziuk, H. *Introduction to Supramolecular Chemistry*, Kluwer Academic Publishers, Dordrecht, The Netherlands 2002. (c) Cram, D. J.; Cram, J. M. *Container Molecules and their Guests, Monographs in Supramolecular Chemistry*; Stoddart, J. F., Ed.; The Royal Society of Chemistry 1994.

2. Bancu, M.; Rai, A. K.; Cheng, P.-C.; Gilardi, R. D.; Scott, L. T. *Synlett* **2004**, 173-176.

3. Georghiou, P. E.; Tran, A. H.; Mizyed, S.; Bancu, M.; Scott, L. T. *J. Org. Chem.* **2005**, *70*, 6158-6163.

4. (a) Tsubake, H.; Furuta, H.; Odani, A.; Takeda, Y.; Kudo, Y.; Liu, Y.; Sakamoto, H.; Kimura, K. in *Comprehensive Supramolecular Chemistry*, Davies, J. E. D.; Ripmeester, J. A., Eds. Elsevier Science, Oxford, 1996; Vol 8, pp 425-482. (b) Connors, K. A. In *Binding Constants* John Wiley & Sons, Inc., 1987.

5. Fielding, L. *Tetrahedron* **2000**, *56*, 6151-6170.

6. Hirose, K. *J. Inc. Phenom.* **2001**, *39*, 193-209.

7. Job, P. *Ann. Chim.* **1928**, *9*, 113-203.

8. Benesi, H. A.; Hildebrand, J. H. *J. Am. Chem. Soc.* **1949**, *71*, 2703-2707.

9. Foster, R.; Fyfe, C. A. *J. Chem. Soc., Chem. Commun.* **1965**, 642.

10. (a) Rose, N. J.; Drago, R. S. *J. Am. Chem. Soc.* **1959**, *81*, 6138-6141. (b) Drago, R. S.; Rose, N. J. *J. Am. Chem. Soc.* **1959**, *81*, 6141-6145. (c) Drago, R. S.; Carlson, R. L.; Rose, N. J.; Wenz, D. A. *J. Am. Chem. Soc.* **1961**, *83*, 3572-3575.

11. Billo, E. J. *Excel for Chemist a Comprehensive Guide,* Wiley VCH, 2001.

12. Dodziuk, H. *Introduction to Supramolecular Chemistry*, Kluwer Academic Publishers, Dordrecht, The Netherlands, 2002 and references cited therein.

13. Scheerder, J.; Fochi, M.; Engbersen, J. F. J.; Reinhoudt, D. N. *J. Org. Chem.* **1994**, *59*, 7815-7820.

14. (a) Oueslati, F.; Dumazet-Bonnamour, I.; Lamartine, R. *New J. Chem.*, **2003**, 27, 644–647. (b) Oueslati, F.; Dumazet-Bonnamour, I.; Lamartine, R. *J. Org. Chem.* **2004**, *69*, 6521-6527.

15. Yoe, J. H.; Harvey, A. E. *J. Am. Chem. Soc.* **1948**, *70*, 648-654.

16. Halouani, H.; Dumazet-Bonnamour,I.; Perrin, M.; Lamartine, R. *J. Org. Chem.* **2004**, *69*, 6521-6527.

17. (a) The C-C distance between adjacent layers of graphite is 3.35 Å: Franklin, R. E. *Acta Cryst.* **1951**, *4*, 253-261. (b) The shortest C-C distance between adjacent molecules of C_{60} in the crystal is 3.11 Å: Buergi, H. B.; Blanc, E.; Schwarzenbach, D.; Liu, S.; Lu, Y. J.; Kappes, M. M.; Ibers, J. A. *Angew. Chem., Int. Ed.* **1992**, *31*, 640-643.

18. (a) Klärner, F.-G.; Panitzky, J.; Preda, D.; Scott, L. T. *J. Molec. Mod.* **2000**, *6*, 318-327. (b) Ansems, R. B. M.; Scott, L. T. *J. Phys. Org. Chem.* **2004**, *17*, 819-823.

19. Mizyed, S.; Georghiou, P.; Bancu, M.; Cuadra, B.; Rai, A. K.; Cheng, P.; Scott, L. T. *J. Am. Chem. Soc.* **2001**, *123*, 12770-12774.

20. Computer-assisted molecular modeling studies were conducted using Spartan'04, V1.0.3 or Spartan Pro V1.1 from Wavefunction, Inc., Irvine, CA, USA. Molecular mechanics (MMFF94) calculations were conducted on the optimized geometry of the hosts and guests and their respective complexes.

21. Cheng, P.-C, *PhD Dissertation*, Boston College, 1996.

22. Very recently, a revealing study of the mechanism of action of the Venus flytrap (*Dionaea muscipula)* entitled *How the Venus Flytrap Snaps* was reported: Forterre, S.; Skotheim, J. M.; Dumais, J.; Mahadevan, L. *Nature* **2005**, *433*, 421-425.

23. Tables 2.1 and 2.2. in: *Fullerenes: Chemistry, Physics and Technology*; Kadish, K. M., Ruoff, R. S., Eds.; John Wiley & Sons: New York, 2000, pp 55-56.

24. An external lock was made by injecting a sample of a deuterated solvent with 5% TMS into a closed-end capillary tube and sealing the open end. For each measurement, the same capillary tube containing the deuterated solvent was inserted into the NMR tube using a specially designed Teflon® insert to provide a lock for the ^{1}H NMR experiments performed in CS_2. This

helps to solve the low solubility of samples measured in the deuterated lock solvent.

25. An internal lock is used to indicate experiments in which a deuterated solvent is injected directly to a CS_2 solution to provide a lock for the ^1H NMR experiments. Using an internal lock, sometimes, will encounter the low solubility of samples measured in the deuterated lock solvent.

26. Mizyed, S.; Georghiou, P. E.; Ashram, M. *J. Chem. Soc., Perkin Trans. 2*, **2000**, 277-280 and references therein.

27. Masci, B. *Tetrahedron* **2001**, *57*, 2841-2845.

28. Tran, A. H.; Miller, D. O.; Georghiou, P. E. *J. Org. Chem.* **2005**, *70*, 1115-1121.

29. For a discussion of a solvophobic effect on the complexation on related systems with C_{60} see Mizyed, S.; Ashram, M.; Miller, D. O.; Georghiou, P. E. *J. Chem. Soc., Perkin Trans. 2*, **2001**, 1916-1919, *and references therein.*

30. (a) Henderson, R. K.; MacNicol, D. D.; McCormack, K. L.; Rowan, S. J.; Yufit, D. S. *Supramol. Chem.* **1998**, *10*, 27-32. (b) Downing, G. A.; Frampton, C. S.; Gall, J. H.; MacNicol, D. D. *Angew. Chem., Int. Ed.* **1996**, *35*, 1547-1549.

Chapter 3

Calix[4]naphthalenes: synthesis, attempted narrow-rim modification, and reinvestigation of complexation studies with [C_{60}]fullerenes

3.1 Introduction

In host-guest recognition studies, calixarenes[1] and calixnaphthalenes[2] are attractive potential hosts for various guests ranging from ions to neutral molecules. The poor affinities of calixarenes towards alkali cations[3] have been improved by completely converting their narrow-rim hydroxyl groups to the corresponding alkoxycarbonylmethoxy groups. For example, the resulting alkoxycarbonylmethoxy ethers **56**–**67** (Figure 3.1), especially the tetrakis(methoxy)- and (ethoxy)carbonylmethoxy ethers, *e.g.* **56**–**59**, demonstrated much higher degrees of phase-transfer affinity for alkali cations than their parent calixarenes in solution,[4] or at the water-air interface of the monolayers of alkoxycarbonylmethoxy ethers.[5]

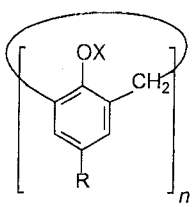

n = 4	n = 6	n = 8
56 R = ^{t}Bu, X = CH_2CO_2Et	**60** R = ^{t}Bu, X = CH_2CO_2Et	**64** R = ^{t}Bu, X = CH_2CO_2Et
57 R = ^{t}Bu, X = CH_2CO_2Me	**61** R = ^{t}Bu, X = CH_2CO_2Me	**65** R = ^{t}Bu, X = CH_2CO_2Me
58 R = H, X = CH_2CO_2Et	**62** R = H, X = CH_2CO_2Et	**66** R = H, X = CH_2CO_2Et
59 R = H, X = CH_2CO_2Me	**63** R = H, X = CH_2CO_2Me	**67** R = H, X = CH_2CO_2Me

Figure 3.1 Alkoxycarbonylmethoxy ether derivatives from calixarenes **56**–**67**.

The Georghiou group has also reported, since 1993, on the preparation of several alkyl ether and ethoxycarbonylmethoxy ether derivatives **68**–**72** from the parent calix[4]naphthalenes **17** and **18** (Scheme 3.1).[6,7] However, no detailed study of the complexation properties of these compounds has yet been made.

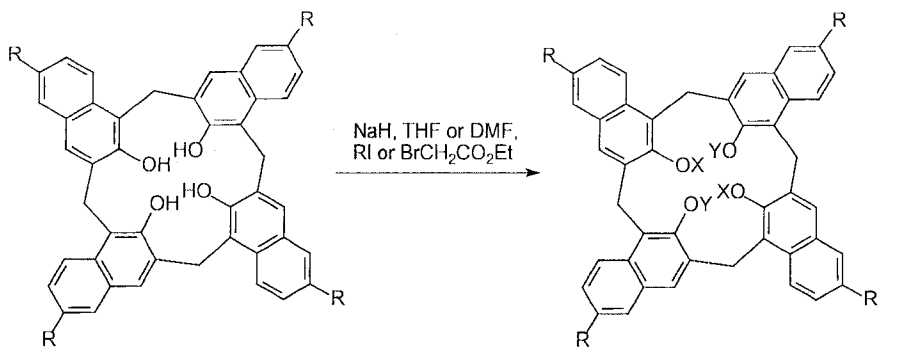

17 R = H
18 R = ^{t}Bu

68 R = H, X = H, Y = CH_2CO_2Et (33%)
69 R = H, X, Y = CH_2CO_2Et (30%)
70 R = ^{t}Bu, X = H, Y = CH_2CO_2Et (25%)
71 R = ^{t}Bu, X = H, Y = ^{i}Pr (56%)
72 R = ^{t}Bu, X = H, Y = ^{n}Pr (36%)

Scheme 3.1 Synthesis of ether and ethoxycarbonylmethoxy ether derivatives of calix[4]naphthalenes **68**–**72**.

In addition to the known *O*-alkylation modification methods, Al-Saraierh *et al.* recently reported[8] that lower-rim hydroxyl groups which have been known to be resistant to Stille[9] and Suzuki-Miyaura[10] reactions can also be partially modified using Sonogashira coupling reactions (Scheme 3.2). Interestingly, in addition to the expected mono- and dialkynyl cross-coupling products **74**–**77**, the previously unknown iodine-containing narrow-rim products **77**–**79** were also formed. Since the corresponding wide-rim arylacetylene derivatives of calixarenes have been reported to have non-linear optical (NLO) properties,[11] the

dialkynyl products resulting from cross coupling of *p-tert*-calix[4]arene 1,3-bistriflate **73** with *p*-nitrophenyl-, *p*-trifluoromethyl- or phenylacetylene were synthesized by Al-Saraierh in our lab and are currently being evaluated for their potential NLO properties.[12]

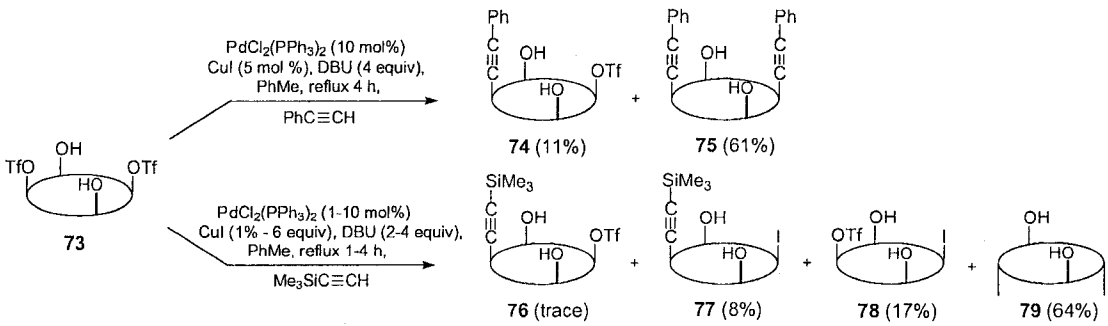

Scheme 3.2 Sonogashira coupling reactions of *p-tert*-butylcalix[4]arene bistriflate **73**.

In order to further contribute to the development of the chemistry of calixnaphthalenes, *e.g.* by application of the Sonogashira reaction to the calixnaphthalenes as was successfully applied to *p-tert*-butylcalix[4]arene (**2**), the synthetic work described in this chapter reports a reinvestigation of the synthesis of calix[4]naphthalenes **17** and **18** (Figure 3.2). Specifically, this study was undertaken to improve the reaction yields and scale, to supply synthetically useful amounts of material. This would allow for reinvestigation of complexation studies with *e.g.* fullerenes, and for attempted modification of their narrow-rim by *O*-alkylation with ethyl bromoacetate, or by use of the Sonogashira reaction. It was anticipated that some of these newly synthesized cyclic compounds might have useful host-guest recognition affinities, or demonstrate NLO activity.

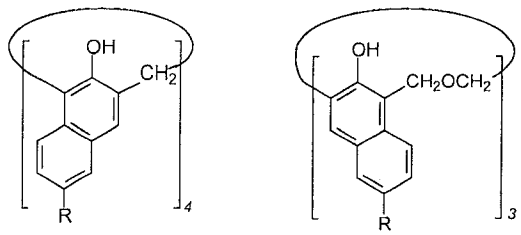

17 R = H
18 R = ^{t}Bu

43

Figure 3.2 Calix[4]naphthalenes **17**, **18** and hexahomotrioxacalix[3]naphthalene **43**.

With respect to the potential host-guest complexation properties, a suitable and reliable method for determining these properties needed to be considered. It is apparent from many studies reported that the use of UV-vis spectroscopy in some cases produced surprisingly large values of $K_{assoc.}$[13] Ideally, K_{assoc} values should be compared with data obtained by another method. The initial UV-vis complexation studies of **17** or **18** with C_{60} were conducted in solvents such as benzene, toluene and CS_2[14] which are commonly used because they can form C_{60} solutions having sufficient concentration[15] (benzene: 2.22–2.58 x 10^{-3} M, toluene: 2.99–4.44 x 10^{-3} M or CS_2: 7.17–16.4 x 10^{-3} M) to enable complexation measurements to be made using absorption spectroscopy. In all three solvents employed, the initial UV-vis results[14] obtained by the Georghiou group suggested the apparent formation of 1:1 complexes of **18** and C_{60} with association constant (K_{assoc}) values of 676 ± 28 (benzene), 295 ± 13 (toluene), and 6920 ± 330 M^{-1} (CS_2). These apparent binding constants were derived from the absorbance changes at λ = 430 nm of the C_{60} solution (ca. 1 x 10^{-4} M) upon titration with the host solutions (ca. 2–10 x 10^{-4} M). This region (λ = 430 nm) is

one that most researchers in the field of fullerene supramolecular host-guest complexation studies using UV-vis spectroscopy use as evidence for complex formation.[16] In order to compare results using two different methods, it was decided to reinvestigate the complexation properties of **17** or **18** with C_{60} using both ^{1}H NMR and UV-vis absorption spectroscopy. Their recognition of C_{70} was also monitored in toluene-d_8 using ^{1}H NMR spectroscopy. The results from the complexation study with C_{60} described in this chapter have been published recently.[17]

3.2 Synthesis of calix[4]naphthalenes 17 and 18

The first synthesis of **17** was reported by Böhmer *et al.*[18] *via* a $TiCl_4$-catalyzed cyclization of 3-(hydroxymethyl)-2-naphthol (**15**). However, Georghiou *et al.* later fully elucidated the structure of cyclic product **17** (Scheme 3.1) by X-ray crystallography. Compound **17** can be considered to be an example of an *endo*-type calix[4]naphthalene (Chapter 1) since all the hydroxyl groups on **17** are situated within the 16-membered annulus.[6,19] The synthesis of **17** (Scheme 3.3) commenced with esterification of commercially available 3-hydroxy-2-naphthoic acid (**80**). With acid catalysis, methyl 3-hydroxy-2-naphthoate (**81**) was easily produced from **80** in 98% yield on a 100 g scale reaction. Reduction of **81** by lithium aluminum hydride gave **15**, the alcohol precursor to **17**, in 95% yield. When **15** was subjected to reaction with $TiCl_4$ in refluxing anhydrous dioxane, calix[4]naphthalene **17** was afforded in 10–15% yields using small- (870 mg) and large (3 g) scale reactions, respectively. The X-ray structure[19] of **17** previously

obtained by Ashram *et al.* revealed that, in a two-molecule unit cell, the naphthalene rings of one molecule are located within the hydrophobic cavity of the other (Figure 3.3).

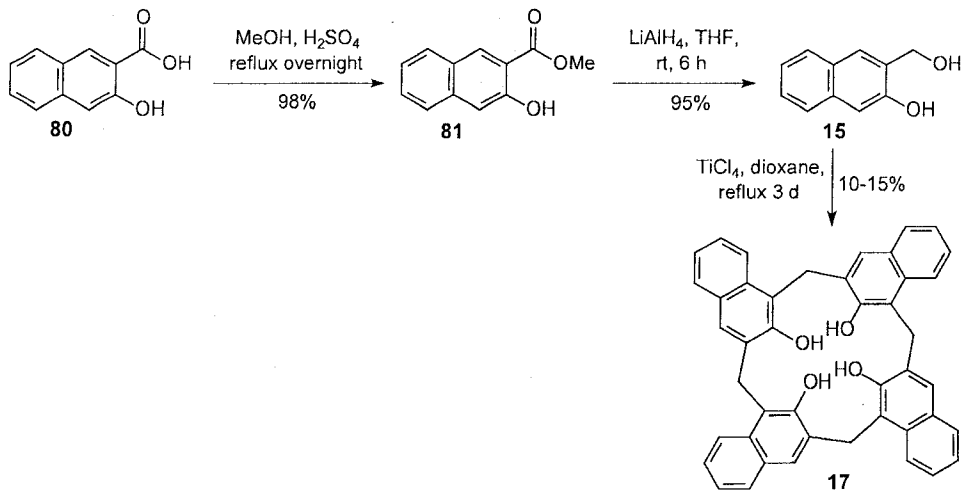

Scheme 3.3 Synthesis of calix[4]naphthalene (**17**).

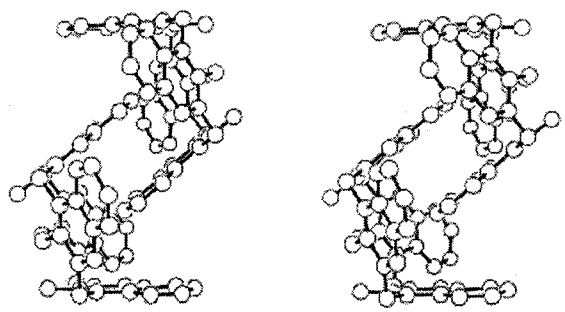

Figure 3.3 X-ray crystal structure of a supramolecular dimer of calix[4]naphthalene **17**.[19]

The synthesis of *tert*-butylcalix[4]naphthalene **18** also commenced from acid **80** using Ashram's procedure (Scheme 3.4).[6] However, in the Friedel-Crafts alkylation step, when the costly and high boiling point solvent, tetrachloroethane (bp 147 °C) was replaced by dichloromethane (bp 40 °C), and with addition of aluminum chloride at low temperature (< –20 °C), yield of intermediate **82** was

improved from 80% to 93%). In addition, dichloromethane could be much more easily removed from the reaction mixture. After the addition of water to the resulting residue, the crude product **82** was easily isolated by suction filtration. The crude product of **82** was purified either by column chromatography on silica gel (93% yield, 2 g scale) or crystallization from methanol (55% yield, 20 g scale). Reduction of **82** by lithium aluminum hydride, followed by $TiCl_4$-catalyzed cyclization of the resulting alcohol **16** furnished *tert*-butylcalix[4]naphthalene (**18**) in 12–21% yield (3 g scale).

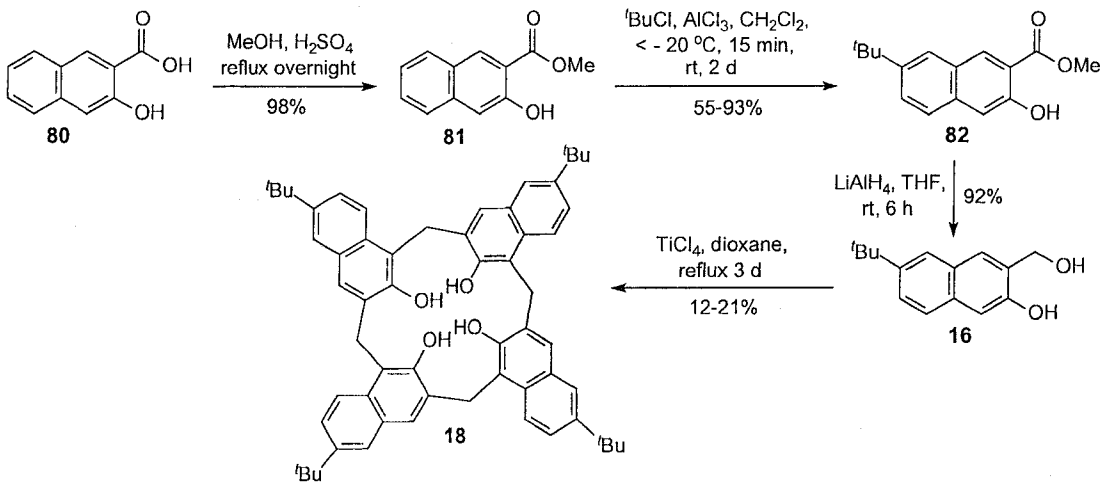

Scheme 3.4 Synthesis of *tert*-butylcalix[4]naphthalene (**18**).

3.3 Attempted modification of the narrow-rim of *tert*-butylcalix[4]-naphthalene (18)

3.3.1 Modification via *O*-alkylations

It is known that narrow-rim alkoxycarbonylmethoxy ether groups of calixarenes exhibit selective inclusion properties with alkali metal cations,[4,5] and that *tert*-butylcalix[4]naphthalene (**18**) is able to encapsulate C_{60}[14,17] to form a

supramolecular complex. In this research, the narrow-rim hydroxyl groups of **18** were converted to ethoxycarbonylmethoxy ether groups via alkylation with ethyl bromoacetate under basic conditions in order to produce a receptor such as **83** for both alkali cationic guests and fullerenes, and which additionally could selectively extract C_{60} or C_{70} by changing the cation guests by potential allosteric contributions.[20] A computer-assisted molecular modeling study[21] (Figure 3.4) revealed that the *cone* conformer of tetrakis(ethoxycarbonylmethoxy) ether **83** ("tetraester") might be able to capture a molecule of C_{60} from the wide-rim, as well as alkali cations such as Li^+ from the narrow-rim. Without the presence of Li^+, the closest distance between the protons of the *tert*-butyl groups and the convex face of C_{60} is 3.20 Å. This would be within an allowable van der Waals contact distance for complexation with C_{60} to occur. When **83** binds an alkali cation, *e.g.* Li^+, Na^+, or K^+, its naphthyl units could become more rigid and the receptor may become locked in a *cone* confomer. This would, therefore, allow a tighter biding between **83** and fullerene guests. Hence, the preparation of calix[4]naphthalene derivative **83** was undertaken.

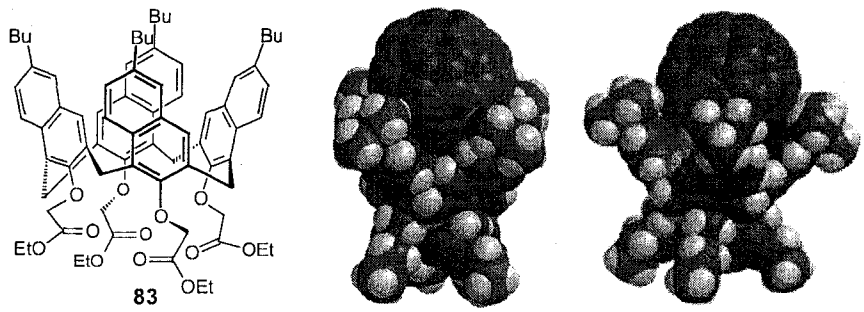

Figure 3.4 *Cone* conformation of **83** (*left*), computer-generated models of a 1:1 **83**:C_{60} complex (middle) and a 1:1:1 **83**:C_{60}:Li^+ complex (*right*).

Ashram[6] and Chowdhury[10] previously reported that treatment of **18** (Scheme 3.1) with sodium hydride and ethyl bromoacetate in THF or DMF gave only mono- and dialkylation products. In the present work, **18** was alkylated under McKervey's conditions[4] by refluxing with ethyl bromoacetate and potassium carbonate in acetone (Scheme 3.5). It is presumed that the "softer" potassium ion associates less tightly than the "harder" sodium ion with the phenoxide ions of the calixarene or calixnaphthalene thereby permitting multiple alkylations.

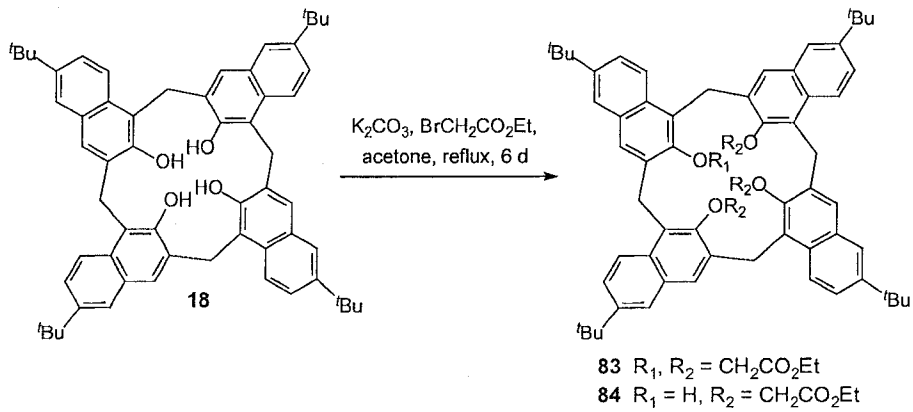

Scheme 3.5 Preparation of tetraester **83**.

Indeed, (+)-APCI MS analysis of the crude product showed the expected molecular ion peak of the tetraester **83** at *m/z* = 1193.5 (100%) (Figure 3.5). However, (–)-APCI MS analysis of the same sample also showed the molecular ion peak of the tris(ethoxycarbonylmethoxy) ether **84** ("triester") at *m/z* = 1105.5 (100%) (Figure 3.6). It is rationalized that triester **84** having a free hydroxyl group was specifically only ionized under negative mode, while the tetraester **83** was ionized under positive mode.

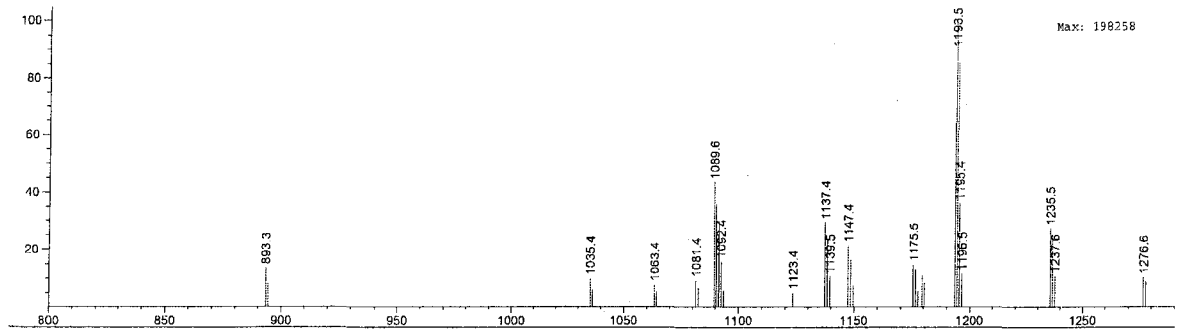

Figure 3.5 (+)-APCI MS of the crude product showing the molecular ion peak of tetraester **83** (calculated *m/z* 1193.5).

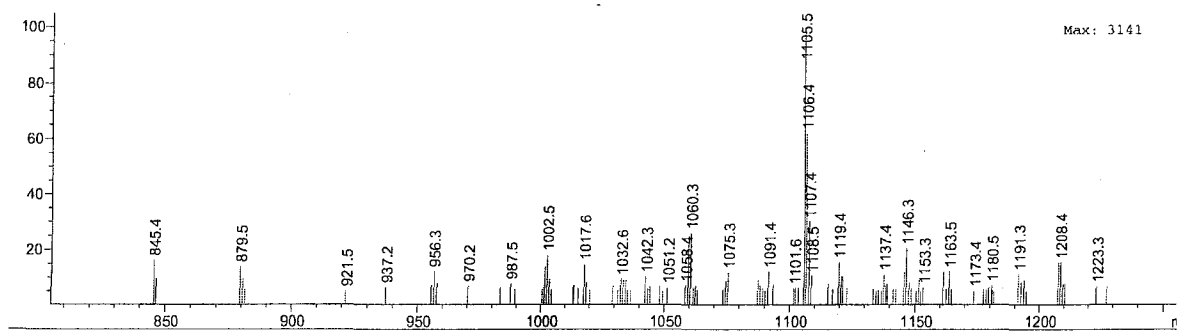

Figure 3.6 (–)-APCI MS of the crude product showing the molecular ion peak of triester **84** (calculated *m/z* 1106.6).

Unfortunately, purification of the crude product by column chromatography or by PLC failed to provide chromatographically-pure products. APCI MS of each fraction, which showed only one spot on TLC, still revealed the presence of the molecular mass ion peak of both tri- and tetraester derivatives. The ^{1}H NMR spectra obtained for these fractions could not be interpreted unambiguously, and appeared to consist of mixtures of different conformations of both **83** and **84**.

The alkylation was then carried out under solvent-free conditions with large excess amounts of ethyl bromoacetate. TLC and APCI MS analysis of the

crude mixture heated at reflux for a week was similar to that of the reaction conducted in acetone. No further attempts were carried out for this *O*-alkylation.

3.3.2 Modification via Sonogashira coupling reactions

The narrow-rim modification of *p-tert*-butylcalix[4]naphthalene (**18**) via Sonogashira coupling reactions commenced with the preparation of *p-tert*-butyl calix[4]naphthalene bistriflate (**85**).[22] Treatment of **18** with triflic anhydride in anhydrous pyridine from 0 °C to room temperature over 1.5 h gave **85** in 60% yield (Scheme 3.6). The formation of **85** was confirmed by (+)-APCI MS analysis, as well as by NMR spectroscopy. When the reaction time was extended to 4 h in order to completely consume the starting material, the reaction yield was unexpectedly reduced to 32% due to the formation of several unidentified side-products.

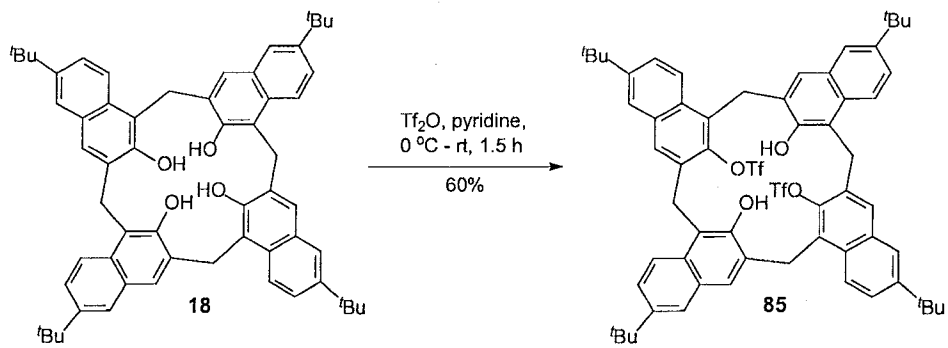

Scheme 3.6 Preparation of bistriflate **85** from *tert*-butylcalix[4]naphthalene (**18**).

In principle, bistriflate **85** could be either the 1,2- or 1,3-substituted product which can adopt one or more of the following usual calixarene-type conformations: *cone*, *piched-cone*, *partial-cone*, *1,2-alternate* and/or *1,3-alternate*

(Figure 3.7, 3.8). It is well-known that ^{1}H NMR signals of each unequivalent bridging methylene proton will appear as a pair of doublet.[23] Based on this fact, the splitting patterns of the bridging methylene signals in each possible conformation of **85** were predicted and are listed in Table 3.1.

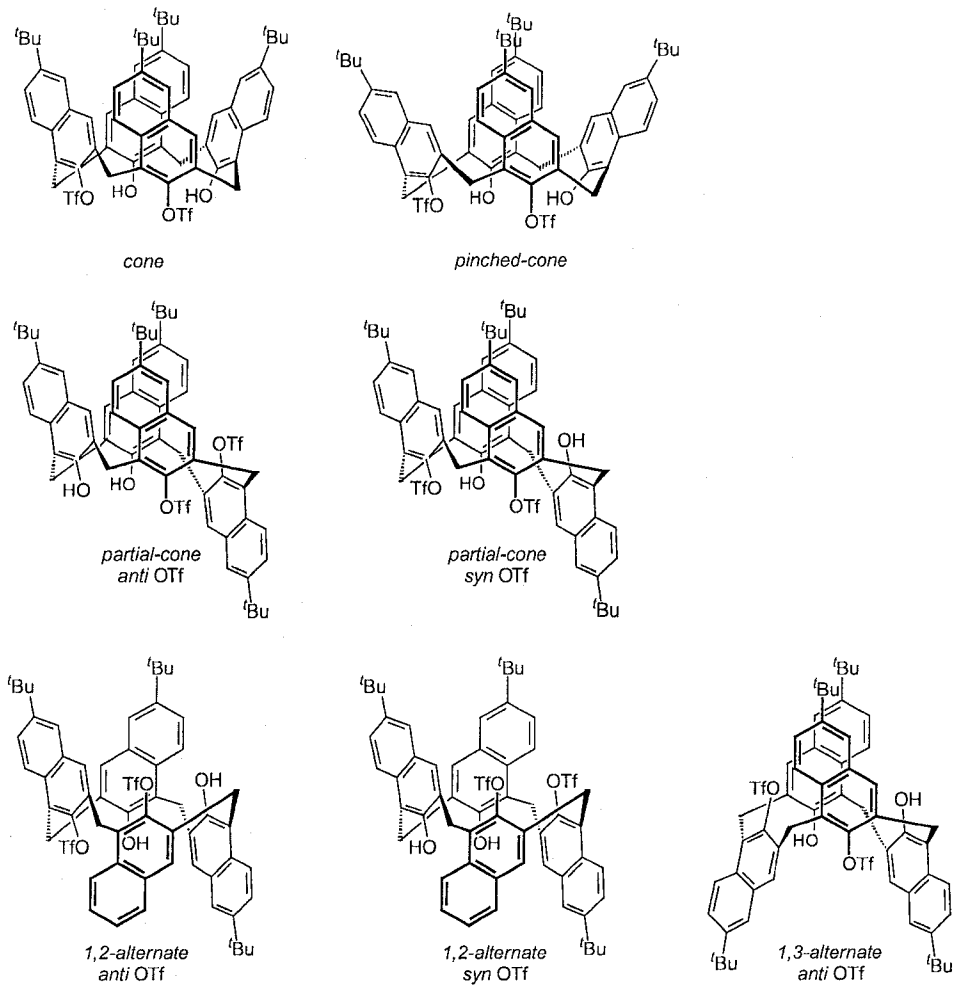

Figure 3.7 Possible conformations of 1,2-bistriflate **85**.

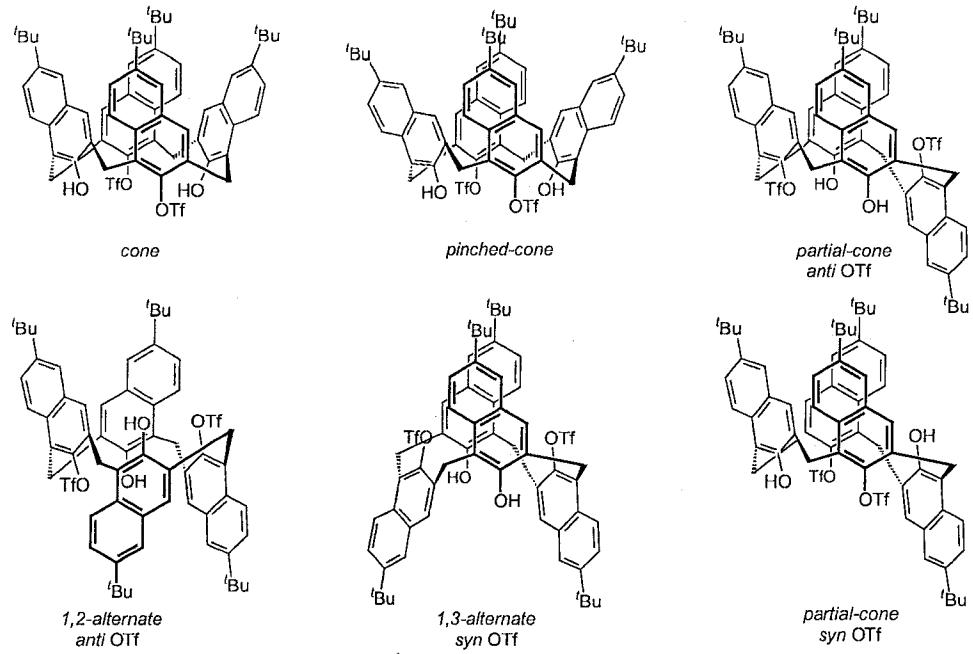

Figure 3.8 Possible conformations of 1,3-bistriflate **85**.

Table 3.1 Predicted splitting pattern of the bridge methylene (CH_2) groups of bistriflate **85**.

Conformation	1,3-bistriflate	1,2-bistriflate
cone or *pinched-cone*	one pair of doublets	three pairs of doublets
partial-cone (*syn*)	**two pairs of doublets**	four pairs of doublets
partial-cone (*anti*)	**two pairs of doublets**	four pairs of doublets
1,2-alternate (*syn*)	----------	three pairs of doublets
1,2-alternate (anti)	**two pairs of doublets**	three pairs of doublets
1,3-alternate (syn)	one pair of doublets	----------
1,3-alternate (anti)	----------	three pairs of doublets

Note: *syn*: when two triflate groups are oriented in the same direction.
anti: when two triflate groups are oriented in the opposite directions.

In fact, the ^{1}H NMR of **85** (Figure 3.9) showed two pairs of doublet for its bridging methylene groups. This indicated the formation of *p-tert*-butylcalix[4]naphthalene 1,3-bistriflate **85** having a *partial-cone* or *1,2-alternate*

conformation. Upon heating from ambient temperature to 328 K, two pairs of doublets are still present. This indicated that 1,3-bistriflate **85** is much more rigid than the parent *p-tert*-butylcalix[4]naphthalene (**18**).

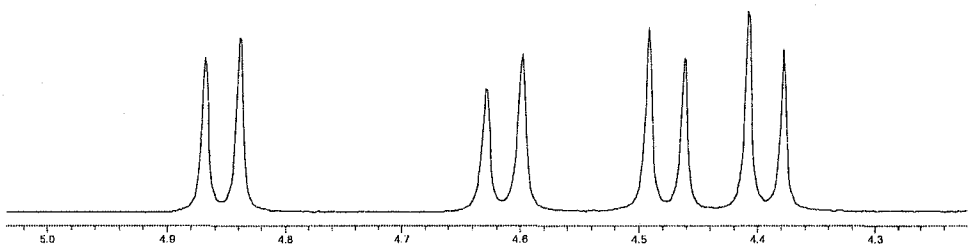

Figure 3.9 ^{1}H NMR of the bridging methylenes in **85** showing two pairs of doublets.

Although the *p-tert*-butylcalix[4]arene bistriflate (**75**) gave fruitful results with phenylacetylene under Sonogashira coupling conditions (Scheme 3.5),[8] no corresponding cross coupling product such as **86** was formed when **85** was subjected to the $PdCl_2(PPh_3)_4$/CuCl-catalyzed coupling reaction with this alkyne (Scheme 3.7). The major product observed was the product of homocoupling of phenylacetylene itself. Addition of LiCl to the reaction mixture gave no improvement.[24] An exhaustive study of alternative Sonogashira coupling conditions was not undertaken due to time constraints on this author.

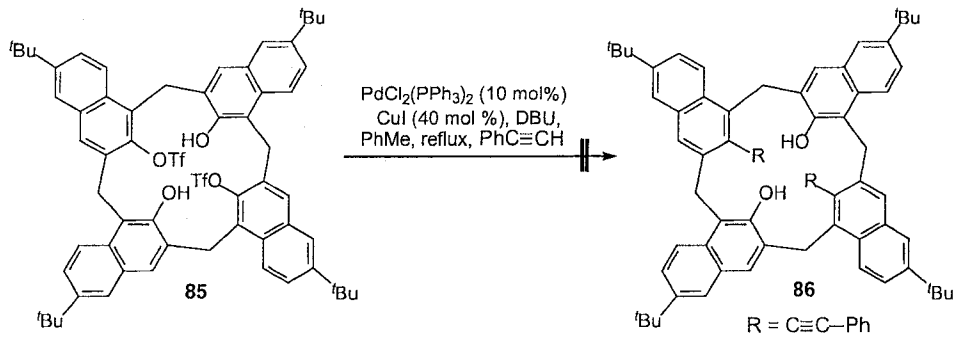

Scheme 3.7 Attempted Sonogashira coupling reaction.

3.4. Results and discussion of solution complexation studies of 17 and 18 hosts

3.4.1 C_{60} as the guest

3.4.1.1 Electronic absorption spectroscopy

UV–vis spectroscopy has been employed to determine the complexation association constants (K_{assoc}) of C_{60} and a variety of host molecules.[14,25,26,27] The success of this determination from UV–vis spectra relies on clear spectroscopic signals attributable to the formation of the host:C_{60} complexes. Complexation causes an increase in absorptivity between λ = 400–470 nm, which has been assigned to resonant inter-fullerene molecular transitions associated with aggregates of C_{60}[28,29] or, in some cases, to charge-transfer (CT) bands.[28] In this chapter, it should be noted that CT bands are defined as being photo-induced electron-transfer transitions from the electron-rich naphthyl moieties of the host studied to the electron-deficient C_{60}. In order to see whether CT bands appear upon mixing the host studied, *e.g.* **18**, and C_{60}, the UV-vis absorption spectra of **18**, C_{60} (Figure 3.10) and mixture of **18** and C_{60} (Figure 3.11) in toluene solution were subsequently measured.

The assignment of electronic transitions and the solvent dependence of the transitions found in C_{60} shown in Figure 3.10 have been published elsewhere.[30] The highly structured band envelope found between λ = 400 nm (25,000 cm^{-1}) to 650 nm (15,400 cm^{-1}) has been assigned to symmetry-forbidden electronic transitions and the symmetry-allowed vibronic transitions.[31] These

transitions have well-defined peaks in aliphatic solvents. However, in aromatic solvents there is extensive broadening and changes in the intensity of these transitions.

The UV–vis absorption spectrum of **18** in toluene solution (Figure 3.10) is dominated by transitions at λ = 327 nm (30,580 cm^{-1}) and 337 nm (29,670 cm^{-1}), which tail out to 420 nm. The structured band centered at λ = 332 nm has been assigned to an $^1A \rightarrow {}^1L_b$ transition to generate a singlet excited state, which is polarized along the long axis based on comparison of the transitions found in 2-hydroxynaphthalene.[32] The molar absorptivity of **18** is approximately four times that found for 2-hydroxynaphthalene itself[34] and the band envelopes have a similar shape, indicating that there is only very weak ground-state electronic coupling between the *tert*-butyl-2-hydroxynaphthyl units in **18**.

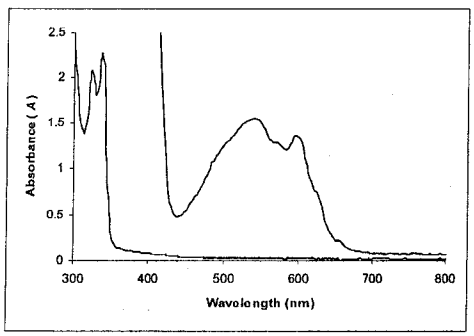

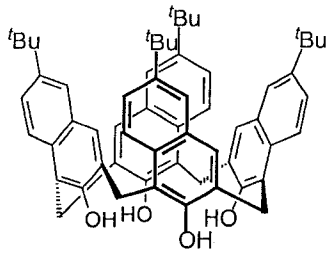

18

Figure 3.10 UV–vis absorption curves of C_{60} (*top*) and of **18** (*bottom*) in toluene.

To determine whether the spectral and colour changes upon mixing **17** or **18** with C_{60} resulted from the charge transfer due to complex formation and not simply from the interaction of the naphthyl units in **18** and C_{60} aggregation, a

solvent-dependent study was undertaken by the D. W. Thompson group at Memorial University. In these experiments, C_{60} was dissolved in three different naphthalene solvents, including 1-chloro-, 1-bromo- and 1-methylnaphthalene[33] and all afforded red-purple solutions similar to the case of toluene or benzene. This supported the conclusion that the solvents studied do not form CT complexes with C_{60}, and the observed enhanced absorptivities are due to resonant inter-fullerene molecular transitions as described previously.[3,28]

In this study, the addition of the red-purple solutions of C_{60} in toluene (or toluene-d_8) or CS_2 to solutions of **17** or **18** in the corresponding solvents, only produced a colour change in the case of **18** and C_{60} in toluene (Figure 3.11a), thus indicating complex formation between **18** and C_{60}. In contrast, no evidence for complexation between **18** and C_{60} was found in CS_2, either by UV-vis or by NMR, and similarly for **17** and C_{60} in CS_2 or in toluene.

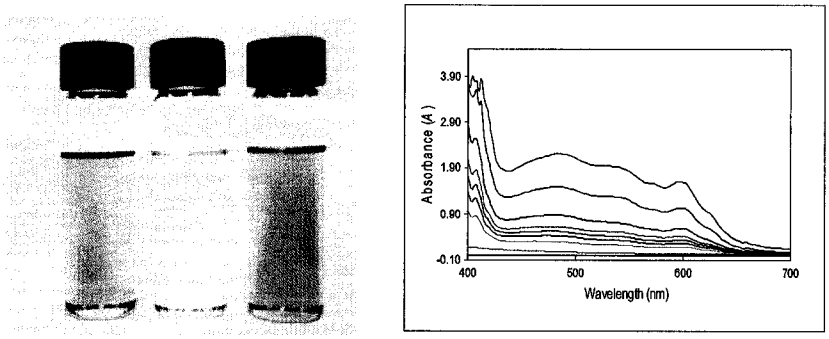

a **b**

Figure 3.11.a Solutions of C_{60} (red-purple, *left*), **18** (colourless, *middle*), **18** and C_{60} (brown, *right*) in toluene.

3.11.b UV–vis titration curves showing the changes in absorption of **18** in toluene solution as a function of increasing [C_{60}].

UV–vis spectroscopic measurements for the titration of **18** in toluene (approximately 2.00 x 10^{-3} M) with increasing amounts of C_{60} are shown in Figure 3.11b. The spectral data at λ = 430 nm[16] were subjected to the Benesi–Hildebrand (Eq 3.4)[34] and Foster-Fyfe (Eq 3.5)[35] treatments (Figure 3.12) (outlined in Chapter 2, Eq 2.21 and Eq 2.22 in which [H] = [**18**] and [G] = [C_{60}]) gave K_{assoc} values, 176 ± 21 M^{-1} and 184 ± 10, respectively (Appendix 3.1) for the **18**:C_{60} complexation.

$$\frac{[\mathbf{18}]_o}{\Delta A} = \frac{1}{K_{assoc} \bullet \Delta\varepsilon_c \bullet [C_{60}]} + \frac{1}{\Delta\varepsilon_c} \qquad \text{(Eq 3.4)}$$

$$\frac{\Delta A}{[C_{60}]} = -K_{assoc} \bullet \Delta A + [\mathbf{18}]_o \bullet K_{assoc} \bullet \Delta\varepsilon_c \qquad \text{(Eq 3.5)}$$

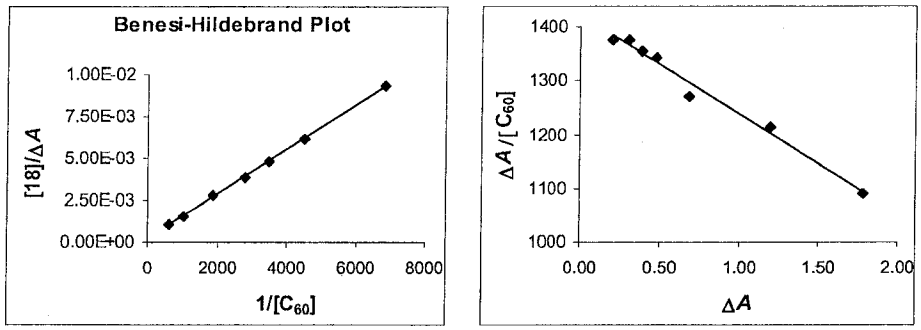

Figure 3.12 Benesi-Hildebrand plot (*left*) and Foster-Fyfe plot (*right*) for the complexation of **18** and C_{60} in toluene measured at λ = 430 nm.

The $\Delta\varepsilon_c$ (4.29 x 10^3 $M^{-1}cm^{-1}$ at λ = 430 nm) value was derived from linear least-squares regression analysis of the Benesi-Hildebrand equation (Eq 3.4) (Appendix 3.1). From Berberan-Santos' argument, it is well known to be difficult to extract accurate values of $\Delta\varepsilon_c$ and K_{assoc} from double-reciprocal plots in the UV-vis

method. In order to validate and to ensure that the $\Delta\varepsilon_c$ and K_{assoc} values obtained were not an artifact, these values were used to calculate back the ΔA values. Both observed and calculated data of ΔA were then replotted according to equation 3.6, which is the non-linear form from which the Benesi-Hildebrand equation was derived. Figure 3.13 shows all data to be in excellent agreement thereby validating the experimental data and analysis (Appendix 3.2).

$$\Delta A_{cal} = \frac{K_{assoc} \cdot \Delta\varepsilon_c \cdot [\mathbf{18}]_o \cdot [C_{60}]}{1 + K_{assoc} \cdot [C_{60}]} \qquad \text{(Eq 3.6)}$$

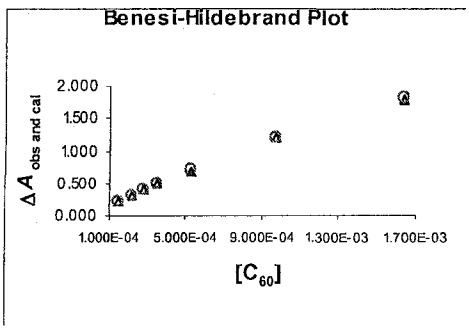

Figure 3.13 Plots of ΔA *vs* $[C_{60}]$ at λ = 430 nm: observed data (▲) and calculated data (o) from non-linear form of the Benesi–Hildebrand plot equation 3.6.

3.4.1.2 ^{1}H NMR spectroscopy

No evidence was found for any complexation of either **17** or **18** with C_{60} in CS_2 solution by ^{1}H NMR spectroscopy. However, the ^{1}H NMR spectra of solutions of **18** in toluene-d_8, to which aliquots of C_{60} were added, showed clear chemical shift changes, especially for the *tert*-butyl protons (Figure 3.14), and afforded reproducible K_{assoc} values.

In these titration experiments, the chemical shifts of all of the proton signals of **18** were affected to some extent. The signals for the *tert*-butyl methyl groups, and the H-5 protons[36] showed the largest relative changes, and were almost identical in magnitude (Figure 3.15, Appendix 3.2).

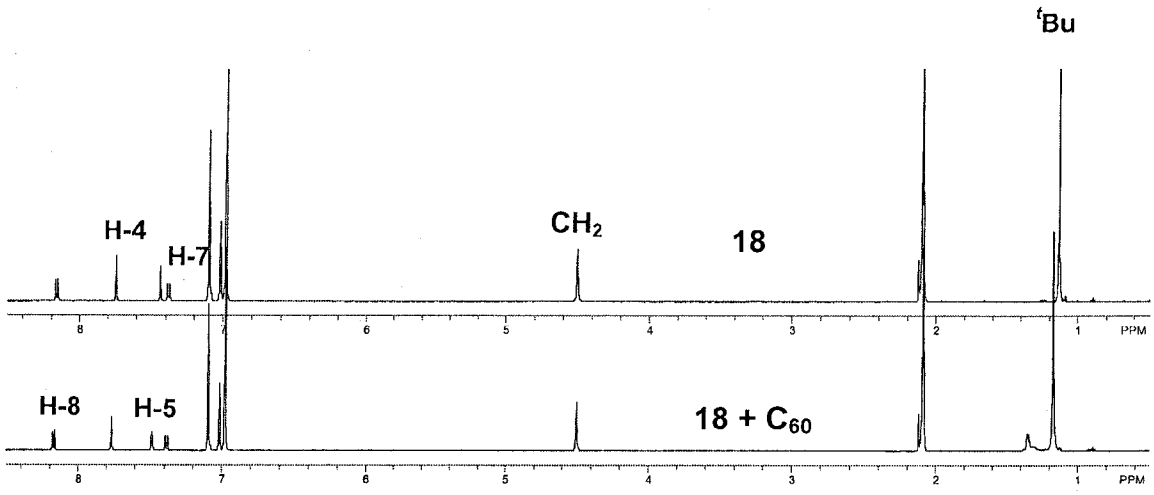

Figure 3.14 ^{1}H NMR spectra of **18** (*top*), mixture of **18** and C_{60} (*bottom*) in toluene-d_8 at room temperature.

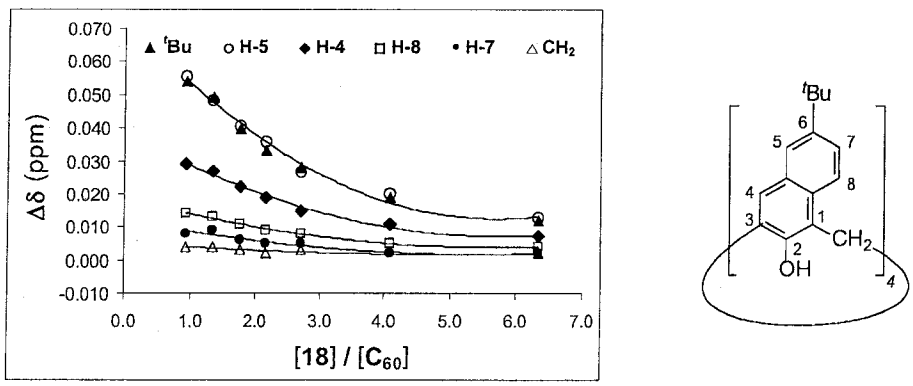

Figure 3.15 Plots of chemical shift changes ($\Delta\delta$) for protons on **18** in toluene-d_8 solution *vs* added C_{60} (*left*), and formula of **18** showing the numbering of positions on the naphthyl ring sub-units (*right*).

These could be rationalized using the results of a computer-assisted molecular modeling study.[21] In the computer-generated model, the fullerene is nestled deeply into the cavity formed by the naphthalene rings in **18** (Figure 3.16). The *tert*-butyl groups tightly embrace the C_{60} molecule, with the closest average distances between a proton on a *tert*-butyl group, and a carbon atom of the fullerene being 3.21 Å. Furthermore, the naphthalene rings are tilted inwards towards the fullerene, with the H-5 protons being closer to the fullerene, than the other, H-7 protons, which are also *ortho* to the *tert*-butyl groups. The closest average distances of the H-5 and H-7 protons of **18** to a carbon atom on the C_{60} are 3.66 *vs* 4.37 Å, respectively (Appendix 3.3). Therefore, the deshielding of the *tert*-butyl and H-5 protons due to electron withdrawal by the electron-deficient C_{60} would be expected to be larger, and thus could account for the observed trends for these protons in the NMR data.

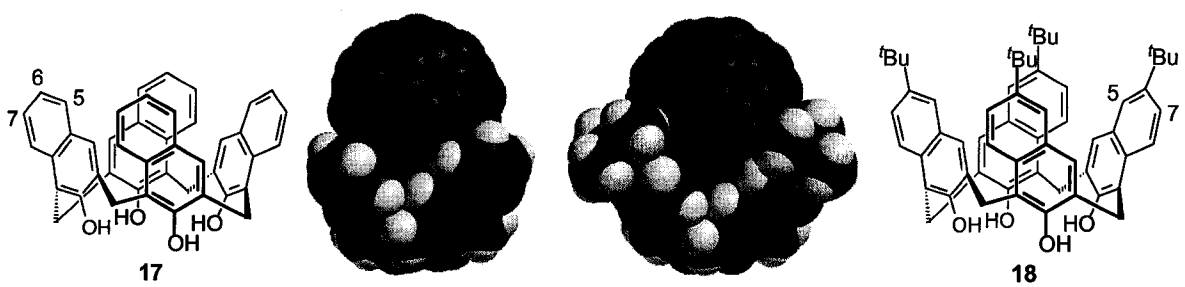

Figure 3.16 Computer-generated 1:1 supramolecular complexes of C_{60} with **17** (*left*) and **18** (*right*).[21]

Mizyed *et al.* previously reported similar observations from the complexation studies of **43** with C_{60}.[37] Computer-aidded molecular mechanics modeling studies on the complex formed between **43** and C_{60} are in agreement

with the actual X-ray structure of this complex (see Chapter 1, Figure 1.13),[37] and show the close contacts between the *tert*-butyl methyl protons and the fullerene. The closest average distance from such protons to a carbon atom on C_{60} is 3.18 Å. An analysis by Shinkai *et al.*[25] of other calixarene supramolecular complexes with C_{60} suggested that the presence of *tert*-butyl groups on such hosts appear to be one of the necessary prerequisites, confirming the importance of π-CH_3 interactions in these systems.

Based upon the largest $\Delta\delta$ values corresponding for the *tert*-butyl protons, K_{assoc} values derived from Benesi-Hildebrand and Foster-Fyfe treatments and regression data analysis for the complexation of C_{60} with **18** in toluene-d_8 at 298 K, were 217 ± 7 M^{-1} and 217 ± 3 M^{-1}, respectively (Figure 3.17, Appendix 3.4). These values are in reasonable agreement with the corresponding K_{assoc} values obtained from the UV–vis absorption determinations (176 ± 21 M^{-1} and 184 ± 10 see above) obtained during this reinvestigation.

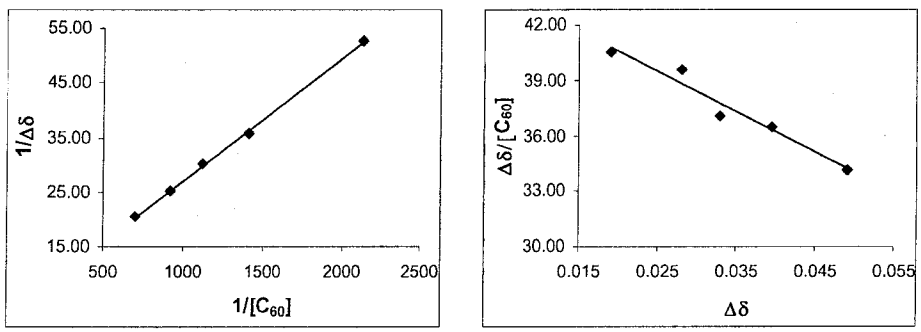

Figure 3.17 Benesi-Hildebrand plot (*left*) and Foster-Fyfe plot (*right*) for the complexation of **18** and C_{60} in toluene-d_8 at 298 K.

A VT ^{1}H NMR experiment using toluene-d_8 solutions was performed. Figure 3.18 shows the temperature-dependence of the chemical shifts of the *tert*-butyl group protons of **18** (Appendix 3.5). Analysis of the data using the Foster–Fyfe method gave a direct measure of K_{assoc} for each of the temperatures indicated in Table 3.2. However, for the higher temperatures examined the fits using either the Benesi–Hildebrand, or Foster–Fyfe treatments are very poor. At higher temperatures it was observed that a dark red-brown precipitate formed over the course of the experiment. Therefore, the K_{assoc} values determined above 338 K should be viewed as lower, imprecise estimates of the true association constants.

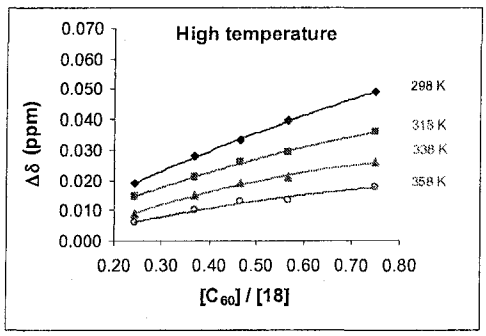

Figure 3.18 Changes in the chemical shifts of the *tert*-butyl group protons in **18** as a function of temperature in toluene-d_8.

The determination of the K_{assoc} values allows a direct measurement of the Gibbs free energy for complexation using $\Delta G° = -RT\ln K_{assoc}$. The free energy of the complexation between **18** and C_{60} has the lowest value at 318 K (Table 3.2, Figure 3.19). This indicates that the complex was formed most easily at this temperature.

Table 3.2 K_{assoc} and $\Delta G°$ for the complexation behavior of **18** with C_{60} *vs* temperature using the Foster–Fyfe treatment of the ^{1}H NMR data.

Run #	K_{assoc}	R^2	T (K)	1/T(x 10^3)	ln K_{assoc}	$\Delta G°$ (kJ mol^{-1})
1	194 ± 21	0.977	278	3.597	5.27	–12.2
1	205 ± 52	0.886	288	3.472	5.32	–12.7
1	215 ± 62	0.859	298	3.356	5.37	–13.3
2	219 ± 26	0.959	298	3.356	5.39	–13.4
2	279 ± 47	0.921	318	3.145	5.63	–14.9
2	72 ± 118	0.110	338	2.959	4.28	–12.0
2	39 ± 127	0.031	358	2.793	3.66	–10.9

Note:[38] Gas constant R = 8.314472 Jmol^{-1}K^{-1}

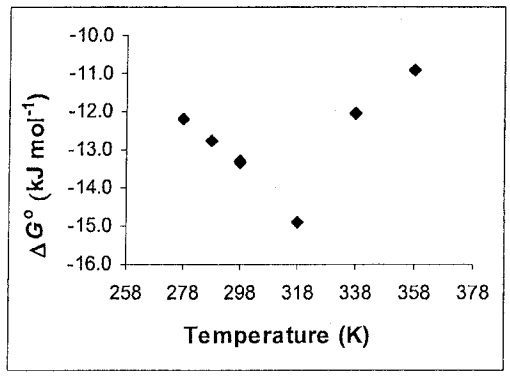

Figure 3.19 $\Delta G°$ free energy of the formation of the 1:1 **18**:C_{60} complex *vs* temperature determined by ^{1}H NMR in toluene-d_8.

As indicated previously, in contrast to the results obtained in toluene-d_8 solutions, addition of C_{60} to solutions of **18** in CS_2 did not reveal any evidence for complexation between the host and guest studied from either UV–vis or ^{1}H NMR determinations. It was hypothesized that the aggregates of C_{60} in CS_2, known to form in this solvent, may be too large to fit, or complex within the relatively small

cavities of either **17** or **18**. However, in other cases with different macrocyclic hosts, $\Delta\delta$ changes may be observed in both CS_2 and toluene-d_8. Therefore, the phenomenon described in the present work is not necessarily a general one, for example, in complexation studies between C_{60} with some concave pentathio-substituted corannulene hosts recently reported by Georghiou *et al.*, K_{assoc} values could be determined in both solvents.[39]

Computer-aidded molecular mechanics modeling (Figure 3.16) also suggested that 1:1 complexation between **17** and C_{60} was feasible,[40] with the closest average distances of the H-5 and H-7 protons to a carbon atom on the fullerene in the **17**:C_{60} complex being very similar to those determined for the **18**:C_{60} complex, (*i.e.*, 3.66 *vs* 3.51 Å, and 4.37 *vs* 4.21 Å, respectively) (Appendix 3.3), and the closest average distances of the H-6 protons being only approximately 3.74 Å. However, the titration experiments in either toluene-d_8 or CS_2 solution, revealed no discernable changes in the chemical shifts of any of its protons. It was presumed that in addition to the known methyl-π interactions which enhance complexation between the **18** and C_{60}, the *tert*-butyl groups also deepen the cavity of **18** sufficiently to better encapsulate C_{60}. In contrast, **17**, which showed no complexation-induced chemical shifts, has no *tert*-butyl groups. These results support the contention that the π–CH_3 interactions are very important for effective complexation with C_{60}. Another factor, which could account for the observed lack of complexation with **17** is suggested by its X-ray structure. It had previously been reported,[19] that the X-ray structure (Figure 3.3) obtained

from crystals of **17** formed from toluene solution, revealed that the unit cell contains two molecules of **17** packed in such a way that a naphthalene ring of one molecule is situated within the hydrophobic cavity of the other. Each of the molecules in this unit cell is in *pinched-cone* conformations, and three molecules of toluene surround the "supramolecular dimer" in the solid state. Also, recently it has been found that **17** shows excimer emission properties in toluene solution, which is evidence to suggest that such dimeric structures might also exist in solution,[41] which could be more competitive than complexation of C_{60} within the cavities of **17**.

3.4.1.3 Proposed mechanism of complexation

In this collaborative study, the following mechanism of complexation between **18** and C_{60} was proposed by D. W. Thompson,[17] at Memorial University. Shown below are seven identifiable chemical processes which could be occurring. Of the processes, ^{1}H NMR monitoring of supramolecular complexation is specific for only the one showing complexation with C_{60} ***(vi)***, where chemical shift differences due to complexation can be discerned. Conversely, steady-state UV–vis spectroscopic methods are sensitive to all of the processes outlined, except for the interconversion of the conformational isomers and desolvation of their cavities, which would require time-resolved spectroscopic methods to discern. The derivation of supramolecular binding constants from UV–vis data and ^{1}H NMR data should agree within experimental error. In many instances, this is not the case, and care should be taken to ascertain the absorption

spectroscopic behaviour of C_{60} to ensure that the spectral changes are indeed attributable to complexation, and are not due to some of the other processes which may be occurring.

	Process	Equilibrium	Equilibrium constant
(i)	Solvation of C_{60}	$C_{60} + nS \underset{k_{-1}}{\overset{k_1}{\rightleftharpoons}} C_{60}(S)_n$	$K_1 = \frac{k_1}{k_{-1}} = \frac{[C_{60}S_n]}{[C_{60}][S]^n}$
(ii)	Aggregation	$nC_{60} \underset{k_a^r}{\overset{k_a^f}{\rightleftharpoons}} (C_{60})_n$	$K_{agg} = \frac{k_a^f}{k_a^r} = \frac{[(C_{60})_n]}{[C_{60}]^n}$
(iii)	Solvation of conformational isomers	$\mathbf{18}^i + nS \underset{k_{-2}}{\overset{k_2}{\rightleftharpoons}} \mathbf{18}^i(S)_n$	$K_2 = \frac{k_2}{k_{-2}} = \frac{[\mathbf{18}^i S_n]}{[\mathbf{18}^i][S]^n}$
(iv)	Interconversion of isomers	$\mathbf{18}^i(S)_n \underset{k_i^r}{\overset{k_i^f}{\rightleftharpoons}} \mathbf{18}^c(S)_x + (n\text{-}x)S$	$K_{int} = \frac{k_i^f}{k_i^r} = \frac{[\mathbf{18}^c S_x][S]^{n-x}}{[\mathbf{18}^i S_n]}$
(v)	Desolvation of cavity	$\mathbf{18}^c(S)_x \underset{k_{+s}}{\overset{k_{-s}}{\rightleftharpoons}} \mathbf{18}^c + xS$	$K_s = \frac{k_{-s}}{k_{+s}} = \frac{[\mathbf{18}^c][S]^x}{[\mathbf{18}^c S_x]}$
(vi)	Complexation of C_{60}	$\mathbf{18}^c + C_{60} \underset{k_c^r}{\overset{k_c^f}{\rightleftharpoons}} \{\mathbf{18}^c // C_{60}\}$	$K_{assoc} = \frac{k_c^f}{k_c^r} = \frac{[\{\mathbf{18}^c // C_{60}\}]}{[\mathbf{18}^c][C_{60}]}$
(vii)	Precipitation	$\{\mathbf{18}^c // C_{60}\} \underset{}{\overset{k_{sp}}{\rightleftharpoons}} \{\mathbf{18}^c // C_{60}\}_{ppt}$	

Scheme 3.8 Kinetics and thermodynamics for supramolecular complexation of **18** and its conformational isomers, $\mathbf{18}^i$, with C_{60} in a solvent (S).

3.4.2 C_{70} as the guest

From the above complexation results, the use of ^{1}H NMR spectroscopy to measure the K_{assoc} emerged as a more reliable method than UV-vis method. Therefore, in the following complexation study with C_{70}, only the ^{1}H NMR method was employed.

It is known that *p-tert*-butylcalix[4]arene (**2**) (Figure 1.1, Chapter 1) does not form complexes with either C_{60} or C_{70}. With calix[4]naphthalenes **17** and **18**,

the formation of a complex between **18** and C_{70} in toluene-d_8 was observed by ^1H NMR spectroscopy while there was no complexation between calix[4]naphthalene **17** and C_{70}. The largest signal shifts were also of the *tert*-butyl protons of **18**. A computer-aided molecular modeling study (Figure 3.20) suggested that a 1:1 complexation between **18** and C_{70} could be formed, with the closest distances of the *tert*-butyl proton, H-5 and H-7 protons of **18** to a carbon atom on C_{70} in the **18**:C_{70} complex being very similar to those determined for the **18**:C_{60} complex, (*i.e.*, 3.00 *vs* 3.21, 3.60 *vs* 3.66, and 4.20 *vs* 4.37 Å, respectively) (Appendix 3.3). The distance between the *tert*-butyl groups of **18** to a carbon on C_{70} are closer than those of C_{60}. In the case of the 1:1 **17**:C_{70} complex, the closest distances of the H-6, H-5 and H-7 protons of **17** to a carbon atom on C_{70} are very similar to those determined for the **17**:C_{60} complex (3.81 *vs* 3.74, 3.55 *vs* 3.51, and 4.20 *vs* 4.21 Å) (Appendix 3.3).

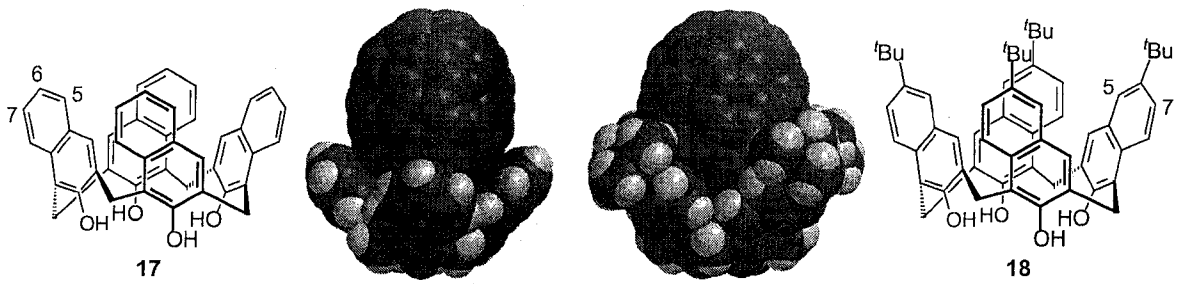

Figure 3.20 Computer-generated 1:1 supramolecular complexes of C_{70} with **17** (*left*) and **18** (*right*).[21]

It was assumed that the complexation stoichiometry of **18** and C_{70} was 1:1, and this would be confirmed later by the agreement of the Foster-Fyfe plot.

This means that if a 1:2 or 2:1 host:guest complexation occur, the Foster-Fyfe plot will not show a good fit between data obtained. The K_{assoc} values for the **18**:C_{70} complex were determined by ^{1}H NMR based on *tert*-butyl protons shifts, in a manner similar to that used with C_{60}. They were 313 ± 20 M^{-1} and 273 ± 1 M^{-1} from Benesi-Hildebrand and Foster-Fyfe treatments, respectively (Figure 3.21, Appendix 3.6). As expected, the hypothesis that a 1:1 complex formation between **18** and C_{70} was gratifyingly confirmed by the good agreement of the data obtained from ^{1}H NMR measurement in the Foster-Fyfe plot (Figure 3.21).

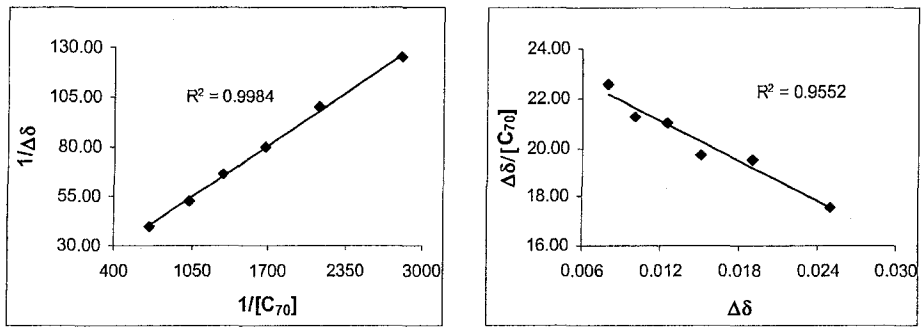

Figure 3.21 Benesi-Hildebrand plot (*left*) and Foster-Fyfe plot (*right*) for the complexation of **18** and C_{70} in toluene-d_8 at 298 K.

In this study, the higher average K_{assoc} values were obtained for the 1:1 complexation of **18** with C_{70} (K_{B-H} 313 ± 20 M^{-1} or K_{F-F} 273 ± 1 M^{-1}) in comparison with C_{60} (K_{B-H} 217 ± 7 M^{-1} or K_{F-F} 217 ± 3 M^{-1}). It could be rationalized that the C_{70} molecule has a more cylindrical shape than C_{60} does, hence C_{70} could be embedded more deeply than C_{60} within the cavity of **18**. However, the C_{70}/C_{60} selectivity of **18** is about 1.4 which is lower than that of calix[5]arene **87** but

higher than that of *p*-allylcalix[5]arene **89** in toluene which were both reported by Gutsche *et al.* (Table 3.3).[42]

Table 3.3 K_{assoc} (M^{-1}) of calix[5]arenes **87**–**89** with fullerenes at 298 K in toluene measured by UV-vis spectroscopy at λ = 430 nm (for C_{60}) and λ = 420 nm (for C_{70}).

Calixarenes	$K_{C_{60}}$	$K_{C_{70}}$	$K_{C_{70}} / K_{C_{60}}$
Calix[5]arene **87**	30 ± 12	51 ± 3	1.7
p-*tert*-butylcalix[5]arene **88**	9 ± 1	-	-
p-allylcalix[5]arene **89**	292 ± 15	141 ± 8	0.5

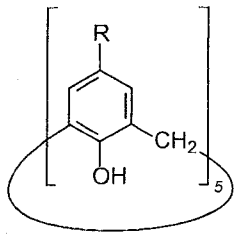

87 R = H
88 R = ^{t}Bu
89 R = Allyl

No complexation between **17** and C_{70} in toluene-d_8 was observed by ^{1}H NMR, presumably also due to the absence of *tert*-butyl groups which appear to be necessary for such complexation.[40] High temperature VT ^{1}H NMR studies of the complexation between **18** and C_{70} gave ambiguous results. It was hypothesized that C_{70} was partially oxidized upon heating.

3.5 Conclusions and proposals for future work

The attempted modifications of the narrow-rim of *tert*-butylcalix[4]-naphthalene **18** by alkylation with ethyl bromoacetate failed to afford clean products suitable for further complexation studies. In the future, this alkylation should be carried out in the presence of akylammonium salts because these alkylammonium ions might bind with the naphthalene units of **18** resulting in it

becoming preorganized into its *cone* conformer during the course of the *O*-alkylation. As a result, this could reduce the number of *O*-alkylation products.

Also, attempted Sonogashira coupling reactions failed to produce the desired narrow-rim-substituted alkynyl-containing calix[4]naphthalenes. To solve this issue, the future coupling should be conducted with different Pd-catalysts such as $Pd(PPh_3)_4/CuI$[43] and/or possibly under microwave-assisted conditions.[24] Using $Pd(PPh_3)_4/CuI$ has been found to give better cross coupling between the *p*-*tert*-butyl calix[4]arene bistriflate **73** with several different terminal akynes studied.[44]

In a complexation study, it had previously been concluded from UV-vis data that both **17** and **18** formed 1:1 complexes with C_{60}.[14] However, in our recent reinvestigation[17] with ^1H NMR support, only **18** was revealed to be a good host for C_{60} and also for C_{70} in toluene-d_8 under the conditions studied. Several factors, including the dilution conditions employed, and a misinterpretation of the significance of the absorbance changes at λ = 430 nm could account for the earlier conclusions.[45] It is suggested and recommended that in future studies, the interpretation of UV-vis absorption data should be undertaken with care and ideally in comparison with ^1H NMR spectroscopic results.

3.6 Experimental section

General methods: All experiments with moisture- or air-sensitive compounds were carried out in anhydrous solvents under Ar or N_2 atmosphere unless otherwise indicated. Organic solvents were evaporated under reduced

pressure using a rotavapor. All synthetic products were dried overnight under vacuum, unless otherwise indicated. Flash chromatography was performed on SAI silica gel, particle size 32–63 μm, pore size 60 Å, Batch number 02826-25. Preparative thin-layer chromatography plates (PLC) were made from SAI F-254 silica gel for TLC (particle size 5–15 μm), Batch number 04860-5. Thin-layer chromatography was performed using precoated SAI F-254 silica gel plates (Plastic Backed TLC, Hard Layer, Batch number 79011), layer thickness 200 μm.

Materials: All chemical reagents were purchased from Aldrich or Fluka. ACS grade solvents purchased from Fisher were dried and distillated according to standard procedures.

Instrumentation: Melting points (mp) were determined on a MEL-TEMP II apparatus and are uncorrected. Mass spectra of compounds were obtained using GCMS (HP 5972 series II), LCMS (HP series 1100) or MALDI-TOF MS (Voyager-DE PRO) machines. MS data were presented as follows: *m/z* (relative intensity), assignment (when appropriate), calculated mass for corresponding formula. Unless otherwise indicated, ^{1}H and ^{13}C NMR spectra were conducted using $CDCl_3$ with the internal standard TMS and recorded on the Bruker Avance 500 spectrometer (otherwise a 300MHz GE GN-300 NB) operated in pulse mode. Data are presented as follows: chemical shift, multiplicity (s = singlet, br = broad, d = doublet, t = triplet, m = multiplet, sept = septet), coupling constant (*J*, Hz), integration (# of H), and assignment (when appropriate). Reported

mutiplicities are apparent. Chemical shifts in the ^{13}C NMR are relative to δ 77.23 ppm for $CDCl_3$

3.6.1 Synthesis of calix[4]naphthalene (17) and *tert*-butylcalix[4]-naphthalene (18).

Methyl 3-hydroxy-2-naphthoate (84)

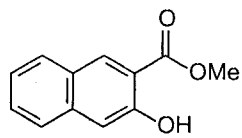

To a suspension of 98% 3-hydroxy-2-naphthoic acid (**83**) (57.60 g, 300.0 mmol) in MeOH (300 mL) was added slowly concentrated H_2SO_4 at 0 °C. The reaction mixture was then heated at reflux with stirring overnight. After the reaction was cooled to room temperature, the resulting yellow precipitate was filtered, washed with deionized water (500 mL), aqueous 10% $NaHCO_3$ and deionized water (500 mL), and dried at 50 °C overnight to give in quantitative yield the crude product as a light yellow powder, which was purified by chromatography (1:99 EtOAc-hexane) to yield **84** (59.45 g, 98%) as a yellow powder: mp 70–71 °C (lit.[6,7] 69–70 °C), ^1H NMR δ 4.03 (s, 3H), 7.32–7.34 (m, 2H), 7.48–7.52 (m, 1H), 7.69 (d, J = 8.2 Hz, 1H), 7.80 (d, J = 8.2 Hz, 1H), 8.50 (s, 1H), 10.4 (s, 1H, disappears upon D_2O addition); ^{13}C NMR δ 52.7, 111.8, 114.3, 124.1, 126.5, 127.2, 129.3, 129.4, 132.6, 138.1, 156.5, 170.4.

3-Hydroxymethyl-2-naphthol (15)

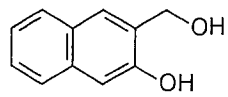

To a stirred suspension of $LiAlH_4$ (1.70 g, 44.9 mmol) in anhydrous THF (120 mL) at 0 °C was added slowly a solution of **84** (4.54 g, 22.5 mmol) in anhydrous THF (90 mL) over 30 min. The reaction mixture was stirred for a further 6 h, and quenched by adding cold aqueous 20% HCl (until the pH reached 1–2) at 0 °C, followed by extraction with diethyl ether (4 x 50 mL). The organic layer was separated, washed with deionized water (2 x 50 mL), brine (1 x 50 mL), dried over anhydrous $MgSO_4$ and filtered. The solvent was removed under reduced pressure to give the crude product (3.91 g, 100%), which was purified by chromatography (1:1 EtOAc-hexane) to yield **15** (3.71 g, 95%) as a pale yellow powder: mp 191–192 °C (lit.[6,7] 185 °C), ^{1}H NMR (DMSO-d_6) δ 4.64 (d, J = 5.0 Hz, 2H), 5.15 (t, J = 5.4 Hz, 1H, disappears upon D_2O addition), 7.09 (s, 1H), 7.23–7.26 (t, J = 7.6 Hz, 1H), 7.32–7.35 (t, J = 7.6 Hz, 1H), 7.64 (d, J = 8.2 Hz, 1H), 7.78 (d, J = 7.5 Hz, 1H), 7.80 (s, 1H), 9.79 (s, 1H disappears upon D_2O addition). ^{13}C NMR (DMSO-d_6) 58.6, 107.9, 122.6, 125.4, 125.6, 127.3, 127.4, 127.7, 131.9, 133.3, 153.1.

Methyl 7-*tert*-butyl-3-hydroxy-2-naphthoate (82)

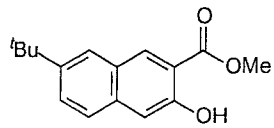

Procedure 1: Using $Cl_2CHCHCl_2$ as solvent

To a solution of **84** (4.04 g, 20.0 mmol) in $Cl_2CHCHCl_2$ (70 mL) at 0 °C was added *tert*-butyl chloride (8.90 mL, 80.0 mmol) and stirred for 10 min, followed by addition of $AlCl_3$ (5.33 g, 40.0 mmol) in two portions. The reaction mixture turned into a brown solution which was stirred at room temperature for a further 2 d. The reaction mixture was quenched by adding cold water (70 mL) at 0 °C. The aqueous layer was extracted with DCM (5 x 50 mL). The combined organic layers were washed with brine (2 x 50 mL), dried over anhydrous $MgSO_4$ and filtered. After the solvent was removed under reduced pressure, the resulting yellow oily liquid was subjected to chromatography (0.5:99.5 EtOAc-hexane) to yield **82** (4.40 g, 85%) as a yellow powder: mp 103–104 °C (lit.[6,7] 102–103 °C), ^{1}H NMR δ 1.39 (s, 9H), 4.02 (s, 3H), 7.27 (s, 1H), 7.61–7.65 (m, 2H), 7.71 (s, 1H), 8.47 (s, 1H), 10.36 (s, 1H disappears upon D_2O addition); ^{13}C NMR δ 31.3, 34.8, 52.7, 111.4, 114.2, 124.1, 126.3, 127.2, 128.6, 132.6, 136.4, 146.7, 156.2, 170.6.

Procedure 2: Using DCM as solvent

To a solution of **84** (2.02 g, 10.0 mmol) in anhydrous DCM (35 mL) at < –20 °C was added *tert*-butyl chloride (4.45 mL, 40.0 mmol) and stirred for 10 min, followed by an addition of $AlCl_3$ (2.67 g, 20.0 mmol) in a portion. The reaction mixture was stirred at room temperature for 2 d. After the solvent was removed under reduced pressure, the reaction mixture was quenched by adding cold water (50 mL) at 0 °C. The resulting precipitate was isolated by suction

filtration, washed several times with deionized water and air dried. The crude product was purified by chromatography (1:99 EtOAc-hexane) to yield **82** (4.80 g, 93%) (MeOH 50% yield) as a yellow powder having identical characterization data to those obtained from the Procedure 1.

6-*tert*-Butyl-3-(hydroxymethyl)-2-naphthol (16)

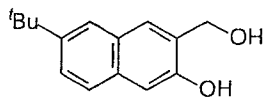

To a stirred suspension of $LiAlH_4$ (0.59 g, 15 mmol) in anhydrous THF (55 mL) at 0 °C was added slowly a solution of **85** (2.00 g, 7.74 mmol) in anhydrous THF (10 mL) over 10 min. The reaction mixture was stirred for a further 6 h at room temperature. The reaction was quenched by adding cold aqueous 20% HCl (until the pH reached 1–2) at 0 °C, followed by extraction with diethyl ether (4 x 50 mL). The organic layer was then separated, washed with deionized water (2 x 50 mL), brine (1 x 50 mL), dried over anhydrous $MgSO_4$ and filtered. The solvent was removed under reduced pressure to give the crude product (1.80 g, 100%), which was purified by chromatography (2:8 EtOAc-hexane) to yield **18** (1.63 g, 92%) as a colourless powder: mp 173–174 °C (lit.[6,7] 174–176 °C); ^{1}H NMR (DMSO-d_6) δ 1.35 (s, 9H), 4.62 (d, J = 5.7 Hz, 2H), 5.08 (t, J = 5.7 Hz, 1H, disappears upon D_2O addition), 7.04 (s, 1H), 7.44 (dd, J = 6.3, 1.9 Hz, 1H), 7.58 (d, J = 8.8 Hz, 1H), 7.66 (s, 1H), 7.76 (s, 1H), 9.64 (s, 1H, disappears upon D_2O addition).

Calix[4]naphthalene (17)

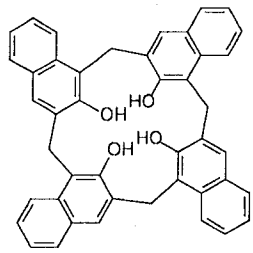

To a stirred solution of **15** (2.96 g, 17.0 mmol) in anhydrous dioxane (350 mL) at room temperature was added neat $TiCl_4$ (1.86 mL, 17.0 mmol) over 15 min. The reaction mixture was heated at reflux with stirring for a further 3 d. After solvent was removed under reduced pressure, the resulting black residue was purified by chromatography (1:1 DCM-hexane) to yield calix[4]naphthalene (0.39 g, 15%) as a light brown powder: mp > 300 °C (dec.) (lit.[6] > 300 °C); ^{1}H NMR δ 4.58 (s, 8H), 7.22–7.25 (m, 4H), 7.48–7.51 (m, 4H), 7.60 (d, *J* = 7.6 Hz, 4H), 7.86 (s, 4H), 8.38 (d, *J* = 8.8 Hz, 4H), 10.95 (s, 1H, disappears upon D_2O addition); ^{13}C NMR δ 25.9, 119.9, 123.0, 123.7, 126.5, 128.6, 129.0, 129.4, 130.1, 131.9, 148.2; (–)-APCI MS *m/z* (relative intensity) 624.2 (M^+, 50) calcd.: 624.2 for $C_{44}H_{32}O_4$.

***tert*-Butylcalix[4]naphthalene (18)**

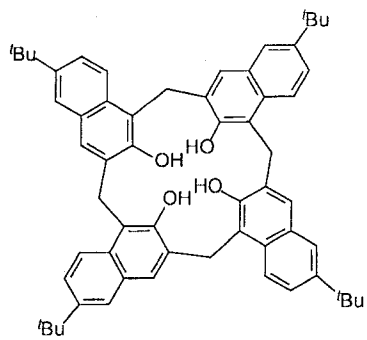

To a stirred, clear and colourless solution of **16** (3.00 g, 13.0 mmol) in anhydrous dioxane (300 mL) at 5–10 °C was added $TiCl_4$ (1.44 mL, 13.0 mmol) over 10 min. The reaction mixture turned to dark brown upon raising temperature. The reaction mixture was heated at reflux with stirring for a further 3 d. After solvent was removed under reduced pressure, the resulting black residue was purified by chromatography (2:8 DCM-hexane) to yield **18** (0.34–0.58 g, 12–21%) as a light yellow powder: mp > 320 °C (dec.) [lit.[10] 246–249 °C (dec.) or[6] > 320 °C], ^{1}H NMR δ 1.32 (s, 36H), 4.52 (s, 8H), 7.52 (s, 4H), 7.57–7.50 (m, 4H), 7.76 (s, 4H), 8.28 (d, *J* = 9.5 Hz, 4H), 10.62 (s, 4H, disappears upon D_2O addition); ^{13}C NMR δ 26.2, 31.4, 34.7, 119.6, 122.9, 123.9, 125.3, 128.4, 129.4, 130.0, 130.2, 146.1, 147.8; (–)-APCI MS *m/z* (relative intensity) 848.5 (M^+, 60) calcd.: 848.5 for $C_{60}H_{64}O_4$.

3.6.2 Attempted modification of the narrow-rim of 18

Attempted preparation of ethoxycarbonylmethoxy ether 83 of calix[4]naphthalene 18

A mixture of **18** (0.11 g, 0.13 mmol), K_2CO_3 (0.42 g, 3.0 mmol) and $BrCH_2CO_2Et$ (0.34 mL, 3.1 mmol) in dry acetone (30 mL) was heated at reflux with stirring over 7 d. After solvent was removed under reduced pressure,

deionized water (40 mL) was added to the resulting yellow residue, The solution was neutralized by aqueous 3 M HCl and extracted with $CHCl_3$ (3 x 25 mL). The organic layer was then separated, washed with deionized water (2 x 30 mL) and brine (1 x 30 mL), dried over anhydrous $MgSO_4$ and filtered. The solvent was removed under reduced pressure to give inseparable mixture.

tert-Butylcalix[4]naphthalene 1,3-bistriflate (85)

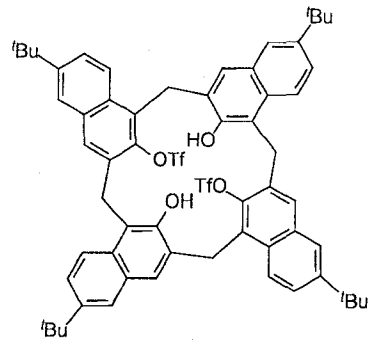

To a stirred solution of **18** (0.51 g, 0.60 mmol) in anhydrous pyridine (25 mL) at 0 °C was added dropwise Tf_2O (0.20 mL, 1.2 mmol) over 15 min. The reaction mixture was stirred for a further 1.5 h at room temperature. The dark yellow reaction mixture was poured into ice water (50 mL) and the solution was neutralized with aqueous 3 M HCl. The resulting light yellow precipitate was filtered, washed several times with deionized water, and dried overnight at 50 °C to give crude product (0.50 g, 75%) as a light yellow powder, which was purified by chromatography (13:87 DCM-hexane) to yield **85** (0.40 g, 60%) as a colourless powder: mp > 385 °C (dec.); ^{1}H NMR δ 1.13 (s, 18H), 1.48 (s, 18H), 4.39 (d, J = 14.8 Hz, 2H), 4.48 (d, J = 15.2, Hz, 2H), 4.62 (d, J = 14.8 Hz, 2H),

4.85 (d, J = 15.0 Hz, 2H), 5.23 (s, 2H, disappears upon D_2O addition), 7.21 (d, J = 1.9 Hz, 2H), 7.31 (s, 2H), 7.42 (dd, J = 6.8, 2.2 Hz, 2H), 7.71 (dd, J = 6.8, 2.2 Hz, 2H), 7.82 (s, 2H), 7.94 (s, 2H), 8.15 (d, J = 8.3 Hz, 2H), 8.27 (d, J = 8.9 Hz, 2H); ^{13}C NMR δ 25.0, 30.7, 31.1, 31.5, 34.8, 34.9, 122.2, 122.7, 123.6, 123.8, 124.6, 125.9, 126.1, 127.1, 127.7, 129.2, 129.7, 129.9, 130.57, 130.63, 131.7, 133.2, 141.2, 146.4, 149.2, 151.0; (+)-APCI MS *m/z* (relative intensity) 1113.3 ($[M+H]^+$, 70) calcd.: 1112.4 for $C_{62}H_{62}F_6O_8S_2$.

3.6.3 Complexation studies

All general methods for complexation studies were similar to those used in Chapter 2 with some differences which are described below.

UV–vis absorption spectroscopy

All UV–vis absorption data were conducted on a HP 8452A diode array spectrophotometer with thermostated cell compartments. Temperatures were recorded to ± 0.1 °C with a thermocouple. Aliquots of solid portions of C_{60} were added to 2.50 mL of solutions, which were approximately 1.00–2.00 $x10^{-3}$ M, of the respective calixnaphthalene, in screw-capped 1.00 cm-pathlength quartz glass cuvettes. After each addition, solutions were sonicated for 10 min, the cuvettes were placed into the thermostated cell compartment, and the resulting spectra were recorded relative to air blanks.

^{1}H NMR spectroscopy

In a typical experiment in toluene-d_8, aliquots of a stock solution of the host calixnaphthalene (1.00 mL, of approximately 1.9 $x10^{-3}$ M solutions) were added to NMR tubes, and the calculated amounts of solid C_{60} were then added in small portions to the host solutions in the NMR tubes. After each addition, the solutions were sonicated for approximately 10 min. ^{1}H NMR measurements were recorded at 298 K at 500 MHz, unless otherwise noted. In the case of the CS_2 determinations, the employed procedure was identical to that in Chapter 2.

3.7 References

1. For recent monographs see: (a) Gutsche, C. D. In *Calixarenes Revisited. Monographs in Supramolecular Chemistry*; Stoddard, J. F., Ed.; Royal Society of Chemistry, Cambridge, 1998. (b) *Calixarenes in Action*; Mandolini, L.; Ungaro, R., Eds. Imperial College Press, London, England, 2000. (c) *Calixarenes2001*; Asfari, Z.; Böhmer, V.; Harrowfield, J.; Vicens, J., Eds. Kluwer Academic Publishers, Dordrecht, 2001

2. (a) Ashram, M.; Mizyed, S.; Georghiou, P. E. *Org. Biomol. Chem.* **2003**,*1*, 599-603. (b) Ashram, M. *Ph.D. Dissertation,* Memorial University of Newfoundland, 1997. (c) Georghiou, P. E.; Mizyed, S.; Chowdhury, S. *Tetrahedron Lett.* **1999**, *40*, 611-614. (b) Georghiou, P. E.; Stroud, S. S. *Unpublished observations.*

3. (a) Gutsche, C. D.; Dhawan, B.; No, K. H.; Muthukrishnan, R. *J. Am. Chem. Soc.* **1981**, *103*, 3782-3792. (b) Izatt, R. M.; Lamb, J. D.; Hawkins, R. T.; Brown, P. R.; Izatt, S. R.; Christensen, J. J. *J. Am. Chem. Soc.* **1983**, *105*, 1782-1785.

4. (a) McKervey, M. C.; Seward, E. M.; Ferguson, G.; Ruhl, B.; Harris, S. J. *J. Chem. Soc., Chem. Commun.* **1985**, 388-390. (b) Ishikawa, Y.; Kunitake, T.; Matsuda, T.; Otsuka, T.; Shinkai, S. *J. Chem. Soc., Chem. Commun.* **1989**, 736-738.

5. Davis, F.; Otoobe, L.; Short, R.; Stirling, C. J. M. *Langmuir* **1996**, *12*, 1892-1894. (b) Dei, L.; Casnati, A.; Lonostro, P.; Baglioni, P. *Langmuir* **1995**, *11*, 1268-1272. (c) Ludwig, R.; Matsumoto, H.; Takeshita, M.; Ueda, K.; Shinkai, S. *Supramol. Chem.* **1995**, *4*, 319-327.

6. Ashram, M. *Ph.D. Dissertation,* Memorial University of Newfoundland, 1997.

7. Chowdhury, S. *Ph.D. Dissertation,* Memorial University of Newfoundland, 2001.

8. Al-Saraierh, H.; Miller, D. O.; Georghiou, P. E. *J. Org. Chem.* **2005**, *70*, 8273-8280.

9. González, J. J.; Nieto, P. M.; Echavarren, A. M.; de Mendoza, *J. Org. Chem.* **1995**, *60,* 7419-7423.

10. (a) Chowdhury, S.; Bridson, J. N.; Georghiou, P. E. *J. Org. Chem.* **2000**, *65,* 3299-3302. (b) Ishiyama, T.; Kizaki, H.; Hayashi, T.; Suzuki, A.; Miyaura, N. *J. Org. Chem.* **1998**, *63,* 4726-4731.

11. Hennrich, G.; Murillo, M. T.; Prados, P.; Song, K.; Asselberghs, I.; Clays, K.; Persoons, A.; Benet-Buchholz, J.; de Mendoza, J. *Chem. Commun.* **2005**, 2747-2749.

12. Al-Saraierh, H.; Georghiou, P. E. *Unpublished results.*

13. (a) Haino, T.; Yanase, M.; Fukunaga, C.; Fukazawa, Y. *Tetrahedron* **2006**, *62,* 2025-2035. (b) Saha, A.; Nayak, S. K.; Chottopadhyay, S.; Mukherjee, A. K. *J. Phys. Chem. B,* **2004**, *108*, 7688-7693. (c) Wang, M.-X.; Zhang, X.-H.; Zheng, Q.-Y. *Angew. Chem. Int. Ed.* **2004**, *43*, 838-842.

14. (a) Georghiou, P. E.; Mizyed, S.; Chowdhury, S. *Tetrahedron Lett.* **1999**, *40*, 611-614. (b) Georghiou, P. E.; Stroud, S. S. *Unpublished observations.*

15. Korobov, M. V.; Smith, A. L. In *Fullerene. Chemistry, Physics and Technology*; Kadish, K. M.; Ruoff, R. S., Eds. 2000, John Wiley & Sons, New York, NY, pp 55-6.

16. Some other studies in which the λ = 430 nm region was used to be their evidence for complex formation with similar systems are as: (a) Haino, T.; Yanase, M.; Fukazawa, Y. *Angew. Chem., Int. Ed. Engl.* **1997**, *36*, 259-260. (b) Haino, T.; Yanase, M.; Fukazawa, Y. *Angew. Chem., Int. Ed. Engl.* **1998**, *37*, 997-998. (c) Tsubaki, K.; Tanaka, K.; Kinoshita, T.; Fuji, K. *Chem. Commun.* **1998**, *37*, 895-896. (d) Ikeda, A.; Yoshimura, M.; Shinkai, S. *Tetrahedron Lett.* **1997**, *38*, 2107-2110. (e) Tucci, F. C.; Rudkevitch, D. M.; Rebek, J. *J. Org. Chem.* **1999**, *64*, 4555-4559. (f) (a) Haino, T.; Yanase, M.; Fukunaga, C.; Fukazawa, Y. *Tetrahedron* **2006**, *62*, 2025–2035.

17. Georghiou, P. E.; Tran, A. H.; Stroud, S. S.; Thompson, D. W. *Tetrahedron* **2006**, *62*, 2036-2044.

18. Andreetti, G. D.; Böhmer, V.; Jordan, J. G.; Tabatabai, M.; Ugozzoli, F.; Vogt, W.; Wolff, A. *J. Org. Chem.* **1993**, *58*, 4023-4032.

19. Georghiou, P. E.; Ashram, M.; Clase, H. J.; Bridson, J. N. *J. Org. Chem.* **1998**, *63*, 1819–1826.

20. Ikeda, A.; Suzuki, Y.; Yoshimura, M.; Shinkai, S. *Tetrahedron* **1998**, *54*, 2497-2508.

21. Computer-assisted molecular modeling studies were conducted using Spartan'04, V1.0.3 from Wavefunction, Inc., Irvine, CA, USA. Molecular mechanics (MMFF94) calculations were conducted on the optimized geometry of the hosts and guests and their respective complexes.

22. (a) González, J. J.; Nieto, P. M.; Prados, P.; Echavarren, A. M.; de Mendoza, J. *J. Org. Chem.* **1995**, *60*, 7419-7423. (b) Csók, Z.; Szalontai, G.; Czira, G.; Kollár, L. *Supramol. Chem.* **1998**, *10*, 69-77. (c) Chowdhury, S.; Bridson, J. N.; Georghiou, P. E. *J. Org. Chem.* **2000**, *65,* 3299-3302.

23. (a) Jaime, C.; de Mendoza, J.; Prados, P.; Nieto, P. M.; Sanchez, C. *J. Org. Chem.* **1991**, *56*, 3372-3376. (b) Mandolini, L.; Ungaro, R. *Calixarenes in Action*, Imperial College Press, London, 2000.

24. (a) Erdélyi, M.; Gogoll., A. *J. Org. Chem.* **2001**, *66,* 4165-4169. (b) Arcadi, A.; Cacchi, S.; Marinelli, F. *Tetrahedron Lett.* **1989**, *30*, 2581-2584.

25. Zhong, Z. -L.; Ikeda, A.; Shinkai, S. Chapter 26, pp 476-495, in *Calixarenes 2001*; Asfari, Z.; Böhmer, V.; Harrowfield, J.; Vicens, J., Eds. Kluwer Academic Publishers, Dordrecht, 2001.

26. (a) Bhattacharya, S.; Nayak, S. K.; Chattopadhyay, S.; Banerjee, M.; Mukherjee, A. K. *J. Chem. Soc. Perkin Trans. 2*, **2001**, 2292-2297; and references therein. (b) Bhattacharya, S.; Nayak, S. K.; Chattopadhyay, S.; Banerjee, M.; Mukherjee, A. K. *J. Phys. Chem. B* **2003**, *107*, 11830-11834; and references therein.

27. Iglesias-Sánchez, J. C.; Fragoso, A.; de Mendoza, J.; Prados, P. *Org. Lett.* **2006**, *8*, 2571-2574.

28. Williams, R, M.; Verhoeven, J. W. *Recl. Trav. Chim. Pays-Bas* **1992**, *111*, 531-532.

29. Atwood, J. L.; Barnes, M. J.; Gardiner, M. G.; Raston, C. L. *Chem. Commun.* **1996**, 1449-1450.

30. Leach, R.S; Tse, D. S.; Despres, A.; Breheret, E.; Hare, J. P.; Dennis, T. J.; Kroto, H. W.; Taylor, R.; Walton, D. R. M. *Chem. Phys.* **1992**, *160*, 451.

31. Gallagher, S. H.; Armstrong, R. S.; Lay, R. A.; Reed, C. A. J. Phys. Chem. **1995**, *99*, 5817-5825.

32. Tolbert, L. M.; Solntsev, K.M. *Acc. Chem. Res.* **2002**, *35*, 19-27.

33. Thompson, D. W. *et al. Unpublished observations.*

34. (a) Benesi, H. A.; Hildebrand, J. H. *J. Am. Chem. Soc.* **1949**, *71*, 2703-2707. (b) Traylor, T. J.; Tsuchiya, S.; Campbell, D.; Mitchell, M.; Stynes, D.; Koga, N. *J. Am. Chem. Soc.* **1985**, *107*, 604-614. (c) Tsubake, H.; Furuta, H.; Odani, A.; Takeda, Y.; Kudo, Y.; Liu, Y.; Sakamoto, H.; Kimura, K. In Davies,

J. E. D., Ripmeester, J. A., Eds.; *Comprehensive Supramolecular Chemistry;* Elsevier Science: Oxford, 1996; *Vol. 8*, pp 425-482. (d) Connors, K. A. *Binding Constants*; Wiley: New York, NY, 1987.

35. (a) Foster, R.; Fyfe, C. A. *J. Chem. Soc., Chem. Commun.* **1965**, 642-643. (b) Fielding, L. *Tetrahedron* **2000**, *56*, 6151-6170. (c) Hirose, K. *J. Inc. Phenom.* **2001**, *39*, 193–209.

36. The numbering for the protons are based upon the naphthalene ring numbering system.

37. Mizyed, S.; Ashram, M.; Miller, D. O.; Georghiou, P. E. *J. Chem. Soc., Perkin Trans. 2*, **2001**, 1916-1919.

38. Petrucci, R. H.; Harwood, W. S.; Herring, F. G.; Madura, J. D. *General Chemistry: Principle and Modern Applications*, Pearson Education Inc., New Jersey, 2007.

39. (a) Mizyed, S.; Georghiou, P. E.; Bancu, M.; Cuadra, B.; Rai, A. K.; Cheng, P.; Scott, L. T. *J. Am. Chem. Soc.* **2001**, *123*, 12770-12774. (b) Georghiou, P. E.; Tran, A. H.; Mizyed, S.; Bancu, M.; Scott, L. T. *J. Org. Chem.* **2005**, *70*, 6158-6163.

40. For a similar absence of experimental evidence for complexation behaviour with C_{60} for a different naphthalene-ring based molecular receptor lacking *tert*-butyl substituents, see: Tran, A. H.; Miller, D. O.; Georghiou, P. E. *J. Org. Chem.* **2005**, *70*, 1115-1121.

41. Thompson, D. W.; Bishop, A.; El-Dali, A. *Unpublished observations.*

42. Wang, J.; Gutsche, C. D. *J. Am. Chem. Soc.* **1998**, *120*, 12226-12231.

43. Nicolaou, K. C.; Dai, W. M.; Hong, Y. P.; Baldridge, K. K.; Siegel, J. S.; Tsay, S. C. *J. Am. Chem. Soc.* **1993**, *115*, 7944-7953.

44. Al-Saraierh, H.; Georghiou, P. E. *Unpublished results.*

45. It should be noted for example, that Tucci *et al.* in their 1999 paper (ref. 16e) also found a discordance between their absorption data based upon absorbance changes at λ = 430 nm, and ^{1}H NMR data for one of their deep-cavitand molecules with C_{60} in toluene solution.

Chapter 4

Ethoxycarbonlymethoxy ethers of homocalix[*n*]naphthalenes: Synthesis and recognition behaviour towards alkali cations

4.1 Introduction

4.1.1 Homocalixarenes and homocalixnaphthalenes

Homocalixarenes such as **90a**–**93g** (Figure 4.1) form a class of calixarenes in which the methylene bridges are partly or completely replaced by ethylene or larger bridges.[1,2,3] As a result, homocalixarenes have larger cavities than those of their calixarene parents. Homocalixarenes and their derivatives have been also shown to be very useful hosts for several different cationic guests such as uranyl ion,[4] transition metal ions,[2,3,5,6] alkaline earth ions[7] and alkali ions.[7,8]

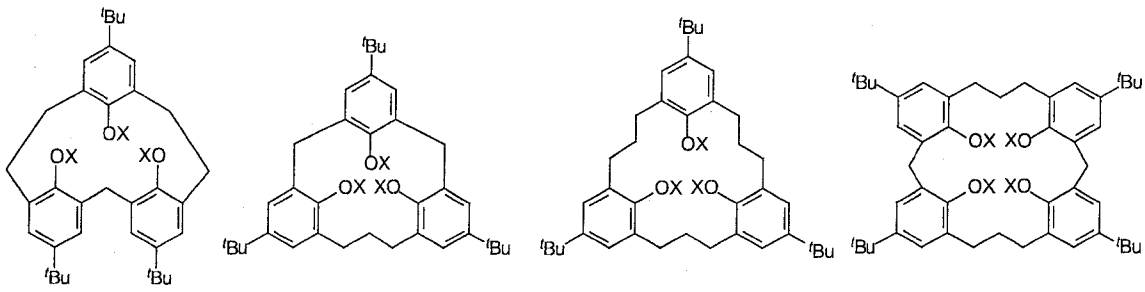

90a X = H
90b X = OMe

91a X = H
91b X = OMe
91c X = CH_2CONEt_2

92a X = Et
92b X = Pr
92c X = Bu
92d X = CH_2CO_2Et
92e X = CH_2CONEt_2
92f X = 2-pyridylmethyl

93a X = Bu
93b X = Bz
93c X = CH_2CO_2Me
93d X = CH_2CO_2Et
93e X = $CH_2CO_2{}^tBu$
93f X = CH_2CONEt_2
93g X = 2-pyridylmethyl

Figure 4.1 Examples of the *n*-homocalixarenes.[1,2]

In 1981, Tashiro and Yamato[9] reported the synthesis of the dihomocalix[4]arene **96** from the bis(iodomethyl) precursor **94** using a Müller-

Röscheisen cyclization, followed by demethylation of tetramethoxydihomocalixarene **95** (Scheme 4.1). This approach was later employed by Vögtle *et al.* to prepare homocalixarenes with various ring sizes.[10]

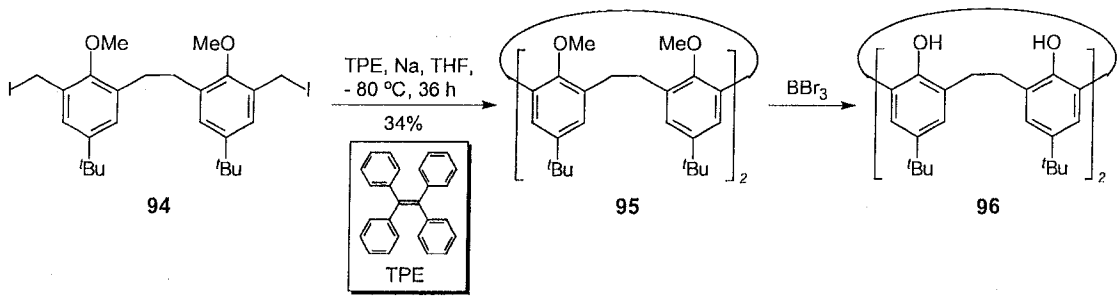

Scheme 4.1 Synthesis of dihomocalix[4]arene **96**.

Extrusion of sulfur atoms on the bridges of thiahomocalixarene precursors has also been another common method to prepare homocalixarenes.[11] For example, in 1990, Tashiro *et al.* reported[11a] that symmetrical homocalix[4]arenes **101a-c** (Scheme 4.2) were obtained from a coupling of bis(mercaptomethyl) **97a-c** and bis(bromomethyl) **98a-c** intermediates, respectively, followed by oxidation with *m*-CPBA and pyrolysis of the resulting sulfones **100a-c**. Demethylation of **101a-c** with BBr_3 yielded homocalixarenes **102a-c** having free hydroxyl groups.

Yamato *et al.* have more recently reported the syntheses of several homocalixarenes[12] using the well-known base-induced cyclocondensation procedure that has been employed to synthesize calixarenes from phenols and formaldehyde. For example, the condensation of phenol **103** and

paraformaldehyde under basic conditions[13] (Scheme 4.3) yielded trihomocalix[6]- **105** and tetrahomocalix[8]arenes **106** in synthetically useful yields. Unexpectedly, no formation of dihomocalix[4]arene **104** was observed.

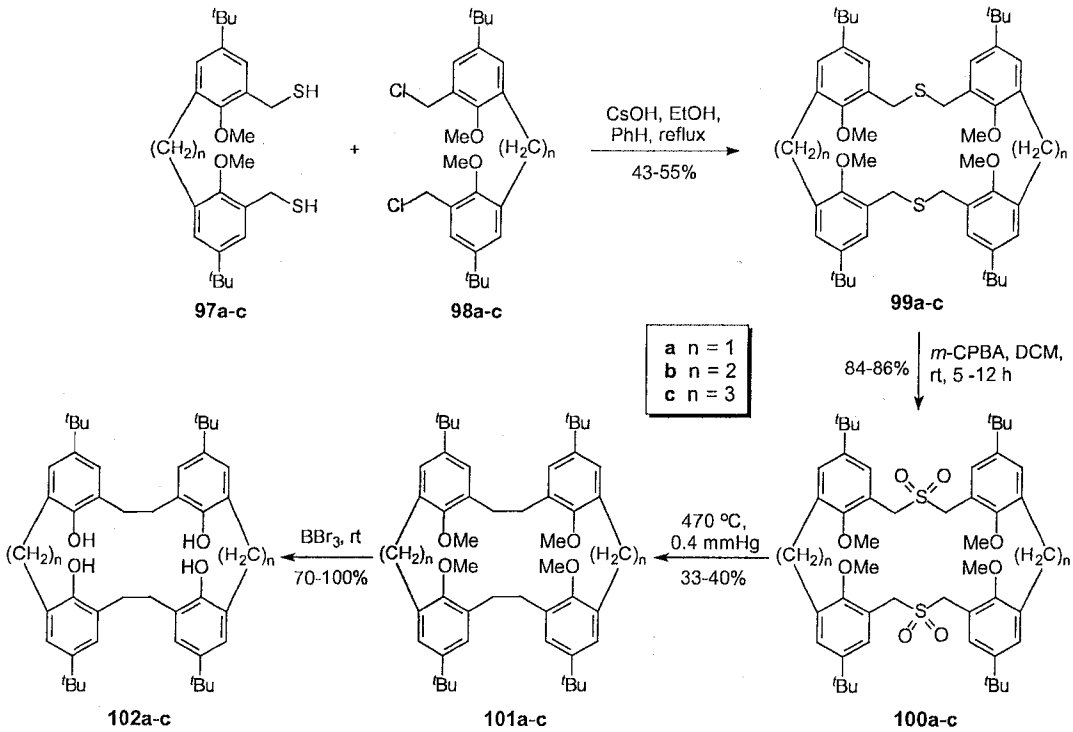

Scheme 4.2 Synthesis of *n*-homocalix[4]arenes **102a-c**.

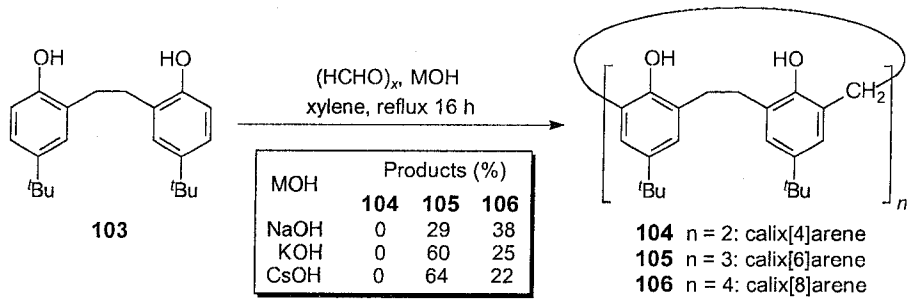

MOH	Products (%)		
	104	**105**	**106**
NaOH	0	29	38
KOH	0	60	25
CsOH	0	64	22

Scheme 4.3 Synthesis of trihomocalix[6]- and tetrahomocalix[8]arenes.

The Georghiou group has reported the synthesis of dihomocalix[4]naphthalenes, *e.g.* **113** and **114**, by photochemical extrusion of the sulfur atoms of the tetrahomodithiacalix[4]naphthalenes **30**, **31** and **111**, which were prepared by high-dilution [1+1] coupling reactions between bis(mercaptomethyl) precursors **107** or **108** and bis(bromomethyl) precursors **109** or **110**, respectively, in the presence of potassium hydroxide (Scheme 4.4). However, attempts to produce dihomocalix[4]naphthalene **112** from tetrahomodithiacalix[4]naphthalene **30** failed to give the desired product either via photochemical extrusion or via oxidation, followed by pyrolysis, presumably due to its low solubility in most of the common organic solvents.[14,15,16]

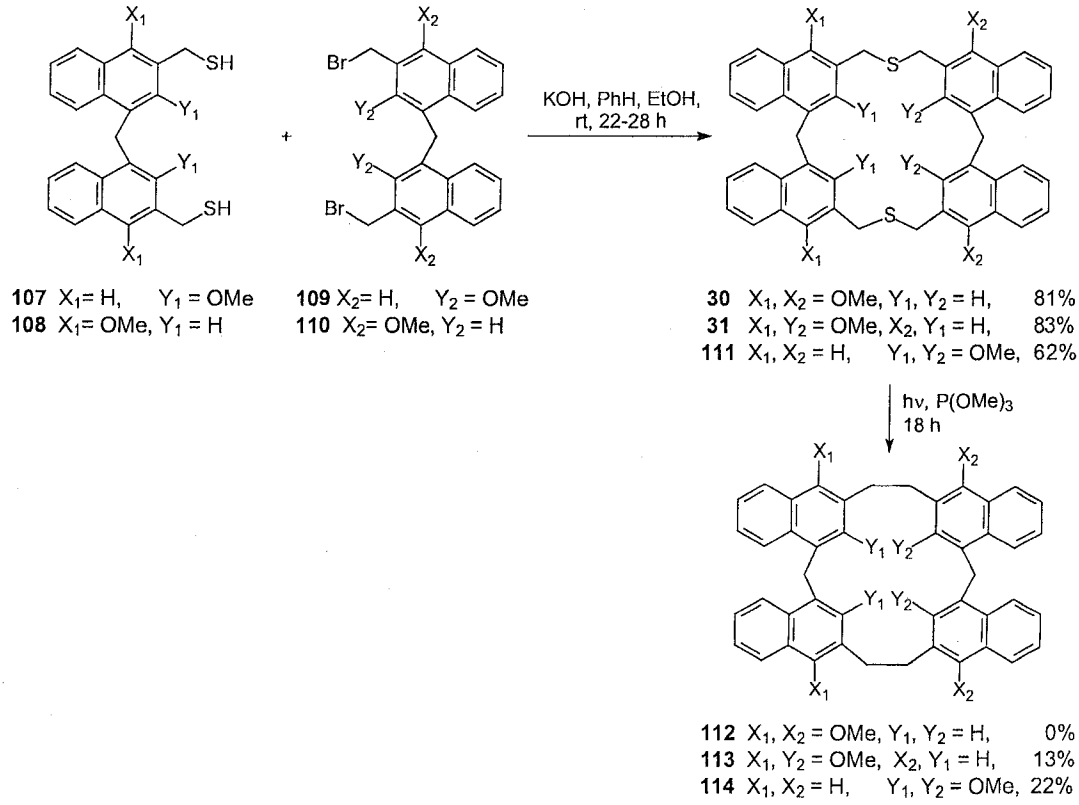

107 X_1= H, Y_1 = OMe
108 X_1= OMe, Y_1 = H

109 X_2= H, Y_2 = OMe
110 X_2= OMe, Y_2 = H

30 X_1, X_2 = OMe, Y_1, Y_2 = H, 81%
31 X_1, Y_2 = OMe, X_2, Y_1 = H, 83%
111 X_1, X_2 = H, Y_1, Y_2 = OMe, 62%

112 X_1, X_2 = OMe, Y_1, Y_2 = H, 0%
113 X_1, Y_2 = OMe, X_2, Y_1 = H, 13%
114 X_1, X_2 = H, Y_1, Y_2 = OMe, 22%

Scheme 4.4 Synthesis of dihomocalix[4]naphthalenes **113** and **114**.

Dihomo- **118** (Scheme 4.5)[8] and tetrahomocalix[4]naphthalenes **122** (Scheme 4.6)[17] were also obtained by the Georghiou group from the corresponding dithia precursors **117** and **121**, respectively, following a procedure similar to that used to form **113** and **114**.

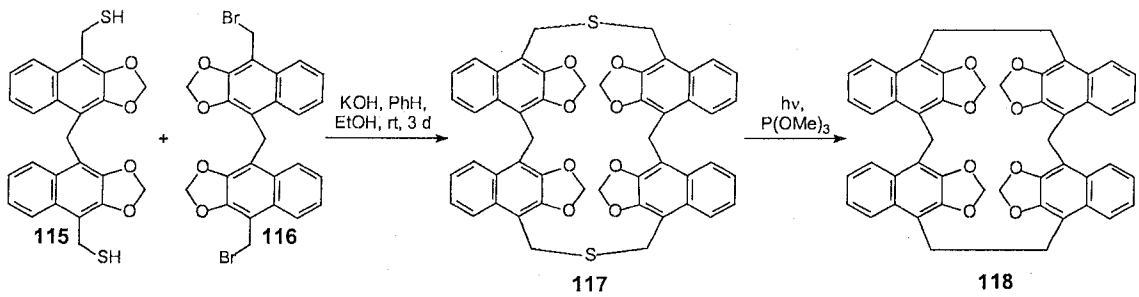

Scheme 4.5 Synthesis of dihomocalix[4]naphthalene **118**.[15]

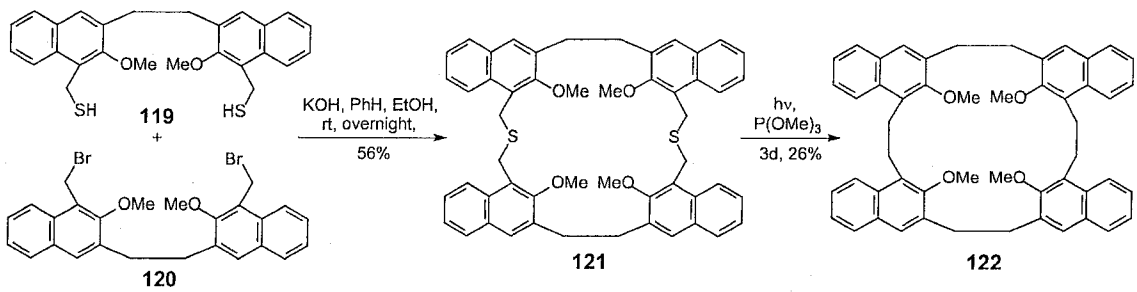

Scheme 4.6 Synthesis of tetrahomocalix[4]naphthalene **122**.[16]

Although the direct photochemical extrusion reaction has one fewer step from the dithiaprecursors compared to the pyrolysis approach, the photochemical extrusion step was only carried out on a small scale and gave either low yields (13–26%) or no product at all. Therefore, in the work described in this chapter, the condensation of 1,2-bis(3-hydroxy-2-naphthyl)ethane (**127**) and formalin, as outlined in the retrosynthetic analysis Scheme 4.7, was employed to synthesize

the trihomocalix[6]- **125** and tetrahomocalix[8]naphthalenes **126** on relatively large scales. *n*-Homocalixnaphthalenes **125** and **126** having free hydroxyl groups were also converted to their corresponding ethoxycarbonylmethoxy ether derivatives **123** and **124** (Scheme 4.7) in order to enhance their solubility in organic solvents, as well as to improve their potential affinities towards alkali cations.

4.1.2 Retrosynthetic analysis of ethoxycarbonylmethoxy ethers 123 and 124 of *n*-homocalixnaphthalenes

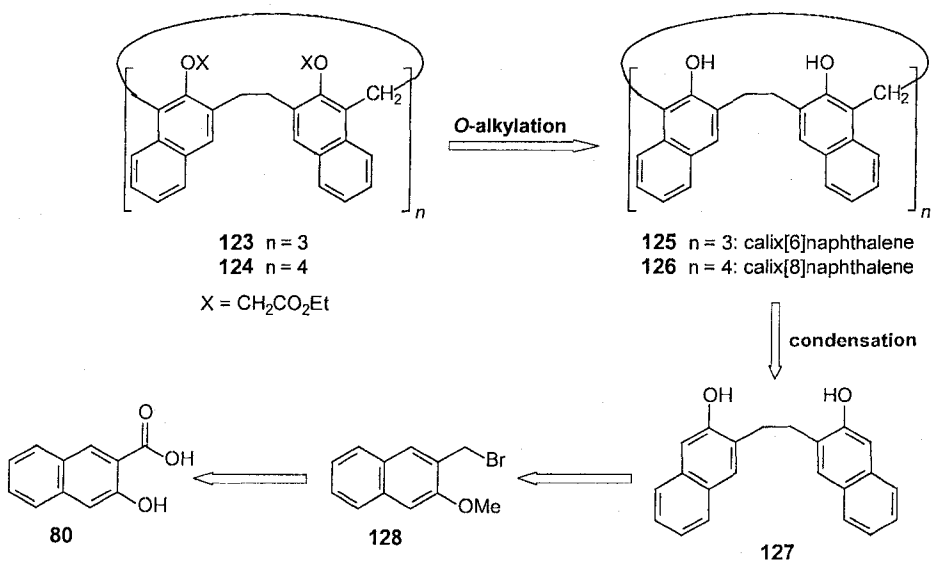

Scheme 4.7 Retrosynthetic analysis of hexaester **123** and octaester **124**

Scheme 4.7 revealed that hexakis(ethoxycarbonylmethoxy) ether of trihomocalix[6]naphthalenes ("hexaester"), **123** and octakis(ethoxycarbonyl-methoxy) ether of tetrahomocalix[8]naphthalenes ("octaester"), **124** could be furnished via alkylation of tri- and tetrahomocalixnaphthalenes **125** and **126**,

respectively, which in turn could conceivably be produced from a base-catalyzed condensation of bis(2-hydroxy-3-naphthyl)ethane (**127**) with formaldehyde. Since the positions ortho to hydroxyl groups on **126** are activated, the cross-coupling should expectedly occur at these positions. The key intermediate **127** could be conveniently obtained via an alkyllithium-assisted coupling of 2-methoxy-3-bromomethylnaphthalene (**128**) followed by demethylation. Intermediate **128** was derived from commercially-available **80** via sequential functional group interconversions, such as dimethylation, reduction and bromination.

4.2 Results and discussion

4.2.1 Synthesis of *n*-homocalixnaphthalenes 123–126

The synthesis of *n*-homocalixnaphthalenes **123**–**126** commenced with the preparation of 1,2-bis(3-hydroxy-2-naphthyl)ethane **127** (Scheme 4.8) from commercially available 3-hydroxy-2-naphthoic acid (**80**). Methylation of **80** with dimethyl sulfate in the presence of sodium hydroxide and only a small amount of PTC, *e.g.* adogen®, smoothly gave methoxy ester **129** as a colourless solid in 96% yield.[17,18] Reduction of the ester group in **129**, followed by bromination with PBr_3, afforded 3-(bromomethyl)-2-methoxynaphthalene (**128**) in 60–90% yield. Reaction on smaller scale gave higher yield of **128**. Intermediate **131** was conveniently formed in 94% yield from an alkyllithium-assisted homocoupling of bromomethyl intermediate **128** at –78 °C. The purity of **128** was found to strongly influence the

purity and yield of the coupling product **131**. Finally, demethylation of **131** with BBr_3 at room temperature quantitatively yielded the key intermediate **127**.

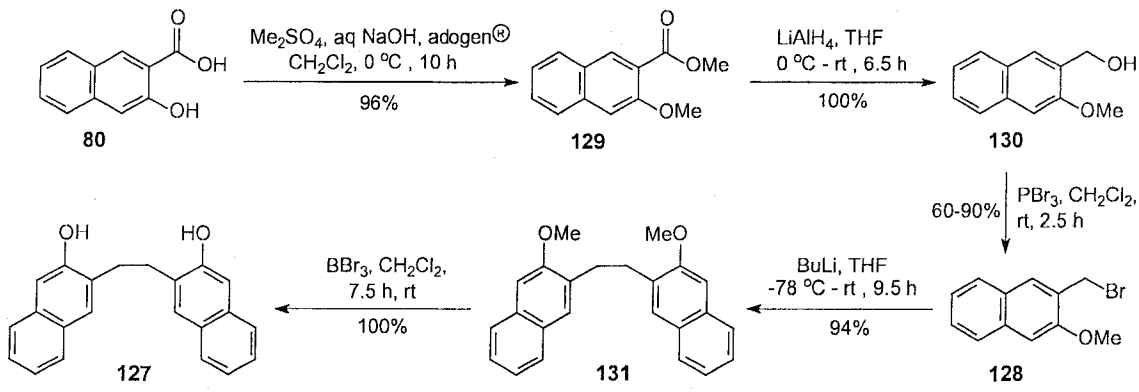

Scheme 4.8 Synthesis of 1,2-bis(3-hydroxy-2-naphthyl)ethane (**127**).

When **127** was subjected to a base-induced condensation reaction (Scheme 4.9) with aqueous 37% formaldehyde in DMF for 1h at 80 °C, a mixture of homocalixnaphthalenes **125** and **126** was afforded as an orange powder, in a total yield of 79%. Due to the low solubility of these products in organic solvents, only a small amount of the crude product could be purified by PLC (1:1 $CHCl_3$: petroleum ether) for characterization purposes. Two products were isolated, and they showed similar ^1H NMR spectra, *i.e.* having two singlets at about δ 3.2 ppm and 4.8 ppm, corresponding to the ethylene and methylene bridges, respectively. In addition, (–)-APCI MS analysis showed the molecular ion peak of trihomocalix[6]naphthalene **125** at *m/z* = 978.3 (Figure 4.2) and that of tetrahomocalix[8]naphthalene **126** at *m/z* = 1304.2 (Figure 4.3), respectively. On TLC, the trihomocalix[6]naphthalene **125** is less polar than tetrahomocalix[8]-naphthalene **126**. These products are the first large-ring homocalixnaphthalenes

synthesized to date. The ^{1}H NMR signals revealed that the larger ring compound **126** is more flexible than compound **125**.

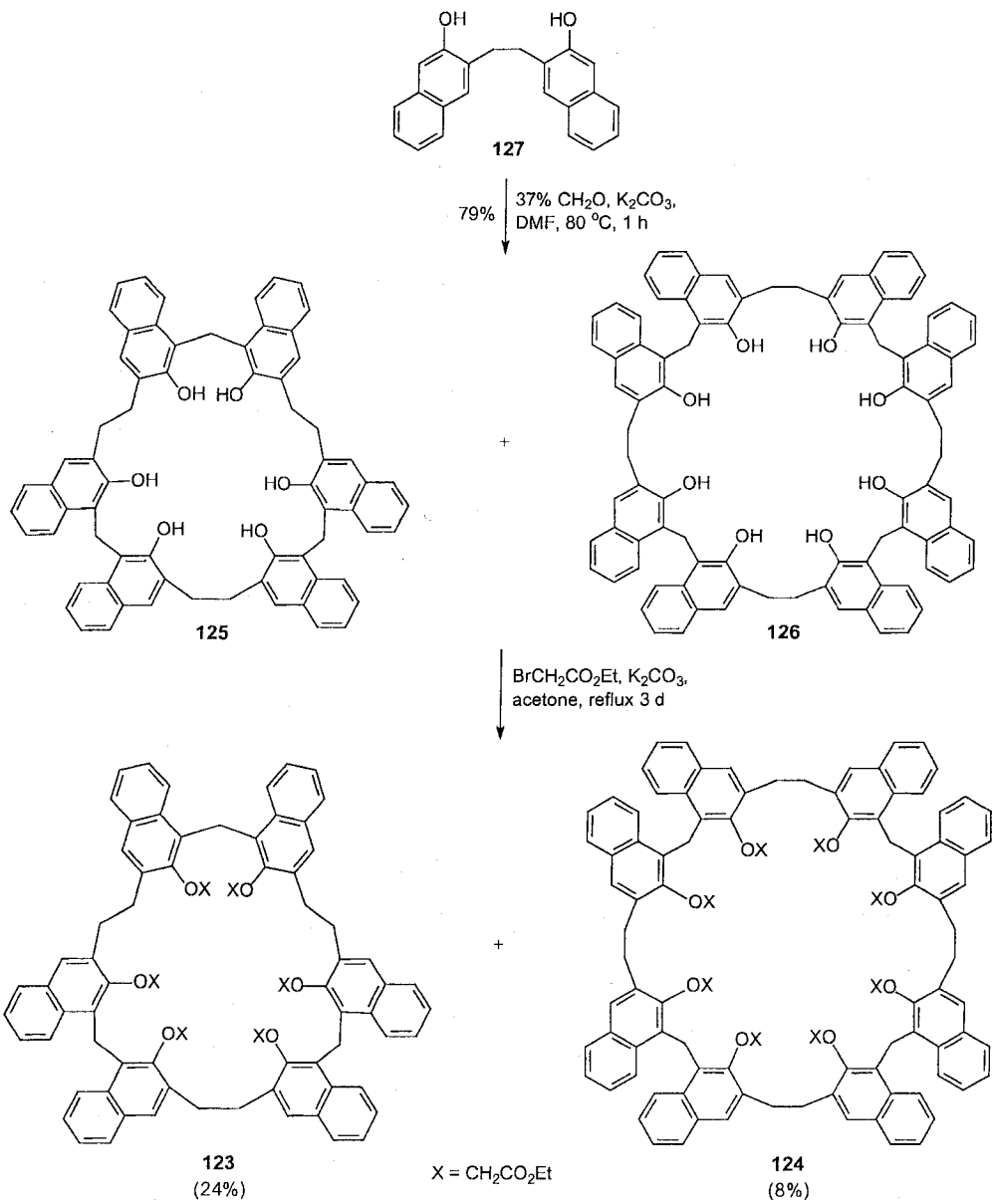

Scheme 4.9 Synthesis of hexaester **123** and octaester **124**.

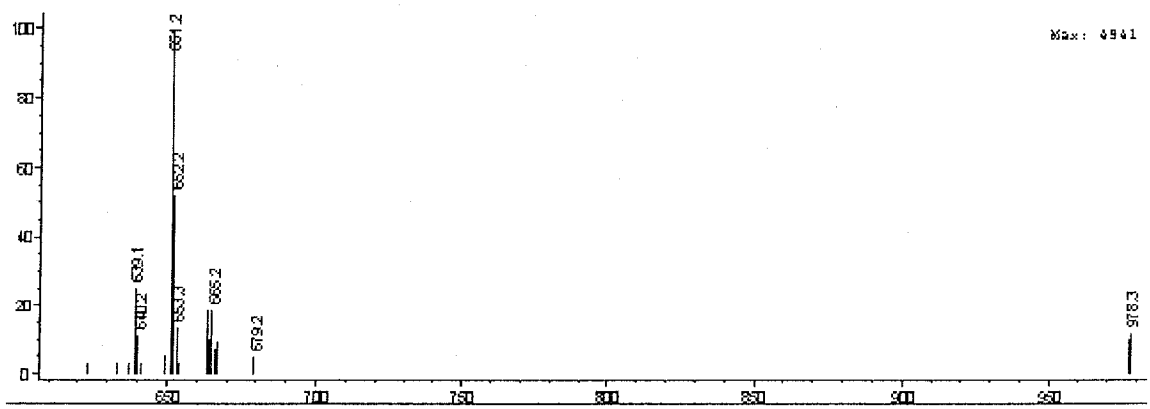

Figure 4.2 (–)-APCI MS spectrum showing the molecular ion peak of trihomocalix[6]naphthalene **125** at *m/z* = 978.3 (calcd.: 979.4 for $C_{69}H_{54}O_6$).

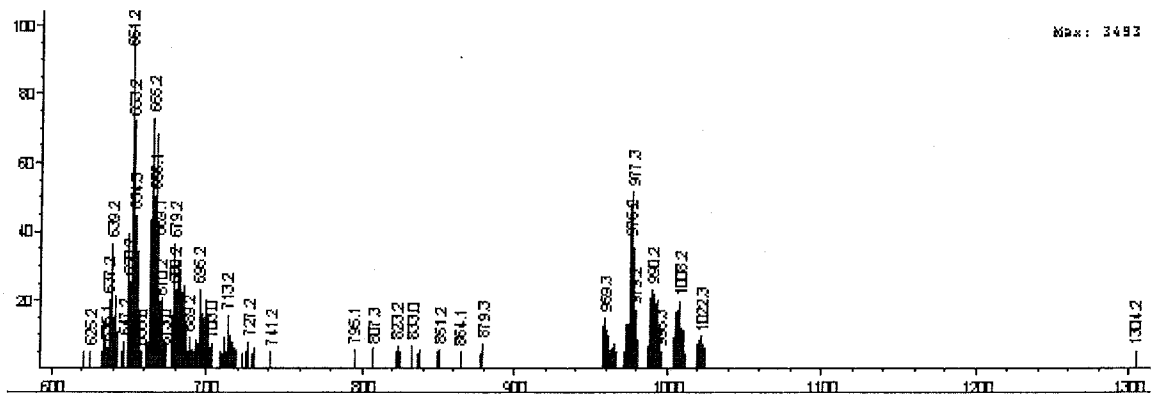

Figure 4.3 (–)-APCI MS spectrum showing the molecular ion peak of tetrahomocalix[8]naphthalene **126** at *m/z* = 1304.2 (calcd.: 1304.5 for $C_{92}H_{72}O_8$).

It is known that the ethoxycarbonylmethoxy ether derivatives of calixarenes[19], homocalixarenes[7,8] or calixnaphthalenes[20] exhibit ionophoric properties. Therefore, the newly formed trihomocalix[6]naphthalenes **125** and tetrahomocalix[8]naphthalene **126** which have very low solubility in organic solvents were converted to their ester derivatives. Indeed, alkylation of the crude

reaction product mixture with an excess amount of ethyl bromoacetate under basic conditions in acetone (Scheme 4.9) afforded the corresponding hexa- **123** and octaesters **124** of *n*-homocalixnaphthalenes as expected, which proved to be more soluble in $CHCl_3$ and could now be chromatographically purified on synthetically useful scales. The two ester derivatives **123** and **124** were isolated from the reaction mixture in 24% and 8% yields, respectively, as pale yellow solids. The hexaester **123** is less polar than the octaester **124** on TLC. In addition to ^{1}H and ^{13}C NMR, the (+)-APCI MS analysis clearly showed the presence of the molecular ion at *m/z* = 1495.8 for **123** (Figure 4.4) and *m/z* = 1994.6 for **124** (Figure 4.5), respectively.

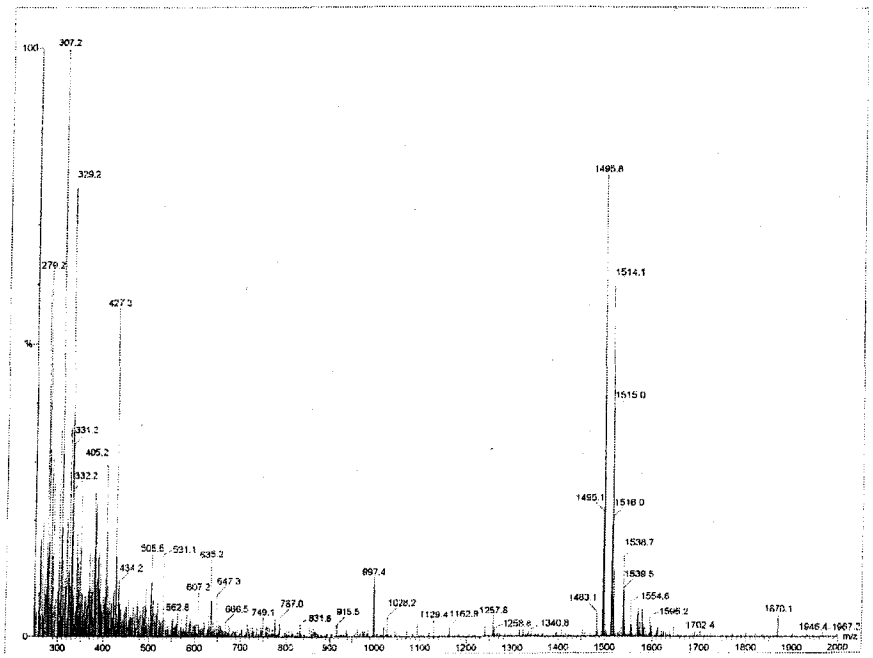

Figure 4.4 (+)-APCI MS spectrum showing the molecular ion peak of hexaester **123** at *m/z* = 1495.8 (calcd.: 1495.7 for $C_{93}H_{90}O_{18}$).

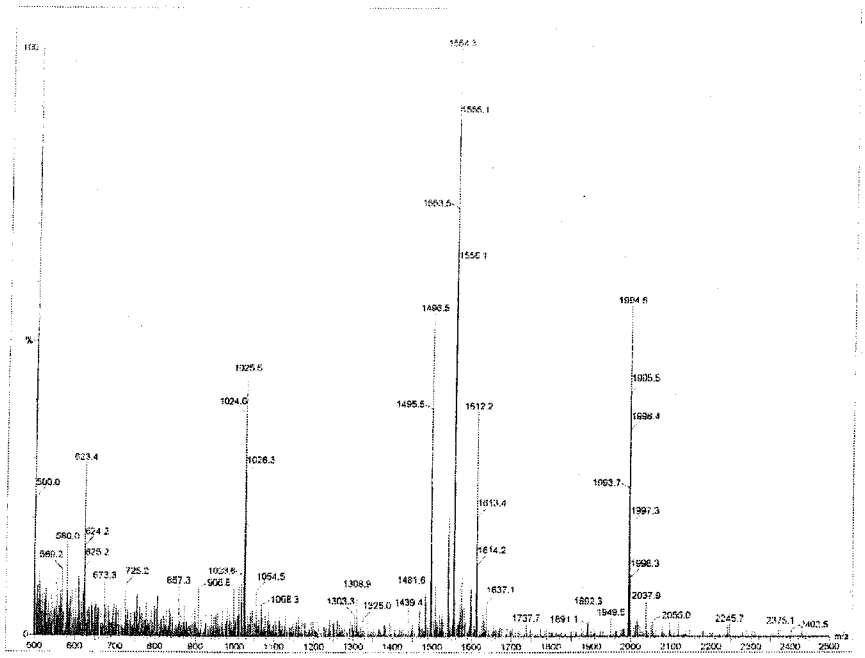

Figure 4.5 (+)-APCI MS spectrum showing the molecular ion peak of octaester **124** at *m/z* = 1994.6 (calcd.: 1994.3 for $C_{124}H_{120}O_{24}$).

4.2.2 Characterization by VT ^{1}H NMR

Ambient temperature ^{1}H NMR spectra revealed that hexaester **123** is conformationally less flexible than octaester **124** because all ^{1}H NMR signals of the former are much broader than those of the latter. To resolve the ^{1}H NMR signals of **123** and **124**, VT ^{1}H NMR experiments were conducted. Upon heating from ambient temperature to 328 K, the spectra of both **123** (Figure 4.6) and **124** (Figure 4.7) revealed sharper and better resolved signals for all of their protons.

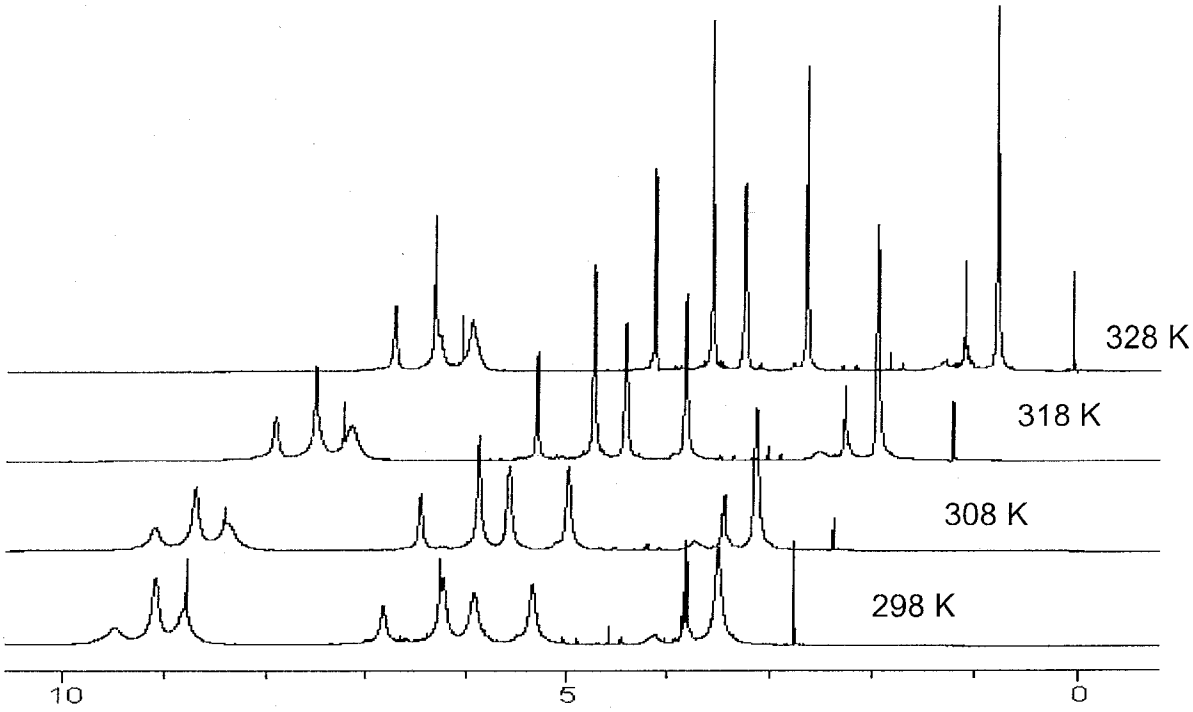

Figure 4.6 VT ^{1}H NMR of hexaester **123**.

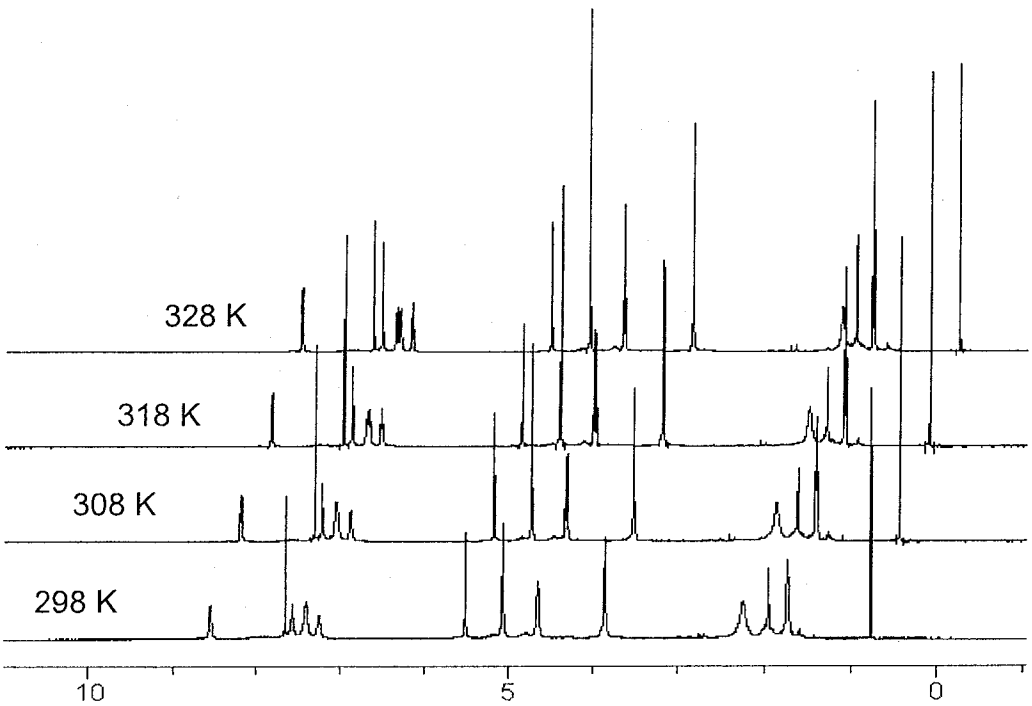

Figure 4.7 VT ^{1}H NMR of octaester **124**.

4.2.3 Solution complexation studies

Preliminary complexation tests of **123** and **124** with neutral guests such as C_{60} and C_{70} in toluene or carbon disulfide solutions were conducted using ^1H NMR spectroscopy. It was obvious that no complexation occurred under the conditions studied. It is possible that the high conformational flexibility of the large annulus could partly account for this observation.

In order to evaluate the extraction capabilities of these newly synthesized ester derivatives, two-phase solvent extraction experiments of metal picrates by **123** and **124** were investigated. These experiments were conducted in collaboration with S. Mizyed, Yarmouk University, Jordan. The extraction capabilities of **123** or **124** were evaluated by the percentage extraction (%*E*) values which are defined by equation 4.1.

$$\%E = \frac{A_o - A}{A_o} \bullet 100\% \qquad \text{(Eq 4.1)}$$

where A_o is the initial absorbance of the pure metal picrate in aqueous solution and A is the absorbance of the same aqueous solution after extraction. The percent extraction (%*E*) values for **123** or **124** towards alkali metal picrates, which were determined by S. Mizyed, are listed in Table 4.1 and described in Figure 4.8. It is obvious that **124** is not an efficient receptor for alkali metal ions under the conditions studied. It slightly extracted Li^+ (%*E* = 2.64) from aqueous solution while **123** proved to be a very good receptor for K^+ (%*E* = 71.36) and a weak host for Na^+ (%*E* = 2.34). Interestingly, **123** exhibits the highest selectivity

towards K^+ comparable with that of 18-crown-6 (**136**), *n*-homocalix[*n*]arenes **133–135** and ester derivatives of calix[*n*]arenes **56**, **57**, **60**, **61**, **64**, **65** and *n*-homocalix[*n*]arenes **132**, **134** (Table 4.2).

Table 4.1 *%E* values for two-phase solvent extraction of alkali metal picrates from queous solution by esters **123** and **124** in $CHCl_3$ at 25 °C.

Entry	Metal picrate / homocalix-naphthalene	Run #1			Run #2			Avarage
		A_o	A	*%E*	A_o	A	*%E*	
1	Li^+/**123**	0.00	0.00	0.00	0.00	0.00	0.00	0.00
2	Na^+/**123**	2.50	2.44	2.32	2.51	2.45	2.35	2.34 ± 0.02
3	K^+/**123**	1.61	0.47	70.65	1.61	0.45	72.08	71.36 ± 1.01
4	Rb^+/**123**	0.00	0.00	0.00	0.00	0.00	0.00	0.00
5	Cs^+/**123**	0.00	0.00	0.00	0.00	0.00	0.00	0.00
6	Li^+/**124**	1.59	1.54	2.90	1.59	1.55	2.39	2.64 ± 0.36
7	Na^+/**124**	0.00	0.00	0.00	0.00	0.00	0.00	0.00
8	K^+/**124**	0.00	0.00	0.00	0.00	0.00	0.00	0.00
9	Rb^+/**124**	0.00	0.00	0.00	0.00	0.00	0.00	0.00
10	Cs^+/**124**	0.00	0.00	0.00	0.00	0.00	0.00	0.00

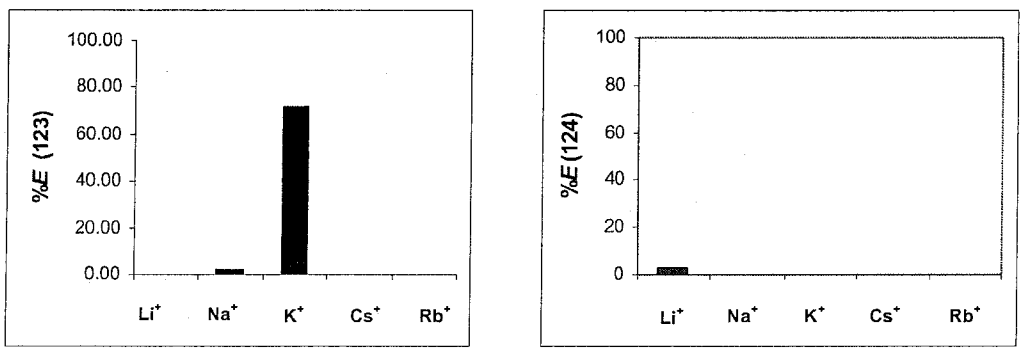

Figure 4.8 *%E* values for **123** (*left*) and **124** (*right*) with alkali metal picrates.

Table 4.2 %*E* values for two-phase solvent extraction of alkali metal picrates from queous solution by various receptors in halogenated solvents at 20–25 °C.

Receptors	Solvents	Li^+	Na^+	K^+	Rb^+	Cs^+
56[19c]	DCM	1.8	60.4	12.9	4.1	10.8
57[19c]	DCM	15.0	94.6	49.1	23.6	48.9
60[19c]	DCM	4.7	10.4	51.3	94.1	94.6
61[19c]	DCM	11.4	50.1	85.9	88.7	100.0
64[19c]	DCM	0.8	7.5	20.2	28.9	30.1
65[19c]	DCM	1.1	6.0	26.0	30.2	24.5
132[8]	DCM	7.6	9.1	11.6	72.0	19.1
133[2]	$CHCl_3$	2.0	1.7	2.0	0.3	-
134[2]	$CHCl_3$	-	2.9	-	-	-
135[2]	$CHCl_3$	-	0.2	-	1.3	-
136[19c]	DCM	8.7	23.1	77.9	77.3	62.9

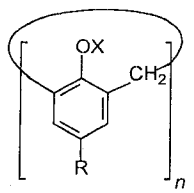

56 n = 4, R = H, X = CH_2CO_2Et
57 n = 4, R = ^{t}Bu, X = CH_2CO_2Et
60 n = 6, R = H, X = CH_2CO_2Et
61 n = 6, R = ^{t}Bu, X = CH_2CO_2Et
64 n = 8, R = H, X = CH_2CO_2Et
65 n = 8, R = ^{t}Bu, X = CH_2CO_2Et

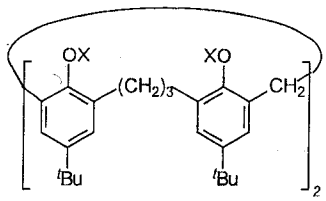

132 X = CH_2CO_2Et

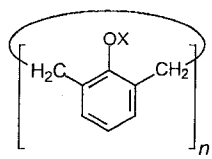

133 n = 5, X = H
134 n = 6, X = CH_2CO_2Me
135 n = 8, X = H

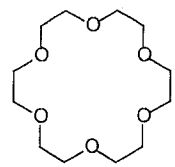

136 18-C-6

4.3 Conclusions

The base-induced condensation of 1,2-bis(3-hydroxy-2-naphthyl)ethane (**127**) and formaldehyde by analogy with procedures commonly utilized for the

synthesis of homocalixarenes, was successfully employed for the synthesis of the *n*-homocalixnaphthalenes **125** and **126**. The synthetic yields were higher than those obtained by the sulfur extrusion approach on a relatively large reaction scale. However, only trihomocalix[6]- and tetrahomocalix[8]naphthalenes were isolated from the condensation of the precursor **127** and formaldehyde. *O*-Alkylation of the homocalixnaphthalenes gave the corresponding hexa- **123** and octaester derivatives **124** having higher solubilities than those of their parent homocalixnaphthalenes. The newly synthesized octaester **123** demonstrated a high selectivity towards K^+ cation under the conditions studied.

4.4 Experimental section

General methods

General methods, materials and instrumentation used are identical to those described in Chapters 2 and 3.

Methyl 3-methoxy-2-naphthoate (129)

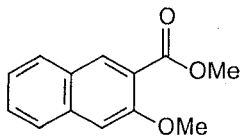

To a stirred solution of 3-hydroxy-2-naphthoic acid (**80**) (37.64 g, 200.0 mmol) in an aqueous solution of NaOH (17.6 g, 440 mmol and 160 mL water) at 0 °C was added adogen® (1.0 mL) and DCM (400 mL), followed by dimethyl sulphate (63 mL, 0.60 mol) over 45 min using a syringe pump. The reaction mixture was stirred for a further 9 h at 0 °C. Aqueous 10% NaOH solution was

added until the pH reached 12, and the mixture was stirred for another 1 h at room temperature. The DCM layer was then separated, washed with saturated aqueous NH_4Cl solution (2 x 50 mL), brine (2 x 50 mL) and distilled water (1 x 50 mL). The organic layer was dried over anhydrous $MgSO_4$ and filtered. After the solvent was evaporated, the resulting yellow solid residue was purified by flash chromatography (2:98 EtOAc-hexane) to yield **129** (41.62 g, 96%) as a colourless solid: mp 49–50 °C (lit.[21] 50–53 °C), ^{1}H NMR δ 3.96 (s, 3H), 4.00 (s, 3H), 7.20 (s, 1H), 7.37 (t, J = 7.5 Hz, 1H), 7.51 (t, J = 7.8, 7.5 Hz, 1H), 7.74 (d, J = 8.0 Hz, 1H), 7.81 (d, J = 8.5 Hz, 1H), 8.30 (s, 1H); ^{13}C NMR δ 52.5, 56.2, 107.0, 122.0, 124.6, 126.7, 127.8, 128.6, 128.9, 133.0, 136.3, 156.0, 166.9; GCMS *m/z* (relative intensity) 216 (M^+, 80), 185 (90), 127 (100), 114 (60).

3-(Hydroxymethyl)-2-methoxynaphthalene (130)

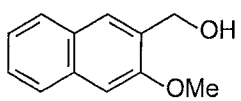

To a suspension of $LiAlH_4$ (10.24 g, 269.8 mmol) in dry THF (250 mL) at 0 °C was added a solution of **129** (33.34 g, 154.2 mmol) in dry THF (60 mL) over 30 min. The reaction was stirred at room temperature for a further 6 h, followed by acidification with cold aqueous 20% HCl at 0 °C (until pH = 1–2) and extraction with diethyl ether (3 x 150 mL). The organic layer was then separated, washed with deionized water (2 x 200 mL) and brine (2 x 50 mL), dried over anhydrous $MgSO_4$ and filtered. The solvent was removed under reduced pressure to give **130** as a colourless solid (29.0 g, 100%): mp 72–73 °C (lit.[17,18]

71–72 °C); ^{1}H NMR δ 2.37 (t, *J* = 6.8 Hz, 1H), 3.98 (s, 3H), 4.83 (d, *J* = 7.0 Hz, 2H), 7.13 (s, 1H), 7.35 (t, *J* = 7.8 Hz, 1H), 7.43 (t, *J* = 7.5 Hz, 1H), 7.73–7.77 (m, 3H); ^{13}C NMR δ 55.5, 62.6, 105.4, 124.1, 126.5, 126.6, 127.7, 127.8, 128.9, 130.7, 134.3, 156.1; GCMS *m/z* (relative intensity) 188 (M^+, 95), 172 (20), 144 (60), 127 (80), 115 (100). Compound **129** was used for the next step without further purification.

3-Bromomethyl-2-methoxynaphthalene (128)

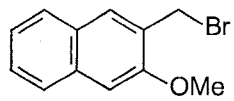

To a stirred solution of **130** (13.18 g, 70.02 mmol) in anhydrous DCM (400 mL) was added dropwise a solution of PBr_3 (2.5 mL, 270 mmol) in anhydrous DCM (7 mL) over 30 min, at room temperature. The solution was stirred for a further 2 h at room temperature and cold water (100 mL) was added. The organic layer was separated, washed with water (2 x 100 mL) and brine (2 x 50 mL), dried over anhydrous $MgSO_4$ and filtered. The crude product (15.81 g, 90%) was filtered through a short column of silica gel eluting with hexane to yield **128** (10.57 g, 60%) as a colourless powder: mp 144 °C (dec.) (lit.[17,18] 142–144 °C); ^{1}H NMR δ 4.01 (s, 3H), 4.71 (s, 2H), 7.13 (s, 1H), 7.34 (t, *J* = 7.0 Hz, 1H), 7.44 (t, *J* = 7.0 Hz, 1H), 7.71–7.75 (m, 2H), 7.82 (s, 1H); ^{13}C NMR δ 29.5, 55.9, 106.0, 124.3, 126.7, 127.2, 127.9, 128.7, 130.6, 135.0, 155.7; GCMS *m/z* (relative

intensity) 252 (M^+ ^{81}Br, 10), 250 (M^+ ^{79}Br, 10), 172 (20), 171 (100), 141 (95), 115 (30).

1,2-Bis(2-methoxy-3-naphthyl)ethane (131)

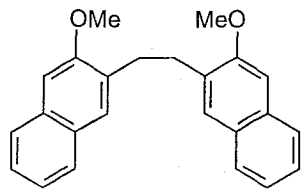

To a stirred solution of **128** (0.51 g, 2.0 mmol) in dry THF (20 mL) at –78 °C was added 1.6 M *n*-BuLi in *n*-hexane (0.62 mL, 1.0 mmol) over 30 min. The reaction mixture was stirred for a further 9 h at –78 °C, then quenched at 0 °C by the addition of cold water (30 mL) and aqueous 10% HCl (10 mL). The resulting colourless precipitate was filtered, washed several times with deionized water and dried at 60 °C overnight to yield **131** (0.32 g, 94%) as colourless powder: mp 209 °C ($CHCl_3$-MeOH) (lit.[17] 184–185.5 °C); ^1H NMR δ 3.13 (s, 4H), 3.93 (s, 6H), 7.10 (s, 2H), 7.30 (t, *J* = 7.5, Hz, 2H), 7.38 (t, *J* = 7.3 Hz, 2H), 7.59 (s, 2H), 7.68–7.72 (m, 4H); ^{13}C NMR δ 31.1, 55.5, 104.9, 123.6, 125.7, 126.5 127.3, 128.3, 129.1, 132.7, 133.7, 156.9; GCMS *m/z* (relative intensity) 342 (M^+, 30), 171 (100), 141 (60), 115 (40), 77 (30).

1,2-Bis(2-hydroxy-3-naphthyl)ethane (127)

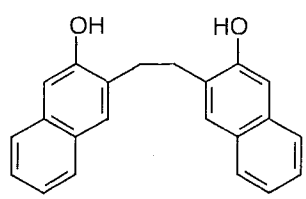

To a suspension of **131** (3.42 g, 10.0 mmol) in anhydrous DCM (95 mL) at room temperature was added dropwise BBr_3 (3.8 mL, 40 mmol) over 30 min. The reaction mixture was stirred for a further 7 h, and then quenched by the addition of cold water (50 mL) at 0 °C. The resulting colourless precipitate was filtered, washed several times with deionized water and dried at 60 °C overnight to yield **127** in quantitative yield as a very light yellow powder: mp 229–230 °C (dec.); ^{1}H NMR (DMSO-d_6) δ 3.06 (s, 4H), 7.15 (s, 2H), 7.22 (t, J = 7.3 Hz, 2H), 7.32 (t, J = 7.3 Hz, 2H), 7.63–7.64 (m, 4H), 7.70 (d, J = 9.0 Hz, 2H), 9.83 (s, 2H, OH, disappears upon D_2O addition); ^{13}C NMR (75 MHz, acetone-d_6) δ 30.8, 108.5, 122.7, 125.2, 125.5, 127.0, 128.2, 128.8, 131.3, 133.7, 154.0; LCMS *m/z* (relative intensity) 314 (M^+, 59), 158 (50), 157 (100).

Trihomocalix[6]naphthalenes 125 and tetrahomocalix[8]naphthalenes 126

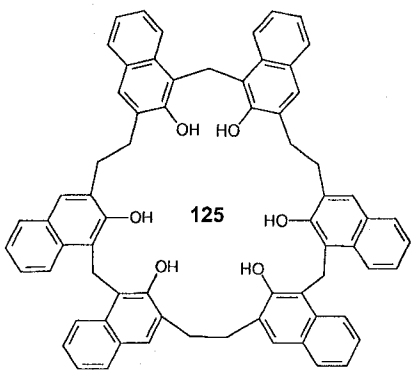

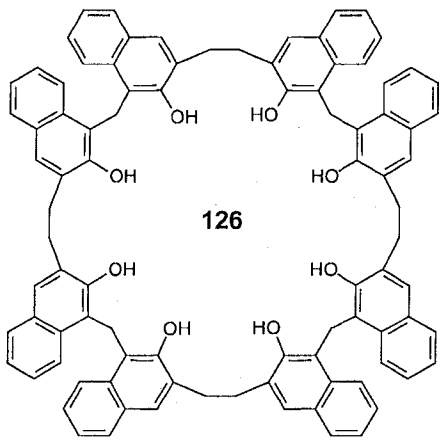

A mixture of **127** (1.26 g, 4.00 mol), aqueous 37% CH_2O (formalin) (0.4 mL) and K_2CO_3 (0.66 g, 4.8 mol) in DMF (40 mL) was heated at 80 °C with

stirring for 1 h. After the solvent was removed under reduced pressure, water (10 mL) was added. The resulting solution was acidified with aqueous 6 M HCl (until the pH reached 1–2) and then treated with $CHCl_3$ (20 mL). The resulting precipitate was isolated by suction filtration. The filtrate was then evaporated to dryness and the residue was treated with another 20 mL of $CHCl_3$, and the newly formed precipitate was also isolated by suction filtration. The precipitates were combined, washed several times with water, and then dried at 50 °C overnight to yield a mixture of **125** and **126** (1.04 g, 79%) as a yellow powder, which was used for the next step without further purification.

Due to the low solubilities of the two isomers in most of the common organic solvents, a small amount of the mixture was dissolved in $CHCl_3$ and purified by PLC (1:1 $CHCl_3$:petroleum ether) to yield **125** as a pale yellow solid: mp 205–210 °C (dec.); ^{1}H NMR (300 MHz, DMSO-d_6) δ 3.21 (s, 12H), 4.84 (s, 6H), 7.04–7.09 (m, 6H), 7.18–7.23 (m, 6H), 7.54–7.57 (m, 12H), 8.16 (d, J = 8.6 Hz, 6H), 9.28 (s, br, 6H, OH); ^{13}C NMR (75 MHz, DMSO-d_6) δ 22.1, 30.4, 119.9, 122.7, 123.4, 125.1, 126.5, 127.8, 128.8, 131.3, 132.0, 150.7; (–)-APCI MS *m/z* (relative intensity) 978.3 ($[M\text{-}1^+]^-$, 15) calcd.: 979.4 for $C_{69}H_{54}O_6$, 651.2 (100); and **126** as pale yellow solid: mp 228–230 °C (dec.); ^{1}H NMR (300 MHz, DMSO-d_6) δ 3.19 (s, 16H), 4.81 (s, 8H), 7.03–7.08 (m, 8H), 7.16–7.22 (m, 8H), 7.55 (s, br, 16H), 8.15 (d, J = 8.4 Hz, 8H), 9.26 (s, br, 8H, OH); ^{13}C NMR (75 MHz, DMSO-d_6) δ 22.6, 31.1, 119.4, 123.2, 123.4, 126.0, 127.0, 128.6, 129.4, 131.8, 132.4,

151.8; (–)-APCI MS: *m/z* (relative intensity) 1304.2 (M^-, 7) calcd.: 1304.5 for $C_{92}H_{72}O_8$, 977.3 (55), 651.2 (100).

Hexaester 123 and octaester 124

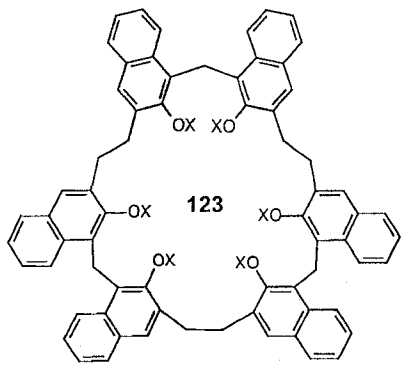

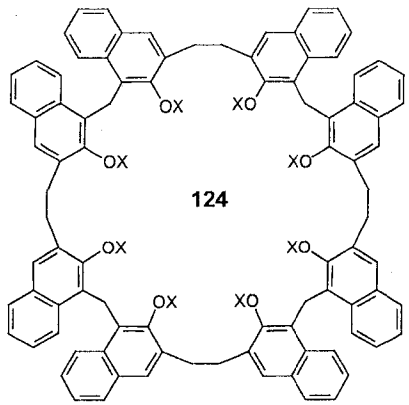

The crude mixture of homocalixnaphthalenes **125** and **126** (0.66 g, 1.0 mmol) obtained in the previous reaction, K_2CO_3 (1.12 g, 8.08 mmol) and ethyl bromoacetate (0.90 mL, 8.0 mmol) in anhydrous acetone (95 mL) were heated at reflux with stirring for 3 d. After the solvent and excess ethyl bromoacetate were removed under reduced pressure, the resulting residue was mixed with water (20 mL), neutralized with aqueous 3 M HCl and extracted with $CHCl_3$ (3 x 60 mL). The organic layers were combined and washed with deionized water (1 x 50 mL) and brine (1 x 50 mL), dried over $MgSO_4$ and filtered. After the solvent was removed under reduced pressure, the resulting yellow residue was purified by flash chromatography (5:19:76 $CHCl_3$-EtOAc-hexane) to yield hexaester **123** (240 mg, 24%) as a pale yellow solid; mp 110–112 °C; ^{1}H NMR ($CDCl_3$) δ 0.88 (s, br, 18H), 3.11 (s, br, 12H), 3.82 (s, br, 12H), 4.19 (s, br, 12H), 4.91 (s, br, 6H),

7.28 (s, br, 12H), 7.62 (s, br, 12H), 8.11 (s, br, 6H); ^{13}C NMR ($CDCl_3$) δ 14.0, 24.0, 29.9, 60.9, 70.4, 124.1, 124.7, 125.6, 127.6, 128.2, 128.7, 131.5, 132.3, 134.3, 153.7, 168.7; (+)-ESI MS *m/z* (relative intensity): 1517.55 ($M+Na^+$, 13) calcd.: 1517.50 for $C_{93}H_{90}O_{18}Na$, 1512.55 ($M^+ + H_2O$, 9) calcd.: 1512.62 for $C_{93}H_{90}O_{18}.H_2O$, 1496.7 (M^+, 100) calcd.: 1495.73 for $C_{93}H_{90}O_{18}$. Further elution with 5:29:66 $CHCl_3$-EtOAc-hexane yielded octaester **124** (8.2 mg, 8%) as a pale yellow solid: mp 130–132 °C; ^1H NMR ($CDCl_3$) δ 1.02 (s, br, 24H), 3.25 (s, 16H), 4.09 (q, *J* = 6.5 Hz, 16H), 4.52 (s, 16H), 4.99 (s, 8H), 6.83 (s, br, 8H), 6.99 (s, br, 8H), 7.17 (s, br, 8H), 8.19 (d, *J* = 8.5, 8H); ^{13}C NMR (75 MHz, $CDCl_3$) δ 13.9, 23.5, 31.0, 61.0, 71.1, 124.3, 124.5, 125.4, 127.6, 128.4, 128.7, 131.1, 132.0, 133.3, 152.9, 168.9; (+)-ESI MS *m/z* (relative intensity) 1994.6 (M^+, 60) calcd.: 1994.3 for $C_{124}H_{120}O_{24}$.

Metal picrate extraction[15,22]

Extractions of alkali metal picrates (Li, Na, K, Cs and Rb) from their aqueous solutions (deionized water) into chloroform (spectrograde) (Figure 4.9 and 4.10) were performed according to the following typical procedure: 5 mL of an aqueous 1.00 x 10^{-4} M solution of the metal picrate and 5 mL of a 1.00 x 10^{-4} M chloroform solution of **123** (or **124**) were mechanically shaken in a Teflon®-lined stoppered glass tube for 24 h. The mixture was then equilibrated in a thermostated water bath at 25.0 ± 0.1 °C for 2 h in order to achieve a good phase separation. The absorbance of the metal picrate remaining in the aqueous phase

was then determined spectrophotometrically at 358 nm using a Unicam UV2 UV-vis spectrophotometer. The percentage extraction (%E) for each solution was calculated from the expression $\%E = 100(A_o\text{-}A)/A_o$. Where A_o is the initial absorbance of the pure metal picrate aqueous solution; and A is the absorbance of the same aqueous solution after extraction. The results are summarized in Table 4.1.

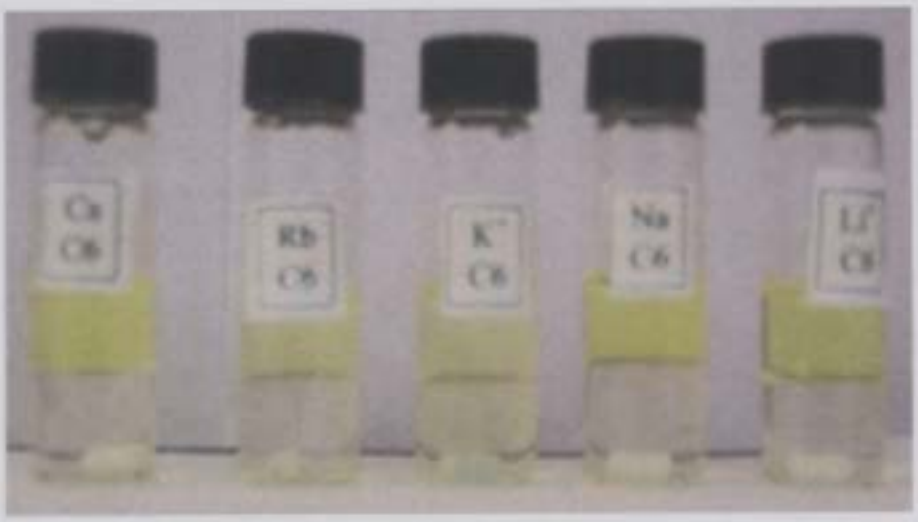

Figure 4.9 Extraction of alkali metal picrates by hexaester **123**.

Figure 4.10 Extraction of alkali metal picrates by octaester **124**.

4.5 References

1. (a) Gutsche, C. D. *Calixarenes, Monographs in Supramolecular Chemistry*; Stoddart, J. F., Ed.; The Royal Society of Chemistry 1989, pp 59-60 and references cited therein; (b) Afari, Z.; Böhmer, V.; Harrowfield, J.; Vicens, J., Eds., *Calixarenes 2001*, Kluwer Acadamic Publishers, Dordrecht, The Netherlands, 2001, pp 219-234 and references cited therein.

2. (a) Brodesser, G.; Vögtle, F. *J. Incl. Phenom. Mol. Recogni. Chem.* **1994**, *19*, 111-135. (b) Schmitz, J.; Vögtle, F.; Nieger, M.; Gloe, K.; Stephen, H.; Heitzsch, O.; Buschmann, H.-J.; Hasse, W.; Cammann, K. *Chem. Ber.* **1993**, *126*, 2483-2491.

3. Ibach, S.; Prautzsch, V.; Vötgle, F. *Acc. Chem. Res.* **1999**, *32*, 729-740.

4. (a) Thuéry, P.; Jeong, T. G.; Yamato, T. *Supramol. Chem.* **2003**, *15*, 359-365. (b) Salmon, L.; Thuéry, P.; Miyamoto, S.; Yamato, T.; Ephritikhine, M. *Polyhedron* **2006**, *62*, 1250-1251.

5. Yamato, T.; Kohno, K.; Tsuchihashi, K. *J. Incl. Phenom. Macro. Chem.* **2002**, *43*, 137-144.

6. Yamato, T. *J. Incl. Phenom. Mol. Recogni. Chem.* **1998**, *32*, 195-207.

7. Yamato, T.; Iwasa, T.; Zhang, F. *J. Incl. Phenom. Macro. Chem.* **2001**, *39*, 285-294.

8. Yamato, T.; Saruwatari, Y.; Yasumatsu, M.; Tsuzuki, H. *New. J. Chem.* **1998**, 1351-1358.

9. Tashiro, M.; Yamato, T. *J. Org. Chem.* **1981**, *46*, 1543-1552.

10. (a) Vötgle, F.; Schmitz, J.; Nieger, M. *Chem. Ber.* **1992**, *125*, 2523-2531. (b) Schmitz, J.; Vötgle, F.; Nieger, M.; Gloe, K.; Stephan, H.; Heitzsch, O.; Buschmann, H. -J.; Hasse, W.; Cammann, K. *Chem. Ber.* **1993**, *126*, 2483-2491.

11. (a) Tashiro, M.; Tsuge, A.; Sawada, T.; Makishima, T.; Horie, S.; Arimura, T.; Mataka, S.; Yamato, T. *J. Org. Chem.* **1990**, *55*, 2404-2409. (b) Tsuge, A.; Sawada, T.; Mataka, S.; Nishiyama, N.; Sakashita, H.; Tashiro, M. *J. Chem. Soc., Chem. Commun.* **1990**, 1066-1068. (c) Tsuge, A.; Sawada, T.; Mataka, S.; Nishiyama, N.; Sakashita, H.; Tashiro, M. *J. Chem. Soc., Perkin Trans. 1*, **1992**, 1489-1494. (c) Yamato, M.; Matsumoto, J.; Tokuhisa, K.; Kajihara, M.; Suehiro, K.; Tashiro, M. *Chem. Ber.* **1992**, *125*, 2443-2454.

12. (a) Yamato, T.; Saruwatari, Y.; Nagayama, S.; Maeda, K.; Tashiro, M. *J. Chem. Soc., Chem. Commun.* **1992**, 861-862. (b) Yamato, T.; Saruwatari, Y.; Yasumatsu, M.; *J. Chem. Soc., Perkin Trans. 1*, **1997**, 1725-1730. (c) Yamato, T.; Saruwatari, Y.; Yasumatsu, M.; *J. Chem. Soc., Perkin Trans. 1*, **1997**, 1731-1737.

13. Yamato, T.; Saruwatari, Y.; Doamekpor, L. K.; Hasegawa, K.; Koike, M. *Chem. Ber.* **1993**, *126*, 2501-2504.

14. Georghiou, P. E.; Miller D. O.; Tran, A. H.; Al-Saraierh, H.; Li, Z.; Ashram, M.; Chowdhury, S.; Mizyed, S. *Synlett* **2005**, *6*, 879-891.

15. Li, Z. *Ph.D. Dissertation,* Memorial University of Newfoundland, 1996.

16. Georghiou, P. E.; Li, Z.; Ashram, M.; Miller, D. O. *J. Org. Chem.* **1996,** *61,* 3865-3869.

17. Ashram, M. *Ph.D. Dissertation,* Memorial University of Newfoundland, 1997.

18. Chowdhury, S. *Ph.D. Dissertation,* Memorial University of Newfoundland, 2001.

19. (a) Gutsche, C. D.; Dhawan, B.; No, K. H.; Muthukrishnan, R. *J. Am. Chem. Soc.* **1981**, *103*, 3782-3792. (b) Izatt, R. M.; Lamb, J. D.; Hawkins, R. T.; Brown, P. R.; Izatt, S. R.; Christensen, J. J. *J. Am. Chem. Soc.* **1983**, *105*, 1782-1785. (c) Mckervey, M. C.; Seward, E. M.; Ferguson, G.; Ruhl, B.; Harris, S. J. *J. Chem. Soc., Chem. Commun.* **1985**, 388-390. (d) Ishikawa, Y.; Kunitake, T.; Matsuda, T.; Otsuka, T.; Shinkai, S. *J. Chem. Soc., Chem. Commun.* **1989**, 736-738. (e) Davis, F.; Otoobe, L.; Short, R.; Stirling, C. J. M. *Langmuir* **1996**, *12*, 1892-1894. (f) Dei, L.; Casnati, A.; Lonostro, P.; Baglioni, P. *Langmuir* **1995**, *11*, 1268-1272. (g) Ludwig, R.; Matsumoto, H.; Takeshita, M.; Ueda, K.; Shinkai, S. *Supramol. Chem.* **1995**, *4*, 319-327. (h) Iwamoto, K.; Shinkai, S. *J. Org. Chem.* **1992**, *57*, 7066-7073.

20. Ashram, M.; Mizyed, S.; Georghiou, P. E. *Org. Biomol. Chem.* **2003**,*1*, 599-603.

21. Aldrich, *Handbook of Fine Chemical and Laboratory Equipment*, 2003-2004, pp 1256.

22. F. Arnaud-Neu, M. J. Schwing-Weill, K. Ziat, S. Cremin, S. J. Harris and M. A. McKervey, *New J. Chem.* **1991**, *15*, 33-37.

Chapter 5

Synthesis and Complexation Properties of "Zorbarene": New homooxaisocalix[*n*]naphthalenes

5.1 Introduction

5.1.1 Homooxacalixarenes

Homooxacalixarenes such as **137**–**141** are examples of calixarenes in which the methylene bridges are replaced by one or more $-CH_2OCH_2-$ groups (Figure 5.1).[1] They can also be considered to be members of the general class of compounds known as cyclophanes, *e.g.* tetraoxa[3.3.3.3](1,4)cyclophane **142**.[2] Homooxacalixarenes have been shown to be good hosts for various types of cations[3,4] and neutral molecules.[5]

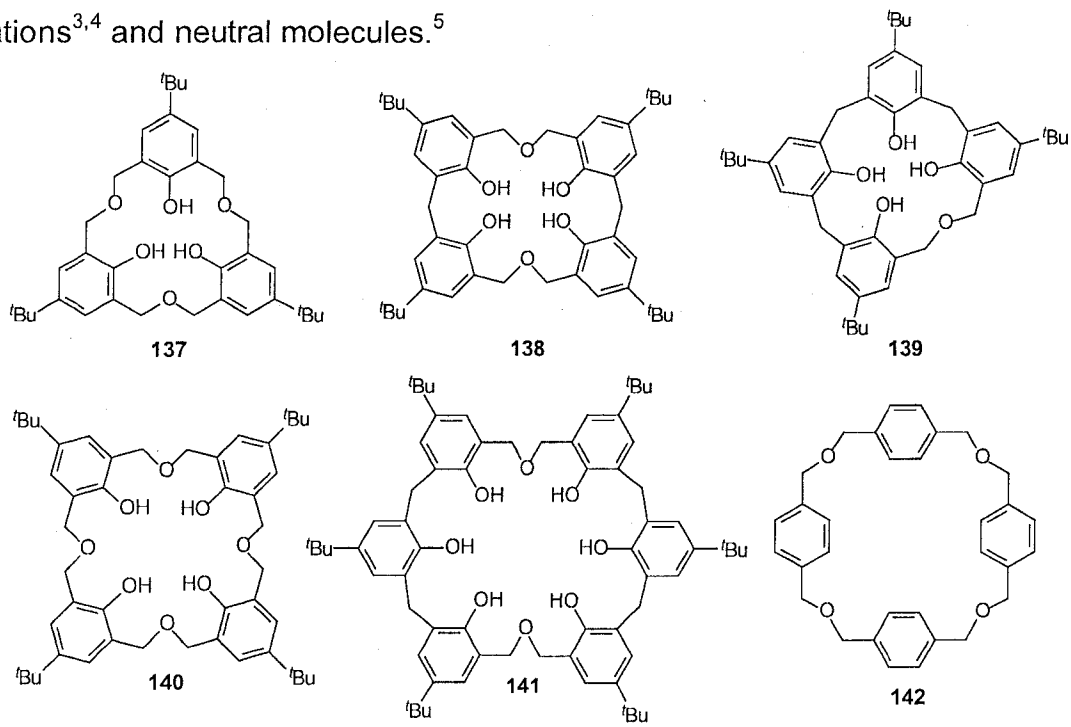

Figure 5.1 Examples of homooxacalixarenes **137**–**141** and the cyclophane **142**.

In 1983, Gutsche *et al.* found that compounds **137**–**141** were formed by thermal intra- and intermolecular dehydrations of suitable bis(hydroxymethyl)-phenol precursors **143**–**145** in boiling xylene (Scheme 5.1).[6] Using different solvent conditions with acid catalysis, Hampton *et al.*[3] produced a family of homooxacalix[3]arene macrocycles **137** with various *p*-substituents such as isopropyl, ethyl, methyl and chloro groups besides the *tert*-butyl group.

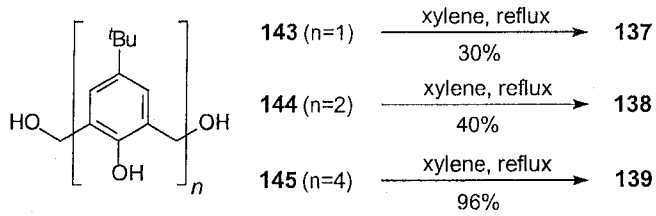

Scheme 5.1 Synthesis of oxacalixarenes **137**–**139** via thermal dehydration.

Another way to synthesize homooxacalixarenes was developed in 1995 by Masci *et al.*,[4] employing the Williamson reaction between 2,6-bis(hydroxymethyl)-4-*tert*-butylphenol (**146**) and 2,6-bis(bromomethyl)-4-*tert*-butylphenol (**147**) under basic conditions to prepare octahomotetraoxa-calix[4]arene **140** (Scheme 5.2).

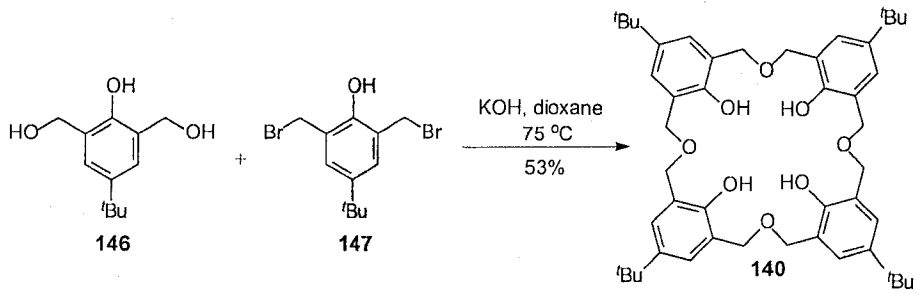

Scheme 5.2 Synthesis of octahomotetraoxacalix[4]arene **140**.

In 2001, Komatsu *et al.* reported a new approach to prepare homooxacalixarenes via the homocoupling reaction of 4-*tert*-butyl-2,6-diformylphenol (**148**) and Et_3SiH in the presence of Me_3SiOTf in DCM (Scheme 5.3).[4] Besides the *tert*-butyl group, derivatives containing other substituents such as methyl, benzyl, phenyl, fluorine, chlorine, bromine and iodine were also prepared this way.[4]

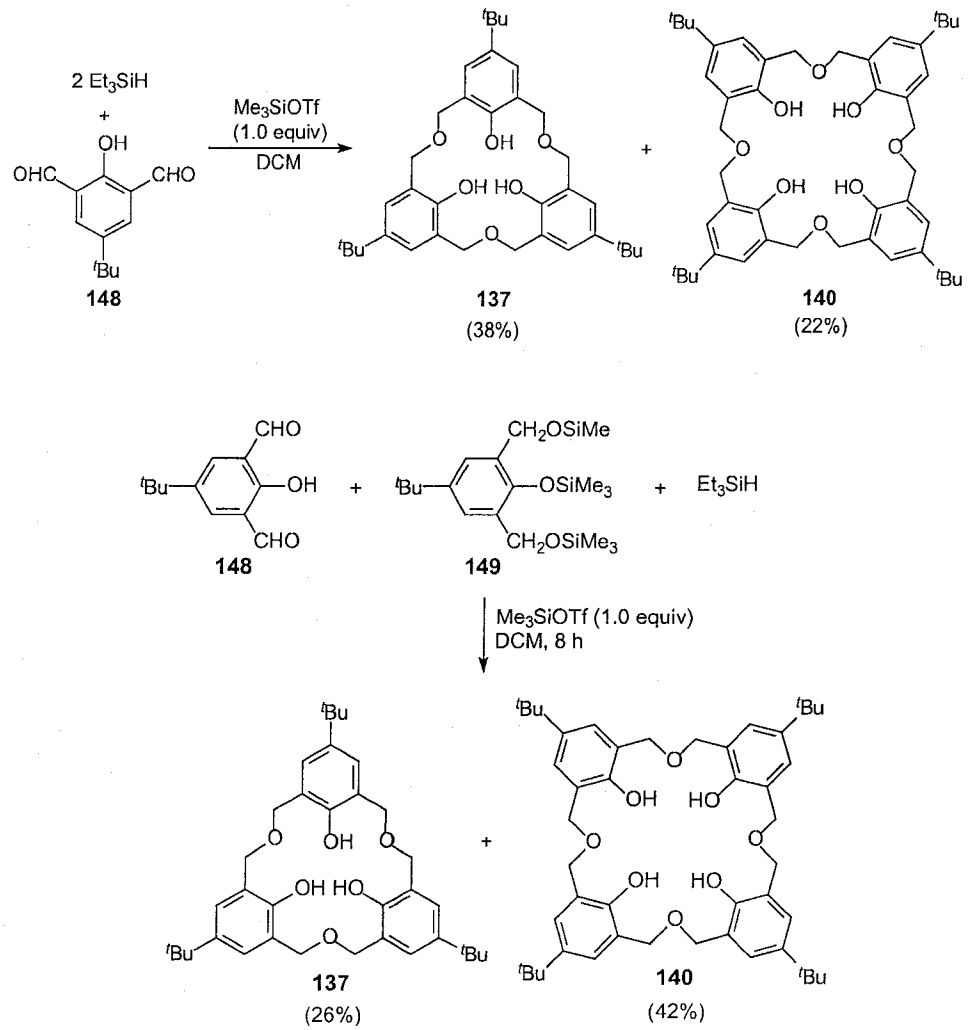

Scheme 5.3 Synthesis of hexahomotrioxacalix[3]arene **137** and octahomotetraoxacalix[4]arene **140** from **148**.

5.1.2 Homooxacalixnaphthalenes[7]

With the aim of producing new cavity-containing cyclic hosts having deeper cavities than those based on calixarenes, the Georghiou group synthesized several new hexahomotrioxacalix[3]naphthalenes (Figure 5.2)[8] and tetrahomodioxacalix[4]naphthalenes (Scheme 5.4, 5.5) derived from 3-hydroxy-2-naphthoic acid or 1-naphthol.

Hexahomotrioxacalix[3]naphthalenes **43**, **43a** and **152** were prepared by two different approaches (Figure 5.2). A cyclocondensation of bis(hydroxymethyl)naphthalene derivatives **150a** and precursor **151** having three naphthalene-based units, using Fuji's 'wet' $CHCl_3/HClO_4$ conditions afforded **43a** and **152** in low 5% and 3% yields, respectively. However, when only **150a** itself was subjected to Fuji's conditions, **43a** was also obtained in 5-6% yield. Similarly, **43** was also afforded from **150** in the same yield using Fuji's conditions.[8]

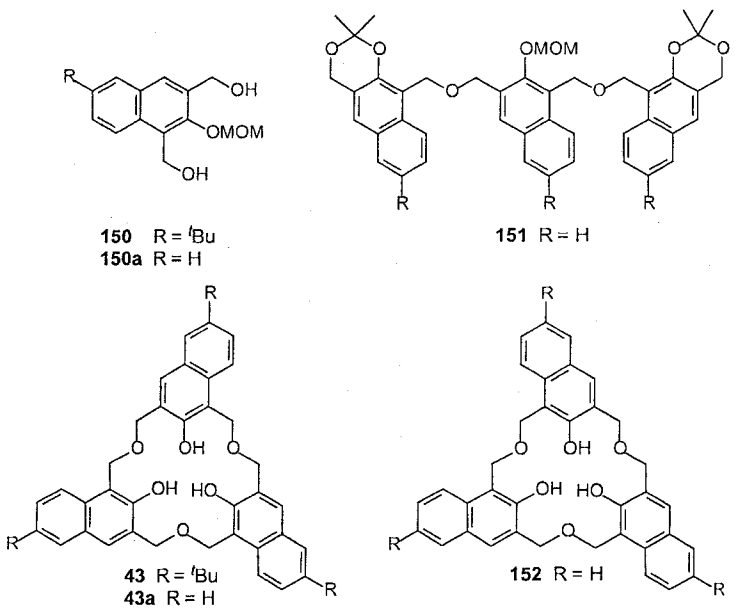

Figure 5.2 Hexahomotrioxacalix[3]naphthalenes and their precursors.

In 2001, Mizyed *et al.* reported the X-ray structure (Fig 1.13, Chapter 1) of a supramolecular complex formed between C_{60} and hexahomotrioxacalix[3]naphthalene **43**. In addition, hexahomotrioxacalix[3]naphthalenes **43** or **43a** were shown to be good hosts for C_{60} in benzene or toluene solutions.[9]

The tetrahomodioxacalix[4]naphthalenes **155a** and **155b** were synthesized via a Williamson reaction between bis(hydroxymethyl)naphthalene precursors **153a** or **153b** and bis(bromomethyl)naphthalene precursors **154a** or **154b**, respectively, in reasonable yields (34% and 23%, respectively) for such macrocyclization (Scheme 5.4).[10]

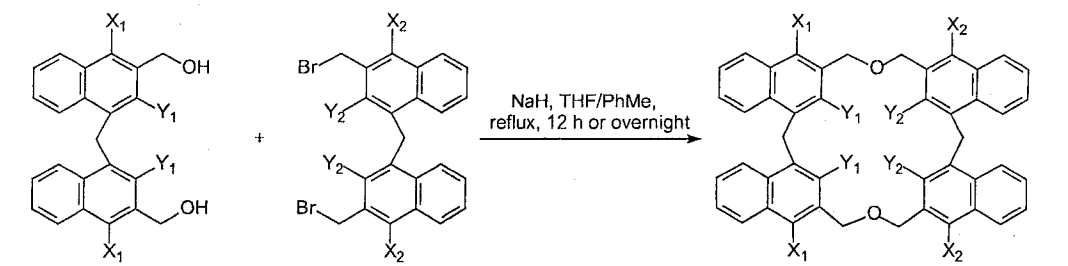

153a X_1= H, Y_1 = OMe **154a** X_2= H, Y_2 = OMe **155a** X_1, X_2 = H, Y_1, Y_2 = OMe, 34%
153b X_1= OMe, Y_1 = H **154b** X_2= OMe, Y_2 = H **155b** X_1, X_2 = OMe, Y_1, Y_2 = H, 23%

Scheme 5.4 Synthesis of tetrahomodioxacalix[4]naphthalenes **155a** and **155b**.[11]

Similarly, hexahomodioxacalix[4]naphthalene **158** was later synthesized via Williamson reactions from bis(hydroxymethyl)naphthalene **156** and bis(bromomethyl)naphthalene **157** precursors (Scheme 5.5).[11] However, the properties of these tetra- and hexahomodioxacalix[4]naphthalenes have not yet been fully investigated.

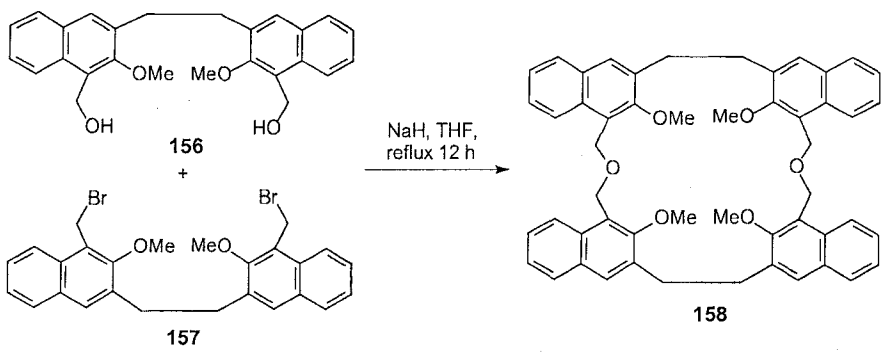

Scheme 5.5 Synthesis of hexahomodioxacalix[4]naphthalene **158**.

5.2 Design and retrosynthetic analysis of "1,4-linked" homooxaiso calix[*n*]naphthalenes 159a-d

5.2.1 Design of target structures

Some other potentially deeper cavity-containing calixnaphthalenes can be envisioned using 2,3-dihydroxynaphthalene sub-units, linked together by $-CH_2OCH_2-$ groups to create new potentially useful receptors such as **159b** whose space-filling structures are shown below (Figure 5.3). Since these compounds are linked via the 1,4-positions on the naphthalene rings and do have calixarene-like structures,[12] they could be considered as members of a new class of "1,4-linked" octahomotetraoxa*iso*calix[4]naphthalenes,[13] and also as "tetraoxa[3.3.3.3](1,4)naphthalenophanes" by analogy with the corresponding benzenoid paracyclophane (**134**) described by Roelens' group.[2] Both CPK models and computer-assisted molecular mechanics modeling[14] suggested that a molecule such as **159b** might be an attractive candidate as a receptor for fullerenes. For example, in **159b** four 2,3-dialkoxynaphthalene (**163**) units are linked in a *para* fashion by $-CH_2OCH_2-$ units and its resulting cavity dimensions

suggested that guests such as C_{60}- and/or C_{70}-fullerenes could be adequately accommodated. In addition, molecular modeling "docking" simulations between, *e.g.*, C_{60} and compounds **159a-d** (Figure 5.3), supported the idea that structures generated using *cone* or *partial-cone* conformers of **159a-d** could form attractive energy minimized host:C_{60} complexes. The computer-assisted molecular modeling observations also suggested that although the host molecules were conformationally flexible, π-π van der Waals interactions between the electron-rich naphthalene rings and the electron-poor fullerenes could result in a conformational reorganization of these structures to adopt conformations which permitted complex formation. The syntheses of these compounds were therefore undertaken. The results from this research have been published recently.[15]

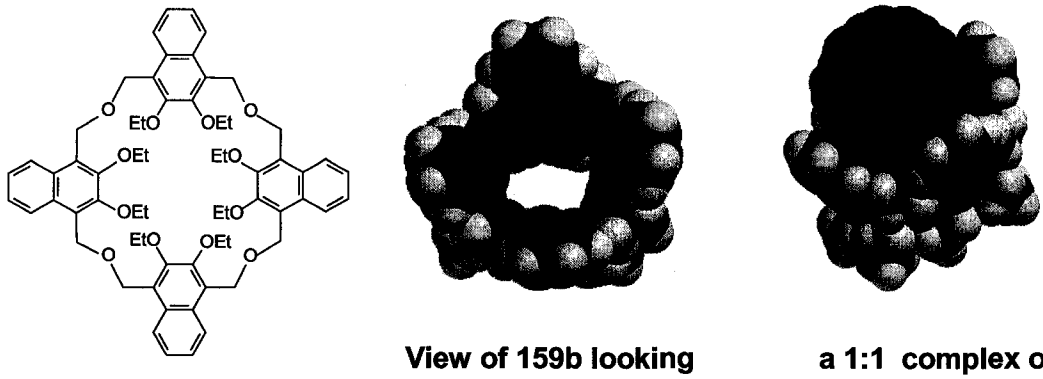

159b | **View of 159b looking down the cavity** | **a 1:1 complex of 159b and C_{60}**

Figure 5.3 Structure (*left*), computer-generated models of **159b** (*middle*) and a 1:1 complex of **159b** and C_{60} (*right*).

5.2.2 Retrosynthetic analysis

Since macrocyclic compounds **159a-d** and **160a-d** are crown ether analogues, a simple retrosynthetic approach can be envisioned via a Williamson

cross-coupling reaction between 1,4-bis(hydroxymethyl)-2,3-dialkoxynaphthalene (**161a-d**) and 1,4-bis(bromomethyl)-2,3-dialkoxynaphthalene (**162a-d**) precursors, respectively (Scheme 5.6). Because of steric hindrance between the alkoxy groups, the calix[4]- and/or calix[6]- products were predicted to be favoured over the possible calix[2]- products.

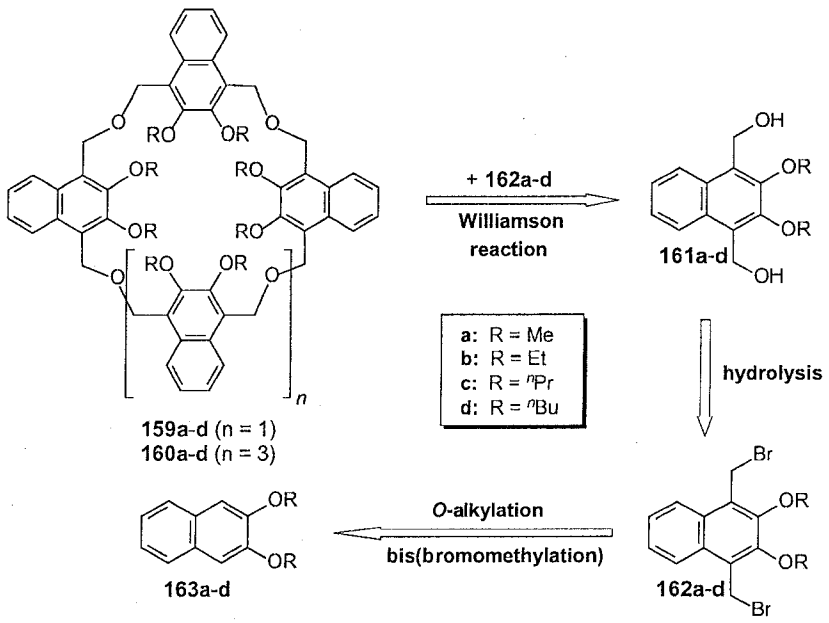

Scheme 5.6 Retrosynthetic analysis of "1,4-linked" homooxaisocalix[*n*]-naphthalenes **159a-d** and **160a-d**.

Under basic conditions, bis(hydroxymethyl)naphthalene intermediate **161a-d** could be obtained respectively via hydrolysis of bis(bromomethyl)-naphthalene derivative **162a-d** which was previously obtained from a bis(bromomethylation) reaction[16,17] of 2,3-diakoxynaphthalene (**163a-d**), respectively. Since the 1- and 4- position of 2,3-dialkoxynaphthalenes (**163a-d**) are activated by the electron-donating alkoxy groups, a bis(bromomethylation)

should easily and selectively take place at these positions to give the desired bis(bromomethyl)naphthalenes **162a-d**. Compounds **163a-d** are, of course, derivable directly from commercially available 2,3-dihydroxynaphthalene (**164**) via *O*-alkylation with an alkyl iodide, or a dialkyl sulfate under basic conditions.[18]

5.3 Results and discussion

5.3.1 Synthesis of "1,4-linked" homooxaisocalix[*n*]naphthalenes 159a-d and 160a-d

The syntheses of the target homooxaisocalixnaphthalenes **159a-d** were accomplished as outlined in Scheme 5.7. Preliminary experiments revealed that bromomethylation of **164** itself only afforded intractable resinous products, hence necessitating the use of alkyl ethers. At first, the larger homologous alkyl ethers (octa-*n*-pentyl- and octa-*n*-hexyl-) were chosen but their subsequent reaction products proved to be difficult to purify and characterize. Therefore, the methyl-, ethyl-, *n*-propyl- and *n*-butyl ethers **163a-d** having smaller alkyl groups were employed instead. Base-mediated alkylation of **164** smoothly gave the di-*O*-alkylated derivatives **163a-d**. The yields of the chromatographically purified products (90-98%) were higher than those obtained by crystallization (70-75%). As expected, double bromomethylation of **163a-d** afforded the corresponding bis(bromomethylated) naphthyl ethers **162a-d**, which, when hydrolyzed with $CaCO_3$ in aqueous dioxane, led to the respective bis(hydroxymethyl)naphthalene analogues **161a-d**. The crude intermediates **161a-d** and **162a-d** were afforded in

high yields (91-98%), which were easily reproduced by MacLachlan at the University of British Columbia.[19]

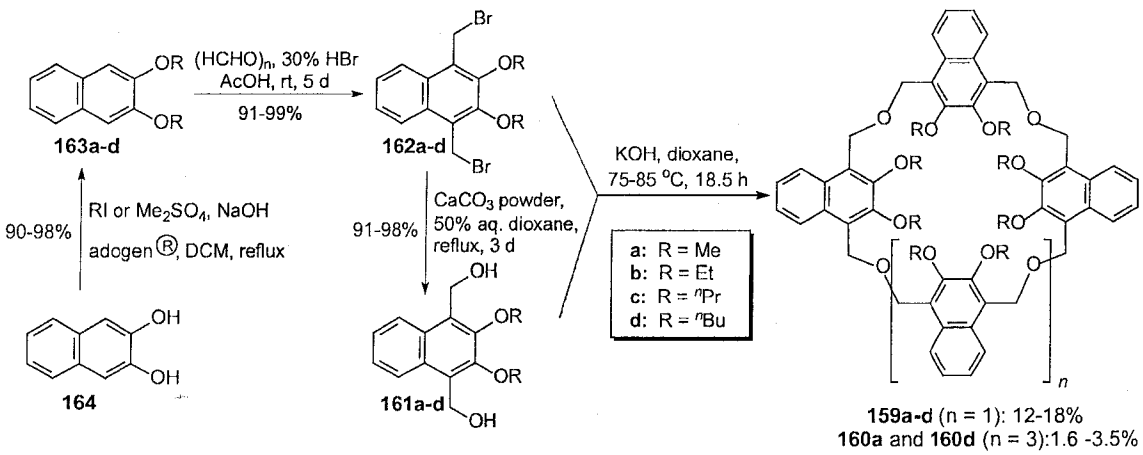

Scheme 5.7 Syntheses of "1,4-linked" homooxaisocalix[*n*]naphthalenes **159a-d**, **160a** and **160d**.

CPK molecular models of either *syn* or *anti* conformers of [3.3](1,4)naphthalenophanes resulting from a [1+1] coupling of **161a-d** and **162a-d**, respectively, suggested that in addition to the steric hindrance between alkoxy groups on the naphthalene rings, the presence of two $-CH_2OCH_2-$ groups would result in too much steric strain, and thus prevent the formation of such products. This was found to be the case as none of these products were detected under the conditions employed. The most difficult experimental conditions to determine were those required for forming the macrocyclic ethers. None of the desired coupling products were obtained using NaH with various solvents such as THF, dioxane and DMF, or KOH in THF or DMF. Nevertheless, after considerable experimentation, optimal conditions based upon Masci's procedure were found.[4] The expected tetrameric octahomotetraoxa-

isocalix[4]naphthalenes (or "tetraoxa[3.3.3.3](1,4)naphthalenophanes") **159a-d**, were obtained in 12-18% isolated yields, respectively. Along with these products, the corresponding hexameric dodecahomohexaoxaisocalix[6]naphthalenes (or "hexaoxa-[3.3.3.3.3.3](1,4)naphthalenophanes") **160a** and **160d** having correct molecular masses [1403.8 ($M+Na^+$, 100%) and 1908 ($M+Na^+$, 25%) respectively], were also isolated albeit in low yields (3.5% and 1.6% respectively). These low yields precluded further detailed structural analyses. None of the corresponding compounds **160b** or **160c** were isolated. On TLC, the calix[4]naphthalenes **159a** and **159d** are less polar than the corresponding calix[6]naphthalenes **160a** and **160d**.

The attempted synthesis of **159e** and **160e** (Scheme 5.8) was unsuccessful due to low solubilities of intermediates **161e** and **162e** under the conditions previously employed for **159a-d**, and in other solvents examined such as DMF and THF.

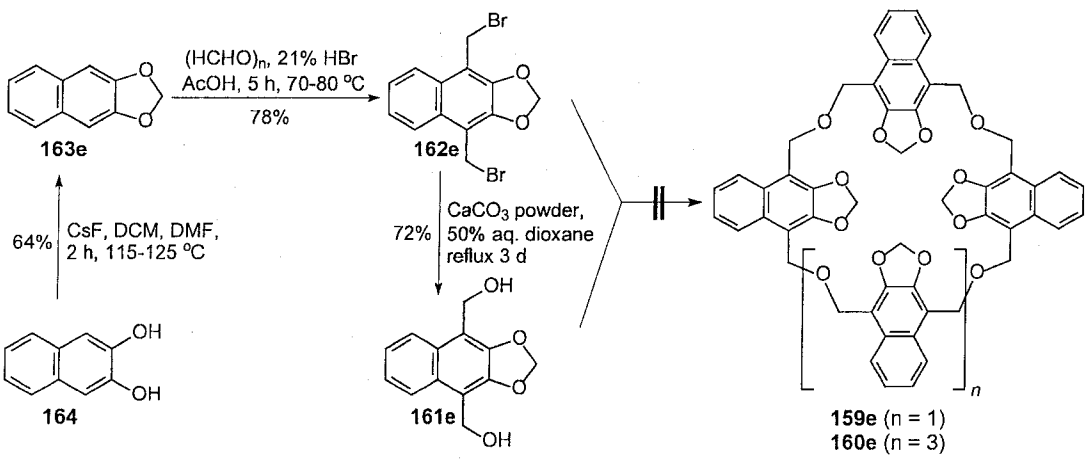

Scheme 5.8 Attempted syntheses of "1,4-linked" homooxaisocalix[*n*]-naphthalenes **159e** and **160e**.

5.3.2 Characterization of 159a-d

All of the new macrocyclic compounds **159**a - **159**d had relatively simple ^{1}H NMR spectra (ambient temperature) which indicated that they were highly symmetrical. Rapid conformational equilibration in solution at ambient temperature was obvious from the fact that all of the signals were sharp, and that the bridging methylene groups of **159a-d** appeared as singlets at 5.04-5.05 ppm. VT ^{1}H NMR experiments conducted on **159d** (Figure 5.4), revealed broadening of all of the signals upon cooling to 223 K, but no coalescence temperature could be observed since the samples precipitated out of solution at lower temperatures. Therefore, it was not possible to gain any insight into the conformations of any of the compounds **159a-d** at the lower temperatures.

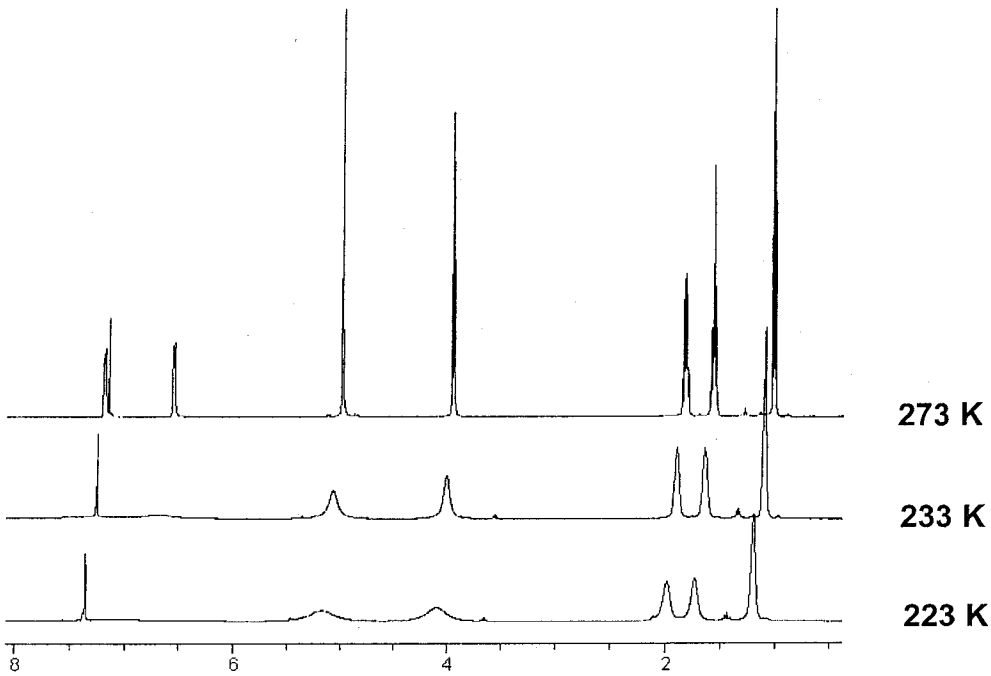

Figure 5.4 VT ^{1}H NMR of **159d** in $CDCl_3$.

When the chemical shifts of the alkoxy protons in the spectra of **159a-d** were compared with those of their respective precursors, only in the cases of **159a** and **159b** were there any significant differences. The position of the CH_3 signal of the methoxy groups in **159a** at δ 3.81 ppm is shifted upfield from that of the corresponding signals in the precursors **161a**, **162a**, and **163a**, which are all at approximately δ 4.00 ppm. The positions of the CH_2 and the CH_3 groups of the ethoxy groups in **159b** at δ 4.03 and 1.41 ppm, respectively, are shifted upfield from the corresponding signals of the precursors **161b**, **162b,** and **163b**, which appear at approximately δ 4.22 and 1.54 ppm, respectively. These observations indicate that in $CDCl_3$ solution, the small alkoxy groups such as methoxy and ethoxy groups in **159a** and **159b**, respectively, could be partially shielded by the "partial cavities" created by the other three naphthalene units. By contrast, the changes in the corresponding chemical shifts in **159c** and **159d** relative to their precursors were less than 0.10 ppm presumably due to less shielded effects of the large alkoxy groups, e.g. *n*-propoxy and *n*-butoxy groups by the naphthalene units.

Although crystals were obtained from solutions of **159a** and **159b**, only those from **159b** were suitable for in an X-ray crystal structure determination (Figure 5.5). Amusingly, the structure generated by the X-ray crystallography can be imagined to resemble a ring of four anthropomorphic dancers. Therefore, this molecule was called a "Zorbarene" in honour of the dance-loving "Zorba" character created by the Greek writer Nikos Kazantzakis (1883-1957) in the

widely-acclaimed and popular book "Zorba the Greek", originally published in 1952.[20]

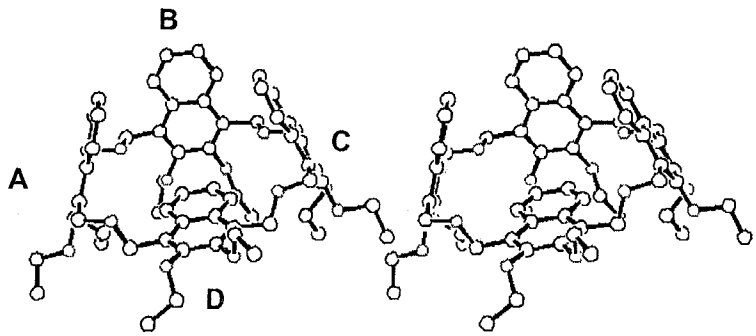

Figure 5.5 X-ray stereoview of **159b** showing its *flattened partial-cone* conformation (solvent molecules were removed for clarity).

The X-ray structure of **159b** (Appendix 5.1) reveals a "*flattened partial-cone*" conformation, in which three naphthalene subunits (**A**, **B**, and **C**) are in a tripodal arrangement. The fourth ring (**D**), which is nearly orthogonal to the *distal* (**B**) naphthyl subunit, has its two ethoxy substituents directed *exo* to the partial cavity, or enclosure defined by the other three naphthyl subunits. The structure therefore contains two "partial cavities", one defined by the half that contains the ethoxy groups of rings **A**, **B**, and **C** and the other by the unsubstituted rings of these naphthyl sub-units. Two acetonitrile guest molecules are contained within this latter enclosure. The methyl groups of each acetonitrile guest are oriented inward toward the aromatic rings, and their nitrogen atoms directed away (Appendix 5.1). These findings are consistent with other well-known π-methyl interactions which have been seen between calixarenes and other methyl group containing guests such as toluene, acetonitrile,[21] and tetramethylammonium salts. A search for the lowest energy conformer (using MMFF94 prior to

geometry optimization at the PM3 level of theory) conducted on **159b** after the X-ray structure was revealed that the *flattened pinched-cone* conformation is indeed the lowest energy conformer. A similar computer-assisted molecular modeling study conducted on the 2:1 acetonitrile:**159b** complex was also in agreement with the X-ray structure, and was of lower energy than a corresponding 2:1 complex in which **159b** was preorganized and locked into a *cone* conformation.

5.3.3 Solution complexation studies

5.3.3.1 C_{60} and C_{70} as the guests

The hexahomotrioxacalix[3]arenes[6] (Chapter 1) and hexahomotriooxacalix[3]naphthalene **43**[10] have been shown to be effective hosts for C_{60},[6,10] and the macrocycles **159a-d** had been predicted on the basis of their molecular architecture and molecular modeling study to also be potentially efficient hosts for C_{60} and/or C_{70}. However, when complexation experiments in toluene and carbon disulfide solutions were conducted with compounds **159a-d**, using either UV-vis or ^{1}H NMR spectroscopic analysis, it was clear that no such complexation occurred because neither change in colour nor in ^{1}H NMR signal shifts was observed upon addition of C_{60} or C_{70} solid to the host solutions under conditions studied. This finding was in contrast to the results previously seen with **43** under similar conditions.[10] It is hypothesized that the supramolecular complexation with these new receptors may be inhibited as a result of an entropic effect arising from the greater flexibility of the larger, 28-membered annulus and the

consequential lack of preorganization of these macrocyles. Another factor may be the lack of a complementary symmetry element[22] between the host and these particular fullerene guest molecules.

5.3.3.2. Tetramethyl ammonium chloride (TMACl) as the guest

Quaternary ammonium salts have been employed as guests in host-guest studies involving cyclophanes in lipophilic solvents, thus demonstrating the importance of cation-π interactions.[23] Masci *et al.* conducted an extensive study on the fine-tuning of the cavity sizes of a series of homooxacalix[4]arenes using various tetraalkylammonium picrate salts as guest probes in organic solvents.[4] Arduini *et al.*[24] also described the use of tetramethylammonium chloride (TMACl) and other TMA salts for binding studies with their particular *p*-substituted calix[4]arene host molecules. A complexation study with **159a** and **159b**, both of which could be obtained in crystalline form was therefore undertaken. More recently, Roelens' group[2] reported a complexation study with various TMA salts, including TMACl, with the related receptor **131** (Chapter 4). Since association constants (K_{assoc}) can be determined on relatively small amounts of compounds with ^{1}H NMR spectroscopy[25] this was the method of choice for this study. In practice, when a solution of pure **159a** (host) in $CDCl_3$ was added to a solution of saturated TMACl (guest), also in $CDCl_3$, changes in chemical shifts were clearly observed for all signals of host and guest (Figure 5.6). Hence, this ^{1}H NMR method was employed to measure the K_{assoc} between **159a** or **159b** with TMACl in $CDCl_3$.

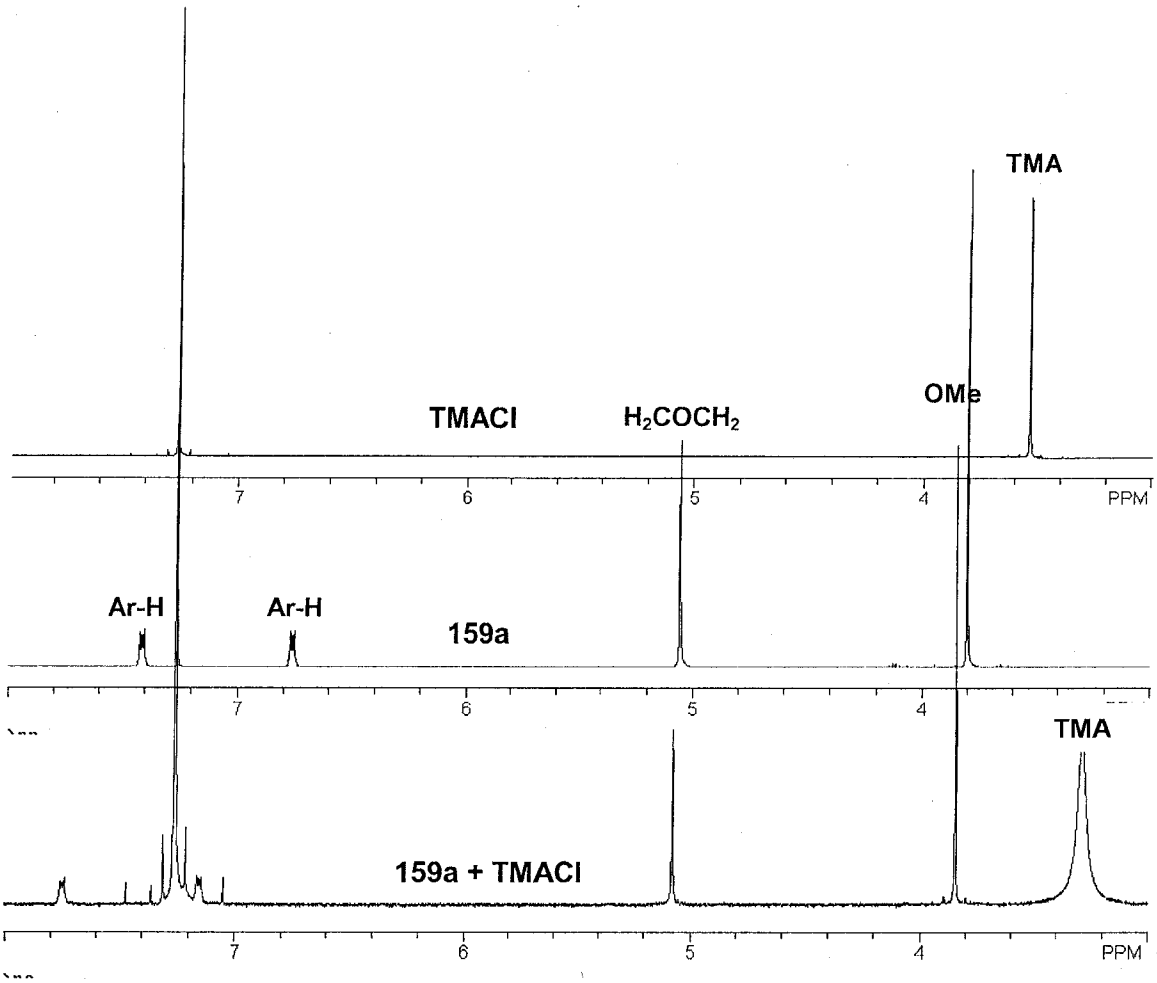

Figure 5.6 ^{1}H NMR spectra of saturated TMACl (*top*), **159a** *(middle)*, and mixture solution of **159a** and TMACl (*bottom*) in $CDCl_3$ at 298 K.

At first, the Job plot method[26] was used to determine the stoichiometry of complexation between **159a** (Appendix 5.2) or **159b** (Appendix 5.3) and TMACl (Figure 5.7), which was found to be 1:1 under the conditions examined, in both cases. The largest change in chemical shifts induced for the receptors **159a** and **159b** ($\Delta\delta_{max}$ = 0.37 and 0.48 ppm, respectively) were for their aromatic signals. Those for the CH_2 groups of the bridging CH_2OCH_2 groups were small ($\Delta\delta_{max}$ =

0.029–0.026 ppm, respectively), as were those for the alkoxy groups (*e.g.*, $\Delta\delta_{max}$ = 0.03 ppm for **159a**). In contrast, the change in chemical shifts induced for the methyl groups of the TMA cation binding with **159a** (Appendix 5.2) and **159b** (Appendix 5.3) were 1.97 and 3.09 ppm, respectively.

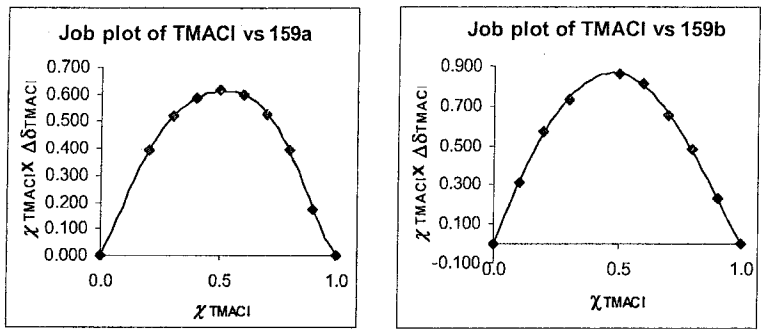

Figure 5.7 Job plot showing the 1:1 stoichiometry of **159a** and TMACl (*left*), and **159b** and TMACl (*right*).

The K_{assoc} values, which were determined from the subsequent titration experiments, were therefore based upon measurements of the $\Delta\delta$ values for the methyl groups of the TMA cation. To determine K_{assoc} values, titration experiments were conducted by adding aliquots of **159a** (Appendix 5.4) or **159b** (Appendix 5.5), respectively, to saturated (*ca.* 10^{-3} M) solutions of TMACl in $CDCl_3$. The [guest]:[host] ratios used in all cases were about 10:1. The changes in the chemical shift of the TMA methyl signal were determined and K_{assoc} values were calculated using both the Benesi-Hildebrand (B-H) and Foster-Fyfe (F-F) treatments (Figure 5.8, 5.9).[25] The results from both methods showed good agreements for both tested receptors (Table 5.1).

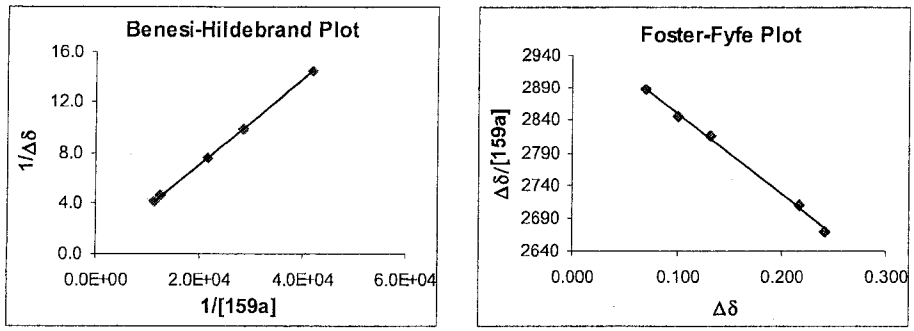

Figure 5.8 Benesi-Hildebrand plot (*left*) and Foster-Fyfe plot (*right*) for the complexation of **159a** and TMACl.

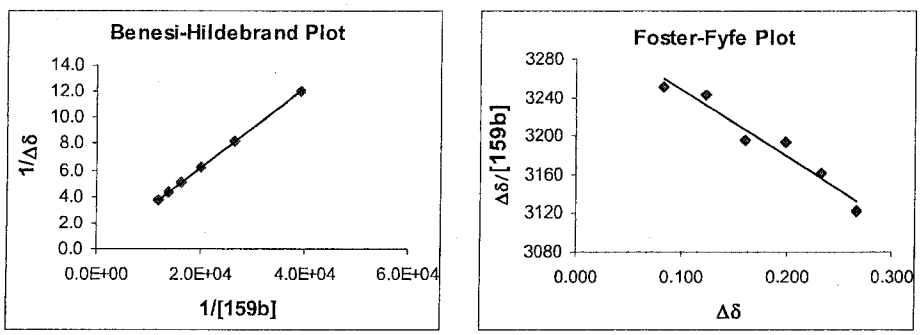

Figure 5.9 Benesi-Hildebrand plot (*left*) and Foster-Fyfe plot (*right*) for the complexation of **159b** and TMACl.

Table 5.1 K_{assoc} values (M^{-1}) for TMACl complexes with **159a** and **159b** in $CDCl_3$ at 298 K.

Complex	Method	Run # 1 (r^2)	Run # 2 (r^2)	Average
159a:TMACl	B–H	1228 (1.000)	1320 (1.000)	1274 ± 65
	F–F	1247 (0.998)	1136 (0.957)	1192 ± 79
159b:TMACl	B–H	636 (1.000)	724 (1.000)	680 ± 62
	F–F	689 (0.956)	607 (0.927)	648 ± 58

The induced chemical shift changes for the methyl groups of TMACl were all to higher fields, thereby demonstrating a shielding effect due to the naphthyl rings. This was also confirmed by the largest change in chemical shifts induced for the aromatic signals, not the methylene-bridge or the alkoxy groups of the receptors **159a** and **159b**. Also noticeable were the line broadening of the TMACl methyl signals upon the addition of the host molecules, although this did not preclude accurate determination of the mean position of the observed signals for the K_{assoc} determinations. Furthermore, the NMR spectra obtained from the complexation solutions were very simple, suggesting the formation of either symmetrical or rapidly interconverting complexes. The K_{assoc} values obtained for **159a** were almost double those for **159b**. In the published account of this work,[15] it was proposed that a possible explanation for these significantly different values is the greater steric requirements of the ethoxy groups which may limit the extent of preorganization of the macrocyclic hosts that must occur in solution in order to permit the TMA cation to enter the cavity. Another factor could be the entropic effects which need to be overcome due to the additional degrees of freedom which the ethoxy groups possess, compared to the methoxy groups. Thus, although no complexation was observed between these new host molecules and C_{60}- or C_{70}-fullerene the smaller, more polar quaternary ammonium salt, TMACl, afforded larger stability constant values than those obtained by Masci for the analogous tetramethoxy octahomotetraoxacalix[4]arenes with TMA picrate. Furthermore, the association constant values which were obtained with **159a** and

159b are approximately 7- and 4-fold larger, respectively, when compared with the value of 165 M^{-1} that Roelens' group reported for the TMACl complex with their unfunctionalized benzenoid tetraoxaparacyclophane **131**.

The computer-generated molecular model of the 1:1 **159b**:TMACl complex (Figure 5.10) indicates a very good fit between the TMA cation and the host, even when compared with the computer-generated model of Roelens' 1:1 TMA:**131** complex.[2] Furthermore, in this **159b**:TMA complex, the receptor is presumably in a symmetrical *cone* conformation which is energetically preferred in this case over a *flattened pinched-cone* conformation. The TMA cation can also be seen to be embedded in the lower half of the receptor, closest to the unsubstituted B-rings of the naphthyl groups.

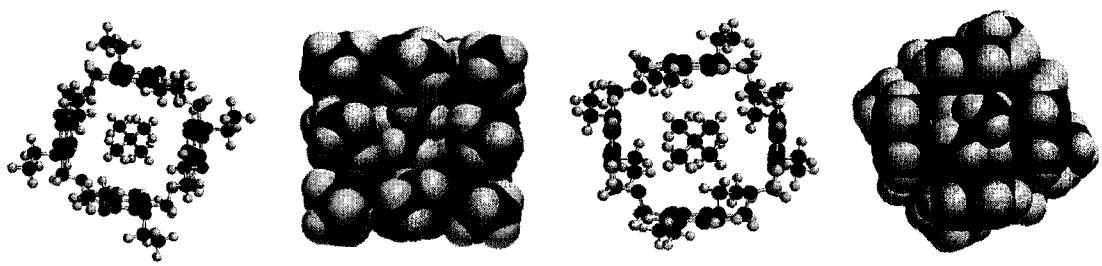

Figure 5.10 Computer-generated model of the complex between **159b** and the TMA cation. *(a) and (b)*: Ball-and-stick and space-filling representations, respectively, of the complex as viewed from the face in which the ethoxy groups can be seen. *(c) and (d)*: Ball-and-stick and space-filling representations, respectively, of the complex as viewed from the opposite face, looking into the cavity defined by the four naphthyl groups.

5.4 Conclusions

A series of new 2,3-dialkoxy-substituted naphthalene-based cavity-containing molecular receptors have been synthesized, and some of their complexation properties have been determined. The syntheses of the octamethoxy and octa-*n*-butoxy macrocyclic compounds **159a** and **159d** were accompanied by small amounts of the corresponding higher hexaoxa homologues, **160a** and **160d**, respectively, but their complexation properties have not yet been determined. The ^{1}H NMR spectra of all of the macrocycles obtained showed clearly that they were highly symmetrical and conformationally flexible. However, suitable crystals of **159b** for single-crystal X-ray crystallography were obtained and the structure revealed it to be in a *flattened partial-cone* conformation. The X-ray structure also revealed it contained two acetonitrile guests, both situated within the same enclosure generated by three naphthalene rings which are in a tripodal arrangement. Although CPK models and molecular modeling suggested that these new receptors had the potential to be suitable hosts for the electron-deficient neutral guest molecules, C_{60}- and C_{70}-fullerenes, solution complexation experiments did not demonstrate any such complexation. With TMACl, however, relatively large stability constant values were observed indicating that cation-π interactions may be more effective than the π-π interactions which are only possible in the case of supramolecular host-fullerene complex formation. A further contributing factor could also be the importance of the symmetry complementarity between the hosts and the tetrahedral TMA cation.

5.5 Experimental section

General methods, materials and instrumentation used are identical to those described in Chapters 2 and 3.

2,3-Dimethoxynaphthalene (163a)

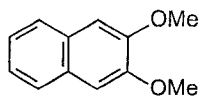

To a stirred solution of 2,3-dihydroxynaphthalene (**164**) (19.2 g, 119 mmol) in aqueous 10% NaOH (98.0 mL, 260 mmol) was added adogen® (0.50 mL) and DCM (300 mL). Dimethyl sulfate (25.0 mL, 264 mmol) was added at 0 °C over 1 h using a syringe pump. The reaction mixture was stirred for a further 9 h. Aqueous 6 M NaOH was added until the pH reached 12, and the mixture was stirred at room temperature for another 1 h. The DCM layer was then separated and washed with saturated aqueous NH_4Cl solution (2 x 50 mL), brine (2 x 50 mL), and distilled water (2 x 50 mL). The organic layer was dried over anhydrous $MgSO_4$ and filtered. After the solvent was removed under reduced pressure, the crude product was purified by chromatography (10:90 EtOAc-hexane) to yield **163a** (21.9 g, 98%) (MeOH-H_2O, 16.56 g, 74%, as colourless prisms): mp 119–120 °C (lit.[18] 115–116 °C, DCM-pentane); ^{1}H NMR (300 MHz) δ 4.00 (s, 6H), 7.12 (s, 2H), 7.32–7.36 (m, 2H), 7.67–7.70 (m, 2H); ^{13}C NMR δ 56.1, 106.5, 124.4, 126.5, 129.4, 149.7; GCMS *m/z* (relative intensity) 188 (M^+, 100), 102

(70), 63 (15).

2,3-Diethoxynaphthalene (163b)

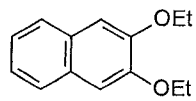

General procedure: To a stirred solution of **164** (6.54 g, 40.8 mmol) in aqueous 10% NaOH (34 mL, 90 mmol) was added adogen® (2 mL) and DCM (150 mL). Ethyl iodide (9.06 mL, 120 mmol) was added over 1 h using a syringe pump. The reaction mixture was heated at reflux with stirring for 3 d. The DCM layer was separated, washed with aqueous 10% K_2CO_3 (1x 50 mL), saturated aqueous NH_4Cl solution (2 x 50 mL), brine (2 x 50 mL), and distilled water (2 x 50 mL), dried over anhydrous $MgSO_4$, and filtered. After the solvent was removed under reduced pressure, the yellow residue was purified by chromatography (5:95 EtOAc-hexane) to yield **163b** (8.38 g, 95%) as a colourless powder (MeOH-H_2O, 6.62 g, 75%, as colourless prisms): mp 96–97 °C (lit.[18] 96 °C, DCM-pentane); ^{1}H NMR (300 MHz) δ 1.54 (t, *J* = 7.1 Hz, 6H), 4.22 (q, *J* = 7.1 Hz, 4H), 7.12 (s, 2H), 7.30–7.33 (m, 2H), 7.65–7.67 (m, 2H); ^{13}C NMR δ 14.6, 64.2, 107.5, 124.0, 126.2, 129.1, 148.9; GCMS *m/z* (relative intensity) 216 (M^+, 30), 188 (15), 160 (100), 102 (20), 77 (20).

2,3-Di-*n*-propoxynaphthalene (163c)

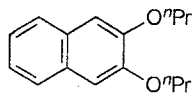

Using the general procedure for **163b**, the reaction of **164** (6.54 g, 40.8 mmol) and *n*-propyl iodide (12.5 mL, 120 mmol) gave a yellow crude product, which was purified by chromatography (1:9 EtOAc-hexane) to yield **163c** (9.17 g, 92%) as a colourless powder (MeOH-H_2O, 6.82 g, 70%, as colourless prisms): mp 75–76 °C; ^{1}H NMR: δ 1.09 (t, *J* = 7.8 Hz, 6H), 1.89–1.96 (m, 4H), 4.07 (t, *J* = 6.8 Hz, 4H), 7.11 (s, 2H), 7.29–7.31 (m, 2H), 7.64–7.66 (m, 2H); ^{13}C NMR δ 10.7, 22.7, 70.5, 108.2, 124.1, 126.4, 129.5, 149.7; GCMS *m/z* (relative intensity) 244 (M^+, 25), 202, 160 (100), 114 (15), 77 (10).

2,3-Di-*n*-butoxynaphthalene (163d)

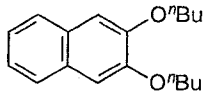

Using the general procedure for **163b**, the reaction of **164** (6.54 g, 40.8 mmol) and *n*-butyl iodide (14.0 mL, 120 mmol) gave a yellow crude product, which was purified by chromatography (5:95 EtOAc-hexane) to yield **163d** (10.0 g, 90%) as a colourless powder (MeOH-H_2O, 8.00 g, 73 %, as colourless prisms): mp 59–60 °C (lit.[18] 56–57 °C, DCM-pentane); ^{1}H NMR δ 1.00 (t, *J* = 7.3 Hz, 6H), 1.52–1.59 (m, 4H), 1.86–1.91 (m, 4H), 4.11 (t, *J* = 6.8 Hz, 4H), 7.12 (s, 2H), 7.29–7.31 (m, 2H), 7.64–7.66 (m, 2H); ^{13}C NMR δ 14.1, 19.5, 31.4, 68.8, 108.1, 124.1, 126.4, 129.5, 149.7; GCMS *m/z* (relative intensity) 272 (M+, 10), 216 (7), 160 (100), 114 (15), 41 (40).

2,3-Methylenedioxynaphthalene (163e)

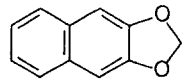

To a stirred mixture of **164** (3.27 g, 20.0 mmol) and CsF (15.34 g, 100.0 mmol) in DMF (60 mL) heated at 115–125 °C was quickly added DCM (1.90 g, 22.0 mmol) with use of a syringe. The dark reaction mixture was stirred for a further 2 h at 115–125 °C and cooled to room temperature. Distilled water (50 mL) was added, and the mixture was extracted with Et_2O (3 x 60 mL). The organic layer was washed with cold brine (2 x 50 mL), cold aqueous 10% NaOH (2 x 30 mL), cold water (1 x 50 mL), again with cold brine (1 x 50 mL), dried over anhydrous $MgSO_4$ and filtered. After the solvents were removed under reduced pressure, the residue was crystallized from MeOH-H_2O to yield **163e** (2.20 g, 64%) as fine prisms: mp 100–101 °C (lit.[17,27] 96–98 °C crude product); ^{1}H NMR δ 6.02 (s, 2H), 7.11 (s, 2H), 7.30–7.32 (m, 2H), 7.64–7.66 (m, 2H); ^{13}C NMR δ 101.2, 104.1, 124.6, 127.2, 130.7, 147.8; GCMS *m/z* (relative intensity) 172 (M^+, 100), 126 (5), 114 (65), 63 (30).

1,4-Bis(bromomethyl)-2,3-dimethoxynaphthalene (162a)

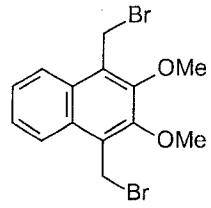

General procedure: To a mixture of **163a** (1.57 g, 8.30 mmol) and 95% paraformaldehyde (1.53 g, 48.0 mmol) in glacial acetic acid (70 mL) was added a solution of HBr in glacial acetic acid (30 wt %, 9.6 mL, 48 mmol of HBr). After being stirred at room temperature for 5 d, the reaction mixture was poured into cold water (200 mL), and the resulting precipitate was filtered, washed with distilled water (2 x 50 mL), aqueous 5% $NaHCO_3$ (2 x 50 mL) and distilled water until the washings were neutral to pH paper, then dissolved in EtOAc (200 mL), dried over anhydrous $MgSO_4$, and filtered. After the solvent was removed under reduced pressure, the crude product (2.80 g, 94%) was crystallized in acetone-hexane to afford **162a** (2.32 g, 78%) as a light yellow fine needles: mp 189 °C (dec.) (lit.[17] 189 °C), ^{1}H NMR (300 MHz) δ 4.05 (s, 6H), 5.04 (s, 4H), 7.58 (m, 2H), 8.08 (m, 2H); ^{13}C NMR δ 24.1, 61.2, 124.3, 126.4, 127.5, 129.4, 150.8.

1,4-Bis(bromomethyl)-2,3-diethoxynaphthalene (162b)

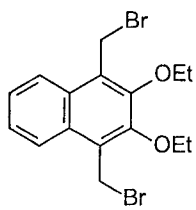

Using the general procedure for **162a**, the reaction of **163b** (2.81 g, 13.0 mmol), 95% paraformaldehyde (2.46 g, 78.0 mmol) and HBr in glacial acetic acid (30 wt %, 16.3 mL, 78 mmol of HBr) gave the crude product (4.97 g, 95%), which was crystallized from acetone-hexane to afford **162b** (3.92 g, 75.0 %) as light yellow fine needles (acetone-hexane): mp 150 °C (dec.); ^{1}H NMR (300 MHz) δ 1.51 (t, *J* = 7.2 Hz, 6H), 4.25 (q, *J* = 7.1 Hz, 4H), 5.05 (s, 4H), 7.57–7.60 (m, 2H), 8.05–8.09 (m, 2H); ^{13}C NMR δ 16.1, 24.5, 69.7, 124.4, 126.3, 127.4, 129.4, 150.1.

1,4-Bis(bromomethyl)-2,3-di-*n*-propoxynaphthalene (162c)

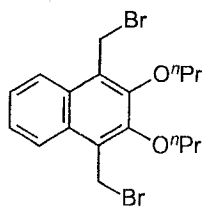

Using the general procedure for **162a,** the reaction of **163c** (3.18 g, 13.0 mmol), 95% paraformaldehyde (2.46 g, 78 mmol) and HBr in glacial acetic acid (30 wt %, 16.3 mL, 78 mmol of HBr) gave the crude product (5.09 g, 91%), which was purified by chromatography (hexane) to afford **162c** (4.19 g, 75%) as a colourless powder: mp 113 °C (dec.); ^{1}H NMR δ 1.13 (t, *J* = 7.3 Hz, 6H), 1.88–1.96 (m, 4H), 4.13 (t, *J* = 6.3 Hz, 4H), 5.05 (s, 4H), 7.57–7.59 (m, 2H), 8.06–8.08 (m, 2H); ^{13}C NMR δ 10.8, 23.9, 24.5, 75.6, 124.3, 126.2, 127.4, 129.5, 150.3.

1,4-Bis(bromomethyl)-2,3-di-*n*-butoxynaphthalene (162d)

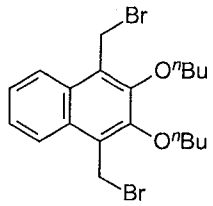

Using the general procedure for **162a**, the reaction of **163d** (3.60 g, 13.0 mmol), 95% paraformaldehyde (2.46 g, 78.0 mmol) and HBr in glacial acetic acid (30 wt %, 16.3 mL, 78.0 mmol of HBr) gave the crude product (5.87 g, 99%), which was purified by chromatography (hexane) to afford **162d** (3.69 g, 62 %) as a white powder: mp 93–94 °C (dec.); ^{1}H NMR δ 1.03 (t, *J* = 7.3 Hz, 6H), 1.57 (m, 4H), 1.87 (m, 4H), 4.15 (t, *J* = 7.0 Hz, 4H), 5.03 (s, 4H), 7.57 (m, 2H), 8.06 (m, 2H); ^{13}C NMR δ 14.2, 19.5, 24.5, 32.7, 73.9, 124.3, 126.2, 127.3, 129.4, 150.3.

1,4-Bis(bromomethyl)-2,3-methylenedioxynaphthalene (162e)

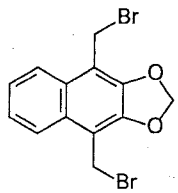

To stirred a solution of **163e** (4.37 g, 25.0 mmol) and paraformaldehyde (1.67 g, 55.0 mmol) in glacial acetic acid (130 mL) was added dropwise 21% HBr in AcOH (103 mL) over 2 h. The reaction mixture was then heated at 70–80 °C with stirring for a further 3 h. The cold reaction mixture was poured into cold water (400 mL), and the resulting precipitate was filtered, washed with

distilled water (2 x 50 mL), aqueous 5% $NaHCO_3$ (2 x 50 mL) and distilled water until the washings were neutral to pH paper, then dissolved in EtOAc (200 mL), dried over anhydrous $MgSO_4$, and filtered. After the solvent was removed under reduced pressure, the crude product (8.70 g, 97%) was crystallized from acetone-hexane to yield **162e** (6.99 g, 78%) as a light yellow fine needle-like solid: mp 202–204 °C (dec.) (lit.[17] 202–204 °C); ^{1}H NMR δ 4.86 (s, 4H), 6.17 (s, 2H), 7.51–7.53 (m, 2H), 7.95–7.97 (m, 2H).

1,4-Bis(hydroxymethyl)-2,3-dimethoxynaphthalene(161a)

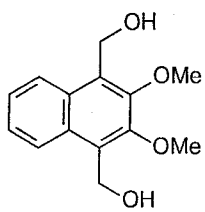

General procedure: A mixture of **162a** (3.74 g, 10.0 mmol) and $CaCO_3$ (10.01 g, 100.0 mmol) in 50% aqueous dioxane (200 mL) was heated at reflux with stirring for 3 d. After the solvent was removed under reduced pressure, the residue was dissolved in aqueous 6 M HCl (25 mL) and extracted with EtOAc (3 x 150 mL). The organic layer was washed with distilled water, dried over anhydrous $MgSO_4$, and filtered. The solvent was removed under reduced pressure to afford crude product (2.43 g, 98%) as a colourless solid, which was purified by chromatography (6:4 EtOAc-hexane) to yield **161a** (1.86 g, 75%) yield as a colourless powder: mp 180–181 °C; ^{1}H NMR (300 MHz) δ 1.88 (t, J = 6.2 Hz, 2H) 3.98 (s, 6H), 5.19 (d, J = 5.7 Hz,

4H), 7.51–7.54 (m, 2H), 8.14–8.17 (m, 2H); ^{13}C NMR δ 56.4, 62.1, 124.5, 126.1, 129.2, 130.3, 150.7; GCMS *m/z* (relative intensity) 248 (M^+, 80), 201 (95), 186 (30), 128 (70), 115 (100).

1,4-Bis(hydroxymethyl)-2,3-diethoxynaphthalene (161b)

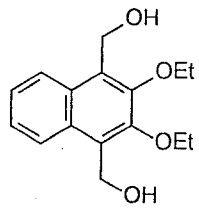

Using the general procedure for **161a**, the reaction of **162b** (2.81 g, 7.00 mmol) and $CaCO_3$ (7.00 g, 70.0 mmol) gave the crude product (1.88 g, 97%) as a colourless solid which was purified by chromatography (3:7 EtOAc-hexane) to yield **161b** (1.39 g, 72%): mp 173–174 °C. ^{1}H NMR (300 MHz) δ 1.44 (t, *J* = 6.9 Hz, 6H), 1.96 (t, *J* = 5.7 Hz, 2H, disappears upon D_2O addition), 4.16 (q, *J* = 6.9 Hz, 4H), 5.18 (d, *J* = 5.7 Hz, 4H), 7.50–7.53 (m, 2H), 8.14–8.17 (m, 2H); ^{13}C NMR δ 16.0, 56.7, 70.5, 124.5, 126.0, 129.4, 130.2, 149.8; GCMS *m/z* (relative intensity) 276 (M^+, 30), 201 (25), 186 (60), 128 (70), 115 (100).

1,4-Bis(hydroxymethyl)-2,3-di-*n*-propoxynaphthalene (161c)

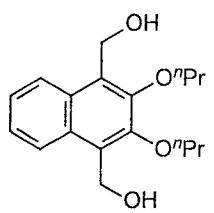

Using the general procedure for **161a**, the reaction of **162c** (3.01 g, 7.00

mmol) and $CaCO_3$ (7.00 g, 70.0 mmol) gave the crude product (2.36 g, 97%) as a colourless solid, which was purified by chromatography (2:8 EtOAc-hexane) to yield **161c** (1.67 g, 71%) as a colourless powder: mp 155–156 °C; ^{1}H NMR δ 1.09 (t, *J* = 7.8 Hz, 6H), 1.83–1.90 (m, 4H), 1.92 (t, *J* = 6.0 Hz, 2H, disappears upon D_2O addition), 4.04 (t, *J* = 6.8 Hz, 4H), 5.18 (d, *J* = 6.0 Hz, 4H), 7.50–7.52 (m, 2H), 8.14–8.16 (m, 2H); ^{13}C NMR δ 10.8, 23.8, 56.6, 76.7, 124.5, 125.9, 129.3, 130.3, 150.1; GCMS *m/z* (relative intensity) 304 (M^+, 60), 215 (10), 186 (100), 128 (40), 115 (40).

1,4-Bis(hydroxymethyl)-2,3-di-*n*-butoxynaphthalene (161d)

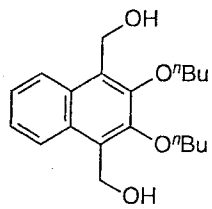

Using the general procedure for **161a**, the reaction of **162d** (3.21 g, 7.00 mmol) and $CaCO_3$ (7.00 g, 70.0 mmol) gave the crude product (2.30 g, 98%) as a colourless solid, which was purified by chromatography (2:8 EtOAc-hexane) to yield **161d** (1.67 g, 72%) as a colourless powder: mp 160 °C; ^{1}H NMR δ 1.01 (t, *J* = 7.5 Hz, 6H), 1.51–1.59 (m, 8H, overlap with HOD exchange signal), 1.80–1.86 (m, 4H), 1.92 (t, *J* = 5.8 Hz, 2H, disappears upon D_2O addition), 4.08 (t, *J* = 6.8 Hz, 4H), 5.18 (d, *J* = 6.0 Hz, 4H), 7.50–7.52 (m, 2H), 8.15–8.17 (m, 2H); ^{13}C NMR δ 14.2, 19.5, 32.6, 56.5, 74.9, 124.5, 125.9, 129.2, 130.2, 150.0; GCMS *m/z* (relative intensity) 332 (M^+, 30), 202 (10),

186 (100).

1,4-Bis(hydroxymethyl)-2,3-methylenedioxynaphthalene (161e)

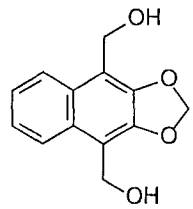

Using the general procedure for **161a**, the reaction of **162e** (2.13 g, 6.00 mmol) and $CaCO_3$ (6.00 g, 60.0 mmol) gave the crude product (1.36 g, 98%) as a colourless solid, which was purified by chromatography (1:1 EtOAc-hexane) to yield **161e** (1.00 g, 72%) as a colourless powder: mp 213–214 °C (lit.[18] 219–220 °C from 95% EtOH), ^{1}H NMR δ 1.70 (t, J = 5.8 Hz, 2H, disappears upon D_2O addition), 5.10 (d, J = 6.0 Hz, 4H), 6.10 (s, 2H), 7.45–7.47 (m, 2H), 8.05–8.07 (m, 2H); ^{13}C NMR (DMSO-d_6) δ 54.0, 100.8, 114.2, 123.9, 124.2, 129.4, 144.4; GCMS *m/z* (relative intensity) 232 (M^+, 100), 185 (100), 128 (70), 115 (80).

"1,4-linked" octahomotetraoxaisocalix[4]-(2,3-dimethoxy)-naphthalene (159a) and "1,4-linked" dodecahomohexaoxaisocalix[6]-(2,3-dimethoxy)-naphthalene (160a).

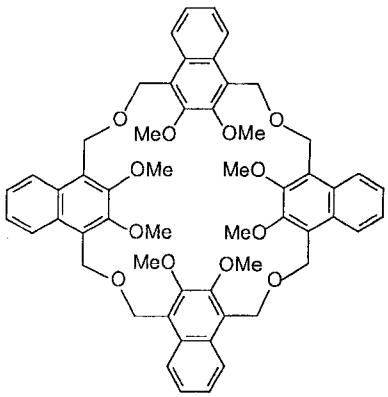

159a

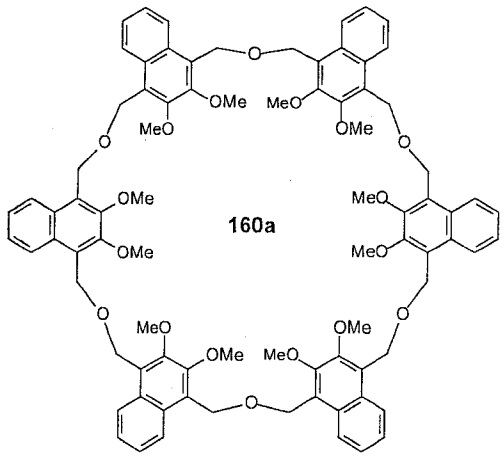

160a

General procedure: To a stirred suspension of powered 85% KOH (1.12 g, 20.0 mmol) in dioxane (20 mL) at 75–85 °C was added a solution of **161a** (496 mg, 2.00 mmol) and **162a** (748 mg, 2.00 mmol) in dry dioxane (40 mL) over 2.5 h using a syringe pump. The reaction mixture was heated at 75–85 °C with stirring for another 16 h. After the solvents were removed under reduced pressure, the residue was added to water (30 mL), and the mixture was neutralized with aqueous 3 M HCl, extracted with $CHCl_3$ (2 x 50 mL), dried over anhydrous $MgSO_4$ and filtered. After the solvent was removed under reduced pressure, the crude product was purified by PLC (3:7 EtOAc-hexane) to yield **159a** (169 mg, 18%) as a colourless powder: mp 152–156 °C (MeCN-MeOH); ^{1}H NMR δ 3.80 (s, 24H), 5.05 (s, 16H), 6.75–6.77 (m, 8H), 7.40–7.42 (m, 8H); ^{13}C NMR δ 62.0, 62.6, 124.2, 125.3, 126.9, 130.5, 151.0; (+)-MALDI-TOF MS *m/z* (relative intensity) 959.0 ($M + K^+$,

32) calcd.: 959.3 for $C_{56}H_{56}O_{12}K$, 943.2 (M + Na^+, 100) calcd.: 943.4 for $C_{56}H_{56}O_{12}Na$; and **160a** (32 mg, 3.5%) as a colourless semisolid: ^1H NMR δ 3.87 (s, 36H), 5.06 (s, 24H), 7.12–7.15 (m, 12H), 7.86–7.88 (m, 12H); ^{13}C NMR δ 62.0, 63.2, 125.0, 125.5, 126.7, 130.8, 151.3; (+)-MALDI-TOF MS *m/z* (relative intensity) 1419.8 (M + K^+, 23) calcd.: 1419.5 for $C_{84}H_{84}O_{18}K$, 1403.8 (M + Na^+,100) calcd.: 1403.6 for $C_{84}H_{84}O_{18}Na$.

"1,4-Linked" octahomotetraoxaisocalix[4]-(2,3-diethoxy)naphthalene (159b).

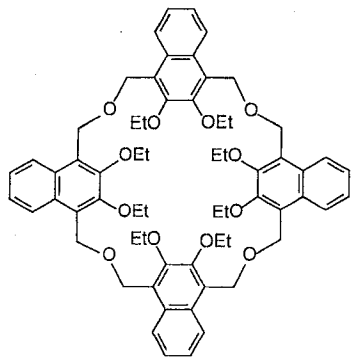

Using the general procedure for **159a**, the coupling reaction between **161b** (276 mg, 1.00 mmol) and **162b** (402 mg, 1.00 mmol) gave the crude product, which was purified by PLC (1.5:8.5 EtOAc-hexane) to yield **159b** (78 mg, 15%) as a colourless powder: mp 120–124 °C (MeCN-MeOH); ^1H NMR (300 MHz) δ 1.41 (t, *J* = 7.4 Hz, 24H), 4.05 (q, *J* = 6.9 Hz, 16H), 5.05 (s, 16H), 6.67–6.71 (m, 8H), 7.31–7.34 (m, 8H); ^{13}C NMR (75 MHz) δ 16.0, 62.8, 70.5, 124.2, 125.2, 127.1, 130.4, 150.1; (+)-MALDI-TOF MS *m/z* (relative intensity) 1072.2 (M + K^+, 100) calcd.: 1072.4 for $C_{64}H_{72}O_{12}K$, 1056.2 (M + Na^+, 33) calcd.: 1056.3 for $C_{64}H_{72}O_{12}Na$.

X-ray Crystal Structure of 159b. A colourless fragment crystal (acetonitrile-methanol) mp 120–124 °C, of $H_{77.25}N_{1.75}O_{12}C_{67.50}$ having approximate dimensions of 0.50 x 0.45 x 0.41 mm was mounted on a glass fiber. Cell constants and an orientation matrix for data collection corresponded to a primitive orthorhombic cell, space group $Pna2_1$ (#33), with dimensions: a = 17.2682(7) Å, b = 14.3146(5) Å, c = 25.106(1) Å, V = 6205.9(4) Å^3. For Z = 4 and F.W. = 1105.11, the calculated density is 1.18 g/cm^3. Intensity data were made at 193 K on a Bruker P4/CCD diffractometer with graphite monochromated Mo-Kα radiation (λ = 0.71073 Å) and a sealed tube source radiation to $2\theta_{max}$ = 52.8°; 44279 reflections converged to a final R_{int} = 0.026 for 12658 unique relections; 10993 observations with $I > 2.00\sigma(I)$. Final R1 and wR2 values were 0.044 and 0.129 respectively and GoF indicator = 1.03.

"1,4-Linked" octahomotetraoxaisocalix[4]-(2,3-*n*-dipropoxy)naphthalene (159c).

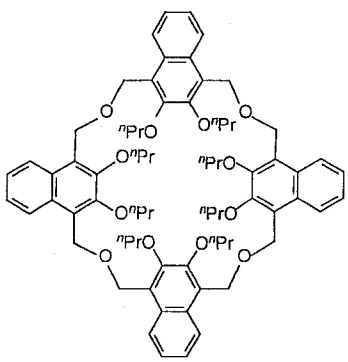

Using the general procedure for **159a**, the coupling reaction between **161c** (304 mg, 1.00 mmol) and **162c** (430 mg, 1.00 mmol) gave the crude, which

product was purified by PLC (1.25:8.75 EtOAc-hexane) to yield **24c** (85.9 mg, 15%) as a colourless powder: mp 98–103 °C; ^{1}H NMR δ 1.08 (t, *J* = 7.5 Hz, 24H), 1.82–1.89 (m, 16H), 3.95 (t, *J* = 6.8 Hz, 16H), 5.05 (s, 16H), 6.65–6.67 (m, 8H), 7.30–7.32 (m, 8H); ^{13}C NMR δ 10.9, 23.8, 62.8, 76.6, 124.2, 125.2, 127.0, 130.5, 150.3; (+)-MALDI-TOF MS (relative intensity) *m/z* 1183.8 (M + K+, 27) calcd.: 1183.6 for $C_{72}H_{88}O_{12}K$, 1167.8 (M + Na^{+}, 100) calcd.: 1167.6 for $C_{72}H_{88}O_{12}Na$.

"1,4-Linked" octahomotetraoxaisocalix[4]-(2,3-*n*-dibutoxy)-naphthalene (159d) and "1,4-linked" dodecahomohexaoxaisocalix[6]-(2,3-*n*-dibutoxy)-naphthalene (160d).

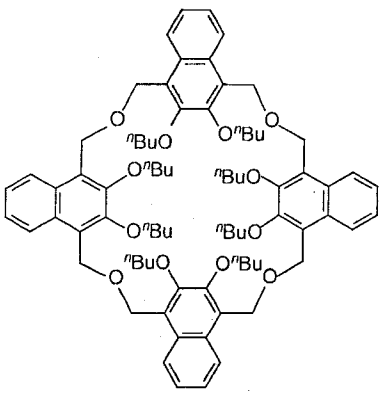

159d

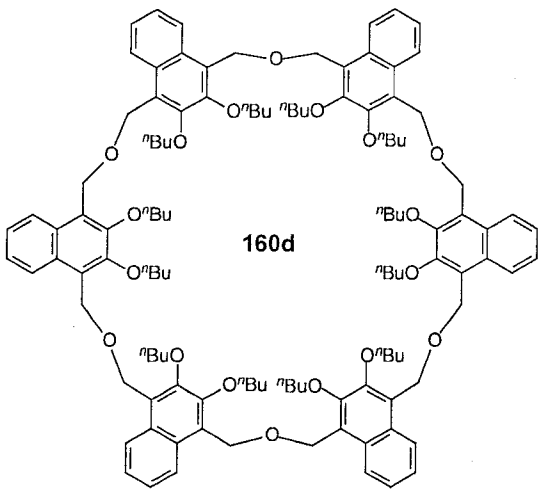

160d

Using the general procedure for **159a**, the coupling reaction between **161d** (332 mg, 1.00 mmol) and **162d** (458 mg, 1.00 mmol) gave the crude product, which was purified by PLC (1:9 EtOAc-hexane) to afford **159d** (76 mg, 12%) as a colourless powder: mp 160–162 °C; ^{1}H NMR δ 0.99 (t, *J* = 7.5

Hz, 24H), 1.51–1.59 (m, 20H, overlap with HOD exchange signal), 1.78–1.84 (m, 16H), 3.98 (t, *J* = 6.5 Hz, 16H), 5.04 (s, 16H), 6.63–6.65 (m, 8H), 7.29–7.31 (m, 8H); ^{13}C NMR δ 14.3, 19.7, 32.7, 62.9, 75.0, 124.2, 125.2, 127.0, 130.5, 150.3; (+)-MALDITOF MS *m/z* (relative intensity) 1296.8 (M + K^+, 100) calcd.: 1296.8 for $C_{80}H_{104}O_{12}K$, 1280.8 (M + Na^+, 96) calcd.: 1280.7 for $C_{80}H_{104}O_{12}Na$. And **160d** (10 mg, 1.6%) as a semisolid: ^{1}H NMR δ 0.99 (t, *J* = 7.5 Hz, 6H), 1.51–1.57 (m, 5H, overlap with HOD exchange signal), 1.79–1.84 (m, 4H), 4.03 (t, *J* = 6.5 Hz, 4H), 5.05 (s, 4H), 7.07–7.09 (m, 2H), 7.81–7.83 (m, 2H); ^{13}C NMR δ 14.3, 19.7, 32.8, 63.6, 75.0, 125.1, 125.3, 126.7, 130.8, 150.7; (+)-MALDI-TOF MS *m/z* (relative intensity) 1908 (M + Na^+, 25) calcd.:1908.1 for $C_{120}H_{156}O_{18}Na$.

Job plot determinations

Job Plot determinations were conducted by varying the mole fractions of TMACl and **159a** or **159b,** using solutions which were *ca.* 8.94 x 10^{-4} M in $CDCl_3$ solution. After mixing, each of the respective solutions (total combined final volumes 1.00 mL) in a series of nine NMR tubes was sonicated for approx. 10 min and then allowed to stand overnight. NMR measurements were recorded at 298 K and 500 MHz, using a 16 K data table, for a 10.0 ppm sweep width having a digital resolution of 0.321 Hz. Job plots were produced by plotting the mole fractions of TMACl against the mole fractions of either **159a** or **159b**, multiplied by the Δδ determined for each set of

chemical shifts present for both the host and guest molecules. In all cases the plots clearly revealed a maximum at 0.5 indicating the formation of 1:1 complexes.

Association constant determinations

The association (stability) constants for the complexation in $CDCl_3$ between **159a** and **159b** with TMACl were determined by ^1H NMR spectroscopy. Changes in the chemical shift ($1/\Delta\delta$) of the methyl signal of TMACl as a function of 1/[**159a**] or [1/**159b**] were determined, and K_{assoc} values were determined using the Benesi-Hildebrand treatment or the Foster-Fyle treatment, by plotting $\Delta\delta$/[**159a**] or $\Delta\delta$ /[**159b**] *vs* $\Delta\delta$. In a typical experiment, aliquots ranging from 20 to 80 μL of approximately 10^{-3} M stock solutions of either **159a** (1.22 x 10^{-3} M) or **159b** (1.30 x 10^{-3} M) were added to a series of individual NMR tubes which each contained 1.00 mL of a saturatured solution of TMACl (*ca.* 8.94 x 10^{-4} M). The resulting solutions were sonicated for *ca.* 10 min, were left overnight before NMR measurements were recorded at 298 K and 500 MHz, as before.

5.6 References and Notes

1. Afari, Z.; Böhmer, V.; Harrowfield, J.; Vicens, J., Eds., *Calixarenes 2001*, Kluwer Acadamic Publishers, Dordrecht, The Netherlands 2001, pp 236-248 and references cited therein.

2. Sarri, P.; Venturi, F.; Cuda, F.; Roelens, S. *J. Org. Chem.* **2004**, *69*, 3654-3661.

3. (a) Hampton, P. D.; Tong, W.; Bencze, Z.; Daitch, C. E. *J. Org. Chem.* **1994**, *59*, 4838-4843. (b) Hampton, P. D.; Daitch, C. E.; Alam, T. M.; Bencze, Z.; Rosay, M. *Inorg. Chem.* **1994**, *33*, 4750-4758. (c) Daitch, C. E.; Hampton, P. D.; Duesler, E. N. *Inorg. Chem.* **1995**, *34*, 5641-5645. (c) Daitch, C. E.; Hampton, P. D.; Duesler, E. N.; Alam, T. M. *J. Am. Chem. Soc.* **1996**, *118*, 7769-7773. (d) Hampton, P. D.; Daitch, C. E.; Alam, T. M.; Pruss, E. A. *Inorg. Chem.* **1997**, *36*, 2879-2883.

4. (a) Masci, B. *Tetrahedron* **1995**, *51*, 5459-5464. (b) Masci, B.; Finelli, M.; Varrone, M. *Chem. Eur. J.* **1998**, *4*, 2018-2030. (c) Masci, B. In *Calixarenes 2001*; Asfari, Z., Bohmer, V., Harrowfield, J., Vicens, J., Eds.; Kluwer Academic Publishers: Dordrecht, The Netherlands, 2001. (d) Masci, B. *J. Org. Chem.* **2001**, *66*, 1497-1499. (e) Masci, B. *Tetrahedron* **2001**, *57*, 2841-2845.

5. (a) Komatsu, N. *Tetrahedron Lett.* **2001**, *42*, 1733-1736. (b) Komatsu, N. *Org. Biomol. Chem.* **2003**, *1*, 204-209.

6. Dhawan, B,; Gutsche, C. D. *J. Org. Chem.* **1983**, *48*, 1536-1539.

7. Georghiou, P. E.; Li, Z.; Ashram, M.; Chowdhury, S.; Mizyed, S.; Tran, A. H.; Al-Saraierh, H.; Miller, D. O. *Synlett*, **2005**, 879-891.

8. Ashram, M.; Mizyed, S.; Georghiou, P. E. *J. Org. Chem.* **2001,** *66,* 1473-1479.

9. Mizyed, S.; Ashram, M.; Miller, D. O.; Georghiou, P. E. *J. Chem. Soc., Perkin Trans. 2*, **2001,** 1916-1919.

10. Ashram, M. *Ph.D. Dissertation,* Memorial University of Newfoundland, 1997.

11. Al-Saraierh, H.; Georghiou, P. E.; *unpublished results.*

12. Calixnaphthalenes and these new homooxa homologues adopt conformations which are similar to those that are typically found for the calixarenes.

13. The name "isocalixnaphthalenes" for these *1,4-* or para-linked compounds was suggested to us by Professor C. David Gutsche, the originator of the name "calixarenes". Personal communication, October 21, 2004.

14. Computer-assisted molecular modeling studies were conducted using Spartan Pro V1.1, from Wavefunction, Inc., Irvine, CA, USA. Calculations at the PM3 level of theory were conducted on the optimized geometry of the host and/or complexes which were obtained through molecular mechanics (MMFF94) conformational searches.

15. Tran, A. H.; Miller, D. O.; Georghiou, P. E. *J. Org. Chem.* **2005**, *70*, 1115-1121.

16. van der Made, A. W.; van der Made, R. H. *J. Org. Chem.* **1993**, *58*, 1262. (b)

17. Li, Z. *Ph.D. Dissertation,* Memorial University of Newfoundland, 1996.

18. Simonet, J.; Patillon, H.; Belloncle, C.; Simonet-Gueguen, N.; Cauliez, P. *Synthetic Metals*, **1995**, *75*, 103-110.

19. Gallant, A.J.; Yun, M.; Sauer, M.; Yeung, C. S.; MacLachlan, M. J. *Org. Lett.* **2005**, *7*, 4827-4830.

20. For an account of the origins of various names coined by organic chemists see Nickon, A.; Silversmith, E. F. *"Organic Chemistry. The Name Game",* Pergamon Books, Inc., U.K., 1987.

21. See Gutsche, C. D. in *Inclusion Compounds, Vol. 4*, Atwood, J. L.; Davies, J. E. D.; MacNicol, D. D. Eds., Oxford University Press, Oxford, U. K., 1991.

22. (a) Atwood, J. L.; Barbour, L. J.; Nichols, P. J.; Raston, C. L.; Sandoval, C. A. *Chem. Eur. J.* **1999**, *5*, 990-996; (b) Steed, J. W.; Junk, P. C.; Atwood, J. L.; Barens, M. J.; Raston, C. L.; Purkhalter, R. S. *J. Am. Chem. Soc.* **1994**, *116*, 10346-10347.

23. Ma, J. C.; Dougherty, D. A. *Chem. Rev.* **1997,** *97*, 1303-1324, *and references cited therein.*

24. Arduini, A.; Giorgi, G.; Pochini, A.; Secchi, A.; Ugozzoli, F. *J. Org. Chem.* **2001**, *66*, 8302-8308.

25. Fielding, L. *Tetrahedron*, **2000**, *56*, 6151-6170.

26. Job, P. *Ann. Chim.* **1928**, *9*, 113-203.

27. Bashall, A. P.; Collins, J. F. *Tetrahedron Lett.* **1975**, 3489-3490.

Chapter 6

An attempted synthesis of a "double-handled" homooxaisocalix[4]naphthalene

6.1 Introduction

Calixcrowns, which are combinations of calixarenes and crown ethers, were first synthesized in 1983 by Ungaro Andreetti *et al.*[1] by refluxing *p-tert*-butylcalix[4]arene **2** in benzene with pentaethylene glycol ditosylate in the presence of potassium *tert*-butoxide (Scheme 6.1). The calixcrown **165** resulting from the dialkylation has both a hydrophilic cavity (from the crown ether) and a lypophilic cavity (from the calixarene). This first calixcrown exhibited selective extraction of alkali cations and ammonium picrates. Furthermore, compound **165** was able to transfer Na^+ and K^+ from an aqueous basic solution into an acidic one, whereas neither was *p-tert*-butylcalix[4]arene (**2**) nor dibenzo-18-crown-6 **166** were able to do so.

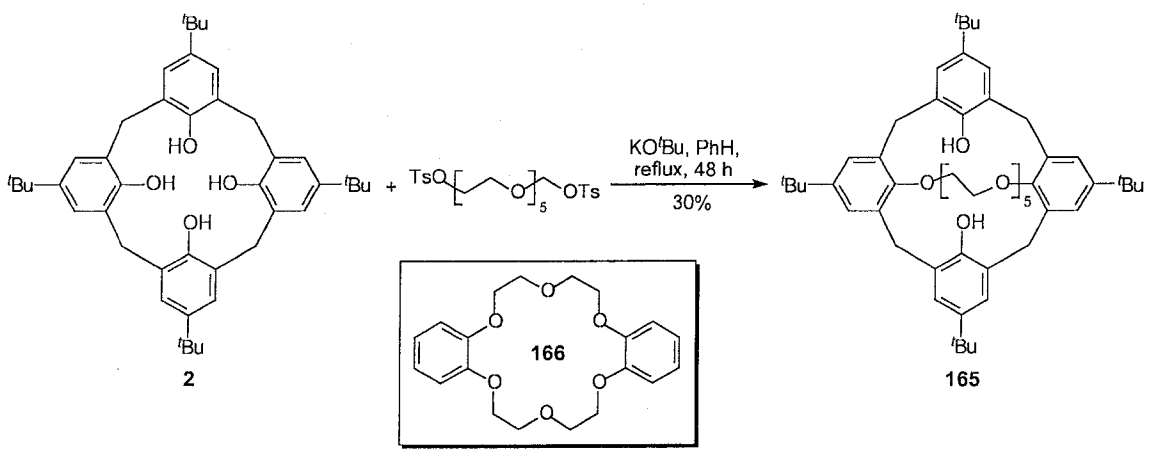

Scheme 6.1 Synthesis of calixcrown **165**.

The initial complexation studies in toluene-d_8, CS_2 or $CDCl_3$ solution, of octahomotetraoxa*iso*calix[4]naphthalene **159a** or **159b** with C_{60} or C_{70} which were monitored by ^1H NMR or UV-vis spectroscopy, did not show any complexation-induced chemical shifts and/or any colour change.[2] Presumably, the loss of entropy, which would result by complex formation between C_{60} and C_{70} and these hosts, is responsible for the absence of complexation (Chapter 5). In order to test the hypothesis that a more rigid calix[4]naphthalene host having lower entropy than those of **159a** and **159b** might be better pre-organized to encapsulate C_{60}- or C_{70}-fullerenes, the synthesis of a "double-handled" octahomotetraoxacalix[4]naphthalene **167** (Figure 6.1) was undertaken.

6.2. Design of a target structure and its retrosynthetic analysis

Target structure

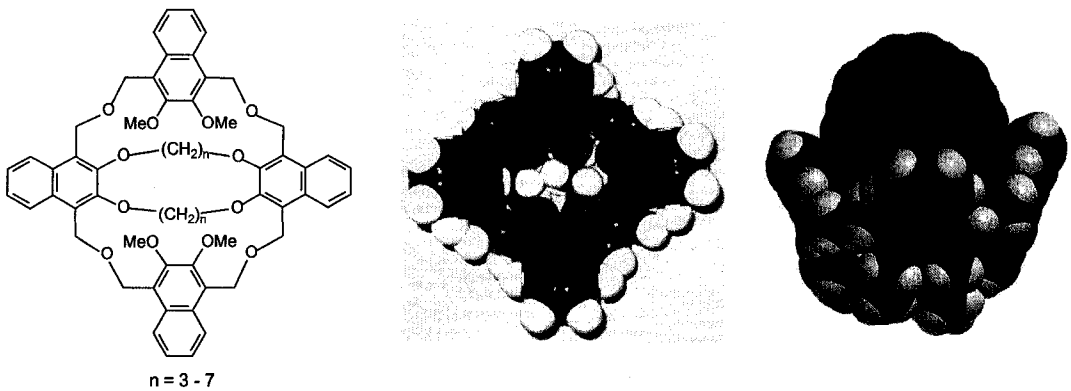

Figure 6.1 Structures (*left*), CPK model of **167** (n = 6) (*middle*), and a computer-generated model of a 1:1 **167**:C_{60} complex (*right*).

CPK model and computer-assisted molecular mechanics modeling using the Spartan'04[3] software were used to determine the optimum length(s) for the alkyl groups required to bridge the four hydroxy groups on the two opposite naphthalene units in structures such as **167** (Figure 6.1). It was concluded that a chain length of n = 3–6 would potentially allow the formation of a double-handled octahomotetraoxacalix[4]naphthalene such as **167**.

Retrosynthetic analysis

The retrosynthetic analysis of the target structure **167** shown in Scheme 6.2 at the indicated bonds via Williamson reactions opened the 28-membered annulus and led back to either tetrakis(hydroxymethyl) cyclic ether **168** and bis(bromomethyl)naphthalene **162a** [path (a)] or tetrakis(bromomethyl) cyclic ether **169** and bis(hydroxymethyl)naphthalene **161a** [path (b)], respectively (Scheme 6.2). Intermediate **168** may be afforded via hydrolysis of **169,** which in turn should be available from tetrakis(bromomethylation) of dinaphtho(β,β)-(b,p)-(1,4,11,14)-tetraoxacycloeicosane (**170**). The 24-membered annulus in **170** could be furnished from commercially available 2,3-dihydroxynaphthalene (**164**) and 1,6-dibromohexane (**171**) also via Williamson reactions.

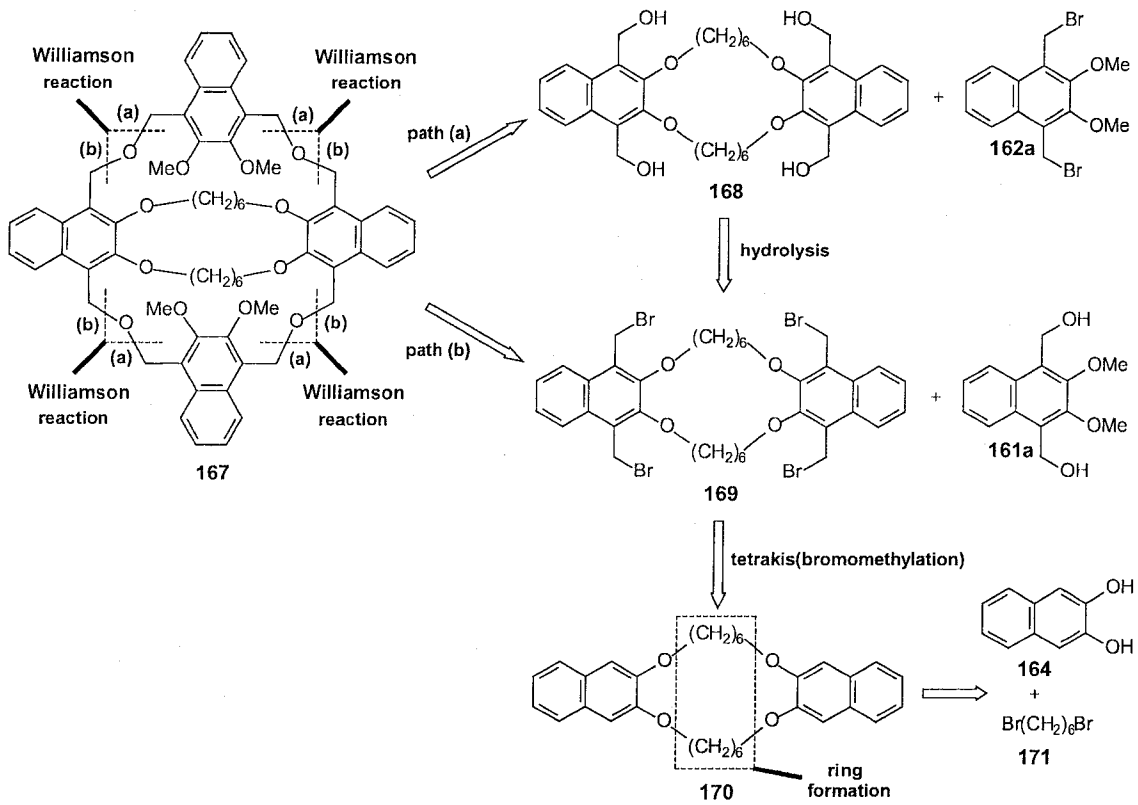

Scheme 6.2 Retrosynthetic analysis of **167**.

6.3 Results and discussion

With the two starting materials 2,3-dihydroxynaphthalene (**164**) and 1,3-dibromopropane (**172**) available in hand, a synthesis of compound **174** was explored first in order to test the possibility of the coupling reaction. Using a mixture of aqueous 10% NaOH and DCM gave only the [1+1] adduct product naphtho(*β*,*β*)-(b,l)-(1,4)-dioxacycloheptane (**173**) in 31% yield, with no evidence for the formation of the desired product dinaphtho(*β*,*β*)-(b,i)-(1,4,8,11)-tetraoxacyclotetradecane (**174**) (Scheme 6.3). It was hypothesized that the

cyclization to form **174** required to be conducted at a higher temperature instead of refluxing of DCM (45 °C).

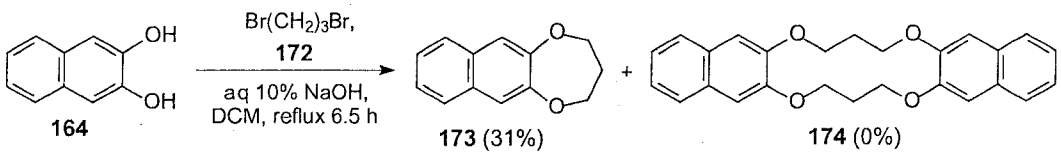

Scheme 6.3 Attempted synthesis of **174**.

A direct coupling reaction between **164** and 1,6-dibromohexane (**171**) under conditions similar to those used in Scheme 6.3 with either NaOH or KOH also failed to afford the desired cyclic product **170**. However, the use of NaH/DMF at 70–80 °C, provided the desired dinaphtho(β,β)-(b,p)-(1,4,11,14)-tetraoxacyclo-eicosane (**170**), albeit in very low yield (5%) along with naphtho(β,β)-(b)-(1,4)-dioxacyclodecane (**175**) in 8% yield (Scheme 6.4).

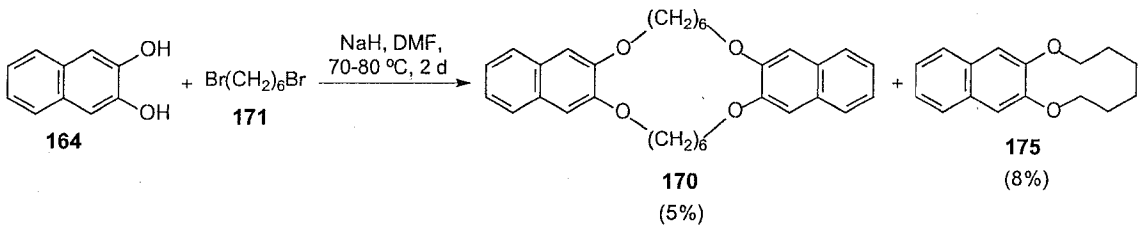

Scheme 6.4 Synthesis of **170** and **175** via direct coupling between **164** and **171**.

Hence, an alternate approach exploiting the coupling of monoprotected intermediates **176a-c** with terminal dibromoalkanes **171** or **172** was pursued. All protecting groups used gave the desired monoprotected intermediates **176a-c** (Scheme 6.5) in synthetically useful yields (Table 6.1).

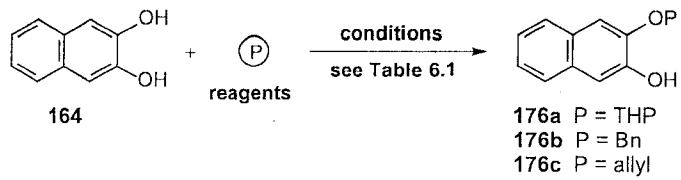

Scheme 6.5 Preparation of monoprotected intermediates **176a-c**.

For example, treatment of **164** with DHP in the presence of PTSA[4] or PPTS[5] gave 2-hydroxy-3-tetrahydropyranyloxynaphthalene (**176a**) in 66% and 53%, respectively. The acidic catalyst PTSA furnished **176a** in slightly higher yield than PPTS. While this study was underway in 2004, Kameta *et al.* reported the use of **176a** in the synthesis of their chiral rotaxanes.[6] However, no details about their experimental conditions or characterization of **176a** were mentioned.[6] Treatment of **164** with benzyl bromide in the presence of K_2CO_3 in acetone afforded 3-benzyloxy-2-hydroxynaphthalene (**176b**) in 69% yield along with diprotected product 2,3-dibenzyloxynaphthalene **176d** (12%) while K_2CO_3/DMF conditions gave **176b** in a slightly lower yield (64%).[7] The K_2CO_3/acetone could be replaced with $NaHCO_3$/DMF[8] or sodium/methanol[9] to give **176b** in 69% or 21% yields, respectively. However, since acetone has a much lower boiling point than that of DMF, it was much more convenient to use as a solvent. Finally, monoprotection of **164** using allyl bromide in the presence of K_2CO_3 in acetone afforded **176c** in 76% yield.

Table 6.1 Monoprotection of 2,3-dihydroxynaphthalene (**164**).

Entry	Reagents	Conditions	Products	Yield (%)
1	DHP	PPTS, DCM, reflux, 25 h	**176a**	53
2	DHP	PTSA, DCM, rt, 25 h	**176a**	66
3	BnBr	K_2CO_3, dry acetone, reflux 13 h	**176b**	69
4	BnBr	K_2CO_3, dry DMF, 85–90 °C, 6 h	**176b**	64
5	$H_2C{=}CHCH_2Br$	K_2CO_3, dry acetone, reflux 13 h	**176c**	76

The stage was now set for attempting Williamson reactions to form the diether **177a-c** or **178a-c** (Scheme 6.6). Unfortunately, none of the intermediates **175a-c** gave the desired products **177a-c** or **178a-c** using K_2CO_3/acetone or NaH/THF. For **176a** and **176b**, the Williamson reactions perhaps need to be conducted at higher temperature. Compound **176c** was not very stable and changed quickly from a yellowish liquid to dark brown upon standing. This instability could be a factor which contributed to the unsuccessful coupling reaction of **176c**.

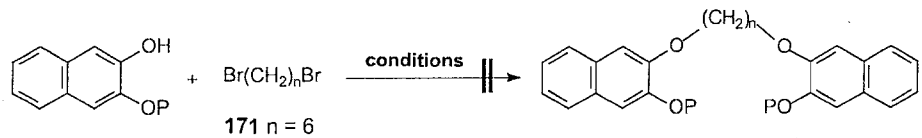

176a P = THP
176b P = Bn
176c P = allyl

171 n = 6
172 n = 3

177a n = 3; P = THP
177b n = 3; P = Bn
177c n = 3; P = allyl
178a n = 6; P = THP
178b n = 6; P = Bn
178c n = 6; P = allyl

Scheme 6.6 Attempted syntheses of intermediates **177a-c** and **178a-c**.

Since the monoprotection of **164** was successfully carried out with benzyl bromide or allyl bromide, a "bis(etherification)" of **164** was, therefore, tested with 1,3-dibromopropane **611** (Scheme 6.7). Gratifyingly, 1,3-bis(3-hydroxy-2-naphthyloxy)propane (**179**) was smoothly furnished in 75% yield. Furthermore since **179**, had free hydroxyl groups, it could conveniently undergo the next step to give the cyclic ether **174** in 73% yield, without requiring a protection-deprotection of **164** (Scheme 6.7).

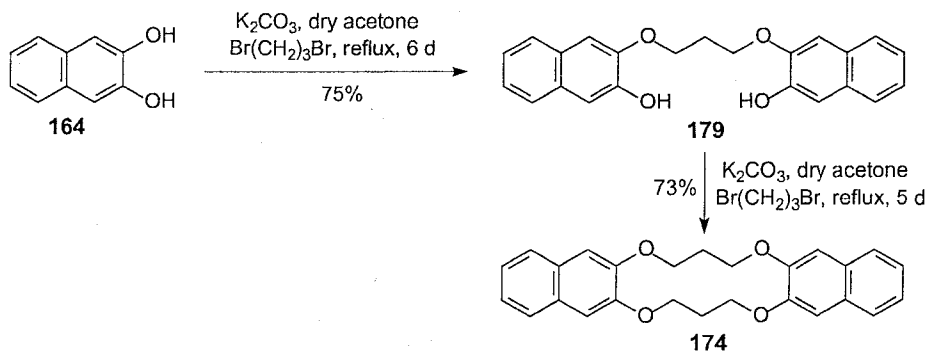

Scheme 6.7 Synthesis of intermediate **174**.

The coupling reaction between **164** and 1,6-dibromohexane (**171**) also easily afforded 1,6-bis(3-hydroxy-2-naphthyloxy)hexane (**180**) in high yield (86%). However, using acetone as the solvent for the ring closure step did not afford any of the cyclic ether **170**. When DMF was used as the solvent, intermediate **170** was formed in 49% yield (Scheme 6.8). Tetrakis(bromomethylation) of **170** with 30% HBr/AcOH and paraformaldehyde required 14 d at 75–80 °C to afford the tetrakis(bromomethyl) intermediate **169** in 96% yield. Hydrolysis of **169** with $CaCO_3$ in aqueous dioxane produced the

tetrakis(hydroxymethyl) intermediate **168** in 99% yield (Scheme 6.8).[3] However, due to their low solubilities in conventional NMR solvents, ^{13}C NMR spectra of **168** and **169** could not be obtained; and only their ^{1}H NMR spectra were successfully recorded. (+)-APCI MS analysis of tetrakis(bromomethyl) **169** (M^+ calcd.: 856.33 for $C_{36}H_{40}Br_4O_4$) did not show the molecular ion peak, but the fragment ions of the molecular ion such as 777 ($M^+ - {}^{81}Br$, 99%) and 775 ($M^+ - {}^{79}Br$, 100%). (+)-APCI MS analysis of tetrakis(hydroxymethyl) **168** showed the molecular ion peak at *m/z* = 603.5 (5%).

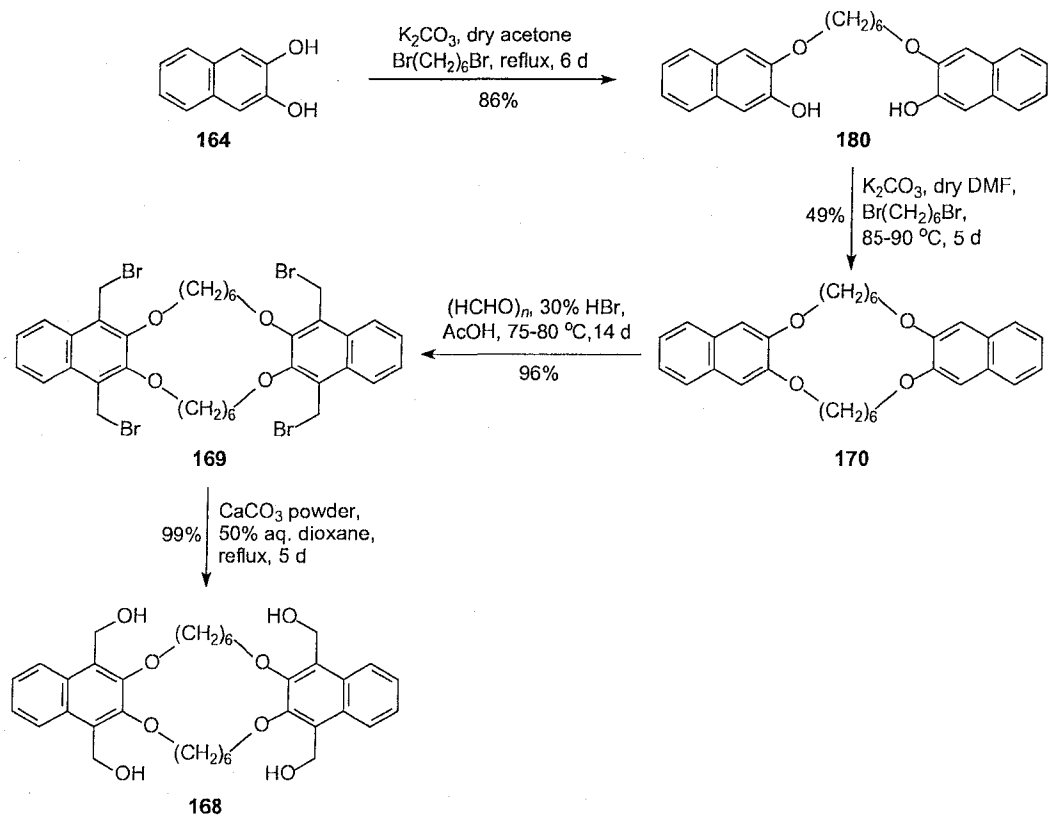

Scheme 6.8 Syntheses of intermediates **168** and **169**.

Unfortunately, the synthesis of **167** using the "[1+2]" coupling (envisioned in Scheme 6.9) between tetrakis(hydroxymethyl) cyclic ether **168** and bis(bromomethyl)naphthalene **162a** or tetrakis(bromomethyl) cyclic ether **169** and bis(hydroxymethyl)naphthalene **161a**, respectively, under conditions similar to those employed for **159a-d** failed to give the desired product. Replacing either solvent (dioxane by DMF or THF), or base (KOH by NaH) did not furnish the desired product **167**. It is possible that the low solubilities of intermediate **168** or **169** may have inhibited the desired macrocyclization to form **167**.

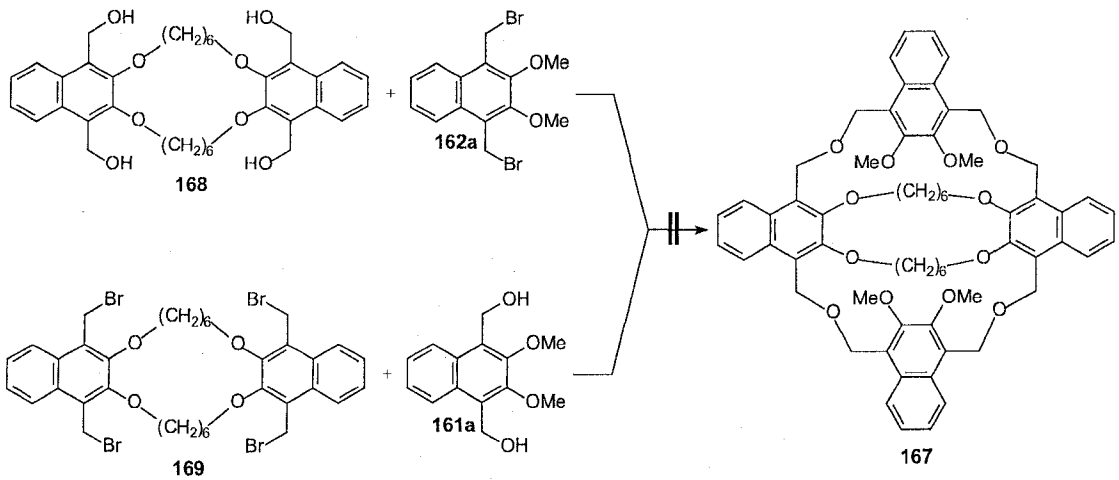

Scheme 6.9 Attempted synthesis of **167**.

6.4 Conclusions and proposals for future work

In summary, the key cyclic ether precursors **168** and **169** which are required for the synthesis of **167** were successfully obtained in synthetically useful yields via a coupling of two 2,3-dihydroxynaphthalene molecules (**164**) with 1,6-dibromohexane (**171**), followed by a tetra(bromomethylation) and hydrolysis, respectively. The coupling step was very useful as it avoids the need

for functional group protections and deprotections. However, due to solubility problems, the final coupling reactions failed to give the target compound **167**.

It is proposed that the final coupling reaction should be attempted in another medium, *e.g.* DMSO, or a suitable ionic liquid, in which the reagents may be more soluble. Furthermore, the $-O(CH_2)_6O-$ "handles" in **167** could be replaced by $-O(CH_2)_2O(CH_2)_2O-$[10] groups in order to form cyclic ether precursors such as **183** and **184** which might have higher solubilities than those of **169** and **168**, respectively (Scheme 6.10).

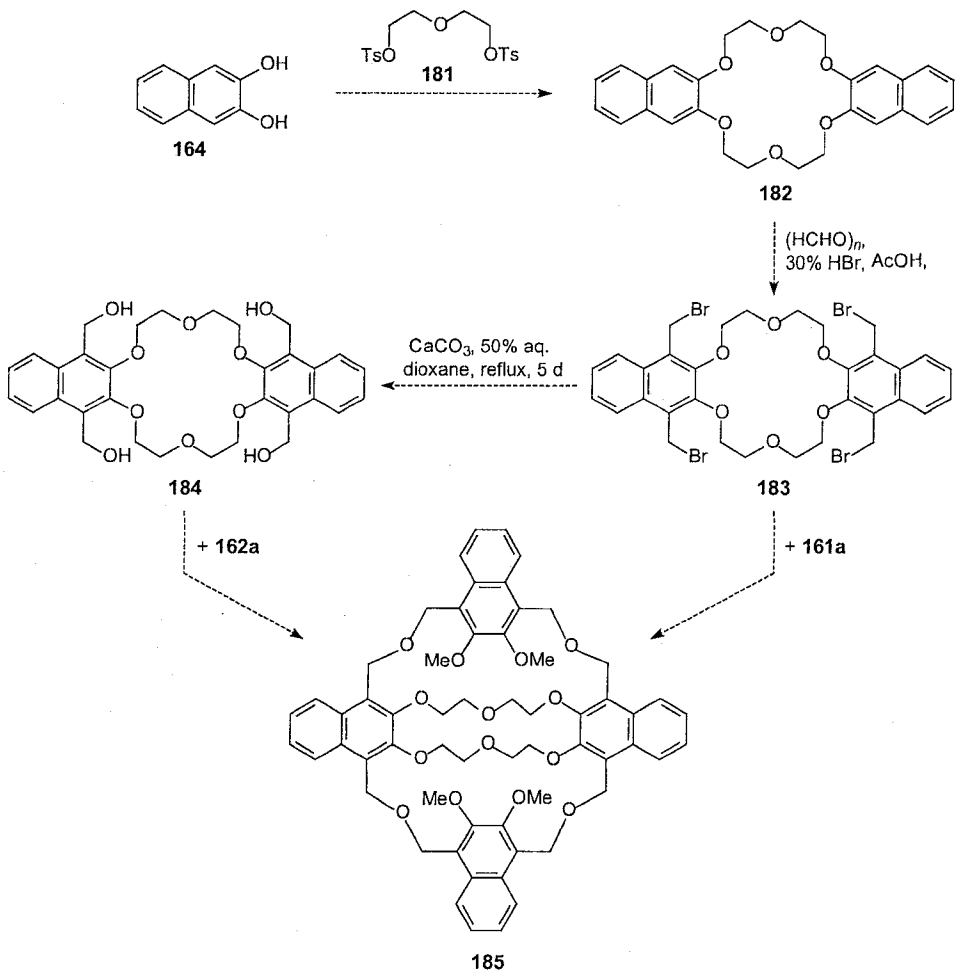

Scheme 6.10 Proposed synthesis of the target structure **185**.

This might help to solve the final coupling reaction, which was the issue in the attempted synthesis of **167**, to form compound **185** which could be a good receptor for alkali metal cations as well as fullerens.

6.5 Experimental section

Naphtho(*β*,*β*)-(b)-(1,4)-dioxacycloheptane (173)

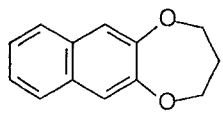

To a stirred mixture of **164** (1.64g, 10.0 mmol) in aqueous 10% NaOH (0.80 g, 0.02 mol and 7.2 g water) and DCM (100 mL) at reflux, was added dropwise 1,3-dibromopropane (**172**) (1.50 g, 8.60 mmol) over 2.5 h using a syringe pump. The reaction mixture was heated at reflux with stirring for a further 4 d. After the reaction mixture was cooled to room temperature, the organic layer was separated and washed with distilled water (1 x 40 mL), saturated aqueous NH_4Cl solution (1 x 40 mL) and brine (2 x 40), dried over anhydrous $MgSO_4$ and filtered. After solvent was removed under reduced pressure, the resulting yellow solid was purified by chromatography (2:8 EtOAc-hexane) to yield **173** (0.60 g, 31%) as a colourless powder: mp 132–133 °C (lit.[11] 132–133 °C from ether); ^{1}H NMR δ 2.24 (m, 2H), 4.27 (t, 4H), 7.33–7.35 (m, 2H), 7.41 (s, 2H), 7.67–7.68 (m, 2H); ^{13}C NMR δ 32.0, 71.1, 118.0, 125.1, 126.9, 130.8, 151.7, GCMS *m/z* (relative intensity) 200 (M^+, 100), 171 (70), 131 (20), 114 (20), 76 (5), 39 (5).

Naphtho(*β*,*β*)-(b)-(1,4)-dioxacyclodecane (175) and dinaphtho(*β*,*β*)-(b,p)-(1,4,11,14)-tetraoxacycloeicosane (170)

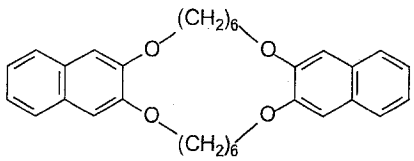

170

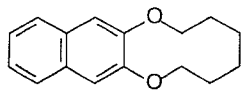

175

To a stirred mixture of **164** (0.82 g, 5.0 mmol) and NaH (0.14 g, 5.5 mmol) in dry DMF (50 mL) at 70 °C, was added dropwise 1,6-dibromohexane (**171**) (1.26 g, 5.00 mmol) over 30 min using a syringe pump. The reaction mixture was heated at 70 °C with stirring for a further 2 d. After the solvent was removed under reduced pressure, the resulting residue was added to water (50 mL) and extracted with EtOAc (3 x 70 mL). The organic layer was combined, washed with distilled water (1 x 40 mL), saturated aqueous NH_4Cl solution (1 x 40 mL) and brine (1 x 40), dried over anhydrous $MgSO_4$ and filtered. After the solvent was removed under reduced pressure, the residue was purified PLC (2:8 EtOAc-hexane) to yield **175** (0.10 g, 8%) as a colourless oil: ^{1}H NMR δ 1.65–1.67 (m, 4H), 1.78–1.79 (m, 4H), 4.25 (t, J = 5.1 Hz, 4H), 7.35–7.36 (m, 2H), 7.40 (s, 2H), 7.69–7.71 (m, 2H); ^{13}C NMR δ 24.4, 27.3, 73.9, 116.7, 124.9, 126.9, 131.0, 151.8; (+)-APCI MS *m/z* (relative intensity) 241.1 (M^+, 100); and **170** (0.05 g, 8%) as a colourless powder: mp 253–254 °C; ^{1}H NMR δ 1.68–1.71 (m, 8H), 1.93 (s, br, 8H), 4.11 (t, J = 6.0 Hz, 8H), 7.13 (s, 4H), 7.29–7.31 (m, 4H), 7.64–7.66 (m, 4H); ^{13}C NMR δ 26.8, 30.1, 69.3, 109.0, 124.1, 126.4, 129.7, 150.1; (+)-APCI MS

m/z (relative intensity) 485.2 (M^+,70) calcd.: 484.6 for $C_{32}H_{36}O_4$, 415 (60), 243 (100).

2-Hydroxy-3-(tetrahydropyranyloxy)naphthalene (176a)

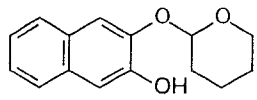

Procedure 1: Using PTSA as the catalyst:

To a stirred mixture of **164** (1.64 g, 10.0 mol) and PTSA.H_2O (0.35 g, 1.8 mmol) in dry DCM (100 mL) at room temperature, was added dropwise a solution DHP (0.94 mL, 10 mmol) in dry DCM (5 mL) over 45 min using a syringe pump. The reaction mixture was stirred at room temperature for a further 24 h. The organic layer was then separated, washed with distilled water (1 x 50 mL), saturated aqueous NH_4Cl solution (2 x 50 mL), dried over anhydrous $MgSO_4$ and filtered. The solvent was then evaporated to afford a light brown solid, which was purified by chromatography (1:9 EtOAc-hexane) to yield **176a** (1.62 g, 66%) as a colourless powder: mp 119 °C; ^{1}H NMR δ 1.72–1.87 (m, 4H), 2.10 (m, 2H), 3.76 (t, 1 H), 4.34 (d, 1H), 5.33 (d, 1H), 6.01 (s, 1H, disappears upon D_2O addition), 7.20 (s, 1H), 7.27–7.32 (m, 2H), 7.58 (d, J = 7.0 Hz, 1H), 7.64–7.66 (m, 1H), 9.58 (s, 1H, disappears upon D_2O addition); ^{13}C NMR δ 23.6, 26.1, 31.9, 70.0, 79.5, 109.3, 117.4, 120.9, 123.7, 124.1, 125.5, 127.7, 129.6, 143.4, 145.8; GCMS *m/z* (relative intensity) 244 (M^+, 100), 160 (35), 115 (50), 71 (80), 31 (40).

Procedure 2: Using PPTS as the catalyst

A stirred mixture of **164** (1.64 g, 10.0 mol) and PPTS (0.08 g, 0.3 mmol) in dry DCM (120 mL) was heated at reflux for 15 min to dissolve completely all reactants and added dropwise DHP (0.94 mL, 10 mmol) over 45 min. The reaction was stirred for a further 24 h. After the reaction mixture was cooled to room temperature, the organic layer was separated, washed with distilled water (1 x 50 mL), saturated aqueous NH_4Cl solution (2 x 50 mL), dried over anhydrous $MgSO_4$ and filtered. The solvent was removed under reduced pressure to leave a light brown solid, which was purified by chromatography (1:9 EtOAc-hexane) to yield (1.30 g, 53%) as a colourless powder having identical characterization data to that obtained from Procedure 1.

2-Hydroxy-3-(benzyloxy)naphthalene (176b) and 2,3-di(benzyloxy)-naphthalene (176d)

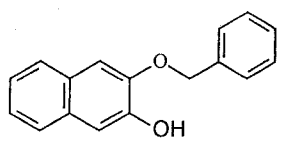

176b

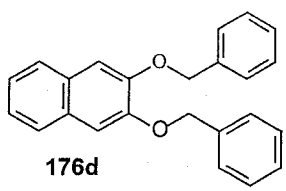

176d

Procedure 1: Using acetone as the solvent:

To stirred mixture of **164** (1.64g, 10.0 mmol) and K_2CO_3 (1.38 g, 10.0 mmol) in dry acetone (40 mL) at reflux, was added dropwise benzyl bromide (1.5 g, 8.6 mmol) over 1 h using a syringe pump. The reaction mixture was heated at reflux for a further 12 h. The solvent was removed under reduced pressure, and the resulting light yellow residue was dissolved in distilled water (100 mL) and

extracted with EtOAc (2 x 50 mL). The organic layer was washed with distilled water (2 x 50 mL), saturated aqueous NH_4Cl solution (1 x 50 mL), dried over anhydrous $MgSO_4$, and filtered. The solvent was then removed under reduced pressure to afford a yellow solid which was purified by chromatography (2:8 EtOAc-hexane) to yield **176d** (0.4 g, 12%) as a colourless powder: mp 139–140 °C; ^{1}H NMR δ 5.28 (s, 4H), 7.21 (s, 2H), 7.30–7.33 (m, 4H), 7.38 (t, *J* = 7.3 Hz, 4H), 7.51 (d, *J* = 7.5 Hz, 4H), 7.63–7.65 (m, 2H); ^{13}C NMR δ 71.0, 109.6, 124.8, 126.6, 127.4, 128.0, 128.7, 129.6, 137.3, 149.4; GCMS *m/z* (relative intensity) 340 (M^+, 10) 249 (15), 181 (10), 91(100), 65 (30). Further elution yielded **176b** (1.50 g, 69%) as a colourless powder: mp 85–87 °C (lit. yellow oil[5] or pale brown solid[6]); ^{1}H NMR 5.25 (s, 2H), 5.93 (s, 1H, disappears upon D_2O addition), 7.21 (s, 1H), 7.28 (s, 1H), 7.30–7.49 (m, 7H), 7.66 (d, *J* = 7.5 Hz, 2H); ^{13}C NMR 71.3, 107.3, 109.8, 124.1, 124.7, 126.6, 126.8, 128.2, 128.8, 129.0, 129.1, 130.0, 136.1, 146.0, 146.8; GCMS *m/z* (relative intensity) 250 (M^+, 20) 131 (25), 91 (100), 65 (30).

Procedure 2: Using DMF as the solvent:

To a stirred mixture of **164** (0.82 g, 5.00 mmol) and K_2CO_3 (0.70 g, 5 mmol) in dry DMF at 85–90 °C, was added dropwise benzyl bromide (0.75 g, 4.3 mmol) over 1 h using a syringe pump. The reaction mixture was stirred and heated at 85–90 °C for a further 5 h. After the solvent was evaporated under reduced pressure, the dark brown residue was poured into cold water (100 mL),

and extracted with EtOAc (2 x 50 mL). The organic layer was separated, washed with distilled water (2 x 50 mL) and saturated aqueous NH_4Cl solution (1 x 50 mL), dried over anhydrous $MgSO_4$ and filtered. The solvent was then evaporated to afford a brown solid, which was purified by chromatography (2:8 EtOAc-hexane) to yield **176b** (0.70 g, 64%) as a colourless powder having identical characterization data to those obtained from Procedure 1.

3-(2-Propenyloxy)-2-hydroxynaphthalene (176c)

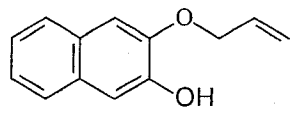

To a stirred mixture of **164** (1.64g, 10.0 mmol) and K_2CO_3 (1.38 g, 10.0 mmol) in dry acetone (40 mL) at reflux was added dropwise allyl bromide (1.07 g, 8.60 mmol) over 1 h using a syringe pump. The reaction mixture was heated at reflux for a further 12 h. After the solvent was removed under reduced pressure, the brown residue was dissolved in distilled water (100 mL), and extracted with EtOAc (2 x 50 mL). The organic layer was washed with distilled water (2 x 50 mL), saturated aqueous NH_4Cl solution (1 x 50 mL), dried over anhydrous $MgSO_4$, and filtered. The solvent was then removed under reduced pressure to give a yellow solid, which was purified by chromatography (5:95 EtOAc-hexane) to yield **176c** (1.31 g, 76%) as a yellowish liquid: ^{1}H NMR δ 4.66 (d, J = 5.0 Hz, 2H), 5.33 (d, J = 10.0 Hz, 1H), 5.42 (d, J = 17.5 Hz, 1H), 5.97 (d, J = 2.0 Hz, 1H, disappears upon D_2O addition), 6.04–6.12 (m, 1H), 7.07 (s, 1H), 7.26 (s, 1H),

7.27–7.31 (m, 2H), 7.62–7.64 (m, 2H); ^{13}C NMR δ 69.8, 107.2, 109.7, 118.9, 124.0, 124.6, 126.5, 126.7, 129.0, 129.9, 132.6, 145.9, 146.4; GCMS *m/z* (relative intensity) 200 (M^+, 100), 183 (35), 115 (55), 76 (30), 39 (30).

1,3-Bis(3-hydroxy-2-naphthyloxy)propane (179)

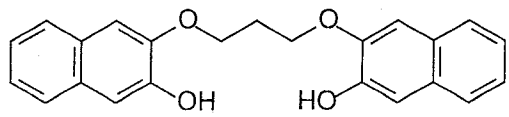

To a stirred mixture of **164** (1.64 g, 10.0 mmol) and K_2CO_3 (4.20 g, 30.0 mmol) in dry acetone (40 mL) at reflux was added dropwise 1,3-dibromopropane (**172**) (1.22 g, 6.00 mmol) over 1 h using a syringe pump. The reaction mixture was heated at reflux with stirring for a further 6 d. After the reaction mixture was cooled to room temperature and added distilled water (200 mL) to dissolve the K_2CO_3, the precipitate was filtered by suction filtration to yield **178** (1.35 g, 75%) as a colourless powder, which was purified by chromatography (4:6 EtOAc-hexane) to yield pure **179** (0.62 g, 34%) as a colourless powder for analytical work: mp 203–6 °C (dec.); ^{1}H NMR δ 2.53 (quintet, *J* = 6.0 Hz, 2H), 4.45 (t, *J* = 6.0 Hz, 4H), 5.86 (s, 2H, disappears upon D_2O addition), 7.16 (s, 2H), 7.29 (s, 2H), 7.30–7.34 (m, 4H), 7.66 (d, *J* = 8.0 Hz, 4H); ^{13}C NMR δ 29.2, 65.8, 107.0, 110.0, 124.2, 124.7, 126.6, 126.7, 129.1, 130.0, 145.7, 146.5; (+)-APCI MS *m/z* (relative intensity) 361.0 (M^+, 20), 201.1 (100).

Dinaphtho(*β*,*β*)-(b,i)-(1,4,8,11)-tetraoxacyclotetradecane (174)

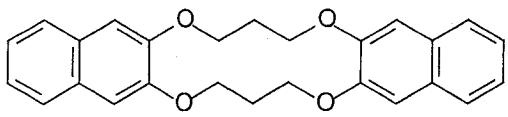

To a stirred mixture of **179** (0.36g, 1.00 mmol) and K_2CO_3 (0.83 g, 6.00 mmol) in dry acetone (70 mL) at reflux was added dropwise **172** (0.22 g, 1.10 mmol) in dry acetone (10 mL) over 2 h using a syringe pump. The reaction mixture was heated at reflux with stirring for a further 5 d. After the reaction mixture was cooled to room temperature and added distilled water (100 mL) to dissolve the K_2CO_3, the precipitate was filtered, and washed several times with distilled water to yield **174** (0.31 g, 77%) as a colourless powder which was chromatographically pure by TLC: mp 280 °C (dec.) (lit.[11] 278–279 °C); ^{1}H NMR δ 2.49 (t, br, J = 4.5 Hz, 4H), 4.38 (t, J = 4.8 Hz, 8H), 7.11 (s, 4H), 7.28–7.30 (m, 4H), 7.63–7.65 (m, 4H); ^{13}C NMR δ 29.0, 68.3, 107.7, 124.1, 126.4, 129.5, 149.8; (+)-APCI MS *m/z* (relative intensity) 401.1 (M^+,100) calcd.: 400.47 for $C_{26}H_{24}O_4$; GCMS *m/z* (relative intensity) 400 (M^+, 60), 241 (30), 200 (100), 171 (40).

1,6-Bis(3-hydroxy-2-naphthyloxy)hexane (180)

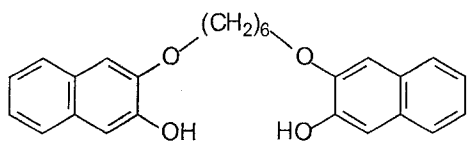

To a stirred mixture of **164** (3.28 g, 20.0 mmol) and K_2CO_3 (1.54 g, 11.0 mmol) in dry acetone (80 mL) at reflux, was added dropwise 1,6-dibromohexane (**171**) (2.16 g, 8.60 mmol) over 1 h using a syringe pump. The reaction mixture

was heated at reflux with stirring for a further 6 d. After the reaction mixture was cooled to room temperature and added distilled water (200 mL) to dissolve K_2CO_3, the precipitate was filtered by suction filtration and washed several with distilled water to yield **180** (3.46 g, 86%) as a light pink powder which was chromatographically pure by TLC: mp 199–201 °C (dec.); ^{1}H NMR δ 1.58 (s, br, 4H), 1.86 (s, br, 4H), 4.11 (t, *J* = 6.3 Hz, 4H), 7.13 (s, 2H), 7.23 (m, 4H) 7.26 (s, 2H), 7.59 (d, *J* = 7.5 Hz, 2H), 7.65 (d, *J* = 8.0 Hz, 2H), 9.29 (s, 2H, disappears upon D_2O addition); ^{13}C NMR δ 25.4, 28.6, 67.9, 107.4, 109.5, 122.8, 123.5, 125.3, 126.2, 128.4, 129.2, 147.5, 148.4; (–)-APCI MS *m/z* (relative intensity) 402.1 ([M+H]$^-$, 30), 401.2 (M$^-$, 100), calcd.: 400.5 for $C_{26}H_{24}O_4$.

Dinaphtho(*β*,*β*)-(b,l)-(1,4,11,14)-tetraoxacycloeicosane (170)

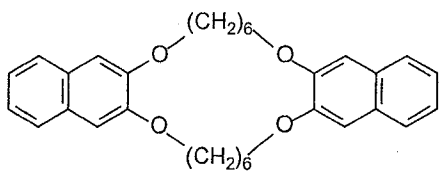

To a stirred mixture of **179** (0.53 g, 1.30 mmol) and K_2CO_3 (7.09 g, 7.80 mmol) in dry DMF (100 mL) at 85–90 °C for 1 h was added dropwise 1,6-dibromohexane (0.35 g, 1.4 mmol) in dry DMF (20 mL) over 2 h using a syringe pump. The reaction mixture was heated at 85–90 °C with stirring for a further 5 d. After the solvent was completely removed under reduced pressure, the brown residue was washed several times with distilled water and methanol (200 mL) to yield **170** (0.31 g, 49%) as a colourless powder which was chromatographically

pure by TLC: mp 253–254 °C; ^{1}H NMR δ 1.68–1.71 (m, 8H), 1.93 (s, br, 8H), 4.11 (t, *J* = 6.0 Hz, 8H), 7.13 (s, 4H), 7.29–7.31 (m, 4H), 7.64–7.66 (m, 4H); ^{13}C NMR δ 26.8, 30.1, 69.3, 109.0, 124.1, 126.4, 129.7, 150.1; (+)-APCI MS *m/z* (relative intensity) 485.2 (M^+, 70) calcd.: 484.6 for $C_{32}H_{36}O_4$, 415 (60), 243 (100).

Tetrakis(bromomethyl) cyclic ether 169

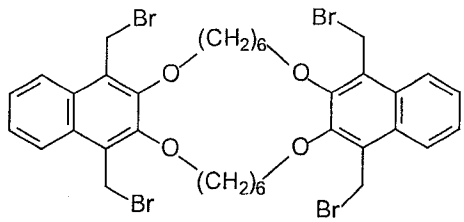

To a stirred suspension of **170** (0.53 g, 1.09 mmol) and paraformaldehyde (1.65 g, 52.5 mmol) in glacial acetic acid (150 mL) at 75–80 °C was added dropwise a solution of HBr in glacial acetic acid (30 wt %, 0.50 mL, 53 mmol of HBr and 5 mL AcOH). After heating at 75–80 °C with stirring for a further 7 d, to the reaction mixture was added another portion of solution of HBr in glacial acetic acid (30 wt %, 3 mL), and also paraformaldehyde (0.53 g, 16.8 mmol), and the reaction mixture was stirred for another 7 d. After cooling to room temperature, the reaction mixture was poured into cold water (200 mL). The resulting precipitate was filtered, washed with distilled water several times, aqueous 5% $NaHCO_3$ (2 x 50 mL), and finally with distilled water, until the washings were neutral to pH paper, and air dried to yield **169** (0.90 g, 96%) as a colourless powder: mp > 205 °C (dec.); ^{1}H NMR δ 1.73 (s, br, 8H), 2.04 (m, 8H), 4.21 (t, *J* = 6.8 Hz, 8H), 5.04 (s, 8H), 7.58–7.60 (m, 4H), 8.06–8.09

(m, 4H); (+)-APCI MS *m/z* (relative intensity) 777 ($M^+ - {}^{81}Br$, 99), 775 ($M^+ - {}^{79}Br$, 100) M^+ calcd.: 856.33 for $C_{36}H_{40}Br_4O_4$.

Tetrakis(hydroxymethyl) cyclic ether 168

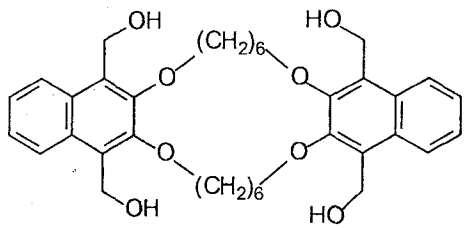

A mixture of **168** (240.0 mg, 0.28 mmol) and $CaCO_3$ (1.00 g, 10.0 mmol) in aqueous 50% dioxane (80 mL) was heated at reflux with stirring for 5 d. After the solvent was completely removed under reduced pressure, the residue was acidified with aqueous 20% HCl until the pH reached 2. The resulting precipitate was filtered, washed with distilled water until the washings were neutral to pH paper, and air dried. The crude product was then washed with 1:9 EtOAc-hexane (5 x 50 mL) and dried at 50 °C to yield **168** (168.4 mg, 99%) as a colourless powder which was chromatographically pure by TLC: mp > 300 °C (dec.); ^1H NMR δ 1.65 (s, br, 8H), 1.92 (s, br, 8H), 4.00 (t, J = 6.0 Hz, 8H), 4.93 (d, J = 4.0 Hz, 8H), 5.06 (t, J = 5.3 Hz, 4H, disappears upon D_2O addition), 7.45–7.47 (m, 4H), 8.15–8.17 (m, 4H); (+)-APCI MS *m/z* (relative intensity) 603.5 (M^+, 5) calcd.: 604.3 for $C_{36}H_{44}O_8$.

6.6 References

1. Alfieri, C.; Dradi, E.; Pochini, A.; Ungaro, R.; Andreetti, G. D. *J. Chem. Soc., Chem. Commun.* **1983**, 1075-1077.

2. Tran, A. H.; Miller, D. O.; Georghiou, P. E. *J. Org. Chem.* **2005**, *70*, 1115-1121.

3. Computer-assisted molecular modeling was conducted using Spartan'04, V1.0.3 from Wavefunction, Inc., Irvine, CA, USA. Calculations were conducted at the PM3 level of theory.

4. Artico, M.; Di Santo, R.; Costi, R.; Novellino, E.; Greco, G.; Massa, S.; Tramontano, E.; Marongiu, M. E.; De Montis, A.; La Colla, P. *J. Med. Chem.* **1998**, *41*, 3948-3960.

5. Ralph, J.; Zhang, Y.; Ede, R. M. *J. Chem. Soc., Perkin Trans. 1*, **1998**, 2609-2613.

6. Kameta, N.; Hiratani, K.; Nagawa, Y. *Chem. Commun.* **2004**, 466-467.

7. Bolchi *et al.* reported, in 2004, the use K_2CO_3 in DMF furnished 2-hydroxy-3-benzyloxynaphthalene (**611b**) in 69% yield: Bolchi, C.; Catalano, P.; Fumagalli, L.; Gobbi, M.; Pallavicini, M.; Pedretti, A.; Villa, L.; Vistoli, G.; Valoti, E. *Bioorg. Med. Chem.* **2004**, *12*, 4937-4951.

8. (a) Tsubaki, K.; Fuji, K.; Tanaka, H.; Morikawa, H. *Jpn. Kokai Tokkyo Koho* **2005**, 5. (b) Tsubaki, K.; Morikawa, H.; Tanaka, H.; Fuji, K. *Tetrahedron: Asymm.* **2003**, *14*, 1393-1396. (c) Weber, E.; Koehler, H. J.; Reuter, H. *Chem. Ber.* **1989**, *122*, 959-967.

9. Colquhoun, H. M.; Goodings, E. P.; Maud, J. M.; Stoddart, J. F.; Wolstenholme, J. B.; Williams, D. J. *J. Chem. Soc., Perkin Trans. 2*, **1985**, 607-624.

10. (a) Pedersen, C.J. *Org. Synth., Coll.* **1988**, *VI*, 395-400. (b) Pedersen, C.J. *J. Am. Chem. Soc.***1967**, *89,* 7017-7036.

11. These references were found recently using SciFinder: (a) Smolinski, S.; Nowicka, J.; Mokrosz, J.; Jamrozik, M.; Jaworski, M.; Wiekieva, E. *Tetrahedron* **1977**, *33,* 1219-1226. (b) Ben Chaabane, T.; Hadou, A. Ould; Meganem, F. *J. Chem. Cryst.* **2000**, *30*, 459-462.

Chapter 7

Synthesis of homothiaisocalix[*n*]naphthalenes and their binding properties

7.1 Introduction

7.1.1 Thiacalixarenes and Homothiacalixarenes

Thiacalixarene **186** is an example of a calixarene in which the methylene bridges between the aromatic units has been replaced by four sulfur atoms.[1,2] These compounds and their derivatives[3] have attracted considerable interest due to their potential applications as molecular hosts for several different soft-to-intermediate hardness metal (*e.g.* Ag^{+}, Zn^{2+}, Cd^{2+}, Hg^{2+}), and alkali or alkali earth metal ions, respectively.[1-4] They have been prepared by either a one-step[5] procedure, from *p-tert*-butylphenol and sulfur, or from a multi-step[6] process via the linear tetramer **187** (Scheme 7.1).

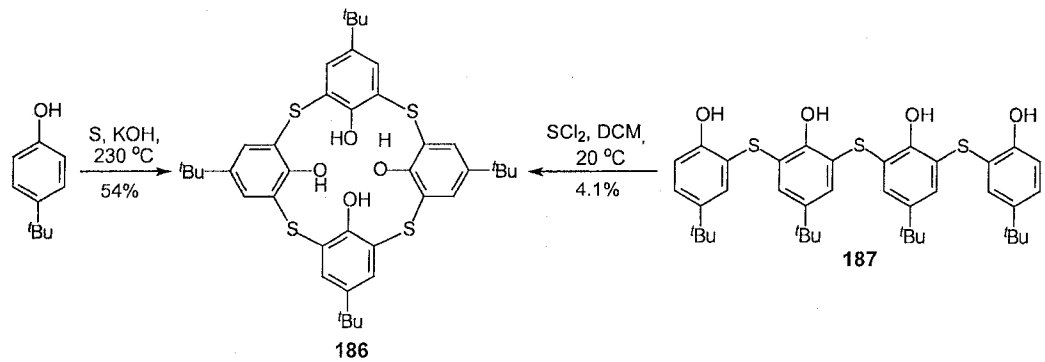

Scheme 7.1 Synthesis of thiacalix[4]arene **186**.

Homothiacalixarenes, for example **188** and **189a-c** (Figure 7.1),[7,8] are also examples of calixarenes, but in such compounds, the methylene bridges between the aromatic units are partly or completely replaced by various alkylthia or alkyldithia groups. To date, homothiacalixarenes, and the analgous homothiacalixnaphthalenes, have received much less attention than calixarenes.

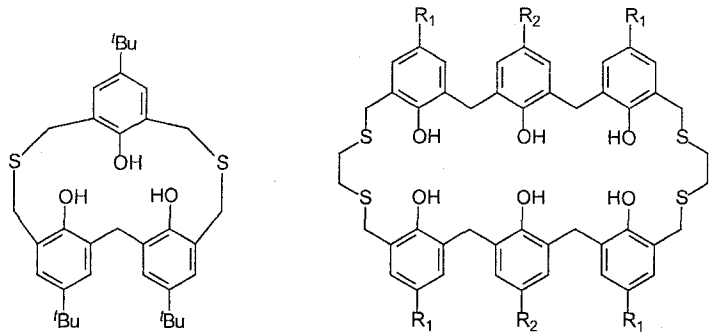

188

189a R_1, R_2 = ^{t}Bu
189b R_1, R_2 = Me
189c R_1= Me, R_2 = ^{t}Bu

Figure 7.1 Examples of *n*-homothiacalixarenes.

In the early 1990s, Tsuge *et al.*[6] reported that under high dilution and basic conditions, both [1+1] coupling reactions of either 2,6-bis(chloromethyl)-4-*tert*-butylanisole (**190**) and bis(3-mercaptomethyl-2-methoxy-5-*tert*-butyl)methane (**191**), or bis(3-chloromethyl-2-methoxy-5-*tert*-butyl)methane (**192**) and 2,6-bis(mercaptomethyl)-4-*tert*-butylanisole (**193**) gave tetrahomodithiacalix[3]arene **194** in synthetically useful yields (Scheme 7.2).

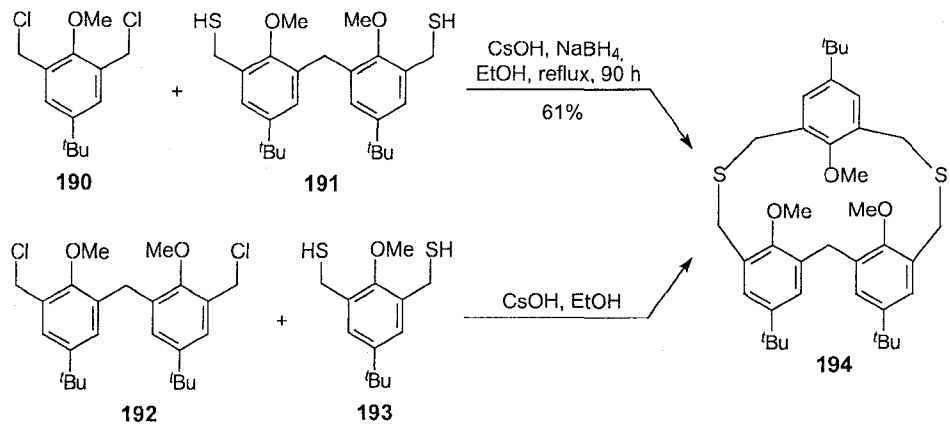

Scheme 7.2 Synthesis of tetrahomothiacalix[3]arene **194**.

In 2000, Ito *et al.* reported the synthesis of analogues of decahomotetrathiacalix[6]arenes **197a-c** from [2+2] cyclizations of 1,2-ethanedithiol (**195**) and *p*-substituted bis(chloromethyl)phenol-formaldehyde trimers **196a-c**, respectively, under very mild conditions (Scheme 7.3) in high yields.[7]

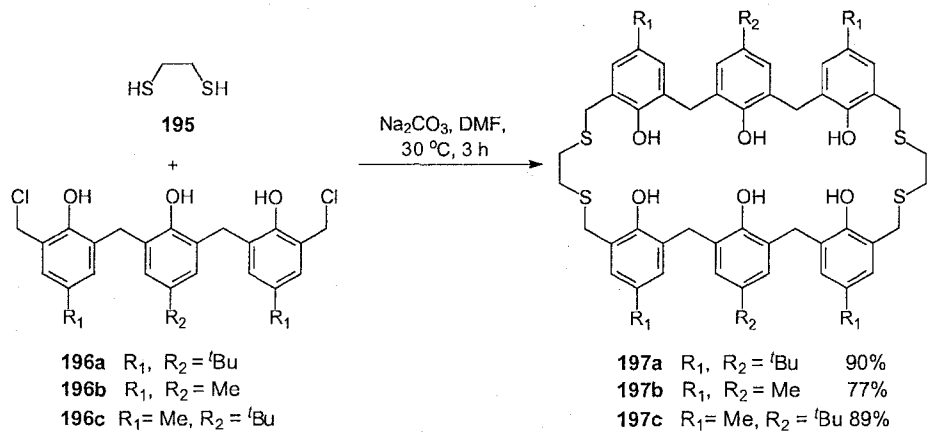

Scheme 7.3 Synthesis of decahomotetrathiacalix[6]arenes **197a-c**.

They also reported the synthesis of hexahomodithiacalix[3]arenes **199a-c** via a coupling reaction between **196a-c** with 1,3-propanedithiol (**198**) under identical conditions (Scheme 7.4).

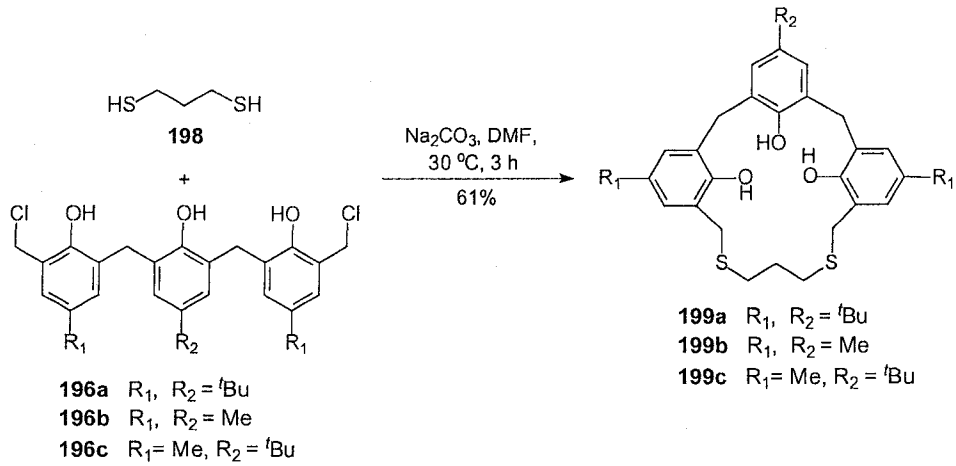

Scheme 7.4 Synthesis of hexahomodithiacalix[3]arenes **199a-c**.

Recently, Kohno and Yamato *et al.* reported[9] that a [1+1] base-mediated coupling of **193** and bis[(5-*tert*-butyl-3-chloromethyl-2-methoxyphenyl)methyl] sulfide (**200**) in refluxing ethanol-benzene over 72 h afforded hexahomotrithiacalix[3]arene **201** in 32% yield (Scheme 7.5).

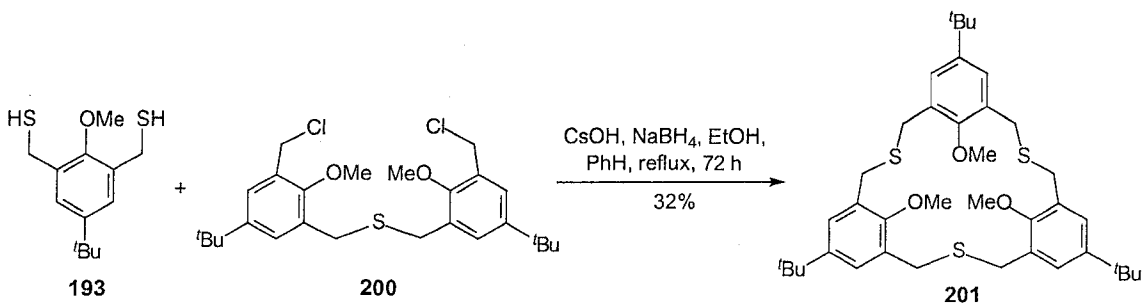

Scheme 7.5 Synthesis of hexahomotrithiacalix[3]arenes **201**.

Compound **201** was shown to be a selective host for Ag^+ among the metal picrates studied[9] which included Na^+, K^+, Cs^+, Ag^+, Ba^{2+}, Co^{2+}, Cd^{2+}, Pb^{2+}, Cu^{2+}, Ni^{2+}, Zn^{2+}, Al^{3+}, Tl^{3+}, Cr^{3+}. The percent extraction (%*E*) from aqueous solution into DCM reported for Ag^+ by **201** was 44% while the %*E* for the others were smaller than 6%.[9]

Recently, Ashram reported[10] the synthesis of hexahomotrithiacalix[3]-arenes **204a-c** via the [1+1] cyclization of 2,6-bis(chloromethyl)-4-*tert*-butylphenol (**202a-c**) and the bis(3-chloromethyl-2-hydroxy)dimethylsulfides **203a-c**, respectively, under high-dilution conditions, in the presence of $Na_2S{\cdot}9H_2O$ in high yields (Scheme 7.6).[10] In addition, **204a** was also afforded in 51% yield via the one-pot reaction of 2,6-bis(chloromethyl)-4-*tert*-butylphenol (**202a**), itself, under identical conditions.

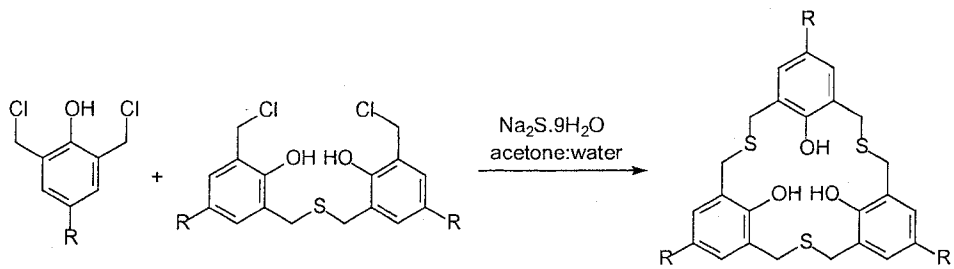

202a R = ^{t}Bu
202b R = Me
202c R = H

203a R = ^{t}Bu
203b R = Me
203c R = H

204a R = ^{t}Bu, 93%
204b R = Me, 60%
204c R = H, 43%

Scheme 7.6 Synthesis of hexahomotrithiacalix[3]arenes **204a-c**.

p-tert-Butylhexahomotrithiacalix[3]arene **204a** was employed to extract alkali metal (Li^+, Na^+, K^+, Rb^+ and Cs^+) and other metal (Cr^{3+}, Mn^{2+}, Co^{2+}, Ni^{2+}, Cu^{2+}, Zn^{2+}, Ag^+, Cd^{2+}, Hg^{2+}, and Pb^{2+}) picrates from aqueous solution into $CHCl_3$.

The percentage efficiencies of the extractions by **204a** were less than 7% in all cases.[10] In contrast, its ether derivative **201** bound Ag^+ with high selectivity. This indicated that the methoxy group has enhanced the interaction between the oxygen atoms and Ag^+ ion to allow binding from the narrow rim. This trend will be discussed subsequently in the host-guest studies reported in this Chapter with octahomotetrathiaisocalix[4]naphthalenes synthesized in this study.

7.1.2 Homothiacalixnaphthalens

The Georghiou group have reported the synthesis of tetrahomo- **30**, **31**, **111**, **117** and hexahomodithiacalix[4]naphthalenes **121** (Figure 7.2) from the [1+1] coupling reactions between corresponding bis(mercaptomethyl)-naphthalene precursors **107**, **108**, **115** or **119** with bis(bromomethyl)naphthalene precursors **109**, **110**, **116** or **120** (Chapter 4, Scheme 4.4–4.6), respectively, under base-mediated high dilution conditions.[11,12,13]

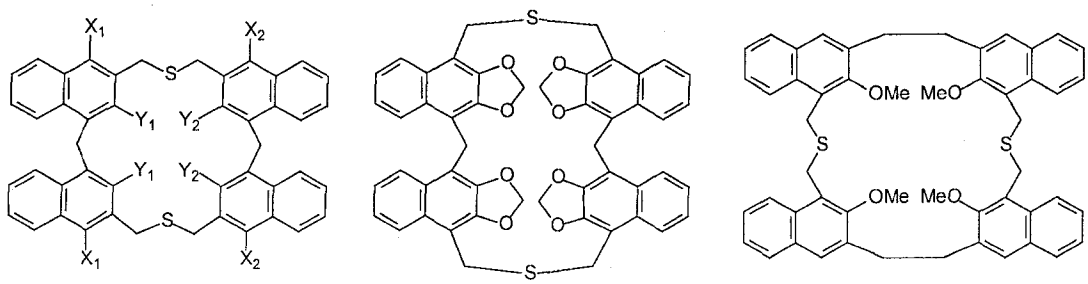

30 X_1, X_2 = OMe, Y_1, Y_2 = H
31 X_1, Y_2 = OMe, X_2, Y_1 = H
111 X_1, X_2 = H, Y_1, Y_2 = OMe

117

121

Figure 7.2 Tetrahomo- **30**, **31**, **111**, **117** and hexahomodithiacalix[4] naphthalenes **121**.

The above homodithiacalix[4]naphthalenes were used as precursors for the syntheses of the corresponding homocalix[4]naphthalenes via the extrusion of the sulfur atoms. Upon treatment with $AgNO_3$ in THF, **30** and **31** formed 1:1 complexes with silver nitrate.[14] However, a detailed complexation study was not reported at the time.

Since the X-ray structure showing the formation of a stable solid 2:1 complex of hexahomotrioxacalix[3]naphthalene (**43**) and C_{60} has been obtained and reported and also because **43** (Figure 7.3) was shown to also be a good host for C_{60} in toluene solutions,[15] we have continued to be interested in the preparation of novel hosts similar to **43** for the complexation of C_{60} and C_{70} fullerenes. The initial solution complexation study of octahomotetraoxaisocalix[4]-naphthalenes **159a** and **159b** indicated that although they were not suitable hosts for the electron-deficient neutral guest molecules, C_{60}- and C_{70}-fullerenes, they were good hosts for tetramethylammonium cation under identical conditions (Figure 7.3).[16]

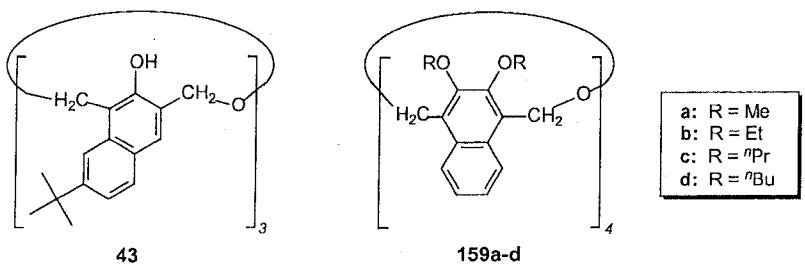

Figure 7.3 Hexahomotriooxacalix[3]naphthalenes **43** and octahomooxaisocalix[4]naphthalenes **159a-d**.

Furthermore, we had previously observed that sulfur atoms in the thiocorannulene derivatives **48**–**53** apparently enhance the binding to fullerenes (Figure 7.4, Chapter 2).[17] Therefore, in order to create new receptors having affinity towards C_{60} or other electron-deficient guests, we hypothesized that replacement of the $-CH_2OCH_2-$ bridges of **159a-d** by $-CH_2SCH_2-$ bridges might produce more electron-rich analogues **205a-d** (Figure 7.5).[18]

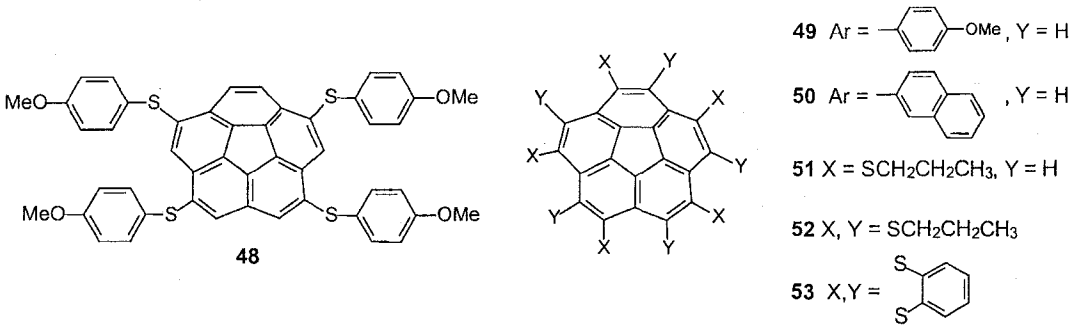

Figure 7.4 Thiocorannulene derivatives **48**–**53**.

In this Chapter the synthesis of **205a-d** and the complexation properties of **205a** and **205b** with Ag^+ are reported. The syntheses of the larger cavity-containing macrocyles, *e.g.* **206b**, **206c**, **207** and **208** (Figure 7.5) are described in this Chapter as well.

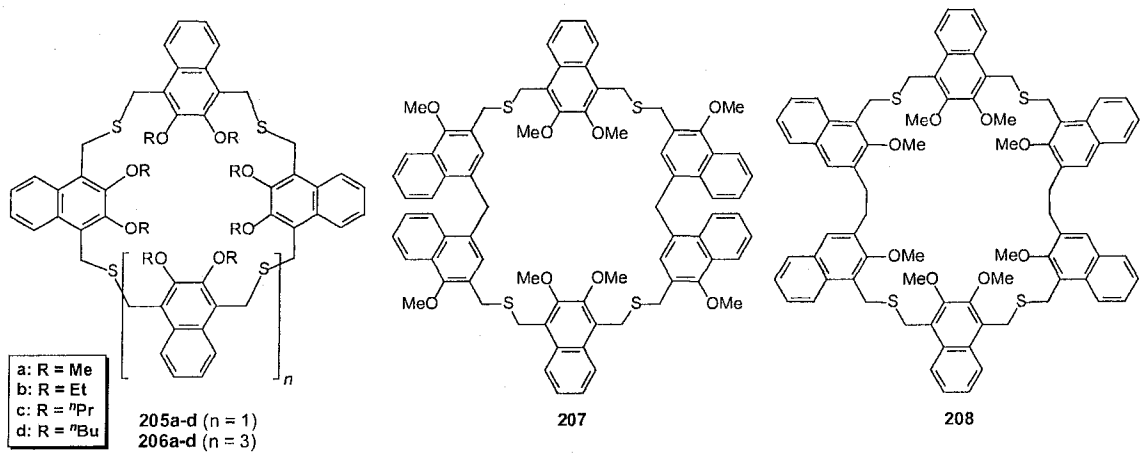

Figure 7.5 Homothiacalix[*n*]naphthalenes **205**–**208**.

7.2 "1,4-Linked" homothiaisocalix[*n*]naphthalenes derived from 2,3-dihydroxynaphthalene

7.2.1 Design of target strutures

Since sulfur has a lower electronegativity and is more polarizable than oxygen, the former can donate its non-bonding electron pair more easily than the latter. Therefore, it was anticipated that replacement of the $-CH_2OCH_2-$ bridges in homooxaisocalix[4]naphathlenes **159a-d** by $-CH_2SCH_2-$ bridges would provide new analogues, the corresponding "1,4-linked" octahomotetrathia-calix[4]naphthalenes **205a-d** ("tetrathia[3.3.3.3](1,4)naphthaleneophanes"), which potentially would be better hosts for electron deficient guests such as fullerenes than **159a-d**.

Both the CPK molecular model and a computer-aided molecular modeling study[19] (Figure 7.6) suggested that a molecule such as **205b** might be an attractive candidate receptor for fullerenes as well as for some cationic guests. The molecular modeling observations also revealed that although **205b** was conformationally flexible, the π-π van der Waals interactions between the electron-rich naphthalene units in **205b** with the electron-poor fullerenes could result in its conformational reorganization enabling it to adopt a conformation which could allow, fullerene encapsulation. The syntheses of these new compounds were therefore undertaken.

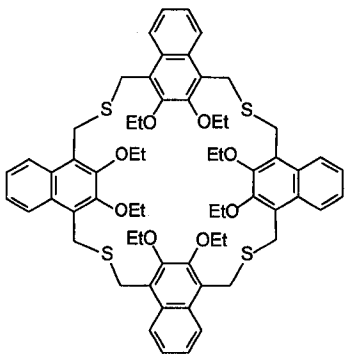

205b

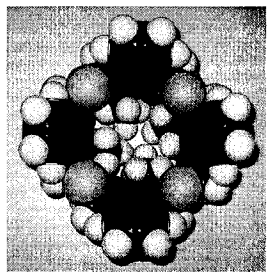

View of 205b looking down the cavity of cone conformer

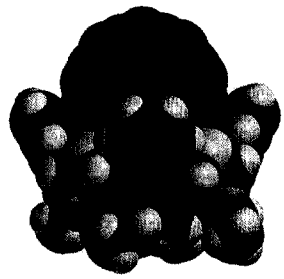

a 1:1 complex of 205b and C_{60}

Figure 7.6 Structure (*left*), CPK model of **205b** (*middle*), and computer-generated models of a 1:1 complex of **205b** and C_{60} (*right*).

7.2.2 Retrosynthetic analysis

The retrosynthetic analysis outlined in Scheme 7.7 indicated that the thia-crown ether-analogous macrocycles **205a-d** and **206a-d**, could be afforded via base-mediated cross-coupling reactions between 1,4-bis(mercaptomethyl)-2,3-dialkoxynaphthalenes (**209a-d**) and 1,4-bis(bromomethyl)-2,3-dialkoxy-naphthalenes (**162a-d**), respectively (Scheme 7.7). Intermediates **209a-d** could be furnished from bis(mercaptolations) of **162a-d**, respectively, which in turn were derivable directly from commercially-available 2,3-dihydroxynaphthalene (**164**). CPK molecular models of either the *syn* or *anti* conformers of [3.3](1,4)naphthalenophanes which could result from [1+1] coupling reactions of **162a-d** and **209a-d**, respectively, suggested that in addition to the steric hindrance presented by the pairs of ortho alkoxy groups on each of the naphthalene rings, that the presence of two $-CH_2SCH_2-$ groups would result in too much steric strain, and thus prevent the formation of such products. As a

result, the calix[4]- and/or calix[6]- products was suggested be favoured over any smaller calix[2]- type products.[20]

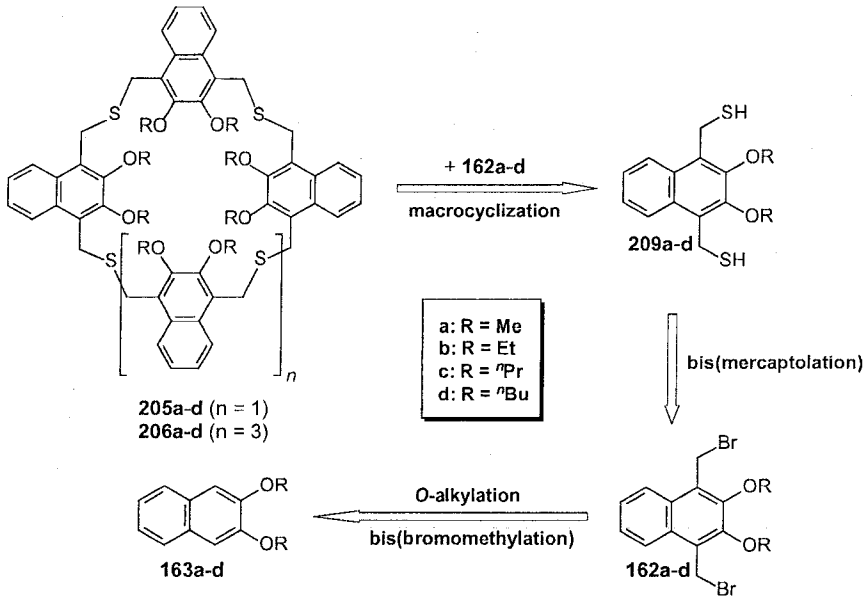

Scheme 7.7 Retrosynthetic analysis of "1,4-linked" homooxaisocalix[*n*]-naphthalenes **205a-d** and **206a-d**.

7.2.3 Results and discussion

7.2.3.1 Synthesis

Employment of Bodwell's one-pot procedure[21] for the reaction 1,4-bis(bromomethyl)-2,3-dialkoxynaphthalenes (**162a-d**) with Na_2S/Al_2O_3 at ambient temperature resulted in no desired product formation but only decomposition of starting material upon heating. Therefore, an alternative procedure involving [2+2] coupling reactions between **162a-d** and 1,4-bis(mercaptomethyl)-2,3-dialkoxynaphthalenes (**209a-d**), respectively, was employed (Scheme 7.8).

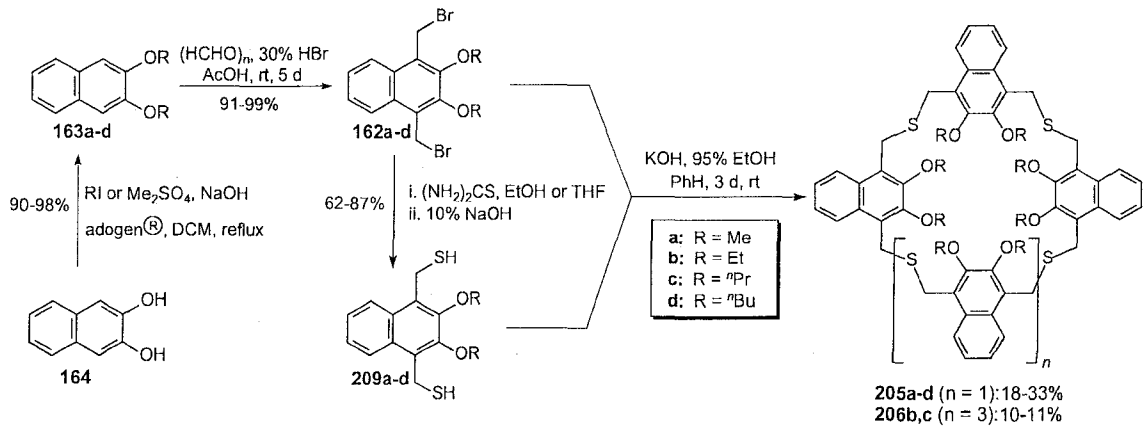

Scheme 7.8 Synthesis of "1,4-linked" homothiaisocalix[*n*]naphthalenes **205a-d, 206b and 206c.**

Treatment of **162a-c** with thiourea, followed by hydrolysis under basic conditions gave intermediates **209a-c** respectively, in 62-87% yields. Unexpectedly, bis(mercaptolation) of **162d** in THF either at ambient temperature or at reflux temperatures gave the crude products as resinous mixtures, which after purification by chromatography afforded **209d** in very low yield (2.5%). Use of 95% EtOH as the reaction solvent, however, produced **209d** in a much better yield (62%). Coupling reactions using equimolar amounts of **162a-d** and **209a-d**, respectively, under basic conditions gratifyingly afforded the corresponding "1,4-linked" octahomotetrathiaisocalix[4]naphthalenes (**205a-d**) in 18-33% isolated yields. Along with these cyclic tetrameric products, "1,4-linked" dodecahomo-hexathiaisocalix[6]naphthalenes (or "hexathia[3.3.3.3.3.3](1,4)naphthaleno-phanes"), **206b** and **206c** were also isolated in 10 and 11% yields, respectively. On TLC, the calix[4]naphthalenes **205b** and **205c** are less polar than the corresponding calix[6]naphthalenes **206b** and **206c**. (+)-APCI MS analysis of

205a-d, **206b** and **206c** all showed molecular ion peaks in agreement with the calculated mass values. As expected, none of the dimeric "[3.3](1,4)naphthaleno-phanes" products were isolated due to steric hindrance.[20]

The unsuccessful synthesis of **205e** and **206e** (Scheme 7.9) could presumably be due to, among other factors, the low solubilities of precursors **162e** and **209e** under conditions previously employed for **205a-d**.

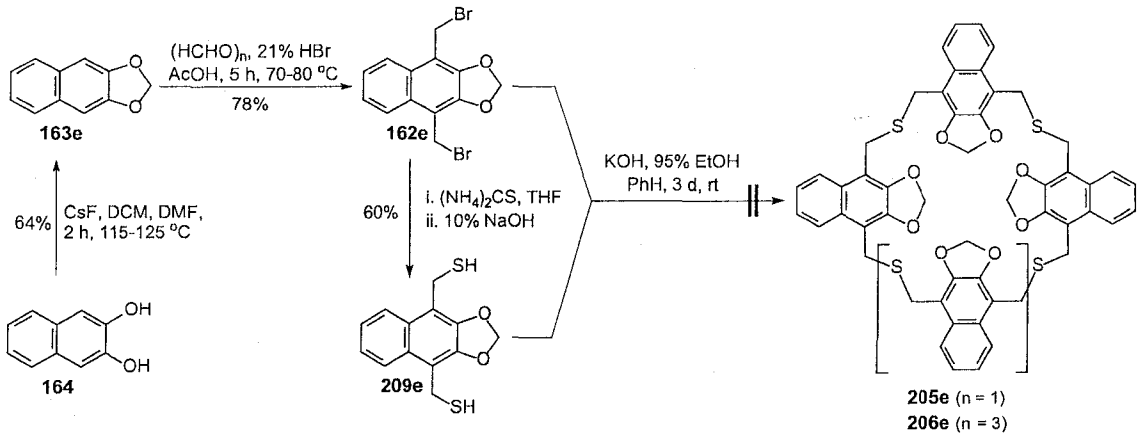

Scheme 7.9 Attempted syntheses of "1,4-linked" homothiaisocalix[*n*]-naphthalenes **205e** and **206e**.

7.2.3.2 Characterization of 205a-d

All of the new macrocyclic compounds **205a-d** had relatively simple ^{1}H NMR spectra at ambient temperature which indicated that they were highly symmetrical. Rapid conformational equilibration in solution at ambient temperature was obvious from the fact that all of the signals were sharp, and that the bridging methylene groups of **205a-d** appeared as singlets at δ 4.30, 4.30, 4.28 and 4.27 ppm, respectively. This is similar to what was also observed with the bridging methylene groups (singlets at δ 5.04-5.05 ppm) of homooxaiso-

calix[4]naphthalenes **159a-d**, which were previously synthesized (Chapter 5). The bridging methylene groups of the homothia analogues **205a-d** were shifted further upfield than those of the homooxa analogues **159a-d**. This indicates that the formers have more electron rich bridges than those of the latters.

When the chemical shifts of the alkoxy protons in the spectra of **205a-d** were compared with those of their respective precursors, only in the cases of **205a** and **205b** were there any significant differences. The position of the CH_3 signal of the methoxy groups in **205a** at δ 3.65 ppm is shifted upfield from that of the corresponding signals in the precursors **162a**, **163a** and **209a**, which are all at approximately δ 4.00 ppm. The positions of the CH_2 and the CH_3 groups of the ethoxy groups in **159b** at δ 4.06 and 1.39 ppm, respectively, are shifted upfield from the corresponding signals of the precursors **162b**, **163b**, and **209b**, which appear at approximately δ 4.22 and 1.48–1.54 ppm, respectively. These indicate that in $CDCl_3$ solution, the small alkoxy groups such as methoxy and ethoxy groups in **205a** and **205b** could be partially shielded by the "partial cavities" created by the other three naphthalene units. By contrast, the changes in the corresponding chemical shifts in **205c** and **205d** relative to their precursors were less than 0.10 ppm presumably due to less shielding of the larger alkoxy groups, *e.g. n*-propoxy and *n*-butoxy groups, by the naphthalene units.

A search for the lowest energy conformer (using molecular modeling with MMFF94 minimization prior to geometry optimization at the PM3 level of the theory)[19] conducted on **205a-d** revealed that their *flattened pinched-cone*

conformations (Figure 7.7), which are almost similar to that of "Zobarene" **159b** (Chapter 5), are of the lowest energy.

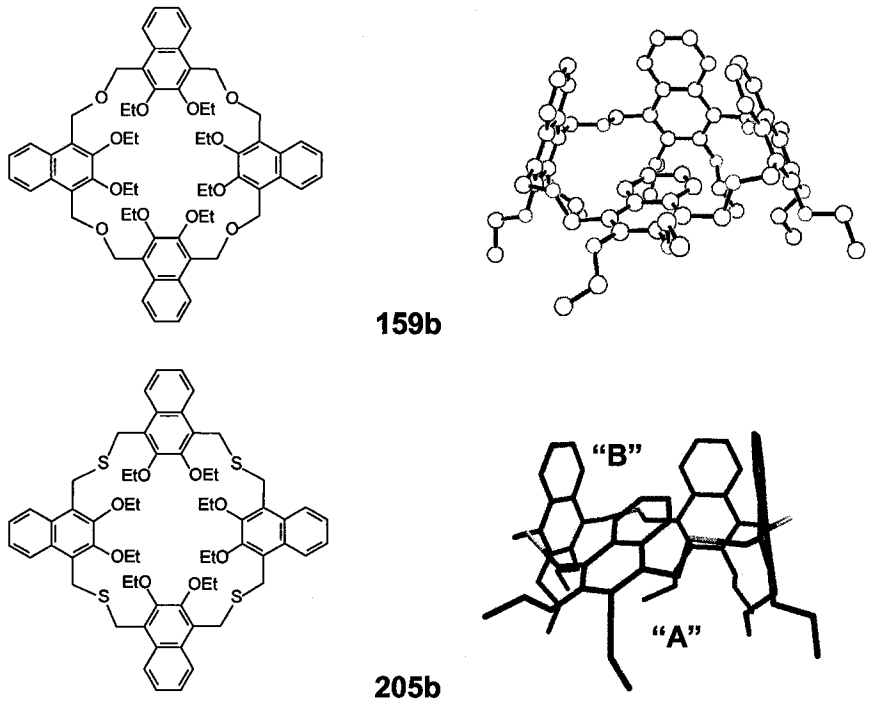

159b

205b

Figure 7.7 Structure and X-ray structure of **159b** showing its *flattened partial-cone* conformation (*top*), structure and computer-generated[19] lowest energy conformer of **205b** (bottom).

In this conformation one naphthyl sub-unit is tilted toward the distal naphthyl unit of the other three sub-units, forming two "partial cavities". One on the top labeled "B", and one at the opposite end labelled "A". The partial cavity A is defined by the space that contains the alkoxy groups of the three near-perpendicular naphthyl sub-units while the partial cavity (B) is defined by the space between the unsubstituted rings of these naphthyl sub-units. This conformer is presumably stabilized by the edge-to-face π–π^* interactions between these naphthalene units.

7.3 Octahomotetrathiaisocalix[6]naphthalene 207 derived from 1-naphthol and 2,3-dihydroxynaphthalene

7.3.1 Retrosynthetic analysis

Retrosynthetic cleavage at the indicated bonds of the cyclic thiaether **207** revealed bis(bromomethyl)naphthalene **210** and bis(mercaptomethyl)-naphthalene **209a** as potential precursors (Scheme 7.10) for a base-mediated [2+2] coupling reaction. Bis(bromomethyl)naphthalene **210**[22] was derived from readily-available 1-naphthol while 1,4-bis(mercaptomethyl)-2,3-dimethoxy-naphthalene **209a** was afforded from 2,3-dihydroxynaphthalene (Scheme 7.8).

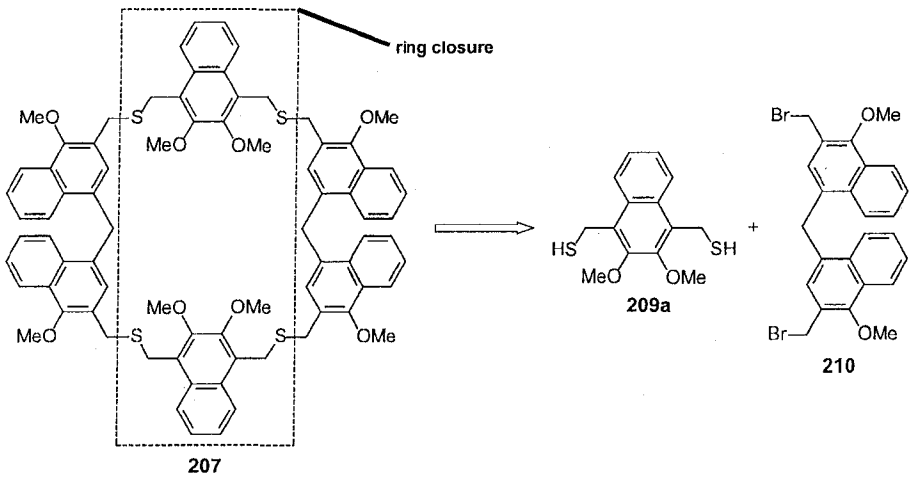

Scheme 7.10 Retrosynthetic analysis of octahomotetrathiaisocalix[6]-naphthalene **207**.

7.3.2 Synthesis and characterization

The synthesis of tetrahomotetrathiaisocalix[6]naphthalene **207** was accomplished as depicted in Scheme 7.11. Methylation[12] of 1-naphthol (**211**) under basic conditions (75% yield), followed by an acid-catalyzed condensation

with paraformaldehyde afforded bis(4-methoxy-1-naphthyl)methane (**213**) in 73% yield.[22] Bis(bromomethylation) of **213** with paraformaldehyde and 31% HBr in AcOH, furnished the desired key intermediate **210**[22a] in a reasonable yield (39%). The yield of this bis(bromomethylation) was lower than usual due to the formation of several unidentified side-products.

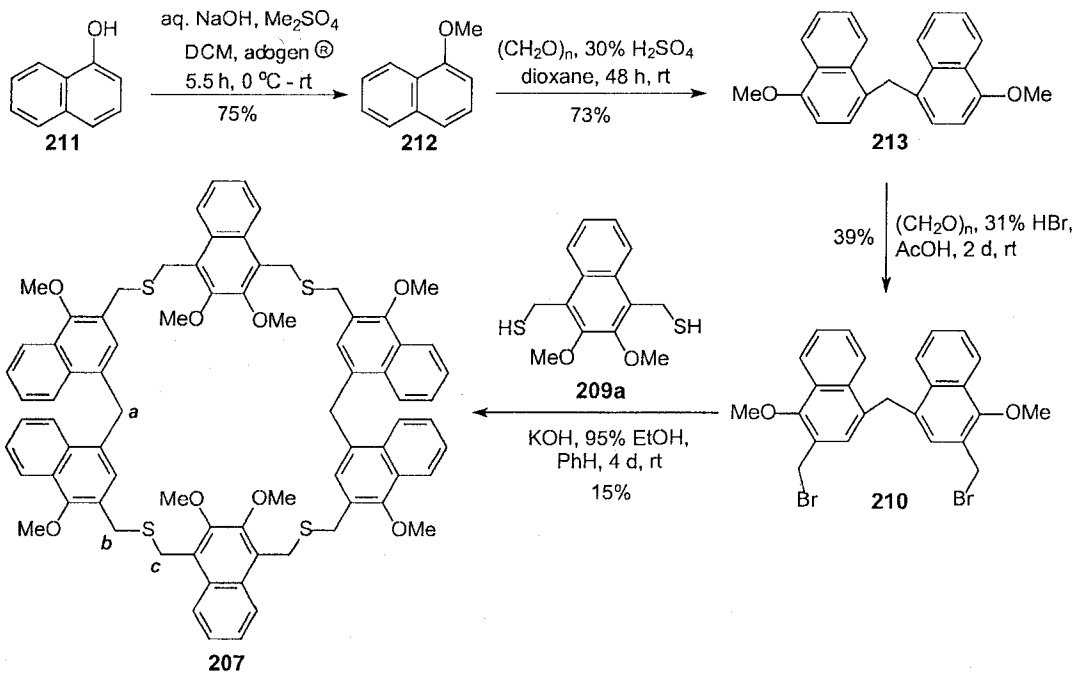

Scheme 7.11 Synthesis of octahomotetrathiaisocalix[6]naphthalene **207**.

Finally, the desired macrocylic **207** was afforded in 15% yield via a base-mediated coupling reaction of the corresponding bis(mercaptomethyl)-naphthalene **209a** and bis(bromomethyl)naphthalene **210** intermediates. (+)-APCI MS analysis showed the molecular ion peak at *m/z* = 1266.4 (80%) (calcd. 1265.7 for $C_{78}H_{72}O_8S_4$).

Tetrathia compound **207** has a relatively simple ^{1}H NMR spectrum at ambient temperature which shows three singlets at approximately δ 3.83, 3.92 and 4.77 ppm for the following three bridging methylene groups (a-c): $ArCH_{2a}Ar$ and $Ar\text{-}CH_{2b}SCH_{2c}\text{-}Ar'$, respectively (Scheme 7.11). In addition, **207** was highly symmetrical and all of the ^{1}H NMR signals were sharp, which indicated rapid conformational equilibration in solution at ambient temperature.

7.4 Decahomotetrathiaisocalix[6]naphthalene 208 derived from 3-hydroxy-2-naphthoic acid and 2,3-dihydroxynaphthalene

7.4.1 Retrosynthetic analysis

Retrosynthetic disassembly of **208** as outlined in Scheme 7.12 provided bis(bromomethyl)naphthalene **214** and 1,4-bis(mercaptomethyl)-2,3-dimethoxy-naphthalene (**209a**) as potential precursors for a [1+1] base-mediated coupling reaction.

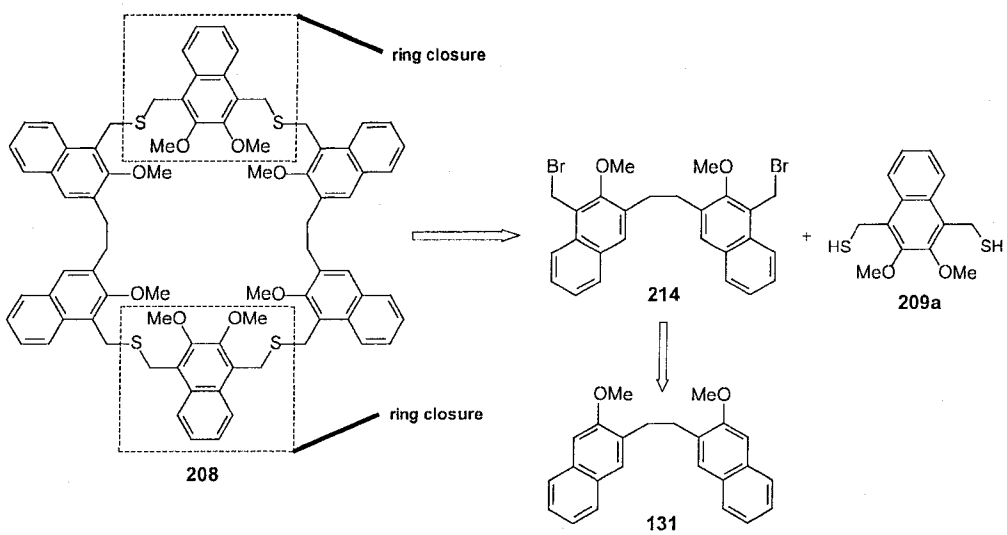

Scheme 7.12 Retrosynthetic analysis of decahomotetrathiaisocalix[6]-naphthalene **208**.

In turn, bis(bromomethyl)naphthalene **214** was directly afforded by bis(bromomethylation) of bis(3-methoxy-2-naphthyl)ethane (**131**)[14] which was synthesized from 3-hydroxy-2-naphthoic acid (**83**) via some functional group manipulations (Scheme 4.8). Bis(mercaptomethyl)naphthalene **209a** was prepared from 2,3-dihydroxynaphthalene (**164**) (Scheme 7.8).

7.4.2 Synthesis and characterization

The synthesis of decahomotetrathiaisocalix[6]naphthalene **208** (Scheme 7.13) commenced with the synthesis of 1,2-bis(3-methoxy-2-naphthyl)ethane (**131**) from 3-hydroxy-2-naphthoic acid (**83**) via the sequence of esterification and methylation, reduction, bromination, and alkyllithium-assisted homocoupling. All steps were carried out in high yields (see Chapter 4). Bis(bromomethylation) of **127** by paraformaldehyde and 31% HBr in AcOH in the usual manner cleanly afforded the desired key intermediate **214** in 93% yield. The coupling reaction of intermediates **214** and **209a** under basic conditions at room temperature over 4 d produced decahomotetrathiaisocalix[6]naphthalene **208** in 25% yield. (+)-APCI MS analysis showed the molecular ion peak at *m/z* = 1293.4 (30%) (calcd. 1293.72 for $C_{80}H_{76}O_8S_4$).

Tetrathia compound **208** had a relatively simple ^{1}H NMR spectrum at ambient temperature due to its symmetry, showing three singlets at approximately δ 3.07, 4.26 and 4.30 ppm for the following bridging methylene groups: $ArCH_{2a}CH_{2a}Ar$ and $Ar\text{-}CH_{2b}SCH_{2c}\text{-}Ar'$, respectively (Scheme 7.13). In

addition, **208** all of the ^{1}H NMR signals were sharp thus indicating rapid conformational equilibration in solution at the ambient temperature.

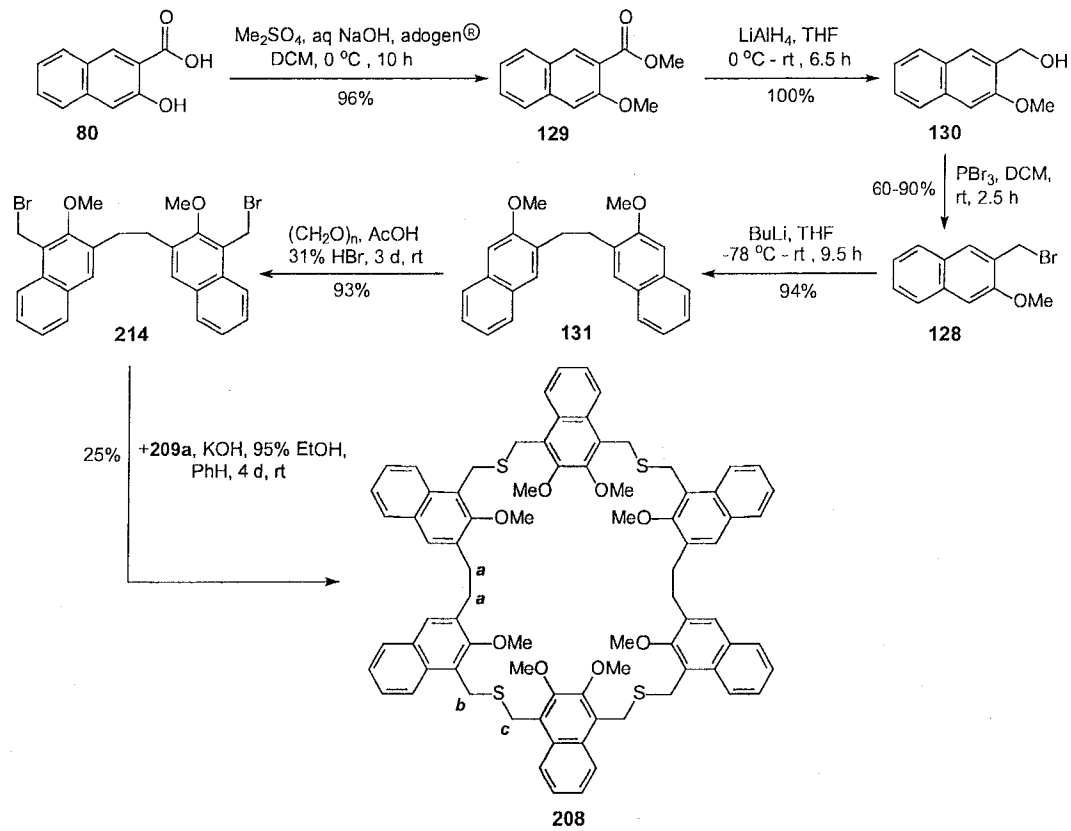

Scheme 7.13 Synthesis of decahomotetrathiaisocalix[6]naphthalene **208**.

7.5 Solution complexation studies

7.5.1 C_{60} and C_{70} as the guests

On the basis of their molecular architecture and molecular modeling, the octahomotetrathiaisocalix[4]naphthalenes **205a-d** had been predicted to be efficient hosts for C_{60} and/or C_{70}. Since **205a** and **205b** were less soluble in benzene or toluene, their complexation experiment studies with fullerenes using ^{1}H NMR spectroscopy could only be conducted in carbon disulfide in which the

solubilities of the fullerenes are also higher. However, in this solvent no complexation occurred since neither change in colour nor in the ^{1}H NMR signal shifts were observed upon addition of C_{60} or C_{70} solid to the host solutions under the conditions studied. This finding was similar to the results previously seen with **159a** and **159b** under similar conditions. It is hypothesized that the supramolecular complexation with these new receptors may also be inhibited as a result of an entropic effect arising from the greater flexibility of the larger, 28-membered annulus and the consequential lack of preorganization of these macrocyles. The lack of a complementary symmetry element between the hosts and fullerene guest molecules may also be a factor.

Similarly, complexation studies of **207** and **208** with C_{60} and C_{70} monitored by ^{1}H NMR spectroscopy in carbon disulfide solutions did not reveal evidence for the formation of any complexes. It is possible that the high conformational flexibility of these hosts could also account for the lack of complexation with the fullerenes examined.

7.5.2 Tetramethylammonium chloride (TMACl) and AgO_2CCF_3 as the guests

TMACl which was shown to be a very good guest for octahomotetraoxaisocalix[4]naphthalenes **159a** and **159b** in $CDCl_3$, was also chosen for complexation studies with the new octahomotetrathia-isocalix[4]naphthalene hosts **205a**, **205b**, **207** and **208**. However, when a pure solution of one of the above hosts in $CDCl_3$ was separately added to a solution of

saturated TMACl (guest), also in $CDCl_3$, there were no changes observed in any of the chemical shifts of either the hosts or guest molecules. It is presumed that the new octahomotetrathiaisocalix[4]naphthalene receptors **205a** and **205b** are much more flexible than the corresponding oxa analogues due to the fact that sulfur atoms (104 pm)[23] are larger than oxygen atoms (73 pm).[23] Therefore, the former may not easily preorganize to allow for a complexation with TMA under the conditions studied. Similar arguments can be made for the absence of complexation between homthiacalix[6]naphthalenes **207** or **208** with TMA in $CDCl_3$ solutions.

Yamato *et al.* recently reported a highly selective binding study of their hexahomotrithiacalix[3]arene **201** with Ag^+ among metal picrates studied.[9] Therefore, it was decided to employ Ag^+ as a guest for **205a** and **205b**. Since octahomotetrathiaisocalix[4]naphthalenes **205a**, and **205b** are less soluble in acetonitrile while AgO_2CCF_3 is less soluble in $CDCl_3$, a mixture of 1:9 CD_3CN-$CDCl_3$ (v/v) was employed as the solvent for the complexation investigation using ^1H NMR spectroscopy. To avoid different solvent effects in these complexation studies, all host and guest solutions which were employed were prepared in the same solvent mixture of 1:9 CD_3CN-$CDCl_3$ (v/v).

Upon addition of guest solutions, *e.g.* Ag^+ (*ca.* 5 x 10^{-3} M) in aliquots to the host solutions, *e.g.* **205a** and **205b**, (*ca.* 5 x 10^{-4} M), the ^1H NMR showed clear changes in the chemical shifts induced for all signals of the hosts (Figure 7.8). When the [G]/[H] ratios ≥ 10:1, the observed chemical shifts almost leveled off,

therefore, the complexation studies were conducted at lower [G]/[H] ratios ranging from 0.54–2.87 ([H]/[G] ratios ranging from 0.35–1.86).

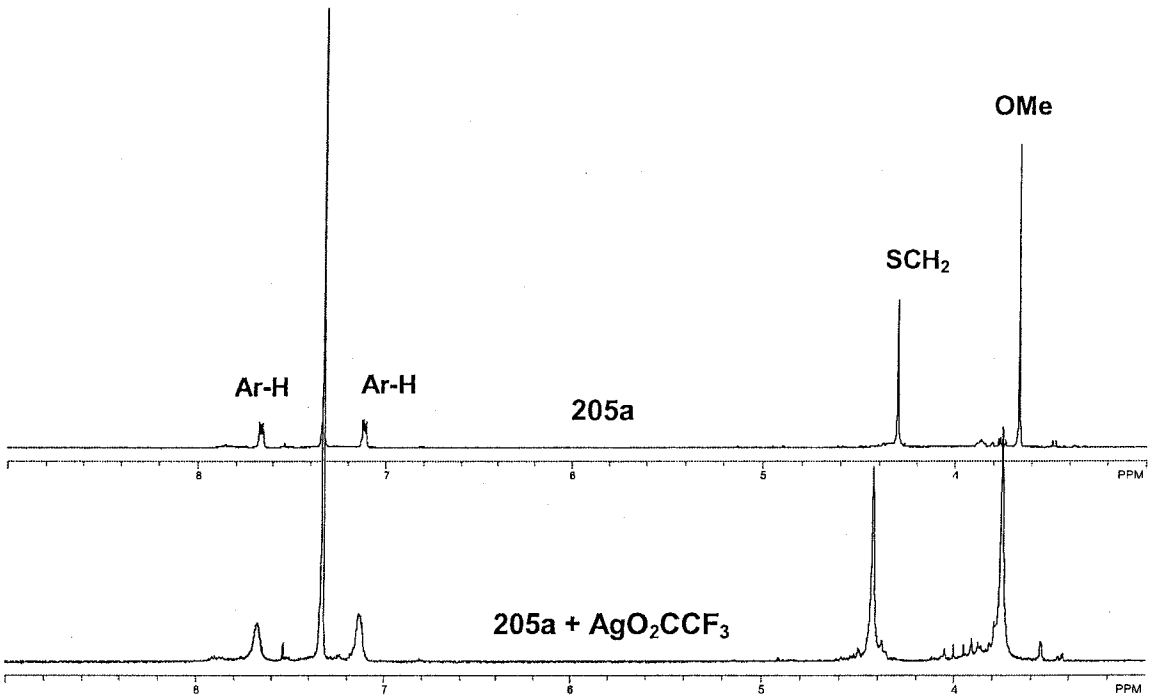

Figure 7.8 ^{1}H NMR spectra of pure **205a** (*top*), and the mixture of **205a** and AgO_2CCF_3 *(middle)* in 1:9 CD_3CN–$CDCl_3$ (v/v) at 298 K.

In these guest-host ranges, upon addition of Ag^+ solutions to the host solutions, all of the host signals were shifted to lower fields. The largest change in chemical shifts for the receptors **205a** (Appendix 7.1) and **205b** (Appendix 7.2) were for the -CH_2- groups of their bridging –CH_2SCH_2– groups ($\Delta\delta_{max}$ = 0.125 and 0.150 ppm, respectively). Those for their alkoxy group signals, *e.g.* OCH_3 or OCH_2, were smaller ($\Delta\delta_{max}$ = 0.088 and 0.035 ppm, respectively) and similarly the changes observed for their aromatic signals were also smaller ($\Delta\delta_{max}$ = 0.012 and 0.100 ppm, respectively). These changes in chemical shifts indicate

that Ag^+, a "soft" cation, binds most tightly with the bridging sulfur atoms rather than with the oxygen atoms of the alkoxy groups or the naphthyl sub-units. Hence, the induced chemical shift changes observed for the bridging methylenes were used for determination of the guest-host stoichiometries of these new receptors with Ag^+ cation by the mole plot ratios method. These signals were also used for determination of the K_{assoc} values.[24] The mole ratio plots in the [G]/[H] ranges studied indicated the formation of 1:1 host-guest complexes between the receptors **205a** (Figure 7.9, Appendix 7.3) or **205b** (Figure 7.10, Appendix 7.4) with Ag^+.

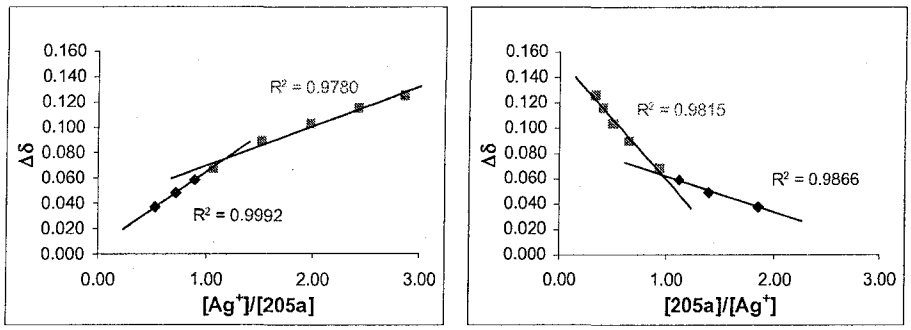

Figure 7.9 Mole ratio plots showing the 1:1 stoichiometry of **205a** and Ag^+.

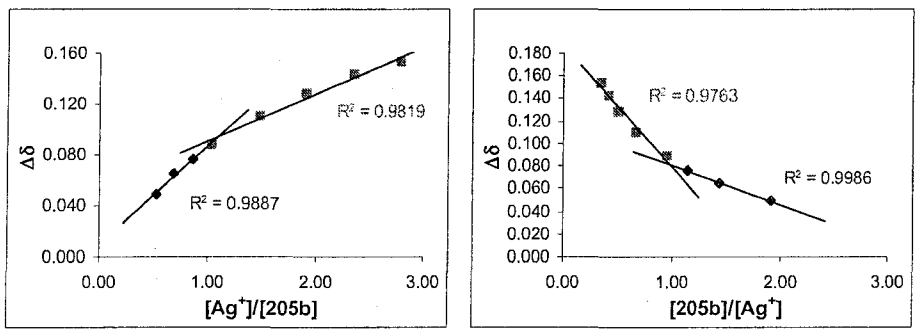

Figure 7.10 Mole ratio plots showing the 1:1 stoichiometry of **205b** and Ag^+.

From the 1:1 host-guest stoichiometry, the above changes in chemical shifts indicate that Ag^+ binds with the bridging sulfur and oxygen atoms of **205a** in its *cone* conformation or from the "A" face of **205a** (Figure 7.7). This is presumed to be the case since the changes in the chemical shifts of the methoxy groups (0.088 ppm) are much larger than those of the protons of the naphthyl sub-units (0.012 ppm). In contrast, with **205b**, due to the steric interactions with the ethyl groups, Ag^+ apparently binds with the sulfur atoms and the unsubstituted rings of the naphthyl sub-units of **205b** in its *cone* conformation or from the "B" face (Figure 7.7) of **205b**. This results in larger changes for the chemical shifts of the naphthyl proton signals (0.100 ppm) than for those of the ethoxy groups (0.035 ppm).

Apparent K_{assoc} values for complex formation between **205a** (Figure 7.11, Appendix 7.3) or **205b** (Figure 7.12, Appendix 7.4) with Ag^+ were calculated by using both the Benesi-Hildebrand (B–H) and Foster-Fyfe (F–F) treatments, respectively.[19,25] The results from both methods which are summarized in Table 7.1 showed good agreement for both receptors tested. The K_{assoc} values which were obtained for **205b** are about 1.4-fold larger than for **205a**. The Foster-Fyfe method gave K_{F-F} values with slightly lower percentage errors and larger K_{assoc} values than those obtained from the Benesi-Hildebrand treatment. These K_{assoc} values for **205a** and **205b** were much smaller than those of **29** (Figure 7.13) in 1:1 $CDCl_3$-CD_3OD (v/v) at – 50 °C, reported by Shinkai *et al.*[26] It was rationalized

that the hosts studied were less conformationally flexible at low temperature, and this allowed a tighter binding between the hosts and silver ions.

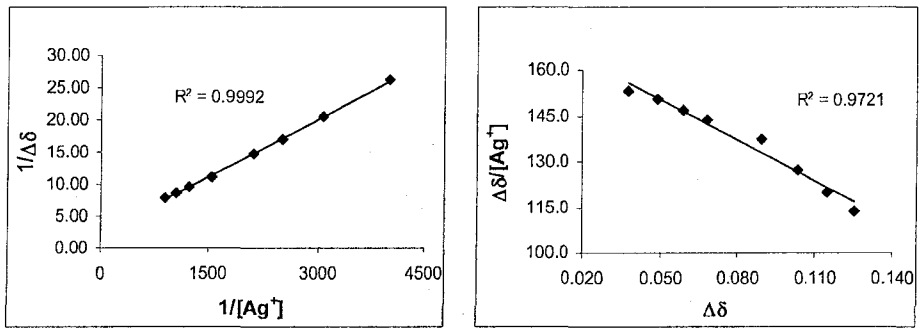

Figure 7.11 Benesi-Hildebrand plot (*left*) and Foster-Fyfe plot (*right*) for the complexation of **205a** and AgO_2CCF_3.

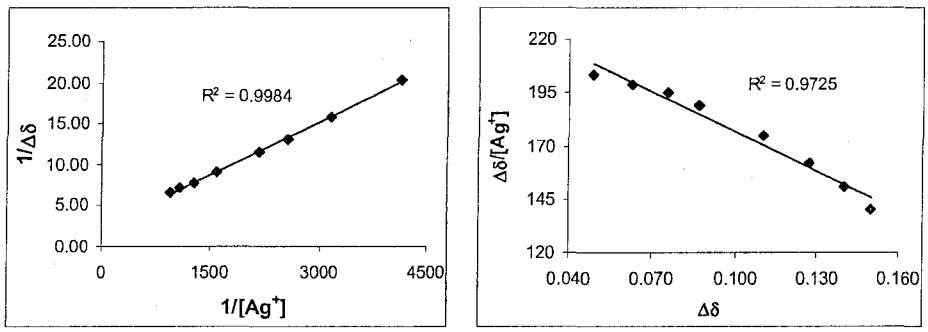

Figure 7.12 Benesi-Hildebrand plot (*left*) and Foster-Fyfe plot (*right*) for the complexation of **205b** and AgO_2CCF_3.

Table 7.1 K_{assoc} values (M^{-1}) for **205a** and **205b** complexes with $AgCF_3CO_2$ in 1:9 CD_3CN-$CDCl_3$ at 298 K.

Complex	Method	Run # 1 (R^2)	Run # 2 (R^2)	Average
205a :Ag^+	B–H	410 ± 26 (0.999)	386 ± 36 (0.999)	398 ± 17
	F–F	450 ± 31 (0.972)	437 ± 32 (0.970)	444 ± 9
205b:Ag^+	B–H	553 ± 51 (0.997)	565 ± 39 (0.998)	559 ± 8
	F–F	616 ± 43 (0.971)	627 ± 43 (0.973)	622 ± 8

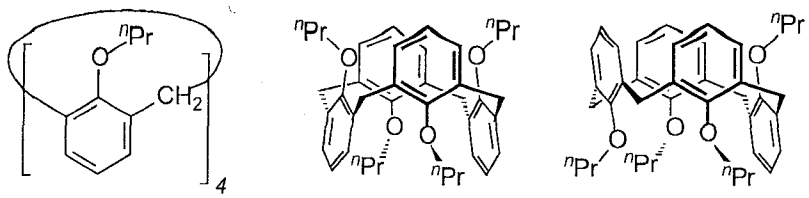

29 *1,3-alternate* *partial cone*

K_{assoc} 3.7×10^3 4.3×10^3

Figure 7.13 Conformations and K_{assoc} values of 1:1 complexes between Ag^+ and conformers of calix[4]arene **29**.

7.6 Conclusions

A series of new octahomotetrathiaisocalix[4]naphthalenes **205a-d** have been synthesized, and some of their complexation properties have also been investigated. The syntheses of the octaethoxy and octa-*n*-propoxy cyclic-tetramers **205b** and **205c** were accompanied by small amounts of the corresponding higher hexathia homologues, **206b** and **206c**, respectively, but the complexation properties of the latter compounds have not yet been elucidated. The ^{1}H NMR spectra of all of the macrocycles obtained showed clearly that they were highly symmetrical and conformationally flexible.

A computer-assisted molecular mechanics modeling showed that the lowest energy conformers of thiacalix[4]naphthalenes are similar to those of "Zobarene" (Chapter 5). Although CPK models and molecular modeling suggested that these new receptors had the potential to be suitable hosts for the electron-deficient neutral guest molecules, *i.e.* C_{60}- and C_{70}-fullerenes, solution complexation experiments did not demonstrate any such binding. Surprisingly, no complexes were observed between these new homothia receptors with TMACl

either. In contrast, the transition metal ion, Ag^+, formed 1:1 host-guest complexes with the octahomotetrathiaisocalix[4]naphthalenes **205a** and **205b** which were studied. These results suggest that the Ag^+-sulfur atom interactions are more dominant than the TMA-π interactions with TMACl, and also for the π-π interactions with fullerene guests.

7.7 Experimental section

General methods, materials and instrumentation used are identical to those described in Chapters 2 and 3.

1,4-Bis(mercaptomethyl)-2,3-dimethoxynaphthalene (209a)

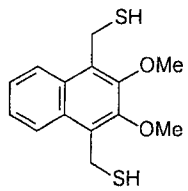

General procedure: A stirred mixture of the crude 1,4-bis(bromomethyl)-2,3-dimethoxynaphthalene (**162a**) (1.87 g, 5.00 mmol) and thiourea (0.98 g, 13 mmol) in dry THF (150 mL) was heated at reflux with stirring for 36 h. After the reaction mixture was cooled to room temperature, the solvent was removed under reduced pressure. The resulting residue was dissolved in distilled water (100 mL), aqueous 10% NaOH solution (20 mL) was added and the mixture was heated at reflux for a further 24 h. After the reaction mixture was cooled to room temperature, the mixture was chilled in an ice bath and was neutralized by the addition of aqueous 10% HCl. The resulting precipitate was isolated by suction

filtration and air-dried to give the crude product (1.22 g, 87% yield) as a light yellow powder, which was purified by chromatography (5:95 EtOAc-hexane) to yield **209a** (0.80 g, 64%) as a colourless powder: mp 120 °C ($CHCl_3$); ^{1}H NMR δ 1.94 (t, *J* = 6.8 Hz, 2H), 4.01 (s, 6H), 4.22 (d, *J* = 6.8Hz, 4H), 7.51–7.53 (m, 2H), 7.97–7.99 (m, 2H); ^{13}C NMR δ 19.1, 61.4, 124.4, 125.9, 129.2, 150.0; GCMS *m/z* (relative intensity) 280 (M^+, 30), 247 (60), 214, 199 (60), 171, 128 (100), 115 (40).

1,4-Bis(mercaptomethyl)-2,3-diethoxynaphthalene (209b)

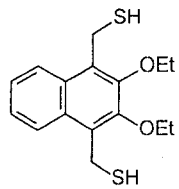

Using the general procedure for **209a**, the reaction of the crude 1,4-bis(bromomethyl)-2,3-diethoxynaphthalene (**162b**) (0.69 g, 1.50 mmol) and thiourea (0.25 g, 3.3 mmol) in dry THF (50 mL) gave the crude product (0.38 g, 68%) as a light yellow powder, which was purified by chromatography (2.5:97.5 EtOAc-hexane) to yield **209b** (0.22 g, 40%) as a colourless powder: mp 119–120 °C ($CHCl_3$); ^{1}H NMR δ 1.48 (t, *J* = 7.0 Hz, 6H), 1.93 (t, *J* = 7.0 Hz, 2H), 4.18–4.23 (m, 8H), 7.50–7.52 (m, 2H), 7.97–7.99 (m, 2H); ^{13}C NMR δ 16.2, 19.3, 69.8, 124.4, 125.7, 129.18, 129.21 149.0; GCMS *m/z* (relative intensity) 308 (M^+, 20), 275 (30), 185 (50), 157 (50), 128 (90), 115 (40).

1,4-Bis(mercaptomethyl)-2,3-dipropoxynaphthalene (209c)

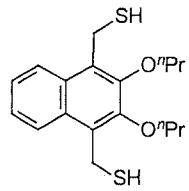

Using the general procedure for **209a**, the reaction of the crude 1,4-bis(bromomethyl)-2,3-dipropoxynaphthalene (**162c**) (1.29 g, 3.0 mmol) and thiourea (0.58 g, 7.8 mmol) in dry THF (150 mL) gave the crude product (0.71 g, 71%) as a light yellow powder, which was purified by chromatography (2:98 EtOAc-hexane) to yield **209c** (0.42 g, 42%) as a colourless powder: mp 72–74 °C ($CHCl_3$); ^{1}H NMR δ 1.12 (t, *J* = 7.5 Hz, 6H), 1.86–1.95 (m, 6H), 4.08 (t, *J* = 6.5 Hz, 4H), 4.22 (d, *J* = 6.9 Hz, 4H), 7.50–7.52 (m, 2H), 7.97–7.99 (m, 2H); ^{13}C NMR δ 10.9, 19.3, 24.0, 75.8, 124.4, 125.7, 129.17, 129.24 149.2; GCMS *m/z* (relative intensity) 336 (M^+, 10), 270 (25), 227 (100), 186 (70), 157 (50), 128 (90), 115 (40).

1,4-Bis(mercaptomethyl)-2,3-dibutoxynaphthalene (209d)

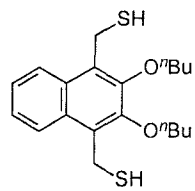

Procedure 1: Using the general procedure for **209a**, **209d** was obtained from 1,4-bis(bromomethyl)-2,3-dibutoxynaphthalene (**162d**) in only 2.5% yield as a colourless powder: mp 41–42 °C; ^{1}H NMR δ 1.03 (t, *J* = 7.4 Hz, 6H), 1.56–1.62

(m, 4H), 1.83–1.88 (m, 4H) 1.93 (t, J = 7.3 Hz, 2H), 4.12 (t, J = 6.3 Hz, 4H), 4.22 (d, J = 6.7 Hz, 4H) 7.50–7.52 (m, 2H), 7.97–7.99 (m, 2H); ^{13}C NMR δ 14.3, 19.3, 19.6, 32.8, 74.1, 124.4, 125.7, 129.1, 129.2 149.2; GCMS *m/z* (relative intensity) 364 (M^+, 1), 298 (30), 241 (100), 225, 186 (100), 186 (100), 157 (50), 128 (70), 115 (41).

Procedure 2: Reaction was conducted at room temperature.

A solution of crude **162d** (0.23 g, 0.50 mmol) and thiourea (0.10 g, 1.3 mmol) in dry THF (25 mL) was stirred at room temperature under N_2 for 30 h. A solution of cold aqueous 10% NaOH (25 mL) was added and stirred for a further 2 h. The reaction mixture was chilled in an ice bath, acidified by aqueous 3 M HCl until the pH reached 2, extracted with $CHCl_3$ (3 x 20 mL), washed with distilled water (1 x 30 mL), brine (1 x 30 mL), dried over anhydrous $MgSO_4$ and filtered. After the solvent was removed under reduced pressure, the resulting residue was purified by chromatography (0.5:99.5 EtOAc-hexane) to yield **209d** (0.07 g, 39%) as a colourless powder having identical characterization data to those obtained from the Procedure 1.

Procedure 3: Using 95% EtOH as the solvent.

A solution of crude **162d** (0.92 g, 2.00 mmol) and thiourea (0.40 g, 5.20 mmol) in 95% EtOH (100 mL) was heated at reflux with stirring under N_2 for 19 h. After cooling to room temperature, the reaction mixture was chilled in an ice bath, then aqueous 10% NaOH (100 mL) was added. The resulting mixture was stirred

for a further 2.5 h, acidified with aqueous 3 M HCl until the pH reached 2, extracted with $CHCl_3$ (3 x 50 mL), dried over anhydrous $MgSO_4$ and filtered. After the solvent was removed under reduced pressure, the resulting residue was purified by chromatography (0.5:99.5 EtOAc-hexane) to yield **209d** (0.45 g, 62%) as a colourless powder having identical characterization data to those obtained from the Procedure 1.

1,4-Bis(mercaptomethyl)-2,3-methylenedioxynaphthalene (209e)

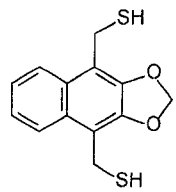

Using the general procedure for **209a**, the reaction of crude **162e** (1.43 g, 4.00 mmol) and thiourea (0.79 g, 10 mmol) in dry THF (200 mL) gave a crude product (1.03 g, 97%) as a light yellow powder, which was purified by chromatography (2.5:97.5 EtOAc-hexane) to yield **209e** (0.64 g, 60%) as a colourless powder: mp 153–154 °C ($CHCl_3$); ^{1}H NMR δ 1.94 (t, J = 7.1 Hz, 2H), 4.09 (d, J = 7.7 Hz, 4H), 6.13 (s, 2H), 7.46–7.48 (m, 2H), 7.88–7.90 (m, 2H); ^{13}C NMR δ 19.0, 101.7, 114.1, 123.5, 125.0, 128.7, 144.5; GCMS *m/z* (relative intensity) 264 (M^+, 20), 231 (40), 198 (100), 185 (25), 141 (100), 115 (40).

"1,4-Linked" octahomotetrathiaisocalix[4]-(2,3-dimethoxy)naphthalene (205a)

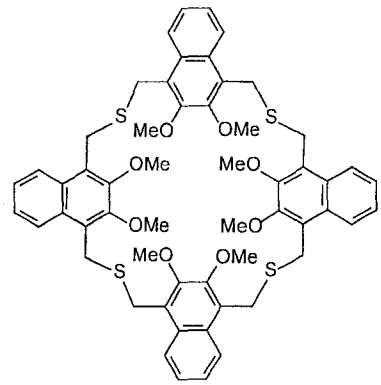

General procedure: To a stirred solution of KOH (0.20 g, 3.0 mmol) in 95% ethanol (20 mL) at room temperature, a solution of **162a** (187 mg, 0.500 mmol) and **209a** (140 mg, 0.500 mmol) in benzene (6 mL) was added over 3.0 h using a syringe pump. The mixture was stirred at room temperature for a further 4 d. After the solvents were evaporated, water (30 mL) was added and the residue was neutralized with aqueous 3 M HCl, extracted with $CHCl_3$ (3 x 50 mL) and dried over anhydrous $MgSO_4$. The solvent was evaporated, and the crude product was purified by PLC (3:7 EtOAc-hexane) to yield **205a** as a colourless powder (63 mg, 25%): mp > 250 °C (dec.); ^{1}H NMR δ 3.65 (s, 6H), 4.03 (s, 4H), 7.11–7.13 (m, 2H), 7.68–7.69 (m, 2H); ^{13}C NMR δ 27.4, 61.2, 124.5, 125.4, 126.3, 129.8, 150.1; (+)-APCI MS *m/z* (relative intensity) 985.3 (M^+, 60) calcd.: 985.3 for $C_{56}H_{56}O_8S_4$, 771.1 (10), 493.1 (100), 338.4 (80);

"1,4-Linked" octahomotetrathiaisocalix[4]-(2,3-diethoxy)naphthalene (205b) and "1,4-linked" dodecahomohexathiaisocalix[6]-(2,3-diethoxy)naphthalene (206b)

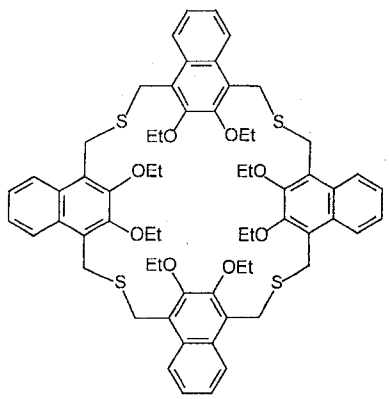

205b

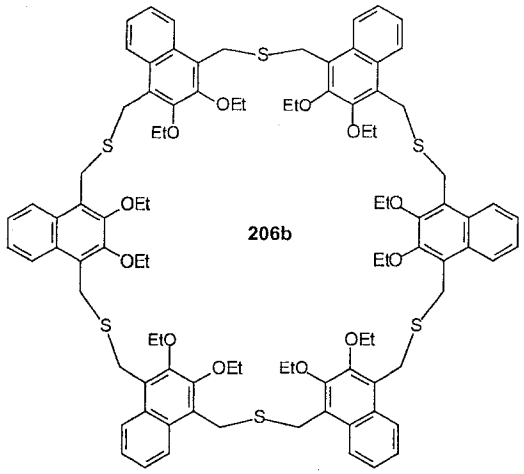

206b

Using the general procedure for **205a**, the coupling reaction between **162b** (201 mg, 0.500 mmol) and **209b** (154 mg, 0.500 mmol) gave the crude product, which was purified by PLC (2:8 EtOAc-hexane) to yield **205b** (76 mg, 28%) as a colourless powder: mp 250 °C (dec.); ^{1}H NMR δ 1.39 (t, *J* = 7.2 Hz, 24H), 4.06 (q, *J* = 6.8 Hz, 16H), 4.30 (s, 16H), 6.90–6.92 (m, 8H), 7.43–7.45 (m, 8H); ^{13}C NMR δ 16.1, 27.7, 70.0, 124.3, 125.3, 126.2, 130.0, 150.0; (+)-APCI MS *m/z* (relative intensity) 1097.4 (M^+, 100) calcd.: 1097.5 $C_{64}H_{72}O_8S_4$, 789.3 (5), 549.3 (7), 338.4 (35); and **206b** (29 mg, 10%) as a colourless powder: mp > 180 °C (dec.); ^{1}H NMR δ ^{1}H NMR δ 1.30 (t, *J* = 7.0 Hz, 36H), 4.06 (q, *J* = 7.1 Hz, 24H), 4.32 (s, 24H), 7.18–7.20 (m, 12H), 7.77–7.78 (m, 12H); ^{13}C NMR δ 16.0, 27.9, 69.9, 124.7, 125.3, 126.0, 130.0, 149.7; (+)-APCI MS *m/z* (relative intensity) 823.3 (M^{2+}, 15) calcd.: 1646.3 for $C_{96}H_{108}O_{12}S_6$, 423.5 (5%), 338.4 (100%).

"1,4-Linked" octahomotetrathiaisocalix[4]-(2,3-dipropoxy)naphthalene (205c) and "1,4-linked" dodecahomohexathiaisocalix[6]-(2,3-*n*-propoxy)-naphthalene (206c)

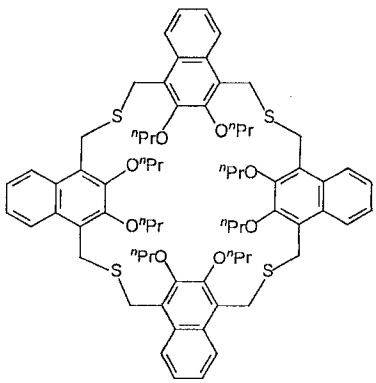

205c

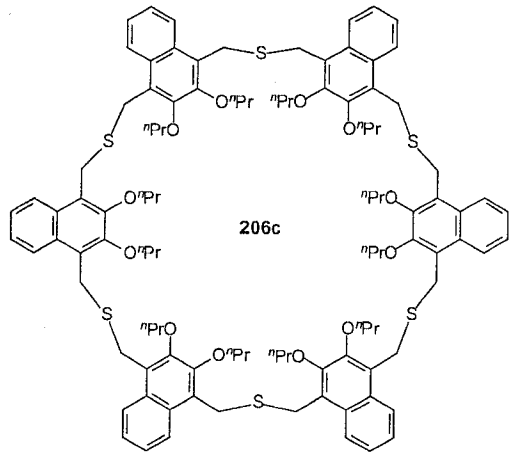

Using the general procedure for **205a**, the coupling reaction between **162c** (168 mg, 0.500 mmol) and **209c** (215 mg, 0.500 mmol) gave the crude product, which was purified by PLC (1:9 EtOAc-hexane) to yield **205c** (100 mg, 33%) as a colourless powder: mp > 180 °C (dec.); ^{1}H NMR δ 1.06 (t, *J* = 7.7 Hz, 24H), 1.81–1.88 (m, 16H), 3.97 (t, *J* = 6.7 Hz 16H), 4.28 (s, 16H), 6.85–6.87 (m, 8H), 7.39–7.41 (m, 8H); ^{13}C NMR δ 10.9, 23.9, 27.5, 76.0, 124.3, 125.2, 126.0, 129.7, 149.8; (+)-APCI MS *m/z* (relative intensity) 1029.4 (M^+, 74) calcd.:1209.7 for $C_{72}H_{88}O_8S_4$, 617.2 (42), 341.2 (100), 338.4 (43); and **206c** (35 mg, 11%) as a colourless powder: mp > 180 °C (dec.); ^{1}H NMR δ 0.89 (t, *J* = 7.3 Hz, 36H), 1.61–1.69 (m, 24H), 3.91 (t, *J* = 6.8 Hz, 24H), 4.32 (s, 24H), 7.19–7.21 (m, 12H), 7.81–7.82 (m, 12H); ^{13}C NMR δ 10.7, 23.7, 27.9, 75.9, 124.7, 125.3, 125.8,

130.1, 149.9; (+)-APCI MS *m/z* (relative intensity) 1813.4 (M^+, 15) calcd.:1814.6 for $C_{108}H_{132}O_{12}S_6$, 715.6 (20), 382.5 (60) 338.4 (100).

"1,4-Linked" octahomotetrathiaisocalix[4]-(2,3-*n*-dibutoxy)naphthalene (205d)

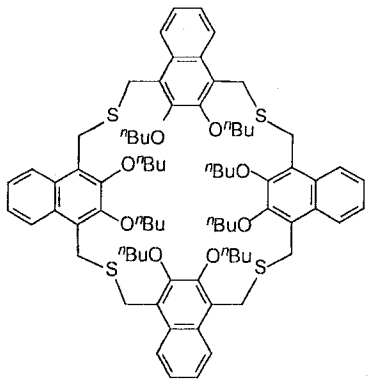

Using the general procedure for **205a**, the coupling reaction between **162d** (182 mg, 0.500 mmol) and **209d** (229 mg, 0.500 mmol) gave the crude product, which was purified by PLC (1:9 EtOAc-hexane) to yield **205d** (59 mg, 18%) as a colourless powder: mp > 200 °C (dec.); ^{1}H NMR δ 0.99 (t, *J* = 7.4 Hz, 24H), 1.49–1.56 (m, 20H, overlap with HOD signal), 1.78–1.84 (m, 16H), 4.01 (t, *J* = 6.4 Hz 16H), 4.27 (s, 16H), 6.83–6.85 (m, 8H), 7.39–7.40 (m, 8H); ^{13}C NMR δ 14.3, 19.6, 27.5, 32.8, 74.3, 124.3, 125.2, 125.9, 129.7, 149.8; (+)-APCI MS *m/z* (relative intensity) 1322.5 (M^+, 100) calcd.: 1321.9 for $C_{80}H_{104}O_8S_4$, 957.3 (10), 705.4 (38), 419.2 (50), 338.4 (70).

1-Methoxynaphthalene (212)

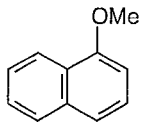

To a stirred solution of 1-naphthol (**211**) (0.58 g, 4.00 mmol) in aqueous 10% NaOH (2 mL, 5.0 mmol) was added adogen® (0.10 mL) and DCM (10 mL). Dimethyl sulfate (0.5 mL, 5.0 mmol) was added dropwise at 0 °C over 10 min. The reaction mixture was stirred for a further 5 h and then added aqueous 6 M NaOH solution until the pH reached 12. The mixture was stirred at room temperature for 30 min. The reaction mixture was extracted with DCM (3 x 10 mL). The organic layer was then washed with aqueous saturated NH_4Cl (1 x 20 mL), brine (2 x 20 mL), and distilled water (2 x 20 mL); dried over anhydrous $MgSO_4$ and filtered. After the solvent was removed under reduced pressure, the yellow oily liquid (quantitative yield) (lit.[13] oily liquid) was purified by chromatography (1:99 EtOAc-hexane) to yield **212** (0.48 g, 75%) as colourless liquid: ^{1}H NMR δ 3.98 (s, 3H), 6.80 (d, J = 7.7 Hz, 1H), 7.35–7.47 (m, 4H), 7.78–7.80 (m, 1H), 8.25–8.27 (m, 1H); GCMS *m/z* (relative intensity) 158 (M^+, 95), 143 (50), 127 (10), 115 (100), 89 (25), 63 (30).

Bis(4-methoxy-2-naphthyl)methane (213)

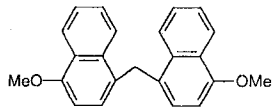

To a solution of **212** (3.16 g, 20 mmol) and paraformaldehyde (0.72 g, 24.0 mmol) in dioxane (20 mL) was added aqueous 30% H_2SO_4 (4 mL) dropwise at room temperature. The reaction mixture was stirred at room temperature for a further 2 d. The resulting precipitate was isolated by suction filtration and crystallized from DCM-MeOH to yield **213** (2.39 g, 73%) as light yellow prisms: mp 154 °C (acetone), (lit.[21] 150.5–152 °C); ^{1}H NMR δ 3.97 (s, 6H), 4.71 (s, 2H), 6.68 (d, *J* = 8.3 Hz, 2H), 6.97 (d, *J* = 7.7 Hz, 2H), 7.48–7.51 (m, 4H), 7.97–7.99 (m, 2H), 8.33–8.35 (m, 2H); ^{13}C NMR δ 35.0, 55.6, 103.7, 122.8, 124.1, 125.1, 126.1, 126.7, 127.1, 128.5, 133.2, 154.6; GCMS *m/z* (relative intensity) 328 (M^+, 100), 297 (40), 265 (30), 128 (50) 114 (30).

Bis[3-(bromomethyl)-4-methoxy-2-naphthyl]methane (210)

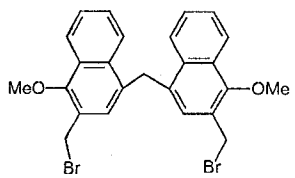

To a stirred suspension of solution of **213** (0.66 g, 2.0 mmol) and paraformaldehyde (0.30 g, 10 mmol) in glacial acetic acid (10 mL) was added 15% HBr in glacial acetic acid (10 mL, 10 mmol). After being stirred for 2 d, the reaction mixture was poured into cold water (100 mL). The resulting precipitate

was then obtained by using a suction filtration, washed with water until the washings were neutral to pH paper, extracted with EtOAc (2 x 150 mL), dried over anhydrous $MgSO_4$ and filtered. After the solvent was evaporated under reduced pressure, the crude product was purified by flash chromatography (2:98 EtOAc-hexane) to yield **210** (0.40 g, 38.8%) as a light yellow powder: mp 144 °C (acetone) (lit.[22a] 138–140 °C, crude product); ^{1}H NMR δ 4.09 (s, 6H), 4.65 (s, 4H), 4.75 (s, 2H), 7.07 (s, 2H), 7.50–7.53 (m, 2H), 7.55–7.58 (m, 2H), 7.99 (d, J = 8.4 Hz, 2H), 8.19 (d, J = 8.4 Hz, 2H); ^{13}C NMR δ 28.6, 35.3, 62.8, 123.5, 124.6, 126.2, 126.4, 127.3, 128.4, 129.2, 132.7, 133.9, 153.7.

Octahomotetrathiaisocalix[6]naphthalene 207

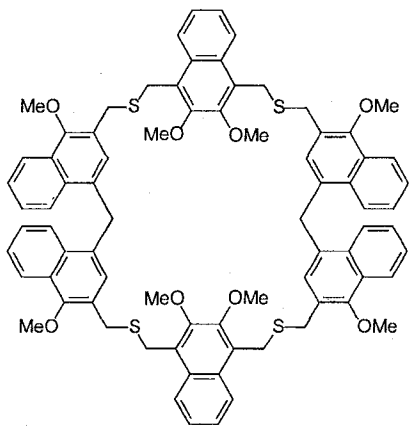

To a stirred, clear solution of KOH (0.20 g, 3.0 mmol) in 95% ethanol (25 mL) at room temperature, a solution of **209a** (140 mg, 0.500 mmol) and **210** (257 mg, 0.500 mmol) in benzene (6 mL) was added over 3.0 h using a syringe pump. The mixture was stirred at room temperature for a further 4 d. After the solvents were evaporated, water (30 mL) was added and the residue was neutralized with

aqueous 3 M HCl, extracted with $CHCl_3$ (3 x 50 mL) and dried over anhydrous $MgSO_4$. The solvent was evaporated, and the crude product was purified by PLC (2:8 EtOAc-hexane) to yield **207** as a colourless powder (46.5 mg, 15%): mp > 180 °C (dec.); ^{1}H NMR δ 3.51 (s, 6H), 3.83 (s, 4H), 3.92 (s, 4H), 3.93 (s, 6H), 4.77 (s, 2H), 7.05–7.06 (m, 2H), 7.17 (s, 2H), 7.46–7.49 (m, 2H), 7.52–7.56 (m, 4H), 8.00 (d, *J* = 8.3 Hz, 2H), 8.16 (d, *J* = 8.3 Hz, 2H); ^{13}C NMR δ 27.1, 31.6, 35.3, 61.1, 62.8, 123.1, 124.5, 124.6, 125.2, 125.8, 126.1, 126.3, 127.0, 128.6, 129.5, 129.7, 132.4, 133.0, 150.0, 153.1; (+)-APCI MS *m/z* (relative intensity) 1266.4 (M^+, 80) calcd.: 1265.7 for $C_{78}H_{72}O_8S_4$, 599.2 (100).

1,2-Bis(1-bromomethyl-2-methoxy-3-naphthyl)ethane (214).

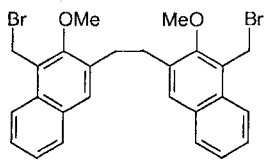

To a suspension of **131** (0.66 g, 1.9 mmol) and paraformaldehyde (0.24 g, 7.7 mmol) in glacial acetic acid (12 mL) was added dropwise a solution of 15% HBr in AcOH (12 mL) at room temperature over 30 min. After being stirred for 3 d, the reaction mixture was poured into cold water (100 mL). The resulting precipitate was then obtained by suction filtration, washed with distilled water (2 x 50 mL), aqueous 5% $NaHCO_3$ (2 x 50 mL) and distilled water until the washings were neutral to pH paper, then dissolved in EtOAc (200 mL), dried over anhydrous $MgSO_4$ and filtered. The solvent was evaporated under reduced pressure to yield **214** (0.95 g, 93%) as a colourless powder: 184–185 °C (DCM-

acetone) (lit.[11] 177–179 °C), ^{1}H NMR δ 3.18 (s, 4H), 4.03 (s, 6H), 5.11 (s, 4H), 7.45 (t, *J* = 7.7 Hz, 2H), 7.57 (t, *J* = 7.4 Hz, 2H), 7.74 (s, 2H), 7.78 (d, *J* = 7.7 Hz, 2H), 8.08 (d, *J* = 8.3 Hz, 2H); ^{13}C NMR δ 25.5, 31.9, 61.9, 123.6, 124.9, 125.6, 126.6, 128.3, 130.7, 131.42, 131.47, 134.9, 156.0.

Dodecahomotetrathiaisocalix[6]naphthalene 208

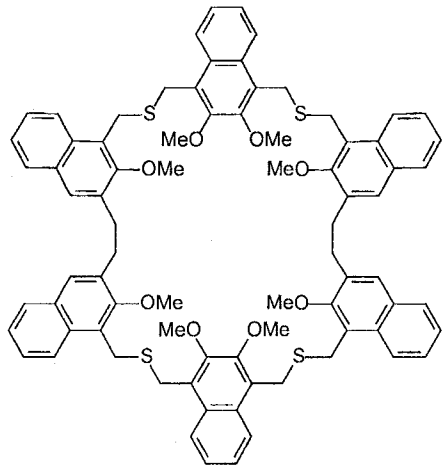

To a stirred, clear solution of KOH (0.20 g, 3.0 mmol) in 95% ethanol (20 mL) at room temperature was slowly added a solution of **209a** (140.2 mg,0.4994 mmol) and **214** (290.6 mg, 0.5500 mmol) in benzene (30 mL) over 5 h using a syringe pump. The mixture was stirred for a further 4 d. After the solvents were removed under reduced pressure water was added to the resulting residue (30 mL), the mixture was neutralized with aqueous 3 M HCl, extracted with $CHCl_3$ (3 x 50 mL), dried over anhydrous $MgSO_4$ and filtered. After the solvent was removed under reduced pressure, the yellow solid residue was purified by flash chromatography (13:87 EtOAc-hexane) to yield **208** (79.0 mg, 25%) as a colourless solid: mp 160 °C (dec.); ^{1}H NMR δ 3.07 (s, 8H), 3.59 (s, 12H), 3.80 (s,

12H), 4.26 (s, 8H), 4.30 (s, 8H), 7.16–7.18 (m, 4H), 7.29 (t, J = 7.4 Hz, 4H), 7.35 (t, J = 7.4 Hz, 4H), 7.60 (s, 4H), 7.64 (d, J = 7.7 Hz, 4H), 7.67–7.69 (m, 4H), 7.96 (d, J = 8.3 Hz,4H); ^{13}C NMR δ 27.3, 27.9, 31.7, 61.46, 61.49, 124.5, 124.7, 125.0, 125.3, 125.8, 125.9, 128.1, 128.5, 128.7, 129.9, 131.4, 131.9, 134.8, 150.3, 155.5; (+)-APCI MS *m/z* (relative intensity) 1310.5 ($[M+H_2O]^+$, 50) calcd.: 1310.45 for $C_{80}H_{76}O_8S_4.H_2O$, 1293.4 (M^+, 30) calcd.: 1293.72 for $C_{80}H_{76}O_8S_4$.

Association constant determinations K_{assoc}

The association constants for the complexation in 1:9 CD_3CN-$CDCl_3$ between **205a** or **205b** with AgO_2CCF_3 were determined by ^{1}H NMR spectroscopy upon the changes in the chemical shift of the methylene bridge SCH_2 signal of **205a** and **205b**. In the Benesi-Hildebrand treatment, K_{assoc} values were derived from plotting $(1/\Delta\delta)$ as a function of $1/[Ag^+]$, or using the Foster-Fyle treatment, by plotting $\Delta\delta/[Ag^+]$ *vs* $\Delta\delta$.

In a typical experiment, aliquots of the guest solutions, *e.g.* AgO_2CCF_3 (5.22×10^{-3}M ranging from 30–885 μL) in 1:9 CD_3CN-$CDCl_3$ (v/v) were added to individual NMR tubes which contained 600 μL of either **205a** (4.84×10^{-4} M), or **205b** (4.84×10^{-4} M). The resulting solutions were sonicated for approx 5 min before NMR measurements were recorded at 298 K at 500 MHz, as in Chapters 3 and 5.

7.8 References and notes

1. Lhoták. P. *Eur. J. Org. Chem.* **2004**, 1675-1692. and references cited therein.

2. (a) Shokova, E. A.; Kovalev, V. V. *Russian J. Org. Chem.* **2003**, *39*, 1-28. (b) Afari, Z.; Böhmer, V.; Harrowfield, J.; Vicens, J., Eds., *Calixarenes 2001*, Kluwer Acadamic Publishers, Dordrecht, The Netherlands 2001, pp 20. and references cited therein.

3. Parola, S.; Desroches, C. *Czech. Chem. Commun.* **2004**, *69*, 966-983.

4. Since 1997: more than 100 publications have been reported on complexation studies of thiacalixarenes and their derivatives with several metal ions, *e.g.* Li^+, Na^+, K^+, Rb^+, Cs^+, Mg^{2+}, Ca^{2+}, Ba^{2+}, Mn^{2+}, Fe^{2+}, Fe^{3+}, Co^{2+}, Ni^{2+}, Pd^{2+}, Cu^{2+}, Ag^+, Au^{3+}, Zn^{2+}, Cd^{2+}, Hg^{2+}, Pb^{2+}, Al^{3+}, Bi^{3+}, etc. For some examples of recent papers: (a) Khomich, E.; Kashapov, M.; Vatsouro, I.; Shokova, E.; Kovalev, V. *Org. Biomol. Chem.* **2006**, *4*, 1555-1560. (b) Yamato, T.; Casas, C. P.; Yamamoto, H.; Elsegood, M. R. J.; Dale, S. H.; Redshaw, C. *J. Incl. Phenom. Macro. Chem.* **2006**, *54*, 261-269. (c) Desroches, C.; Pilet, G.; Szilagyi, P. A..; Molnar, G.; Borshch, S. A.; Bousseksou, A.; Parola, S.; Luneau, D. *Eur. J. Inorg. Chem.* **2006**, 357-365. (d) Morohashi, N.; Yokomakura, K.; Hattori, T.; Miyano, S. *Tetrahedron Lett.* **2006**, *47*, 1157-1161.

5. (a) Kumagai, H.; Hasegawa, M.; Miyanari, S.; Sato, Y.; Hori, T.; Ueda, S.; Kamiyama, H.; Miyano, S. *Tetrahedron Lett.* **1997**, *38*, 3971-3972. (b) Iki, H.; Kabuto, C.; Fukushima, T.; Kumagai, H.; Takeya, H.; Miyanari, S.; Miyashi, T.; Miyano, S. *Tetrahedron* **2000**, *56*, 1437-1443.

6. Sone, T.; Ohba, Y.; Moriya, K.; Kumada, H.; Ito, K. *Tetrahedron* **1997**, *53*, 10689-10698.

7. (a) Tsuge, A.; Sawada, T.; Mataka, S.; Nishiyama, N.; Skashita, H.; Tashiro, M. *J. Chem. Soc., Perkin Trans. 1*, **1992**, 1489-1994. (b) Tsuge, A.; Sawada, T.; Mataka, S.; Nishiyama, N.; Skashita, H.; Tashiro, M. *J. Chem. Soc., Perkin Trans. 1*, **1990**, 1066-1068.

8. Ito, K.; Yamamori, Y.; Ohba, Y.; Sone, T. *Synth. Commun.* **2000**, *30*, 1167-1177.

9. Kohno, K.; Takeshita, M.; Yamato, T. *J. Chem. Res.* **2006**, 251-253.

10. Ashram, M. *J. Incl. Phenom. Macro. Chem.* **2006**, *54*, 253-259.

11. Georghiou, P. E.; Miller D. O.; Tran, A. H.; Al-Saraierh, H.; Li, Z.; Ashram, M.; Chowdhury, S.; Mizyed, S. *Synlett* **2005**, *6*, 879-891.

12. Li, Z. *Ph.D. Dissertation,* Memorial University of Newfoundland, 1996.

13. Georghiou, P. E.; Li, Z.; Ashram, M.; Miller, D. O. *J. Org. Chem.* **1996**, *61,* 3865-3869.

14. Ashram, M. *Ph.D. Dissertation,* Memorial University of Newfoundland, 1997.

15. Mizyed, S.; Ashram, M.; Miller, D. O.; Georghiou, P. E. *J. Chem. Soc., Perkin Trans. 2*, **2001**, 1916.

16. Tran, A. H.; Miller, D. O.; Georghiou, P. E. *J. Org. Chem.* **2005**, *70*, 1115-1121.

17. Georghiou, P. E.; Tran, A. H.; Mizyed, S.; Bancu, M.; Scott, L. T. *J. Org. Chem.* **2005**, *70*, 6158-6163.

18. The idea of replacing the $-CH_2OCH_2-$ bridges of **159a-d** by $-CH_2SCH_2-$ bridges in order to produce the more electron-rich analogues **205a-d**, **206a** and **206d** was suggested by Dr. Graham J. Bodwell at the "*Soccer 2004, 1st Summer Organic Chemistry Conference on Everybody's Research*", St. John's, NL, Canada, August 4th, 2004.

19. Computer-assisted molecular modeling studies were conducted using Spartan'04, V1.0.3, from Wavefunction, Inc., Irvine, CA, USA. Calculations at the PM3 level of theory were conducted on the optimized geometry of the host and/or complexes which were obtained through molecular mechanics (MMFF94) conformational searches.

20. By way of contrast, the analogous reaction between 1,4-bis(bromomethyl)-naphthalene and 1,4-bis(mercaptomethyl)naphthalene produced the corresponding dithia[3,3](1,4)naphthaleneophane. See Otsubo, T.; Boekelheide, V. *J. Org. Chem.* **1977**, *42,* 1085-1087.

21. Bodwell, G. J.; Houghton, T. J.; Koury, H. E.; Yarlagadda, B. *Synlett* **1995**, 751-752.

22. (a) Georghiou, P. E.; Ashram, M.; Li, Z.; Chaulk, S. G. *J. Org. Chem.***1995**, *60*, 7284-7289. (b) Schreiber, K. C.; Kennedy, M. C. *J. Org. Chem.* **1956**, *21*,1310-1311.

23. Petrucci, R. H.; Harwood, W. S.; Herring, F. G.; Madura, J. D. *General Chemistry: Principle and Modern Applications*, Pearson Education Inc., New Jersey, 2007, pp 352.

24. For further discussion, see Chapter 2.

25. Fielding, L. *Tetrahedron*, **2000**, *56*, 6151-6170.

26. (a) Ikeda, A.; Tsuzuki, H.; Shinkai, S. *J. Chem. Soc., Perkin Trans 2*, **1994**, 2073-2080. (b) Ikeda, A.; Shinkai, S. *J. Am. Chem. Soc.* **1994**, *116*, 3102-3110.

Chapter 8

Calixarene-like azacyclophanes resulting from an attempted synthesis of *N*-substituted-homoazaisocalix[4]naphthalenes

8.1 Introduction

Homoazacalixarenes such as **215a–218** form an expanded class of calixarenes in which the methylene bridges are partly or completely replaced by $-CH_2NRCH_2-$ groups (R = H, alkyl, benzyl, etc...) (Figure 8.1).[1-10]

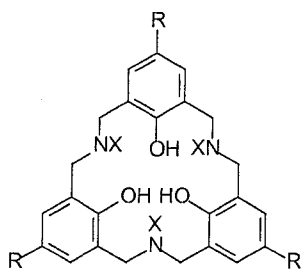

215a R = Me, X = *i*Bu
215b R = Me, X = Bn
215c R = Me, X = (*S*)-CHMePh
215d R = Me, X = Allyl
215e R = Me, X = CH_2-2-pyridyl
215f R = Me, X = CH_2CO_2Me
215g R = Me, X = H
215h R = *t*-Bu, X = Bn
215i R = Cl, X = Bn

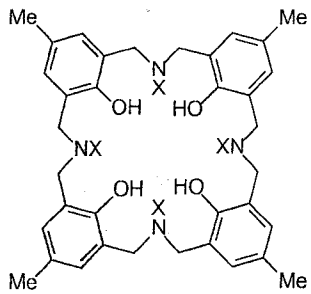

216a X = H
216b X = CH_2CO_2Me

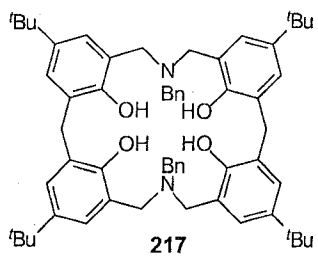

217

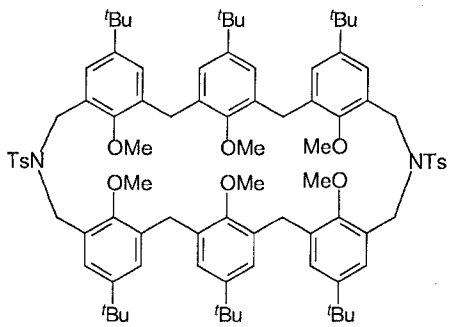

218

Figure 8.1 Examples of homoazacalixarenes.

Several useful methods for preparation of homoazalixarenes and their derivatives have recently been reported. Homoazacalixarenes have been shown to be moderate receptors for various guests such as alkali metal ions,[2] UO_2^{2+},[2,3] Zn^{2+},[4] Co^{3+},[4] Nd^{3+},[5], Yb^{3+},[6] ammonium[7] anion and various fluorescent molecules.[8]

In 1990, Robson *et al.* developed a novel, efficient method to synthesize octahomotetraazacalix[4]arene **216a** via reduction of Schiff base **221** which was prepared in high yield (71%) from the condensation of 2,6-bis(aminomethyl)-4-methylphenol (**219**) and 2,6-diformyl-4-methylphenol (**220**) in the presence of $Ni(OAc)_2$ or $Zn(OAc)_2$ (Scheme 8.1).[4,9]

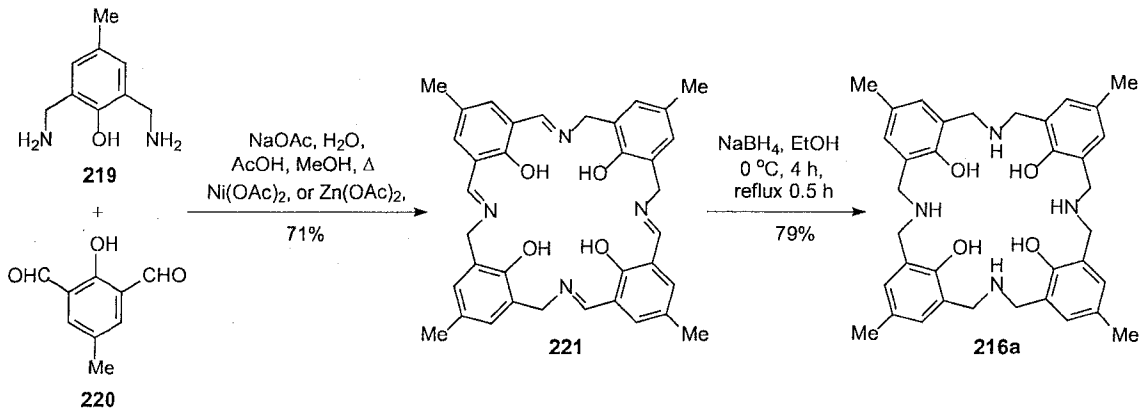

Scheme 8.1 Synthesis of octahomotetraazacalix[4]arene **216a** via reduction of Schiff base **221**.

In 1992, Takemura *et al.*[10] reported that *N,N',N''*-tribenzylhexahomotriaza-calix[3]arene **215b** was afforded in acceptable yield upon prolonged heating of 2,6-bis(hydroxymethyl)-4-methylphenol (**222**) with benzylamine (**223**) in refluxing toluene (Scheme 8.2).

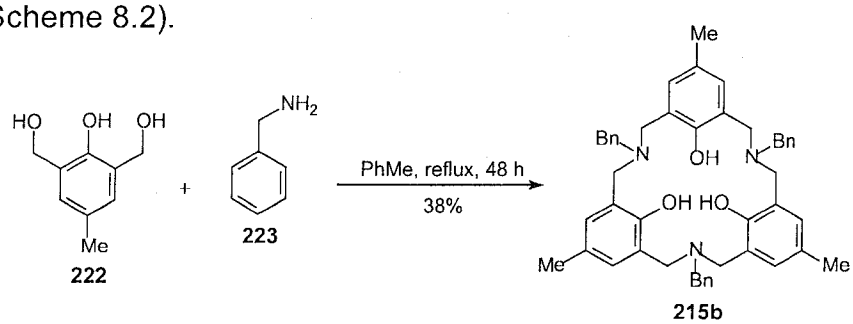

Scheme 8.2 Synthesis of *N*-benzylhexahomotriazacalix[4]arene **215b**.

Exploiting the Inazu[11] approach to azacyclophanes, in 1994, Takemura *et al.*[12] synthesized *N,N',N'',N'''*-tetratosyloctahomotetraaza-*p-tert*-butylcalix[4]arene (**227**) in 13% yield, along with *N,N'*-ditosyl-2,11-diaza[3.3](1,3)cyclophane **226** (10%) from the coupling of 2,6-bis(bromomethyl)-4-*tert*-butylanisole (**224**) and *p*-toluenesulfonamide (**225**) (Scheme 8.3).

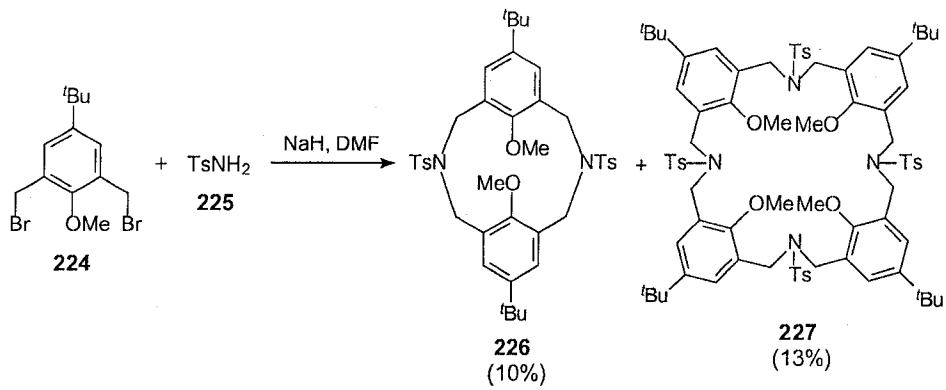

Scheme 8.3 Synthesis of octahomotetraazacalix[4]arene **227**.

In 1995, Shinmyozu *et al.*[13] reported a different method to prepare *N*-substitutedhomoazacalix[4]arene, *e.g.* **230**, via alkylation of commercially available cyanamide (**228**) with several bis(bromomethyl)benzene derivatives, *e.g.* **224** (Scheme 8.4). *N,N',N'',N'''*-tetracyanooctahomotetraaza-*p-tert*-butylcalix[4]arene (**230**) in 10% yield along with *N,N'*-dicyano-5,14-dimethoxy-2,11-diaza[3.3](1,3)cyclophane (**229**) (16%). Although this method still encountered the problem of low yield of macrocyclization, it used mild conditions.

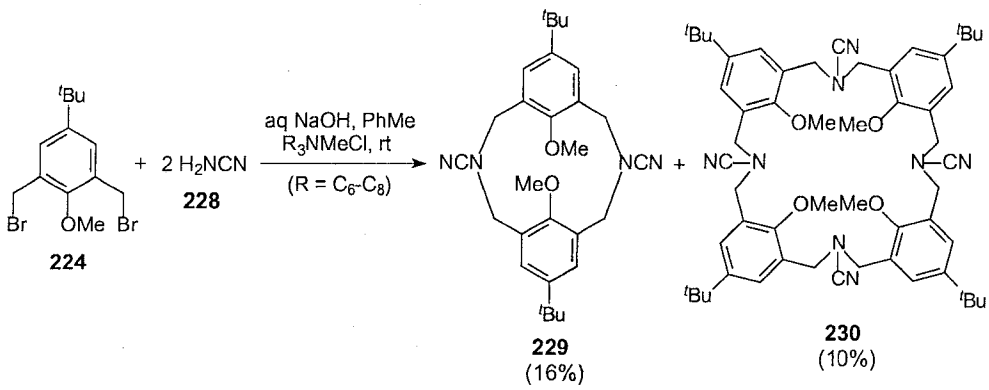

Scheme 8.4 Synthesis of octahomotetraazalcalix[4]arene **230**.

In 1996, Hampton *et al.* reported[2] that the thermal condensation of 2,6-bis(chloromethyl)-4-methylphenol (**231**) with glycine methyl ester hydrochloride (**232**) under basic and high dilution conditions afforded a mixture of *N,N',N''*-tris(methoxycarbonylmethyl)hexahomotriazacalix[3]arene (**215f**) and *N,N',N'',N'''*-tetrakis(methoxycarbonylmethyl)octahomotetraazacalix[4]arene (**216b**), which was purified by chromatography to afford **215f** in 19% yield along with **216b** (Scheme 8.5).

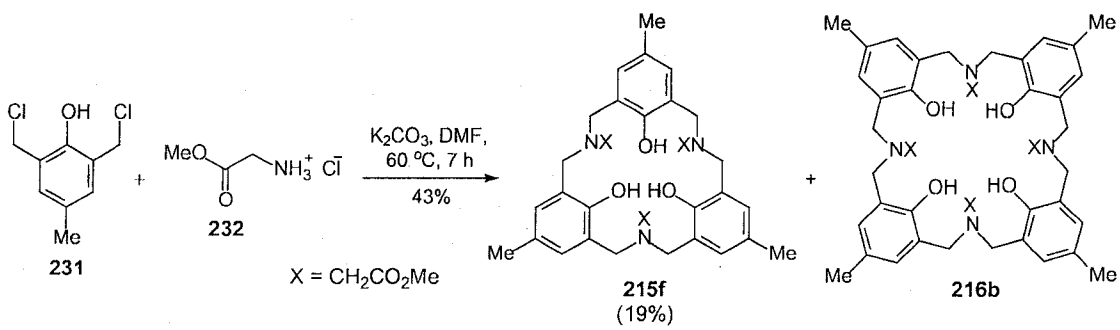

Scheme 8.5 Synthesis of homoazacalix[4]arenes **215f** and **216b**.

Using this approach, in 2000 Ito *et al.* reported the successful synthesis of chiral tetrahomodiazacalix[4]arenes, *e.g.* **235a-f**, in 10–22% yields via

condensation of bis(chloromethyl)phenol-formaldehyde dimers (**233a** or **233b**) with the corresponding (*S*)-amino acid methyl esters (**234a-d**) under basic conditions (Scheme 8.6).[7]

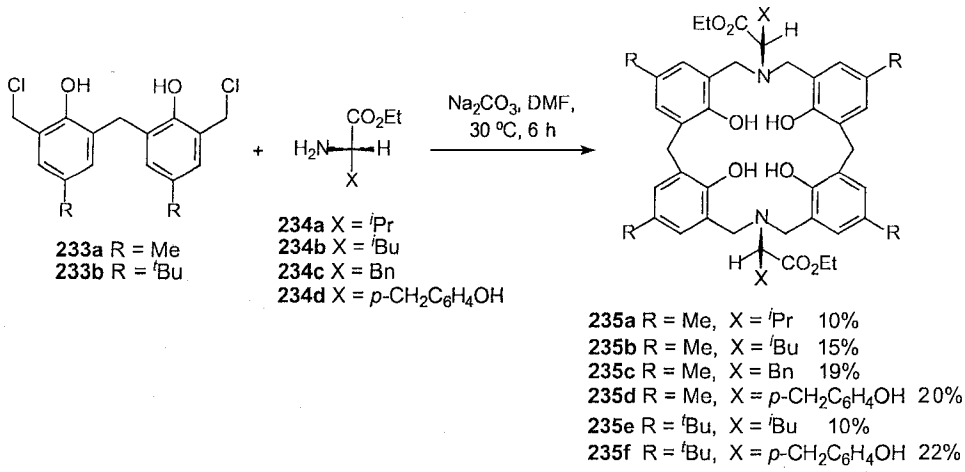

Scheme 8.6 Synthesis of tetrahomodiazacalix[4]arenes **235a-f**.

In the same year, Hampton *et al.* also reported the synthesis of *N,N',N''*-trisubstituted-hexahomtriazacalix[3]arenes (**238a-d**) in very high yields (90-95%) via a mild coupling between bis(chloromethyl)-4-methylphenol (**231**) but with triamines **237a-d** (Scheme 8.7).[14]

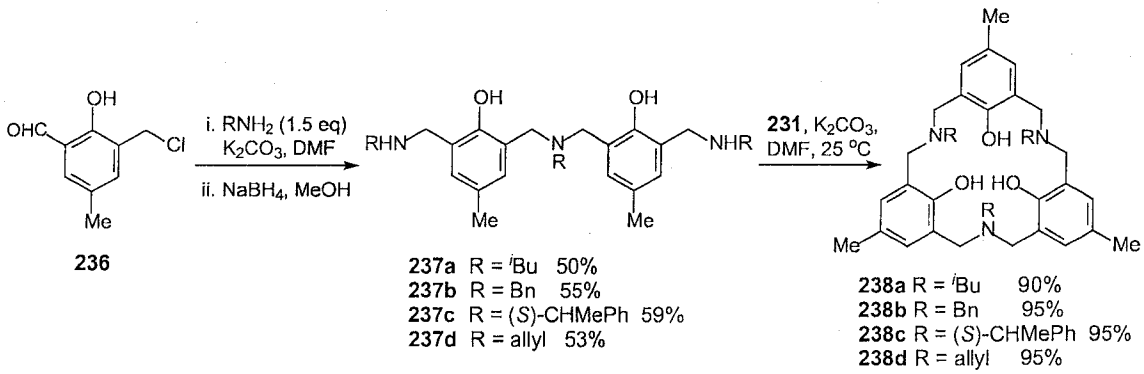

Scheme 8.7 Synthesis of hexahomotriazacalix[4]arene **237a-d**.

Furthermore, Anslyn *et al.* reported in 1999 the preparation of octahomotetraazacalix[4]arene **242**, containing the wide-rim primary methylamino groups, in reasonably high yield (40%). The synthesis was achieved via a one-step cyclization from 1,3,5-tris(aminomethyl)-2,4,6-ethylbenzene (**239**) and 1,3-bis(bromomethyl)-5-azidomethyl-2,4,6-ethylbenzene (**240**), in the presence of triethylamine at room temperature, followed by reduction of the azido groups in **241** (Scheme 8.8).[15]

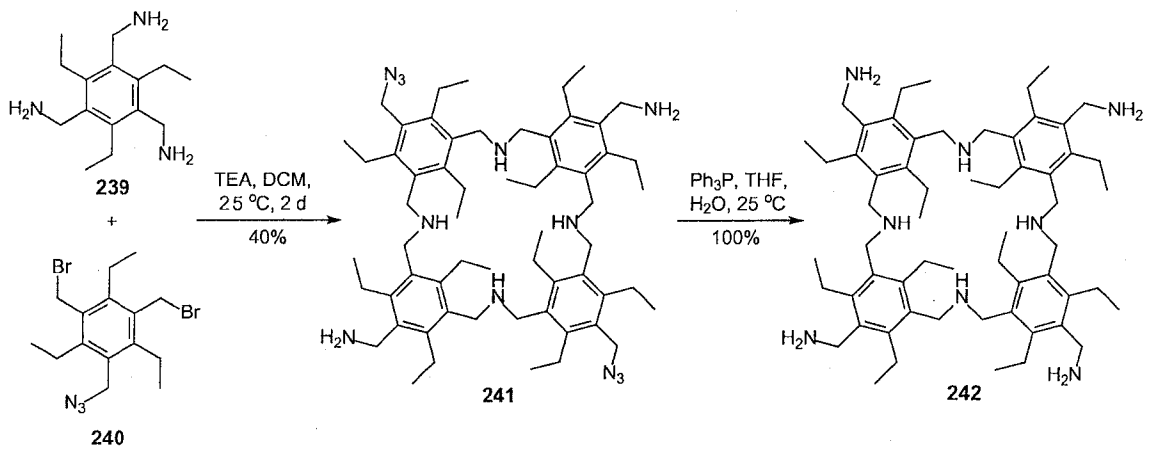

Scheme 8.8 Synthesis of octahomotetraazacalix[4]arene **242**.

Octahomotetraazacalix[4]arene **242** was shown to be a weak receptor for fluorescent indicators **243**, **244** and phosphorylated carbohydrates **245**-**247** (Figure 8.2), all with 1:1 binding ratios under the conditions studied.

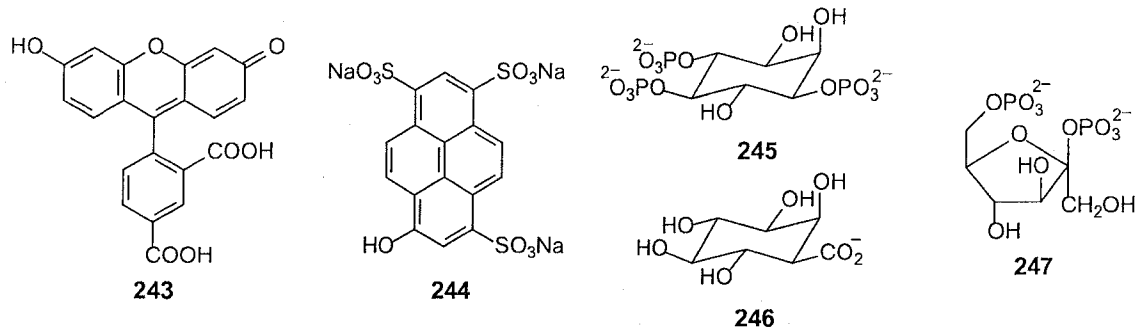

Figure 8.2 Structures of guests **243-247**.

To date, there has been no report dealing with the analoguos homoazacalixnaphthalenes and/or their derivatives. In order to expand the class of homohetero-bridged calixnaphthalenes besides the homoxa-[16] and homothia-analogues,[17] attempted syntheses of octahomotetraazaisocalix[4]naphthalenes and *N,N',N'',N'''*-tetrasubstituted-octahomotetraazacalix[4]naphthalenes were, therefore, undertaken and these endeavours are described in this chapter. These new target compounds could serve as potentially useful receptors for ionic and/or neutral guests.

8.2 Design and retrosynthetic analysis of "1,4-linked" octahomotetraazaisocalix[4]naphthalenes 248a-d and "1,4-linked" *N,N',N'',N'''*-tetratosyloctahomotetraazaisocalix[4]naphthalenes 249a-d

8.2.1 Design of target structures

The CPK model and computer-aidded molecular modeling studies[18] both suggested that the octahomotetraazaisocalix[4]naphthalenes **248a-d**, are quite flexible. This is similar to what was also observed with the homooxa- **159a-d** and homothiaisocalix[4]naphthalenes **205a-d**, which were previously synthesized.

However, when tosyl groups were attached on the bridging nitrogen atoms of **248a-d**, the resulting *N,N',N'',N'''*-tetratosyloctahomotetraazaisocalix[4]-naphthalenes **249a-d** were shown to be less flexible than their parent compounds (Figure 8.3). It was anticipated that these new, more rigid homoazacalixnaphthalenes **249a-d** could serve as better hosts for host-guest binding studies than the homooxa- and homothia-analogues synthesized. Hence, the attempted syntheses of these new homoaza receptors were undertaken.

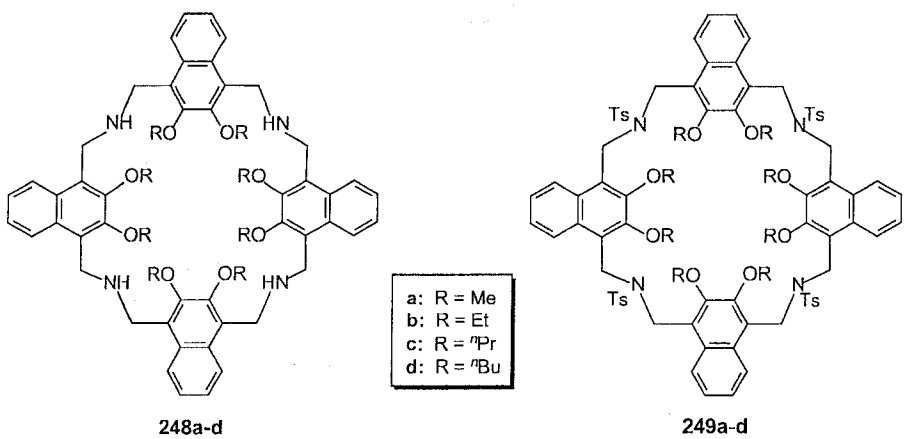

Figure 8.3 Octahomotetraazaisocalix[4]naphthalenes **248a-d** (*left*); *N,N',N'',N'''*-tetratosyloctahomotetraazaisocalix[4]naphthalenes **249a-d** (*right*).

8.2.2 Retrosynthetic analysis

Retrosynthetic analysis as outlined in Scheme 8.9 indicated that tetra(*N*-tosylation) of octahomotetraazaisocalix[4]naphthalenes **248a-d** could produce *N,N',N'',N'''*-tetratosyloctahomotetraazaisocalix[4]naphthalenes **249a-d**. From several known routes available for the synthesis of homoazacalixarenes which have been mentioned above, the two highest yield approaches, including

Anslyn's procedure,[15] and via reduction of intermediate cyclic Schiff bases,[4,9] were selectively employed to prepare the precursors **248a-d**.

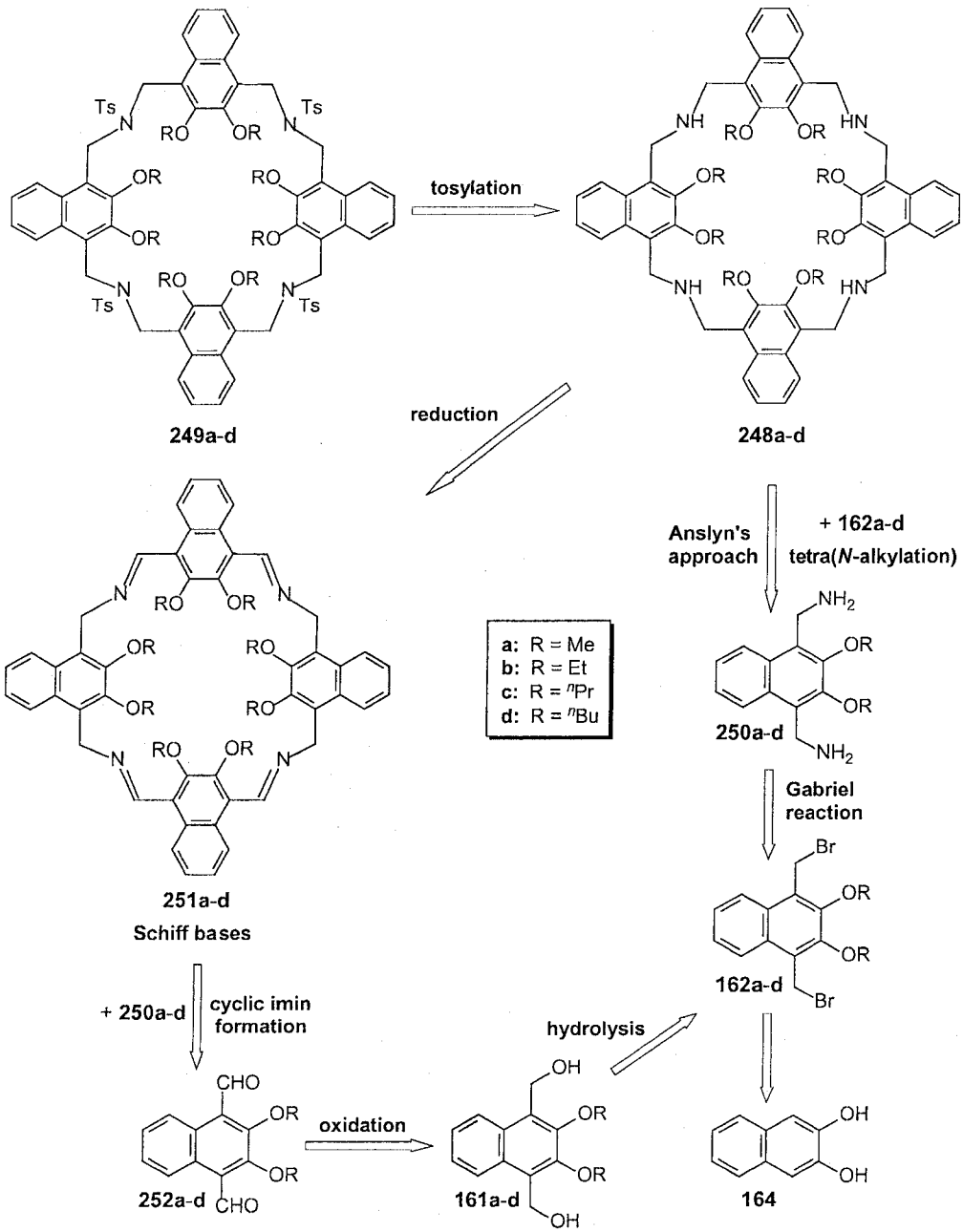

Scheme 8.9 Retrosynthetic analysis of azacalixnaphthalenes **248a-d** and **249a-d**.

In turn, it was anticipated that tetra(*N*-alkylation) of 1,2-bis(aminomethyl)-2,3-dialkoxynaphthalenes (**250a-d**) by 1,4-bis(bromomethyl)-2,3-dialkoxy-naphthalenes (**162a-d**) might afford the cyclic product **248a-d**. Employment of the Gabriel reaction with **162a-d** would give intermediate **250a-d** having two primary amine functional groups. The precursors **162a-d** were directly derivable from commercially available 2,3-dihydroxynaphthalene (**164**). In the alternate approach, **248a-d** could be afforded via reduction of the cyclic Schiff bases **251a-d** which would result from the condensation of **250a-d** and 1,4-diformyl-2,3-dialkoxynaphthalenes (**252a-d**), respectively. Intermediates **252a-d** were also derivable directly from **162a-d** via hydrolysis and oxidation.

8.3 Results and discussion

8.3.1 Synthesis of 1,4-diformyl-2,3-dimethoxynaphthalene (252a) and 1,4-bis(aminomethyl)-2,3-dialkoxynaphthalenes (250a-d)

Both approaches involved coupling reactions between 1,2-bis(aminomethyl)-2,3-dialkoxynaphthalenes (**250a-d**) with 1,4-bis(bromomethyl)-2,3-dialkoxynaphthalens (**162a-d**), or condensation between intermediates **250a-d** with diformylnaphthalenes **252a-d**, respectively. Hence, intermediates **250a-d** and only **252a** were synthesized in order to test the cyclization methodology.

Oxidation of 1,4-bis(hydroxymethyl)-2,3-dimethoxynaphthalene **161a** derived from 2,3-dihydroxynaphthalene (**164**) by PCC[19] at room temperature in 3 h gave pure **252a** in 95% yield (Scheme 8.10). This approach proved to be

reproducible.[20] On the other hand, a direct diformylation of 2,3-dimethoxynaphthalene (**163a**) exploiting a dilithiation of the naphthyl diether[21,22] gave **252a** in only 10% yield.

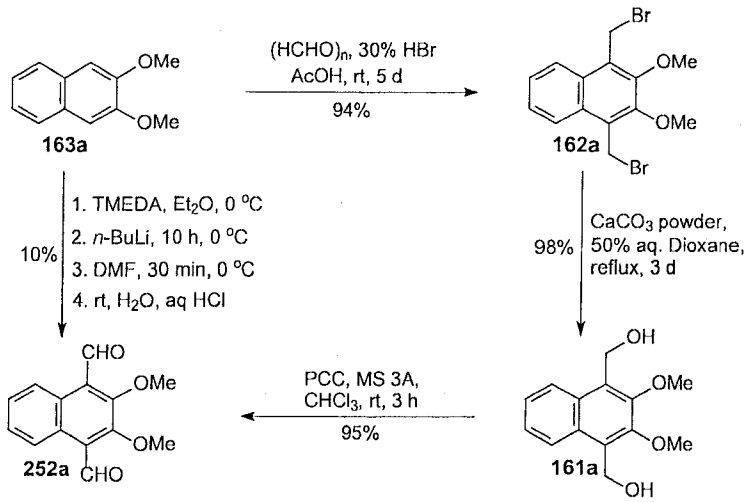

Scheme 8.10 Synthesis of 1,4-diformyl-2,3-dimethoxynaphthalene (**252a**).

Intermediates **250a-d** were afforded from **162a-d** via two-step Gabriel reactions (Scheme 8.11).[23] At first, treatment of each of **162a-d** with potassium phthalimide (**253**) in refluxing DMF in 3.5 h gave the corresponding 1,4-bis(*N*-phthalimidomethyl)-2,3-dialkoxynaphthalenes **254a-d**, each in high yields (70-93%). Hydrolysis reaction of each of **254a-d** in the presence of H_2NNH_2 in refluxing methanol in 4 h yielded the corresponding products **250a-d** in 65-100% yields. In the case of **250b**, using ethanol as solvent afforded a lower reaction yield (63%) than that obtained when methanol was used as solvent (100% yield).

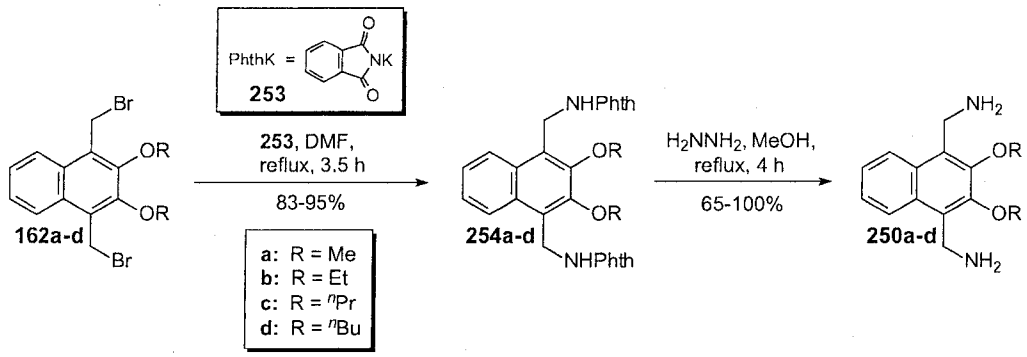

Scheme 8.11 Synthesis of 1,4-bis(aminomethyl)-2,3-dialokoxynaphthalenes (**250a-d**).

8.3.2 Attempted synthesis of 248a, 248b, 249a and 249b

Addition of 1,4-bis(bromomethyl)-2,3-diethoxynaphthalene (**162b**) to the mixture of 1,4-bis(aminomethyl)-2,3-dimethoxynaphthalene (**250b**) and TEA in DCM at room temperature following Anslyn's procedure,[15] gave an intractable resinous mixture (Scheme 8.12). The expected cyclization, therefore, failed to form desired cyclic product, *e.g.* **248b**.

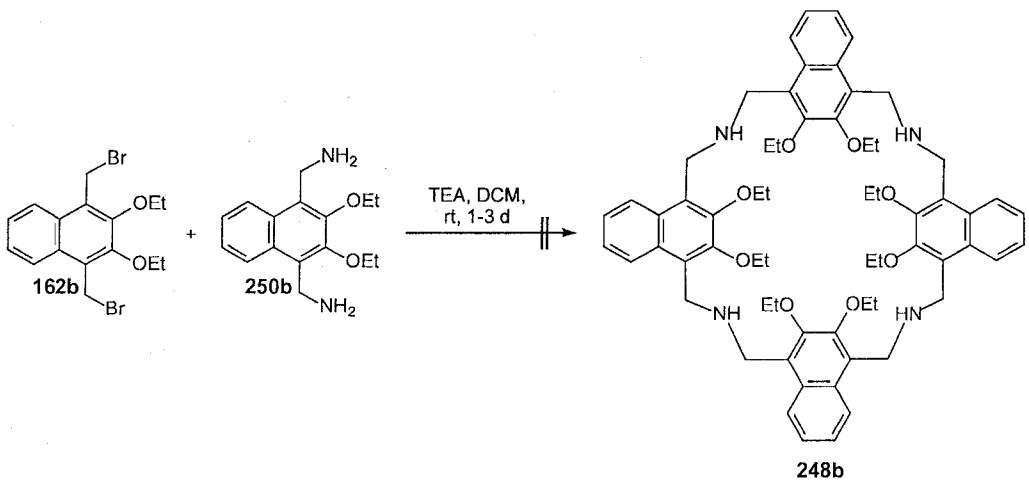

Scheme 8.12 Attempted synthesis of **248b**.

Hence, the alternate approach via Schiff bases was exploited without using a cationic template (Scheme 8.13) following Kuhnert's procedure.[22] However, heating a mixture of **250a** and **252a** in DCM at reflux over 2-12 h produced no reaction at all. Both TLC and ^{1}H NMR showed only the presence of starting materials. It was presumed that the cyclization of **250a** and **252a** required a higher reaction temperature. However, when DCM replaced by benzene, no cyclization was observed with or without use of a Dean-Stark apparatus in order to shift the reaction equilibrium towards the cylic product direction. No improvement was found using acetonitrile following Akine's procedure[24] either at ambient temperature or heating at reflux. Employment of acetonitrile-chloroform conditions found by MacLachlan[25] and heating at reflux for 2 h gave an unidentified resinous mixture which was not soluble in most of the common organic solvents.

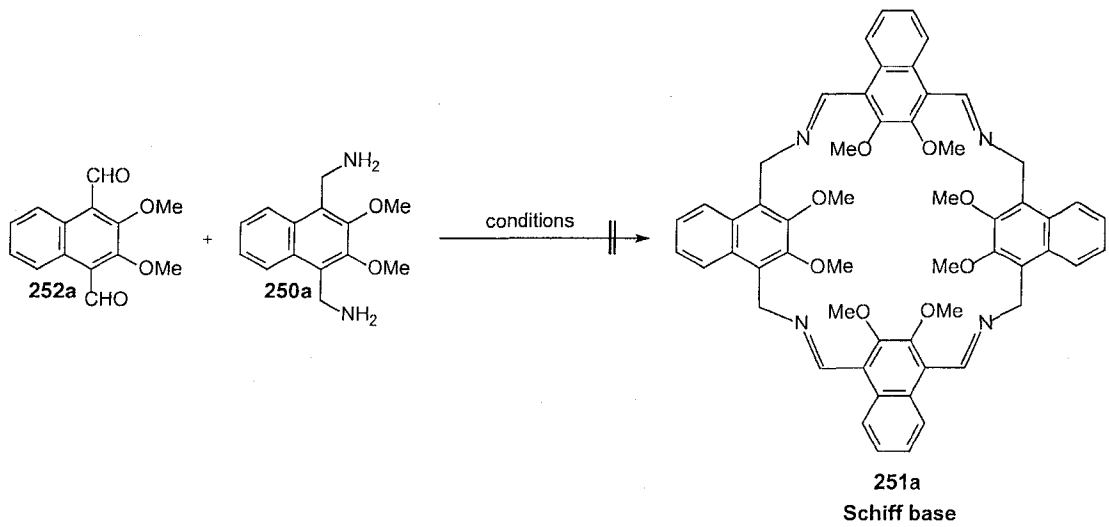

251a
Schiff base

Scheme 8.13 Attempted synthesis of Schiff base **251a**.

It was then hypothesized[24] that the reaction to form the cyclic Schiff base might be facilitated by having free hydroxy phenol groups on **255a**. Specifically, the hydrogen bonding could facilitate formation of intermediates **256a** or **257a** which could gradually lead to the formation of cyclic Schiff base **258a**. (Scheme 8.14). The free hydroxy groups in **258a** could be very useful since they could form intramolecular hydrogen bonds to reduce the flexibility of **258a**. Therefore, a condensation between 1,4-bis(aminomethyl)-2,3-dimethoxy-naphthalene **250a** and 1,4-diformyl-2,3-dihydroxnaphthalene **255a** was explored to form **258a**.

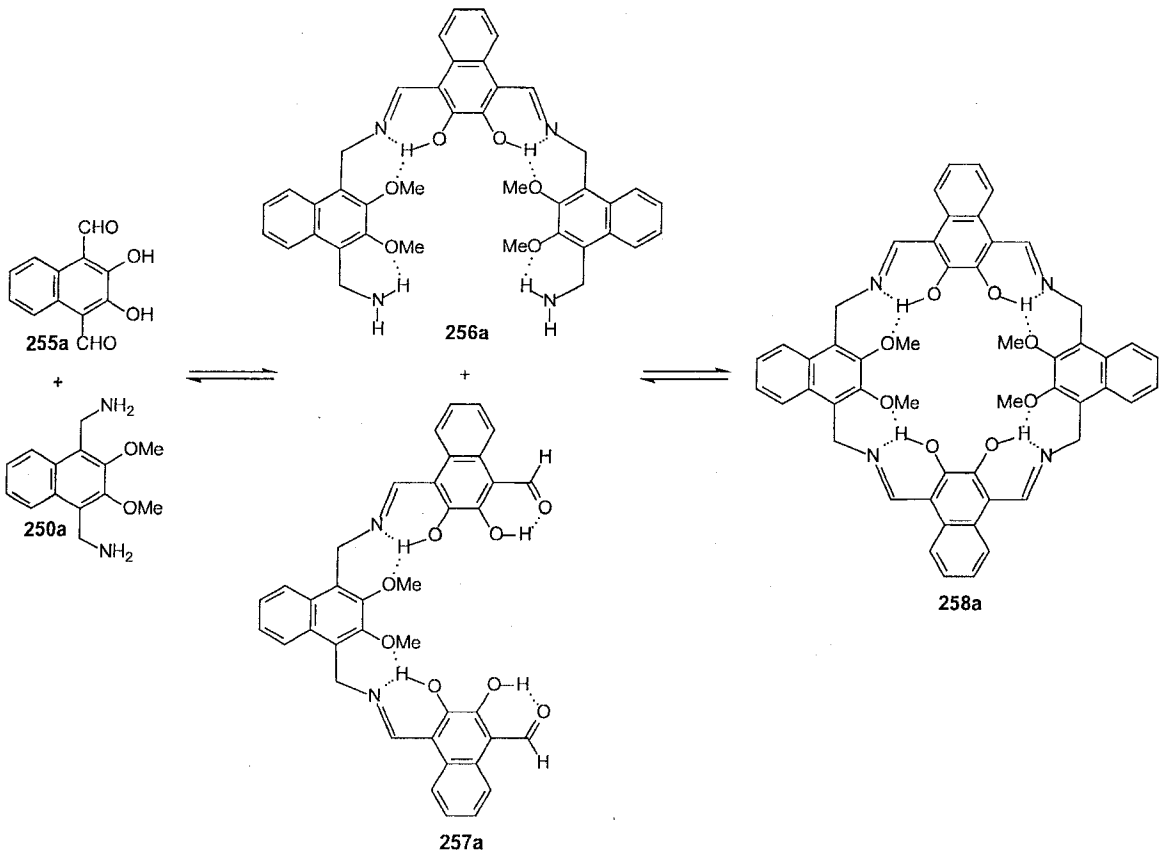

Scheme 8.14 A proposed condensation 1,4-bis(aminomethyl)-2,3-dimethoxy-naphthalene (**250a**) and 1,4-diformyl-2,3-dihydroxynaphthalene (**255a**) to form cyclic Schiff base **258a**.

Demethylation of 1,4-bis(hydroxymethyl)-2,3-dimethoxynaphthalene (**252a**) by BBr_3 in DCM at room temperature gave intermediate **255a** in 98% yield (Scheme 8.15). This approach proved to be more reproducible[20] than the Reinhoudt procedure.[26] Employment of the Skattebøl formylation,[27] however, failed to give **255a** directly from 2,3-dihydroxynaphthalene (**164**).

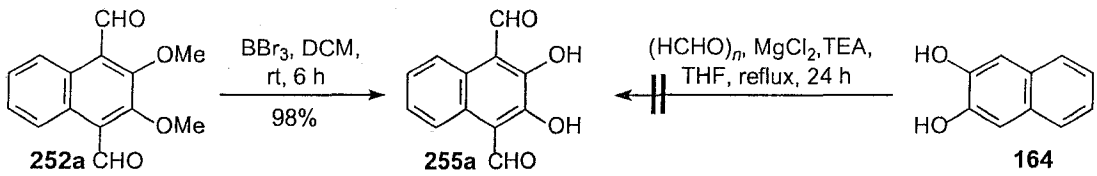

Scheme 8.15 Preparation of 1,4-diformyl-2,3-dihydroxynaphthalene **255a**.

The condensation of 1,4-diformyl-2,3-dimethoxynaphthalene (**255a**) and 1,4-bis(aminomethyl)-2,3-dimethoxynaphthalene (**250a**) (Scheme 8.15) was tested in several solvents (CH_2Cl_2,[22] CH_3CN,[24] 1:1 CH_3CN-$CHCl_3$,[20b,25,28] 1:1 MeOH-CH_3CN[26]) by the dropwise addition of solutions of **255a** to solutions of **250a** in the same solvent, or *vice versa*, or using a two-syringe pump in order to add both solutions at the same rate. The reactions were conducted at either room temperature (3-14 d) or at reflux (2-4 h). The starting materials were completely consumed under the conditions employed, but reactions produced intractable and unidentified mixtures which were not soluble in most of the common organic solvents. It was presumed that the oligomeric or polymeric products were formed instead of the desired cyclic products.

Reinhoudt *et al.* reported[26] the use of Ba^{2+} as a template ion for the condensation of 1,4-diformyl-2,3-dimethoxynaphthalene (**255a**) with diamine

259a-d to synthesize calixsalens **260a-c** and **261** in 60-70% yields (Scheme 8.16). Therefore, the condensation of **255a** and 1,4-bis(aminomethyl)-2,3-dimethoxynaphthalene (**250a**) (Scheme 8.15) was then reinvestigated using $Ba(CF_3SO_2)$ or $Ba(SCN)_2$ as the source of the Ba^{2+} template in a variety of solvents (CH_2Cl_2,[22] CH_3CN,[24] 1:1 CH_3CN-$CHCl_3$,[20b,25,28] 1:1 MeOH-CH_3CN[26]) either at room temperature (1-3 d) or at reflux temperature (1-4 h). However, the resulting brown or orange precipitates could not be identified since they were not soluble in most common organic solvents. No further attempts were carried out with this approach.

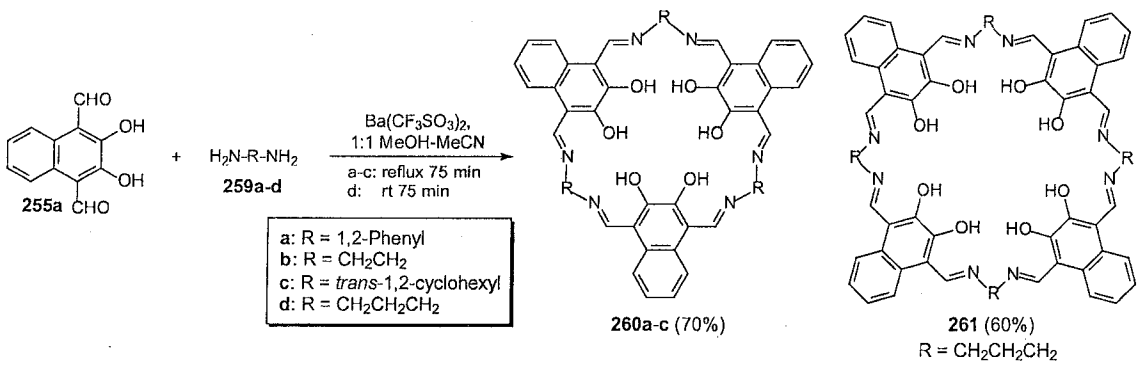

Scheme 8.16 The Reinhoudt syntheses of calixsalens **260a-c** and **261**.

8.3.3 Calixarene-like *N,N*-ditosyldiaza[3.3](1,4)naphthalenophanes 264a-d resulting from an attempted synthesis of 249a-d

8.3.3.1 Retrosynthetic analysis and synthesis

Since both Anslyn's procedure[15] and the Schiff base approach[4,9] failed to give the desired product **248a-d**, a new route involving a coupling of 1,4-bis(*p*-tolylsulfonylaminomethyl)-2,3-dialkoxynaphthalenes **262a-d** and 1,4-bis-

(bromomethyl)-2,3-dialkoxynaphthalenes **162a-d** was employed (Scheme 8.17) to synthesize **149a-d**.[29]

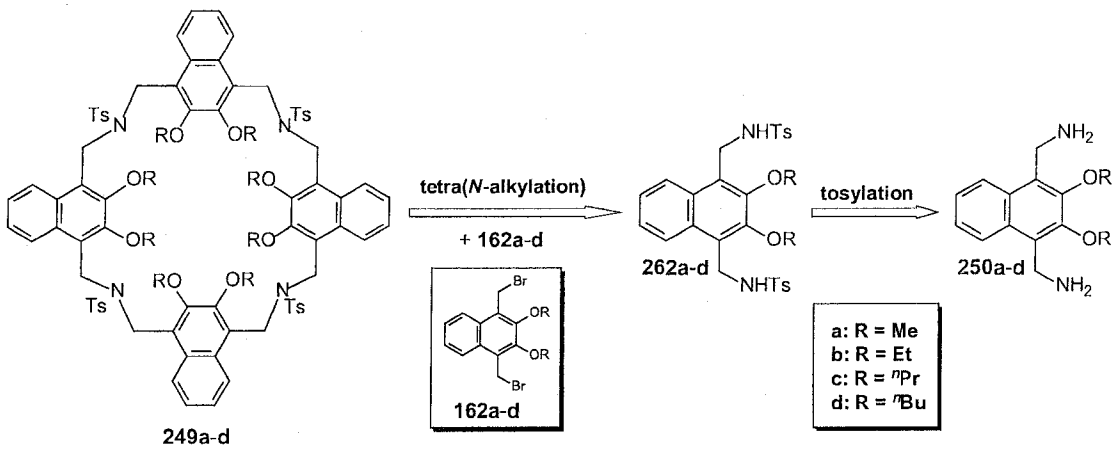

Scheme 8.17 New retrosynthetic analysis for **249a-d**.

It was envisioned that under basic conditions, the amide in **262a-d** could be deprotonated to generate anion which would undergo S_N2 displacement with **162a-d** to give **249a-d**. Intermediates **262a-d** could be derivable directly from **250a-d**, respectively, via ditosylation reactions.

Ditosylation of **250a** by TsCl under various conditions using organic bases such as TEA/THF,[29] pyridine/THF or DCM,[30] or neat TEA-pyridine,[30] unfortunately, gave no reaction or produced unidentifiable reaction mixtures. It was presumed that the organic bases under conditions used were not strong enough to deprotonate the amine groups needed to form 1,4-bis(*p*-tolylsulfonylaminomethyl)-2,3-dimethoxynaphthalene (**262a**). When Hart's protocol[31] using a two-phase system consisting of aqueous NaOH and DCM was

employed at room temperature, compounds **262a-d** were formed in 73-83% yields over reaction times of 20-40 h (Scheme 8.18).

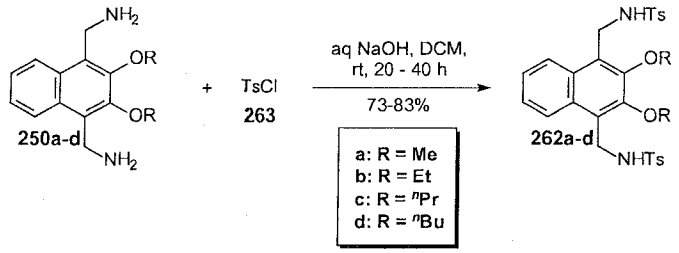

Scheme 8.18 Ditosylation of **250a** using Hart's protocol to prepare **262a-d**.

The stage was set for another attempted synthesis of compounds **249a-d** via the coupling reaction of intermediates **162a-d** and **262a-d** under basic conditions (Scheme 8.19). CPK models suggested that the formation of *N,N*-ditosyldiaza[3.3](1,4)naphthalenophanes **264a-d**, which are [1+1] products, from the above coupling reaction would be inhibited due to steric strain. Therefore, it was anticipated that [2+2] coupling products would be the dominant products instead, as was observed with the synthesis of octahomtetraoxa-**159a-d** and octahomotetrathiacalix[4]naphthalenes **205a-d**.

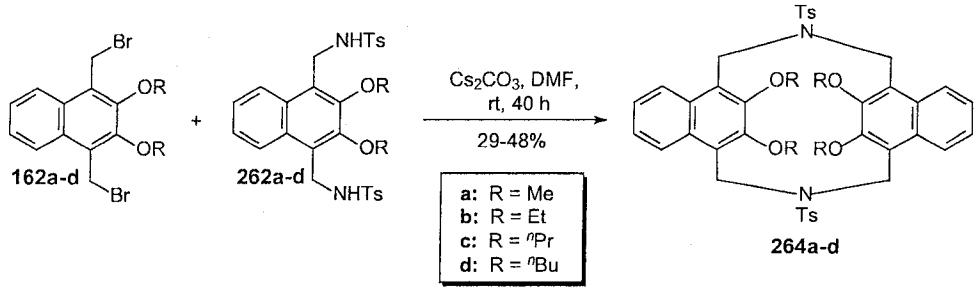

Scheme 8.19 Synthesis of *N,N*-ditosyldiaza[3.3](1,4)naphthalenophanes **264a-d**.

Unexpectedly, the coupling between these above intermediates in DMF in the presence of Cs_2CO_3 specifically gave *N,N*-ditosyl-diaza[3.3](1,4)-naphthalenophanes **264a-d** as products instead of the desired [2+2] coupling products, *N,N',N'',N'''*-tetratosyloctahomotetraazaisocalix[4]naphthalenes **249a-d**. (+)-APCI MS analysis all showed the molecular ion peaks of **264a-d**, respectively, at *m/z* = 767, 823.3, 879.5, and 935.4 at 100% relative intensities. The formation of **264a** was also confirmed by its X-ray structure (Figure 8.4). The X-ray structure of **264c** (Figure 8.5) was also obtained but with low refinement.

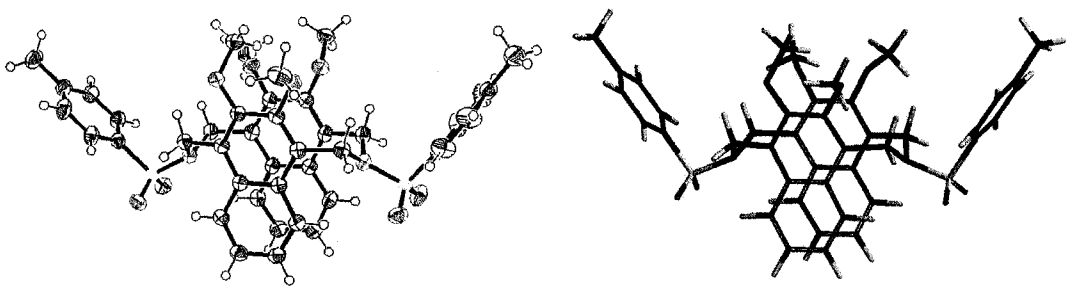

Figure 8.4 X-ray stereoview of **264a** showing its "*1,3-alternate*"[32] conformation (*left*) (solvent molecules were removed for clarity) identical with its computer-generated lowest energy conformer[18] (*right*).

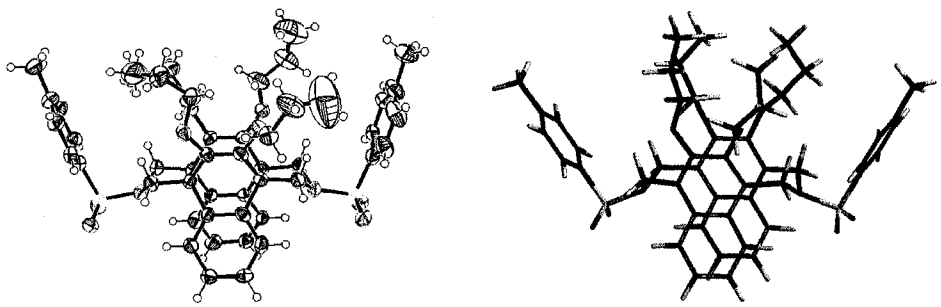

Figure 8.5 X-ray stereoview of **264c** showing its "*1,3-alternate*"[33] conformation (*left*) (solvent molecules were removed for clarity) identical with its computer-generated lowest energy conformer[18] (*right*).

Pappalardo *et al.*[33] also found that the coupling reaction between 1,4-bis(chloromethyl)-2,3,5,6-tetramethylbenzene (**265**) and monosodium *p*-toluenesulfonamide (**266**) *N,N*-ditosyl-5,6,8,9,14,15,17,18-octamethyl-2,11-diaza[3.3](1,4)cyclophane (**267**) in 15% yield along with 1,4-bis(tosylamino-methyl)durene (**268**) in 36% yield (Scheme 8.20).

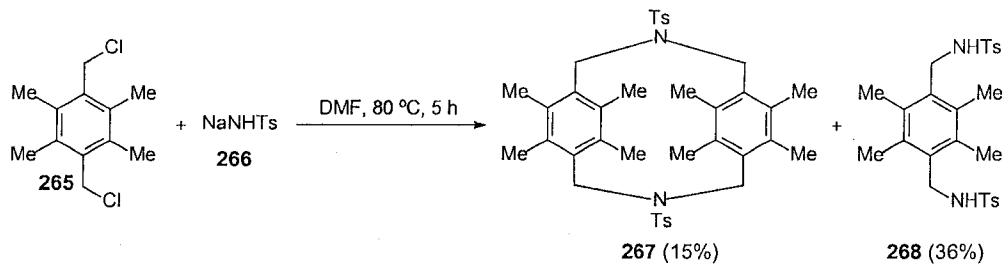

Scheme 8.20 The Pappalardo synthesis of **267**.

8.3.3.2 Characterization of *N,N*-ditosyldiaza[3.3](1,4)naphthalenophanes 264a-d

All of these new macrocyclic compounds had relatively simple ambient temperature ^{1}H NMR spectra which indicated that they were highly symmetrical. In addition, the ^{1}H NMR spectra for compounds **264a-d** all revealed AB type doublet system for their bridging methylene groups, at 4.19 and 5.29 ppm, 4.13 and 5.24 ppm, 4.11 and 5.23 ppm, 4.09 and 5.23 ppm, respectively. This indicates that **264a-d** are much more rigid than the homooxa and homothia analogues which only show singlet signals for their bridging methylene groups. Furthermore, the bridging methylene groups of **264a-d** were slightly more shielded in the following order: **264a** > **264b** > **264c** > **264d**.

The X-ray structure of **264a** revealed that it is in a "*1,3-alternate* conformation"[33] in the solid state (Figure 8.4). This conformation was also found for compound **264c** in the solid state (Figure 8.4). A search for the lowest conformer (using MMFF94 prior to geometry optimization at the PM3 level of theory)[18] conducted on **264a** and the other structures **264b-264d** was consistent with the *1,3-alternate* conformation being the lowest energy conformer.

8.4 Conclusions and proposals for future complexation work

In summary, both the *N*-alkylation[15] and cyclic Schiff base[4,9] approaches failed to afford the desired products *N,N',N'',N'''*-tetratosyloctahomotetraaza-isocalix[4]naphthalene **249a-d** but instead give resinous intractable products. The coupling between 1,4-bis(*p*-tolylsulfonylamino-methyl)-2,3-dialkoxy-naphthalenes (**262a-d**) and 1,4-bis(bromomethyl)-2,3-dialkoxy-naphthalenes (**162a-d**), respectively, gave a series of new corresponding *N,N*-ditosyldiaza[3.3](1,4)naphthalenephanes (**264a-d**) (or "tetrahomodiazacalix[2]-naphthalenes"), respectively, in reasonable yields (29-48%) for such macrocyclizations. The ^{1}H NMR spectra of all of the macrocycles obtained showed clearly that they were highly symmetrical and also conformationally rigid. The X-ray structures of **264a** and **264b** also revealed that the *1,3-alternate* conformations are most likely the dominant ones.

The complexation studies of these new tetrahomodiazacalix[2]-naphthalenes should be investigated with alkali metal ions[2] and transition metal

(Ag^+, Hg^{2+}, Cu^{2+}, etc.)[4-6,34] and to evaluate their binding properties for potential applications.

8.5 Experimental section

1,4-Diformyl-2,3-dimethoxynaphthalene (252a)

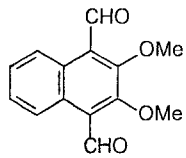

Procedure 1: Oxidation of 1,4-bis(hydroxymethyl)-2,3-dimethoxy-naphthalene (**161a**).

To a stirred suspension of PCC (1.86 g, 3.72 mmol) and 3 Å molecular sieves (2.8 g) in $CHCl_3$ (30 mL) at room temperature was added a solution of **161a** (0.51 g, 2.0 mmol) in $CHCl_3$ (100 mL). The reaction mixture was stirred for a further 3 h, filtered through a Florisil® pad, and the residue was washed with $CHCl_3$ (3 x 30 mL). The organic layer was dried over anhydrous $MgSO_4$ and filtered. After the solvent was removed under reduced pressure, the crude product was purified by chromatography (1:9 EtOAc-hexane) to yield **252a** (0.46 g, 92%) as a yellow solid: mp 100–101 °C (acetone-hexane) (lit.[20] 101–102 °C); ^{1}H NMR δ 4.11 (s, 6H), 7.60–7.62 (m, 2H), 9.02–9.04 (m, 2H), 10.8 (s, 2H); ^{13}C NMR δ 63.2, 125.1, 128.2, 128.8, 129.0, 158.4, 192.2; GCMS *m/z* (relative intensity) 244 (M^+, 85), 229 (30), 169 (65), 102 (100).

Procedure 2: Direct diformylation[22] of 2,3-dimethoxynaphthalene (**163a**)

To a stirred solution of **163a** (0.75 g, 4.00 mmol) and TMEDA (3.0 mL, 20 mmol) in anhydrous Et_2O (25 mL) at 0 °C was added dropwise 1.6 M *n*-BuLi in hexane (13 mL, 20 mmol), and the reaction mixture was then heated at reflux for a further 10 h and cooled to room temperature. To the reaction mixture DMF (1.6 mL, 20 mmol) was added dropwise, and the mixture was stirred for a further 30 min. Cool water (20 mL) was added to the mixture, followed by aqueous 3 M HCl (4.0 mL). The mixture was extracted with Et_2O (3 x 40 mL). The organic layers were combined, washed with brine (1 x 40 mL), dried over $MgSO_4$ and filtered. After the solvent was removed under reduced pressure, the resulting residue was purified by chromatography (2:98 EtOAc-hexane) to yield **252a** (0.10 g, 10%) having identical characterization data to those obtained from Procedure 1.

1,4-Bis(*N*-phthalimidomethyl)-2,3-dimethoxynaphthalene (254a)

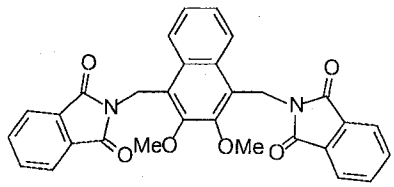

General procedure: To a stirred solution of crude **162a** (3.74 g, 10.0 mmol) in DMF (100 mL), was added potassium phthalimide (**253**) (4.07 g, 22.0 mmol). The reaction mixture was heated at reflux (153–160 °C) with stirring for 3.5 h, cooled to room temperature and then poured into cold water (500 mL). The resulting precipitate was filtered and dried at 60 °C to afford crude product (4.20 g, 83%) as a light yellow powder, which was purified by chromatography (5:95

EtOAc–DCM) to yield **254a** (3.34 g, 66%) as also a light yellow powder: mp 270–272 °C; ^{1}H NMR δ 4.09 (s, 6H), 5.37 (s, 4H), 7.37–7.39 (m, 2H), 7.64–7.66 (m, 4H), 7.77–7.78 (m, 4H), 8.06–8.08 (m, 2H); ^{13}C NMR δ 33.8, 61.0, 123.4, 124.0, 124.4, 125.7, 129.5, 132.2, 134.1, 152.0, 168.4; (+)-APCI MS *m/z* (relative intensity) 507.0 (M^+, 40), calcd.: 506.51 for $C_{30}H_{22}N_2O_6$, 360.1 (100)

1,4-Bis(*N*-phthalimidomethyl)-2,3-diethoxynaphthalene (254b)

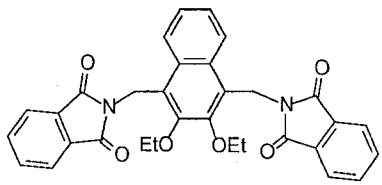

Using the general procedure for **254a**, the reaction of the crude **162b** (2.81 g, 6.99 mmol) and **253** (2.76 g, 14.9 mmo) gave the crude product (3.11 g, 83%) as a light yellow powder, which was purified by chromatography (3:7 EtOAc-hexane) to yield **254b** (2.94 g, 79%) as a colourless powder: mp 238–240 °C; ^{1}H NMR δ 1.46 (t, *J* = 7.1 Hz, 6H), 4.34 (q, *J* = 7.1 Hz, 4H), 5.38 (s, 4H), 7.36–7.38 (m, 2H), 7.64–7.65 (m, 4H), 7.76–7.78 (m, 4H), 8.03–8.05 (m, 2H); ^{13}C NMR δ 16.0, 34.1, 69.4, 123.3, 124.1, 124.3, 125.6, 129.5, 132.2, 134.0, 151.3, 168.3; (+)-APCI MS *m/z* (relative intensity) 535.1 (M^+, 70), calcd.: 534.37 for $C_{32}H_{26}N_2O_6$, 388.1 (100)

1,4-Bis(*N*-phthalimidomethyl)-2,3-di-*n*-propoxynaphthalene (254c)

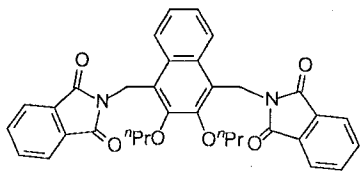

Using the general procedure for **254a**, the reaction of the crude **162c** (3.44 g, 8.00 mmol) and **253** (3.16 g, 17.1 mmol) gave crude product (4.20 g, 93%) as a yellow powder, which was purified by chromatography (DCM) to yield **254c** (3.12 g, 69%) as a light yellow powder: mp 193–195 °C; ^{1}H NMR δ 1.07 (t, *J* = 7.5 Hz, 6H), 1.87–1.94 (m, 4H), 4.24 (t, *J* = 6.5 Hz, 4H), 5.39 (s, 4H), 7.34–7.35 (m, 2H), 7.64–7.66 (m, 4H), 7.76–7.78 (m, 4H), 7.99–8.01 (m, 2H); ^{13}C NMR δ 10.8, 23.8, 34.1, 75.3, 123.4, 124.0, 124.3, 125.5, 129.5, 132.2, 134.0, 151.5, 168.3; (+)-APCI MS *m/z* (relative intensity) 563.1 (M^+, 40), calcd.: 562.62 for $C_{34}H_{30}N_2O_6$, 416.1 (100).

1,4-Bis(*N*-phthalimidomethyl)-2,3-di-*n*-butoxynaphthalene (254d)

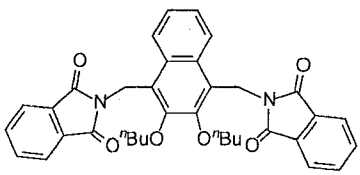

Using the general procedure for **254a**, the reaction of the crude **162d** (5.50 g, 12.0 mmol) and **253** (4.89 g, 26.4 mmol) gave crude product (6.77 g, 95%) as a yellow powder, which was purified by chromatography (DCM) to yield

254d (4.96 g, 70%) as a light yellow powder: mp 184–185 °C; ^{1}H NMR δ 0.99 (t, *J* = 7.4 Hz, 6H), 1.49–1.57 (m, 4H), 1.83–1.89 (m, 4H), 4.28 (t, *J* = 6.7 Hz, 4H), 5.38 (s, 4H), 7.33–7.35 (m, 2H), 7.63–7.65 (m, 4H), 7.76–7.77 (m, 4H), 7.99–8.00 (m, 2H); ^{13}C NMR δ 14.3, 19.6, 32.7, 34.0, 73.7, 123.4, 124.0, 124.3, 125.5, 129.5, 132.2, 134.0, 151.6, 168.3; (+)-APCI MS *m/z* (relative intensity) 591.1 (M^+, 70), calcd.: 590.68 for $C_{36}H_{34}N_2O_6$, 444.2 (100).

1,4-Bis(aminomethyl)-2,3-dimethoxynaphthalene (250a)

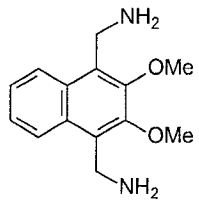

General procedure: The suspension of **254a** (3.04 g, 6.00 mmol) and hydrate hydrazine (2.4 mL, 48 mmol) in MeOH (85 mL) was heated at reflux with stirring for 4 h. After the solvent was removed under reduced pressure, the residue was dissolved in distilled water (50 mL) and extracted with $CHCl_3$ (3 x 50 mL). The organic layers were combined, washed with distilled water (2 x 50 mL), brine (1 x 50 mL), dried over anhydrous $MgSO_4$ and filtered. After the solvent was removed under reduced pressure, the residue was dried overnight on a vacuum pump, to yield **250a** (1.29 g, 88%) as a yellow oily liquid: ^{1}H NMR δ 1.59 (s, br, 4H, disappears upon D_2O addition), 3.96 (s, 6H), 4.29 (s, 4H), 7.47–7.50 (m, 2H), 8.05–8.07 (m, 2H); ^{13}C NMR δ 36.7, 61.5, 124.1, 125.6, 130.0, 130.9, 150.0; GCMS *m/z* (relative intensity) 246 (M^+, 45), 202 (95), 171 (70), 128

(60), 115 (100).

1,4-Bis(aminomethyl)-2,3-diethoxynaphthalene (250b)

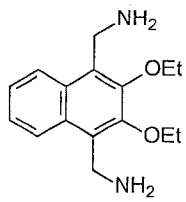

Procedure 1: Using the general procedure for **250a**, the reaction of **254b** (3.21 g, 6.00 mmol) and H_2NNH_2 (2.4 mL, 48 mmol) gave **250b** (1.65 g, 100%) as a yellow oily liquid: ^{1}H NMR δ 1.46 (t, *J* = 7.1 Hz, 6H), 1.54 (s, br, 4H, disappears upon D_2O addition), 4.14 (q, *J* = 7.0 Hz, 4H), 4.30 (s, 4H), 7.47–7.49 (m, 2H), 8.05–8.07 (m, 2H); ^{13}C NMR δ 16.1, 37.0, 69.9, 124.2, 125.5, 130.0, 131.1, 149.2; GCMS *m/z* (relative intensity) 274 (M^+, 45), 257 (20), 201 (100), 184 (40), 115 (100).

Procedure 2: Using 95% EtOH as solvent instead of MeOH afforded **250b** (63%) having identical characterization data to those obtained by Procedure 1.

1,4-Bis(aminomethyl)-2,3-di-*n*-propoxynaphthalene (250c)

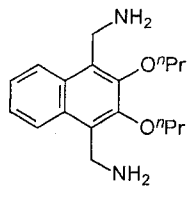

Using the general procedure for **250a**, the reaction of **254c** (2.25 g, 4.00 mmol) and H_2NNH_2 (1.6 mL, 32 mmol) gave **250c** (1.21 g, 100%) as a yellow

semisolid: mp 50–51 °C; ^{1}H NMR δ 1.10 (t, *J* = 7.3, 6H), 1.59 (s, br, 4H, disappears upon D_2O addition), 1.84–1.91 (m, 4H), 4.02 (t, *J* = 6.8 Hz, 4H), 4.29 (s, 4H), 7.47–7.49 (m, 2H), 8.05–8.07 (m, 2H); ^{13}C NMR δ 10.8, 23.9, 37.0, 76.1, 124.2, 125.5, 130.0, 131.1, 149.5; GCMS *m/z* (relative intensity) 302 (M^+, 60), 257 (20), 226 (60), 215 (100), 200 (63), 184 (45), 128 (50), 115 (60).

1,4-Bis(aminomethyl)-2,3-di-*n*-butoxynaphthalene (250d)

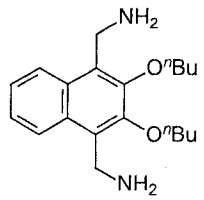

Using the general procedure for **250a**, the reaction of **254d** (2.95 g, 5.00 mmol) and H_2NNH_2 (2.0 mL, 40 mmol) gave **250d** (1.08 g, 65%) as a light yellow liquid: ^{1}H NMR δ 1.01 (t, *J* = 7.4 Hz, 6H), 1.51 (s, br, 4H, disappears upon D_2O addition), 1.53–1.60 (m, 4H), 1.80–1.86 (m, 4H), 4.06 (t, *J* = 6.7 Hz, 4H), 4.29 (s, 4H), 7.47–7.49 (m, 2H), 8.06–8.08 (m, 2H); ^{13}C NMR δ 14.2, 19.6, 32.8, 37.0, 74.4, 124.3, 125.5, 130.0, 131.1, 149.5; GCMS *m/z* (relative intensity) 330 (M^+, 60), 285 (20), 240 (84), 229 (100), 184 (65), 128 (67), 115 (60).

1,4-Diformyl-2,3-dihydroxynaphthalene (255a)

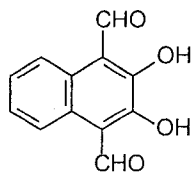

To a stirred solution of **252** (1.12 g, 4.50 mmol) in dry DCM (45 mL) was

added dropwise a solution of BBr_3 (1.7 mL, 18 mmol) in dry DCM (17 mL) over 1 h. The reaction mixture was stirred for a further 5 h, and cold water (100 mL) was then added at 0 °C. The mixture was acidified with aqueous 6 M HCl until pH reached 1–2, extracted with $CHCl_3$ (3 x 60 mL), dried over anhydrous $MgSO_4$ and filtered. After the solvent was removed under reduced pressure, the residue was dried over night on a vacuum pump to yield crude product (0.99 g, 100%), which was purified by chromatography (2:8 EtOAc-hexane) to yield **255a** (0.72g, 73%) as a yellow solid: mp 205 °C (dec.) [lit.[20] > 180 °C (dec.)]; ^{1}H NMR δ 7.58–7.60 (m, 2H), 8.39–8.41 (m, 2H), 10.9 (s, 2H), 13.0 (s, 2H, disappears upon D_2O addition); ^{13}C NMR δ 115.6, 120.2, 126.4, 127.0, 155.2, 194.6; GCMS *m/z* (relative intensity) 216 (M^+, 100), 188 (100).

2,3-Diethoxy-1,4-bis(*p*-tolylsulfonylaminomethyl)naphthalene (262a)

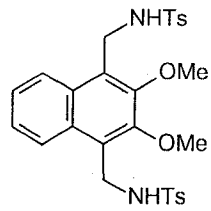

General procedure: To a stirred solution of **250a** (0.25 g, 1.0 mmol) in DCM (1 mL) at room temperature was added an aqueos solution of 0.2 M NaOH (10 mL, 2.00 mmol). The reaction mixture was stirred at room temperature a futher 10 min, and a solution of TsCl (0.39 g, 2.00 mmol) in DCM (9 mL) was added dropwise over 20 min. The reaction mixture was stirred for another 20 h, and water (100 mL) was added to the mixture. The resulting precipitate was

filtered, washed several times with DCM and dried at 50 °C to afford **262a** (0.44 g, 80%) as a light yellow powder: mp > 257 °C (dec.); ^{1}H NMR δ 2.42 (s, 6H), 3.65 (s, 6H), 4.32 (d, *J* = 5.3 Hz, 4H), 7.43 (d, *J* = 8.0 Hz, 4H), 7.46–7.48 (m, 2H), 7.76 (d, *J* = 8.7 Hz, 4H), 7.80 (t, *J* = 5.4 Hz, 2H, disappears upon D_2O addition), 7.95–7.97 (m, 2H); ^{13}C NMR δ 21.0, 37.1, 60.8, 124.4, 124.5, 125.4, 126.7, 129.3, 129.6, 137.0, 142.7, 150.3; (–)-APCI MS *m/z* (relative intensity) 553.0 (M^+, 100), calcd.: 554.67 for $C_{28}H_{30}N_2O_6S_2$.

2,3-Diethoxy-1,4-bis(*p*-tolylsulfonylaminomethyl)naphthalene (262b)

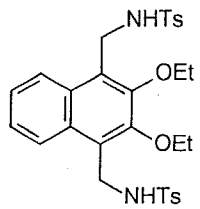

General procedure: To a stirred solution of **250b** (1.75 g, 6.37 mmol) in DCM (2.0 mL) at room temperature was added an aqueous solution of 0.3 M NaOH (63.0 mL, 19.0 mmol). The reaction mixture was stirred for another 10 min, and a solution of TsCl (3.65 g, 19.1 mmol) in DCM (75 mL) was added dropwise over 30 min at room temperature. The reaction mixture was stirred for a further 40 h. The organic layer was separated, and the aqueous layer was extracted with $CHCl_3$ (3 x 50 mL). The organic layers were combined, washed with water (2 x 50 mL), brine (1 x 50 mL), dried over $MgSO_4$ and filtered. After the solvent was removed under reduced pressure, the resulting residue was purified by chromatography (2:98 EtOAc-DCM) to yield **262b** (2.88 g, 77%) as a

colourless powder: mp 210–211 °C; ^{1}H NMR δ 1.23 (t, *J* = 7.0 Hz, 6H) 2.41 (s, 6H), 3.89–3.94 (q, *J* = 7.1 Hz, 4H), 4.51 (d, *J* = 5.3 Hz, 4H), 4.64 (t, *J* = 4.8 Hz, 2 H, disappears upon D_2O addition) 7.23 (d, *J* = 8.0 Hz, 4H), 7.40–7.42 (m, 2H), 7.72 (d, *J* = 7.7 Hz, 4H) 7.77–7.79 (m, 2H); ^{13}C NMR δ 15.9, 21.7, 38.6, 70.0, 124.0, 125.2, 126.4, 127.5, 129.6, 129.8, 136.7, 143.7, 149.9; (–)-APCI MS *m/z* (relative intensity) 581.1 ([M-1]$^-$, 100), calcd.: 582.7 for $C_{30}H_{34}N_2O_6S_2$.

2,3-Di-*n*-propoxy-1,4-bis(*p*-tolylsulfonylaminomethyl)naphthalene (262c)

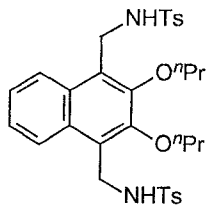

Using the general procedure for **262b**, the crude product from the reaction of **250c** (0.50 g, 1.65 mmol) with TsCl (0.94 g, 2.0 mmol) was purified by chromatography (2:98 EtOAc-DCM) to yield **262c** (0.83 g, 83%) as a colourless powder: mp 199–200 °C; ^{1}H NMR δ 0.91 (t, *J* = 7.2 Hz, 6H), 1.58–1.65 (m, 4H), 2.41 (s, 6H), 3.78 (t, *J* = 6.7 Hz, 4H), 4.51 (d, *J* = 5.5 Hz, 4H), 4.62 (t, *J* = 5.8 Hz, 2H, disappears upon D_2O addition), 7.22 (d, *J* = 8.1 Hz, 4H), 7.41–7.43 (m, 2H), 7.72 (d, *J* = 8.1 Hz, 4H), 7.79–7.81 (m, 2H); ^{13}C NMR δ 10.6, 21.7, 23.6, 38.5, 76.1, 124.0, 125.0, 126.4, 127.5, 129.6, 129.8, 136.7, 143.7, 150.1; (–)-APCI MS *m/z* (relative intensity) 609.1 ([M-1$^-$], 100), calcd.: 610.8 for $C_{32}H_{38}N_2O_6S_2$.

2,3-Di-*n*-butoxy-1,4-bis(*p*-tolylsulfonylaminomethyl)naphthalene (262d)

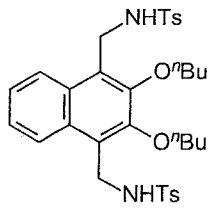

Using the general procedure for **262b**, the crude product from the reaction of **250d** (0.83 g, 2.5 mmol) with TsCl (0.30 g, 7.5 mmol) was purified by chromatography (5:95 EtOAc–DCM) to yield **262d** (1.17 g, 73%) as a colourless powder: mp 190–192 °C; ^{1}H NMR δ 0.92 (t, *J* = 7.4 Hz, 6H), 1.30–1.37 (m, 4H), 1.54–1.60 (m, 5H, overlap with HOD signal), 2.41 (s, 6H), 3.82 (t, *J* = 6.8 Hz, 4H), 4.50 (d, *J* = 6.4 Hz, 4H), 4.63 (t, *J* = 5.9 Hz, 2H, disappears upon D_2O addition), 7.23 (d, *J* = 8.5 Hz, 4H), 7.41–7.43 (m, 2H), 7.72 (d, *J* = 8.6 Hz, 4H), 7.81–7.83 (m, 2H); ^{13}C NMR δ 14.2, 19.4, 21.7, 32.5, 38.6, 74.4, 124.0, 125.0, 126.4, 127.5, 129.6, 129.8, 136.7, 143.6, 150.1; (–)-APCI MS *m/z* (relative intensity) 637.2 ([M-1]$^-$, 100), calcd.: 638.2 for $C_{34}H_{42}N_2O_6S_2$.

Bis(*N*-tosylamide)azaisocalix[2]-2,3-dimethoxynaphthalene (264a)

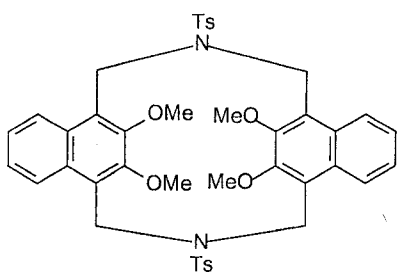

General procedure: To a suspension of Cs_2CO_3 (0.36 g, 1.1 mmol) in dry DMF (5 mL) was added dropwise a solution of **162a** (187 mg, 0.500 mmol) and **262a** (277 mg, 0.500 mmol) in dry DMF (15 mL) at room temperature over 5 h using a syringe pump. The reaction mixture was stirred for a further 40 h at room temperature. After the solvent was removed under reduced pressure, to the resulting residue was added distilled water (30 mL), and the mixture was extracted with $CHCl_3$ (3 x 30 mL). The organic layer was combined and washed with distilled water (2 x 40 mL) and brine (1 x 40 mL), dried over $MgSO_4$ and filtered. After the solvent was removed under reduced pressure, the residue was purified by chromatography (DCM) to yield **264a** (0.14 g, 37%) as a light yellow powder: mp > 290 °C ($CHCl_3$-acetone) (dec.); ^{1}H NMR δ 2.56 (s, 3H), 3.64 (s, 6H), 4.19 (d, *J* = 13.5 Hz, 2H), 5.29 (d, *J* = 13.5 Hz, 2H), 7.01–7.03 (m, 2H), 7.49 (d, *J* = 7.5 Hz, 2H), 7.94 (d, *J* = 7.5 Hz, 2H), 8.05–8.08 (m, 2H); ^{13}C NMR δ 21.9, 45.9, 63.1, 123.0, 125.3, 125.4, 128.1, 130.3, 130.5, 134.5, 144.1, 150.0; (+)-APCI MS *m/z* (relative intensity) 767.0 (M^+, 100) calcd.:766.9 for $C_{42}H_{42}N_2O_8S_2$.

X-ray Crystal Structure of 264a. A colorless prism crystal of $C_{45.50}H_{45.50}Cl_{10.50}N_2O_8S_2$ having approximate dimensions of 0.50 x 0.30 x 0.20 mm was mounted on a glass fiber. All measurements were made on a Rigaku Saturn CCD area detector with graphite monochromated Mo-Ka radiation. Indexing was performed from 0 images that were exposed for 0 seconds. The crystal-to-detector distance was 35.07 mm. Cell constants and an

orientation matrix for data collection corresponded to a primitive triclinic cell with dimensions: a = 12.9568(11) Å, α = 92.4503(16)^{o}, b = 14.4422(14) Å, β = 103.0694(12)^{o}, c = 15.5453(12) Å, γ = 112.024(2)^{o}, V = 2600.5(4) Å^{3}. For Z = 2 and F.W. = 1184.75, the calculated density is 1.513 g/cm^{3}. The data were collected at a temperature of –120 ± 1 °C to a maximum 2θ value of 61.5^{o}. A total of 714 oscillation images were collected. The crystal-to-detector distance was 35.07 mm. Readout was performed in the 0.137 mm pixel mode. The final cycle of full-matrix least-squares refinement on F was based on 13377 observed reflections and 641 variable parameters and converged (largest parameter shift was 0.00 times its esd) with unweighted and weighted agreement factors of: R1 = 0.0795 and wR2 = 0.2094. The standard deviation of an observation of unit weight was 1.10. Unit weights were used. The maximum and minimum peaks on the final difference Fourier map corresponded to 1.63 and –1.52 e^{-}/Å^{3}, respectively.

Bis(*N*-tosylamide)azaisocalix[2]-2,3-diethoxynaphthalene (264b)

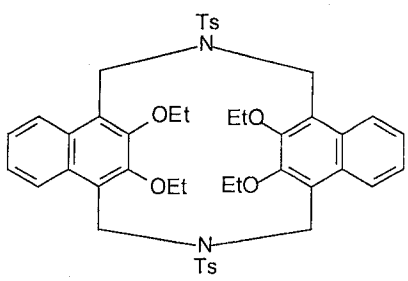

Using the general procedure for **264a**, the coupling reaction between **162b** (0.20 g, 0.50 mmol) and **262b** (0.29 g, 0.50 mmol) gave the crude product, which

was purified by chromatography (DCM) to yield **264b** (0.12 g, 29%) as a light yellow powder: mp > 260 °C ($CHCl_3$-acetone) (dec.); ^{1}H NMR δ 1.18 (t, *J* = 7.3 Hz, 6H), 2.55 (s, 3H), 3.69–3.75 (m, 2H), 3.87–3.92 (m, 2H), 4.13 (d, *J* = 13.5 Hz, 2H), 5.24 (d, *J* = 13.5 Hz, 2H), 8.99–7.00 (m, 2H), 7.49 (d, *J* = 7.2 Hz, 2H), 7.93 (d, *J* = 8.0 Hz, 2H), 7.99–8.01 (m, 2H); ^{13}C NMR δ 15.7, 21.9, 46.4, 70.6, 122.8, 125.0, 125.3, 128.1, 130.0, 130.3, 134.1, 144.0, 148.9; (+)-APCI MS *m/z* (relative intensity) 823.3 (M^+, 100) calcd.: 823.0 for $C_{46}H_{50}N_2O_8S_2$.

Bis(*N*-tosylamide)azaisocalix[2]-2,3-dipropoxynaphthalene (264c)

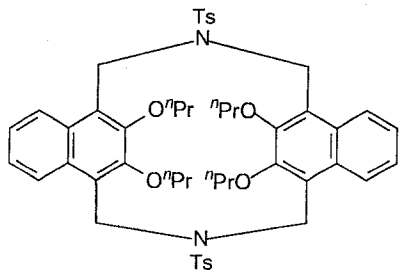

Using the general procedure for **264a**, the coupling reaction between **162c** (0.21 mg, 0.50 mmol) and 1,4-bis(*p*-tolylsulfonylaminomethyl)-2,3-dipropoxynaphthalene **262c** (0.31 g, 0.50 mmol) gave the crude product, which was purified by chromatography (DCM) to give **264c** (0.21 g, 48%) as a colourless powder: mp > 280 °C ($CHCl_3$-CH_3CN) (dec.); ^{1}H NMR δ 0.88 (t, *J* = 7.5 Hz, 6H), 1.55–1.65 (m, 4H), 2.53 (s, 3H), 3.50–3.55 (m, 2H), 3.79–3.83 (m, 2H), 4.11 (d, *J* = 13.4 Hz, 2H), 5.23 (d, *J* = 13.4 Hz, 2H), 6.99–7.01 (m, 2H), 7.47 (d, *J* = 8.8 Hz, 2H), 7.92 (d, *J* = 8.1 Hz, 2H), 7.97–7.99 (m, 2H); ^{13}C NMR δ 10.7, 21.8, 23.7, 46.3, 76.6, 122.7, 125.0, 125.3, 128.0, 129.9, 130.3, 133.8, 143.9,

149.0; (+)-APCI MS *m/z* (relative intensity) 879.5 (M^+, 100) calcd.: 879.1 for $C_{50}H_{58}N_2O_8S_2$.

X-ray Crystal Structure of 264c. A colorless prism crystal of $C_{51}H_{58}N_2O_8S_2Cl_3$ having approximate dimensions of 0.20 x 0.20 x 0.20 mm was mounted on a glass fiber. All measurements were made on a Rigaku Saturn CCD area detector with graphite monochromated Mo-Kα radiation.Indexing was performed from 360 images that were exposed for 8 seconds. The crystal-to-detector distance was 35.02 mm. Cell constants and an orientation matrix for data collection corresponded to a primitive monoclinic cell with dimensions: a = 14.4291(17) Å, b = 19.034(2) Å, β = 94.676(3)°, c = 18.175(2) Å, V = 4975.1(10) $Å^3$. For Z = 4 and F.W. = 997.51, the calculated density is 1.332 g/cm^3. The data were collected at a temperature of –120 ± 1 °C to a maximum 2θ value of 61.6°. A total of 720 oscillation images were collected. The exposure rate was 16.0 [sec./°]. The crystal-to-detector distance was 35.02 mm. Readout was performed in the 0.137 mm pixel mode. The final cycle of full-matrix least-squares refinement on F was based on 8753 observed reflections and 596 variable parameters and converged (largest parameter shift was 0.00 times its esd) with unweighted and weighted agreement factors of: R1 = 0.1607, wR2 = 0.4569. The standard deviation of an observation of unit weight was 1.75. Unit weights were used. The maximum and minimum peaks on the final difference Fourier map corresponded to 2.05 and –1.24 $e^-/Å^3$, respectively.

Bis(*N*-tosylamide)azaisocalix[2]-2,3-dibutoxynaphthalene (264d)

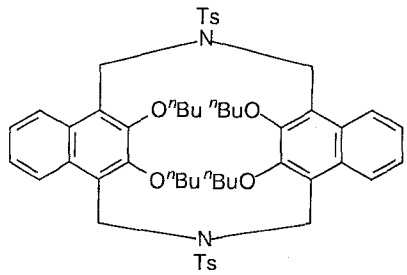

Using the general procedure for **264a**, the coupling reaction between **162d** (0.23 g, 0.50 mmol) and **262d** (0.32 g, 0.50 mmol) gave the crude product, which was purified by chromatography (1:9 EtOAc-hexane) to yield **264d** (0.15 g, 31%) as a colourless powder: mp > 290 °C ($CHCl_3$-CH_3CN) (dec.); ^{1}H NMR δ 0.89 (t, *J* = 7.3 Hz, 6H), 1.26–1.34 (m, 2H), 1.36–1.43 (m, 2H) 1.47–1.52 (m, 2H), 1.55–1.62 (m, 2H), 2.54 (s, 3H), 3.52–3.57 (m, 2H), 3.81–3.85 (m, 2H), 4.09 (d, *J* = 13.3 Hz, 2H), 5.23 (d, *J* = 13.7 Hz, 2H), 6.99–7.01 (m, 2H), 7.48 (d, *J* = 8.7 Hz, 2H), 7.92 (d, *J* = 7.9 Hz, 2H), 7.98–8.00 (m, 2H); ^{13}C NMR δ 14.2, 19.6, 21.8, 32.7, 46.3, 74.8, 122.7, 125.0, 125.3, 128.0, 130.0, 130.3, 133.8, 143.8, 149.1; (+)-APCI MS *m/z* (relative intensity) 935.4 (M^+, 100) calcd.: 935.3 for $C_{54}H_{66}N_2O_8S_2$.

8.6 References and notes

1. (a) Gutsche, C. D. *Calixarenes Revisited,* In *Supramolecular Chemistry*; Stoddard, J. F., Ed.; Royal Society of Chemistry: Cambridge, 1998, pp 25, 26 (b) Afari, Z.; Böhmer, V.; Harrowfield, J.; Vicens, J., Eds., *Calixarenes 2001*, Kluwer Acadamic Publishers, Dordrecht, The Netherlands 2001, pp 245-249 and references cited therein. (b) Chirakul, P.; Hampton, P. D.; Duesler, E. N. *Tetrahedron Lett.* **1998**, *39*, 5473-5476. (c) Takemura, H. *J. Incl. Phenom. Mol. Recog. Chem.* **1994**, *19*, 193-206. (d) Takemura, H. *J. Incl. Phenom. Macro. Chem.* **2002**, *42*, 169-186.

2. Hampton, P. D.; Tong, W. D.; Wu, S.; Duesler, E. N. *J. Chem. Soc., Perkin Trans. 2*, **1996**, 1127-1130.

3. (a) Thuéry, P.; Nierlich, M.; Vicens, J.; Masci, B.; Takemura, H. *Eur. J. Inorg. Chem.* **2001**, 637-643. (b) Thuéry, P.; Nierlich, M.; Vicens, J.; Masci, B.; Takemura, H. *Polyhedron* **2001**, *20*, 3183-3187.

4. Grannas, M. J.; Hoskins, B. F.; Robson, R. *Inorg. Chem.* **1994**, *33*, 1071-1079.

5. Thuéry, P.; Nierlich, M.; Vicens, J.; Takemura, H. *J. Chem. Soc., Dalton Trans.* **2000**, 279-283.

6. Thuéry, P.; Nierlich, M.; Vicens, J.; Masci, B.; Takemura, H. *Polyhedron* **2000**, *19*, 2673-2678.

7. Ito, K.; Ohta, T.; Ohba, Y.; Sone, T. *J. Heterocyclic Chem.* **2000**, *37*, 79-85.

8. Tanaka, A.; Fujiyoshi, S.; Motomura, K.; Hayashida, O.; Hisaeda, Y.; Murakami, Y. *Tetrahedron* **1998**, *54*, 5178-5206.

9. (a) Bell, M.; Edwards, A. J.; Hoskins, B. F.; Kachab, E. H.; Robson, R. *J. Am. Chem. Soc.* **1989**, *111*, 3603-3610. (b) Edwards, A. J.; Hoskins, B. F.; Kachab, E. H.; Markiewicz, A.; Murray, K. S.; Robson, R. *Inorg. Chem.* **1992**, *31*, 3585-3591.

10. (a) Takemura, H.; Yoshimura, K.; Khan, I. U.; Shinmyozu, T.; Inazu, T. *Tetrahedron Lett.* **1992**, *33*, 5775-5778. (b) Khan, I. U.; Takemura, H.; Suenaga, M.; Shinmyozu, T.; Inazu, T. *J. Org. Chem.* **1993**, *58*, 3158-3161.

11. Takemura, H.; Suenaga, M.; Sakai, K.; Shinmyozu, T.; Miyahara, Y.; Inazu, T. *J. Incl. Phenom.* **1984**, *2*, 207-214.

12. Takemura, H.; Shinmyozu, T.; Miura, H.; Khan, I. U.; Inazu, T. *J. Inclusion Phenom.* **1994**, *19*, 193-206.

13. Wen, G.; Matsunaga, M.; Matsunaga, T.; Takemura, H.; Shinmyozu, T. *Synlett* **1995**, 947-948.

14. Chiraku, P.; Hampton, P.; Bencze, Z. *J. Org. Chem.* **2000**, *65*, 8297-8300.

15. Niikura, K.; Anslyn, E. V. *J. Chem. Soc., Perkin Trans. 2*, **1999**, 2769-2775.

16. Tran, A. H.; Miller, D. O.; Georghiou, P. E. *J. Org. Chem.* **2005**, *70*, 1115-1121.

17. A preliminary account of this work was presented at "*ISNA-11: 11th International Symposium on Novel aromatic compounds*", St. John's, NL, Canada, August 14-18th, 2005; and "*Soccer 2005, 2nd Summer Organic Chemistry Conference on Everybody's Research*", St. John's, NL, Canada, August 11-12th, 2005.

18. Computer-assisted molecular modeling were conducted using Spartan'04, V1.0.3, from Wavefunction, Inc., Irvine, CA, USA. Calculations at the PM3 level of theory were conducted on the optimized geometry of the host and/or complexes which were obtained through molecular mechanics (MMFF94) conformational searches.

19. Li, Z. *Ph.D. Dissertation,* Memorial University of Newfoundland, 1996.

20. (a) The simple routes to 1,4-diformyl-2,3-dimethoxynaphthalene and 1,4-diformyl-2,3-dihydroxynaphthalene were concomitantly presented at "*ISNA-11: 11th International Symposium on Novel aromatic compounds*", St. John's, NL, Canada, August 14-18th, 2005. (b) Gallant, A.J.; Yun, M.; Sauer, M.; Yeung, C. S.; MacLachlan, M. J. *Org. Lett.* **2005**, *7*, 4827-4830.

21. Crowther, G. P.; Sundberg, R. J.; Sarpeshkar, A. M. *J. Org. Chem.* **1984**, *49*, 4657-4663.

22. Kuhert, N.; Rossignolo, G. M.; Lopez-Periago, A. *Org. Biomol. Chem.* **2003**,*1*, 1157-1170.

23. Campaigne, E.; Bosin, T. R. *J. Med. Chem.* **1968**, *11*, 178-180.

24. Akine, S.; Taniguchi, T.; Nabeshima, T. *Tetrahedron Lett.* **2001**, *42*, 8861-8864.

25. Gallant, A. J.; MacLachlan, M. *Angew. Chem. Int. Ed.* **2003**, *42*, 5307-5310.
26. Huck, W. T. S.; van Veggel, F. C. J. M.; Reinhoudt, D. N. *Recl. Trav. Chim. Pays-Bas* **1995**, *114*, 273-276.

27. (a) Hofsløkkhen, N. U.; Skattebøl, L. *Acta Chem. Scand.* **1999**, *53*, 258-262. (b) Ogata, Y.; Kawasaki, A. Sugiura, F. *Tetrahedron* **1968**, *24*, 5001-5010.

28. Gallant *et al.*, *J. Org. Chem.* **2004**, *69*, 8739-8744.

29. Paker, D., Ed., *Macrocycle synthesis: a practical approach,* New York: Oxford University Press, 1996.

30. Lanman, B. A.; Myers, A.G. *Org. Lett.* **2004**, *6*, 1045-1047.

31. Vinod, T. K.; Hart, H. *J. Org. Chem.* **1990**, *55*, 5461-5466.

32. In this chapter, a *1,3-alternate* conformation is a conformation in which two naphthyl sub-units and two phenyl sub-units are oriented in opposite directions.

33. Bottino, F.; Grazia, M. D.; Finocchiaro, P.; Fronczek, F. R.; Mamo, A.; Pappalardo, S. *J. Org. Chem.* **1988**, *53*, 3521-3529.

34. Garcia-Espana, E.; Latorre, J.; Luis, S. V.; Miravet, J. F.; Pozuelo, P. E.; Ramirez, J. A.; Soriano, C. *Inorg. Chem.* **1996**, *35*, 4591-4596.

Appendix A

Complexation data for compounds studied in Chapter order and PLUTO figure for compound **159b**

Appendix 2.1 Determination of Complexation stoichiometry for **53** *vs* C_{60}.

• Using Job Plot method

[**53**] = [C_{60}] = 7.86 x 10^{-4} M in CS_2 using DMSO-d_6 as external lock.

(Δδ are absolute values).

χ	δ values (ppm) for the lower-field multiplet				Average δ (ppm)	Δδ (ppm)	χ x Δδ
1.0	7.393	7.384	7.382	7.374	7.383	0.000	0.00
0.9	7.395	7.389	7.383	7.377	7.386	-0.003	2.47 x 10^{-3}
0.8	7.396	7.390	7.386	7.378	7.388	-0.004	3.40 x 10^{-3}
0.7	7.400	7.394	7.391	7.382	7.392	-0.009	5.95 x 10^{-3}
0.6	7.403	7.396	7.393	7.385	7.394	-0.011	6.60 x 10^{-3}
0.5	7.407	7.401	7.395	7.389	7.398	-0.015	7.38 x 10^{-3}
0.4	7.409	7.402	7.397	7.391	7.400	-0.016	6.60 x 10^{-3}
0.3	7.413	7.406	7.402	7.395	7.404	-0.021	6.23 x 10^{-3}
0.2	7.416	7.409	7.405	7.398	7.407	-0.024	4.75 x 10^{-3}
0.1	7.417	7.409	7.407	7.399	7.408	-0.025	2.48 x 10^{-3}
0.0					0.000	0.000	0.00

χ: mol fraction of **53**.

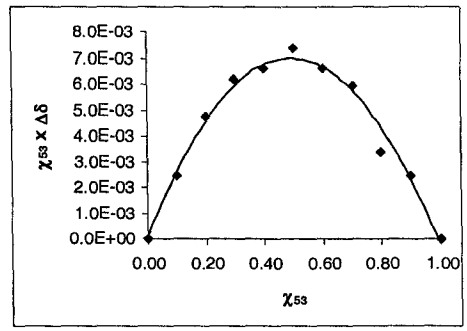

• Using mole ratio plot method

[**53**] = 7.86 x 10^{-4} M in CS_2 using DMSO-d_6 as external lock.

C_{60} was added as solid aliquots. (Δδ are absolute values)

[C_{60}]/[53]	Δδ (ppm)
0.00	0.000
0.36	0.012
0.78	0.020
1.12	0.024
1.79	0.028
2.29	0.031
2.70	0.032
3.74	0.035

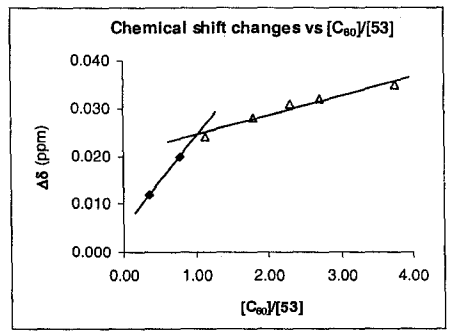

Appendix 2.2 Determination of K_{assoc} for **53**:C_{60} complex in CS_2 using DMSO-d_6 as external lock; C_{60} was added as solid aliquots. ($\Delta\delta$ are absolute values).

• **Run #1**: [**53**] = 7.86 x 10^{-4} M

Entry#	$[C_{60}]$	[53]	$[C_{60}]/[53]$	$1/[C_{60}]$	$1/\Delta\delta$	$\Delta\delta$ (ppm)	$\Delta\delta/[C_{60}]$
1	0.00	7.86 x 10^{-4}	0.00	0	0.0	0.000	0.0
2	2.80 x 10^{-4}	7.86 x 10^{-4}	0.36	3578	83.3	0.012	42.9
3	6.11 x 10^{-4}	7.86 x 10^{-4}	0.78	1638	50.0	0.020	32.8
4	8.84 x 10^{-4}	7.86 x 10^{-4}	1.12	1131	41.7	0.024	27.1
5	1.41 x 10^{-4}	7.86 x 10^{-4}	1.79	710	35.7	0.028	19.9
6	1.80 x 10^{-3}	7.86 x 10^{-4}	2.29	554	32.3	0.031	17.2
7	2.13 x 10^{-3}	7.86 x 10^{-4}	2.70	471	31.3	0.032	15.1
8	2.94 x 10^{-3}	7.86 x 10^{-4}	3.74	340	28.6	0.035	11.9

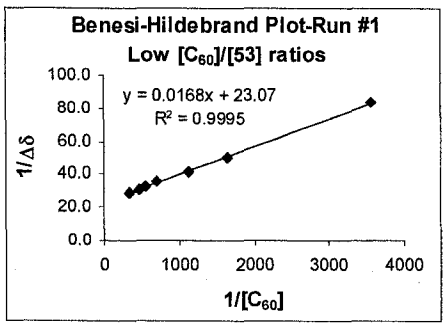

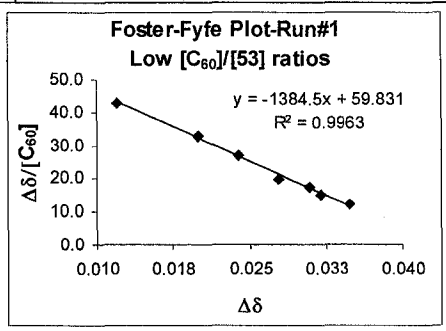

• **Run #2**: [**53**] = 1.05 x 10^{-4} M

Entry#	$[C_{60}]$	[53]	$[C_{60}]/[53]$	$1/[C_{60}]$	$1/\Delta\delta$	$\Delta\delta$ (ppm)	$\Delta\delta/[C_{60}]$
1	0.00	1.05 x 10^{-4}	0.00	0	0.0	0.0000	0.0
2	1.05 x 10^{-4}	1.05 x 10^{-4}	9.92	957	41.7	0.0240	23.0
3	1.18 x 10^{-4}	1.05 x 10^{-4}	11.2	845	40.4	0.0248	20.9
4	1.67 x 10^{-3}	1.05 x 10^{-4}	15.8	601	35.4	0.0283	17.0
5	1.88 x 10^{-3}	1.05 x 10^{-4}	17.8	532	33.9	0.0295	15.7
6	2.20 x 10^{-3}	1.05 x 10^{-4}	20.8	455	33.3	0.0300	13.7
7	2.72 x 10^{-3}	1.05 x 10^{-4}	25.8	368	31.5	0.0318	11.7
8	3.14 x 10^{-3}	1.05 x 10^{-4}	29.8	319	31.3	0.0320	10.2

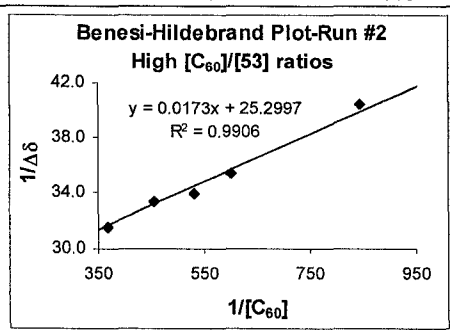

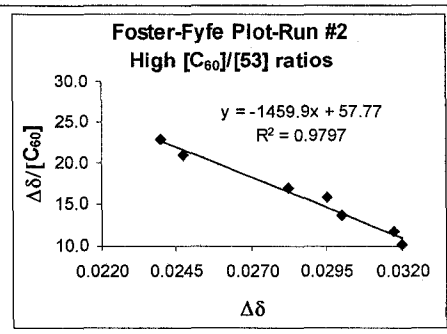

	$[C_{60}]/[53]$	slope	intercept	K(B-H)	R^2	K(F-F)	R^2
Run #1	0.36–3.74	0.0168	23.07 ± 0.28	1373 ± 17	0.9995	1384 ± 38	0.9963
Run #2	9.92–29.78	0.0173	25.20 ± 0.47	1462 ± 27	0.9906	1460 ± 94	0.9797
			Average:	**1420**		**1420**	
			SD:	**64**		**54**	

Appendix 2.3 Determination of K_{assoc} for **53**:C_{70} complex in CS_2 using DMSO-d_6 as external lock; C_{70} was added as solid aliquots. ($\Delta\delta$ are absolute values).

• **Run #1**: [**53**] = 7.96 x 10^{-4} M

Entry #	$[C_{70}]$	[53]	$[C_{70}]/[53]$	$1/[C_{70}]$	$1/\Delta\delta$	$\Delta\delta$ (ppm)	$\Delta\delta / [C_{70}]$
1	0.00	7.96 x 10^{-4}	0.00	0.0	0.0	0.000	0
2	2.34 x 10^{-4}	7.96 x 10^{-4}	0.29	4275	160.0	0.006	26.7
3	5.51 x 10^{-4}	7.96 x 10^{-4}	0.69	1815	88.9	0.011	20.4
4	7.04 x 10^{-4}	7.96 x 10^{-4}	0.88	1421	75.5	0.013	18.8
5	1.13 x 10^{-4}	7.96 x 10^{-4}	1.42	883	57.1	0.018	15.5
6	1.72 x 10^{-3}	7.96 x 10^{-4}	2.16	583	46.0	0.020	12.7
7	2.73 x 10^{-3}	7.96 x 10^{-4}	3.43	367	44.0	0.023	8.3

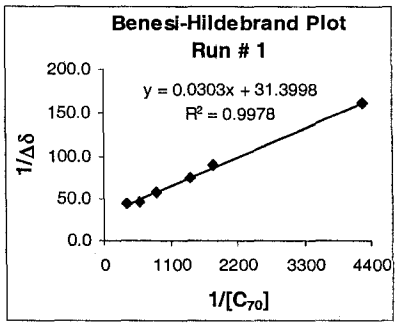

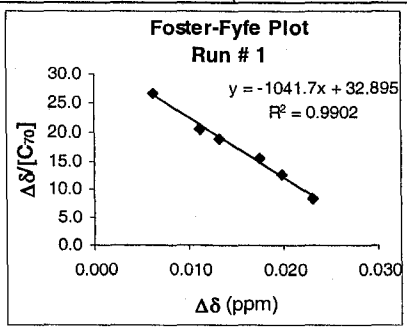

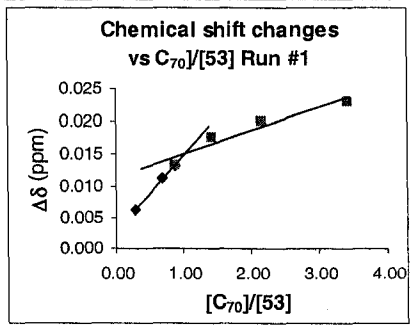

• **Run #2**: [**53**] = 7.77 x 10^{-4} M

Entry #	$[C_{70}]$	[53]	$[C_{70}]/[53]$	$\Delta\delta$ (ppm)	$\Delta\delta / [C_{70}]$	$1/[C_{70}]$	$1/\Delta\delta$
1	0.00	7.73 x 10^{-4}	0.00	0.000	0	0	0.0
2	2.83 x 10^{-4}	7.73 x 10^{-4}	0.37	0.008	27.3	3528	129.0
3	5.29 x 10^{-4}	7.73 x 10^{-4}	0.68	0.011	21.3	1889	88.9
4	7.18 x 10^{-4}	7.73 x 10^{-4}	0.93	0.014	19.2	1394	72.7
5	1.35 x 10^{-3}	7.73 x 10^{-4}	1.75	0.019	14.1	741	52.6
6	1.62 x 10^{-3}	7.73 x 10^{-4}	2.09	0.020	12.3	617	50.0
7	2.06 x 10^{-3}	7.73 x 10^{-4}	2.67	0.022	10.7	485	45.5
8	2.55 x 10^{-3}	7.73 x 10^{-4}	3.29	0.024	9.4	393	41.7

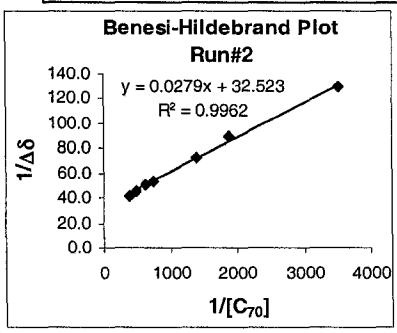

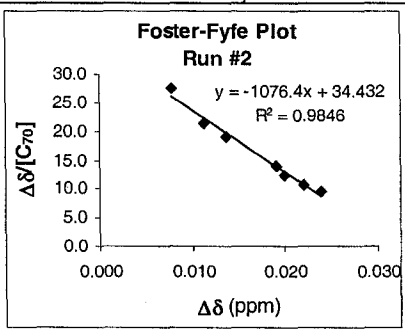

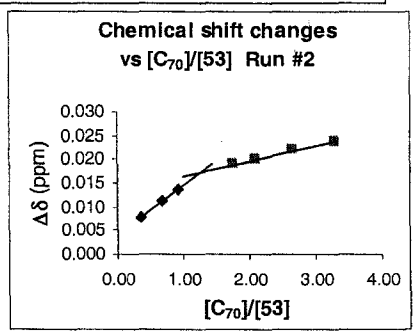

	$[C_{70}]/[53]$	slope	intercept	*K*(B-H)	R^2	*K*(F-F)	R^2
Run #1	0.29–3.43	0.0303	31.40 ± 1.44	1040 ± 48	0.9962	1042 ± 52	0.9902
Run #2	0.37–3.29	0.0279	32.52 ± 1.28	1170 ± 46	0.9978	1076 ± 60	0.9846
			Average:	**1101**		**1059**	
			SD:	**92**		**24**	

Appendix 2.4 Determination of K_{assoc} for **51**:C_{60} complex in CS_2 using DMSO-d_6 as external lock; C_{60} was added as solid aliquots. ($\Delta\delta$ are absolute values).

Run #1: [**51**] = 7.90 x 10^{-4} M

Entry #	[C_{60}]	[51]	[C_{60}]/[51]	1/[C_{60}]	1/$\Delta\delta$	$\Delta\delta$ (ppm)	$\Delta\delta$ / [C_{60}]
1	0.00	7.90 x 10^{-4}	0.00	0	0.0	0.000	0.0
2	5.55 x 10^{-4}	7.90 x 10^{-4}	0.70	1802	142.9	0.007	12.6
3	8.28 x 10^{-4}	7.90 x 10^{-4}	1.05	1208	100.0	0.010	12.1
4	1.33 x 10^{-3}	7.90 x 10^{-4}	1.69	751	62.5	0.016	12.0
5	1.78 x 10^{-3}	7.90 x 10^{-4}	2.25	562	50.0	0.020	11.2
6	2.28 x 10^{-3}	7.90 x 10^{-4}	2.88	439	40.0	0.025	11.0
7	2.77 x 10^{-3}	7.90 x 10^{-4}	3.51	361	32.3	0.031	11.2

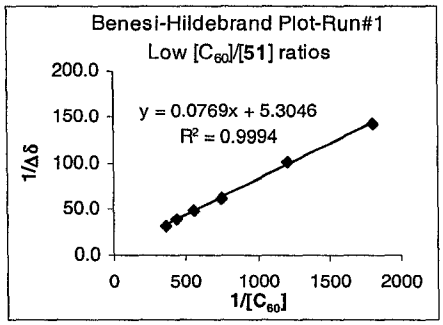

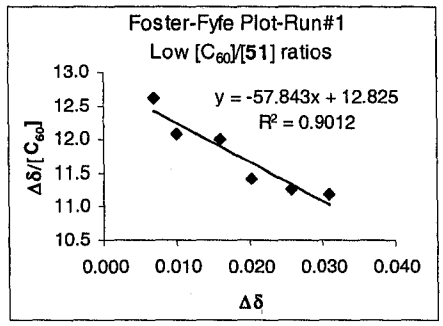

Run #2: [**51**] = 1.18 x 10^{-4} M

Entry #	[C_{60}]	[51]	[C_{60}]/[51]	1/[C_{60}]	1/$\Delta\delta$	$\Delta\delta$ (ppm)	$\Delta\delta$ / [C_{60}]
1	0.00	1.18 x 10^{-4}	0.00	0	0.0	0.000	0.0
2	1.23 x 10^{-3}	1.18 x 10^{-4}	10.4	813	66.7	0.015	12.2
3	1.59 x 10^{-3}	1.18 x 10^{-4}	13.4	628	52.6	0.019	11.9
4	1.84 x 10^{-3}	1.18 x 10^{-4}	15.5	544	45.5	0.022	12.0
5	2.29 x 10^{-3}	1.18 x 10^{-4}	19.3	436	37.0	0.027	11.8
6	2.99 x 10^{-3}	1.18 x 10^{-4}	25.2	335	29.4	0.034	11.4
7	3.51 x 10^{-3}	1.18 x 10^{-4}	29.6	285	25.6	0.039	11.1
8	4.22 x 10^{-3}	1.18 x 10^{-4}	35.6	237	22.2	0.045	10.7

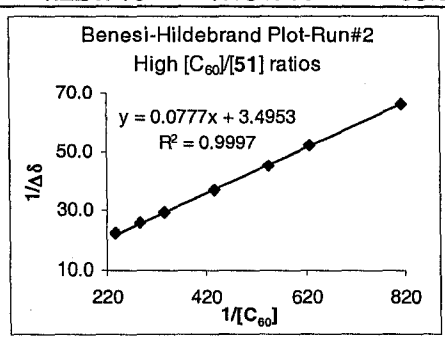

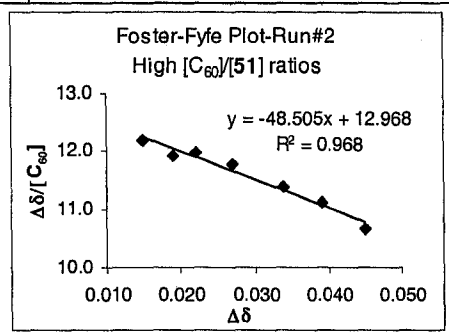

	[C_{60}]/[51]	slope	intercept	*K*(B-H)	R^2	*K*(F-F)	R^2
Run #1	0.70–3.51	0.0765	5.30 ± 0.95	69 ± 12	0.9992	58 ± 9	0.9012
Run #2	10.4–35.6	0.0777	3.49 ± 0.31	45 ± 4	0.9997	49 ± 4	0.9683
			Average:	**62**		**53**	
			SD:	**23**		**6**	

Appendix 2.5 Determination of K_{assoc} for **51**:C_{70} complex in CS_2 using DMSO-d_6 as external lock; C_{70} was added as solid aliquots. ($\Delta\delta$ are absolute values).

- **Run #1**: [**51**] = 7.90 x 10^{-4} M

Entry #	[C_{70}]	[51]	[C_{70}]/[51]	1/[C_{70}]	1/$\Delta\delta$	$\Delta\delta$ (ppm)	$\Delta\delta$/[C_{70}]
1	0.00	7.90 x 10^{-4}	0.00	0.0	0.0	0.000	0.0
2	4.18 x 10^{-4}	7.90 x 10^{-4}	0.53	2391	83.3	0.012	28.7
3	6.03 x 10^{-4}	7.90 x 10^{-4}	0.76	1659	58.8	0.017	28.2
4	8.96 x 10^{-4}	7.90 x 10^{-4}	1.13	1116	40.0	0.025	27.9
5	1.18 x 10^{-3}	7.90 x 10^{-4}	1.50	847	31.3	0.032	27.1
6	1.52 x 10^{-3}	7.90 x 10^{-4}	1.92	658	25.0	0.040	26.3
7	1.93 x 10^{-3}	7.90 x 10^{-4}	2.44	518	20.0	0.050	25.9
8	3.13 x 10^{-3}	7.90 x 10^{-4}	3.96	320	13.5	0.074	23.7

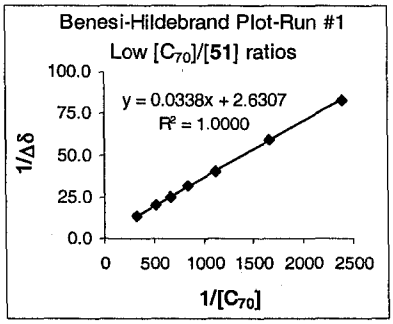

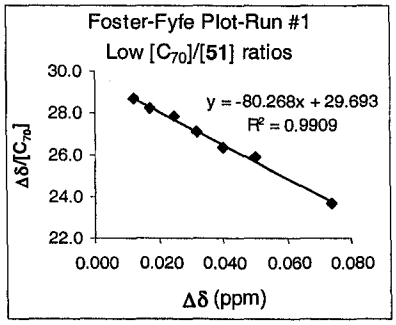

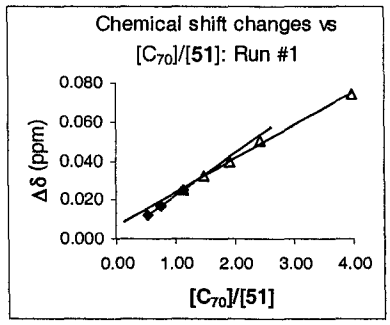

- **Run #2**: [**51**] = 7.90 x 10^{-4} M

Entry #	[C_{70}]	[51]	[C_{70}]/[51]	1/[C_{70}]	1/$\Delta\delta$	$\Delta\delta$ (ppm)	$\Delta\delta$/[C_{70}]
7	0.00E+00	1.19 x 10^{-4}	0.0	0	0.0	0.000	0
6	1.26 x 10^{-3}	1.19 x 10^{-4}	10.7	791	29.4	0.034	26.9
5	1.85 x 10^{-3}	1.19 x 10^{-4}	15.6	541	20.8	0.048	26.0
4	2.36 x 10^{-3}	1.19 x 10^{-4}	20.0	423	16.9	0.059	24.9
3	2.94 x 10^{-3}	1.19 x 10^{-4}	24.8	340	14.5	0.069	23.5
2	3.61 x 10^{-3}	1.19 x 10^{-4}	30.5	277	12.5	0.080	22.1
1	4.40 x 10^{-3}	1.19 x 10^{-4}	37.1	228	10.9	0.092	20.9

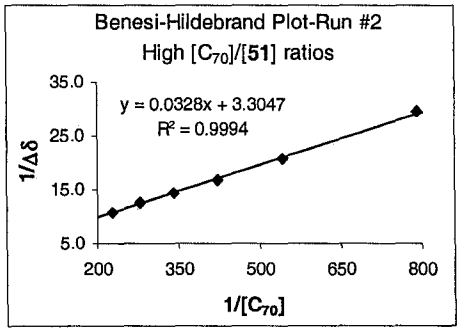

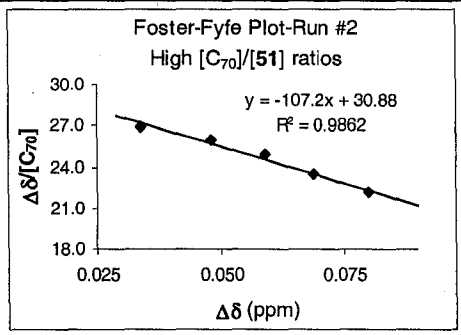

	[C_{70}]/[51]	slope	intercept	*K*(B-H)	R^2	*K*(F-F)	R^2
Run #1	0.53–3.96	0.0338	2.63 ± 0.13	78 ± 5	0.9999	80 ± 3	0.9909
Run #2	10.7–37.1	0.0328	3.30 ± 0.20	101 ± 6	0.9994	107 ± 6	0.9862
			Average:	**90**		**94**	
			SD:	**16**		**19**	

Appendix 2.6 Determination of K_{assoc} for **50**:C_{60} complex in CS_2 using DMSO-d_6 as external lock; C_{60} was added as solid aliquots. ($\Delta\delta$ are absolute values).

- **Run #1**: [**50**] = 7.94 x 10^{-4} M

Entry #	$[C_{60}]$	[50]	$[C_{60}]/[50]$	$1/[C_{60}]$	$1/\Delta\delta$	$\Delta\delta$ (ppm)	$\Delta\delta/[C_{60}]$
1	0.00	7.94 x 10^{-4}	0.00	0	0.0	0.000	0.0
2	2.75 x 10^{-4}	7.94 x 10^{-4}	0.35	3634	333	0.003	10.9
3	8.58 x 10^{-3}	7.94 x 10^{-4}	1.08	1165	125	0.008	9.3
4	1.19 x 10^{-3}	7.94 x 10^{-4}	1.49	843	100	0.010	8.4
5	1.45 x 10^{-3}	7.94 x 10^{-4}	1.83	689	83	0.012	8.3
6	1.99 x 10^{-3}	7.94 x 10^{-4}	2.51	502	67	0.015	7.5
7	2.49 x 10^{-3}	7.94 x 10^{-4}	3.13	402	59	0.017	6.8

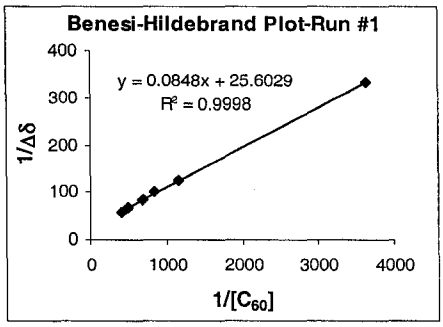

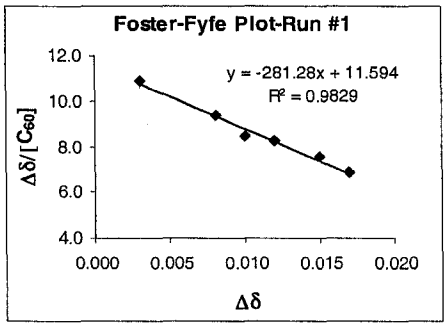

- **Run #2**: [**50**] = 7.94 x 10^{-4} M

Entry #	$[C_{60}]$	[50]	$[C_{60}]/[50]$	$1/[C_{60}]$	$1/\Delta\delta$	$\Delta\delta$ (ppm)	$\Delta\delta/[C_{60}]$
1	0.00	7.94 x 10^{-4}	0.00	0	0.00	0.000	0.0
2	2.68 x 10^{-4}	7.94 x 10^{-4}	0.34	3728	333	0.003	11.18
3	5.90 x 10^{-4}	7.94 x 10^{-4}	0.74	1696	167	0.006	10.17
4	8.28 x 10^{-4}	7.94 x 10^{-4}	1.04	1208	132	0.008	9.18
5	1.16 x 10^{-3}	7.94 x 10^{-4}	1.47	860	100	0.010	8.60
6	1.45 x 10^{-3}	7.94 x 10^{-4}	1.82	691	83	0.012	8.29
7	1.97 x 10^{-3}	7.94 x 10^{-4}	2.48	509	67	0.015	7.63
8	3.10 x 10^{-3}	7.94 x 10^{-4}	3.90	323	54	0.019	6.00

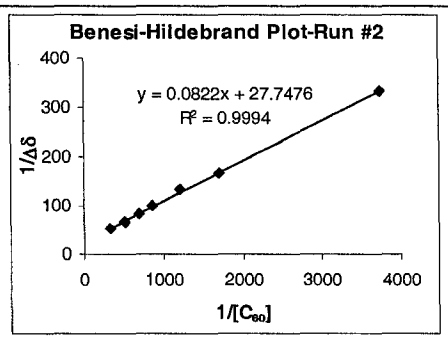

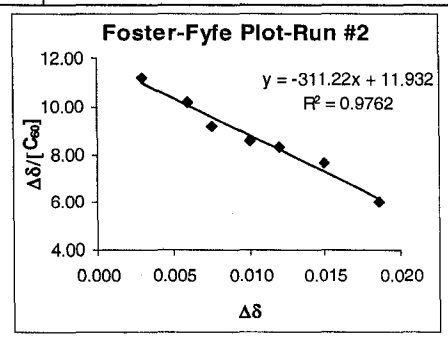

	$[C_{60}]/[50]$	slope	intercept	*K*(B-H)	R^2	*K*(F-F)	R^2
Run #1	0.35–3.13	0.0848	25.60 ± 1.06	302 ± 13	0.9998	281 ± 19	0.9829
Run #2	0.34–3.90	0.0822	27.75 ± 1.53	338 ± 19	0.9994	311 ± 19	0.9762
			Average:	**320**		**296**	
			SD:	**25**		**21**	

Appendix 2.7 Determination of K_{assoc} for **50**:C_{70} complex in CS_2 using DMSO-d_6 as external lock; C_{70} was added as solid aliquots. ($\Delta\delta$ are absolute values).

- **Run #1**: [**50**] = 7.94×10^{-4} M

Entry #	$[C_{70}]$	[50]	$[C_{70}]/[50]$	$1/[C_{70}]$	$1/\Delta\delta$	$\Delta\delta$ (ppm)	$\Delta\delta/[C_{70}]$
1	0.00	7.94×10^{-4}	0.00	0	0.0	0.000	0.0
2	5.67×10^{-4}	7.94×10^{-4}	0.71	1764	143	0.007	12.3
3	1.16×10^{-3}	7.94×10^{-4}	1.46	862	71	0.014	12.1
4	1.49×10^{-3}	7.94×10^{-4}	1.87	672	59	0.017	11.4
5	1.97×10^{-3}	7.94×10^{-4}	2.49	506	45	0.022	11.1
6	2.47×10^{-3}	7.94×10^{-4}	3.11	405	38	0.026	10.5
7	3.11×10^{-3}	7.94×10^{-4}	3.91	322	31	0.032	10.3

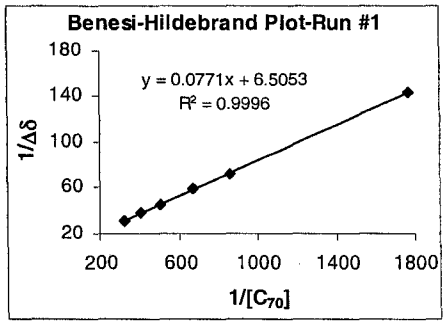

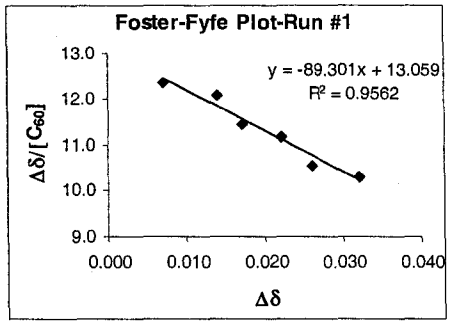

- **Run #2**: [**50**] = 7.94×10^{-4} M

Entry #	$[C_{70}]$	[50]	$[C_{70}]/[50]$	$1/[C_{70}]$	$1/\Delta\delta$	$\Delta\delta$ (ppm)	$\Delta\delta/[C_{70}]$
1	0.0	7.94×10^{-4}	0.00	0	0.00	0.000	0.0
2	8.52×10^{-4}	7.94×10^{-4}	1.07	1173	96	0.010	12.3
3	1.18×10^{-3}	7.94×10^{-4}	1.48	849	71	0.014	12.0
4	1.52×10^{-3}	7.94×10^{-4}	1.91	658	59	0.017	11.2
5	3.14×10^{-3}	7.94×10^{-4}	3.95	318	32	0.031	9.9
6	3.74×10^{-3}	7.94×10^{-4}	4.71	267	28	0.036	9.6

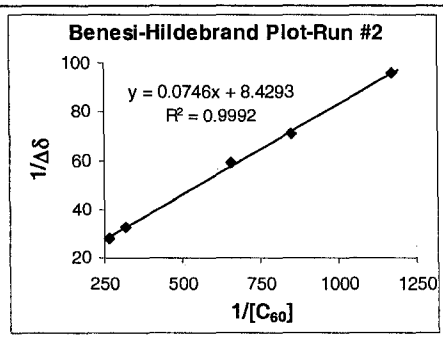

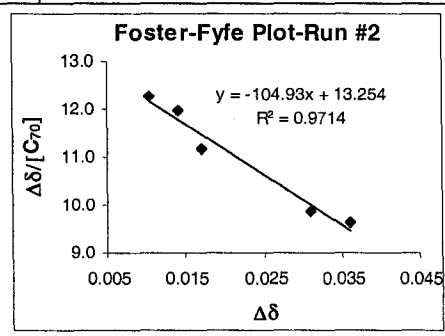

	$[C_{70}]/[50]$	slope	Intercept	*K*(B-H)	R^2	*K*(F-F)	R^2
Run #1	0.71–3.91	0.077	6.51 ± 0.69	84 ± 9	0.9996	89 ± 10	0.9562
Run #2	1.07–4.71	0.075	8.43 ± 0.92	113 ± 12	0.9992	105 ± 10	0.9714
			Average:	**99**		**97**	
			SD:	**20**		**11**	

Appendix 3.1 Determination of K_{assoc} for **18**:C_{60} complex in toluene using UV-vis spectroscopy. C_{60} added as solid aliquots. (ΔA values are absolute values measured at λ = 430 nm) and [**18**] = 1.88 x 10^{-3} M.

Entry #	$[C_{60}]$	[18]	$[18]/[C_{60}]$	$1/[C_{60}]$	$[18]/\Delta A$	ΔA	$\Delta A/[C_{60}]$	ΔA_{cal}
1	1.47 x 10^{-4}	1.88 x 10^{-3}	12.83	6818	9.32 x 10^{-3}	0.202	1376	0.203
2	2.22 x 10^{-4}	1.88 x 10^{-3}	8.47	4500	6.15 x 10^{-3}	0.306	1376	0.304
3	2.87 x 10^{-4}	1.88 x 10^{-3}	6.56	3488	4.84 x 10^{-3}	0.389	1355	0.388
4	3.60 x 10^{-4}	1.88 x 10^{-3}	5.23	2778	3.89 x 10^{-3}	0.483	1342	0.481
5	5.36 x 10^{-4}	1.88 x 10^{-3}	3.51	1867	2.76 x 10^{-3}	0.681	1272	0.695
6	9.81 x 10^{-4}	1.88 x 10^{-3}	1.92	1020	1.58 x 10^{-3}	1.190	1214	1.188
7	1.64 x 10^{-3}	1.88 x 10^{-3}	1.15	610	1.05 x 10^{-3}	1.787	1090	1.808

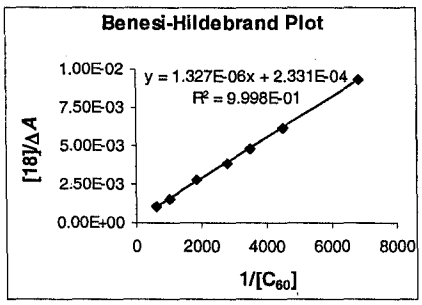

a

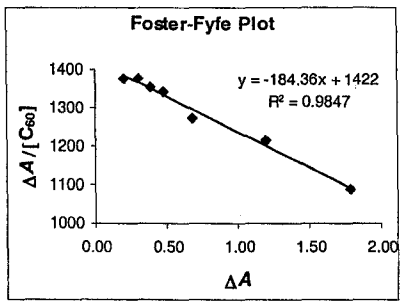

b

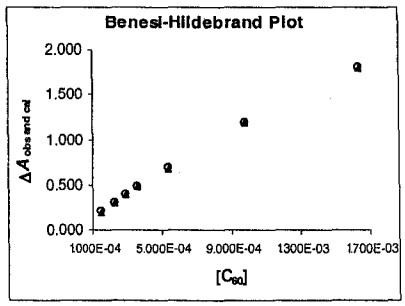

c

Figure a. Benesi-Hilderbrand plot

Figure b. Foster-Fyfe plot

Figure c. Plots of ΔA *vs* $[C_{60}]$ (*left*): observed data (▲) and calculated data (o) from non-linear form of the Benesi– Hildebrand plot (eq 3.6).

$[18]/[C_{60}]$	slope	intercept	*K*(B-H)	R^2	*K*(F-F)	R^2
1.15–12.83	1.33 x 10^{-6}	2.33 x 10^{-4}	176 ± 21	0.9998	184 ± 10	0.9847

$\Delta\varepsilon_c$ = 1/ intercept = 4.29 x 10^3 M^{-1} cm^{-1}

$$\Delta A_{cal} = \frac{K_{assoc} \bullet \Delta\varepsilon_c \bullet [\mathbf{18}]_o \bullet [C_{60}]}{1 + K_{assoc} \bullet [C_{60}]} \quad \text{(eq 3.6)}$$

Appendix 3.2 Plots of chemical shift changes ($\Delta\delta$) for protons on **18** in toluene-d_8 solution *vs* added C_{60} (*left*), and formula of **18** showing the numbering of positions on the naphthyl ring sub-units (right).

Entry #	$[C_{60}]$	[18]	$[18]/[C_{60}]$	$\Delta\delta$ ^{t}Bu	$\Delta\delta$ H-5	$\Delta\delta$ H-4
1	3.03×10^{-4}	1.92×10^{-3}	6.33	0.012	0.013	0.007
2	4.69×10^{-4}	1.92×10^{-3}	4.08	0.019	0.020	0.011
3	7.08×10^{-4}	1.92×10^{-3}	2.71	0.028	0.027	0.015
4	8.89×10^{-4}	1.92×10^{-3}	2.15	0.033	0.036	0.019
5	1.08×10^{-3}	1.92×10^{-3}	1.77	0.040	0.041	0.022
6	1.43×10^{-3}	1.92×10^{-3}	1.34	0.049	0.048	0.027
7	2.05×10^{-3}	1.92×10^{-3}	0.94	0.054	0.056	0.029

Entry #	$[C_{60}]$	[18]	$[18]/[C_{60}]$	$\Delta\delta$ H-8	$\Delta\delta$ H-7	$\Delta\delta$ CH_2
1	3.03×10^{-4}	1.92×10^{-3}	6.33	0.004	0.002	0.002
2	4.69×10^{-4}	1.92×10^{-3}	4.08	0.005	0.002	
3	7.08×10^{-4}	1.92×10^{-3}	2.71	0.008	0.005	0.003
4	8.89×10^{-4}	1.92×10^{-3}	2.15	0.009	0.005	0.002
5	1.08×10^{-3}	1.92×10^{-3}	1.77	0.011	0.006	0.003
6	1.43×10^{-3}	1.92×10^{-3}	1.34	0.013	0.009	0.004
7	2.05×10^{-3}	1.92×10^{-3}	0.94	0.014	0.008	0.004

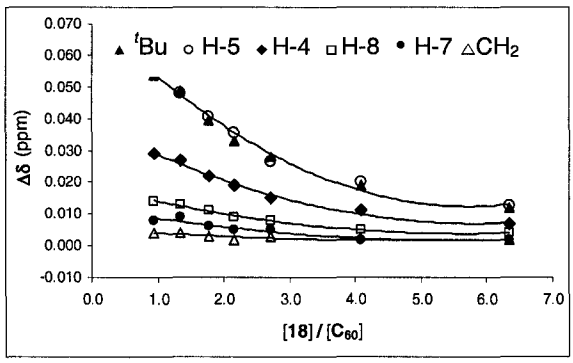

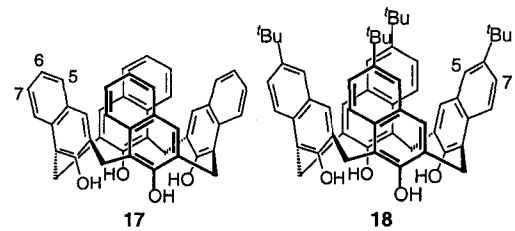

17 18

Appendix 3.3 The closest distances (Å) between **17** or **18** hosts to C_{60} or C_{70} guests in their computer-generated 1:1 complexes.

1:1 host:guest complexes	*tert*-butyl or H-6	H-5	H-7
17:C_{60}	3.74	3.51	4.21
17:C_{70}	3.81	3.55	4.20
18:C_{60}	3.21	3.66	4.37
18:C_{70}	3.00	3.60	4.20

Appendix 3.4 Determination of K_{assoc} for **18**:C_{60} complex in toluene at 298 K using ^{1}H NMR. C_{60} added as solid aliquots. ($\Delta\delta$ values are absolute values)

• **Run #1**: [**18**] = 1.93x 10^{-3} M.

Entry #	$[C_{60}]$	[18]	$[18]/[C_{60}]$	$1/[C_{60}]$	$1/\Delta\delta$	$\Delta\delta$ (ppm)	$\Delta\delta/C_{60}$
1	0.00	1.93 x 10^{-3}	0.00	0	0.0	0.0000	0.0
2	4.52 x 10^{-4}	1.93 x 10^{-3}	4.27	2211	55.6	0.018	39.8
3	6.99 x 10^{-4}	1.93 x 10^{-3}	2.76	1430	38.5	0.026	37.2
4	8.81 x 10^{-4}	1.93 x 10^{-3}	2.19	1135	30.3	0.033	37.5
5	1.13 x 10^{-3}	1.93 x 10^{-3}	1.71	888	25.6	0.039	34.6

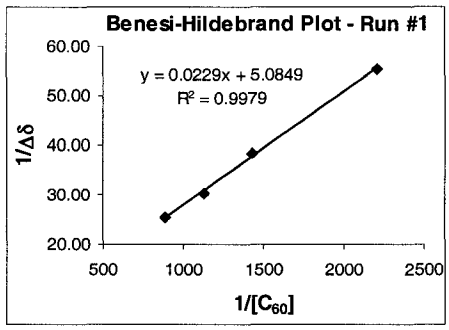

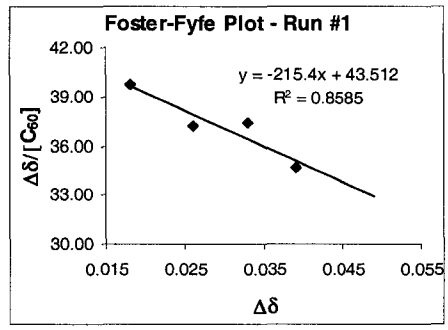

• **Run #2**: [**18**] = 1.92x 10^{-3} M.

Entry #	$[C_{60}]$	[18]	$[18]/[C_{60}]$	$1/[C_{60}]$	$1/\Delta\delta$	$\Delta\delta$ (ppm)	$\Delta\delta/C_{60}$
1	0.00	1.92 x 10^{-3}	0.00	0	0.0	0.0000	0.0
2	4.69 x 10^{-4}	1.92 x 10^{-3}	4.08	2132	52.6	0.019	40.5
3	7.08 x 10^{-4}	1.92 x 10^{-3}	2.71	1413	35.7	0.028	39.6
4	8.89 x 10^{-4}	1.92 x 10^{-3}	2.15	1124	30.3	0.033	37.1
5	1.08 x 10^{-3}	1.92 x 10^{-3}	1.77	923	25.3	0.040	36.4
6	1.43 x 10^{-3}	1.92 x 10^{-3}	1.34	697	20.4	0.049	34.2

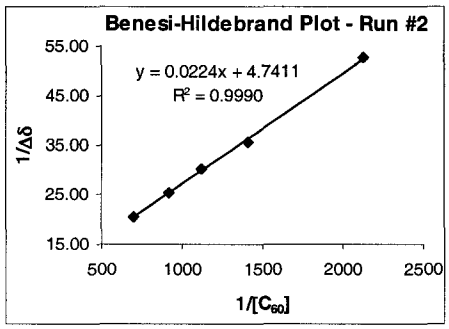

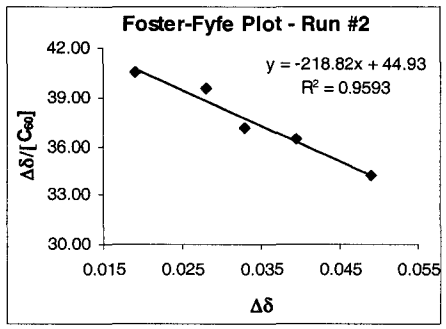

	$[18]/[C_{60}]$	slope	intercept	K(B-H)	R^2	K(F-F)	R^2
Run #2	1.71–4.27	0.0229	5.08 ± 1.10	222 ± 48	0.9979	215 ± 62	0.8585
Run #1	1.34–4.08	0.0224	4.74 ± 0.56	212 ± 25	0.9990	219 ± 26	0.9593
			Average:	217		217	
			SD:	7		3	

Appendix 3.5 Plots of change in the chemical shifts of the *t*-butyl group protons in **18** and K_{assoc} (Foster-Fyfe treatment) of **18**:C_{60} complex as a function of temperature.

Run #1: Low temperature [**18**] = 1.93 x 10^{-3} M

Entry#	[G]/[H]	278 K		288 K		298 K	
		Δδ (ppm)	Δδ / [C_{60}]	Δδ (ppm)	Δδ / [C_{60}]	Δδ (ppm)	Δδ / [C_{60}]
1	0.23	0.026	57.5	0.021	46.4	0.018	39.8
2	0.36	0.038	54.3	0.032	45.8	0.026	37.2
3	0.46	0.047	53.3	0.038	43.1	0.033	37.5
4	0.55	0.055	51.7	0.045	41.8	0.039	34.6
5	0.76	0.066	45.0	0.053	35.8	0.045	29.3

Run #2: High temperature [**18**] = 1.92 x 10^{-3} M

Entry#	[G]/[H]	298 K		318 K		338 K		358 K	
		Δδ (ppm)	Δδ / [C_{60}]	Δδ (ppm)	Δδ / [C_{60}]	Δδ (ppm)	Δδ / [C_{60}]	Δδ (ppm)	Δδ / [C_{60}]
1	0.24	0.019	40.5	0.015	30.9	0.009	19.2	0.006	12.8
2	0.37	0.028	39.6	0.021	29.7	0.015	21.2	0.010	14.1
3	0.46	0.033	37.1	0.026	29.2	0.019	21.4	0.013	14.6
4	0.57	0.040	36.4	0.029	26.8	0.021	19.4	0.014	12.5
5	0.75	0.049	34.2	0.036	25.1	0.026	18.1	0.018	12.5

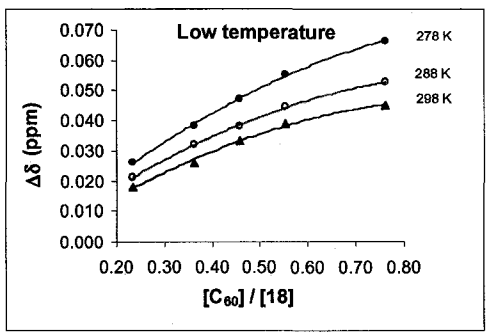

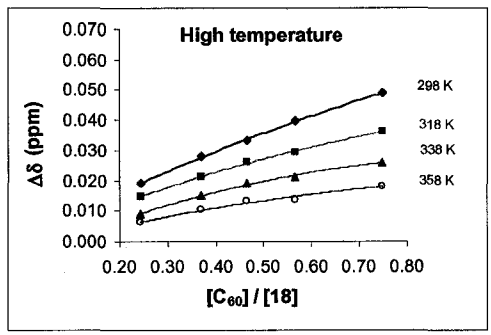

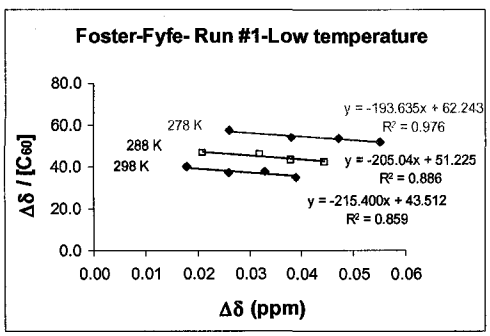

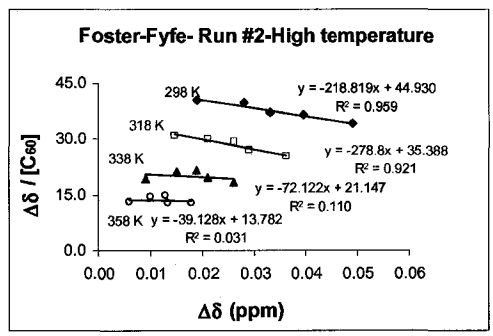

Appendix 3.6 Determination of K_{assoc} for **18**:C_{70} complex in toluene using ^{1}H NMR at 298 K. C_{60} added as solid aliquots. ($\Delta\delta$ values are absolute values).

• **Run #1**: [**18**] = 1.93x 10^{-3} M

Entry #	$[C_{70}]$	[18]	$[18]/[C_{70}]$	$1/[C_{70}]$	$1/\Delta\delta$	$\Delta\delta$ (ppm)	$\Delta\delta/[C_{70}]$
1	0.00	1.93 x 10^{-3}	0.00	0	0.0	0.000	0.0
2	3.45 x 10^{-4}	1.93 x 10^{-3}	5.59	2899	125.0	0.008	23.2
3	4.70 x 10^{-4}	1.93 x 10^{-3}	4.11	2129	100.0	0.010	21.3
4	6.14 x 10^{-4}	1.93 x 10^{-3}	3.14	1629	76.9	0.013	21.2
5	7.95 x 10^{-4}	1.93 x 10^{-3}	2.43	1259	62.5	0.016	20.1
6	1.01 x 10^{-3}	1.93 x 10^{-3}	1.91	989	52.6	0.019	18.8
7	1.45 x 10^{-3}	1.93 x 10^{-3}	1.33	691	38.5	0.026	18.0

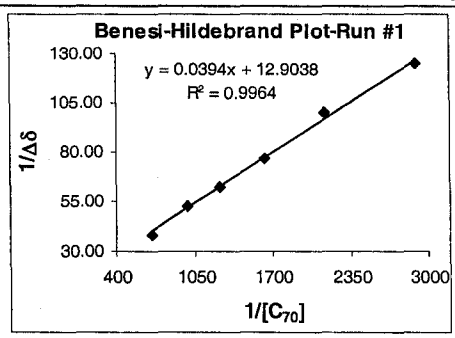

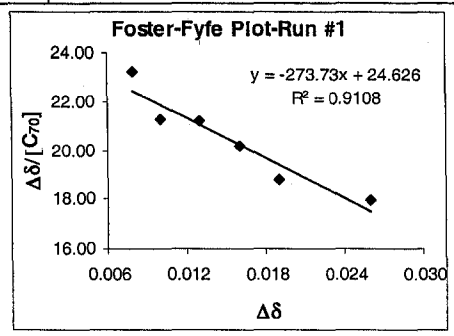

• **Run #2**: [**18**] = 1.92x 10^{-3} M

Entry #	$[C_{70}]$	[18]	$[18]/[C_{70}]$	$1/[C_{70}]$	$1/\Delta\delta$	$\Delta\delta$ (ppm)	$\Delta\delta/[C_{70}]$
1	0.00	1.92 x 10^{-3}	0.00	0	0.0	0.000	0.0
2	3.54 x 10^{-4}	1.92 x 10^{-3}	5.41	2821	125.0	0.008	22.6
3	4.70 x 10^{-4}	1.92 x 10^{-3}	4.08	2129	100.0	0.010	21.3
4	5.96 x 10^{-4}	1.92 x 10^{-3}	3.21	1678	80.0	0.013	21.0
5	7.60 x 10^{-4}	1.92 x 10^{-3}	2.52	1316	66.7	0.015	19.7
6	9.73 x 10^{-4}	1.92 x 10^{-3}	1.97	1028	52.6	0.019	19.5
7	1.43 x 10^{-3}	1.92 x 10^{-3}	1.34	701	40.0	0.025	17.5

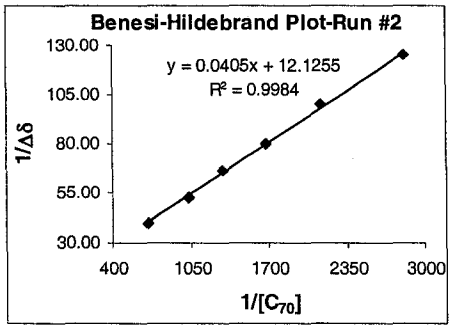

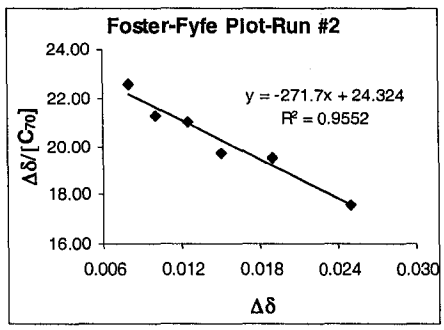

	$[18]/[C_{70}]$	slope	intercept	K(B-H)	R^2	K(F-F)	R^2
Run #1	1.33–5.59	0.0394	12.9 ± 2.09	328 ± 53	0.9964	274 ± 43	0.9108
Run #2	1.34–5.41	0.0405	12.1 ± 1.42	300 ± 35	0.9984	272 ± 29	0.9552
			Average:	313		273	
			SD:	20		1	

Appendix 5.1

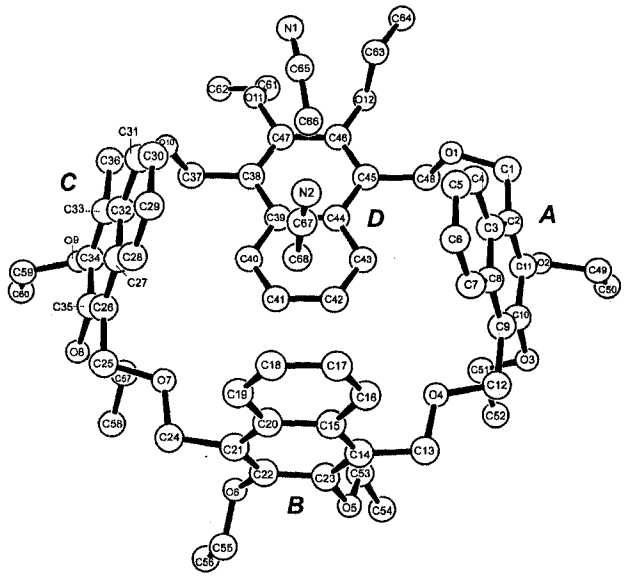

(a) PLUTO figure for **159b** showing the numbering system employed for the X-ray structure determination. Also shown are the label ***A-D*** used to for the naphthyl sub-units.

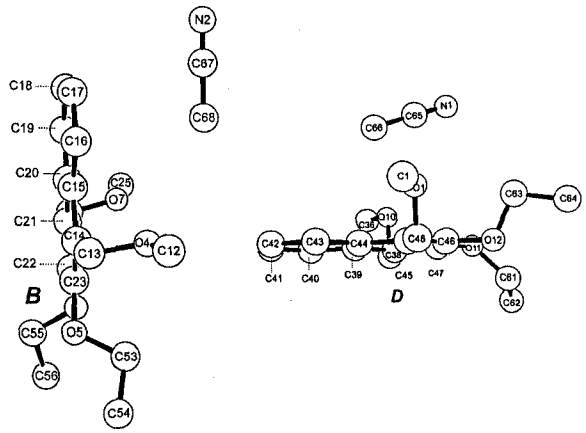

(b) Partial PLUTO figures describe from the X-ray structure determination of **159b** showing (a) The orientation of one of the acetoniltrile guest molecules which respective to the "***B***"–naphthyl sub-unit and (b) The orientation of the other acetonitrile guest molecule which respective to the "***D***" –naphthyl sub-unit.

Appendix 5.2 Determination of Complexation stoichiometry for **159a** vs TMACl using Job plot method.
[**159a**] = [TMACl] = 8.94 x 10^{-4} M

TMACl signal δ = 3.534 ppm				Aromatic signals of **159a** δ = 7.427 ppm				Aromatic signals of **159a** δ = 6.761 ppm			-H_2C-O-CH_2- signals of **159a** δ = 5.052 ppm		
χ_{TMACl}	δ (ppm)	Δδ (ppm)	χ_{TMACl} x Δδ	χ_{159a}	δ (ppm)	Δδ (ppm)	χ_{159a} xΔδ	δ (ppm)	Δδ (ppm)	χ_{159a} x Δδ	δ (ppm)	Δδ (ppm)	χ_{159a} x Δδ
1.0	**3.534**	0.000	0.000	0.0	0.000	0.000	0.000	0.000	0.000	0.000	0.000	0.000	0.000
0.9	3.338	0.196	0.176	0.1	7.729	-0.302	-0.030	7.131	-0.370	-0.037	5.081	-0.029	-0.003
0.8	3.044	0.490	0.392	0.2	7.685	-0.258	-0.052	7.089	-0.328	-0.066	5.075	-0.023	-0.005
0.7	2.782	0.752	0.526	0.3	7.649	-0.222	-0.067	7.053	-0.292	-0.088	5.073	-0.021	-0.006
0.6	2.540	0.994	0.596	0.4	7.623	-0.196	-0.078	7.016	-0.255	-0.102	5.070	-0.018	-0.007
0.5	2.302	1.232	0.616	0.5	7.585	-0.158	-0.079	6.971	-0.210	-0.105	5.068	-0.016	-0.008
0.4	2.073	1.461	0.584	0.6	7.549	-0.122	-0.073	6.931	-0.170	-0.102	5.066	-0.014	-0.008
0.3	1.799	1.735	0.521	0.7	7.515	-0.088	-0.061	6.889	-0.128	-0.089	5.062	-0.010	-0.007
0.2	1.560	1.974	0.395	0.8	7.475	-0.048	-0.038	6.842	-0.081	-0.065	5.061	-0.009	-0.007
0.0			0.000	0.9	7.436	-0.009	-0.008	6.798	-0.037	-0.033	5.058	-0.006	-0.005
				1.0	**7.427**	0.000	0.000	**6.761**	0.000	0.000	**5.052**	0.000	0.000

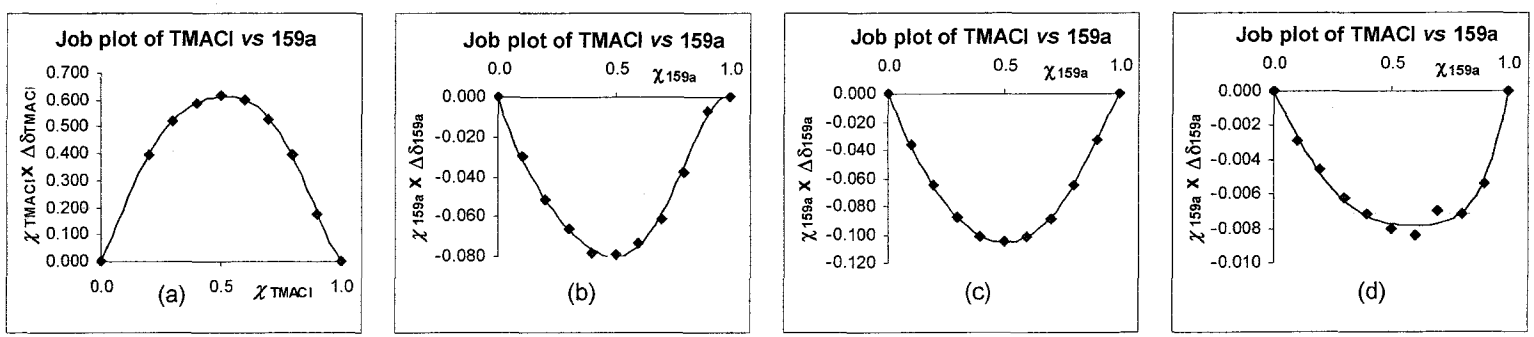

Figure (a) is a plot of mole fraction of TMACl versus Δδ of the methyl signal of TMACl (δ = 3.534 ppm).
Figure (b) is a plot of mole fraction of TMACl versus Δδ of the for the δ = 7.427 ppm signal of **159a**.
Figure (c) is a plot of mole fraction of TMACl versus Δδ of the for the δ = 6.761 ppm signal of **159a**.
Figure (d) is a plot of mole fraction of TMACl versus Δδ of the for the δ = 5.052 ppm signal of **159a**.

Appendix 5.3 Determination of Complexation stoichiometry for **159b** vs TMACl using Job plot method.
[**159b**] = [TMACl] = 8.94 x 10^{-4} M

TMACl signal δ = 3.534 ppm				Aromatic signals of **159b** δ = 7.323 ppm				Aromatic signals of **159b** δ = 6.721 ppm			-H_2C-O-CH_2- signals of **159b** δ = 5.051 ppm		
χ_{TMACl}	δ (ppm)	Δδ (ppm)	χ_{TMACl} x Δδ	χ_{159a}	δ (ppm)	Δδ (ppm)	χ_{159a} xΔδ	δ (ppm)	Δδ (ppm)	χ_{159a} x Δδ	δ (ppm)	Δδ (ppm)	χ_{159a} x Δδ
1.0	**3.534**	0.000	0.000	0.0	0.000	0.000	0.000	0.000	0.000	0.000	0.000	0.000	0.000
0.9	3.274	0.260	0.234	0.1	7.799	-0.476	-0.048	7.185	-0.464	-0.046	5.077	-0.026	-0.003
0.8	2.936	0.598	0.478	0.2	7.748	-0.425	-0.085	7.134	-0.413	-0.083	5.071	-0.020	-0.004
0.7	2.602	0.932	0.652	0.3	7.720	-0.397	-0.119	7.102	-0.381	-0.114	5.069	-0.018	-0.005
0.6	2.178	1.356	0.814	0.4	7.666	-0.343	-0.137	7.078	-0.357	-0.143	5.068	-0.017	-0.007
0.5	1.810	1.724	0.862	0.5	7.607	-0.284	-0.142	7.016	-0.295	-0.148	5.065	-0.014	-0.007
0.3	1.100	2.434	0.730	0.6	7.548	-0.225	-0.135	6.949	-0.228	-0.137	5.061	-0.010	-0.006
0.2	0.695	2.839	0.568	0.7	7.494	-0.171	-0.120	6.881	-0.160	-0.112	5.059	-0.008	-0.006
0.1	0.445	3.089	0.309	0.8	7.421	-0.098	-0.078	6.787	-0.066	-0.053	5.055	-0.004	-0.003
0.0			0.000	0.9	7.370	-0.047	-0.042	6.747	-0.026	-0.023	5.052	-0.001	-0.001
				1.0	**7.323**	0.000	0.000	**6.721**	0.000	0.000	**5.051**	0.000	0.000

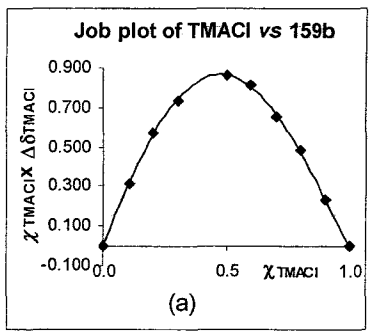

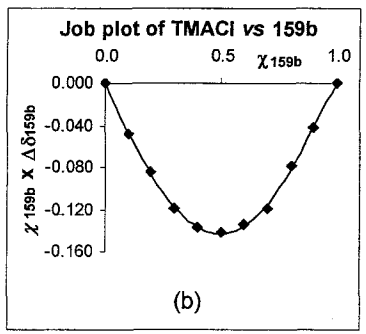

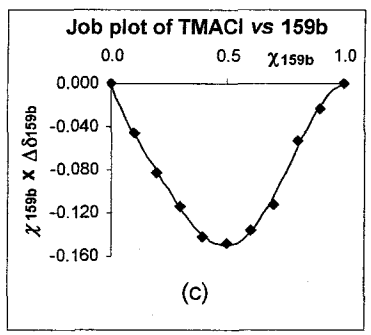

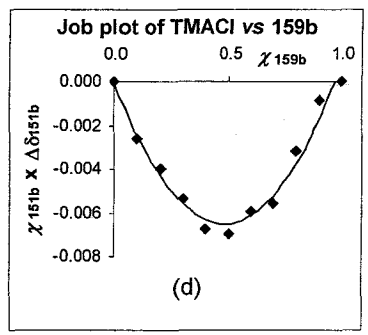

Figure (a) is a plot of mole fraction of TMACl versus Δδ of the methyl signal of TMACl (δ = 3.534 ppm).
Figure (b) is a plot of mole fraction of TMACl versus Δδ of the for the δ = 7.323 ppm signal of **159b**.
Figure (c) is a plot of mole fraction of TMACl versus Δδ of the for the δ = 6.721 ppm signal of **159b**.
Figure (d) is a plot of mole fraction of TMACl versus Δδ of the for the δ = 5.051 ppm signal of **159b**.

Appendix 5.4 Determination of K_{assoc} for **159a**:TMACl complex in $CDCl_3$ at 298 K; **159a** was added as aliquots. ($\Delta\delta$ are absolute values).

Entry #	159a (μL)	Total vol. (mL)	[159a] (M)	[TMACl] (M)	[TMACl] / [159a]	Run #1 δ (ppm)	Run #2 δ (ppm)
1	0	1	0	8.94×10^{-4}	0.00	3.542	3.542
2	20	1.02	2.39×10^{-5}	8.77×10^{-4}	36.7	3.473	3.473
3	30	1.03	3.55×10^{-5}	8.68×10^{-4}	24.5	3.441	3.442
4	40	1.04	4.69×10^{-5}	8.60×10^{-4}	18.3	3.410	3.412
5	70	1.07	7.97×10^{-5}	8.36×10^{-4}	10.5	3.326	3.326
6	80	1.08	9.03×10^{-5}	8.28×10^{-4}	9.2	3.301	3.301

Run #1				Run #2			
1/[159a]	1/Δδ	Δδ (ppm)	Δδ/[159a]	1/[159a]	1/Δδ	Δδ (ppm)	Δδ/[159a]
0.00	0.000	0.000	0.000	0.00	0.00	0.000	0.000
4.18×10^{4}	14.49	0.069	2.89×10^{3}	4.18×10^{4}	14.49	0.069	2.89×10^{3}
2.82×10^{4}	9.90	0.101	2.85×10^{3}	2.82×10^{4}	10.00	0.100	2.82×10^{3}
2.13×10^{4}	7.58	0.132	2.82×10^{3}	2.13×10^{4}	7.69	0.130	2.78×10^{3}
1.25×10^{4}	4.63	0.216	2.71×10^{3}	1.25×10^{4}	4.63	0.216	2.71×10^{3}
1.11×10^{4}	4.15	0.241	2.67×10^{3}	1.11×10^{4}	4.15	0.241	2.67×10^{3}

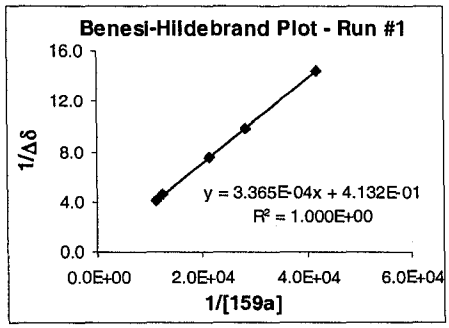

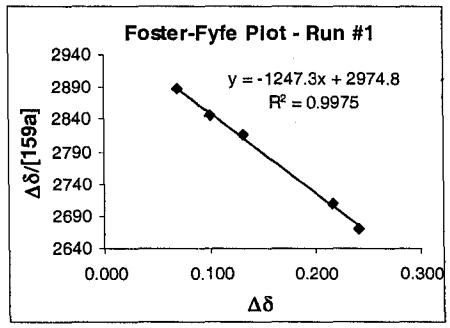

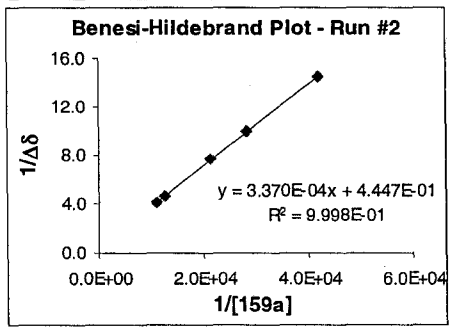

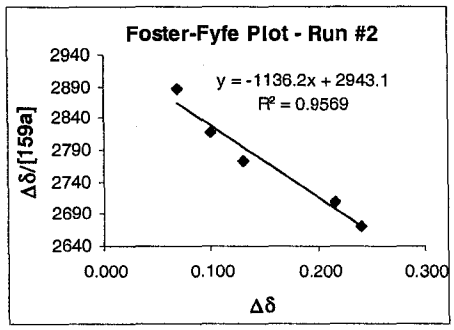

	slope	intercept	K(B-H)	R^2	K(F-F)	R^2
Run#1	3.365×10^{-4}	0.413 ± 0.012	1228 ± 36	1.0000	1247 ± 36	0.9975
Run#2	3.370×10^{-4}	0.445 ± 0.066	1320 ± 196	0.9998	1136 ± 139	0.9569
		Average	1274	**Average**	1192	
		SD	65	**SD**	79	

Appendix 5.5 Determination of K_{assoc} for **159b**:TMACl complex in $CDCl_3$ at 298 K; **159b** was added as aliquots. ($\Delta\delta$ are absolute values).

Entry #	159b (μL)	Total vol. (mL)	[159b] (M)	[TMACl] (M)	[TMACl] / [159b]	Run #1 δ (ppm)	Run #2 δ (ppm)
1	0	1	0	8.94×10^{-4}	0.0	3.542	3.541
2	20	1.02	2.55×10^{-5}	8.77×10^{-4}	34.3	3.459	3.457
3	30	1.03	3.79×10^{-5}	8.68×10^{-4}	22.9	3.419	3.418
4	40	1.04	5.01×10^{-5}	8.60×10^{-4}	17.2	3.382	3.380
5	50	1.05	6.20×10^{-5}	8.51×10^{-4}	13.7	3.344	3.343
6	60	1.06	7.37×10^{-5}	8.43×10^{-4}	11.4	3.309	3.306
7	70	1.07	8.52×10^{-5}	8.36×10^{-4}	9.8	3.276	3.271

Run #1				Run #2			
1/[159b]	1/Δδ	Δδ (ppm)	Δδ/[159b]	1/[159b]	1/Δδ	Δδ (ppm)	Δδ/[159b]
0.00	0.00	0.000	0.00	0.00	0.00	0.000	0.00
3.92×10^{4}	12.05	0.083	3.25×10^{3}	3.92×10^{4}	11.90	0.084	3.29×10^{3}
2.64×10^{4}	8.13	0.123	3.24×10^{3}	2.64×10^{4}	8.13	0.123	3.24×10^{3}
2.00×10^{4}	6.25	0.160	3.19×10^{3}	2.00×10^{4}	6.21	0.161	3.21×10^{3}
1.61×10^{4}	5.05	0.198	3.19×10^{3}	1.61×10^{4}	5.05	0.198	3.19×10^{3}
1.36×10^{4}	4.29	0.233	3.16×10^{3}	1.36×10^{4}	4.26	0.235	3.19×10^{3}
1.17×10^{4}	3.76	0.266	3.12×10^{3}	1.17×10^{4}	3.70	0.270	3.17×10^{3}

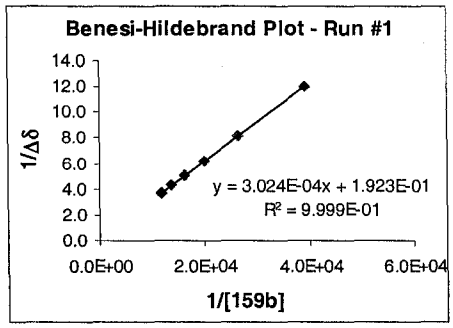

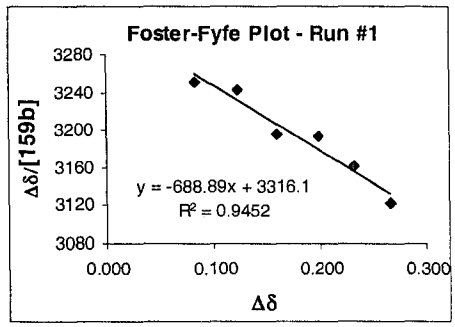

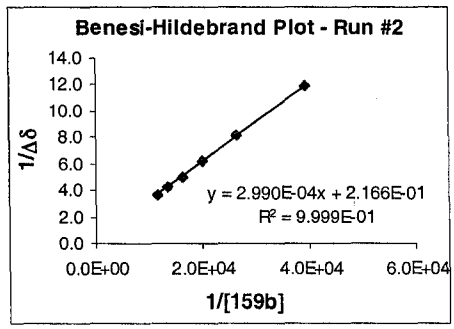

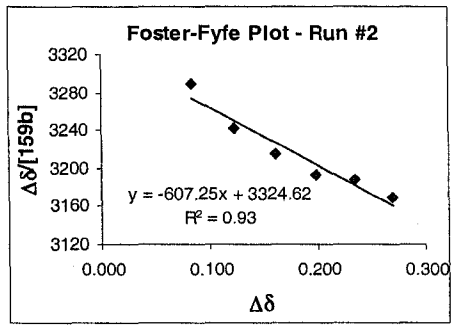

	slope	intercept	K(B-H)	R^2	K(F-F)	R^2
Run#1	3.024×10^{-4}	0.192 ± 0.025	636 ± 83	1.0000	689 ± 83	0.9564
Run#2	2.990×10^{-4}	0.217 ± 0.028	724 ± 94	0.9997	607 ± 85	0.9269
		Average	680	**Average**	648	
		SD	62	**SD**	58	

Appendix 7.1 Chemical shift changes ($\Delta\delta$) for protons on **205a** in 1:9 CD_3CN-$CDCl_3$ at 298 K *versus* added AgO_2CCF_3 solution (5.22×10^{-3} M) ($\Delta\delta$ are absolute values).

Run #1:

Entry	$[Ag^+]$	[205a]	$\frac{[Ag^+]}{[205a]}$	$\frac{[205a]}{[Ag^+]}$	δ_{Ar} (ppm)	$\Delta\delta_{Ar}$ (ppm)	δ_{SCH_2} (ppm)	$\Delta\delta_{SCH_2}$ (ppm)	δ_{OCH_3} (ppm)	$\Delta\delta_{OCH_3}$ (ppm)
1	0.00	4.84×10^{-4}	0.00	0.00	**7.115**	0.000	**4.301**	0.000	**3.666**	0.000
2	2.48×10^{-4}	4.61×10^{-4}	0.54	1.86	7.121	0.005	4.339	0.038	3.699	0.033
3	3.26×10^{-4}	4.54×10^{-4}	0.72	1.39	7.120	0.005	4.351	0.050	3.707	0.041
4	4.01×10^{-4}	4.47×10^{-4}	0.90	1.11	7.124	0.008	4.361	0.060	3.713	0.047
5	4.74×10^{-4}	4.40×10^{-4}	1.08	0.93	7.124	0.009	4.370	0.069	3.717	0.051
6	6.47×10^{-4}	4.24×10^{-4}	1.53	0.66	7.124	0.009	4.390	0.089	3.728	0.062
7	8.08×10^{-4}	4.09×10^{-4}	1.97	0.51	7.126	**0.010**	4.406	0.105	3.738	0.072
8	9.58×10^{-4}	3.95×10^{-4}	2.42	0.41	not clear	-	4.418	0.117	3.745	0.079
9	1.10×10^{-3}	3.82×10^{-4}	2.87	0.35	not clear	-	4.428	**0.127**	3.751	**0.085**

Run #2:

Entry	$[Ag^+]$	[205a]	$\frac{[Ag^+]}{[205a]}$	$\frac{[205a]}{[Ag^+]}$	δ_{Ar} (ppm)	$\Delta\delta_{Ar}$ (ppm)	δ_{SCH_2} (ppm)	$\Delta\delta_{SCH_2}$ (ppm)	δ_{OCH_3} (ppm)	$\Delta\delta_{OCH_3}$ (ppm)
1	0.00	4.84×10^{-4}	0.00	0.00	7.116	0.000	**4.301**	**0.000**	3.666	0.000
2	2.48×10^{-4}	4.61×10^{-4}	0.54	1.86	7.121	0.005	4.339	0.038	3.700	0.034
3	3.26×10^{-4}	4.54×10^{-4}	0.72	1.39	7.124	0.008	4.350	0.049	3.708	0.042
4	4.01×10^{-4}	4.47×10^{-4}	0.90	1.11	7.126	0.010	4.360	0.059	3.716	0.050
5	4.74×10^{-4}	4.40×10^{-4}	1.08	0.93	7.126	0.010	4.369	0.068	3.722	0.056
6	6.47×10^{-4}	4.24×10^{-4}	1.53	0.66	7.128	**0.012**	4.390	0.089	3.735	0.069
7	8.08×10^{-4}	4.09×10^{-4}	1.97	0.51	not clear	-	4.404	0.103	3.744	0.078
8	9.58×10^{-4}	3.95×10^{-4}	2.42	0.41	not clear	-	4.416	0.115	3.752	0.086
9	1.10×10^{-3}	3.82×10^{-4}	2.87	0.35	not clear	-	4.426	**0.125**	3.758	**0.092**

Appendix 7.2 Chemical shift changes ($\Delta\delta$) for protons on **205b** in 1:9 CD_3CN-$CDCl_3$ at 298 K *versus* added AgO_2CCF_3 solution (5.07×10^{-3} M) ($\Delta\delta$ are absolute values).

Run #1:

Entry	$[Ag^+]$	[205b]	$\frac{[Ag^+]}{[205b]}$	$\frac{[205b]}{[Ag^+]}$	δ_{Ar} (ppm)	$\Delta\delta_{Ar}$ (ppm)	δ_{SCH_2} (ppm)	$\Delta\delta_{SCH_2}$ (ppm)	δ_{OCH_2} (ppm)	$\Delta\delta_{OCH_2}$ (ppm)
1	0.00	4.84×10^{-4}	0.00	0.00	**6.930**	0.000	**4.304**	0	**4.069**	0.000
2	2.41×10^{-4}	4.61×10^{-4}	0.52	1.91	6.964	0.034	4.353	0.049	4.083	0.014
3	3.17×10^{-4}	4.54×10^{-4}	0.70	1.43	6.977	0.047	4.369	0.065	4.088	0.018
4	3.90×10^{-4}	4.47×10^{-4}	0.87	1.15	6.982	0.052	4.380	0.076	4.089	0.019
5	4.61×10^{-4}	4.40×10^{-4}	1.05	0.96	6.988	0.058	4.392	0.088	4.092	0.023
6	6.29×10^{-4}	4.24×10^{-4}	1.48	0.67	7.002	0.072	4.414	0.110	4.095	0.026
7	7.85×10^{-4}	4.09×10^{-4}	1.92	0.52	7.017	0.087	4.432	0.128	4.099	0.029
8	9.31×10^{-4}	3.95×10^{-4}	2.35	0.42	7.021	0.091	4.446	0.142	4.102	0.032
9	1.07×10^{-3}	3.82×10^{-4}	2.79	0.36	7.029	**0.099**	4.457	**0.153**	4.103	**0.034**

Run #2:

Entry	$[Ag^+]$	[205b]	$\frac{[Ag^+]}{[205b]}$	$\frac{[205b]}{[Ag^+]}$	δ_{Ar} (ppm)	$\Delta\delta_{Ar}$ (ppm)	δ_{SCH_2} (ppm)	$\Delta\delta_{SCH_2}$ (ppm)	δ_{OCH_2} (ppm)	$\Delta\delta_{OCH_2}$ (ppm)
1	0.00	4.84×10^{-4}	0.00	0.00	**6.931**	0.000	**4.306**	0.000	**4.069**	0.000
2	2.41×10^{-4}	4.61×10^{-4}	0.52	1.91	6.963	0.032	4.355	0.049	4.084	0.015
3	3.17×10^{-4}	4.54×10^{-4}	0.70	1.43	6.976	0.045	4.369	0.063	4.088	0.019
4	3.90×10^{-4}	4.47×10^{-4}	0.87	1.15	6.985	0.054	4.382	0.076	4.092	0.023
5	4.61×10^{-4}	4.40×10^{-4}	1.05	0.96	6.990	0.059	4.393	0.087	4.092	0.023
6	6.286×10^{-4}	4.24×10^{-4}	1.48	0.67	7.003	0.072	4.416	0.110	4.097	0.027
7	7.85×10^{-4}	4.09×10^{-4}	1.92	0.52	7.015	0.084	4.433	0.127	4.102	0.033
8	9.31×10^{-4}	3.95×10^{-4}	2.35	0.42	7.026	0.095	4.446	0.140	4.105	0.036
9	1.07×10^{-3}	3.82×10^{-4}	2.79	0.36	7.031	**0.100**	4.456	**0.150**	4.108	**0.039**

Appendix 7.3 Determination of stoichiometry and K_{assoc} for **205a**:Ag^+ complex in 1:9 CD_3CN-$CDCl_3$ at 298 K. AgO_2CCF_3 (5.22 x 10^{-3} M) solution was added as aliquots.

Entry	$[Ag^+]$	[205a]	$\frac{[Ag^+]}{[205a]}$	Run #1			
				$1/[Ag^+]$	$1/\Delta\delta$	$\Delta\delta_{SCH_2}$	$\Delta\delta/[Ag^+]$
1	0	4.84 x 10^{-4}	0	0	0.00	0.000	0.0
2	2.48 x 10^{-4}	4.61 x 10^{-4}	0.54	4027	26.32	0.038	153.0
3	3.26 x 10^{-4}	4.54 x 10^{-4}	0.72	3068	20.41	0.049	150.3
4	4.01 x 10^{-4}	4.47 x 10^{-4}	0.90	2493	16.95	0.059	147.1
5	4.74 x 10^{-4}	4.40 x 10^{-4}	1.08	2109	14.71	0.068	143.4
6	6.47 x 10^{-4}	4.24 x 10^{-4}	1.53	1545	11.24	0.089	137.5
7	8.08 x 10^{-4}	4.09 x 10^{-4}	1.97	1238	9.71	0.103	127.5
8	9.58 x 10^{-4}	3.95 x 10^{-4}	2.42	1044	8.70	0.115	120.1
9	1.10 x 10^{-3}	3.82 x 10^{-4}	2.87	911	8.00	0.125	113.9

Entry	$[Ag^+]$	[205a]	$\frac{[205a]}{[Ag^+]}$	Run #2			
				$1/[Ag^+]$	$1/\Delta\delta$	$\Delta\delta_{SCH_2}$	$\Delta\delta/[Ag^+]$
1	0	4.84 x 10^{-4}	0.00	0	0.00	0.000	0.0
2	2.48 x 10^{-4}	4.61 x 10^{-4}	1.86	4027	26.32	0.038	153.0
3	3.26 x 10^{-4}	4.54 x 10^{-4}	1.39	3068	20.00	0.050	153.4
4	4.01 x 10^{-4}	4.47 x 10^{-4}	1.11	2493	16.67	0.060	149.6
5	4.74 x 10^{-4}	4.40 x 10^{-4}	0.93	2109	14.49	0.069	145.6
6	6.47 x 10^{-4}	4.24 x 10^{-4}	0.66	1545	11.24	0.089	137.5
7	8.08 x 10^{-4}	4.09 x 10^{-4}	0.51	1238	9.52	0.105	130.0
8	9.58 x 10^{-4}	3.95 x 10^{-4}	0.41	1044	8.55	0.117	122.2
9	1.10 x 10^{-3}	3.82 x 10^{-4}	0.35	911	7.87	0.127	115.7

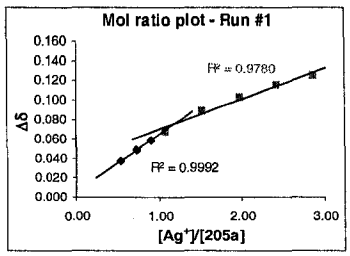

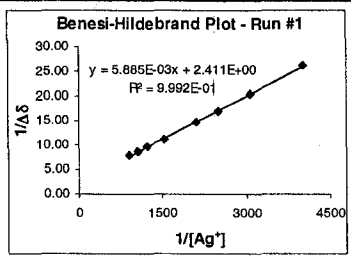

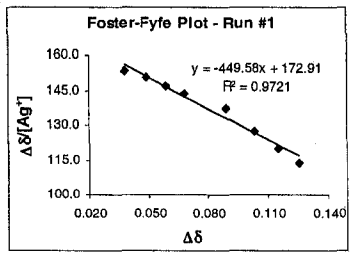

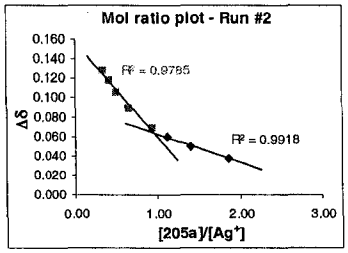

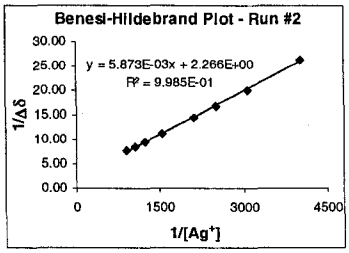

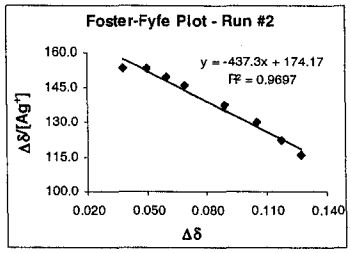

205a:Ag+	slope	intercept	K(B-H)	R^2	K(F-F)	R^2
Run#1	5.885E-03	2.411 ± 0.153	410 ± 26	0.9992	450 ± 31	0.9721
Run#2	5.873E-03	2.266 ± 0.211	386 ± 36	0.9985	437 ± 32	0.9697
		Average	398	**Average**	444	
		SD	17	**SD**	9	

Appendix 7.4 Determination of stoichiometry and K_{assoc} for **205b**:Ag^+ complex in 1:9 CD_3CN-$CDCl_3$ at 298 K. AgO_2CCF_3 (5.07 x 10^{-3} M) solution was added as aliquots.

Entry	[Ag^+]	[205b]	[Ag^+]/[205b]	Run #1			
				1/[Ag^+]	1/Δδ	$\Delta\delta_{SCH_2}$	Δδ/[Ag^+]
1	0.00	4.84 x 10^{-4}	0.00	0	0.00	0.000	0.0
2	2.41 x 10^{-4}	4.61 x 10^{-4}	0.52	4145	20.41	0.049	203.1
3	3.17 x 10^{-4}	4.54 x 10^{-4}	0.70	3158	15.38	0.065	205.3
4	3.90 x 10^{-4}	4.47 x 10^{-4}	0.87	2566	13.16	0.076	195.0
5	4.61 x 10^{-4}	4.40 x 10^{-4}	1.05	2171	11.36	0.088	191.1
6	6.29 x 10^{-4}	4.24 x 10^{-4}	1.48	1591	9.09	0.110	175.0
7	7.85 x 10^{-4}	4.09 x 10^{-4}	1.92	1274	7.81	0.128	163.1
8	9.31 x 10^{-4}	3.95 x 10^{-4}	2.35	1075	7.04	0.142	152.6
9	1.07 x 10^{-3}	3.82 x 10^{-4}	2.79	938	6.54	0.153	143.5

Entry	[Ag^+]	[205b]	[205b]/[Ag^+]	Run #2			
				1/[Ag^+]	1/Δδ	$\Delta\delta_{SCH_2}$	Δδ/[Ag^+]
1	0.00	4.84 x 10^{-4}	0.00	0	0.00	0.000	0.0
2	2.41 x 10^{-4}	4.61 x 10^{-4}	1.91	4145	20.41	0.049	203.1
3	3.17 x 10^{-4}	4.54 x 10^{-4}	1.43	3158	15.87	0.063	199.0
4	3.90 x 10^{-4}	4.47 x 10^{-4}	1.15	2566	13.16	0.076	195.0
5	4.61 x 10^{-4}	4.40 x 10^{-4}	0.96	2171	11.49	0.087	188.9
6	6.29 x 10^{-4}	4.24 x 10^{-4}	0.67	1591	9.09	0.110	175.0
7	7.85 x 10^{-4}	4.09 x 10^{-4}	0.52	1274	7.87	0.127	161.8
8	9.31 x 10^{-4}	3.95 x 10^{-4}	0.42	1075	7.14	0.140	150.5
9	1.07 x 10^{-3}	3.82 x 10^{-4}	0.36	938	6.67	0.150	140.6

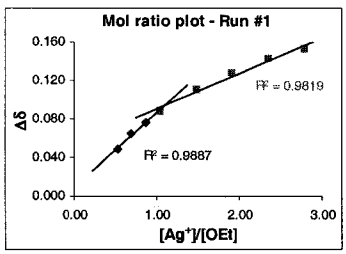

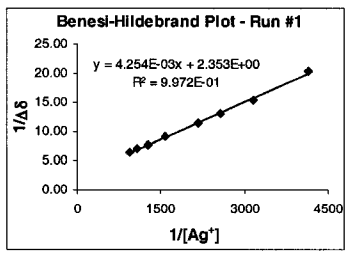

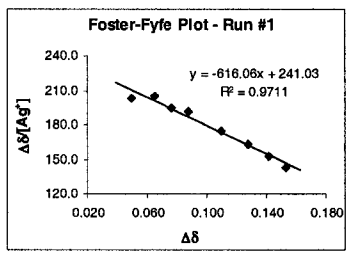

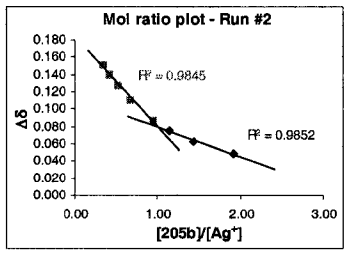

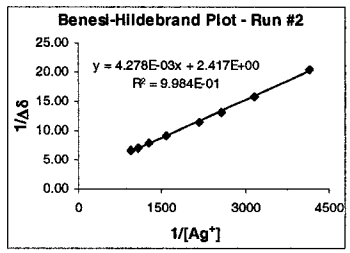

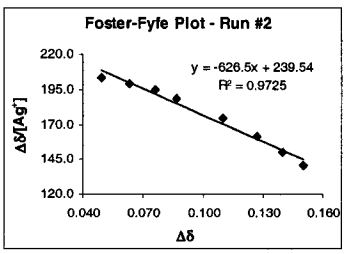

205b:Ag+	slope	intercept	K(B-H)	R^2	K(F-F)	R^2
Run#1	4.254E-03	2.353 ± 0.219	553 ± 51	0.9972	616 ± 43	0.9711
Run#2	4.278E-03	2.417 ± 0.165	565 ± 39	0.9984	627 ± 43	0.9725
		Average	559	**Average**	622	
		SD	8	**SD**	8	

Appendix B

Selected NMR spectra for synthesized compounds in numerical order

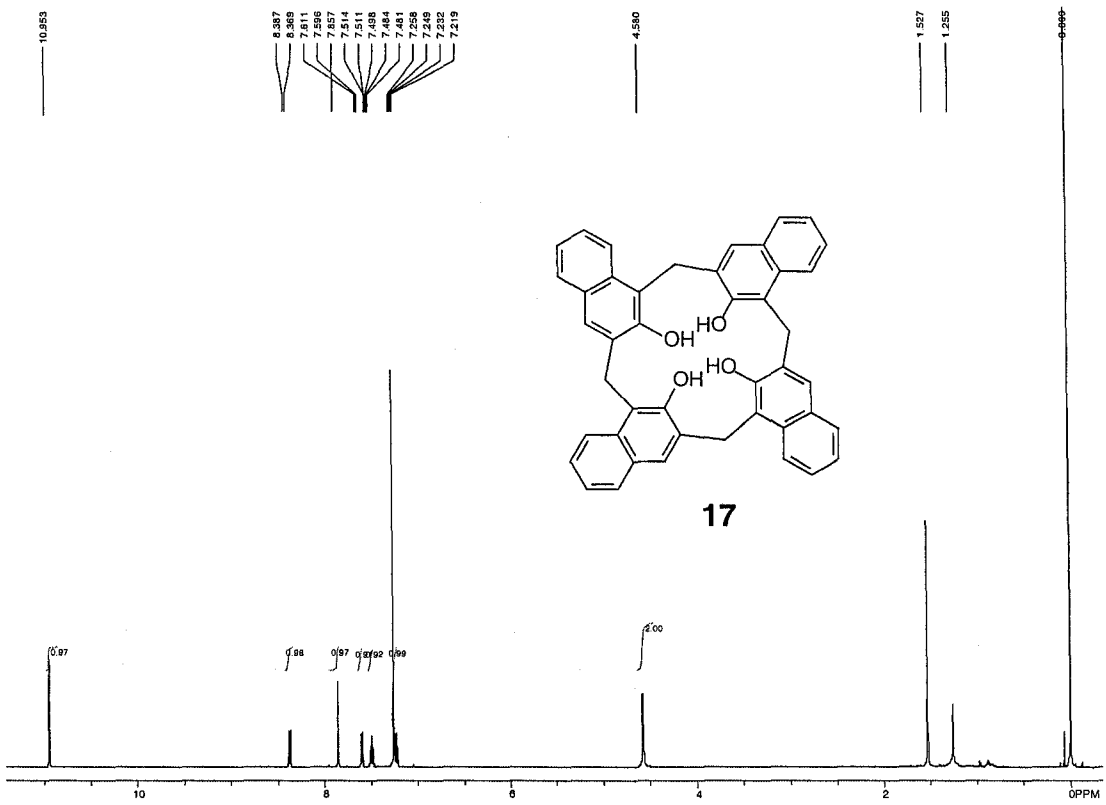
10.953
8.387
8.369
7.611
7.596
7.557
7.514
7.511
7.498
7.484
7.481
7.258
7.249
7.232
7.219
4.580
1.527
1.255
0.000
OH
HO
OH
HO
17
0.97
0.98
0.97
0.92
0.99
2.00
10
8
6
4
2
0PPM

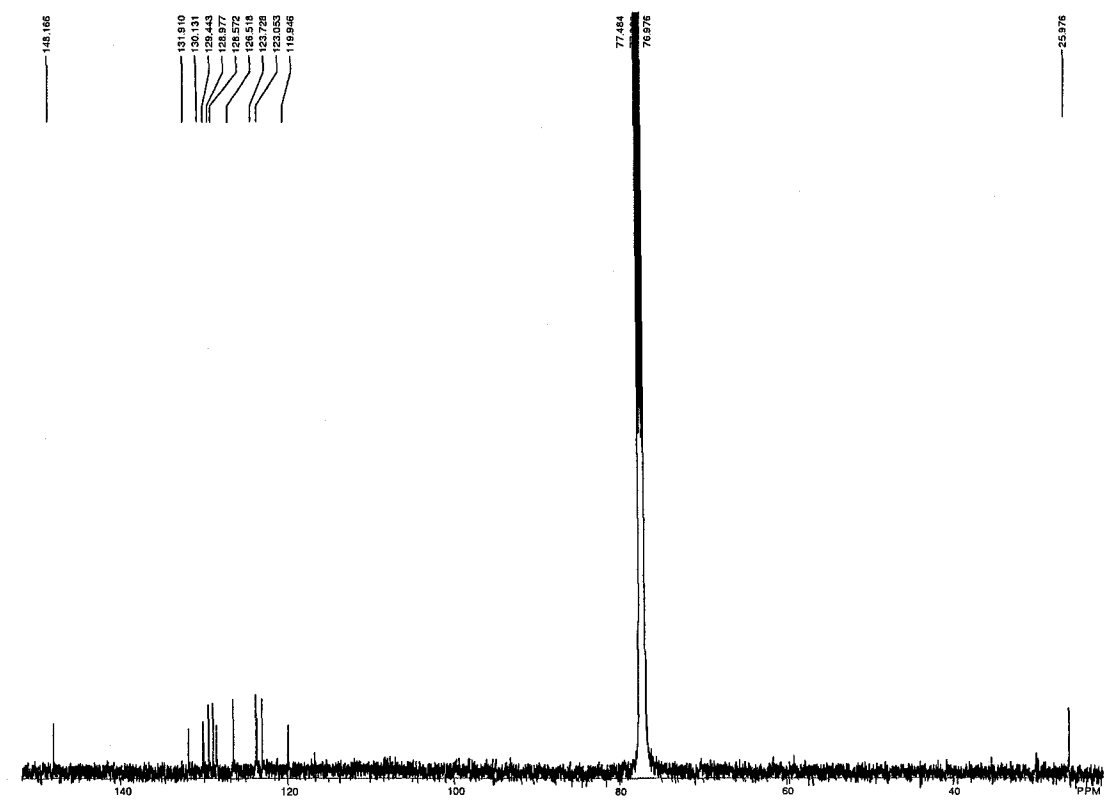
148.165
131.910
130.131
129.443
128.977
126.572
126.518
123.728
123.053
119.946
77.484
77.160
76.976
25.976
140
120
100
80
60
40
PPM

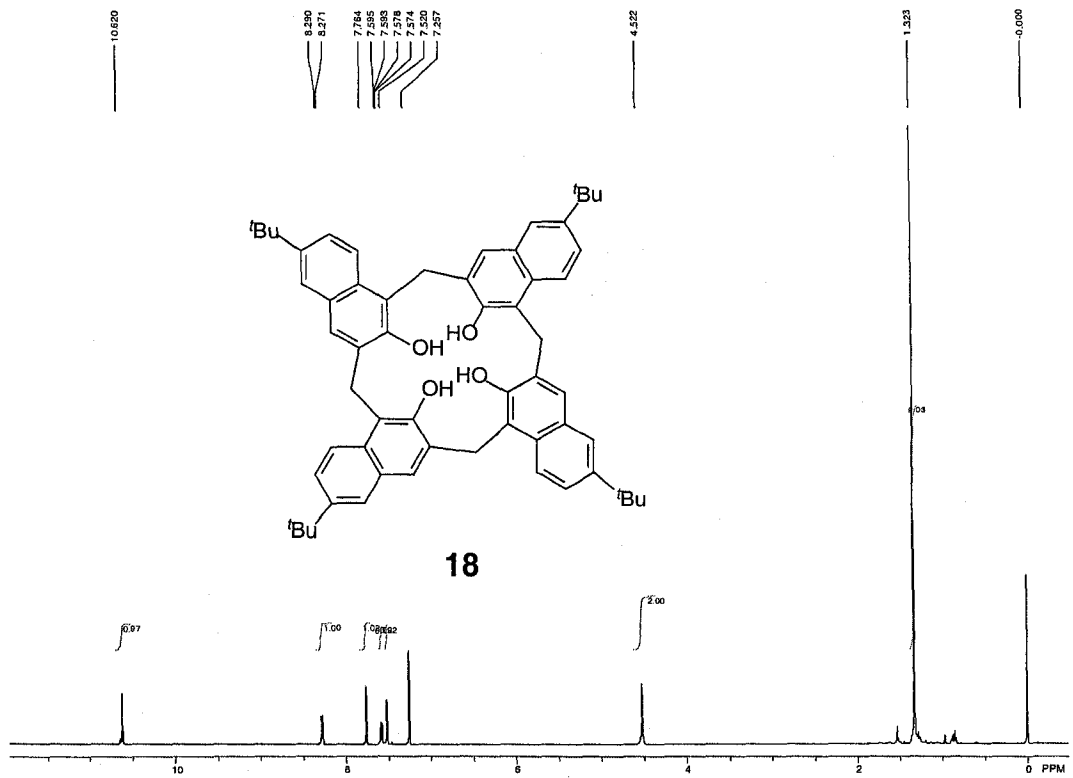
10.620
8.290
8.271
7.764
7.585
7.565
7.578
7.574
7.520
7.257
4.522
1.323
-0.000
tBu
tBu
tBu
tBu
HO
OH
HO
OH
18
0.97
1.00
2.00
4.03
10
8
6
4
2
0 PPM

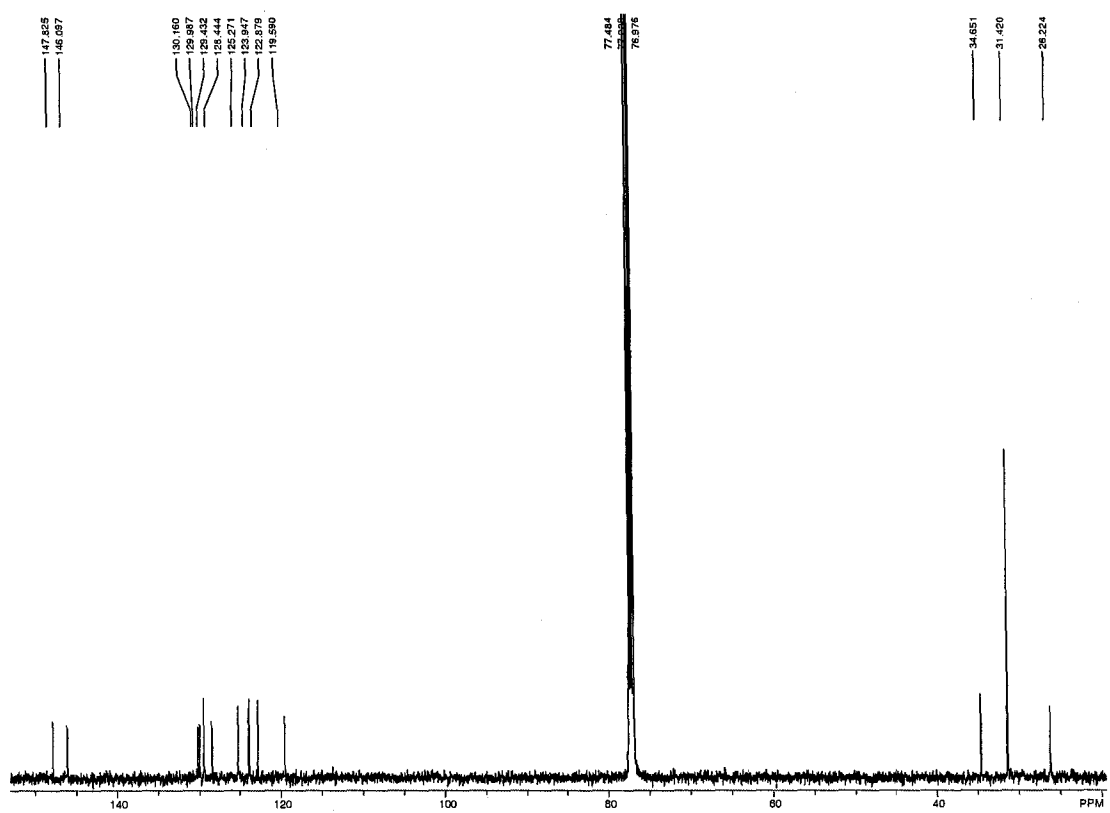
147.825
146.097
130.160
129.987
129.432
128.444
125.271
123.947
122.879
119.590
77.484
77.158
76.976
34.651
31.420
28.224
140
120
100
80
60
40
PPM

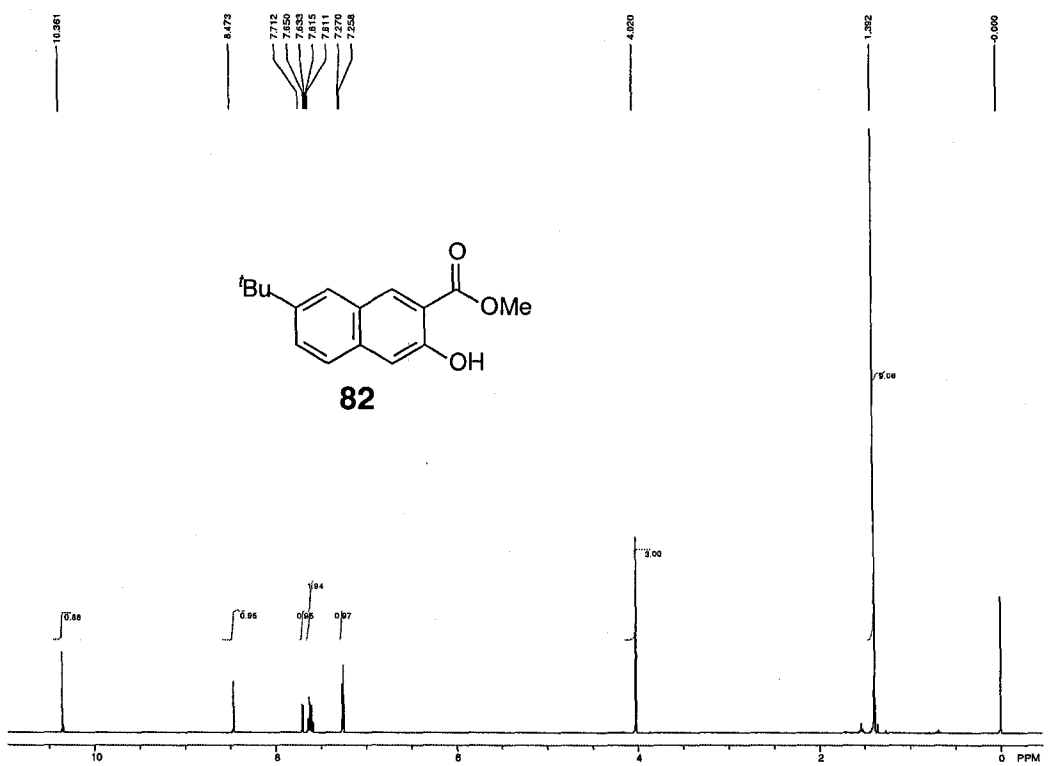
10.361
8.473
7.712
7.650
7.633
7.615
7.511
7.270
7.258
4.020
1.392
-0.000
tBu
O
OMe
OH
82
0.88
0.95
0.94
0.97
3.00
9.08
10
8
6
4
2
0
PPM

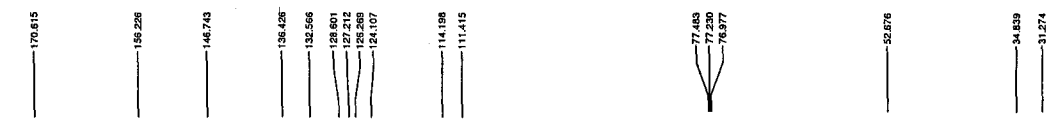
170.615
156.226
146.743
136.425
132.566
128.601
127.212
125.268
124.107
114.198
111.415
77.483
77.230
76.977
52.576
34.539
31.274

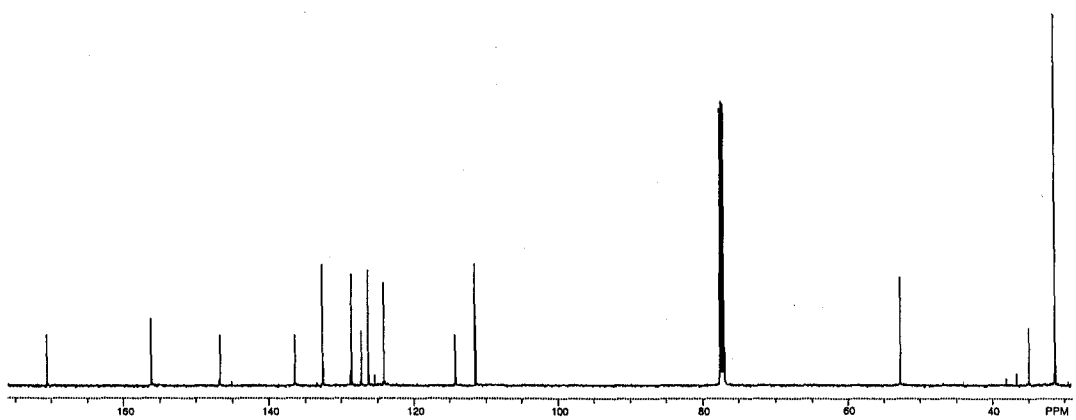
160
140
120
100
80
60
40
PPM

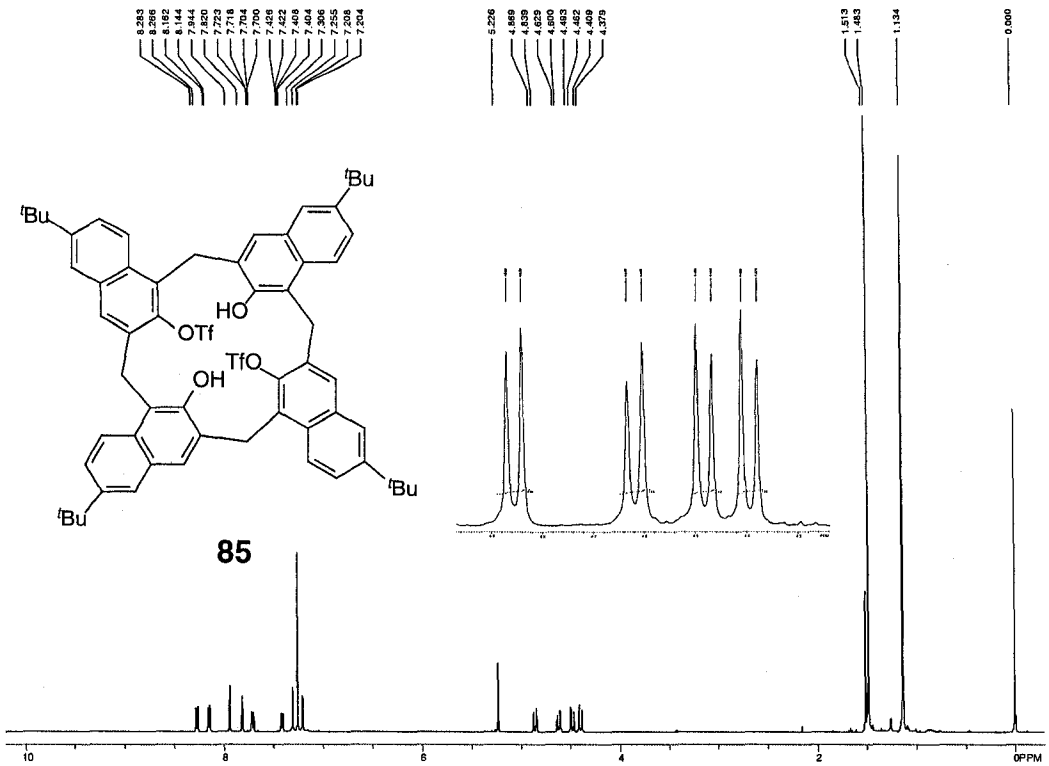
tBu
tBu
HO
OTf
TfO
OH
tBu
tBu
85
10
8
6
4
2
0PPM

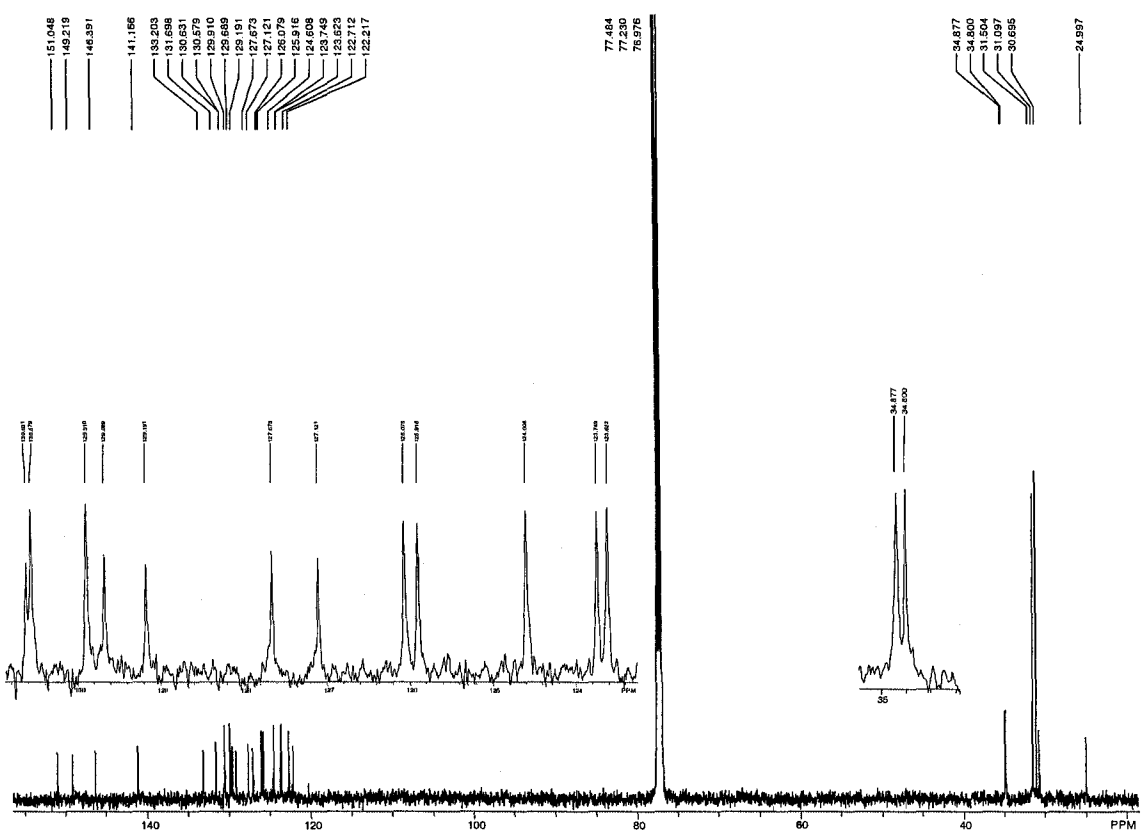
140
120
100
80
60
40
PPM

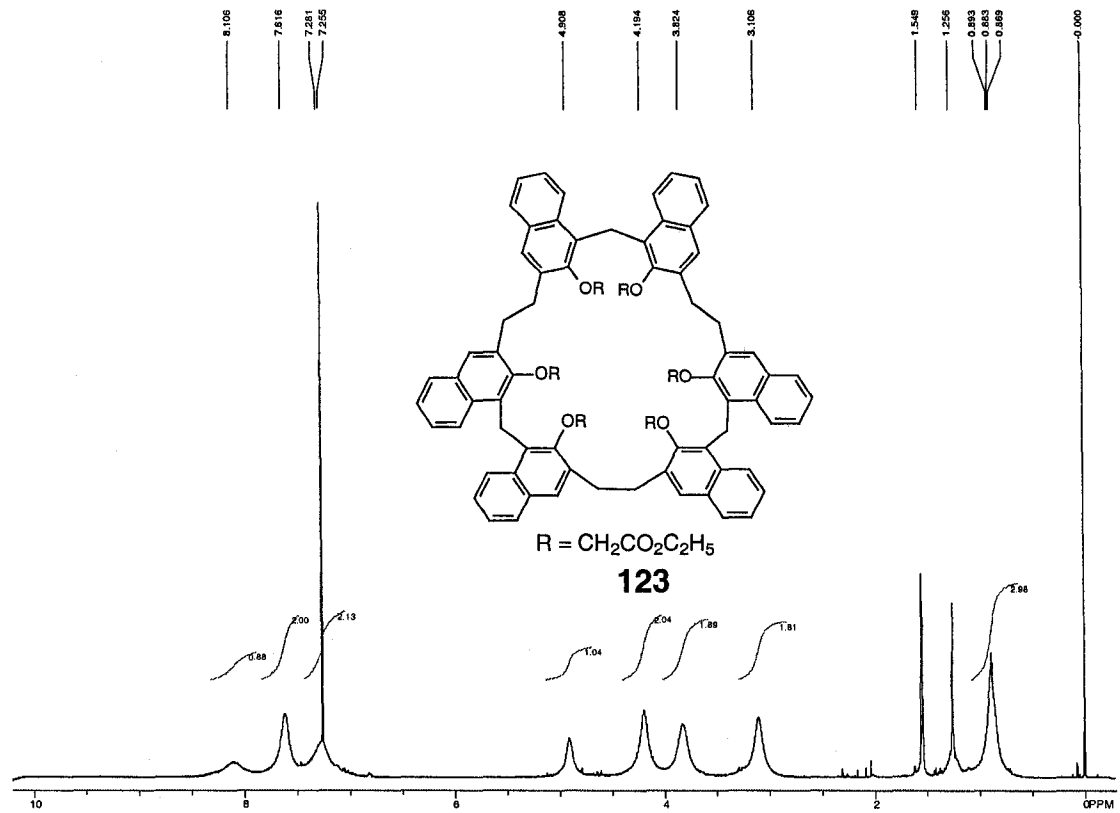

$R = CH_2CO_2C_2H_5$

123

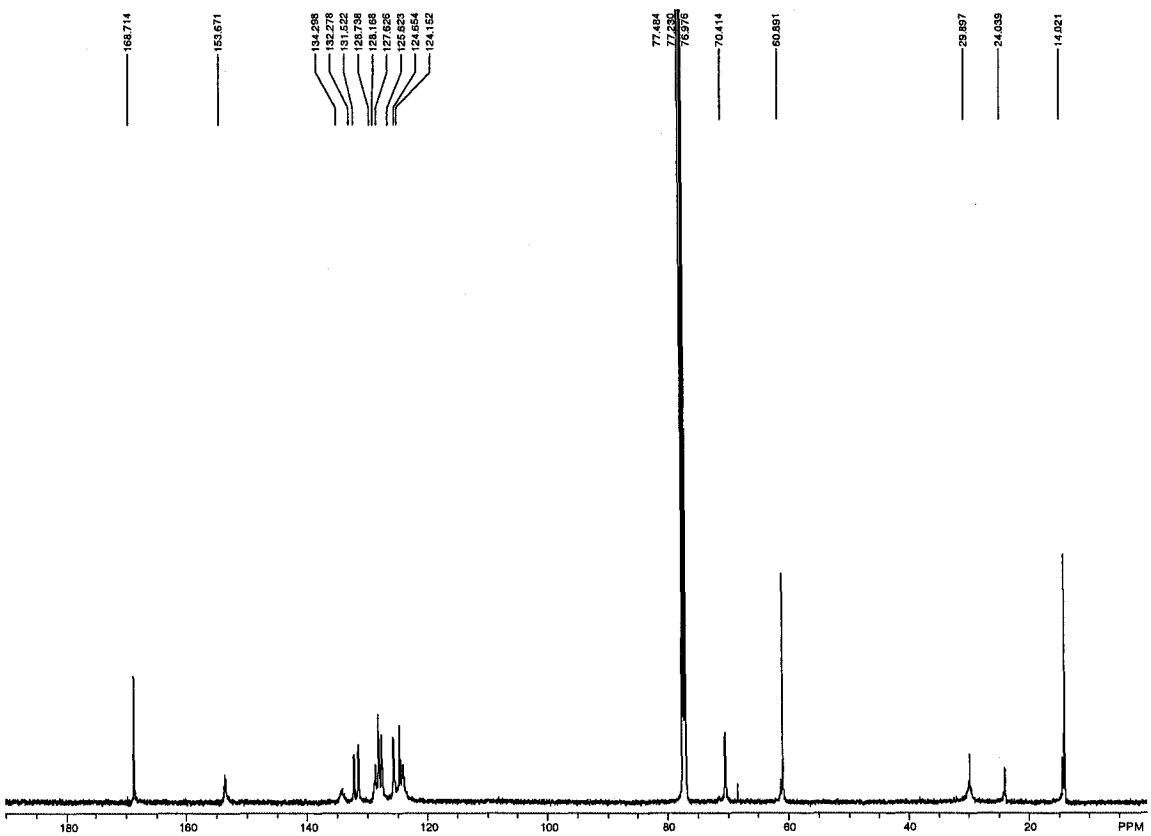

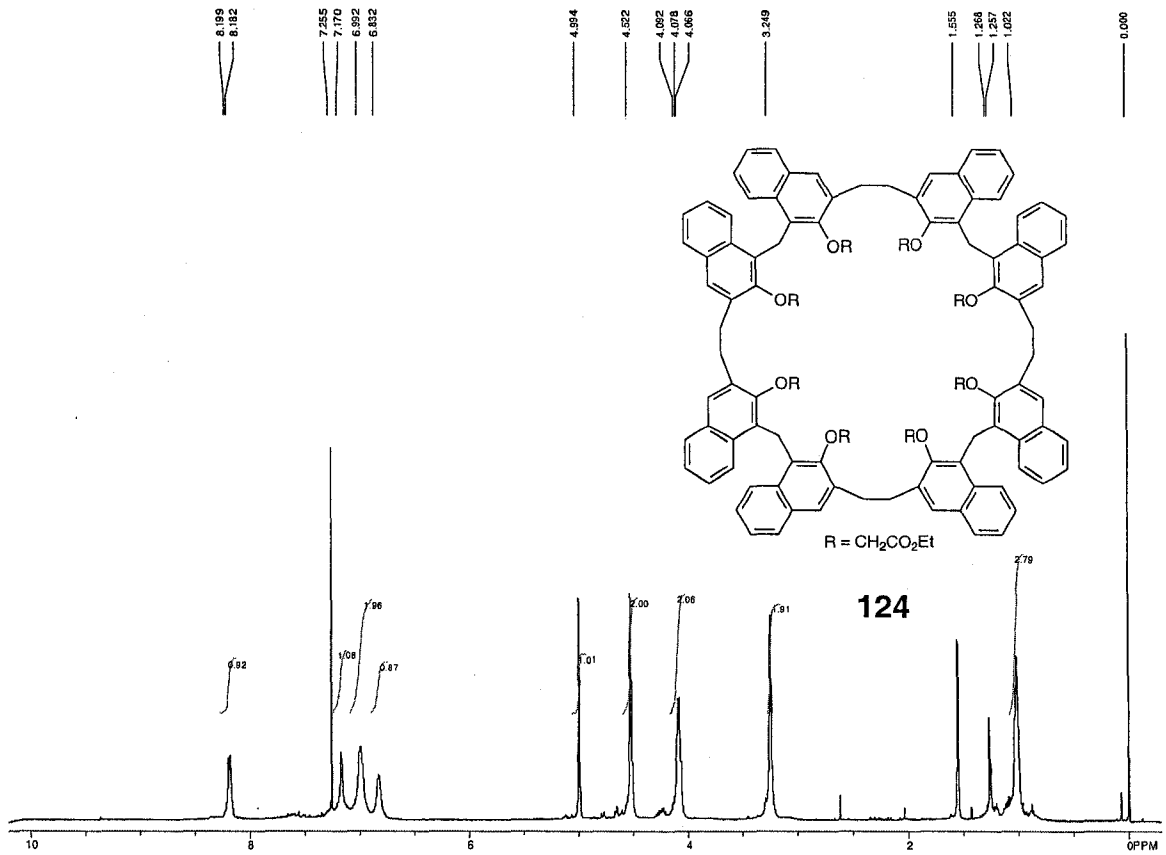
8.199
8.182
7.255
7.170
6.992
6.832
4.994
4.522
4.092
4.078
4.066
3.249
1.555
1.268
1.257
1.022
0.000
OR
RO
R = CH2CO2Et
124
0.92
1.08
0.87
1.01
2.00
2.08
1.91
2.79
10
8
6
4
2
0PPM

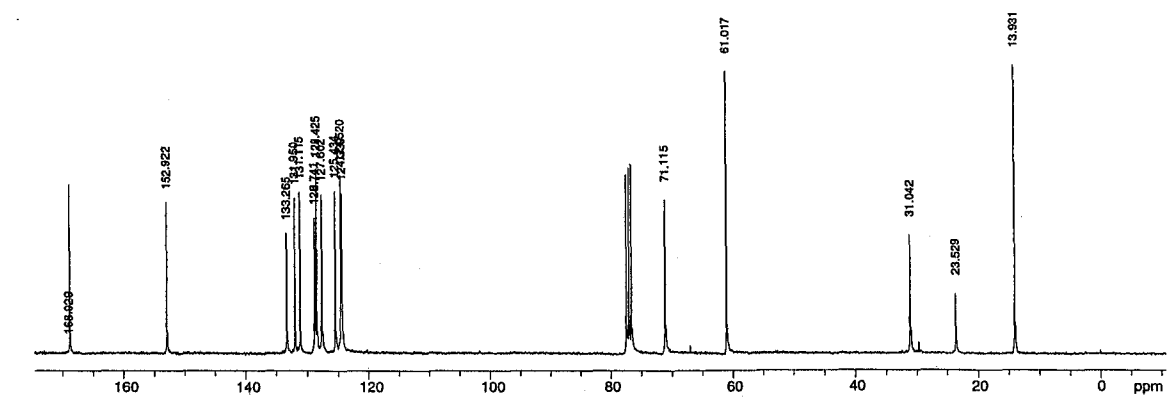
168.639
152.922
133.265
71.115
61.017
31.042
23.529
13.931
160
140
120
100
80
60
40
20
0
ppm

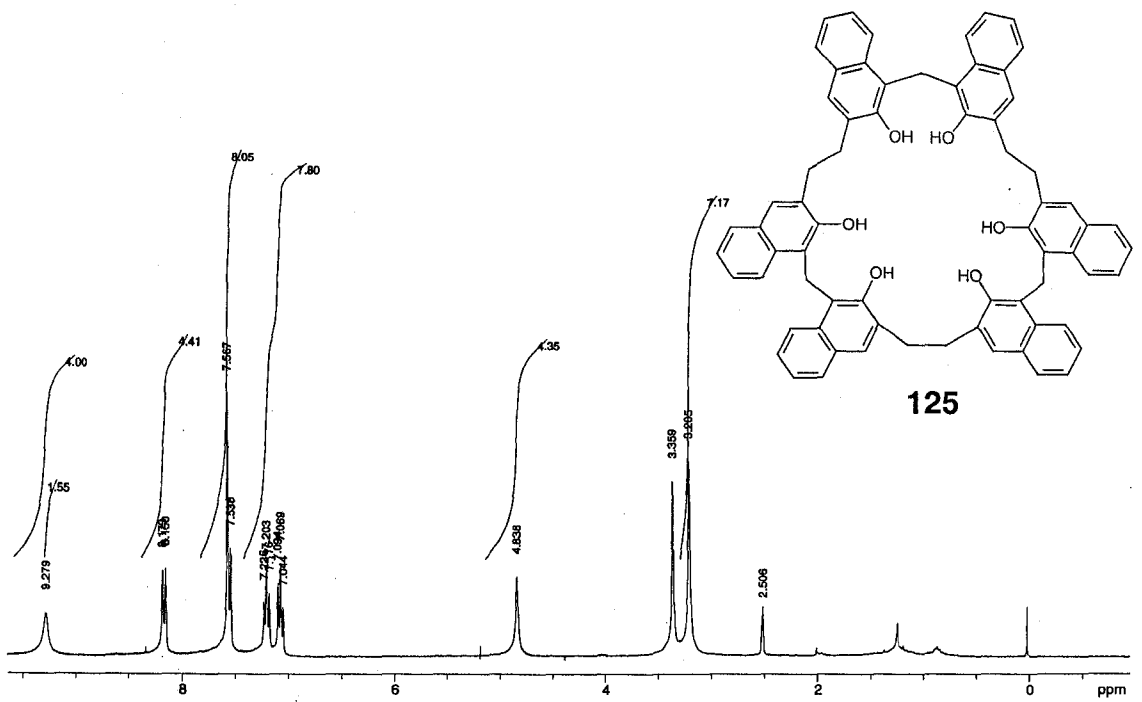
OH
HO
OH
HO
OH
HO
125
4.00
4.41
7.567
8.05
7.80
4.35
7.17
3.359
9.205
1.55
9.279
7.336
4.838
2.506
8
6
4
2
0
ppm

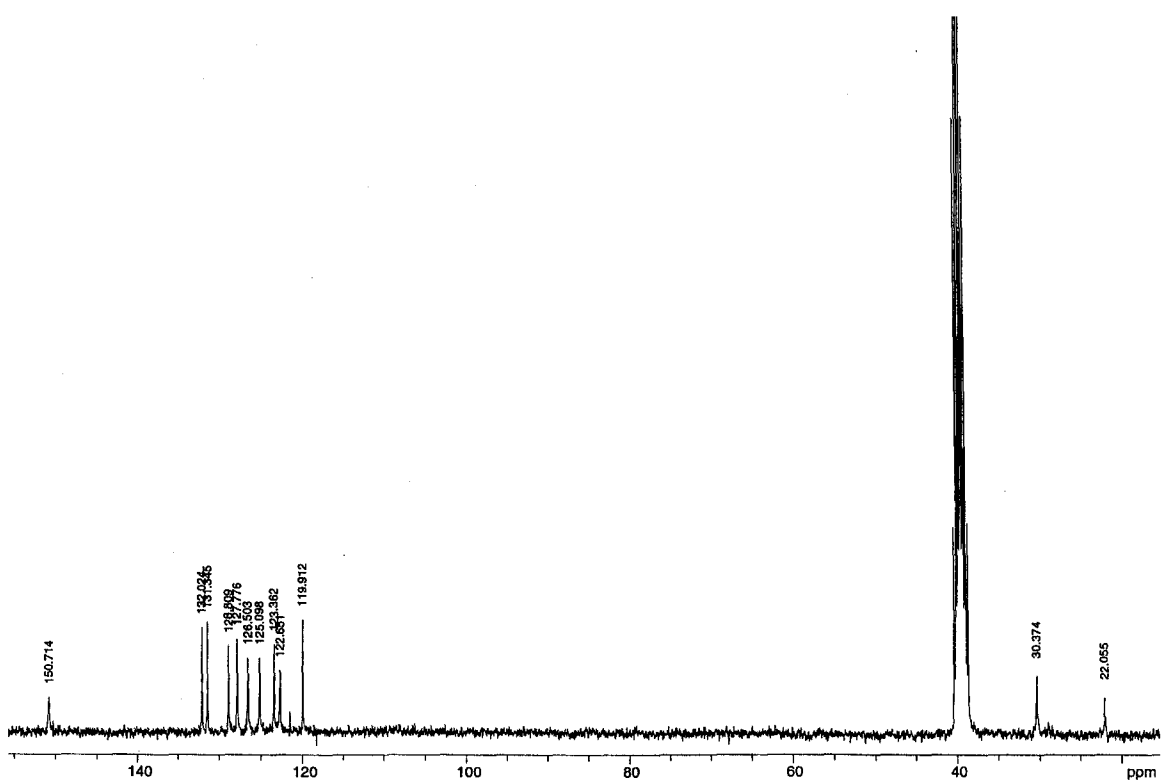
150.714
131.345
128.776
126.503
125.098
123.362
122.651
119.912
30.374
22.055
140
120
100
80
60
40
ppm

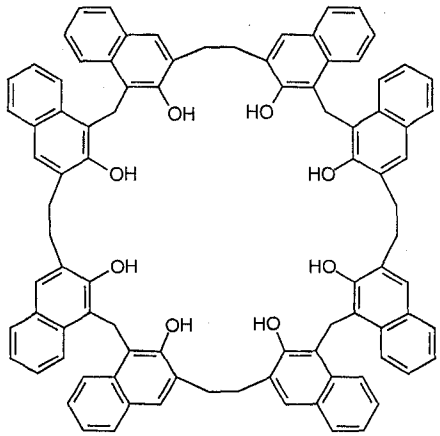
OH
HO
OH
HO
OH
HO
OH
HO

126

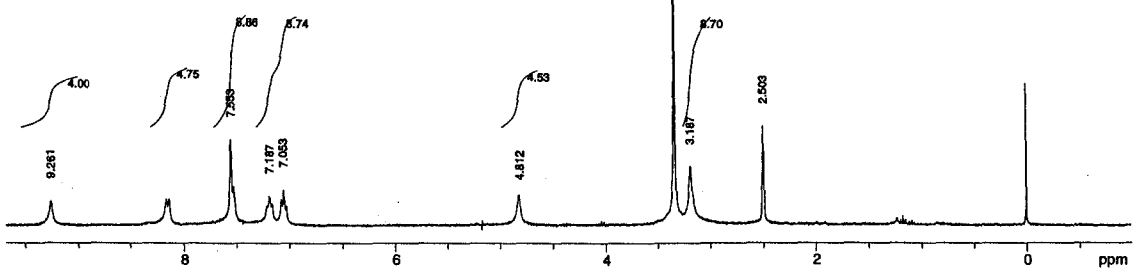
4.00
4.75
8.86
8.74
4.53
8.70
9.261
7.393
7.187
7.053
4.812
3.187
2.503
8
6
4
2
0
ppm

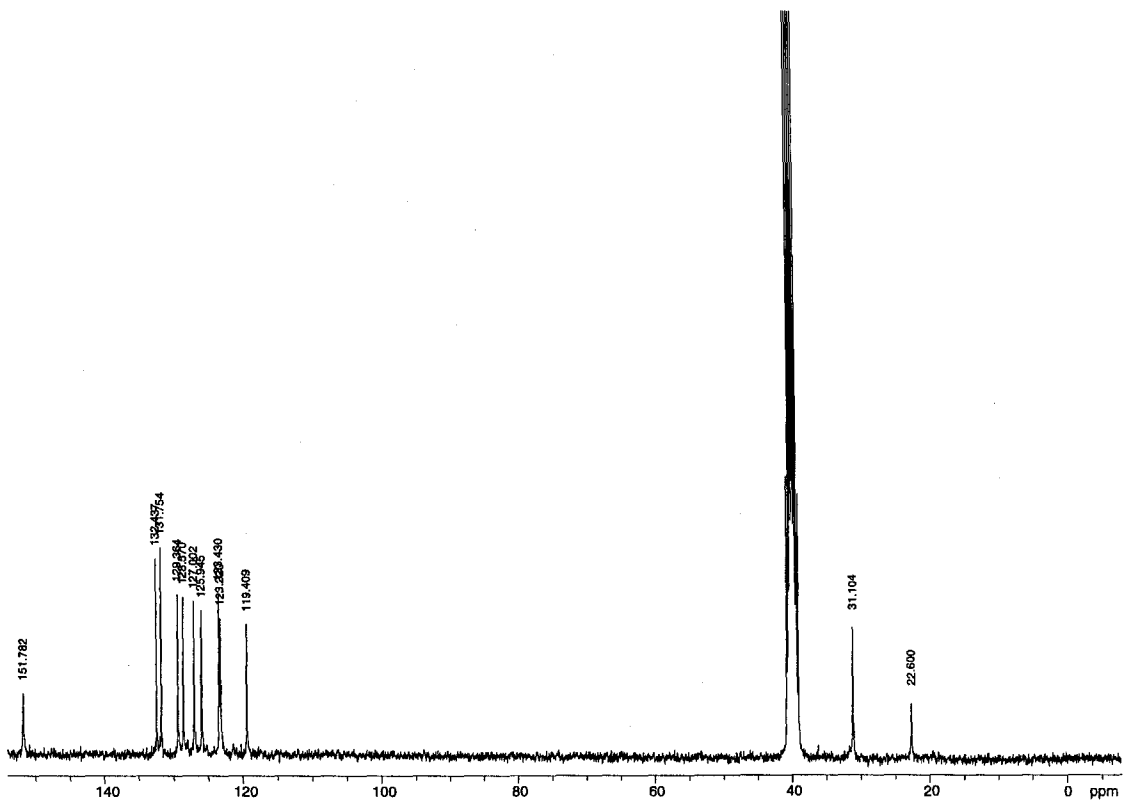
151.782
130.437
131.754
119.409
31.104
22.600
140
120
100
80
60
40
20
0
ppm

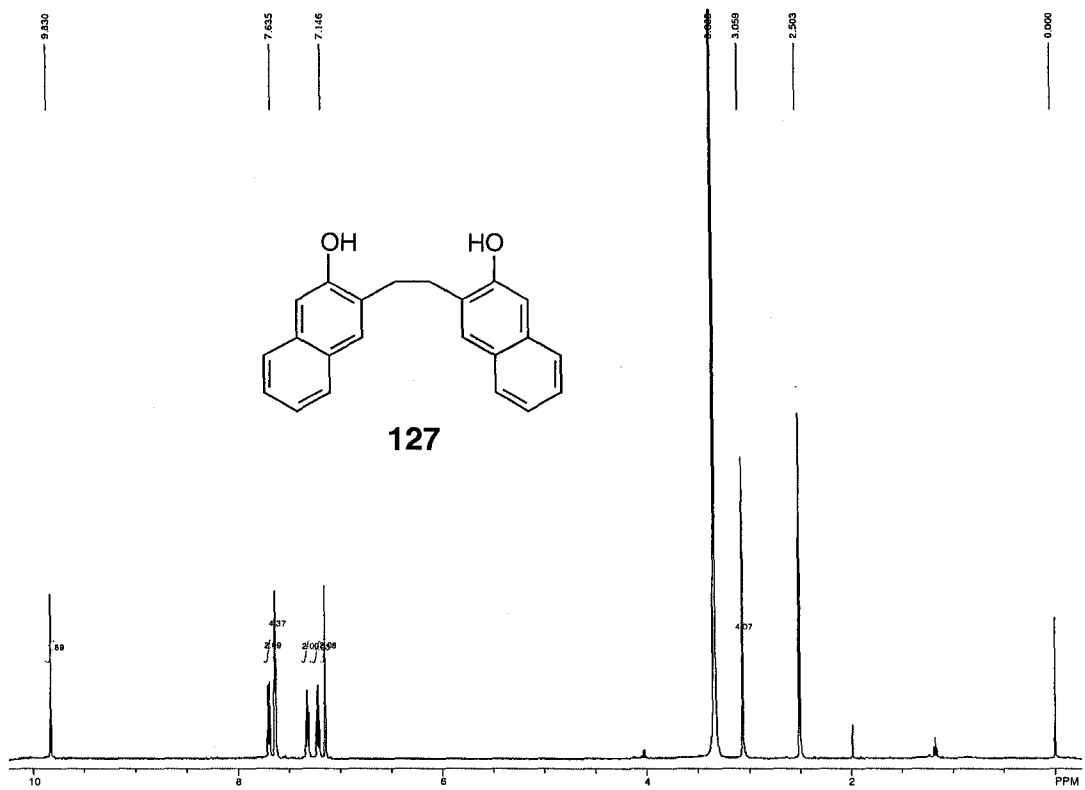
9.830
7.635
7.146
3.059
2.503
0.000
OH
HO
4.07
10
8
6
4
2
PPM

127

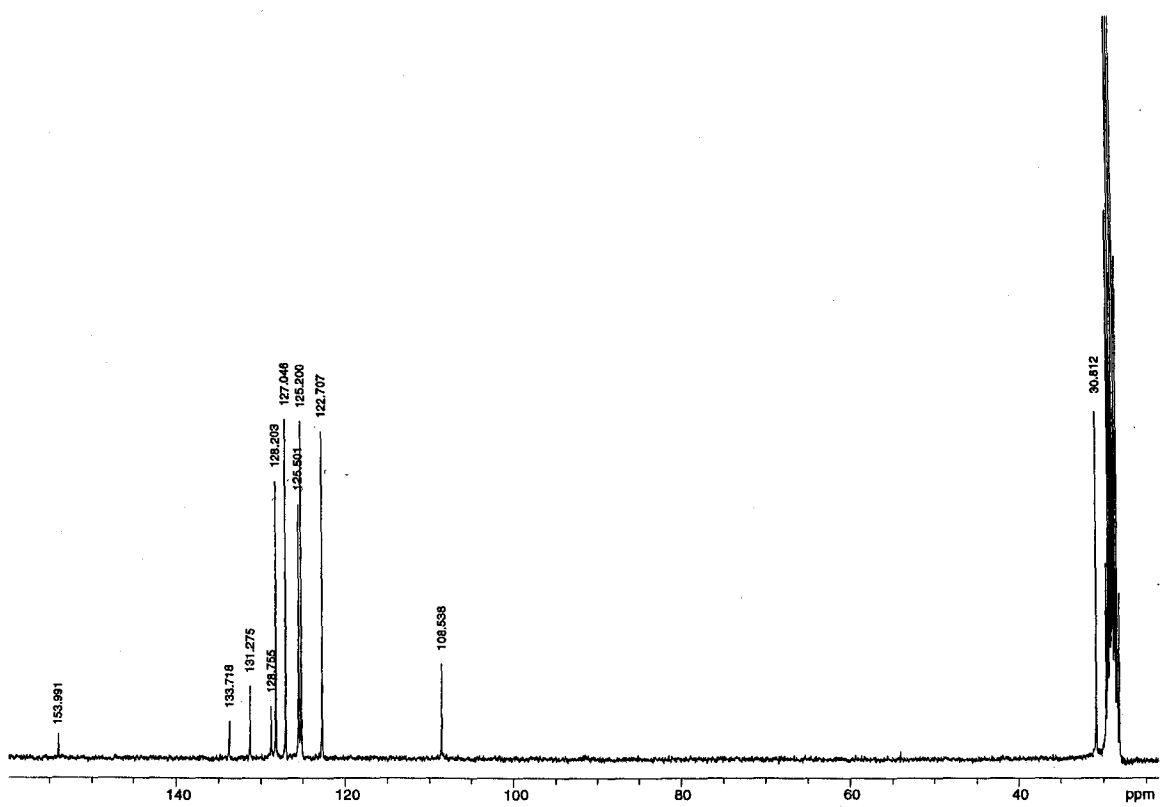
153.991
133.718
131.275
128.755
128.203
127.048
125.501
125.200
122.707
108.538
90.812
140
120
100
80
60
40
ppm

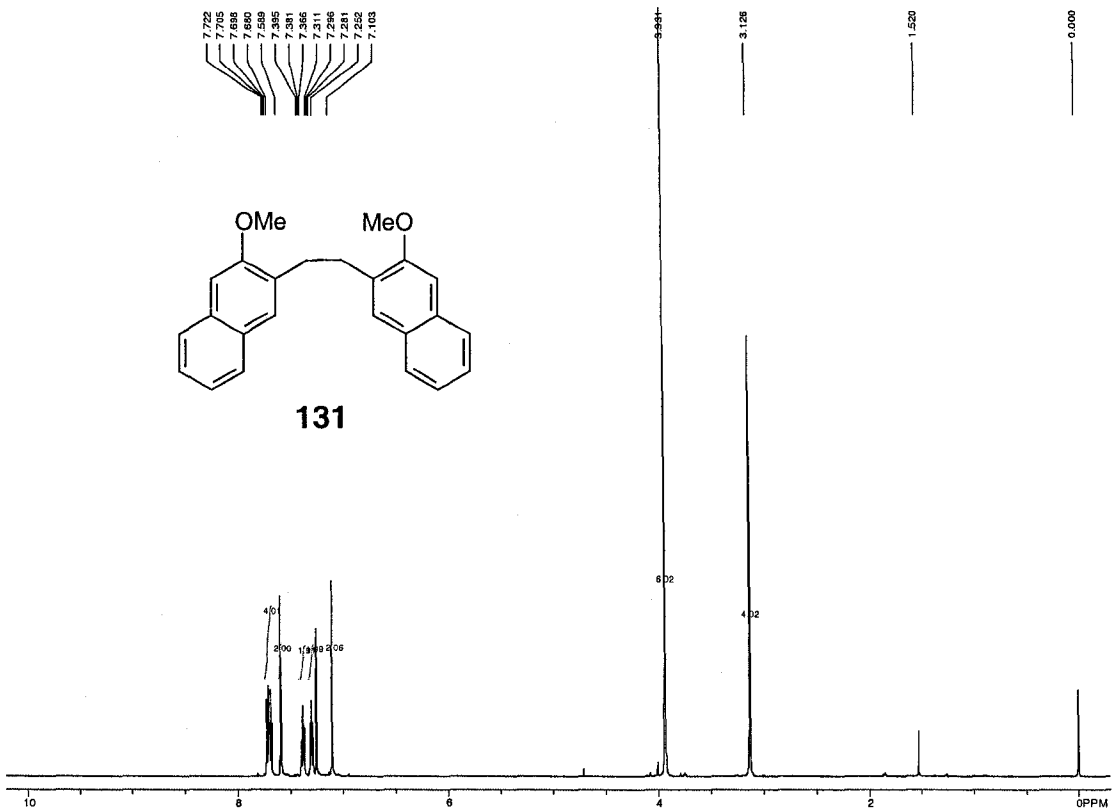
7.722
7.705
7.698
7.680
7.589
7.395
7.381
7.366
7.311
7.296
7.281
7.252
7.103
3.331
3.125
1.520
0.000
OMe
MeO
8.02
4.02
4.01
2.00
2.06
10
8
6
4
2
0PPM

131

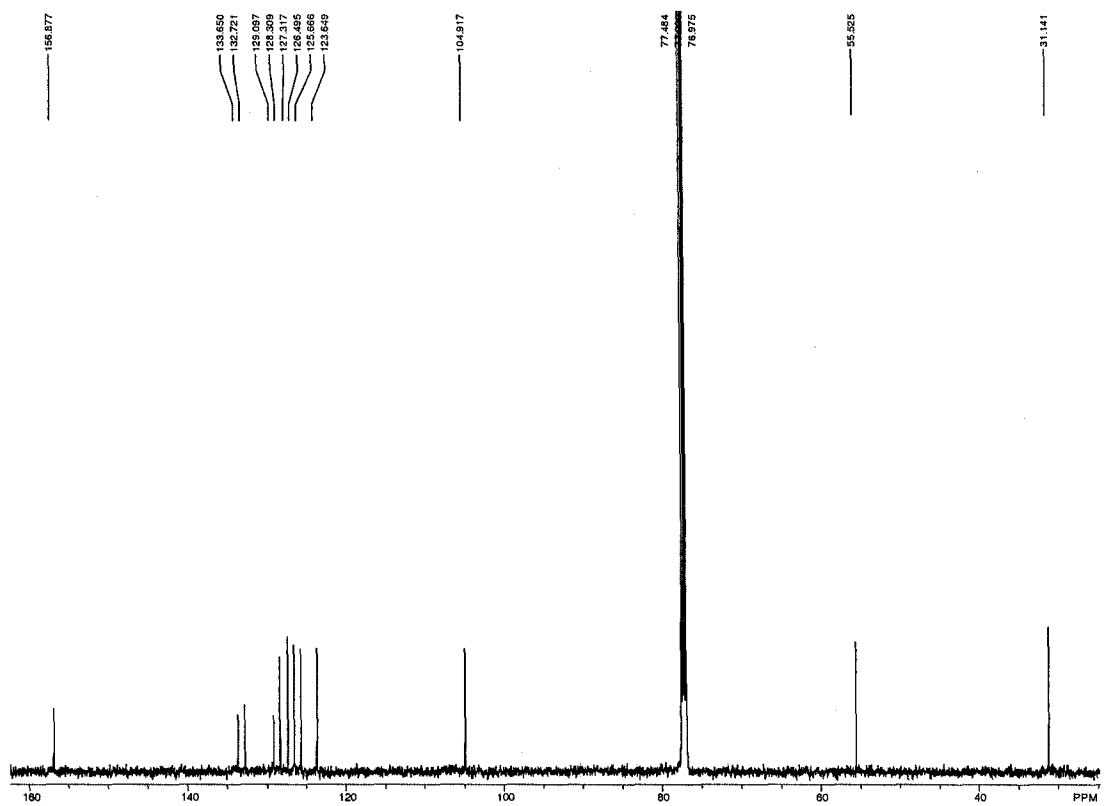
156.877
133.650
132.721
129.097
128.309
127.317
126.495
125.666
123.649
104.917
77.484
76.975
55.525
31.141
160
140
120
100
80
60
40
PPM

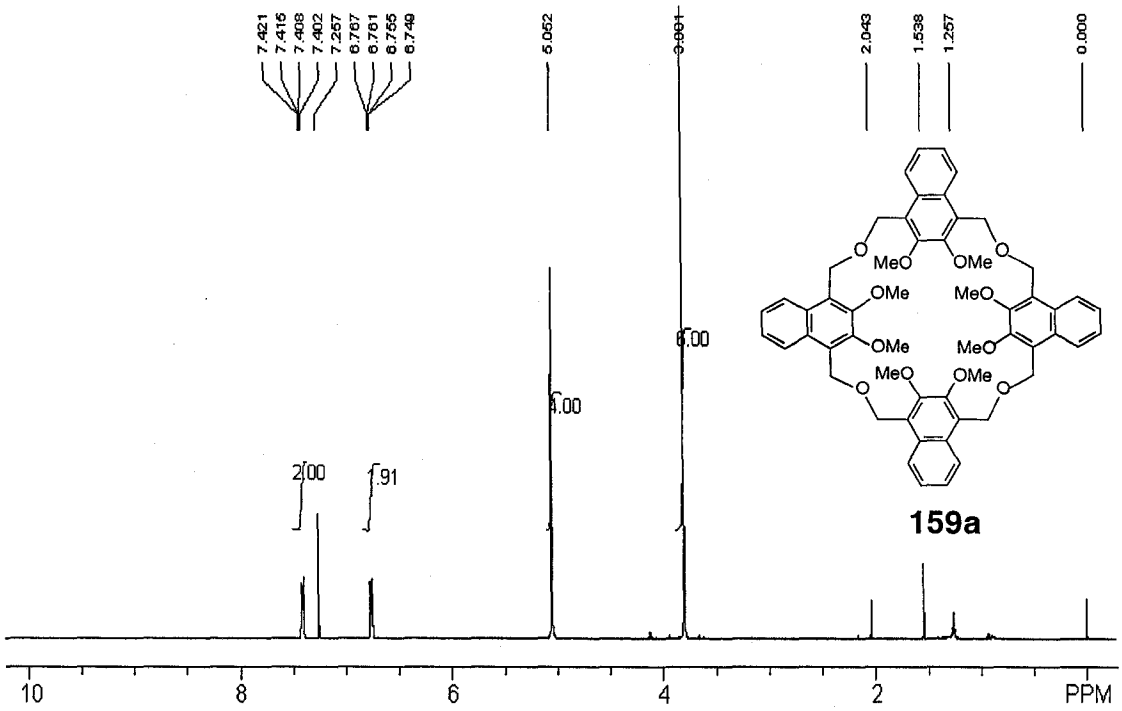
7.421
7.416
7.408
7.402
7.257
6.767
6.761
6.755
6.749
5.052
3.861
2.043
1.538
1.257
0.000
2.00
1.91
4.00
6.00
MeO
OMe
159a
10
8
6
4
2
PPM

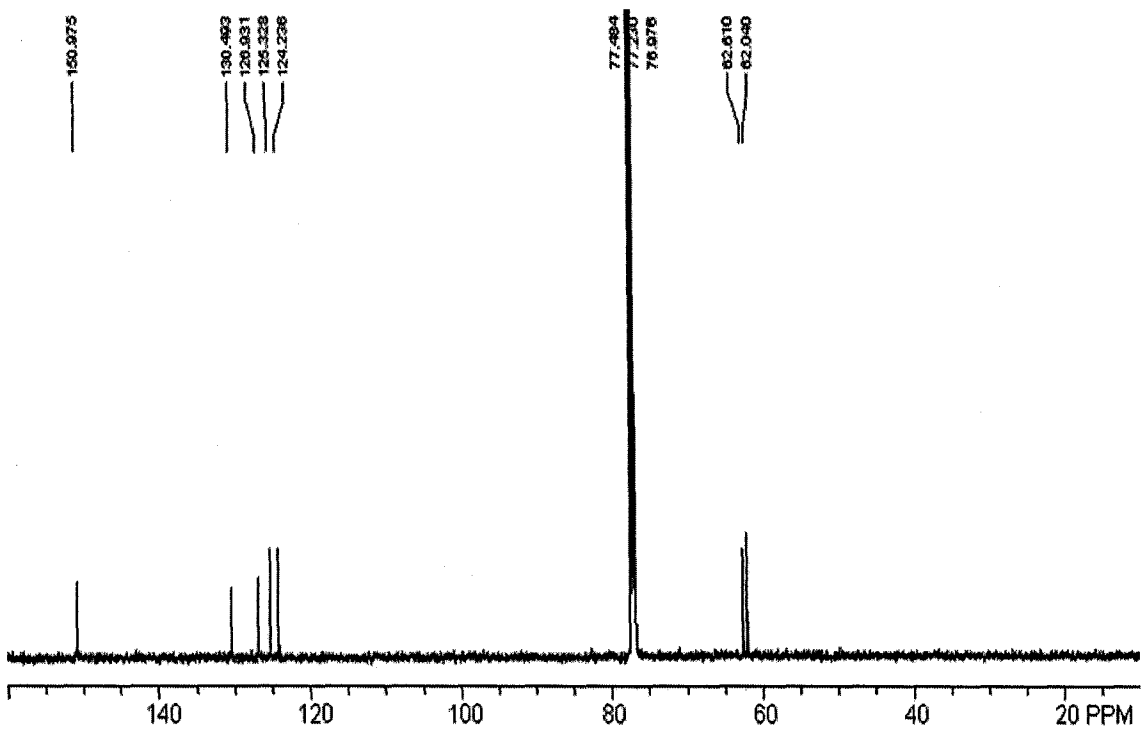
150.975
130.493
126.831
125.328
124.236
77.484
77.230
76.976
62.610
62.049
140
120
100
80
60
40
20 PPM

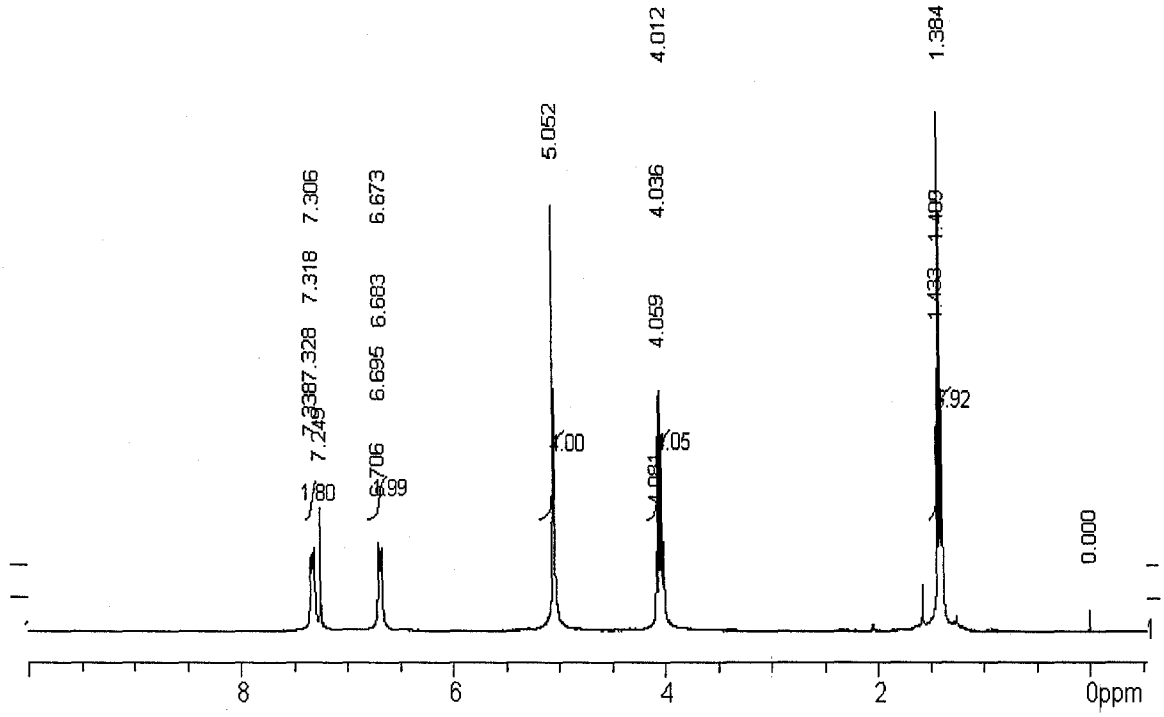
7.306
7.318
7.328
7.387
7.749
6.673
6.683
6.695
6.706
5.052
4.012
4.036
4.059
1.384
1.400
1.433
1.80
1.00
1.05
1.92
0.000
8
6
4
2
0ppm

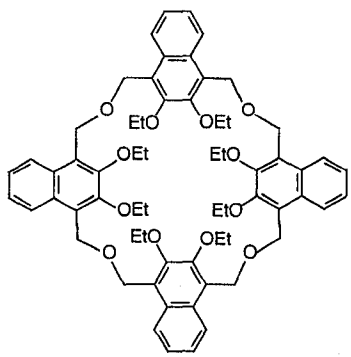
EtO
OEt
OEt
EtO
OEt
EtO
EtO
OEt

159b

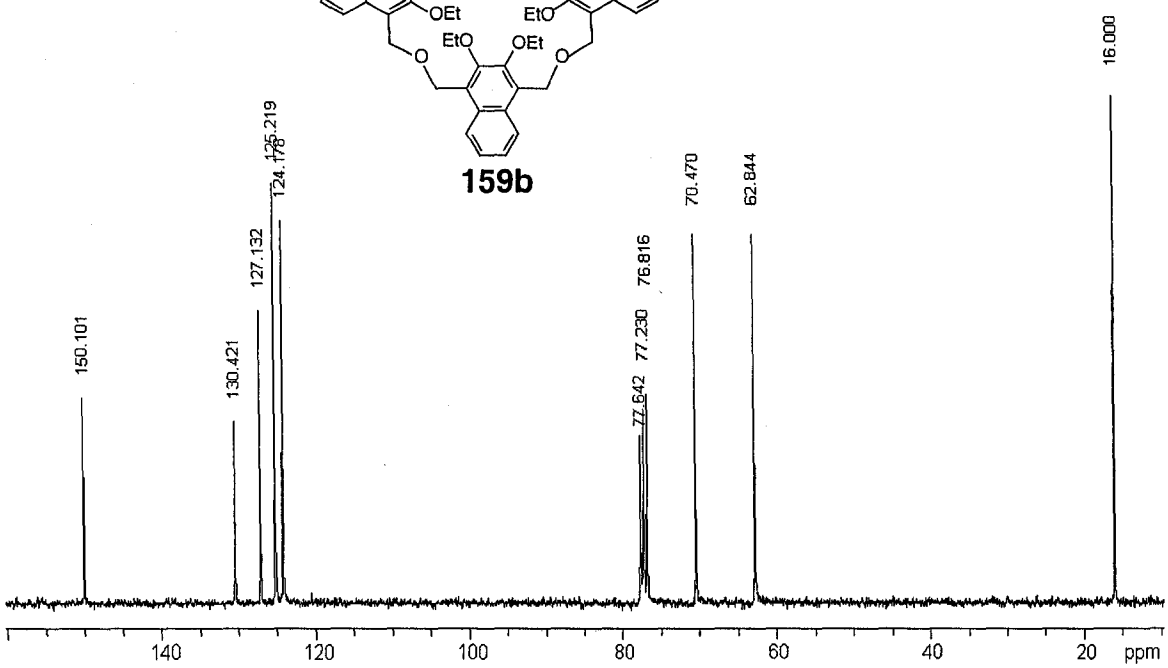
150.101
130.421
127.132
125.219
124.178
76.816
77.230
77.642
70.470
62.844
16.000
140
120
100
80
60
40
20
ppm

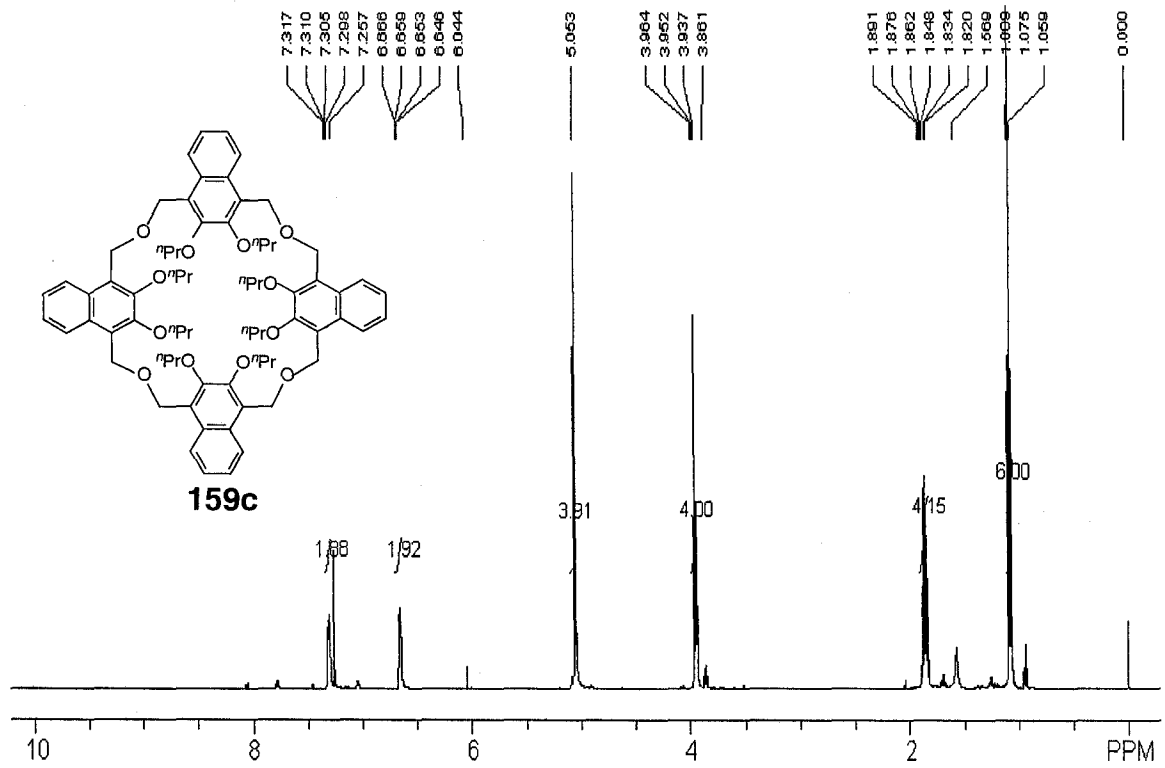
7.317
7.310
7.305
7.298
7.257
6.866
6.859
6.853
6.846
6.044
5.053
3.964
3.952
3.937
3.861
1.881
1.876
1.862
1.848
1.834
1.820
1.569
1.069
1.075
1.059
0.000
nPrO
OnPr
3.91
4.00
4.15
6.00
1.88
1.92
10
8
6
4
2
PPM

159c

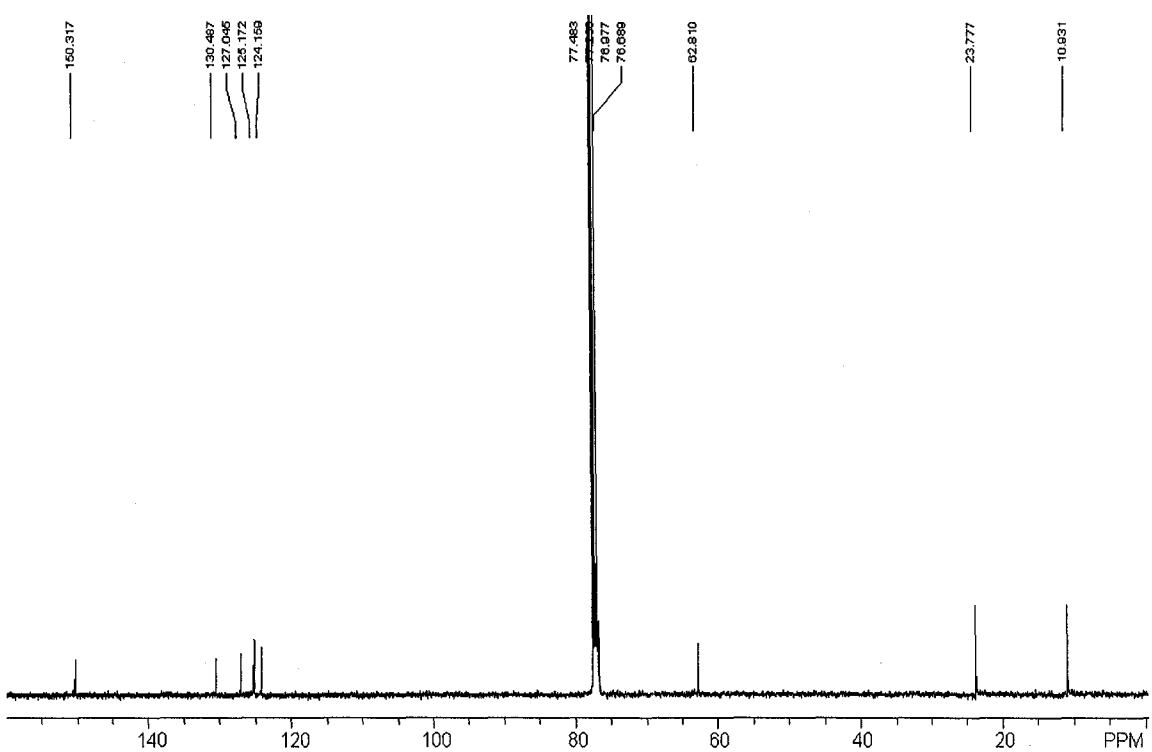
150.317
130.467
127.046
125.172
124.159
77.483
76.877
76.689
62.810
23.777
10.931
140
120
100
80
60
40
20
PPM

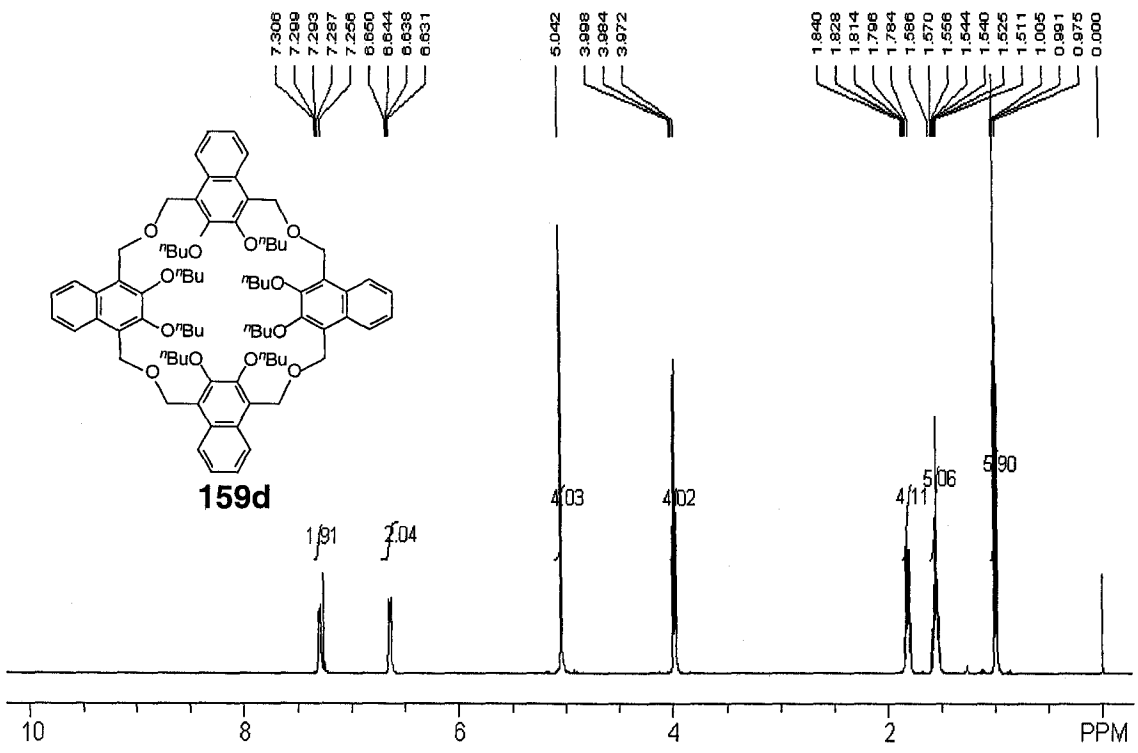
7.306
7.299
7.293
7.287
7.256
6.650
6.644
6.638
6.631
5.042
3.998
3.984
3.972
1.840
1.828
1.814
1.796
1.784
1.586
1.570
1.556
1.544
1.540
1.525
1.511
1.005
0.991
0.975
0.000
nBuO
nBu
159d
1.91
2.04
4.03
4.02
4.11
5.06
5.90
10
8
6
4
2
PPM

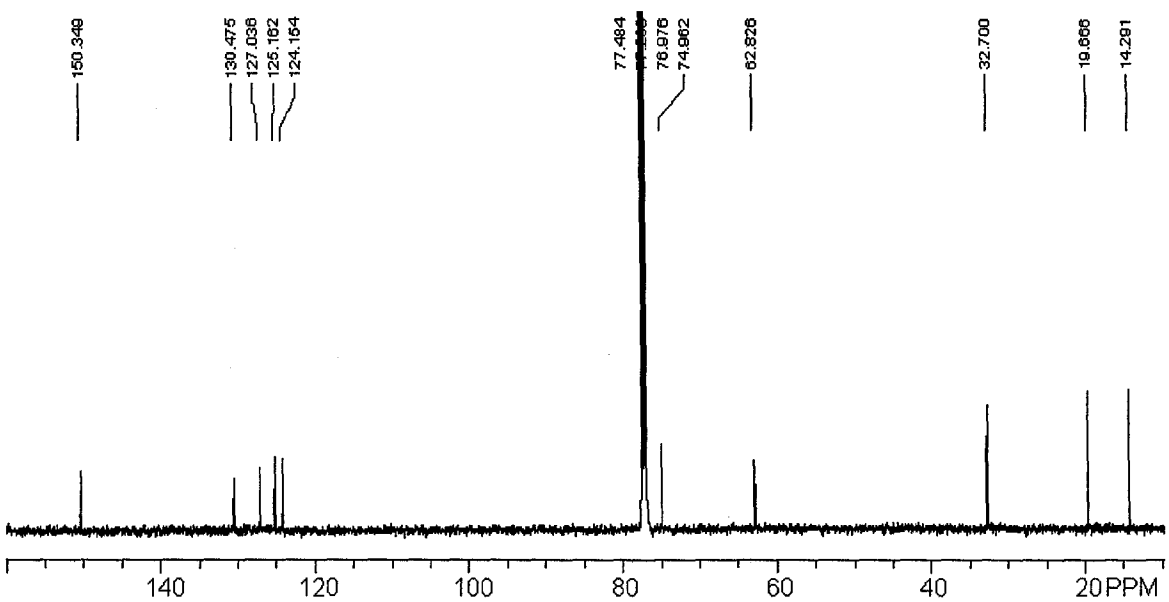
150.349
130.475
127.036
125.162
124.164
77.484
76.976
74.962
62.826
32.700
19.666
14.291
140
120
100
80
60
40
20PPM

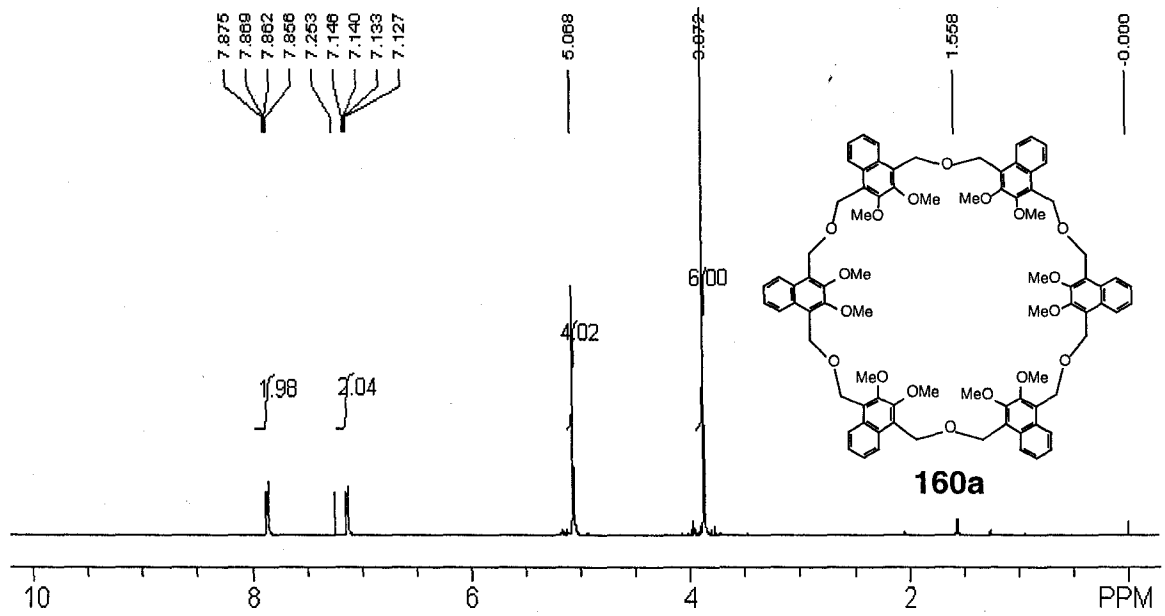
7.875
7.869
7.862
7.856
7.253
7.146
7.140
7.133
7.127
5.068
3.872
1.558
-0.000
1.98
2.04
4.02
6.00
OMe
MeO
10
8
6
4
2
PPM

160a

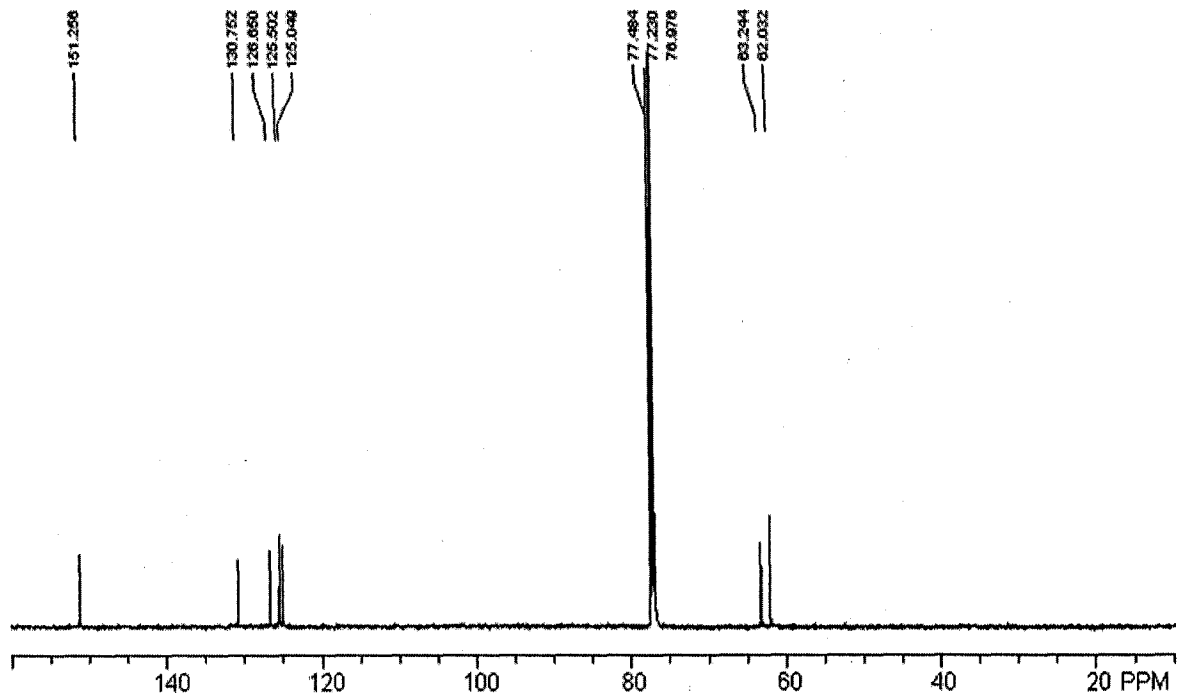
151.256
130.752
126.650
125.502
125.049
77.484
77.230
76.976
63.244
62.032
140
120
100
80
60
40
20 PPM

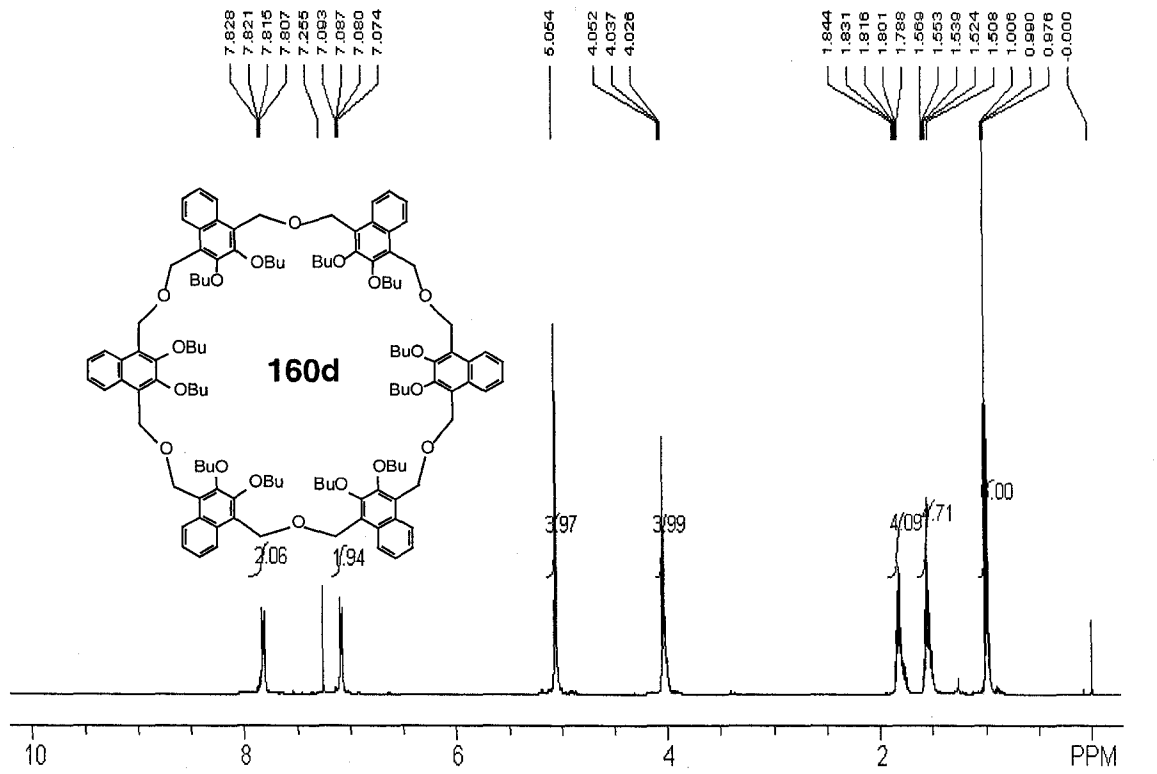
7.828
7.821
7.815
7.807
7.255
7.093
7.087
7.080
7.074
5.054
4.052
4.037
4.026
1.844
1.831
1.816
1.801
1.788
1.569
1.553
1.539
1.524
1.508
1.006
0.990
0.976
-0.000
160d
BuO
OBu
3.97
3.99
4.09
4.71
6.00
2.06
1.94
10
8
6
4
2
PPM

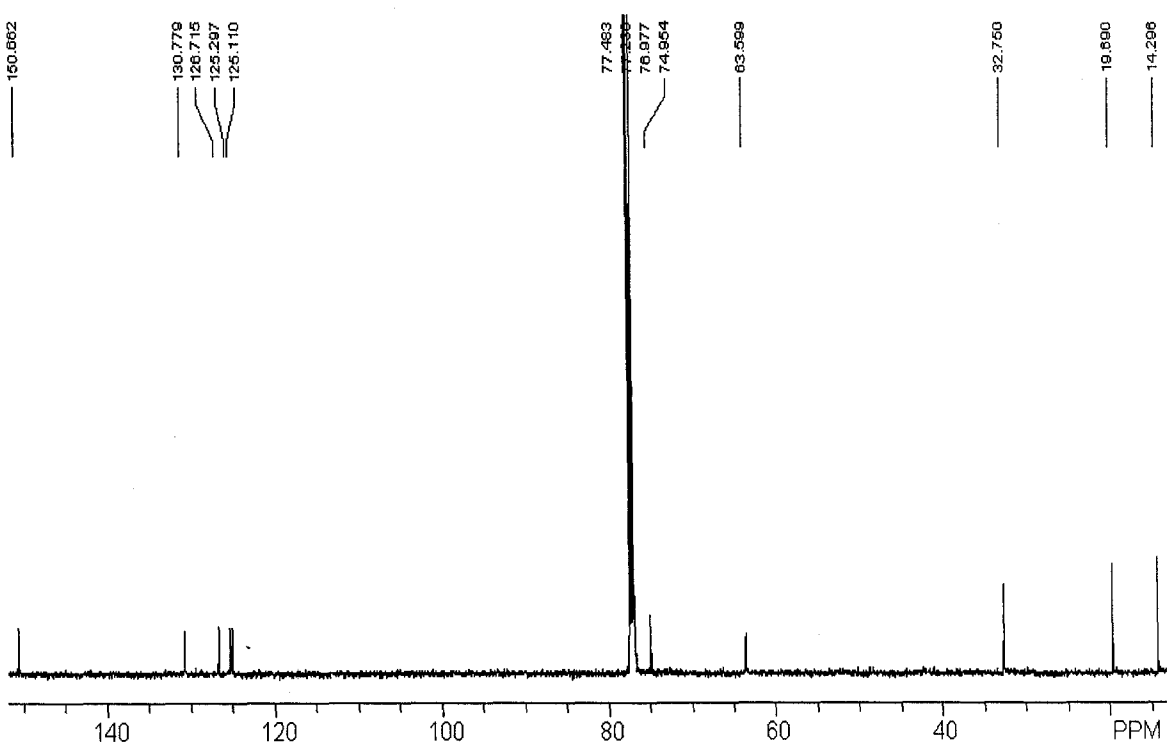
150.662
130.779
126.715
125.297
125.110
77.483
76.977
74.954
63.599
32.750
19.690
14.296
140
120
100
80
60
40
PPM

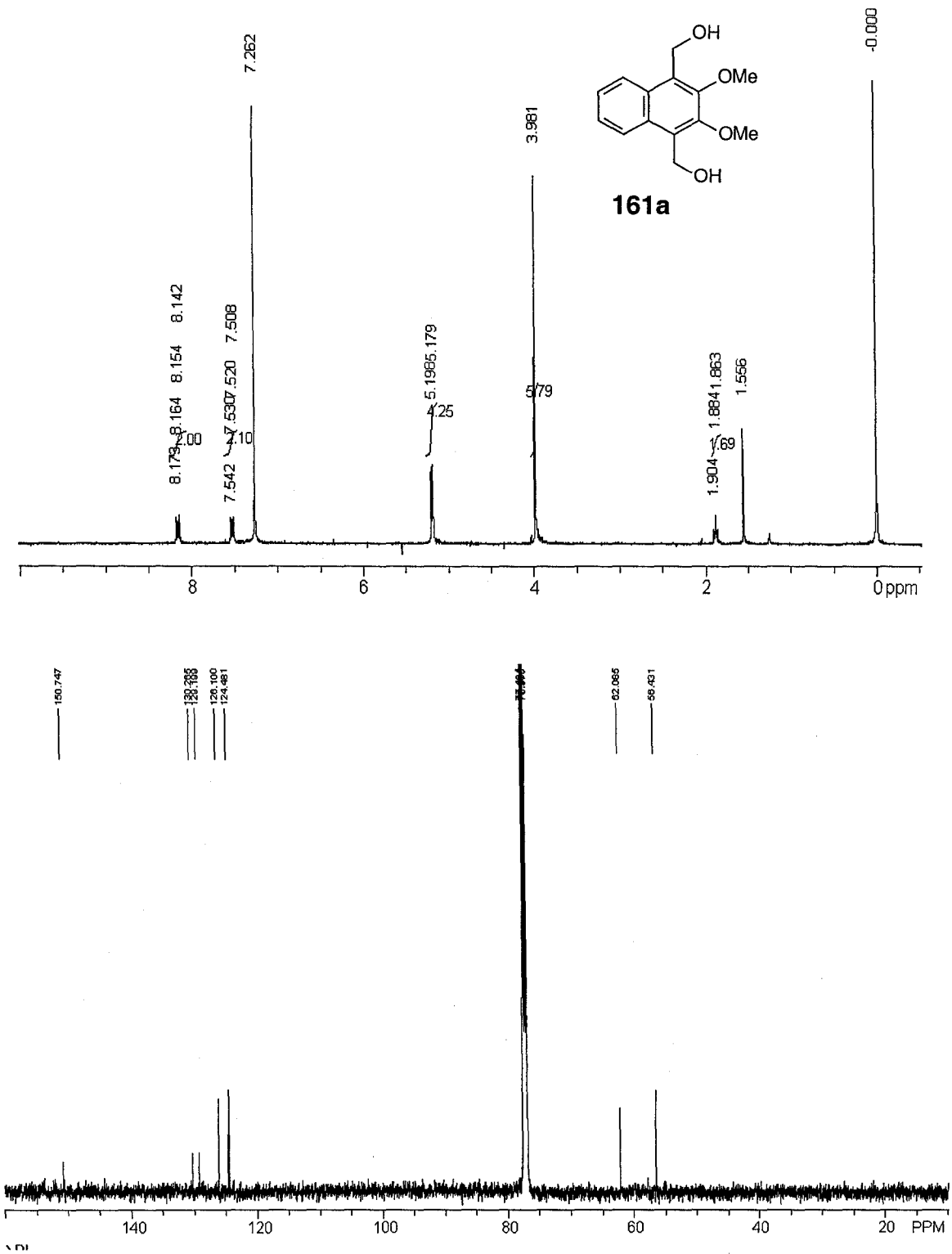
OH
OMe
OMe
OH
161a
8.164
8.154
8.142
8.179
7.542
7.530
7.520
7.508
7.262
5.179
5.1985.179
4.25
3.981
1.904
1.8841.863
1.69
1.556
-0.000
2.00
2.10
8
6
4
2
0 ppm
150.747
130.285
129.188
128.100
124.481
62.065
58.491
140
120
100
80
60
40
20
PPM

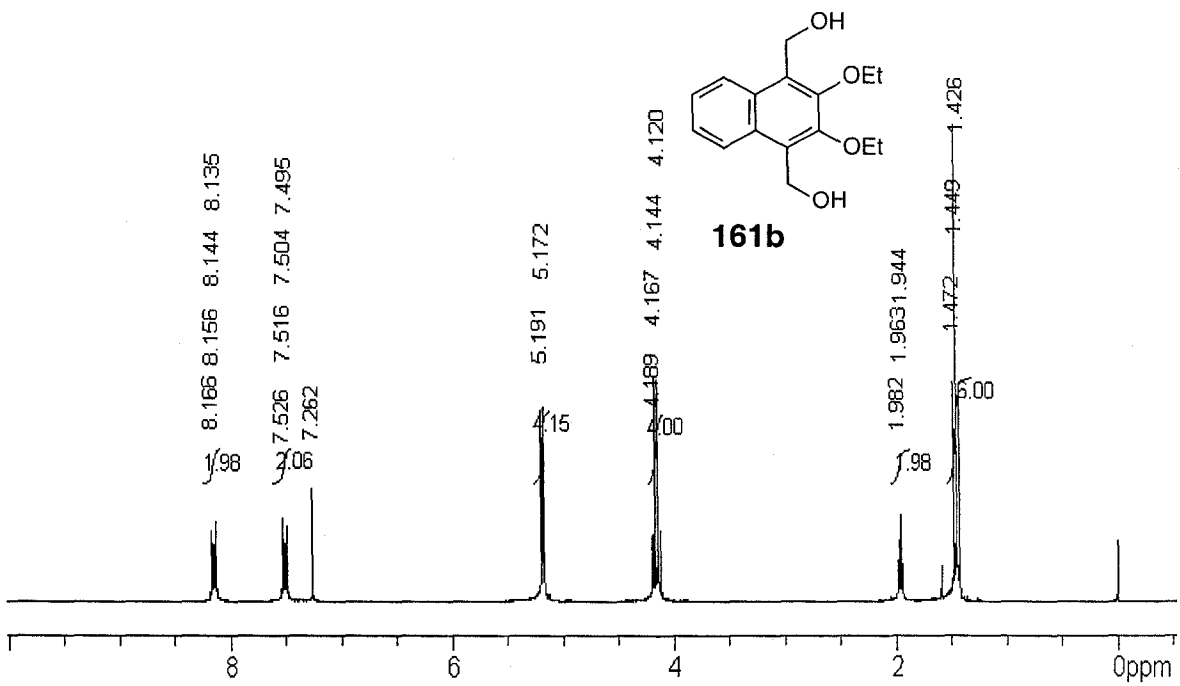
OH
OEt
OEt
OH
161b
8.166 8.156 8.144 8.135
7.526 7.516 7.504 7.495
7.262
5.191 5.172
4.167 4.144 4.120
1.982 1.963 1.944
1.472 1.449 1.426
1.98
2.06
4.15
4.00
1.98
6.00
8
6
4
2
0ppm

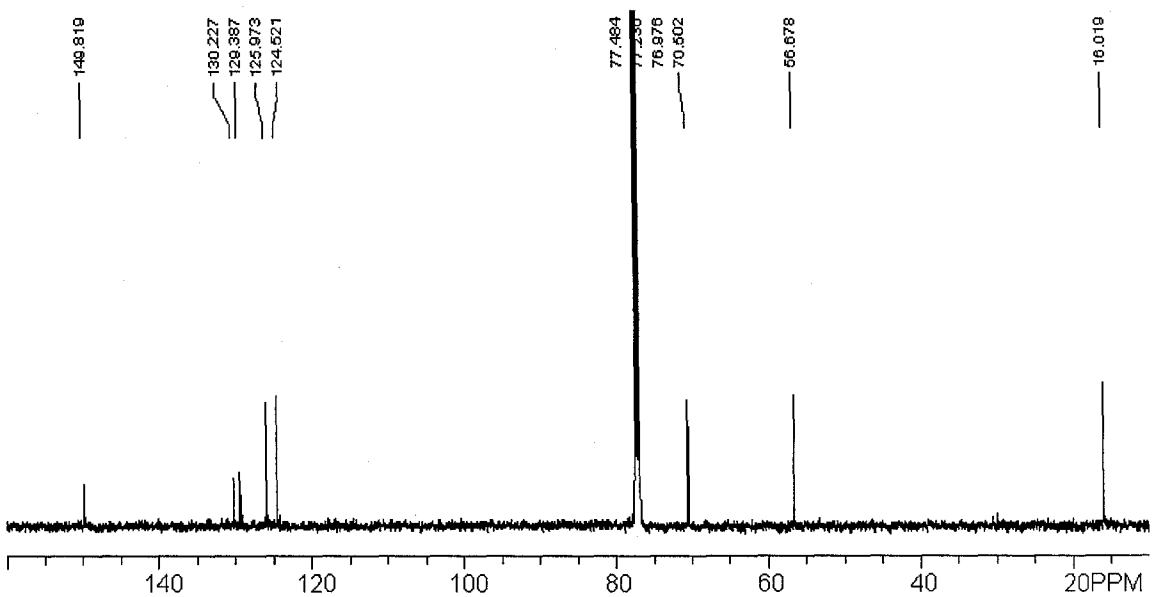
149.819
130.227
129.387
125.973
124.521
77.484
77.230
76.976
70.502
55.678
16.019
140
120
100
80
60
40
20PPM

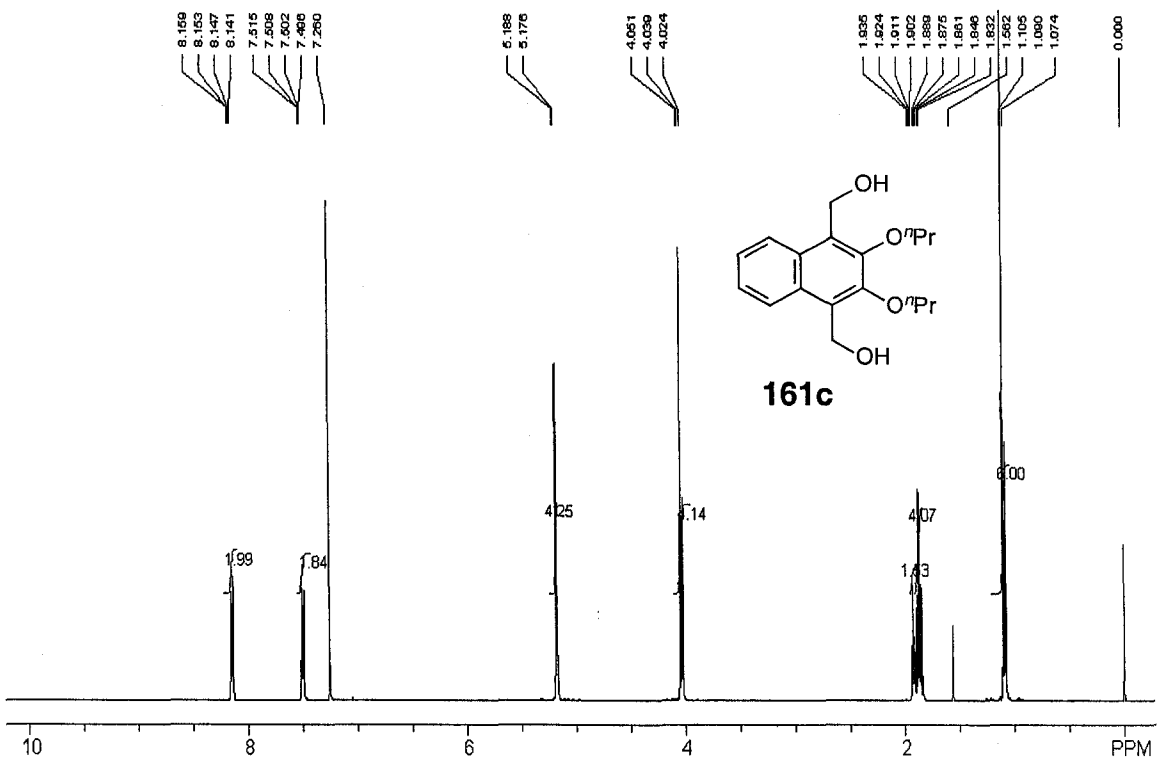
8.159
8.153
8.147
8.141
7.515
7.508
7.502
7.486
7.260
5.188
5.176
4.051
4.039
4.024
1.935
1.924
1.911
1.902
1.889
1.875
1.861
1.846
1.832
1.562
1.105
1.090
1.074
0.000
OH
O^{n}Pr
O^{n}Pr
OH
161c
1.99
1.84
4.25
4.14
4.07
1.83
6.00
10
8
6
4
2
PPM

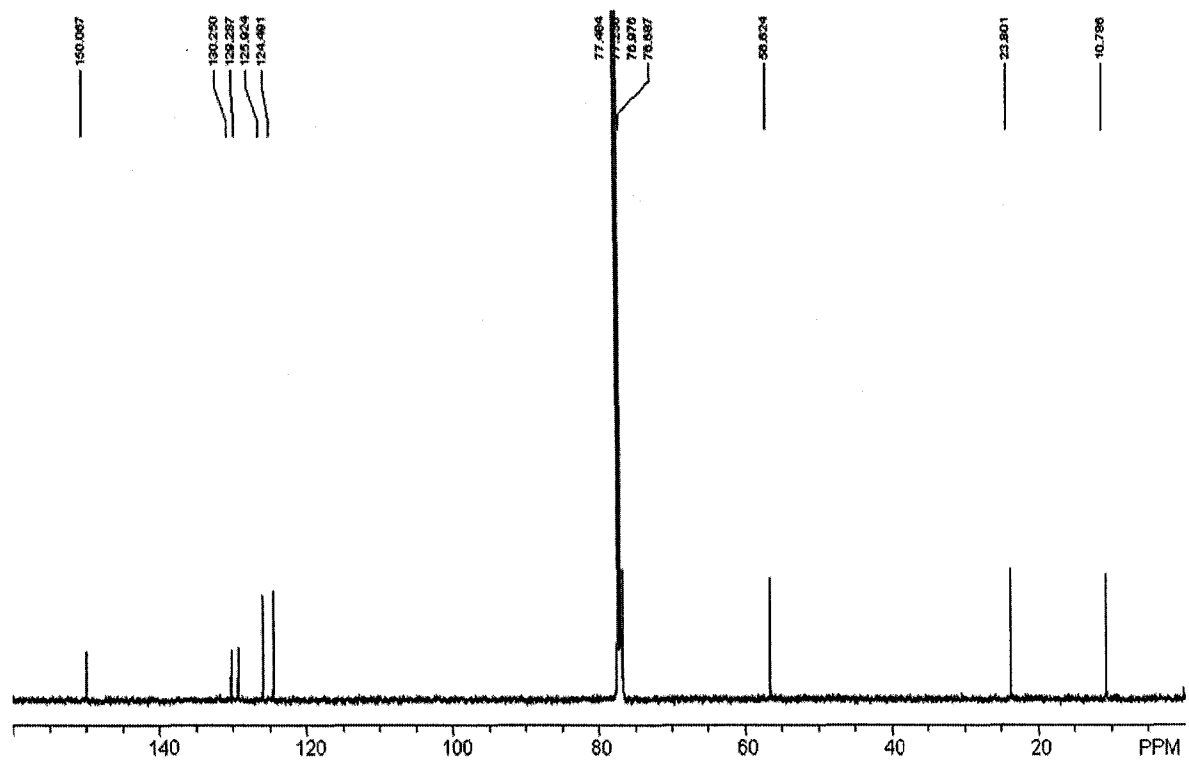
150.067
130.250
129.287
125.924
124.491
77.484
77.239
76.876
76.587
58.824
23.901
10.786
140
120
100
80
60
40
20
PPM

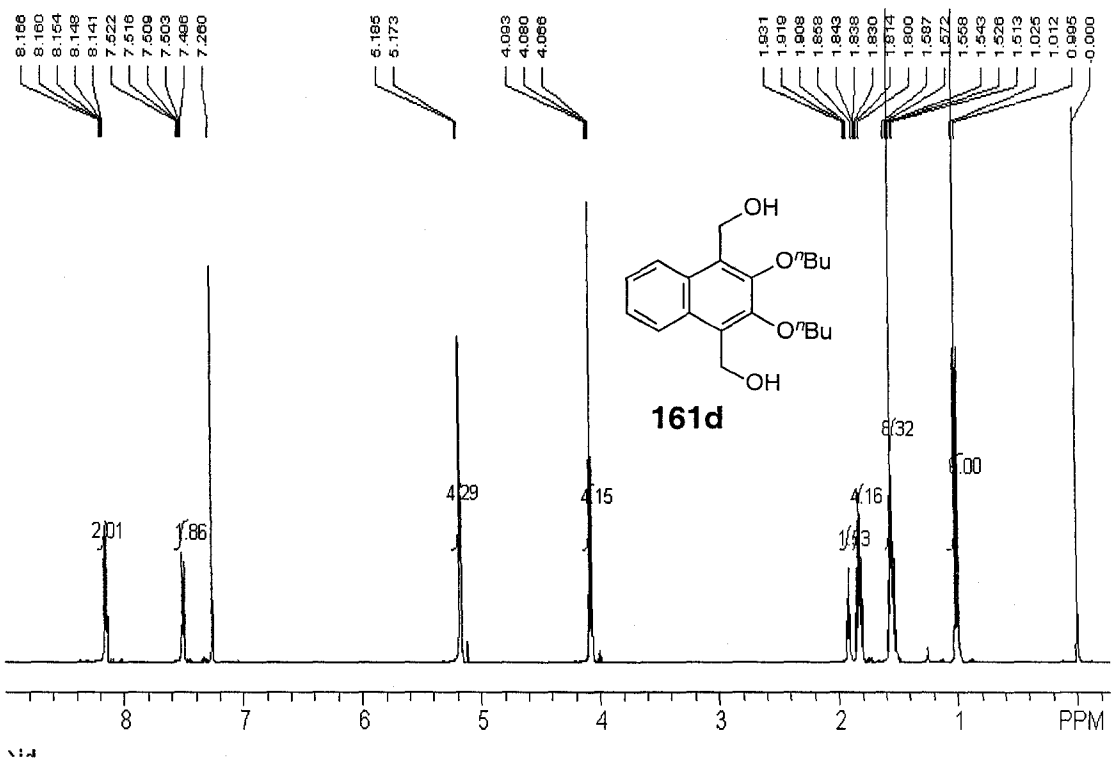
8.166
8.160
8.154
8.148
8.141
7.522
7.516
7.509
7.503
7.496
7.260
5.185
5.173
4.093
4.080
4.066
1.931
1.919
1.908
1.858
1.843
1.838
1.830
1.814
1.800
1.587
1.572
1.558
1.543
1.526
1.513
1.025
1.012
0.995
0.000
OH
O^{n}Bu
O^{n}Bu
OH
161d
2.01
1.86
4.29
4.15
4.16
1.53
8.32
9.00
8
7
6
5
4
3
2
1
PPM

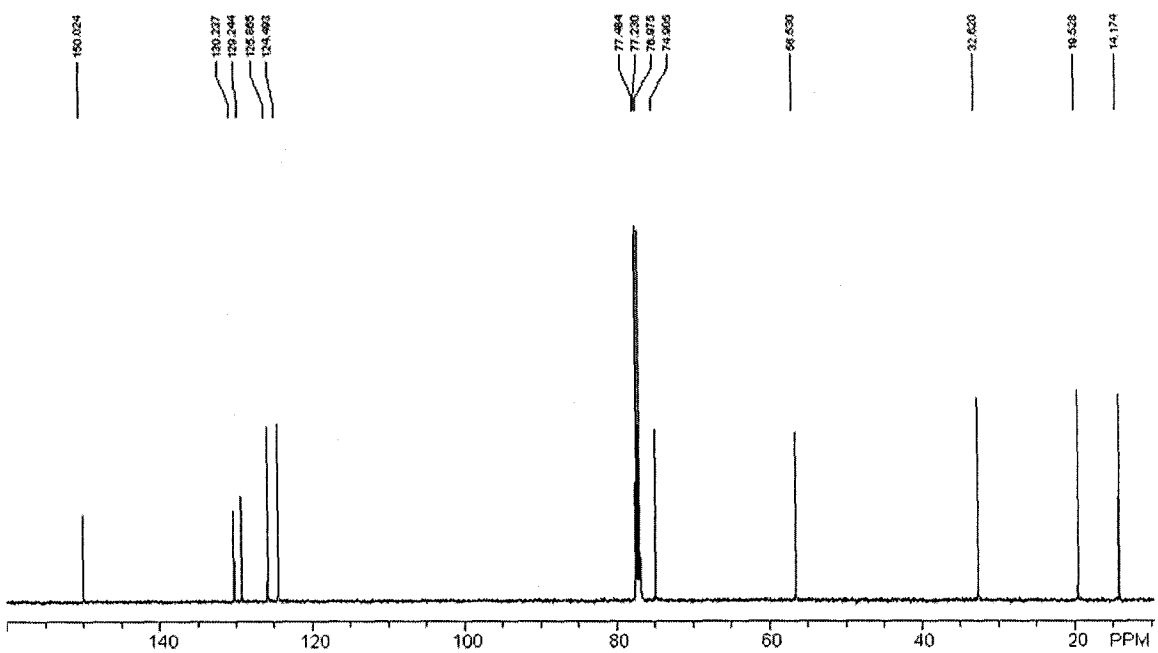
150.024
130.237
129.244
125.885
124.493
77.484
77.230
76.975
74.905
68.530
32.620
19.528
14.174
140
120
100
80
60
40
20
PPM

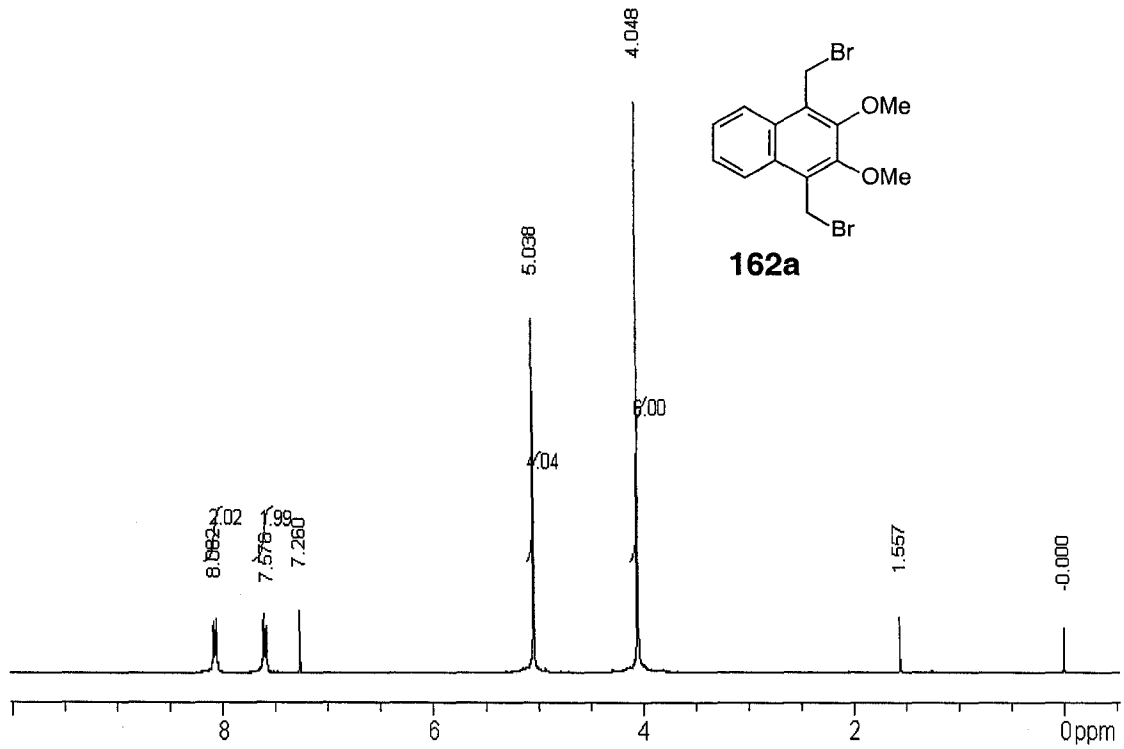
4.048
Br
OMe
OMe
Br
5.038
162a
6.00
4.04
2.02
1.99
7.576
7.260
1.557
-0.000
8
6
4
2
0ppm

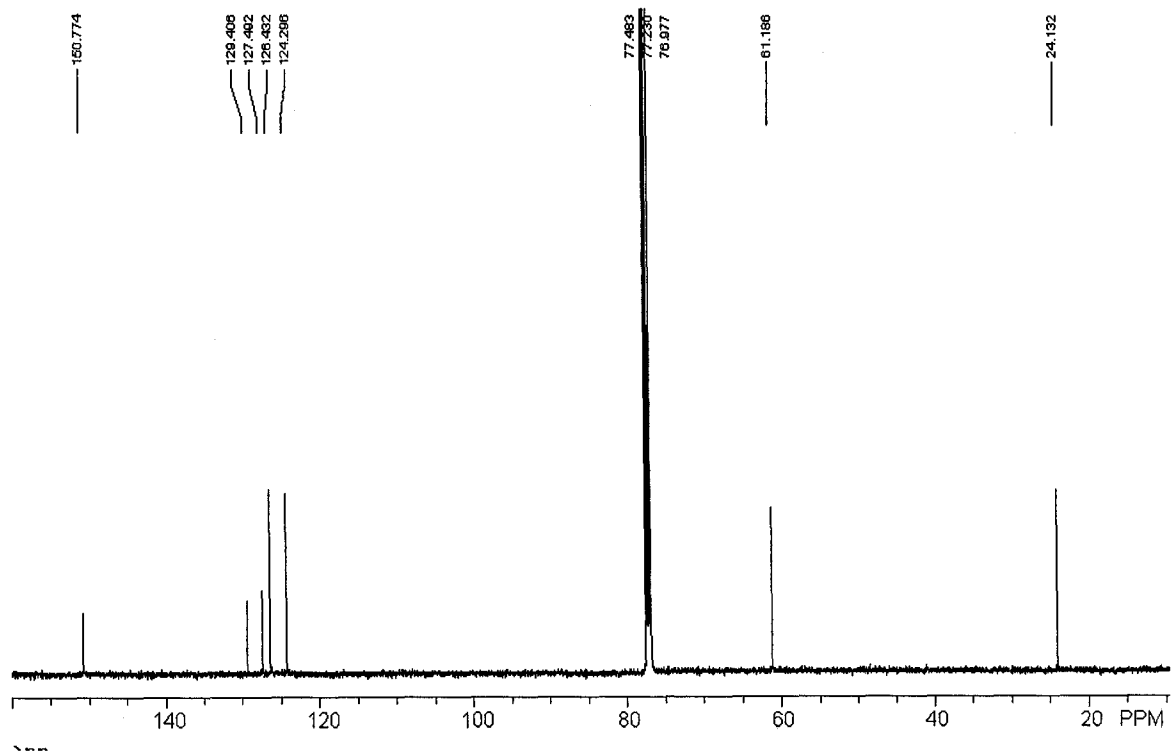
150.774
129.405
127.492
126.432
124.296
77.483
77.230
76.977
61.186
24.132
140
120
100
80
60
40
20
PPM

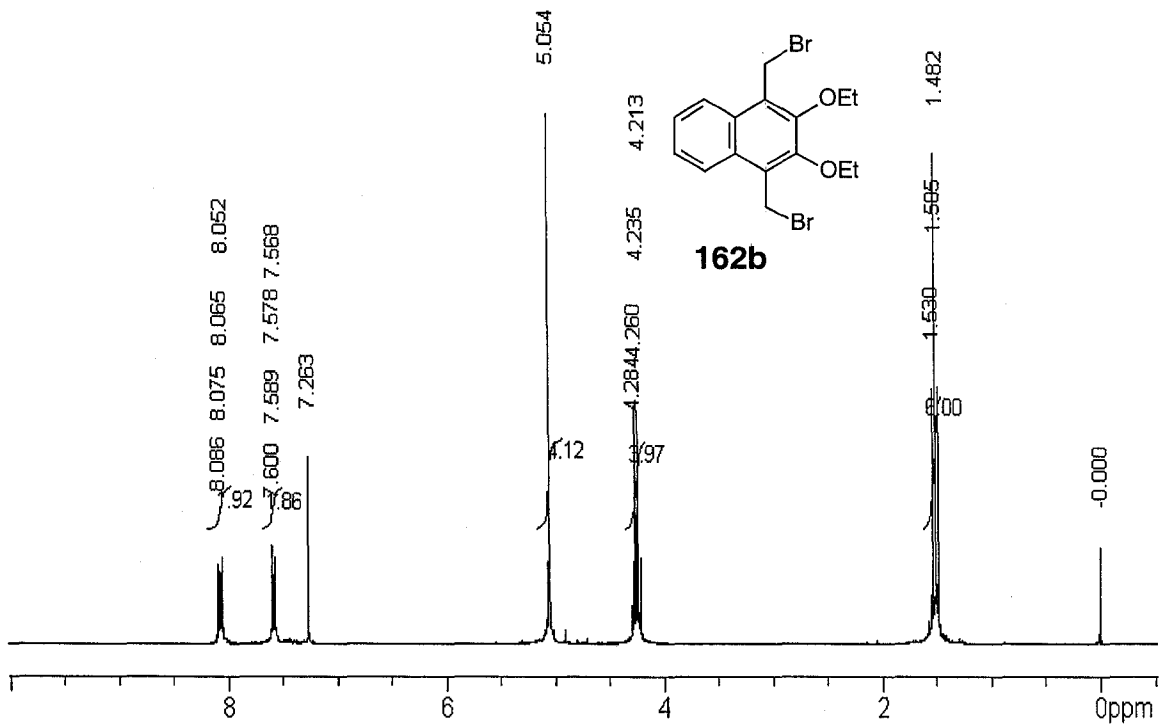
8.086
8.075
8.065
8.052
7.600
7.589
7.578
7.568
7.263
5.054
4.284
4.260
4.235
4.213
1.530
1.482
-0.000
Br
OEt
OEt
Br
162b
8
6
4
2
0ppm

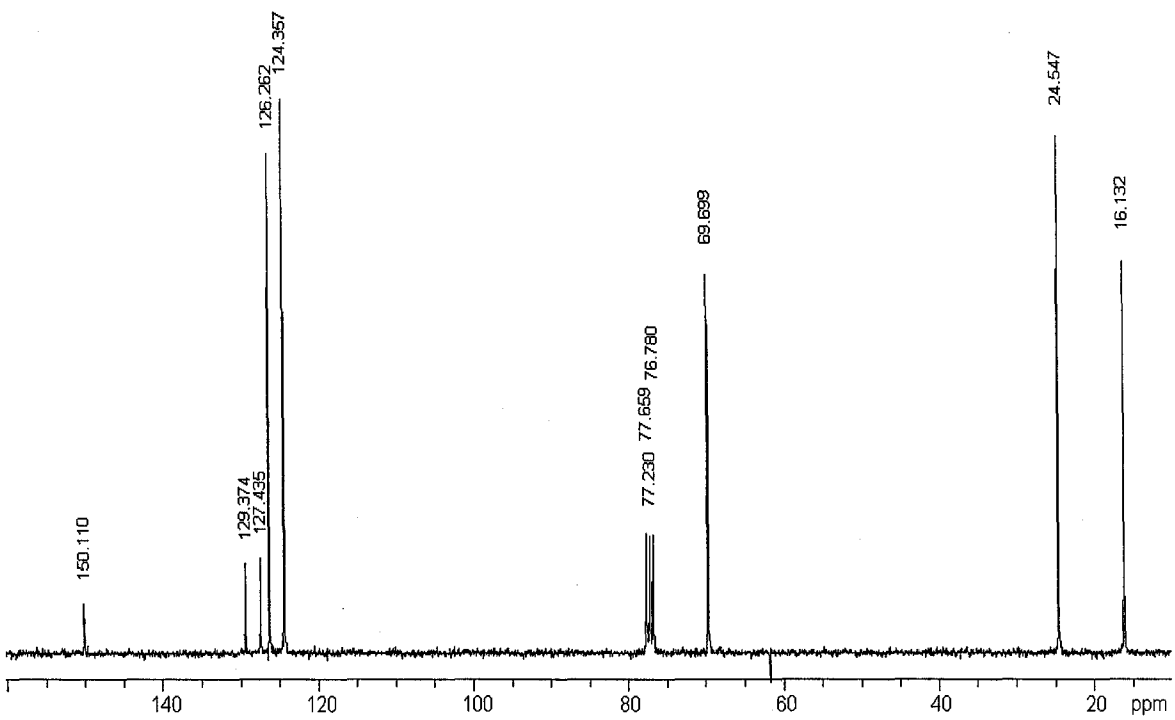
150.110
129.374
127.435
126.262
124.357
77.230
77.659
76.780
69.699
24.547
16.132
140
120
100
80
60
40
20
ppm

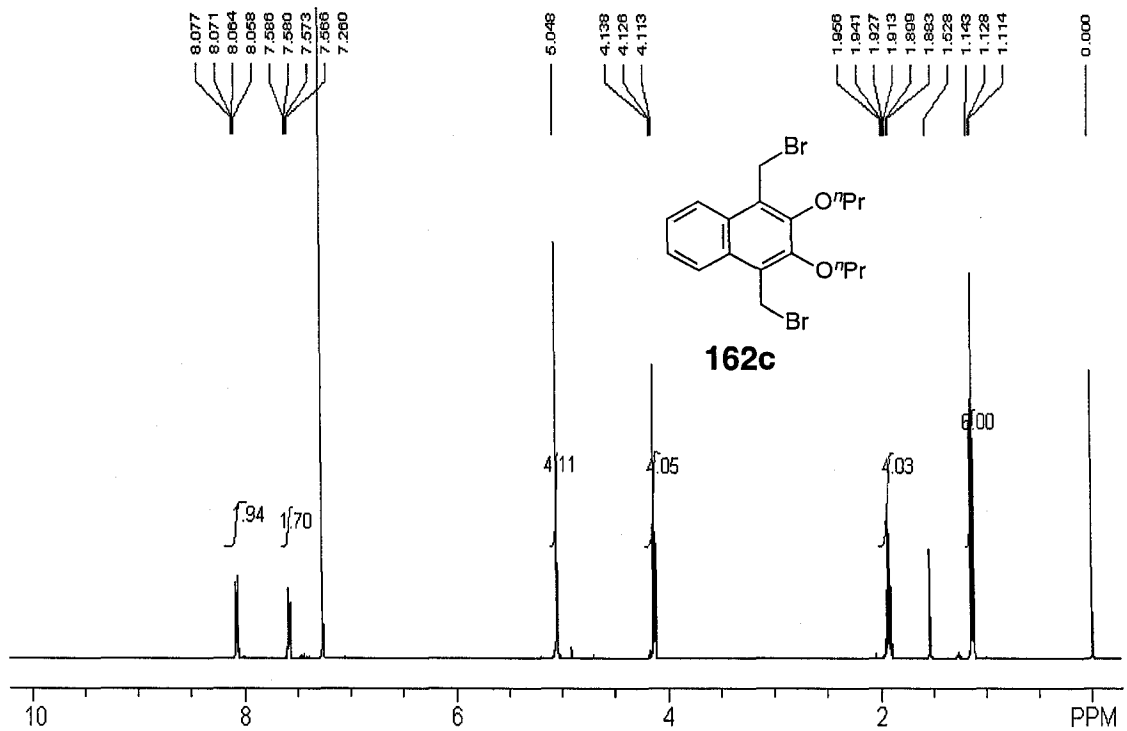
8.077
8.071
8.064
8.058
7.586
7.580
7.573
7.566
7.260
5.048
4.138
4.126
4.113
1.956
1.941
1.927
1.913
1.899
1.883
1.528
1.143
1.128
1.114
0.000
Br
O^{n}Pr
O^{n}Pr
Br
162c
1.94
1.70
4.11
4.05
4.03
6.00
10
8
6
4
2
PPM

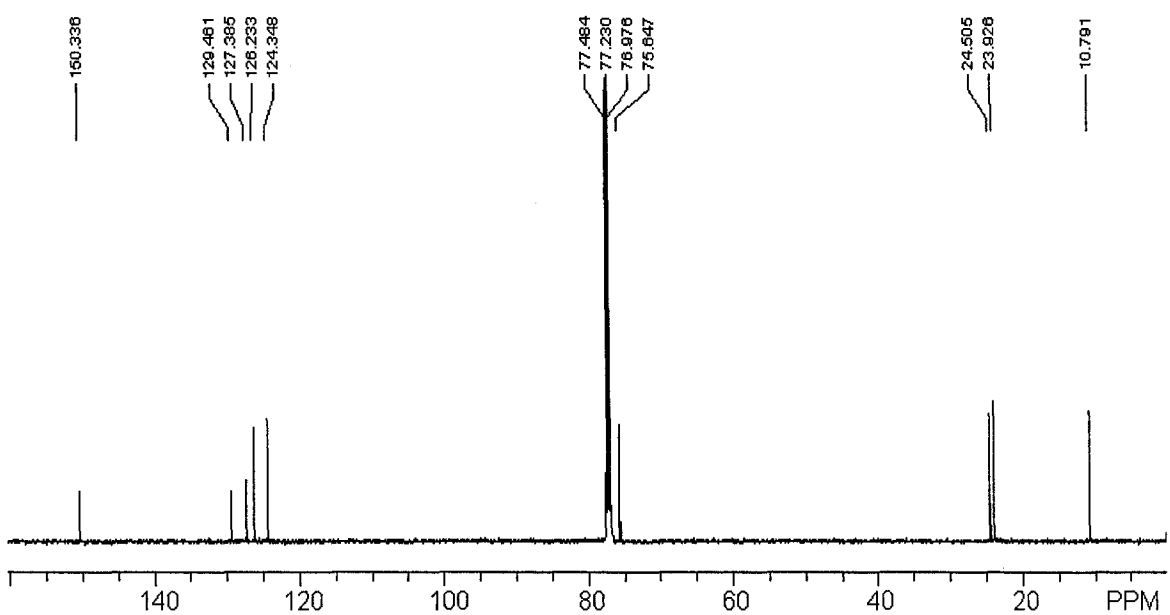
150.336
129.461
127.385
126.233
124.348
77.484
77.230
76.976
75.647
24.505
23.926
10.791
140
120
100
80
60
40
20
PPM

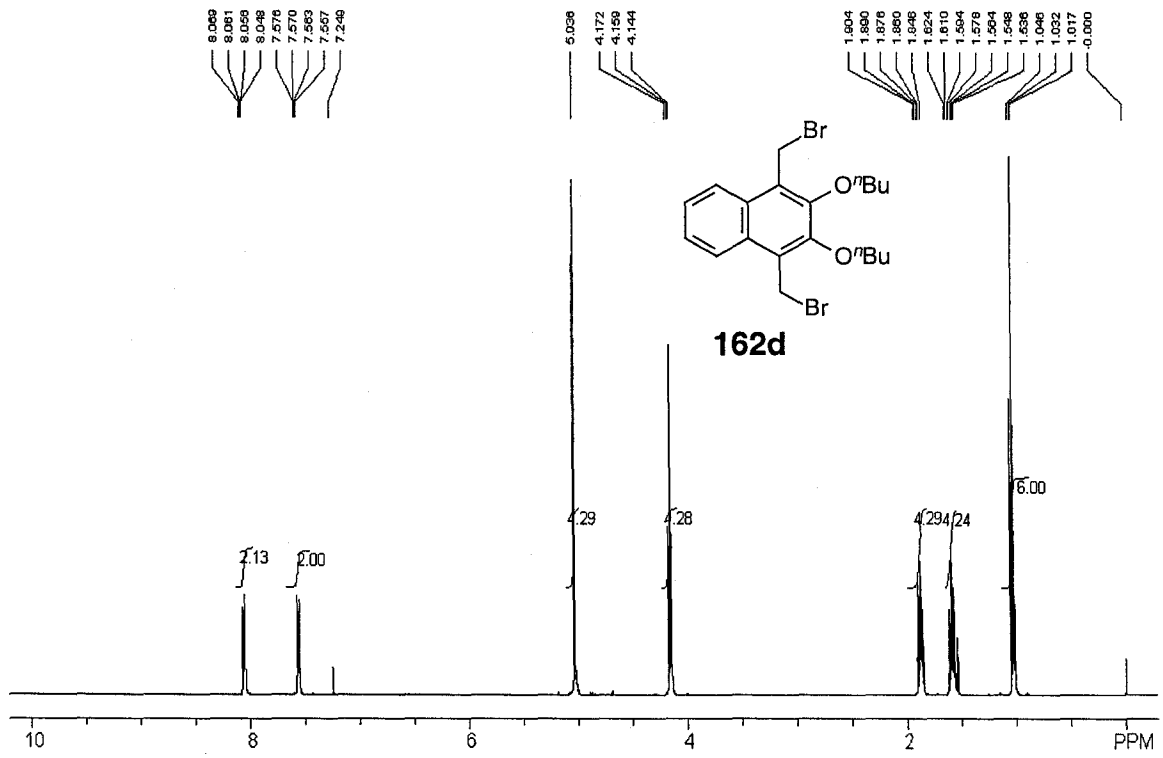
8.069
8.061
8.059
8.048
7.576
7.570
7.563
7.557
7.249
5.036
4.172
4.159
4.144
1.904
1.890
1.876
1.860
1.846
1.824
1.810
1.594
1.578
1.564
1.548
1.536
1.046
1.032
1.017
0.000
Br
O^{n}Bu
O^{n}Bu
Br
2.13
2.00
4.29
4.28
4.29
4.24
6.00
10
8
6
4
2
PPM

162d

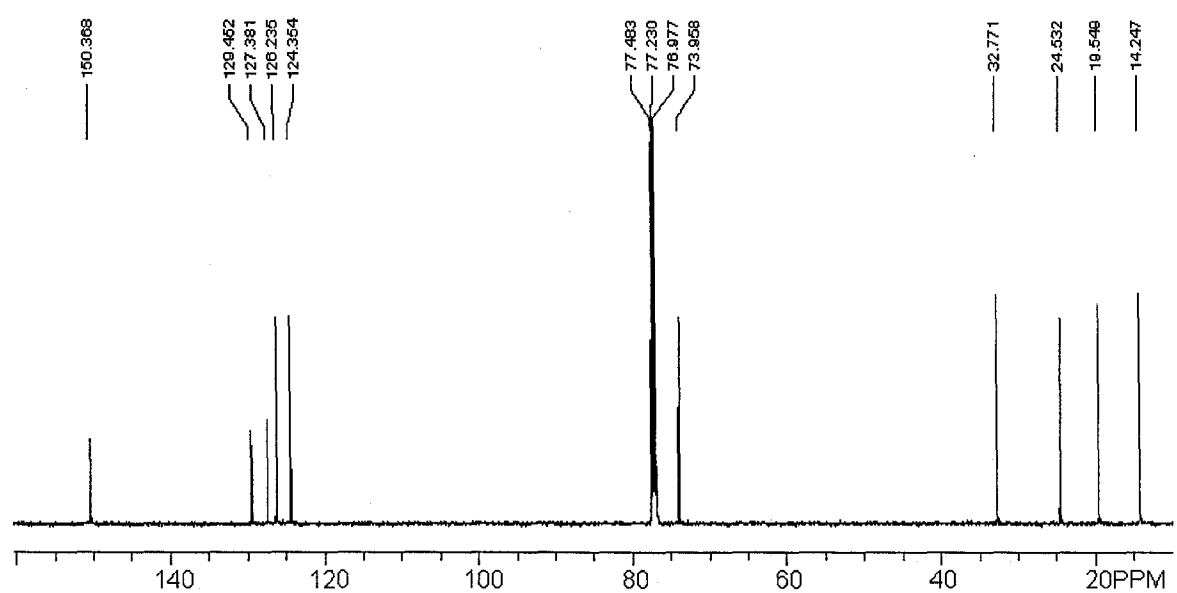
150.368
129.462
127.381
126.235
124.354
77.483
77.230
76.977
73.958
32.771
24.532
19.548
14.247
140
120
100
80
60
40
20PPM

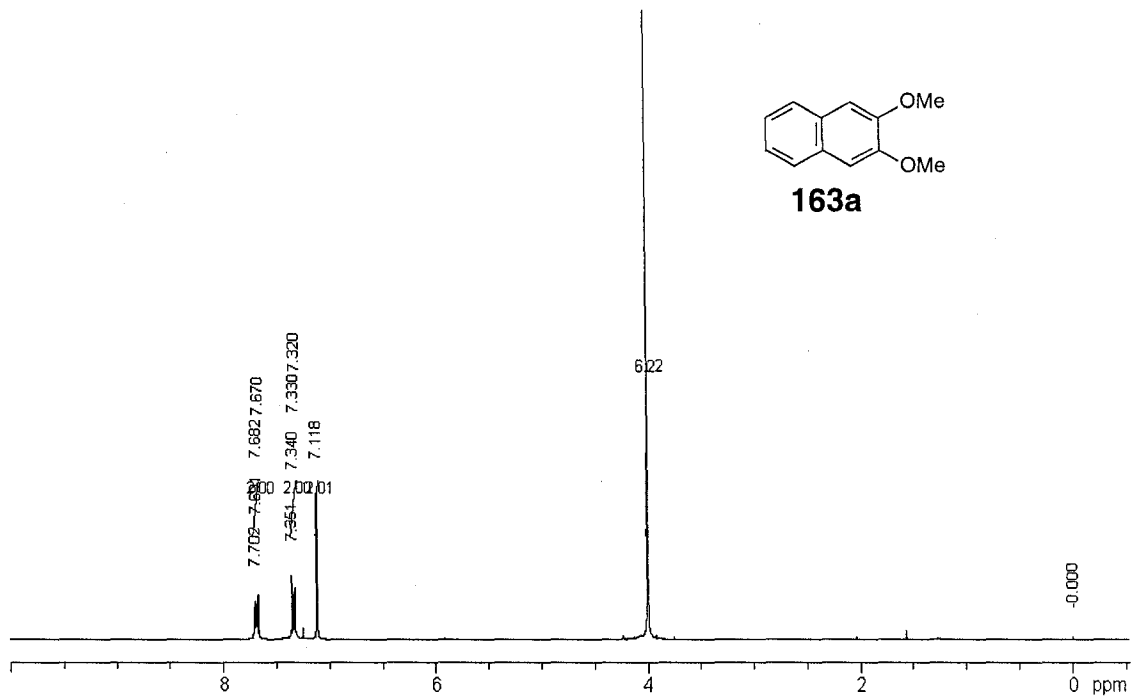
OMe
OMe
163a
7.682
7.670
7.330
7.320
7.340
7.118
7.702
7.351
6.22
-0.000
8
6
4
2
0 ppm

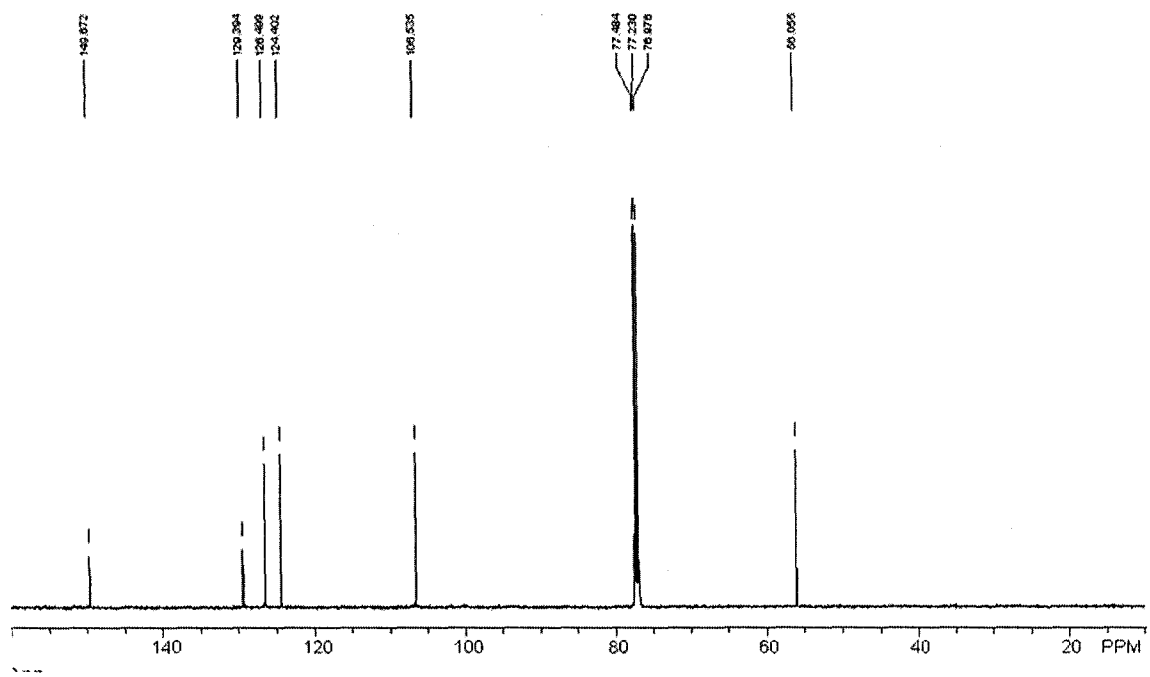
140.672
129.364
126.469
124.402
106.535
77.484
77.230
76.976
55.656
140
120
100
80
60
40
20 PPM

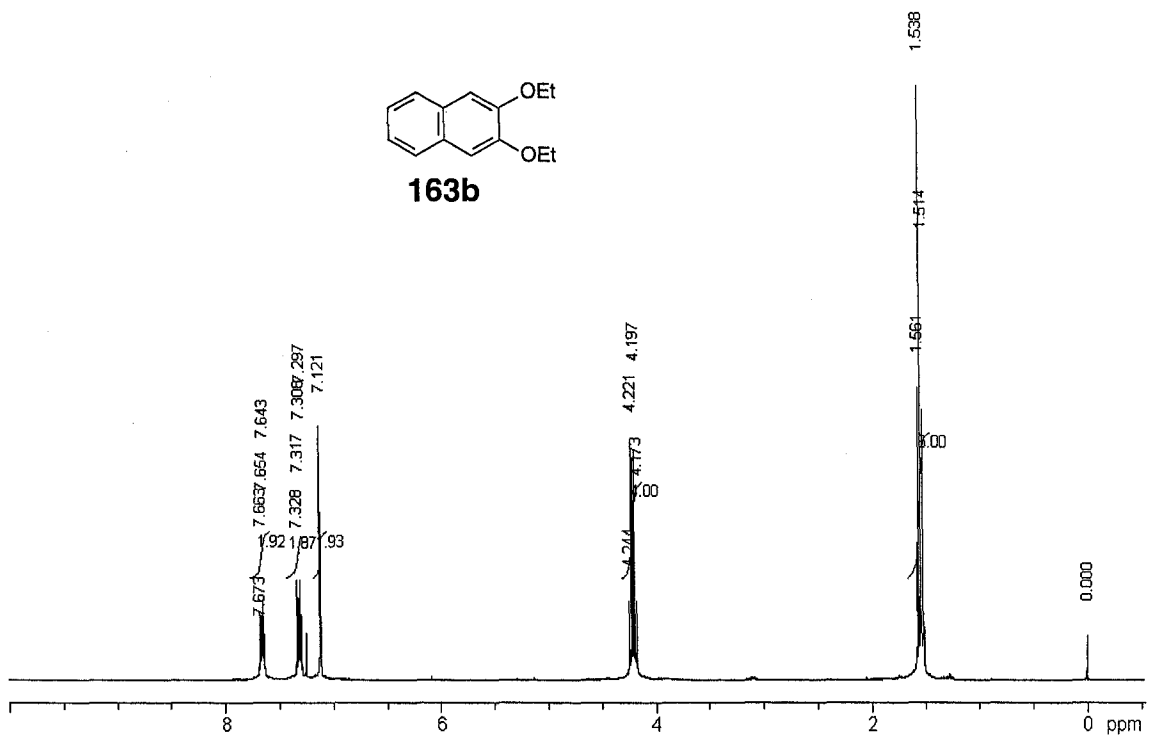
OEt
OEt
163b
1.538
1.514
1.561
7.643
7.654
7.663
7.328
7.317
7.306
7.297
7.121
4.221
4.197
4.173
0.000
8
6
4
2
0 ppm

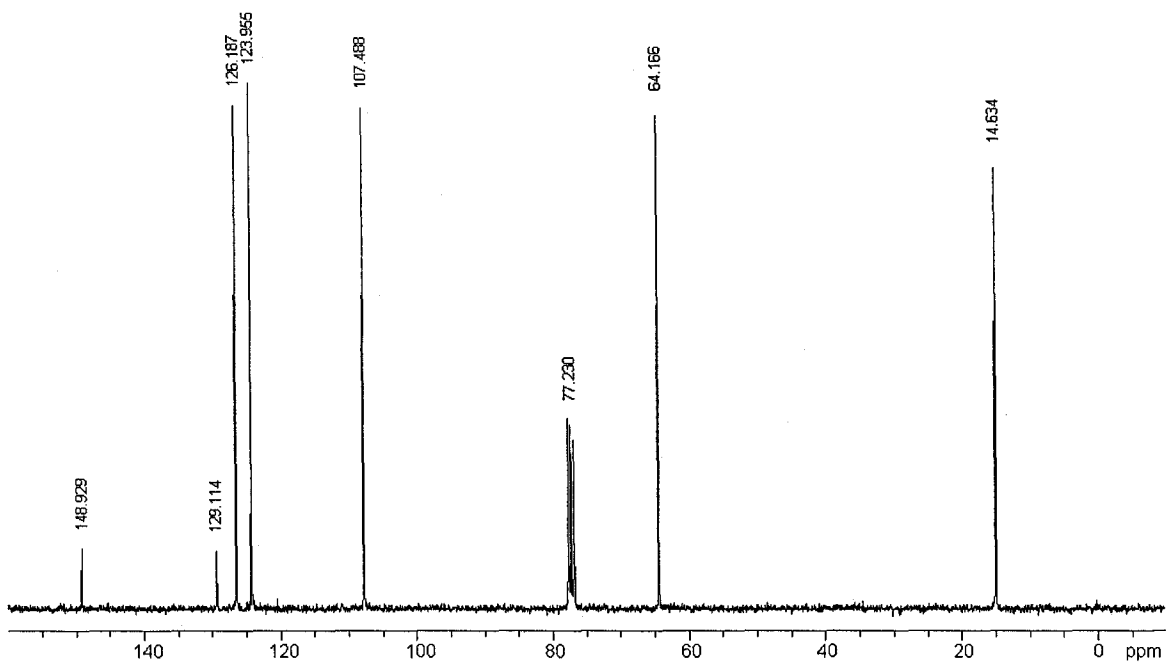
148.929
129.114
126.187
123.955
107.488
77.230
64.166
14.634
140
120
100
80
60
40
20
0 ppm

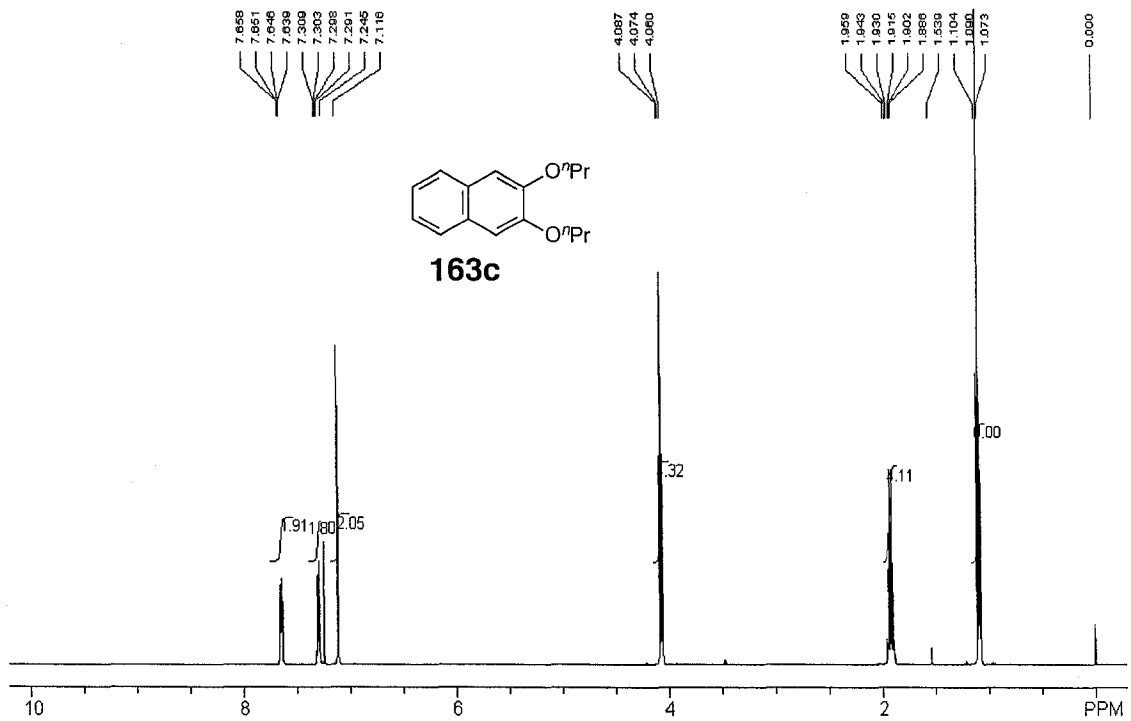
7.658
7.651
7.646
7.639
7.309
7.303
7.298
7.291
7.245
7.116
4.087
4.074
4.060
1.959
1.943
1.930
1.915
1.902
1.886
1.539
1.104
1.090
1.073
0.000
O^{n}Pr
O^{n}Pr
163c
1.91
1.80
2.05
4.32
3.11
6.00
10
8
6
4
2
PPM

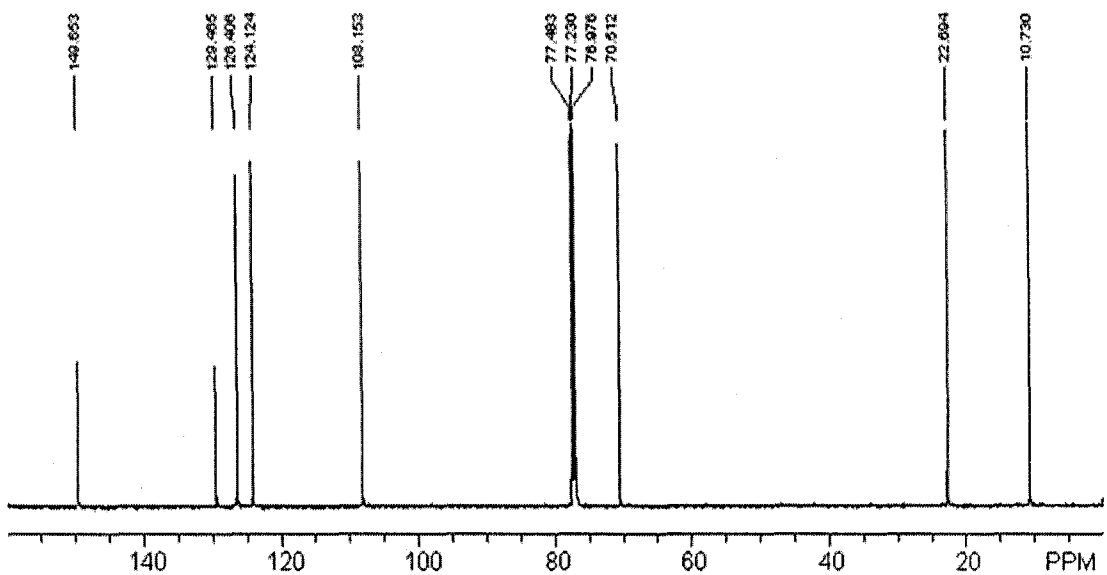
149.653
129.495
126.406
124.124
108.153
77.483
77.230
76.976
70.512
22.684
10.730
140
120
100
80
60
40
20
PPM

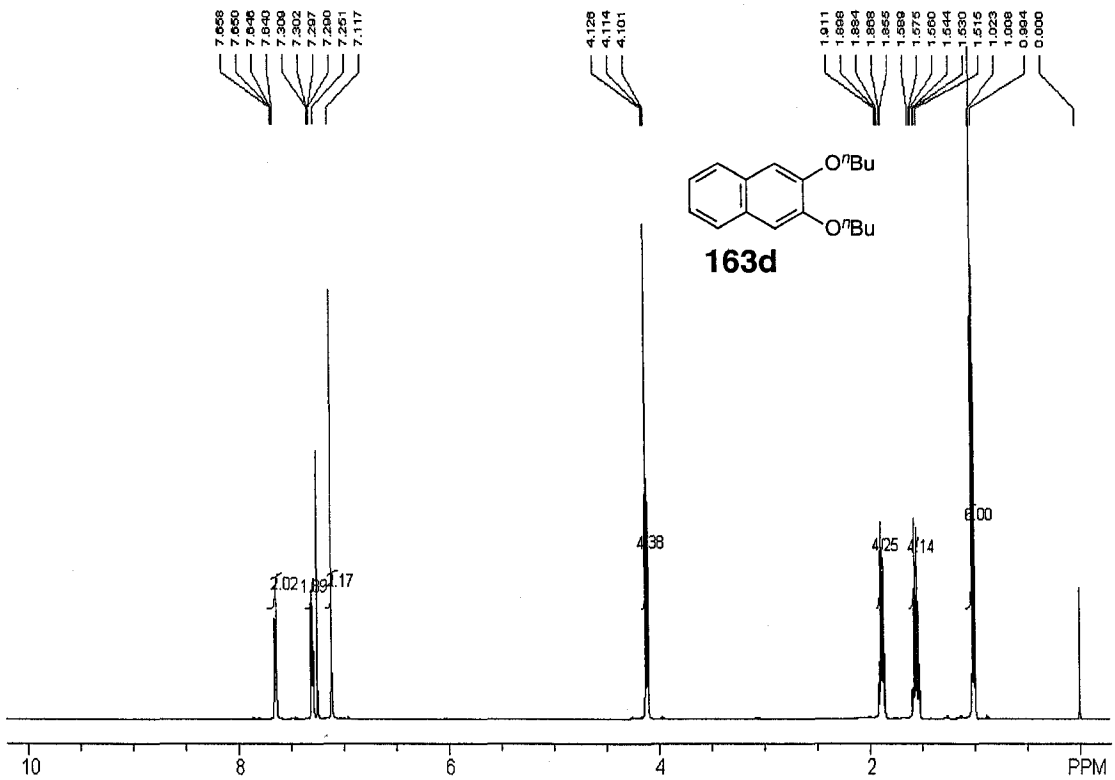
7.658
7.650
7.646
7.640
7.306
7.302
7.297
7.290
7.251
7.117
4.126
4.114
4.101
1.911
1.898
1.884
1.868
1.855
1.589
1.575
1.560
1.544
1.530
1.515
1.023
1.008
0.994
0.000
O^{n}Bu
O^{n}Bu
163d
2.02
1.99
2.17
4.38
4.25
4.14
8.00
10
8
6
4
2
PPM

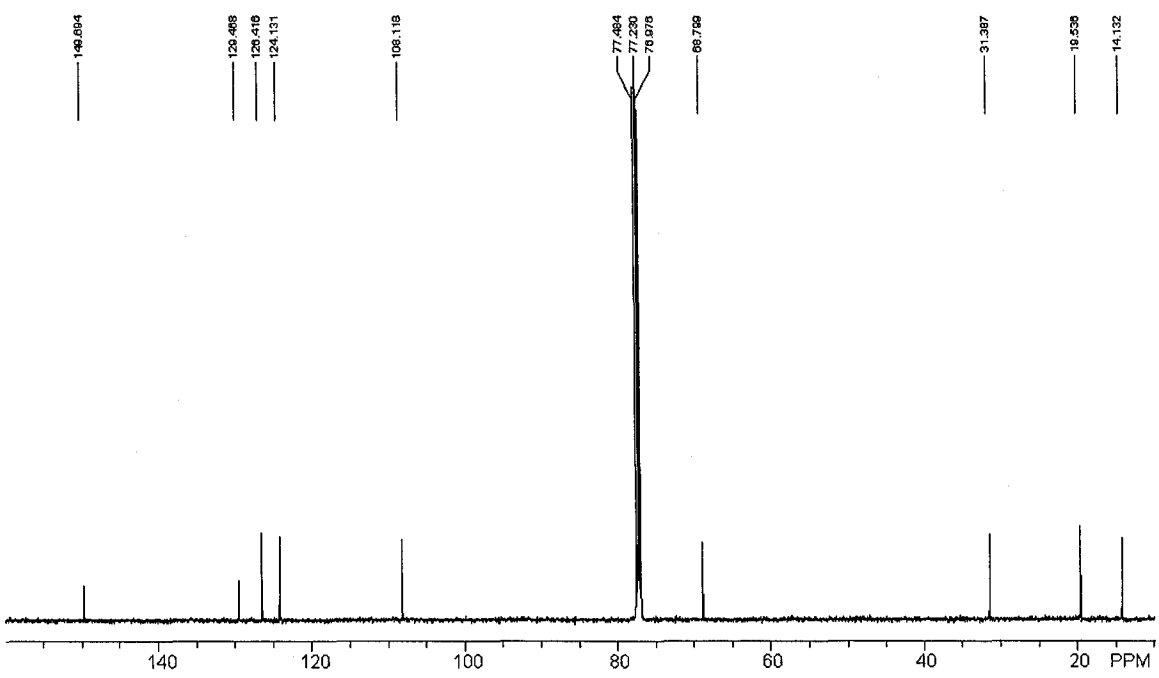
149.694
129.466
129.416
124.131
109.118
77.484
77.230
76.976
68.799
31.387
19.536
14.132
140
120
100
80
60
40
20
PPM

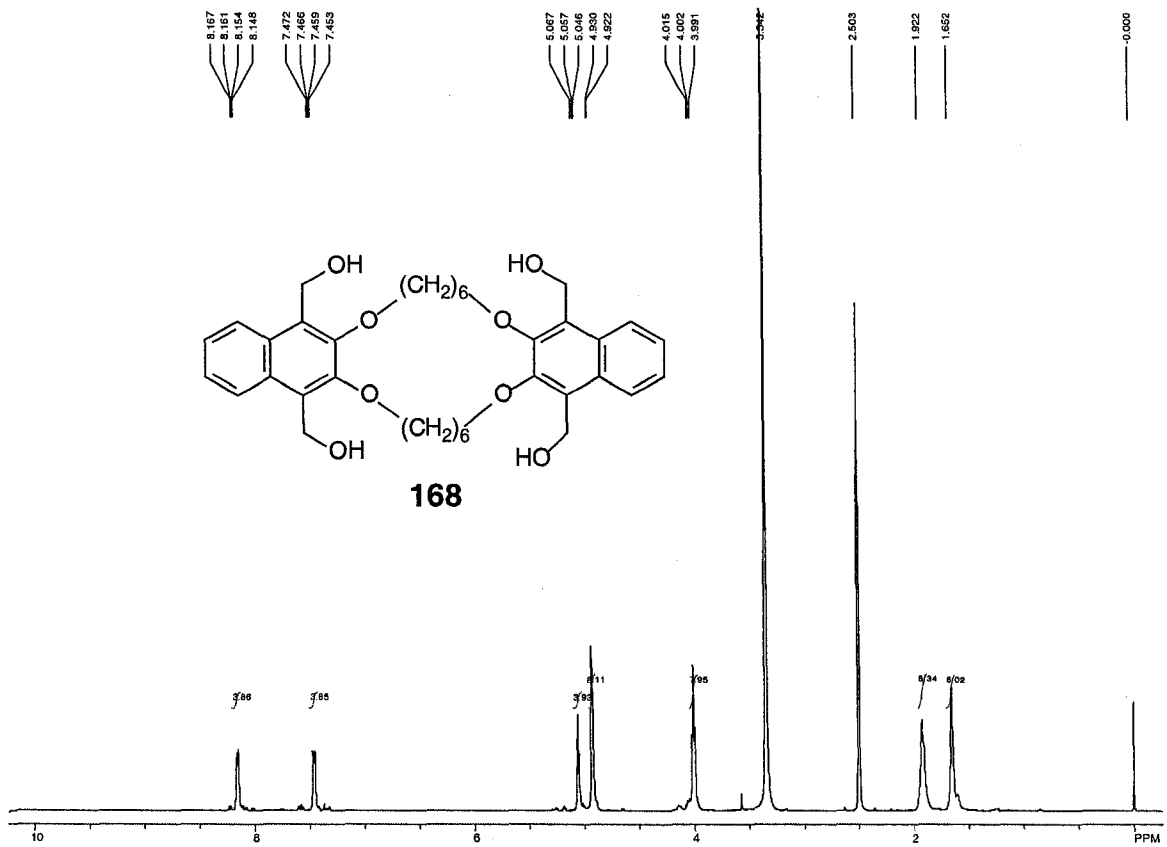
8.167
8.161
8.154
8.148
7.472
7.466
7.459
7.453
5.067
5.057
5.046
4.930
4.922
4.015
4.002
3.991
2.503
1.922
1.652
0.000
OH
HO
(CH2)6
O
O
O
O
(CH2)6
OH
HO
3.86
3.85
3.93
3.95
3.34
3.02
10
8
6
4
2
PPM

168

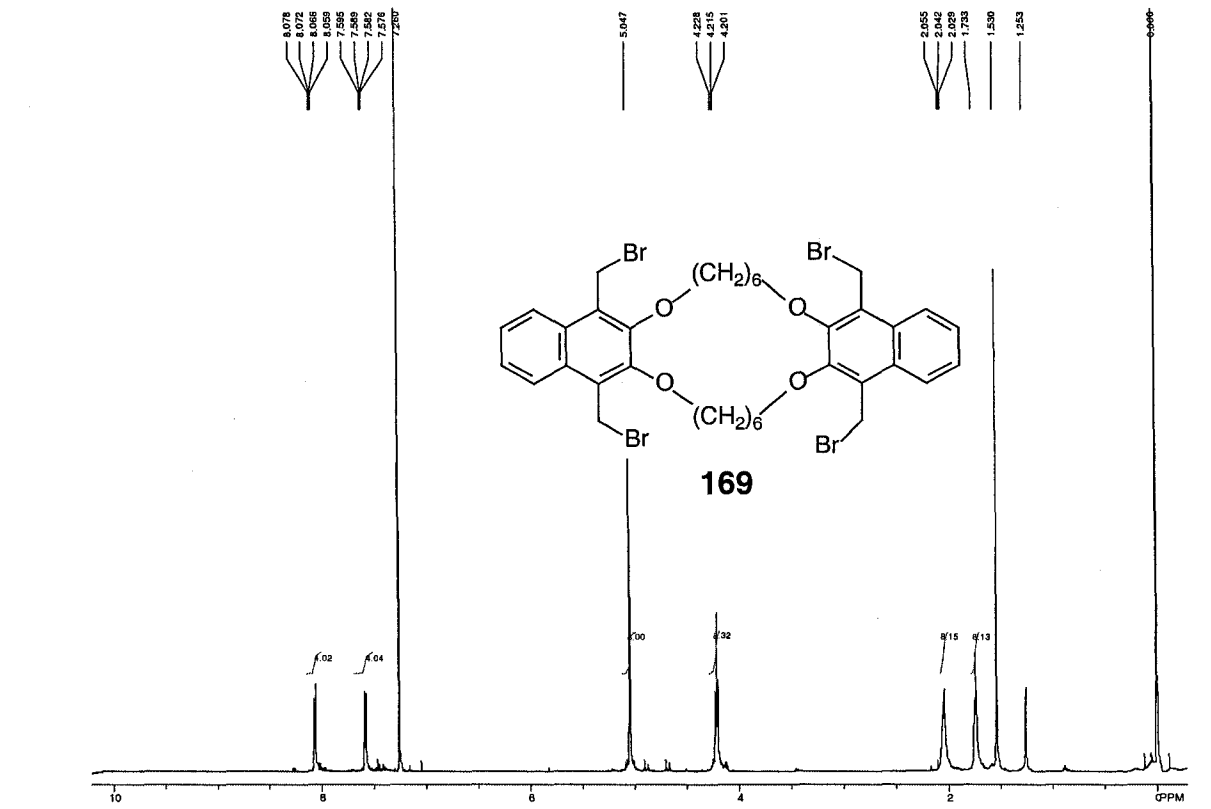
8.078
8.072
8.066
8.059
7.595
7.589
7.582
7.576
7.257
5.047
4.228
4.215
4.201
2.055
2.042
2.029
1.733
1.530
1.253
0.000
Br
(CH2)6
O
O
O
O
(CH2)6
Br
Br
Br
1.02
4.04
2.00
3.32
3.15
3.13
10
8
6
4
2
PPM

169

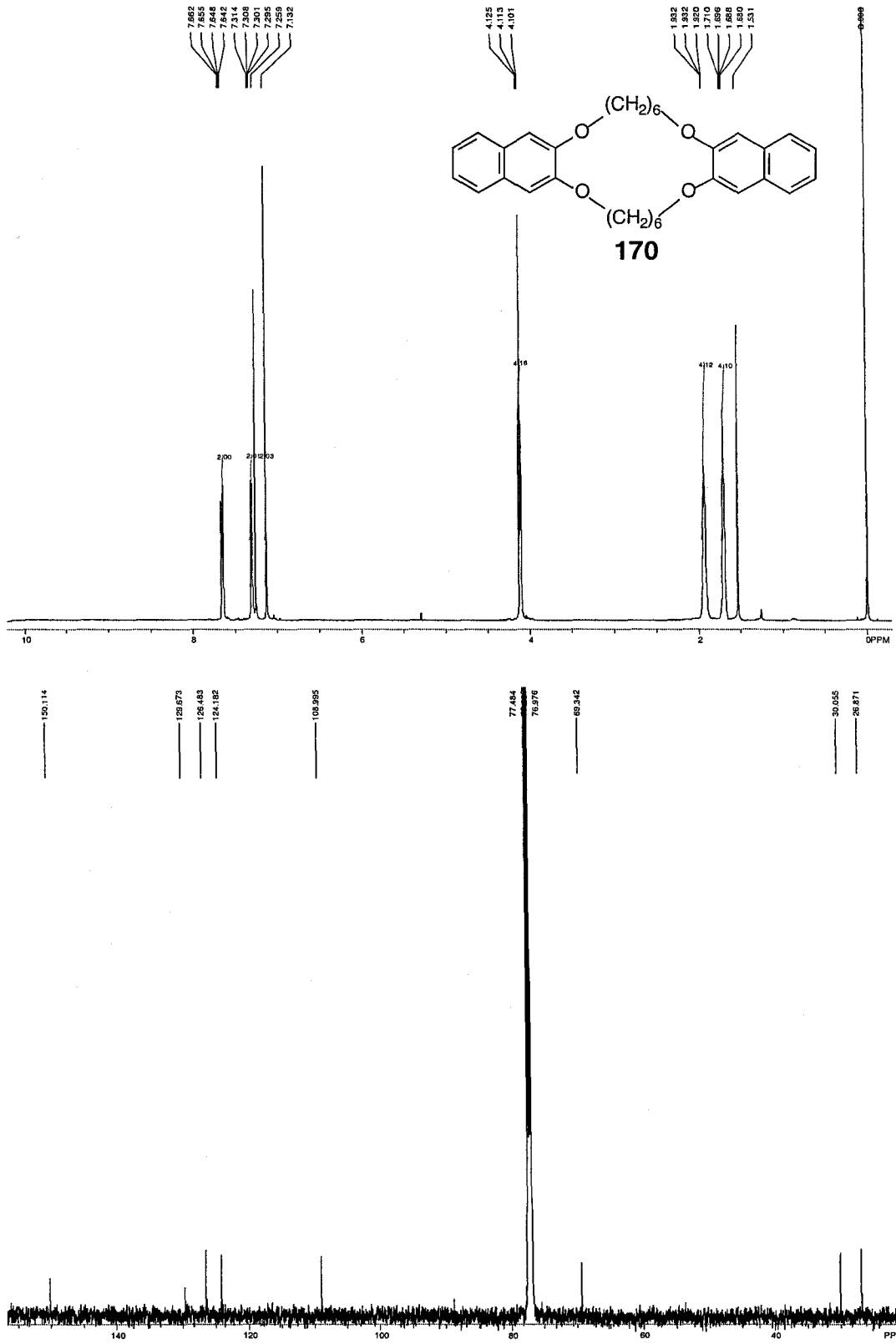
7.662
7.655
7.648
7.642
7.314
7.308
7.301
7.295
7.259
7.132
4.125
4.113
4.101
1.932
1.932
1.920
1.710
1.696
1.688
1.680
1.531
(CH2)6
O
O
O
O
(CH2)6
170
4.16
4.12
4.10
2.00
2.12
2.03
10
8
6
4
2
0PPM
150.114
129.673
126.483
124.182
108.995
77.484
76.976
69.342
30.055
26.871
140
120
100
80
60
40
PPM

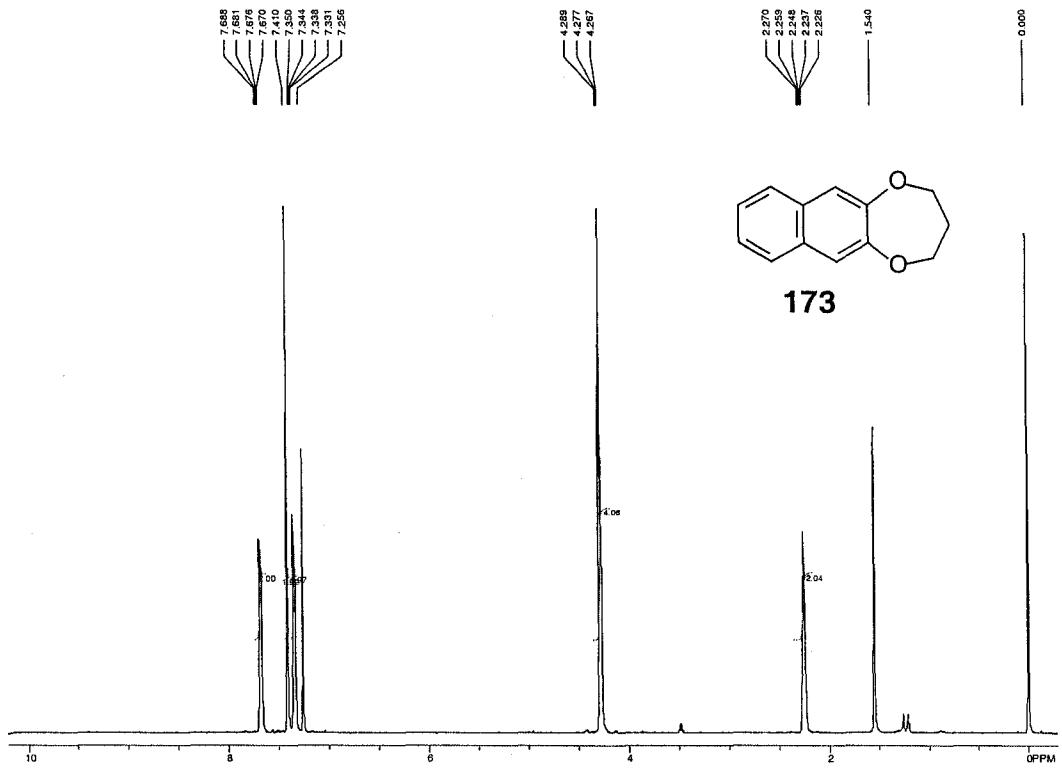
7.688
7.681
7.676
7.670
7.410
7.350
7.344
7.338
7.331
7.256
4.289
4.277
4.267
2.270
2.259
2.248
2.237
2.226
1.540
0.000
4.06
2.04
10
8
6
4
2
0PPM

173

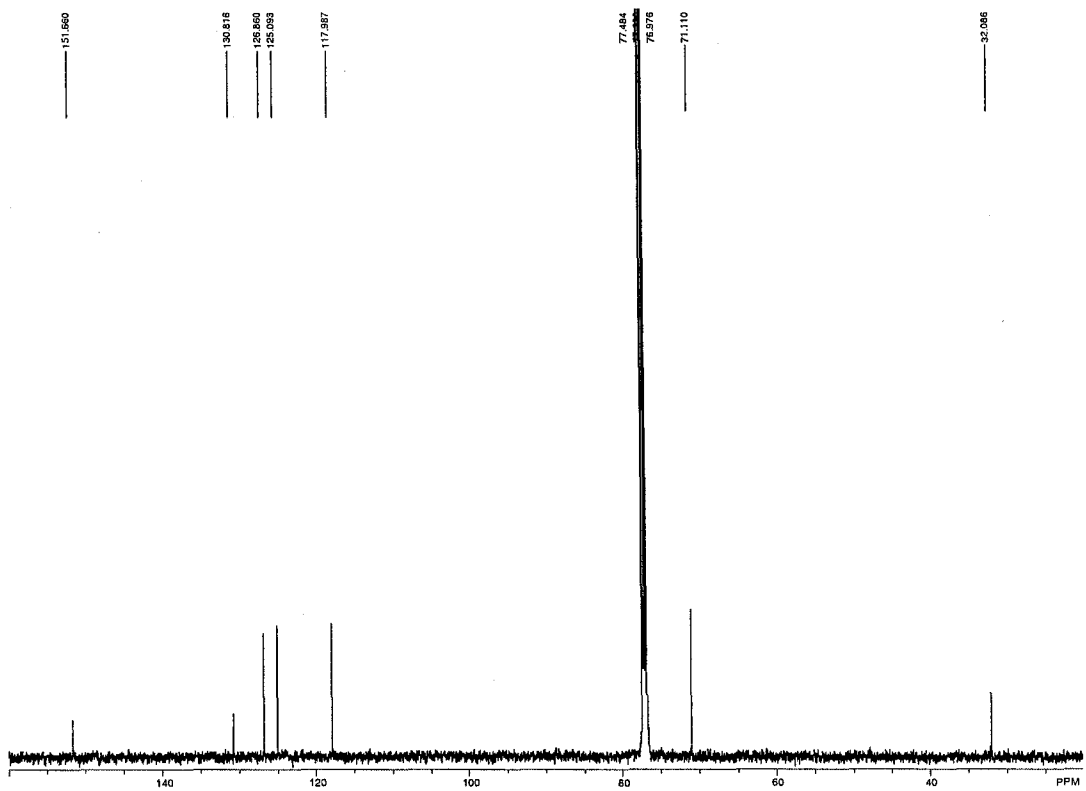
151.660
130.818
126.860
125.093
117.987
77.484
76.578
71.110
32.086
140
120
100
80
60
40
PPM

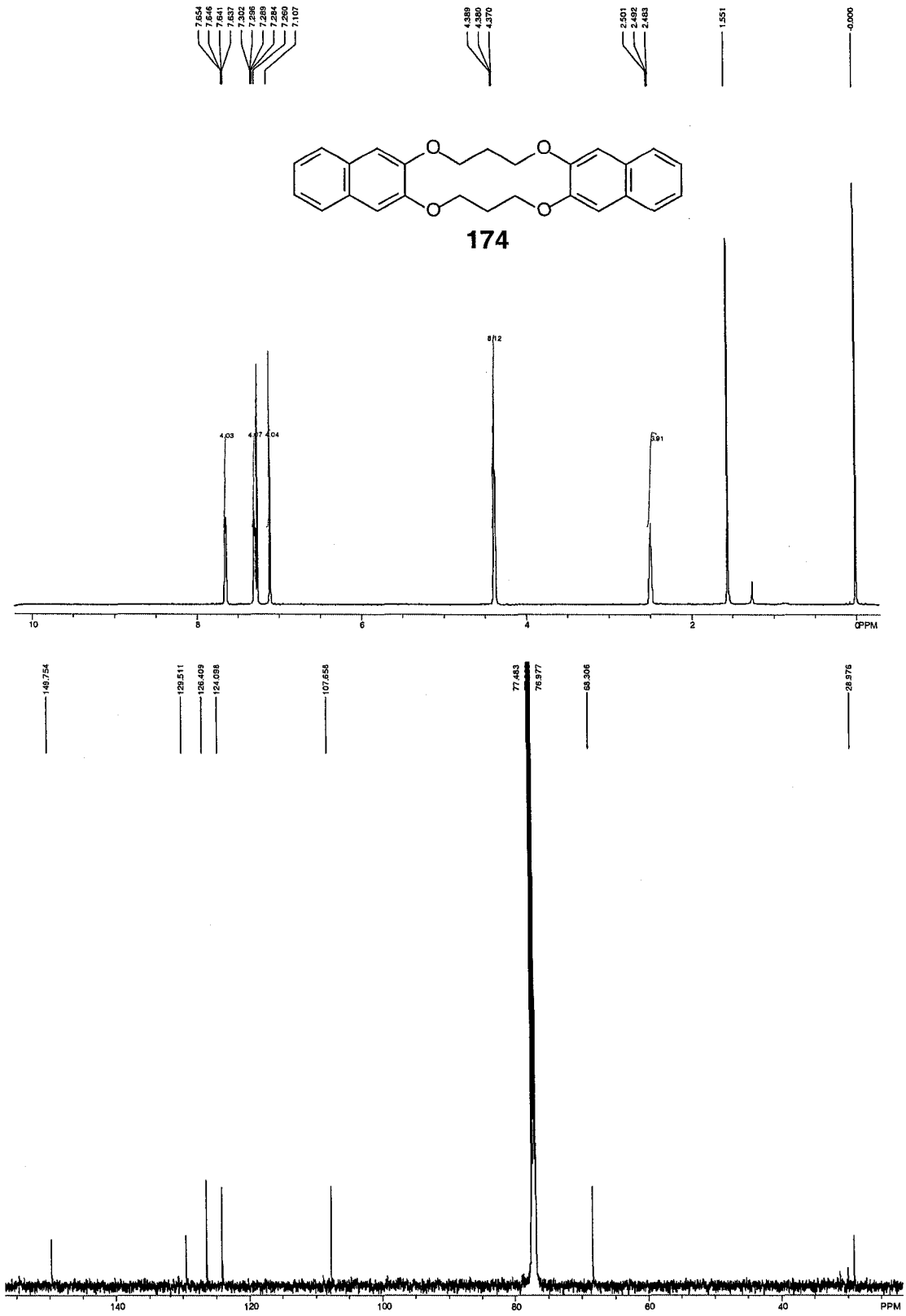
7.654
7.646
7.641
7.637
7.302
7.296
7.289
7.284
7.260
7.107
4.389
4.380
4.370
2.501
2.492
2.483
1.551
0.000
174
8.12
4.03
4.04
3.91
10
8
6
4
2
0PPM
149.754
129.511
126.409
124.098
107.658
77.483
76.977
69.306
29.976
140
120
100
80
60
40
PPM

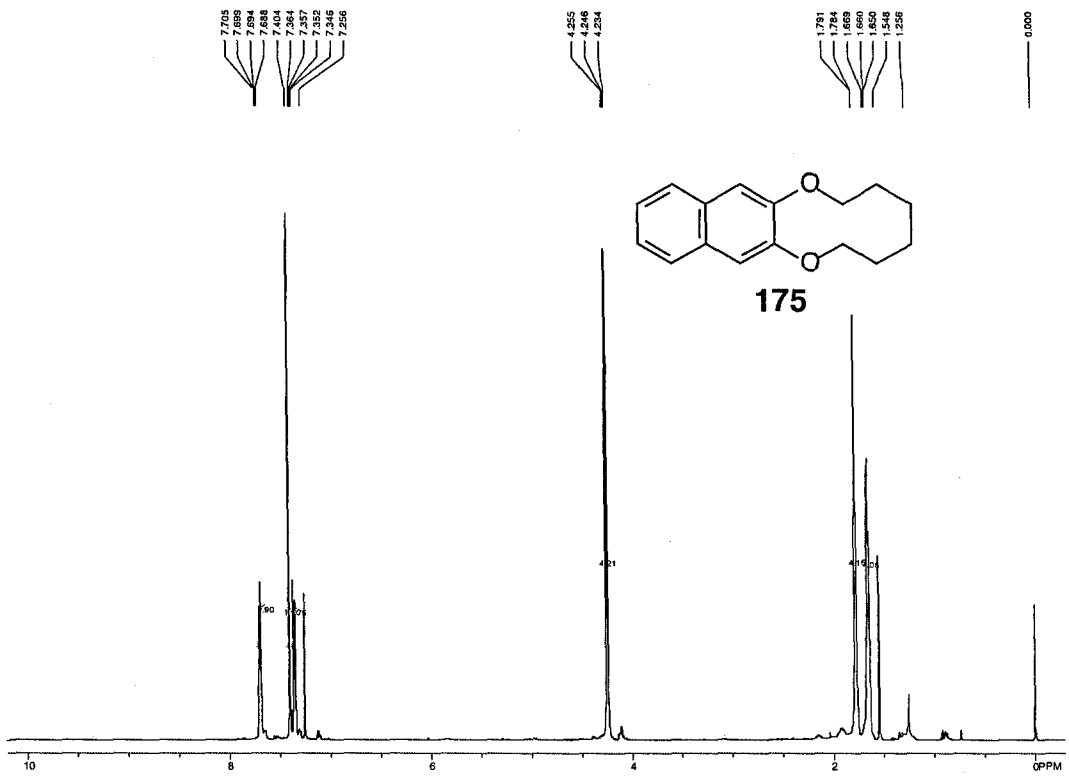
7.705
7.699
7.694
7.688
7.404
7.364
7.357
7.352
7.346
7.256
4.255
4.246
4.234
1.791
1.784
1.658
1.650
1.548
1.256
0.000
O
O
175
4.21
10
8
6
4
2
0PPM

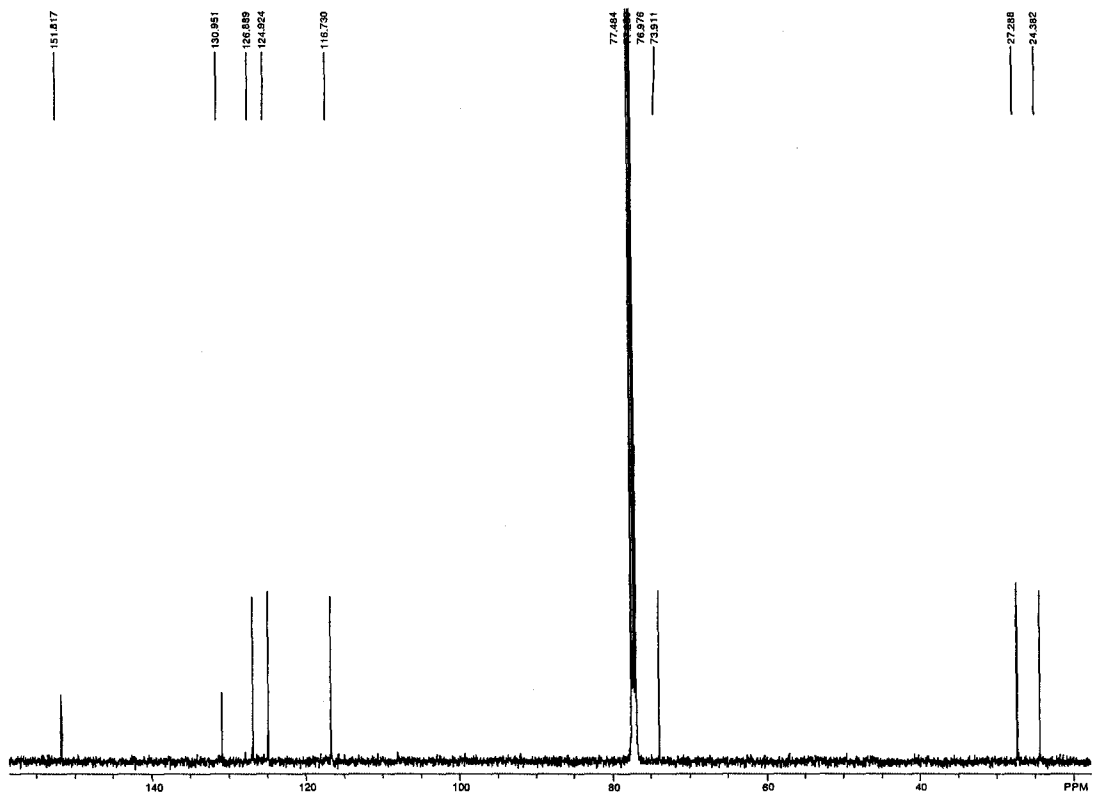
151.817
130.951
126.589
124.924
116.730
77.484
76.876
73.911
27.288
24.382
140
120
100
80
60
40
PPM

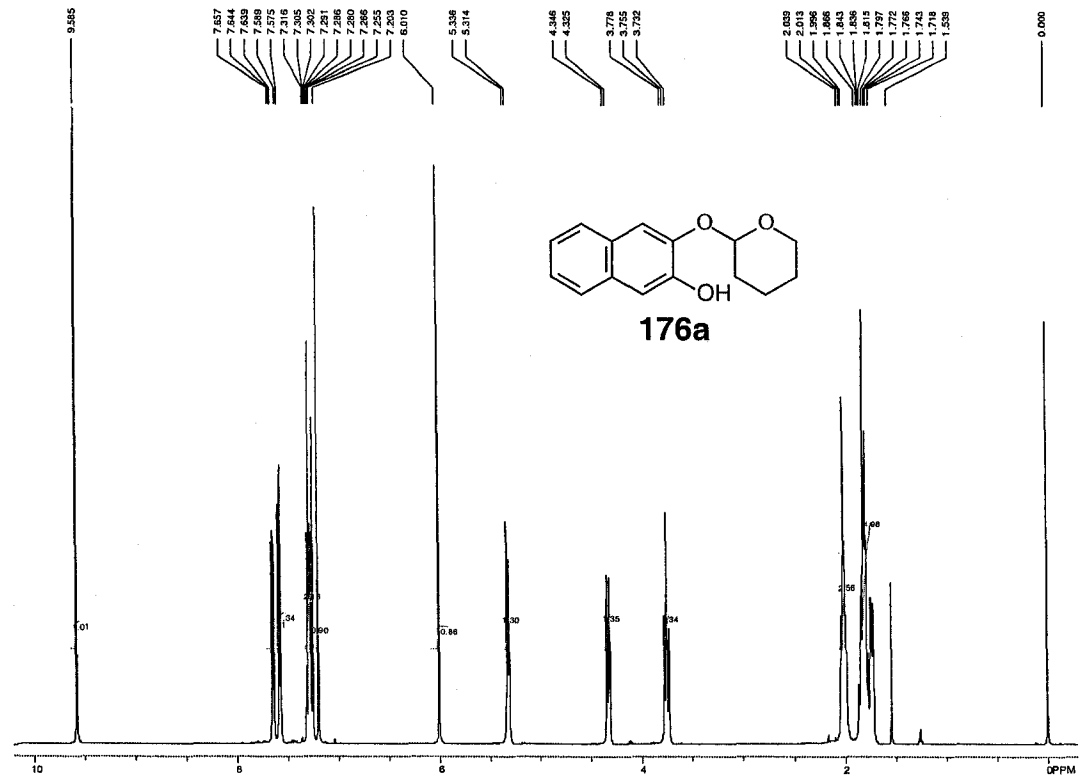
9.565
7.657
7.644
7.639
7.589
7.575
7.316
7.305
7.302
7.291
7.285
7.280
7.266
7.253
7.203
6.010
5.338
5.314
4.346
4.325
3.778
3.755
3.732
2.039
2.013
1.995
1.866
1.843
1.836
1.815
1.797
1.772
1.766
1.743
1.718
1.538
0.000
O
O
OH
176a
1.01
1.34
2.91
3.60
0.86
1.30
1.35
1.34
3.56
4.68
10
8
6
4
2
0PPM

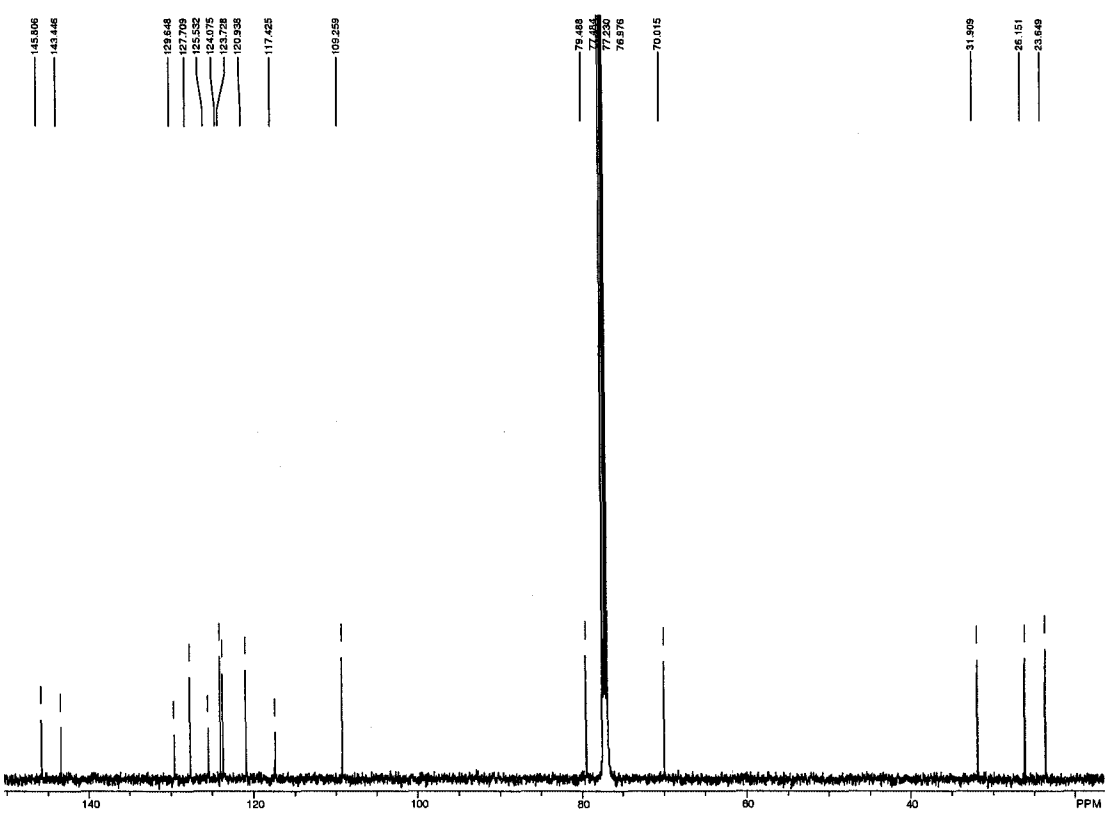
145.806
143.446
129.648
127.709
125.532
124.075
123.728
120.938
117.425
109.259
79.488
77.230
76.976
70.015
31.909
26.151
23.649
140
120
100
80
60
40
PPM

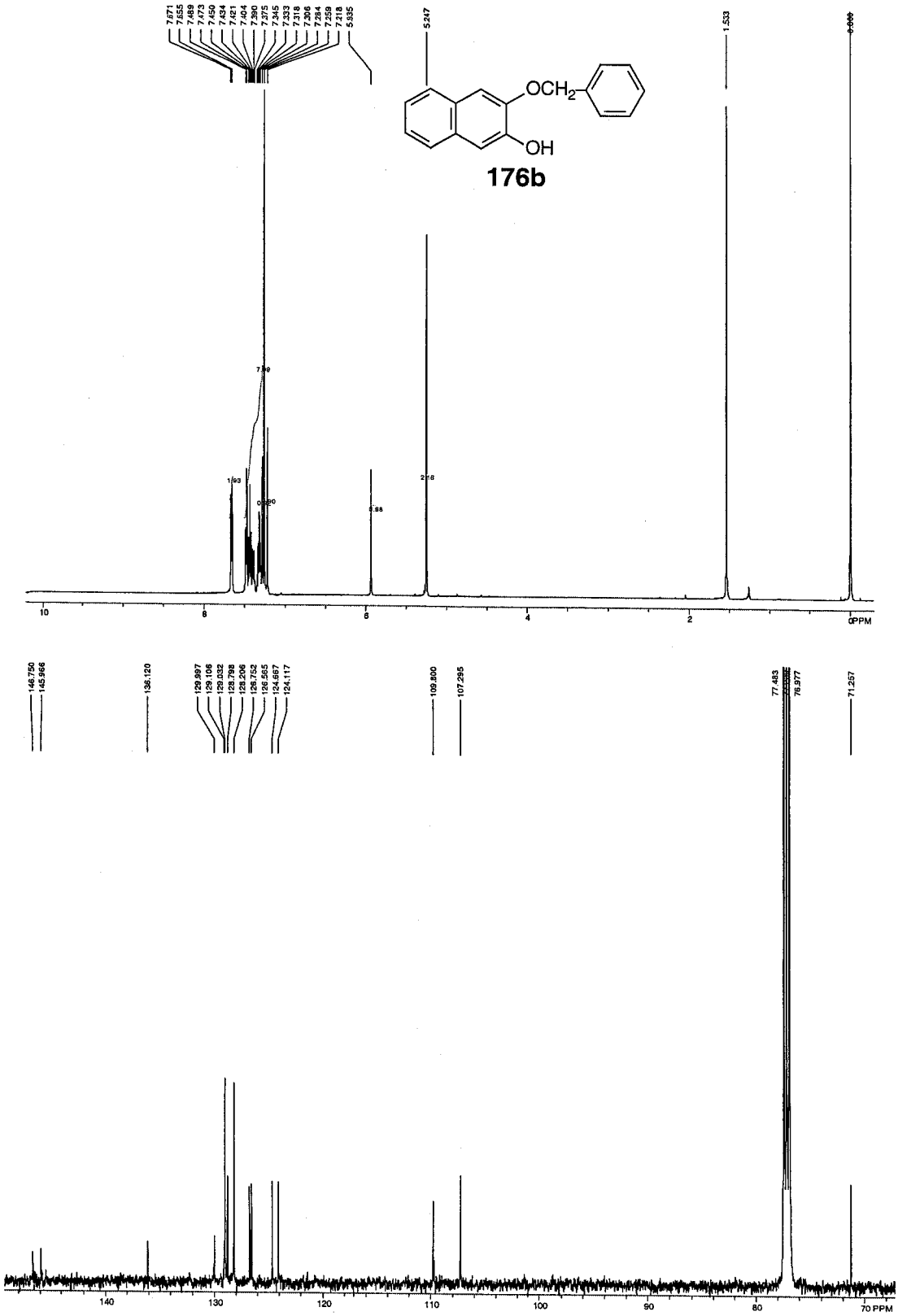
OCH2
OH
176b

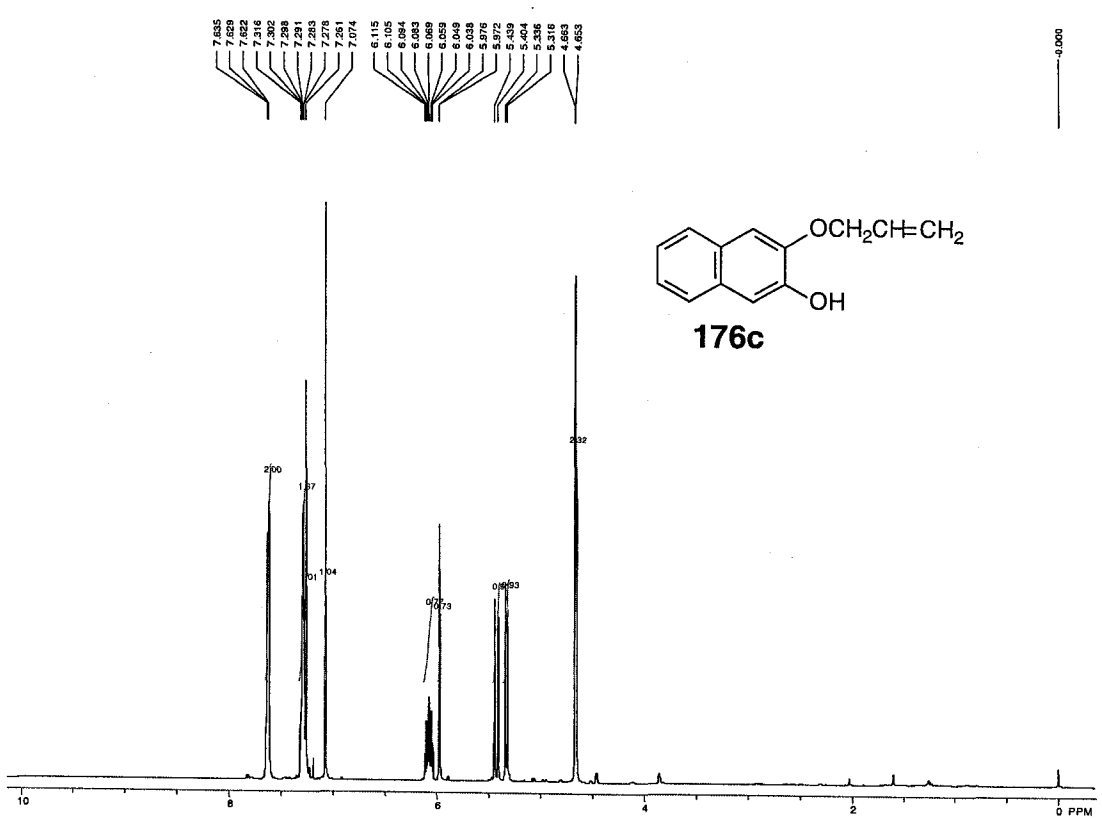
7.835
7.829
7.822
7.316
7.302
7.298
7.291
7.283
7.278
7.261
7.074
6.115
6.105
6.094
6.083
6.069
6.059
6.049
6.038
5.976
5.972
5.439
5.404
5.336
5.318
4.663
4.653
0.000
OCH2CH=CH2
OH
176c
2.00
1.37
1.01
1.04
2.32
10
8
6
4
2
0 PPM

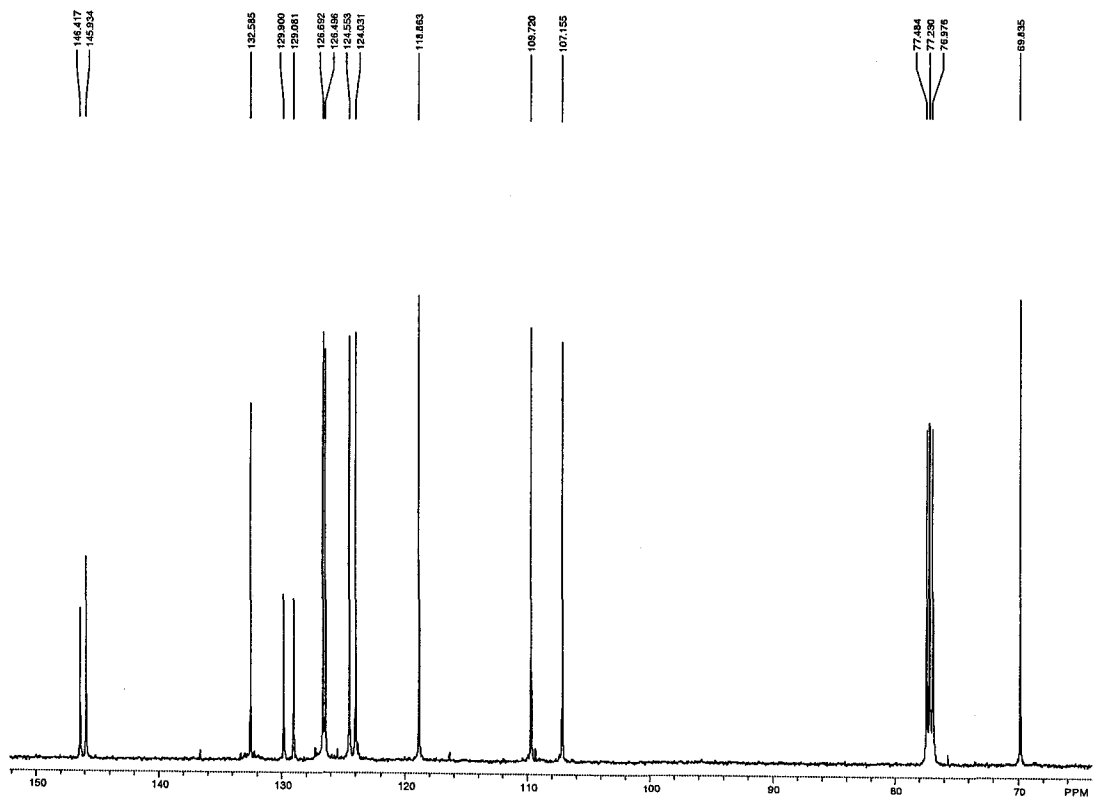
146.417
145.934
132.585
129.900
129.061
126.692
126.486
124.553
124.031
118.863
109.720
107.155
77.484
77.230
76.976
69.835
150
140
130
120
110
100
90
80
70
PPM

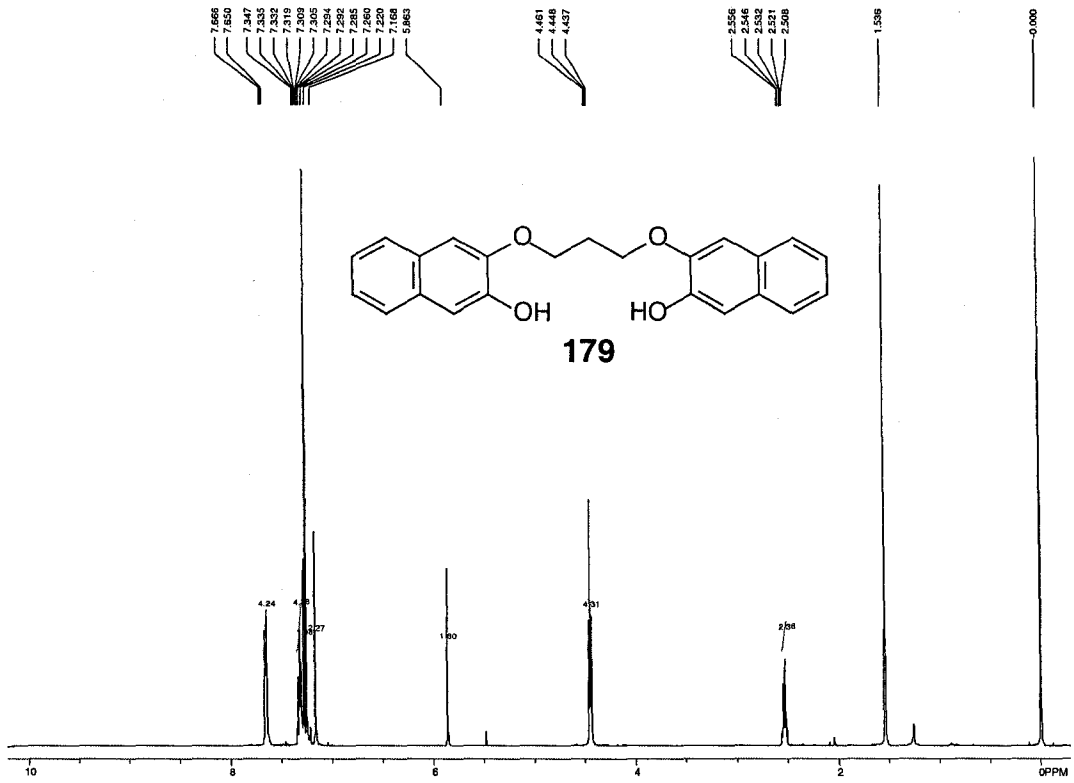
7.666
7.650
7.347
7.335
7.332
7.319
7.309
7.305
7.294
7.292
7.285
7.260
7.220
7.168
5.863
4.461
4.448
4.437
2.556
2.546
2.532
2.521
2.508
1.356
0.000
OH
HO
4.24
4.27
1.00
4.31
2.08
10
8
6
4
2
0PPM

179

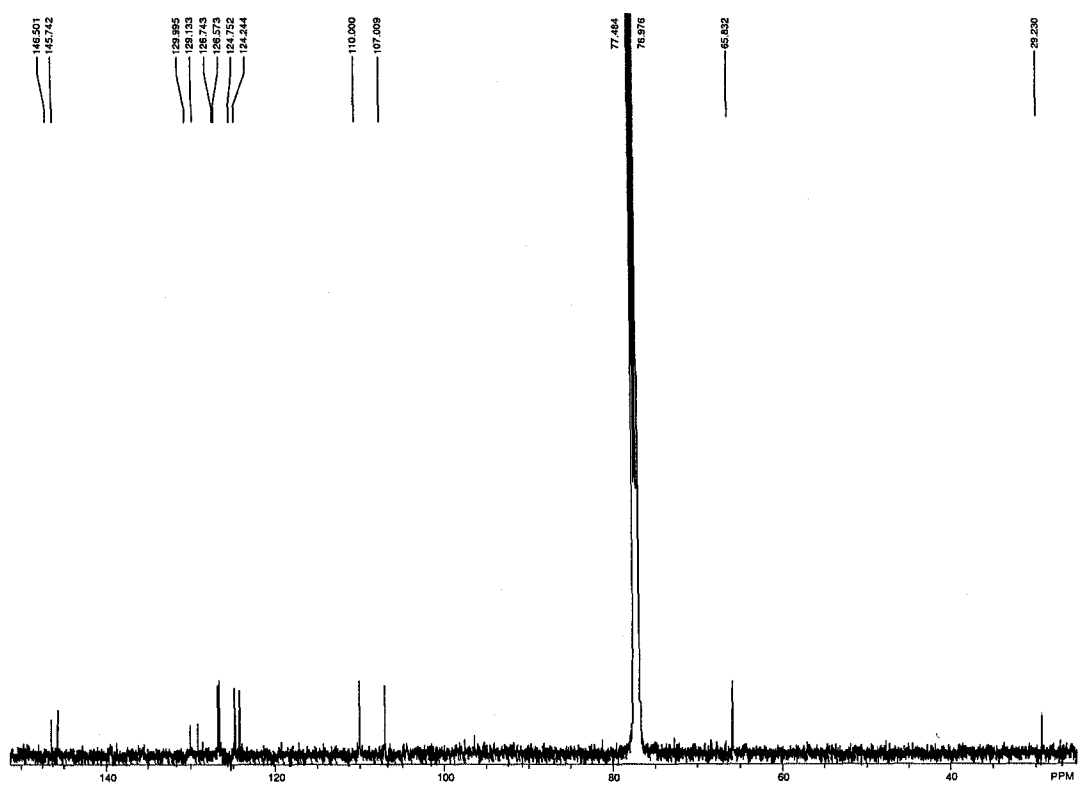
146.501
145.742
129.995
129.133
126.743
126.573
124.752
124.244
110.000
107.009
77.484
76.976
65.832
29.230
140
120
100
80
60
40
PPM

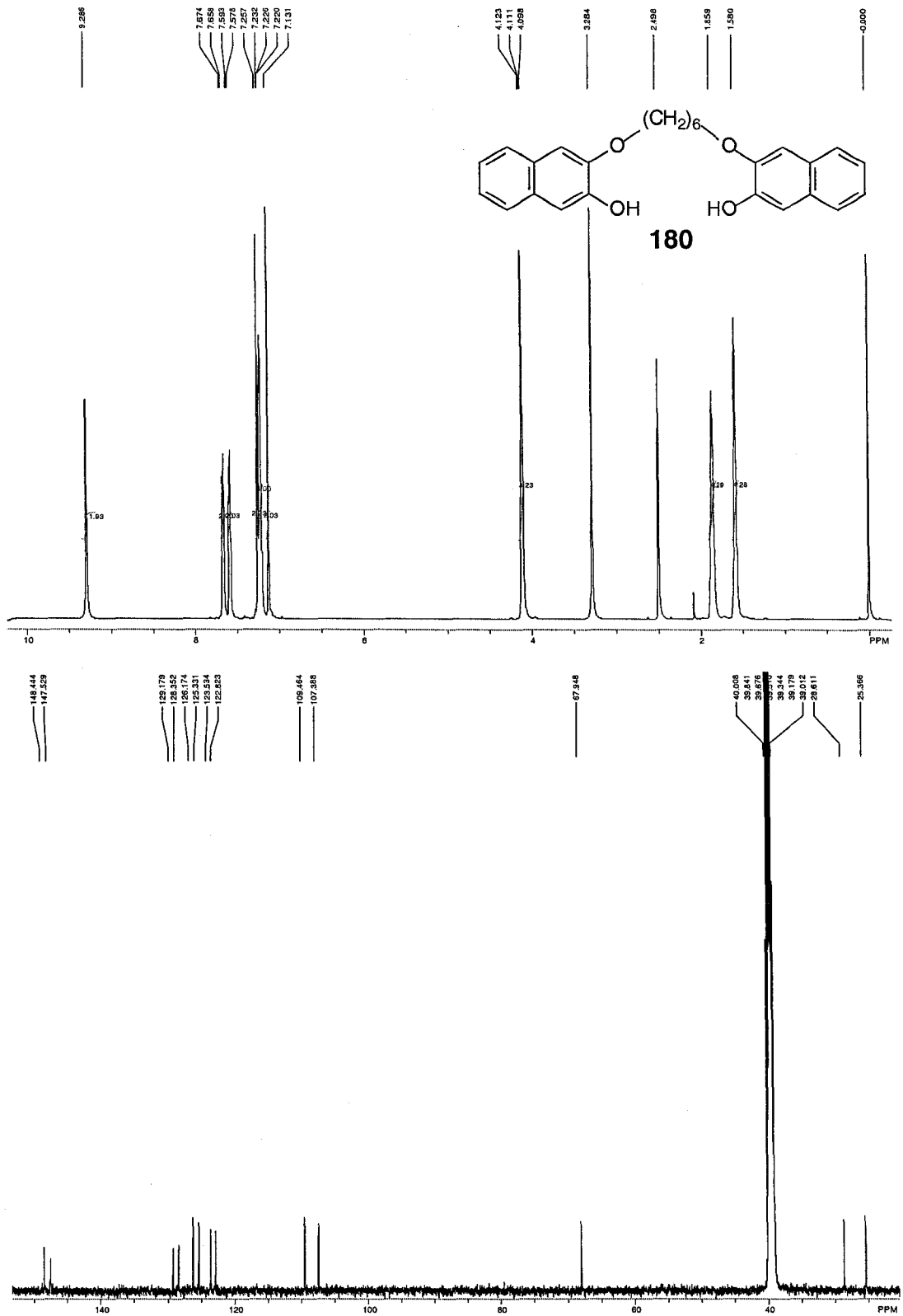
9.286
7.674
7.658
7.593
7.578
7.257
7.232
7.226
7.220
7.131
4.123
4.111
4.098
3.284
2.498
1.559
1.550
0.000
(CH2)6
O
O
OH
HO
180
1.93
2.03
2.03
4.23
2.29
2.28
10
8
6
4
2
PPM
148.444
147.529
129.179
128.352
126.174
125.331
123.534
122.823
109.464
107.388
67.948
40.008
39.841
39.676
39.510
39.344
39.179
39.012
29.611
25.366
140
120
100
80
60
40
PPM

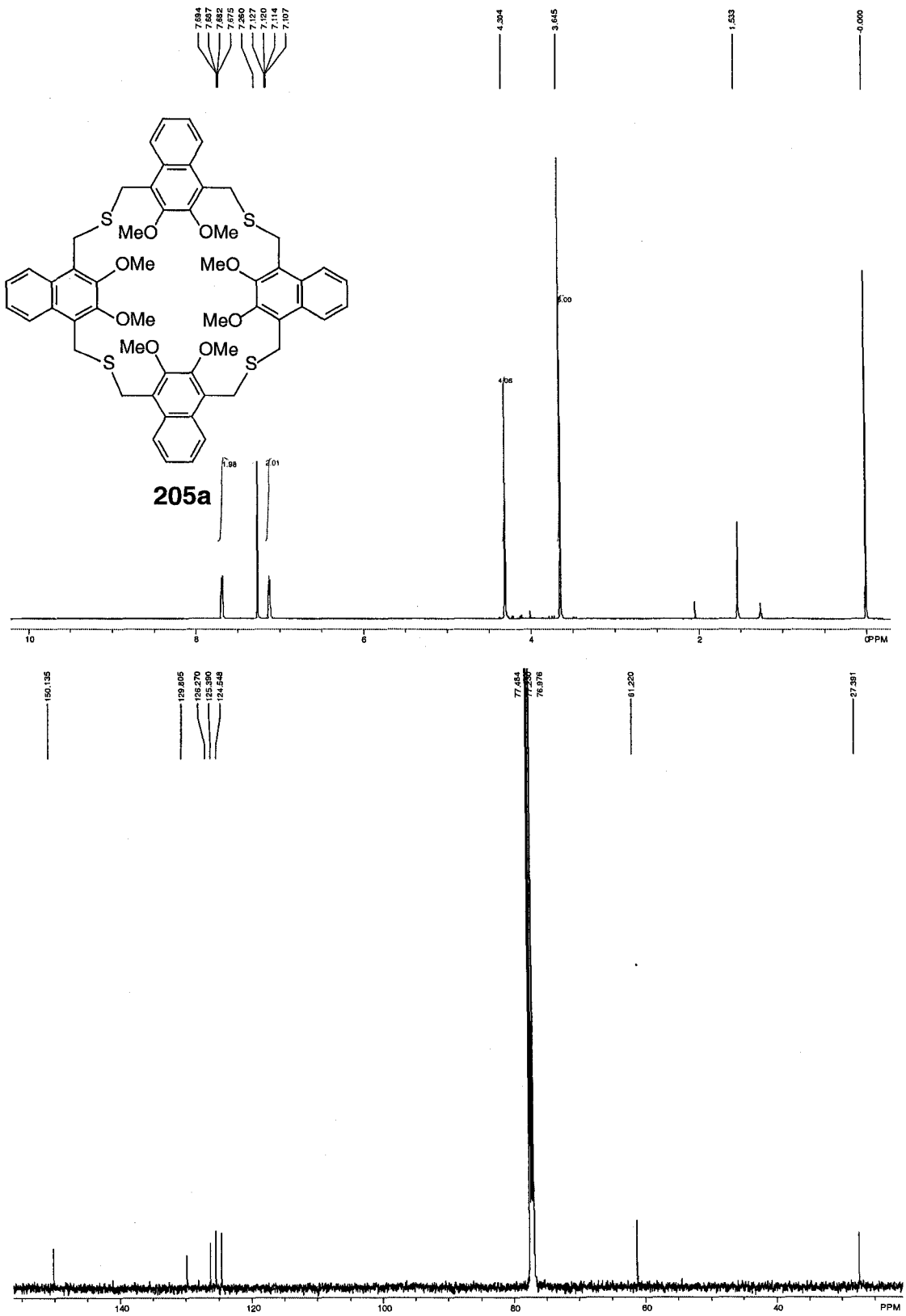
7.894
7.887
7.882
7.875
7.560
7.127
7.120
7.114
7.107
4.394
3.645
1.533
0.000
MeO
OMe
OMe
MeO
OMe
MeO
MeO
OMe
S
S
S
S
205a
1.98
2.01
4.06
6.00
10
8
6
4
2
PPM
150.135
129.805
128.270
125.390
124.548
77.484
77.268
76.976
61.220
27.391
140
120
100
80
60
40
PPM

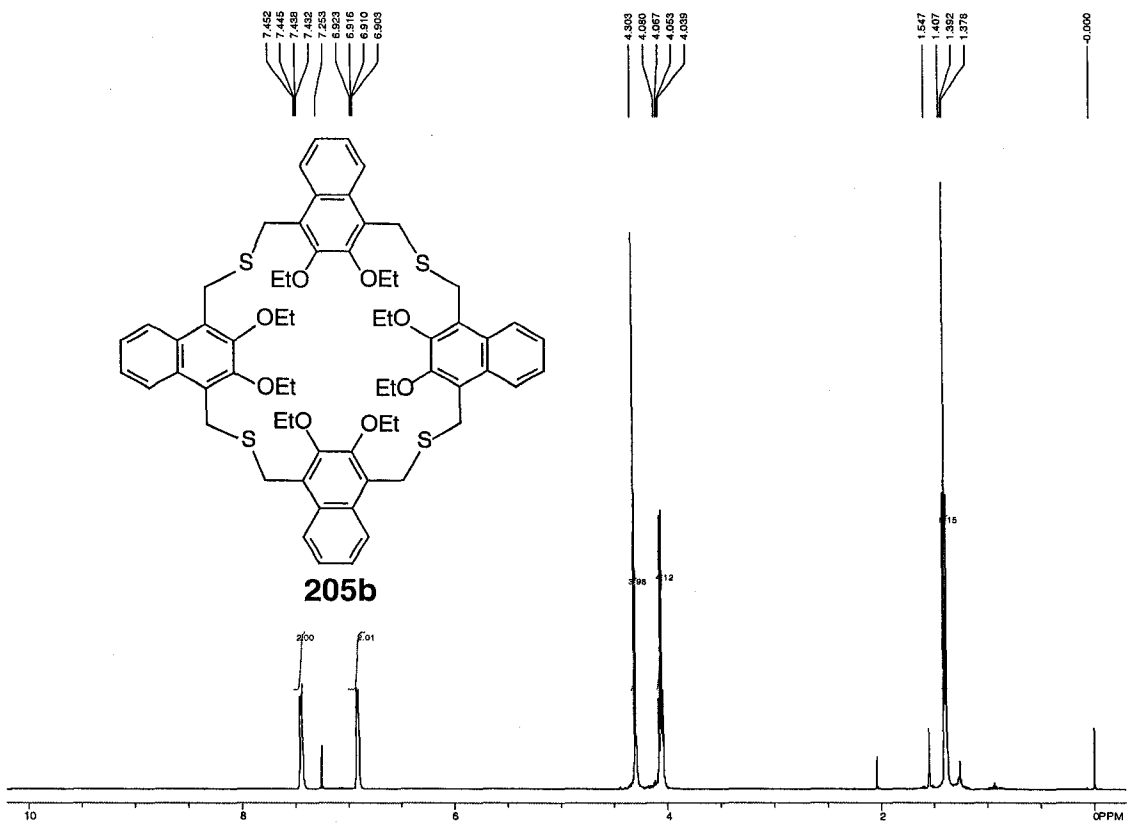
7.452
7.445
7.438
7.432
7.253
6.923
6.916
6.910
6.903
4.303
4.080
4.067
4.053
4.039
1.547
1.407
1.392
1.378
0.000
S
EtO
OEt
S
OEt
EtO
OEt
EtO
EtO
OEt
S
S
205b
2.00
2.01
3.95
4.12
6.15
10
8
6
4
2
0PPM

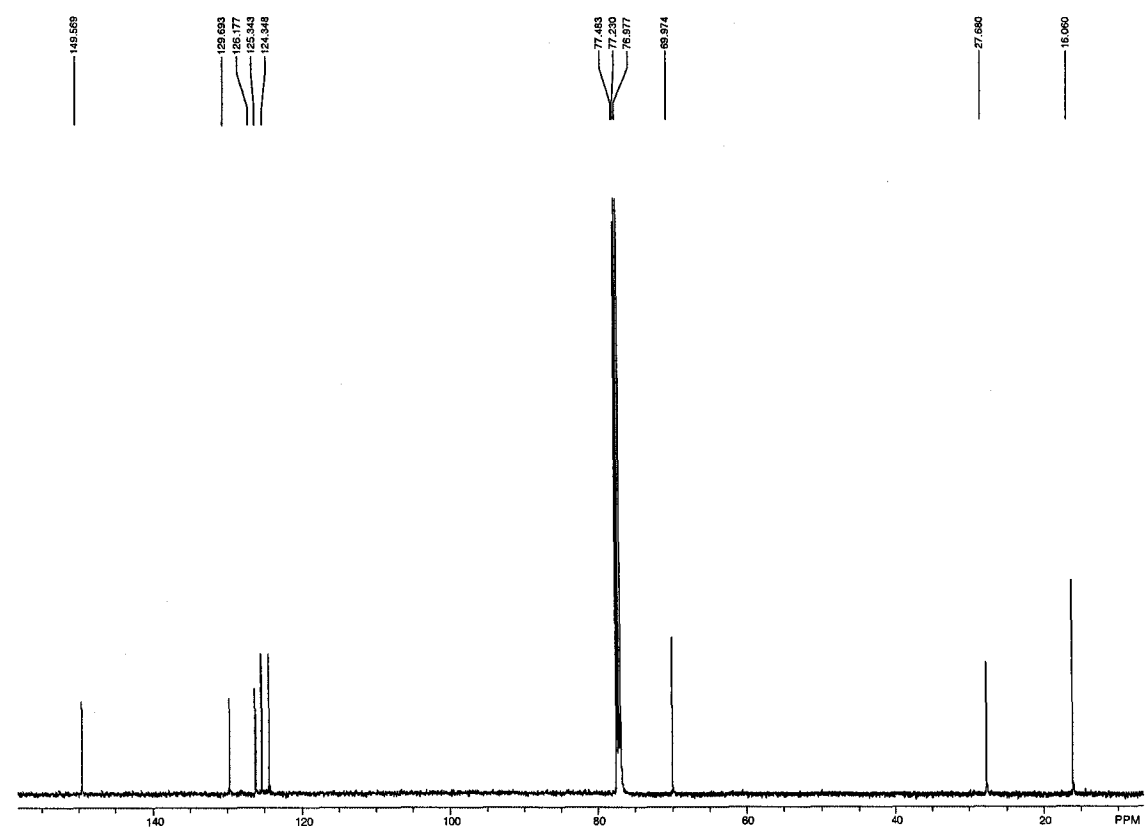
149.569
129.693
126.177
125.343
124.348
77.483
77.230
76.977
69.974
27.680
15.060
140
120
100
80
60
40
20
PPM

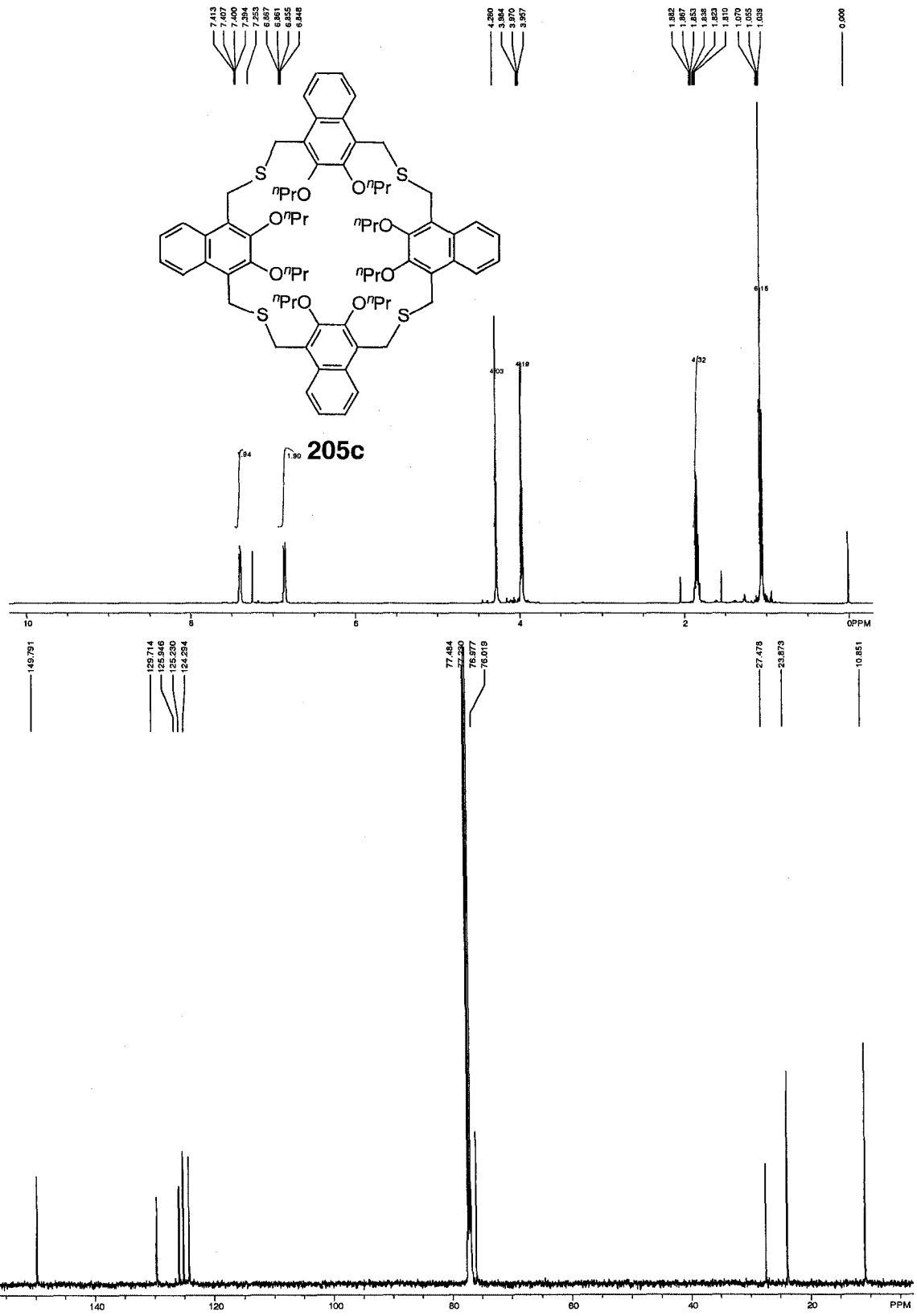
7.413
7.407
7.400
7.394
7.253
6.861
6.855
6.848
4.280
3.984
3.970
3.957
1.882
1.867
1.853
1.838
1.823
1.810
1.070
1.055
1.039
0.000
S
S
S
S
nPrO
OnPr
nPrO
OnPr
OnPr
nPrO
OnPr
nPrO
205c
6.15
4.03
4.19
4.32
1.94
1.80
10
8
6
4
2
0PPM
149.791
129.714
125.946
125.230
124.294
77.484
77.230
76.977
76.019
27.478
23.873
10.851
140
120
100
80
60
40
20
PPM

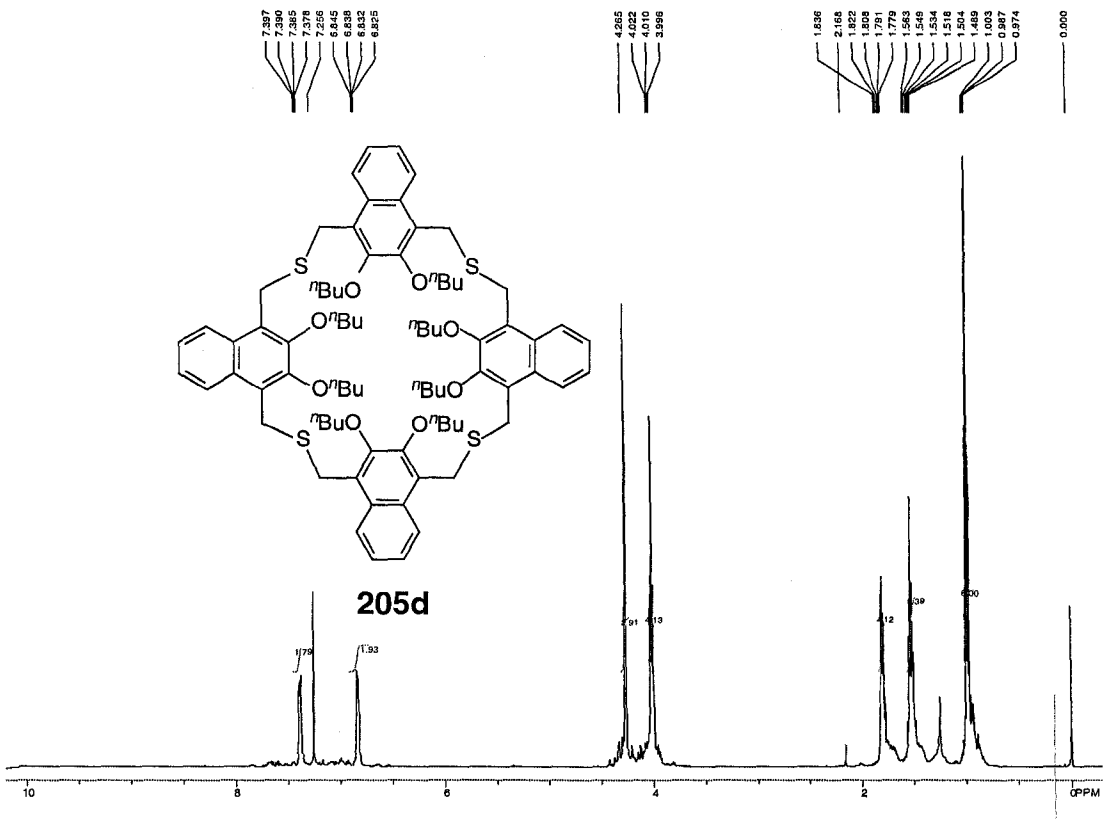
7.397
7.390
7.385
7.378
7.256
6.845
6.838
6.832
6.825
4.265
4.022
4.010
3.996
1.836
2.168
1.822
1.808
1.791
1.779
1.563
1.549
1.534
1.518
1.504
1.489
1.003
0.987
0.974
0.000
S
nBuO
OnBu
OnBu
nBuO
OnBu
nBuO
nBuO
OnBu
S
S
S
205d
1.79
1.93
2.91
4.13
4.12
6.39
10.00
10
8
6
4
2
0PPM

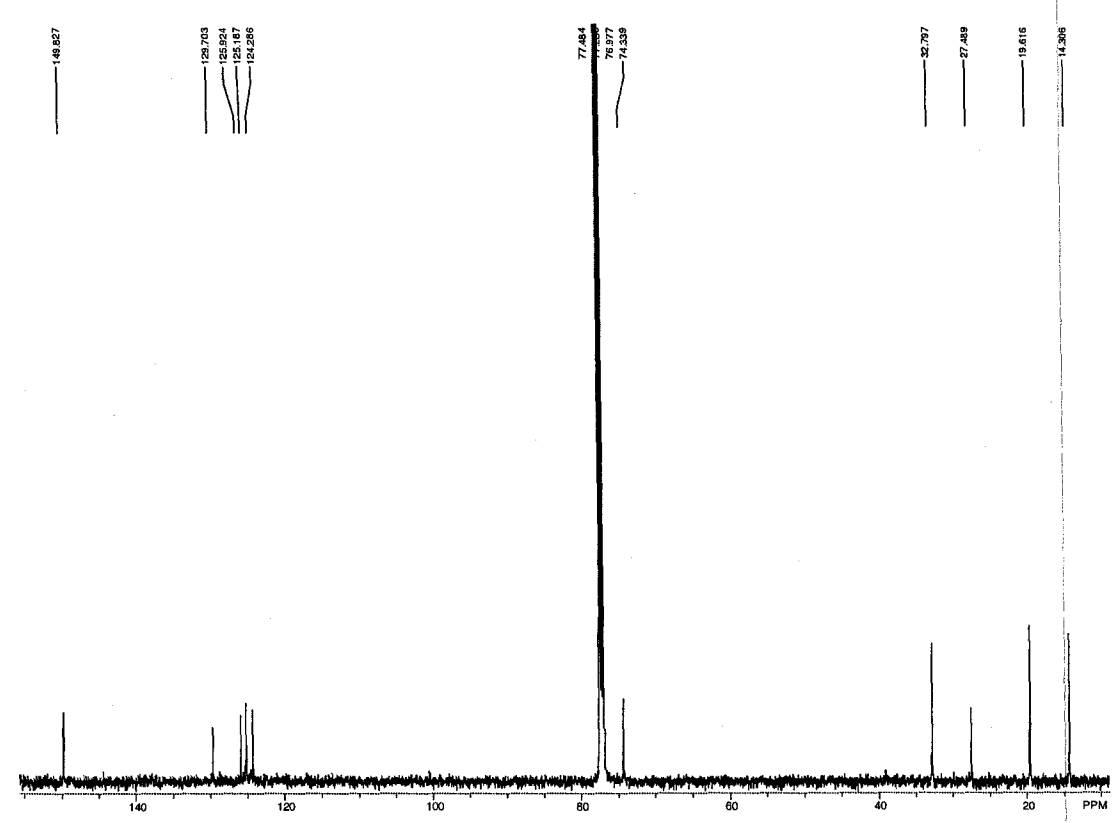
149.827
129.703
125.924
125.187
124.286
77.484
76.977
74.339
32.797
27.489
19.616
14.306
140
120
100
80
60
40
20
PPM

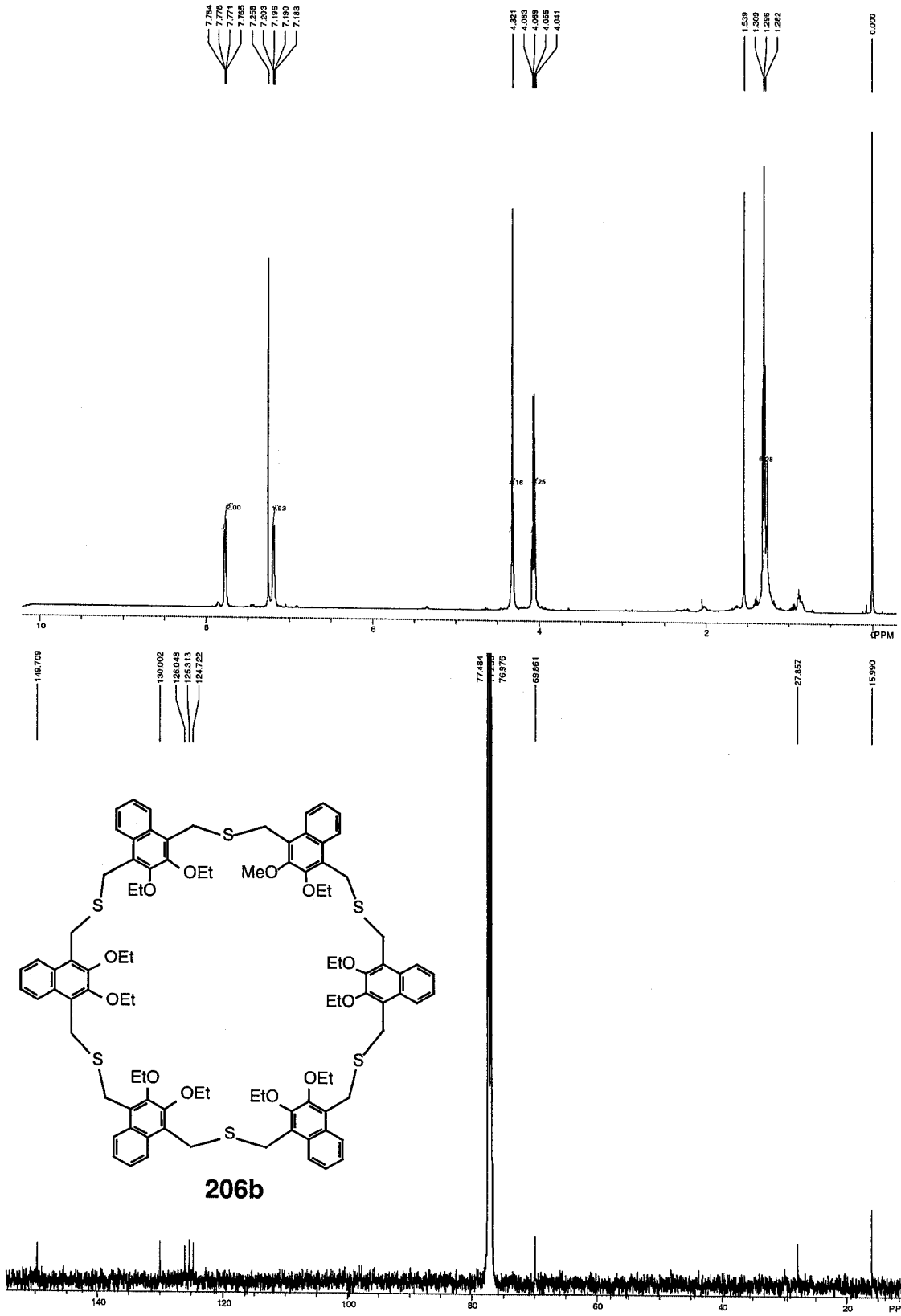
7.784
7.778
7.771
7.765
7.238
7.203
7.196
7.190
7.163
4.321
4.083
4.069
4.055
4.041
1.539
1.309
1.296
1.282
0.000
2.00
1.93
4.16
4.25
6.28
10
8
6
4
2
PPM
149.709
130.002
126.048
125.313
124.722
77.484
76.376
69.861
27.857
15.990
S
OEt
EtO
MeO
206b
140
120
100
80
60
40
20
PPM

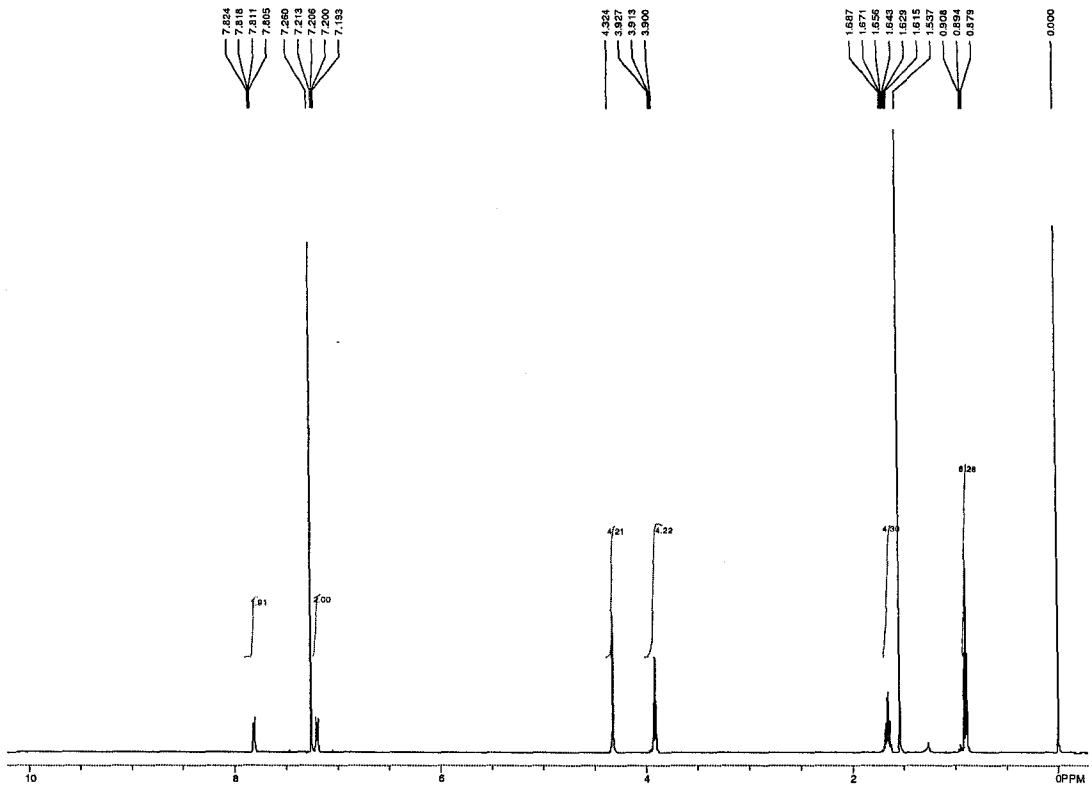

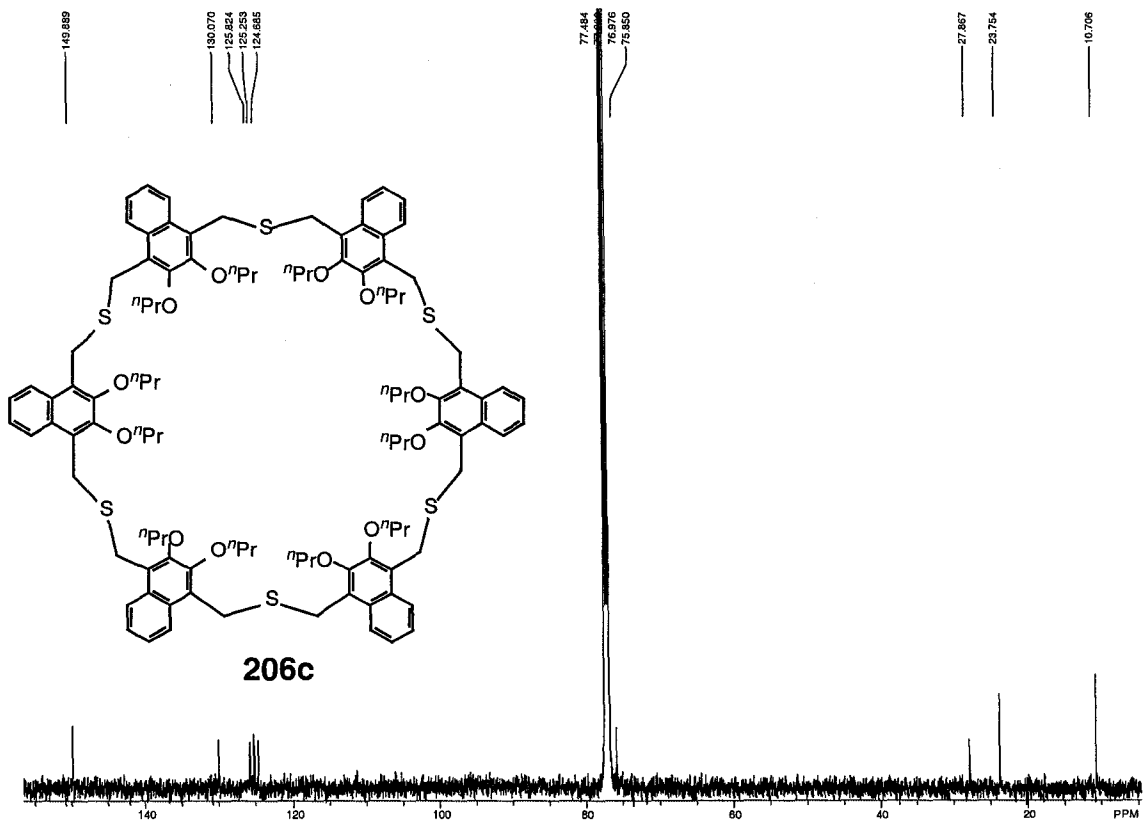

206c

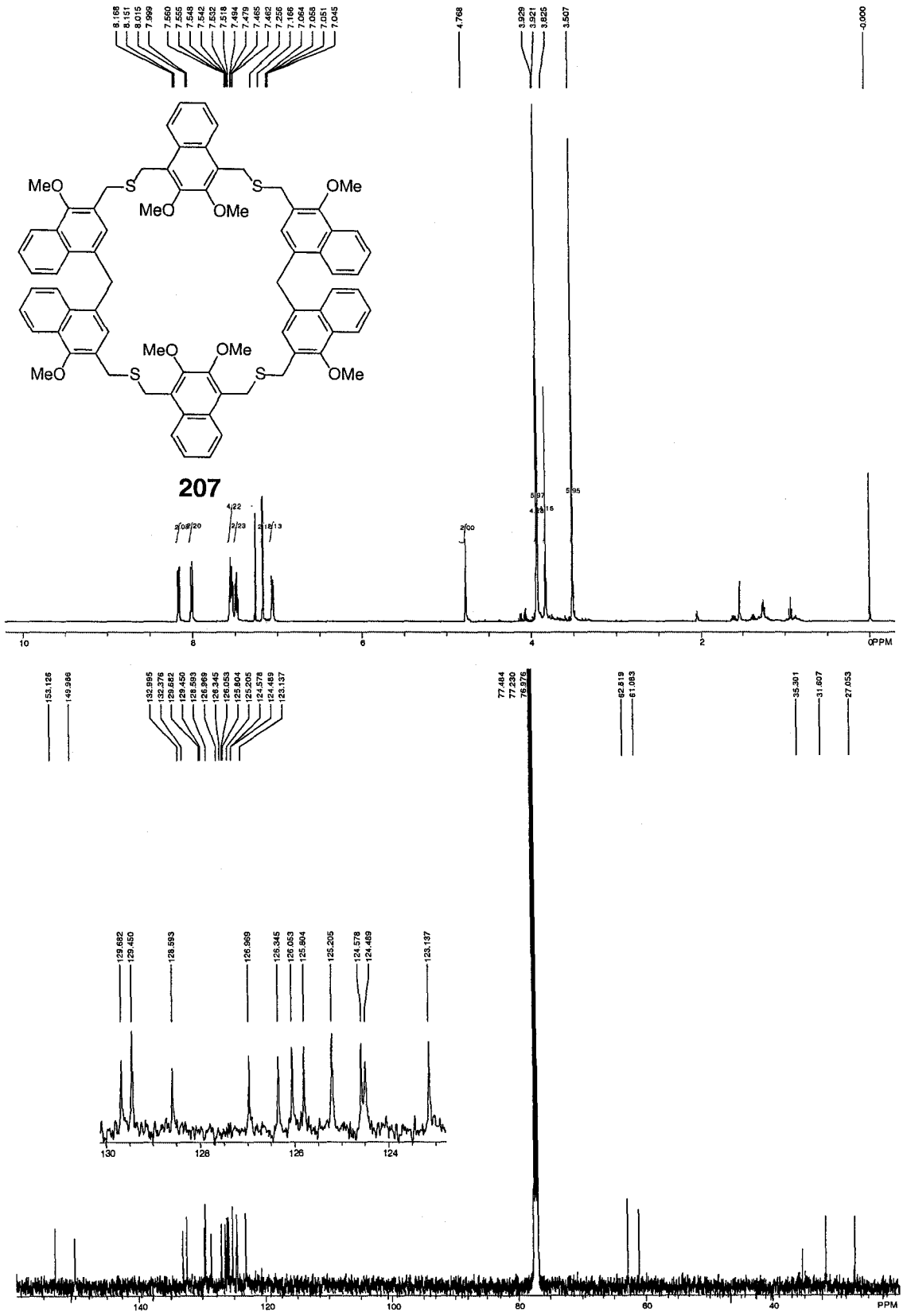
8.168
8.151
8.015
7.999
7.560
7.555
7.548
7.542
7.532
7.518
7.494
7.479
7.465
7.462
7.236
7.166
7.064
7.058
7.051
7.045
4.768
3.929
3.921
3.825
3.507
2.000
MeO
S
OMe
MeO
OMe
207
4.22
2.23
2.18
2.13
2.08
2.20
2.00
5.97
5.95
10
8
6
4
2
0PPM
153.126
149.986
132.995
132.376
129.682
129.450
128.593
126.969
126.345
126.053
125.804
125.205
124.578
124.489
123.137
77.484
77.200
76.916
62.819
61.083
35.301
31.607
27.053
130
128
126
124
140
120
100
80
60
40
PPM

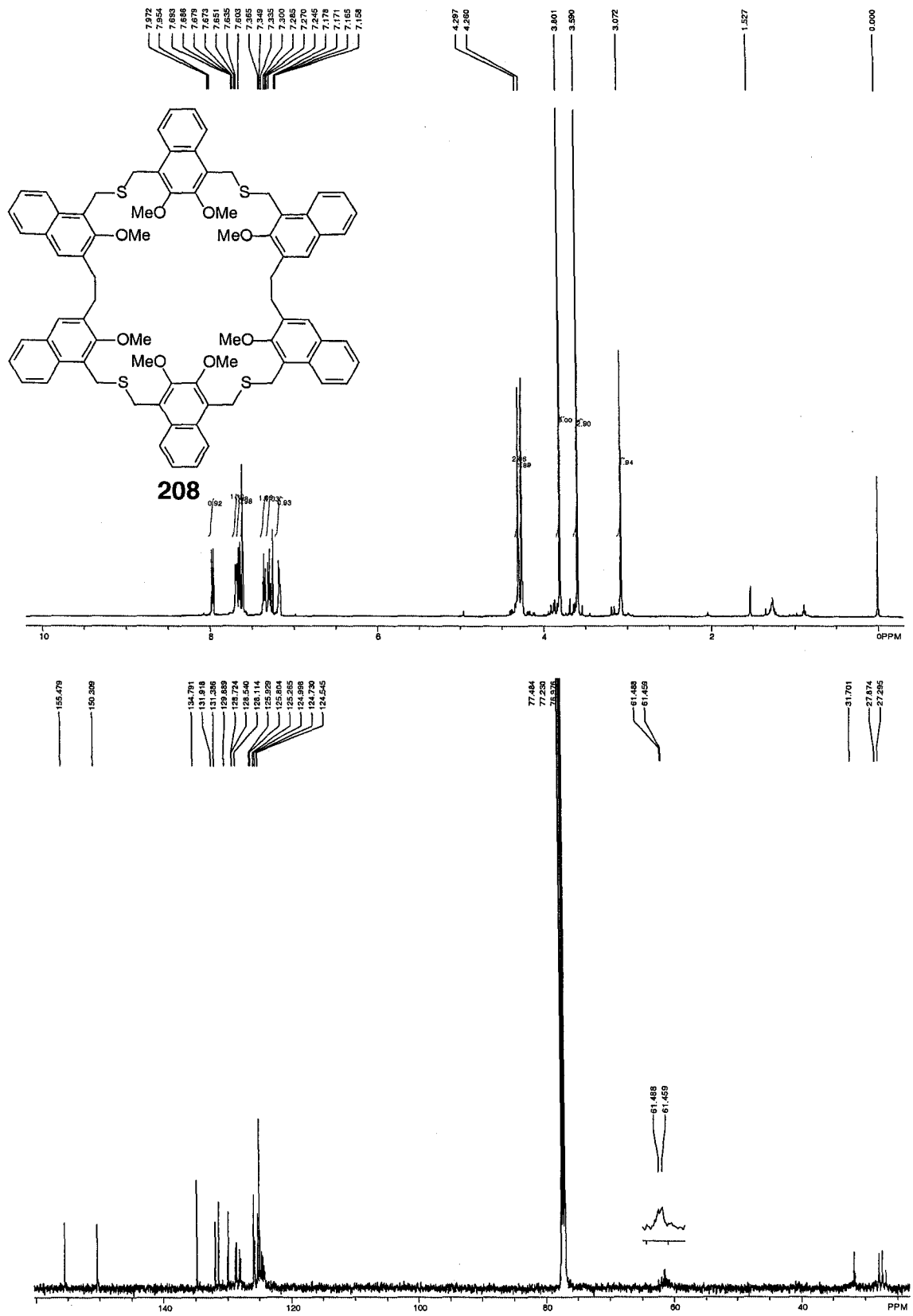
208
MeO
OMe
S
10
8
6
4
2
0PPM
140
120
100
80
60
40
PPM

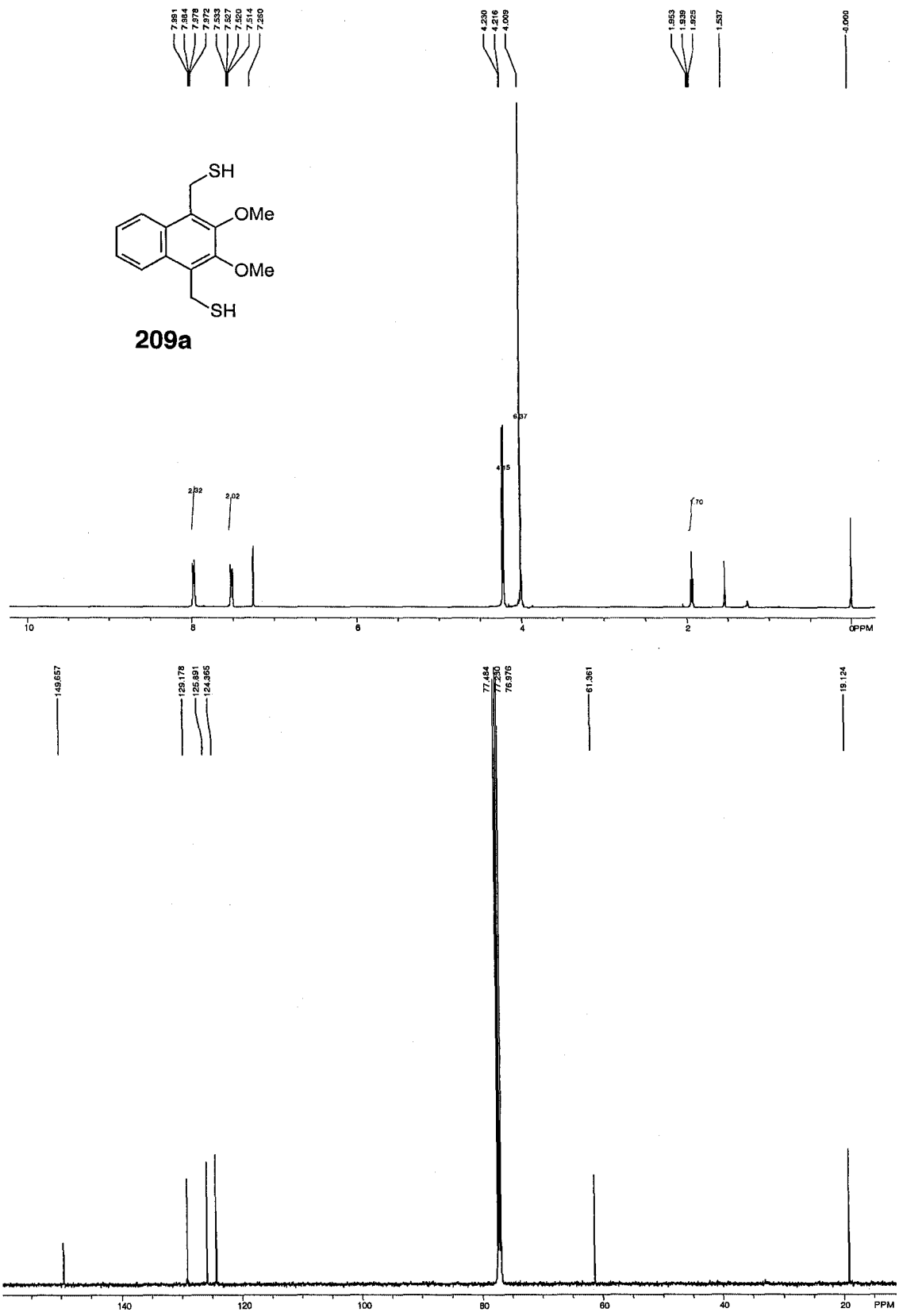
7.981
7.984
7.978
7.972
7.533
7.527
7.520
7.514
7.260
4.230
4.216
4.009
1.953
1.939
1.925
1.537
3.000
SH
OMe
OMe
SH
209a
6.37
4.35
2.32
2.02
1.70
10
8
6
4
2
0PPM
149.657
129.178
125.891
124.365
77.484
77.260
76.976
61.361
19.124
140
120
100
80
60
40
20
PPM

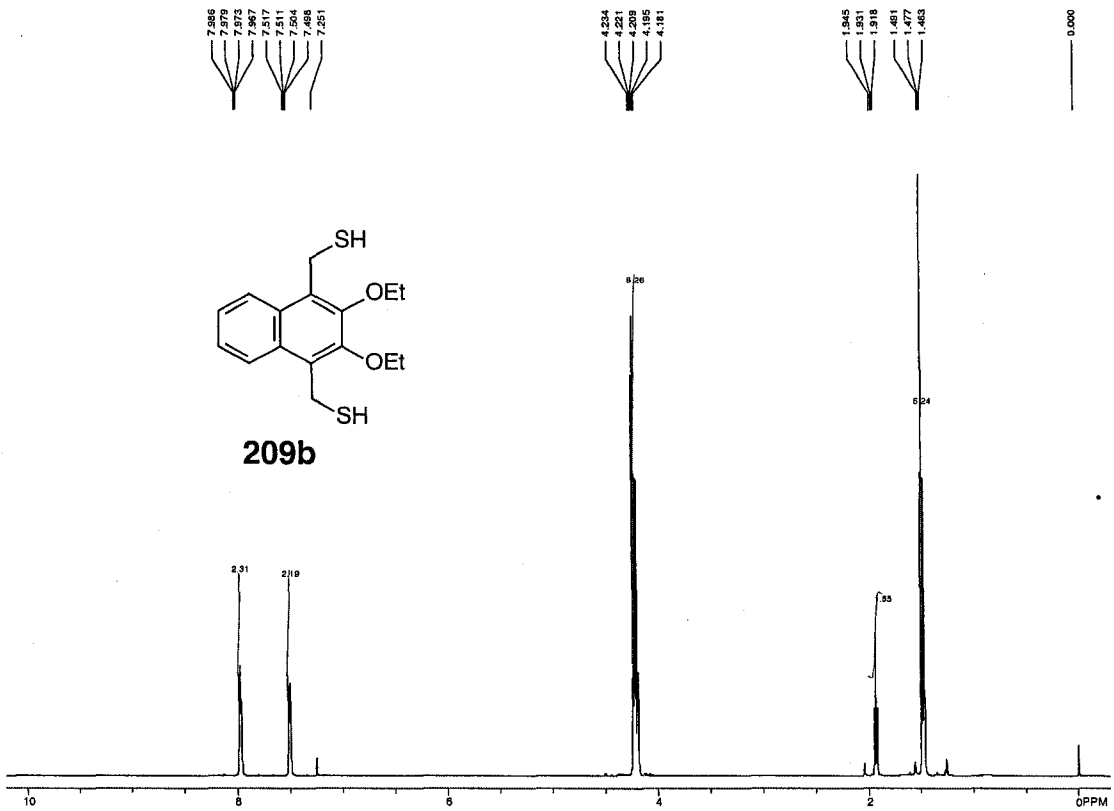
7.986
7.979
7.973
7.967
7.517
7.511
7.504
7.488
7.251
4.234
4.221
4.208
4.195
4.181
1.945
1.931
1.918
1.481
1.477
1.463
0.000
SH
OEt
OEt
SH
8.26
6.24
2.31
2.19
1.55
10
8
6
4
2
0PPM

209b

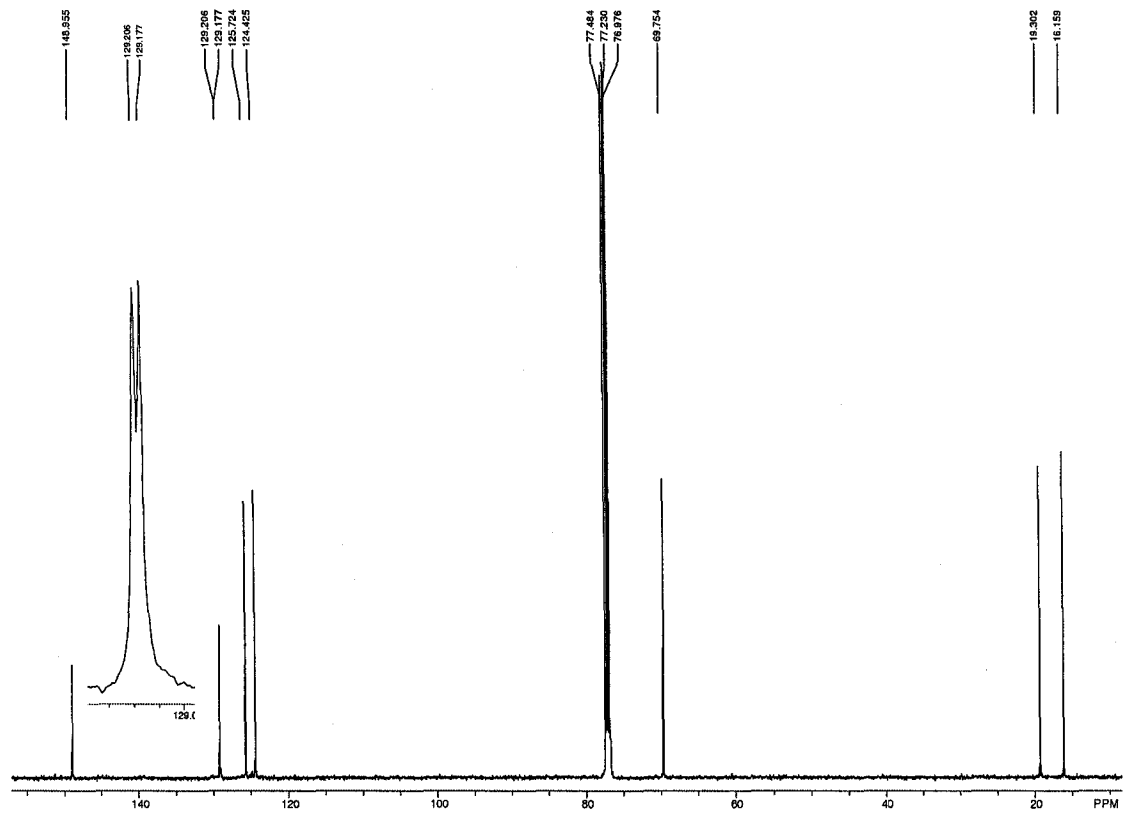
146.955
129.206
129.177
125.724
124.425
77.484
77.230
76.976
69.754
19.302
16.159
140
120
100
80
60
40
20
PPM

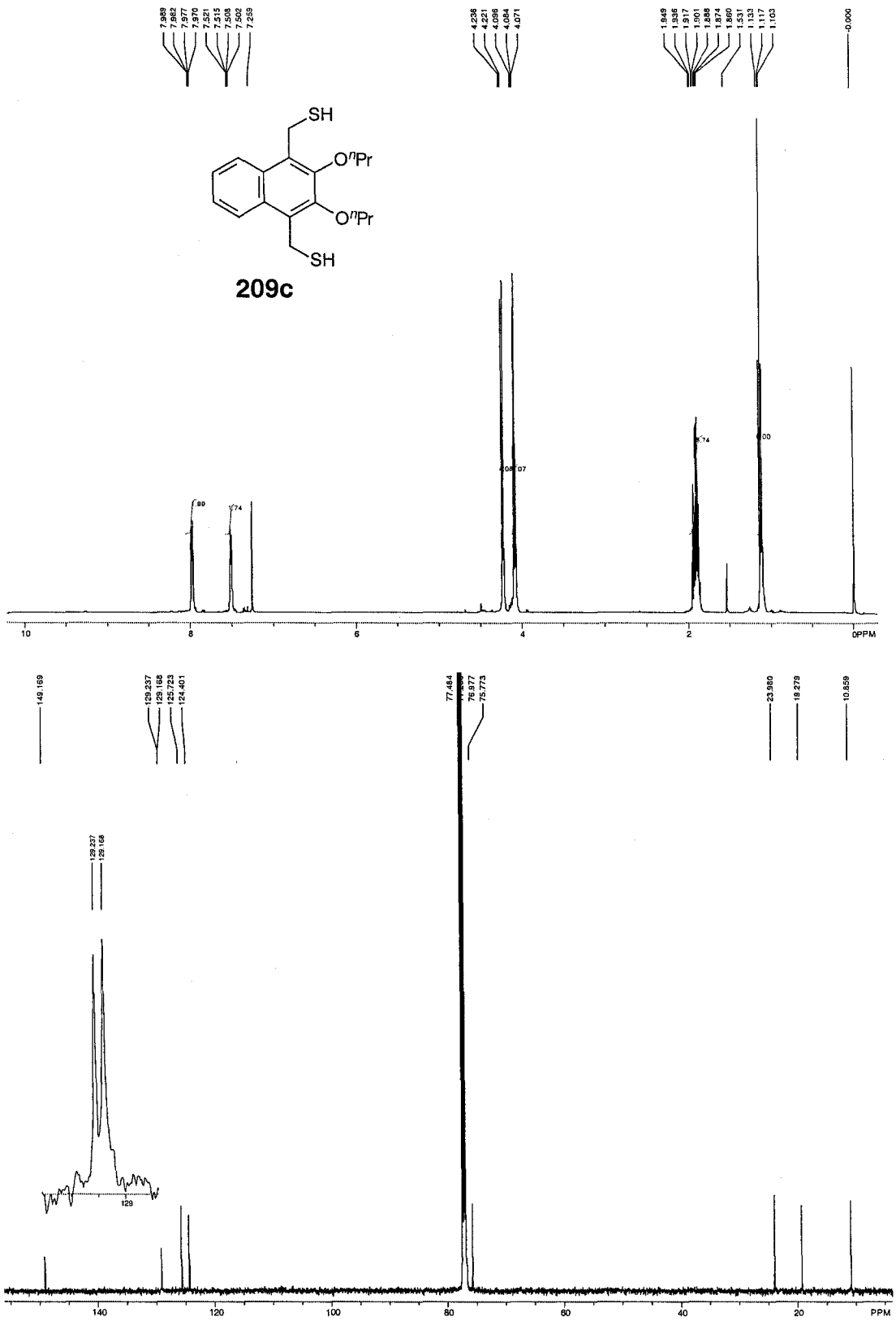
SH
O^{n}Pr
O^{n}Pr
SH
209c

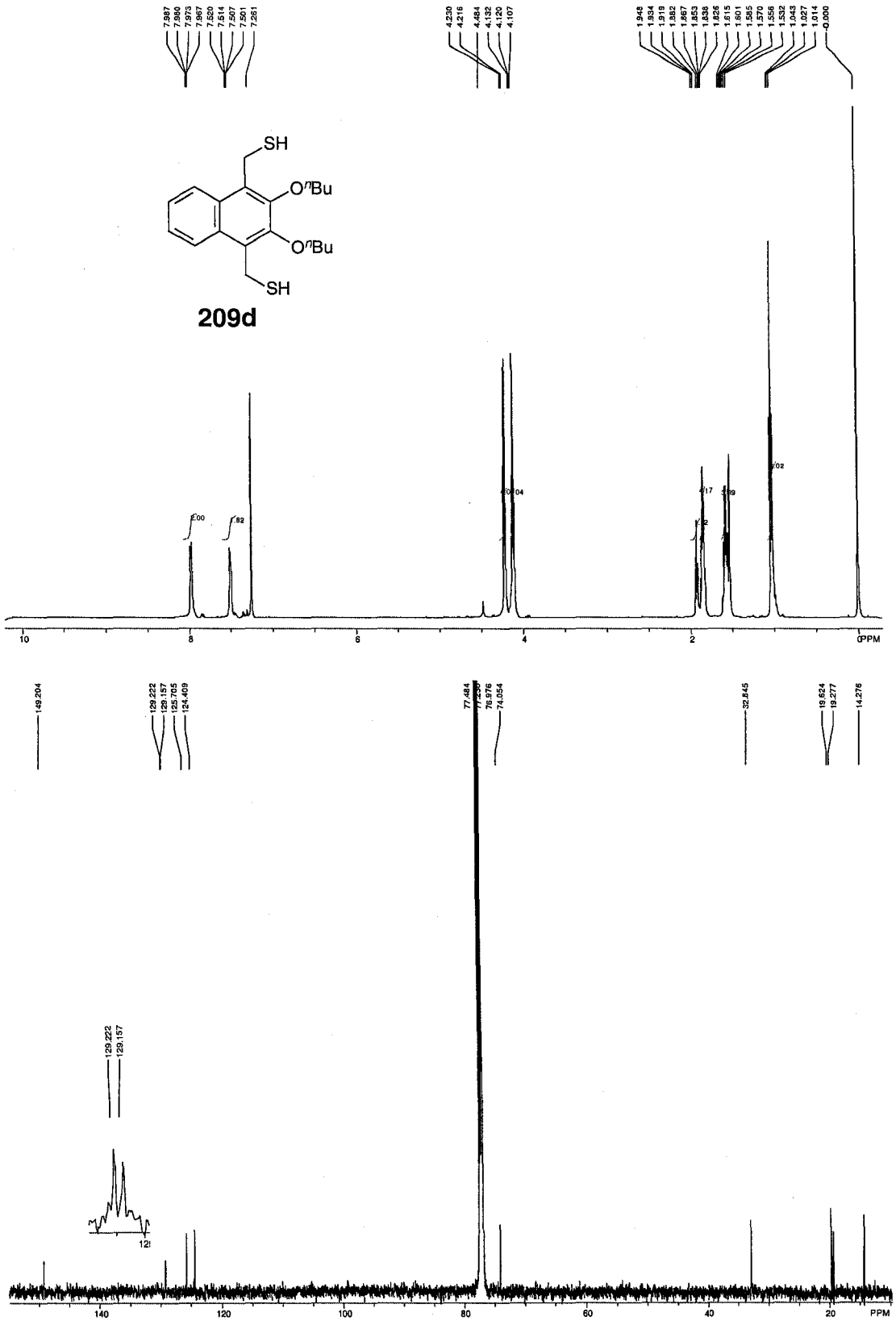
SH
O^{n}Bu
O^{n}Bu
SH
209d
PPM
PPM

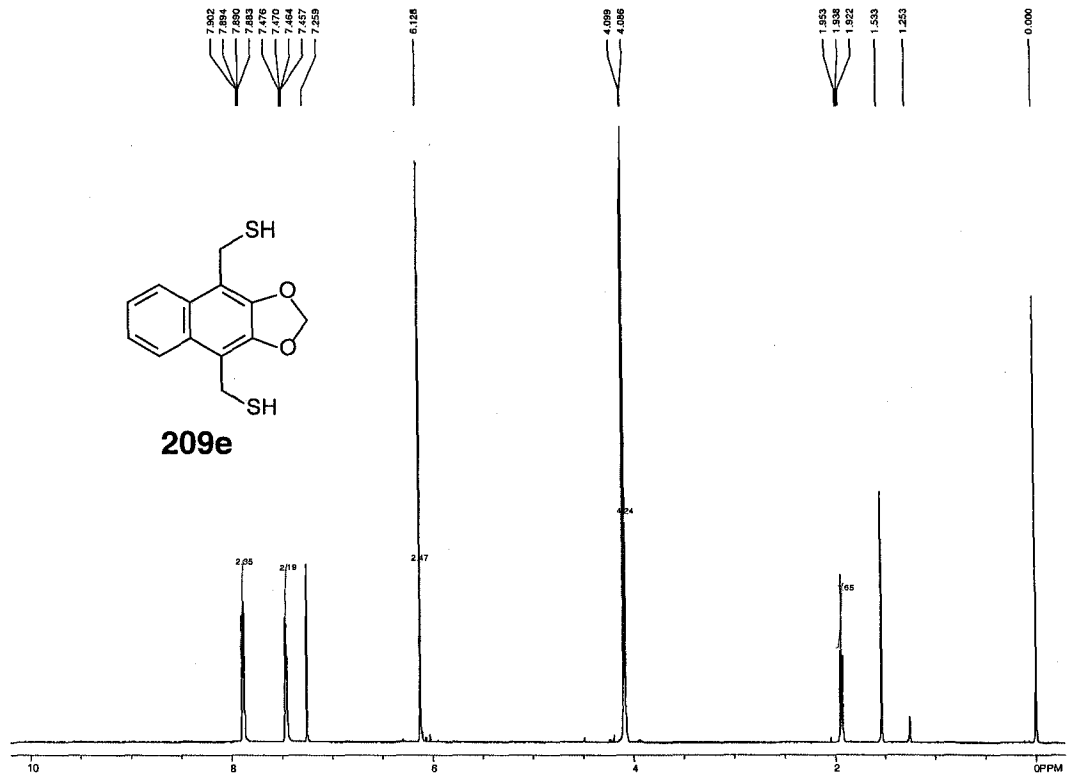
7.902
7.894
7.890
7.883
7.476
7.470
7.464
7.457
7.259
6.128
4.099
4.086
1.953
1.938
1.922
1.533
1.253
0.000
SH
O
O
SH
209e
2.05
2.19
2.47
4.24
1.65
10
8
6
4
2
0PPM

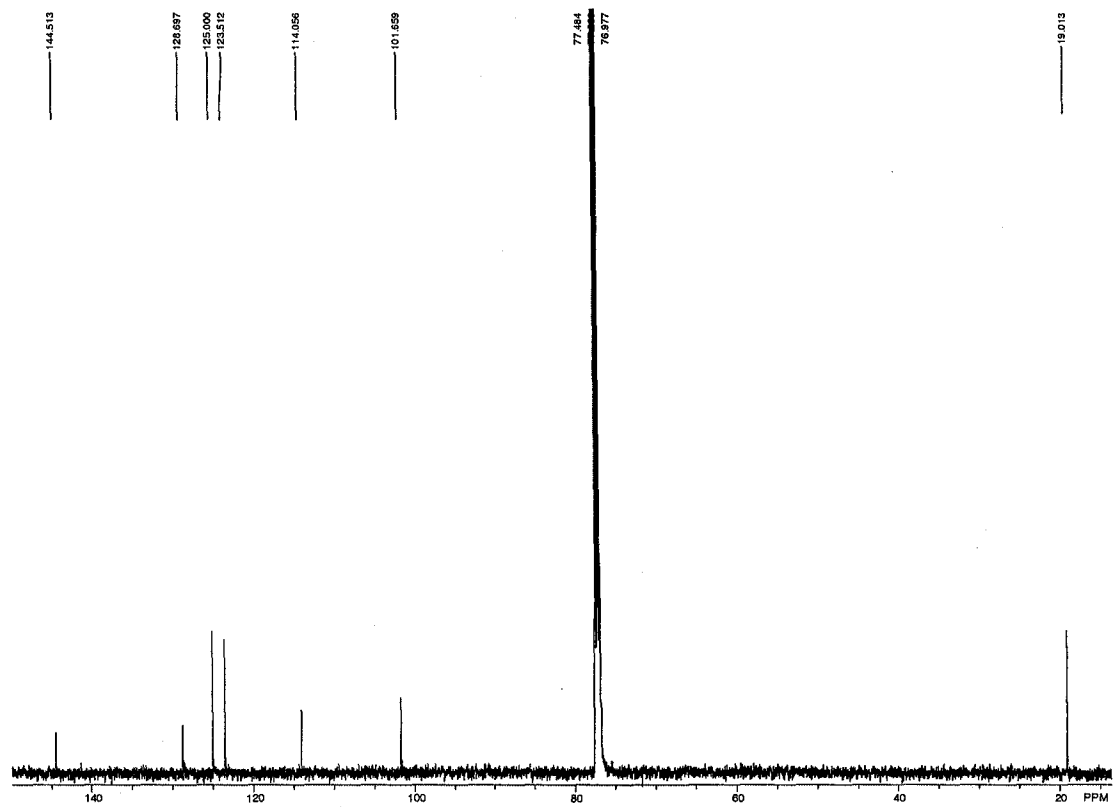
144.513
128.697
125.000
123.512
114.056
101.659
77.484
76.977
19.013
140
120
100
80
60
40
20
PPM

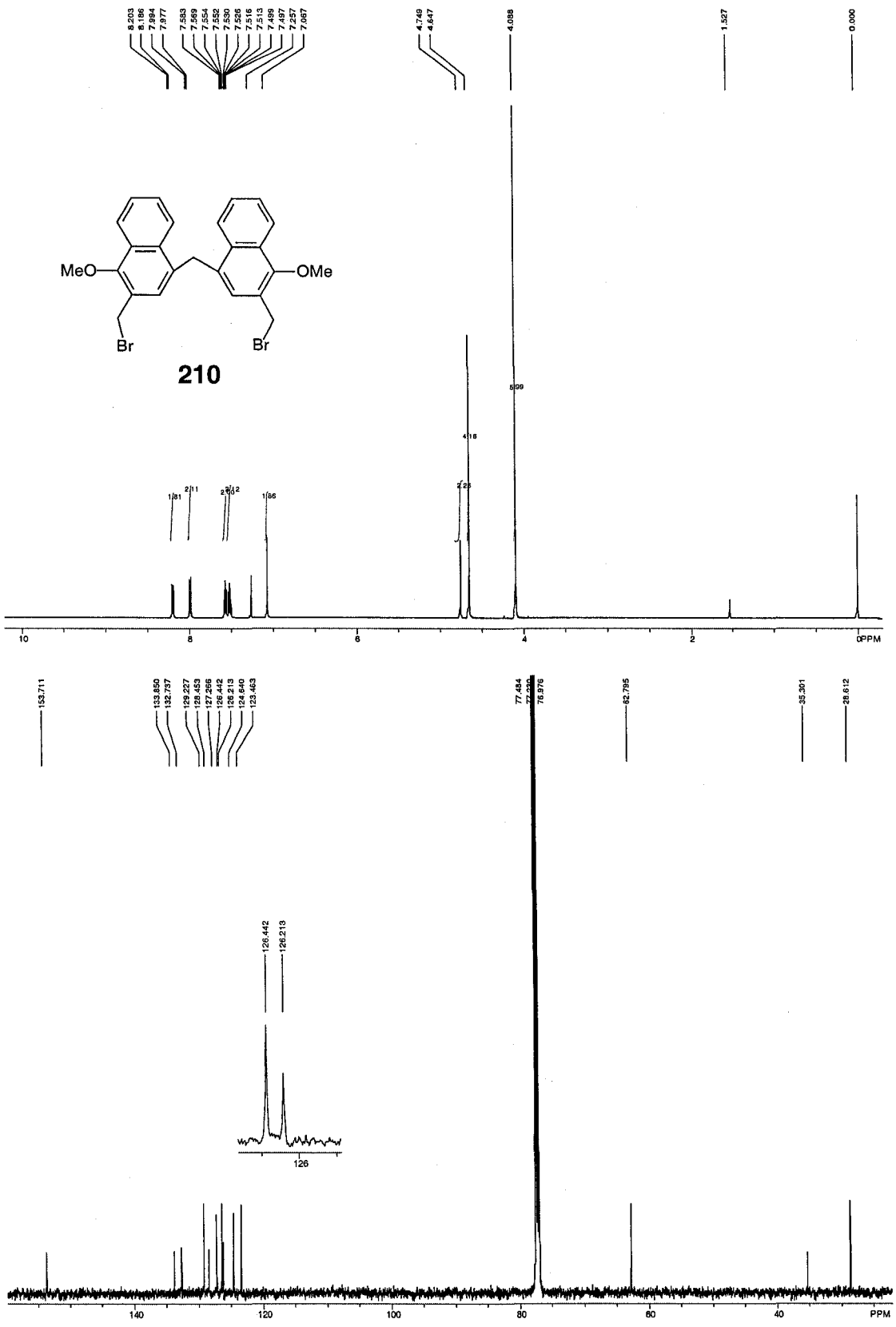
MeO
OMe
Br
Br
210

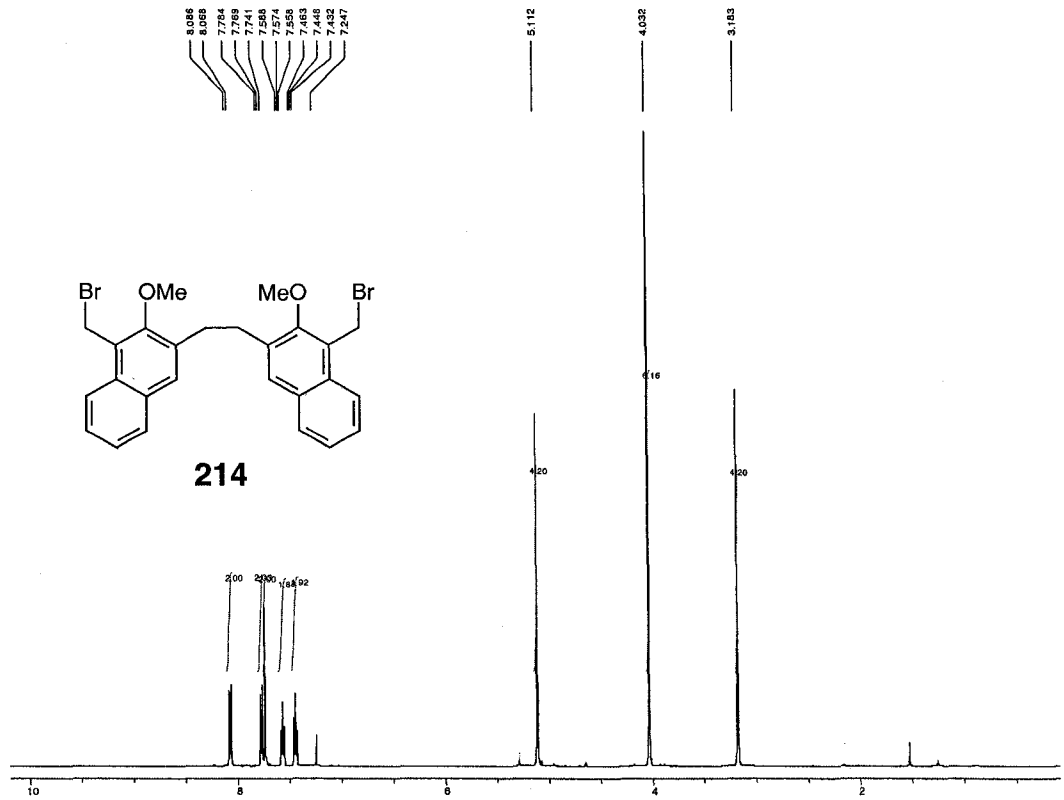
8.086
8.065
7.794
7.769
7.741
7.588
7.574
7.558
7.463
7.446
7.432
7.247
5.112
4.032
3.183
Br
OMe
MeO
Br
214
4.20
4.16
4.20
2.00
2.00
1.84
1.92
10
8
6
4
2

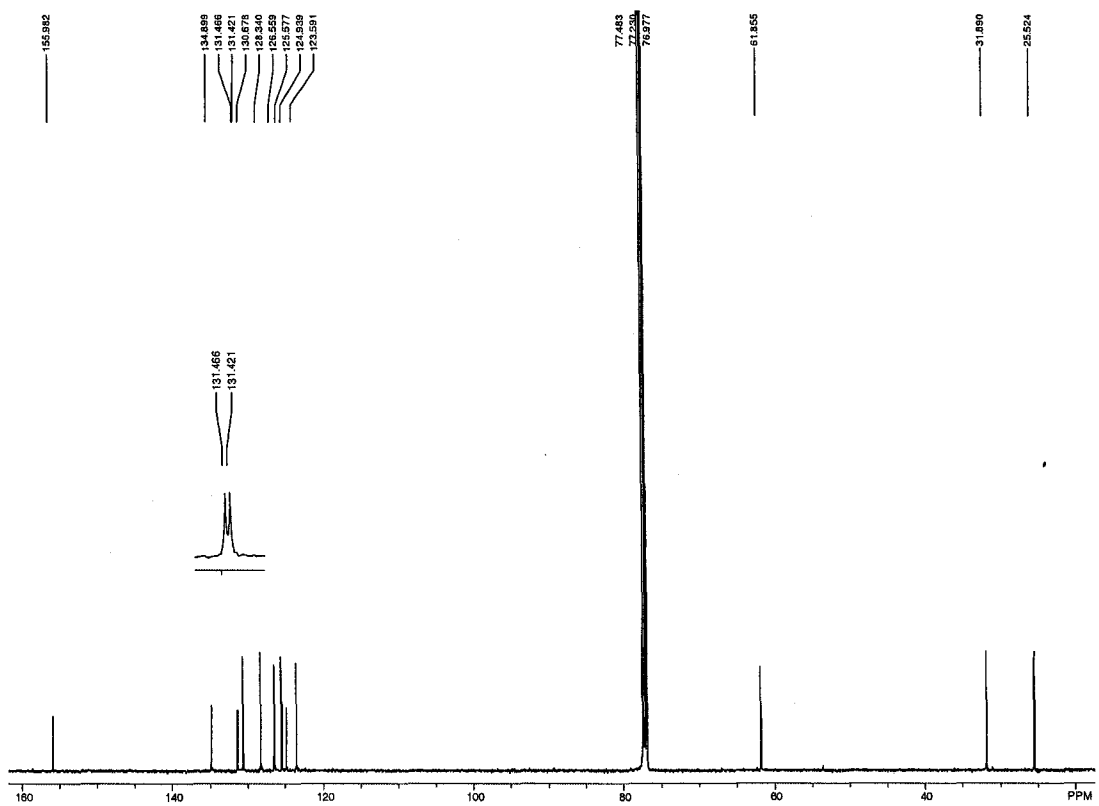
155.982
134.899
131.466
131.421
130.678
128.340
126.559
125.577
124.939
123.591
77.483
77.266
76.977
61.855
31.890
25.524
131.466
131.421
160
140
120
100
80
60
40
PPM

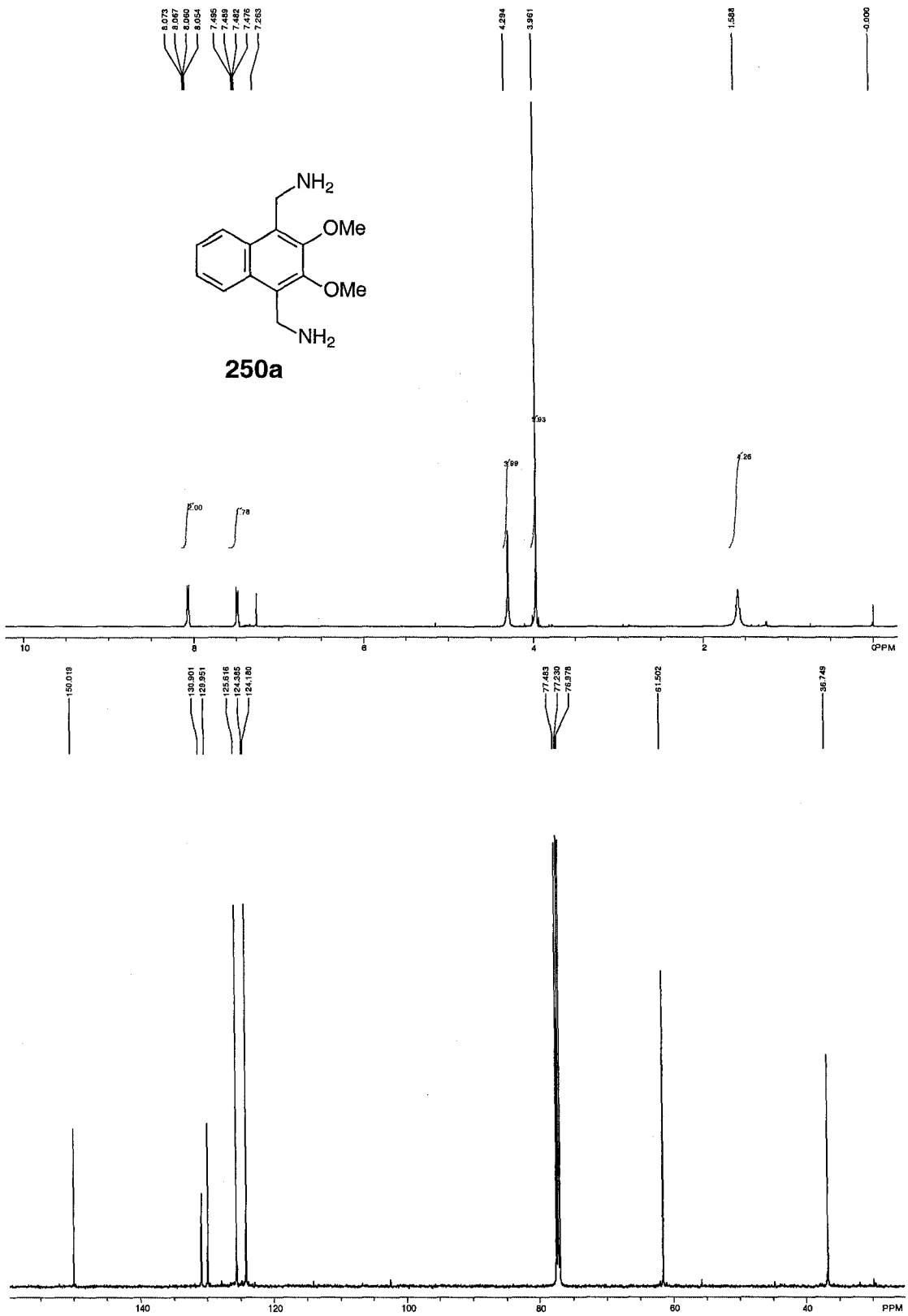
8.073
8.067
8.060
8.054
7.495
7.489
7.482
7.476
7.263
4.294
3.961
1.588
0.000
NH2
OMe
OMe
NH2
250a
2.00
1.78
3.99
1.93
4.26
10
8
6
4
2
0PPM
150.018
130.901
129.951
125.616
124.385
124.180
77.483
77.230
76.978
61.502
36.749
140
120
100
80
60
40
PPM

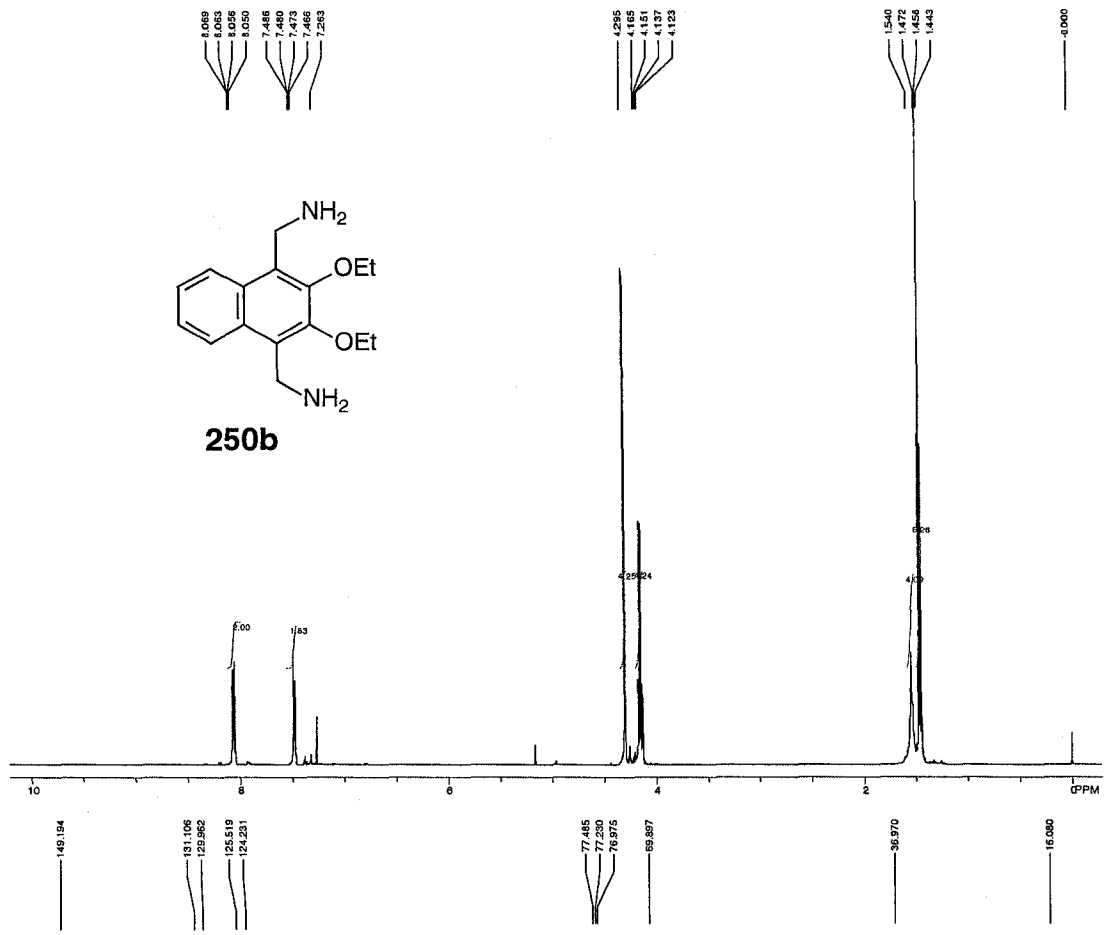
8.069
8.063
8.056
8.050
7.486
7.480
7.473
7.466
7.263
4.295
4.165
4.151
4.137
4.123
1.540
1.472
1.458
1.443
0.000
NH2
OEt
OEt
NH2
250b
5.00
1.63
10
8
6
4
2
0PPM
149.194
131.106
129.962
125.519
124.231
77.485
77.230
76.975
69.897
36.970
16.080

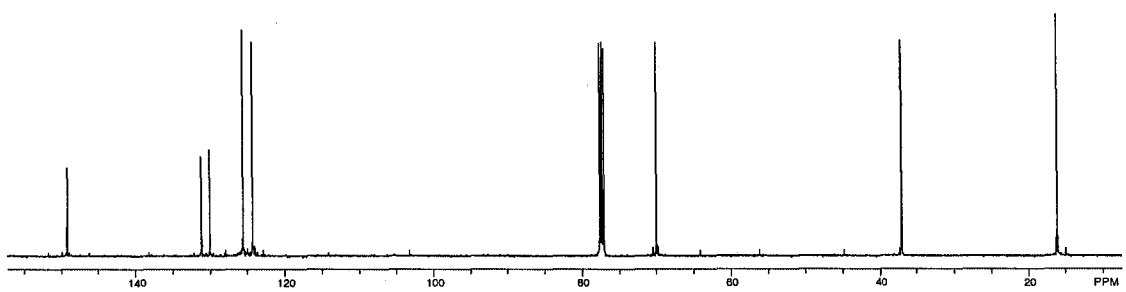
140
120
100
80
60
40
20
PPM

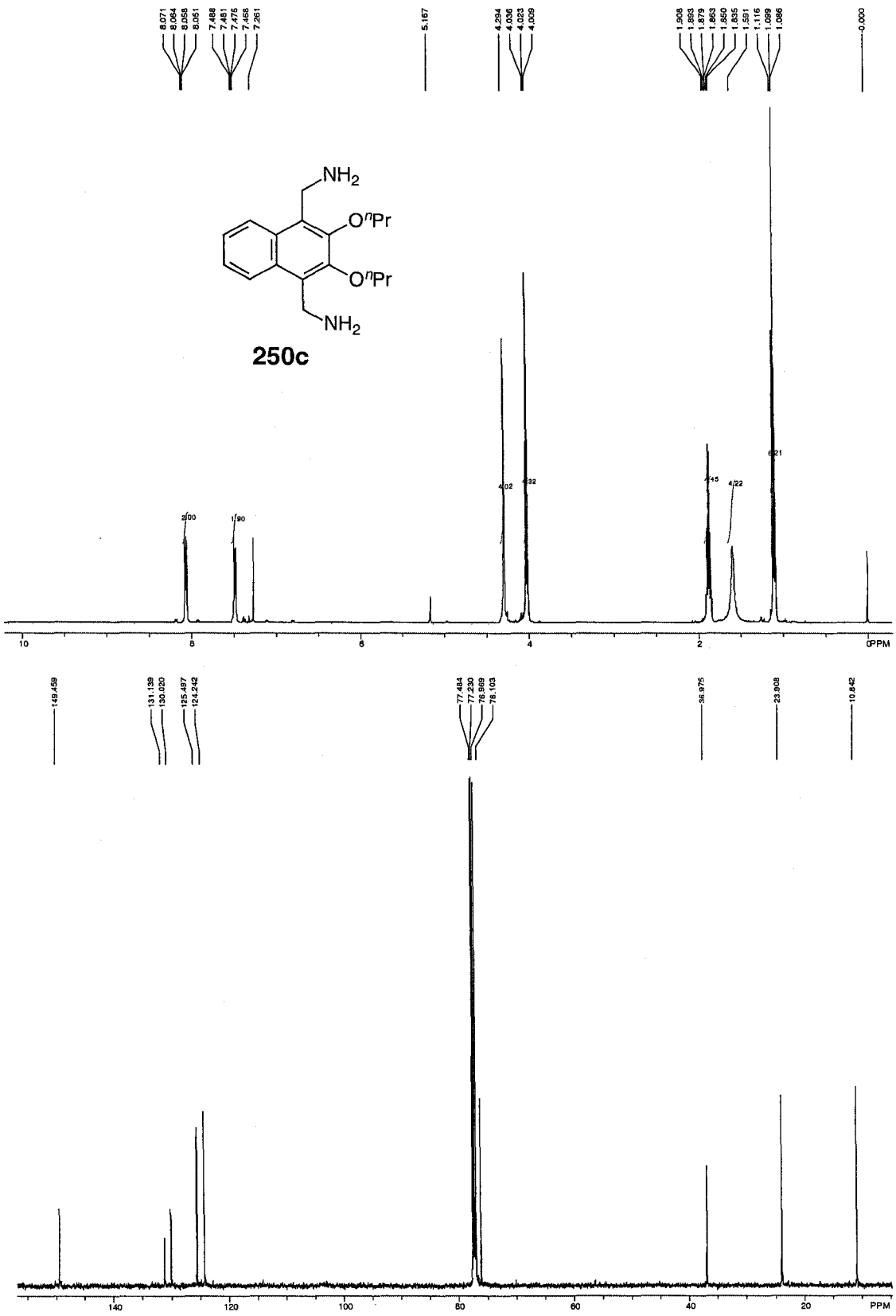
8.071
8.064
8.058
8.051
7.488
7.481
7.475
7.468
7.261
5.167
4.294
4.036
4.023
4.009
1.908
1.893
1.879
1.863
1.850
1.835
1.591
1.116
1.099
1.086
0.000
NH2
OnPr
OnPr
NH2
250c
2.00
1.90
4.02
4.32
4.45
4.22
6.21
10
8
6
4
2
0PPM
149.459
131.139
130.020
125.497
124.242
77.484
77.230
76.969
76.103
36.975
23.908
10.842
140
120
100
80
60
40
20
PPM

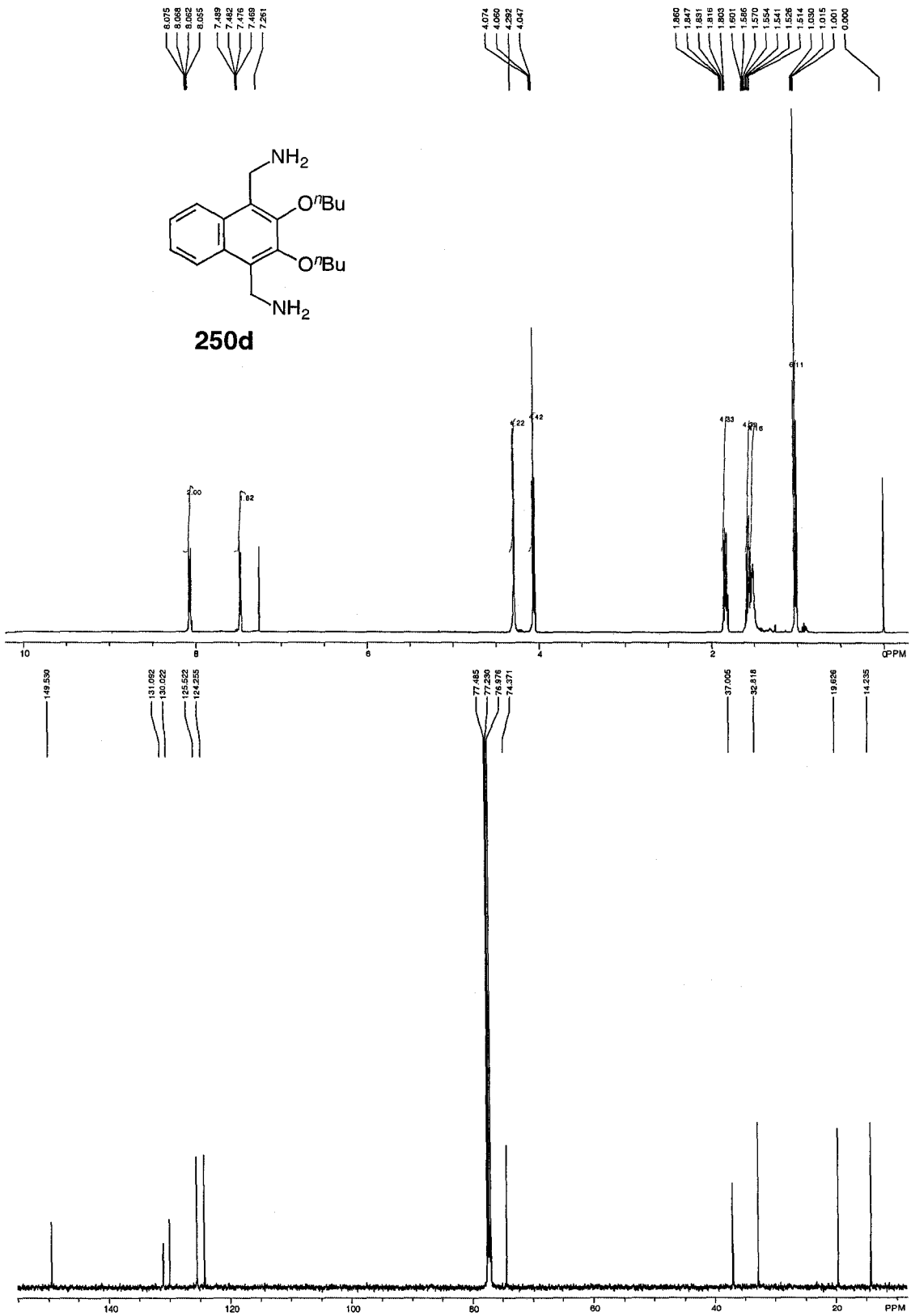
8.075
8.068
8.062
8.055
7.489
7.482
7.476
7.469
7.261
4.074
4.060
4.292
4.047
1.860
1.847
1.831
1.816
1.803
1.601
1.586
1.570
1.554
1.541
1.526
1.514
1.030
1.015
1.001
0.000
NH2
OnBu
OnBu
NH2
250d
2.00
1.82
4.22
4.12
4.33
4.28
4.16
6.11
10
8
6
4
2
0
PPM
149.530
131.092
130.022
125.522
124.255
77.485
77.230
76.976
74.371
37.005
32.818
19.626
14.235
140
120
100
80
60
40
20
PPM

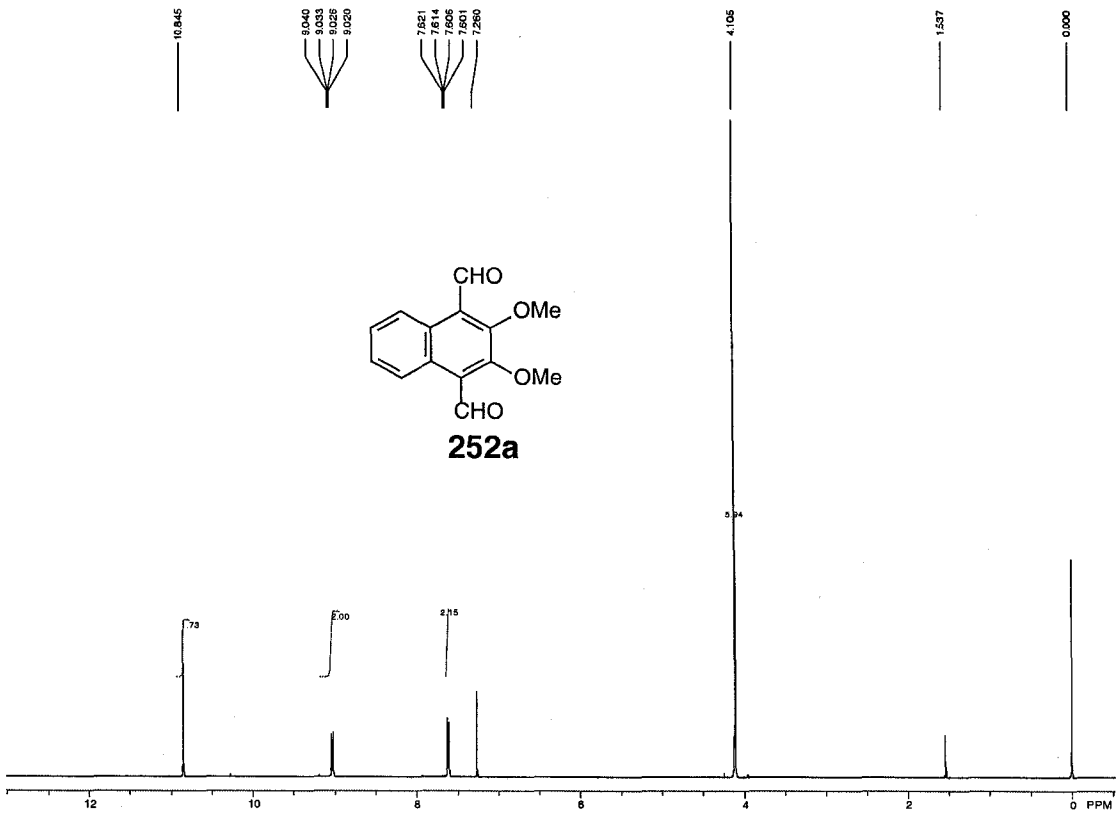
10.845
9.040
9.033
9.026
9.020
7.621
7.614
7.606
7.601
7.260
4.106
1.537
0.000
CHO
OMe
OMe
CHO
252a
5.94
1.73
2.00
2.15
12
10
8
6
4
2
0 PPM

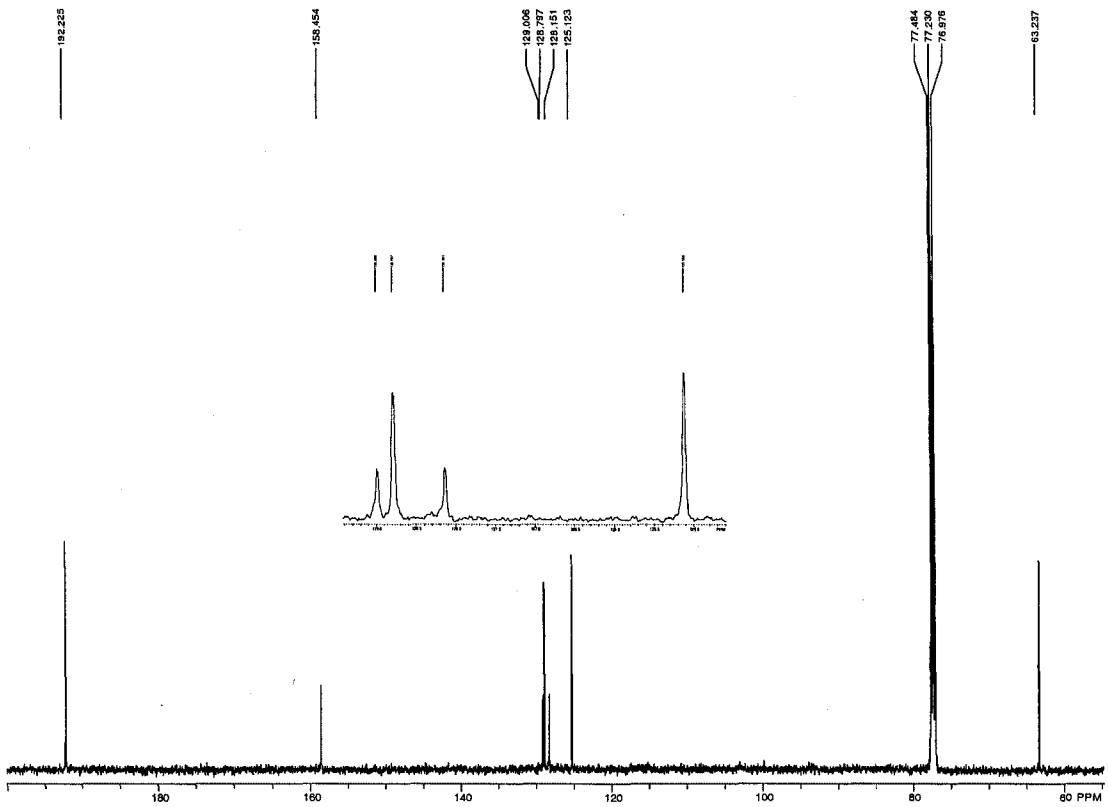
192.225
158.454
129.006
128.797
128.151
125.123
77.484
77.230
76.976
63.237
180
160
140
120
100
80
60 PPM

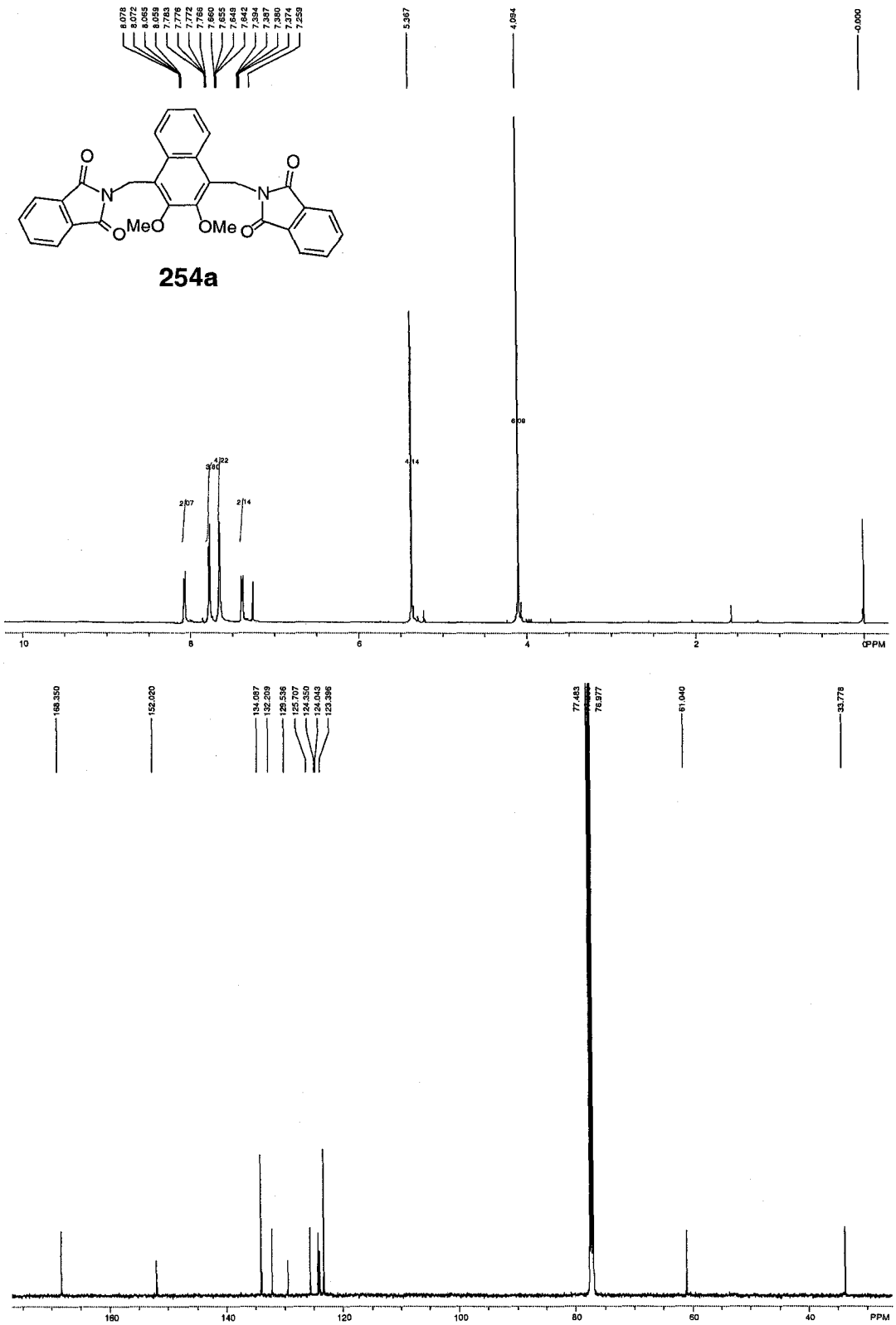
8.078
8.072
8.065
8.059
7.783
7.776
7.772
7.766
7.660
7.655
7.648
7.642
7.394
7.387
7.380
7.374
7.259
5.367
4.094
0.000
O
N
O
MeO
OMe
O
N
O
O
254a
6.08
4.14
4.22
3.80
2.07
2.14
10
8
6
4
2
0PPM
168.350
152.020
134.087
132.209
129.536
125.707
124.350
124.043
123.396
77.483
77.158
76.977
61.040
33.778
180
140
120
100
80
60
40
PPM

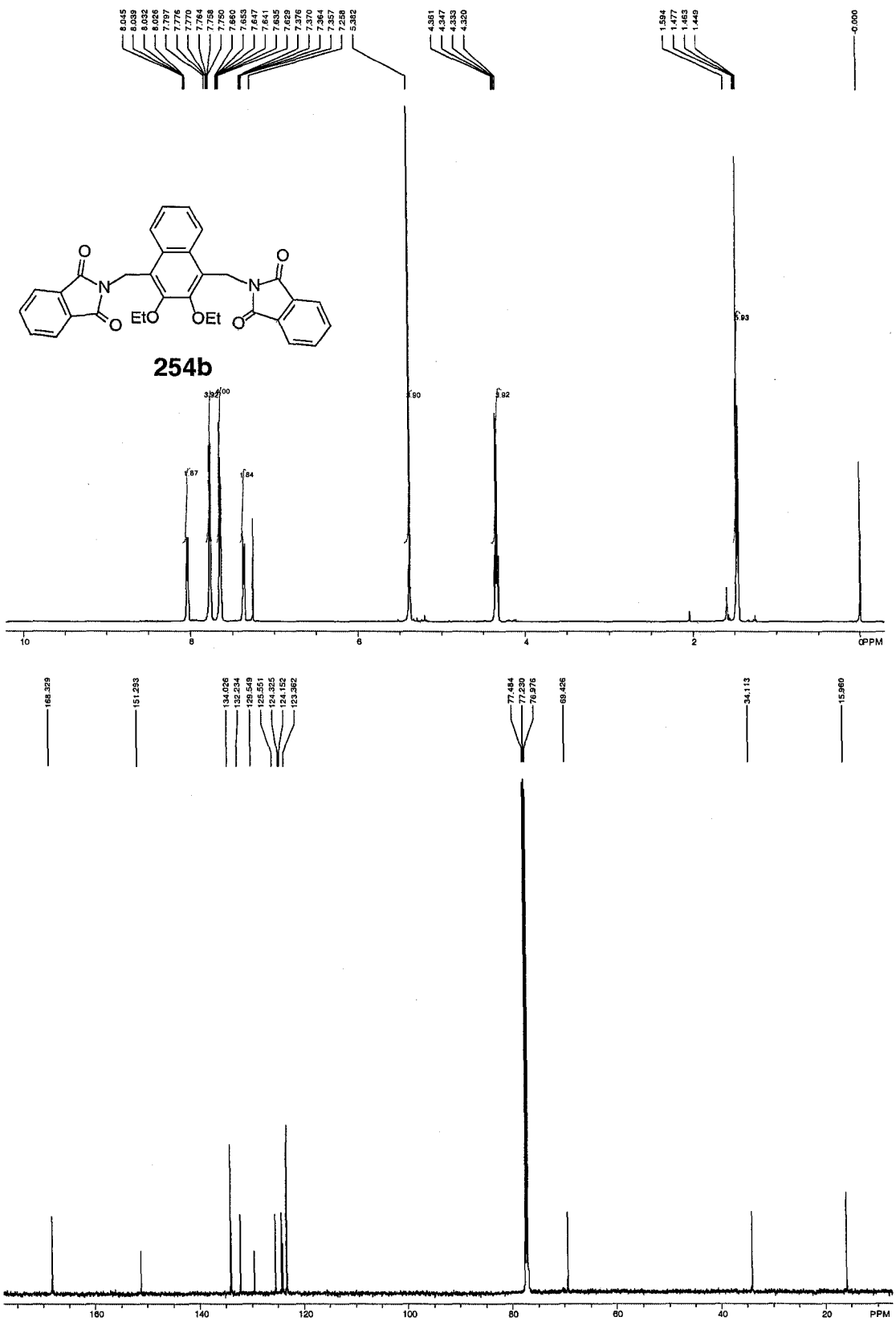
8.045
8.039
8.032
8.026
7.797
7.776
7.770
7.764
7.758
7.750
7.660
7.653
7.647
7.641
7.635
7.629
7.376
7.370
7.364
7.357
7.258
5.382
4.361
4.347
4.333
4.320
1.594
1.477
1.463
1.449
0.000
EtO
OEt
254b
3.92
4.00
1.87
1.84
3.90
3.92
6.93
10
8
6
4
2
0PPM
168.329
151.293
134.026
132.234
129.549
125.551
124.325
124.152
123.362
77.484
77.230
76.976
69.426
34.113
15.960
180
140
120
100
80
60
40
20
PPM

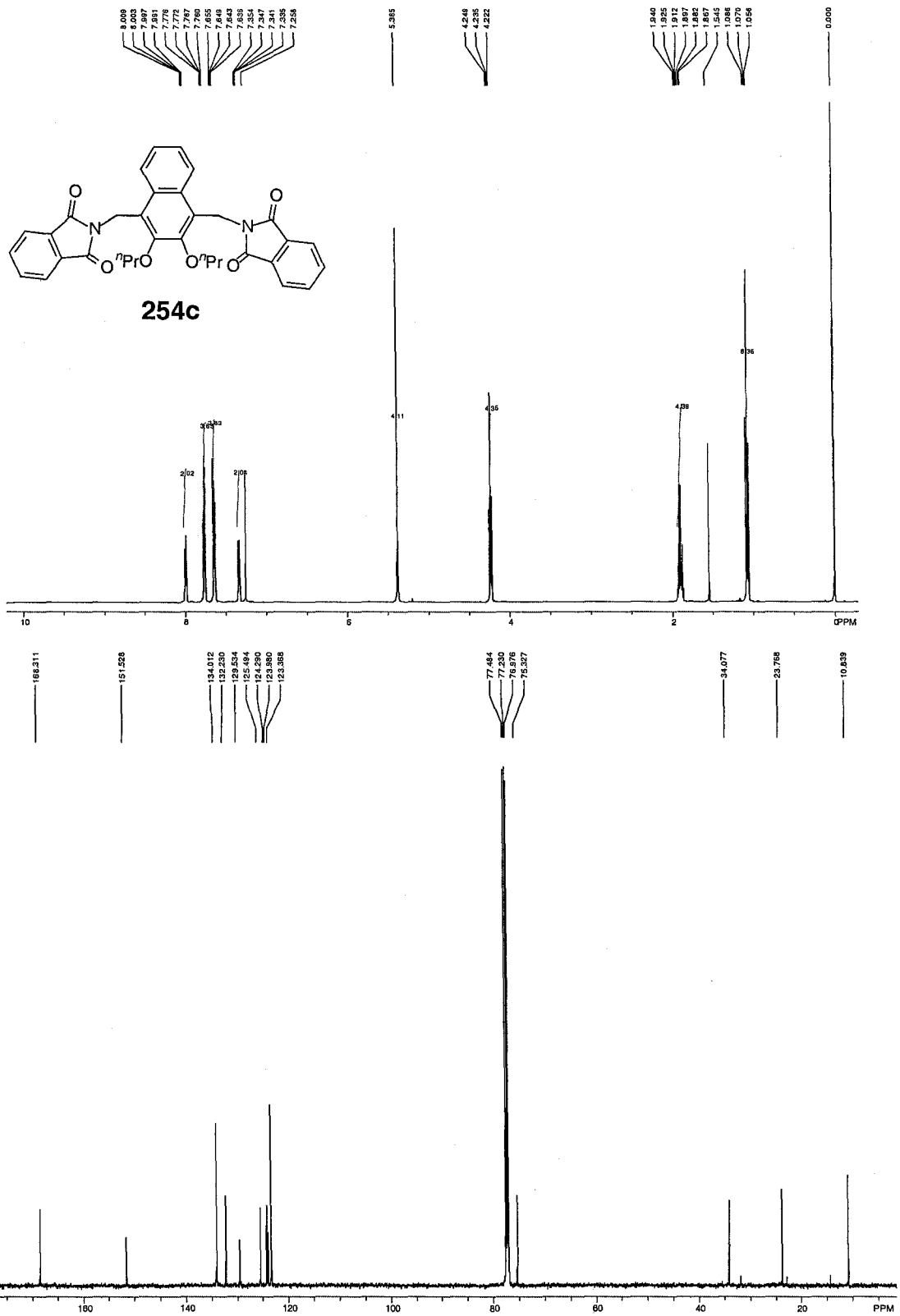
8.009
8.003
7.997
7.991
7.778
7.772
7.767
7.760
7.655
7.649
7.643
7.358
7.354
7.347
7.341
7.335
7.258
5.365
4.248
4.235
4.222
1.940
1.925
1.912
1.897
1.882
1.867
1.545
1.086
1.070
1.054
0.000
O
N
O
O
O
O
O
N
O
O
nPr
nPr
254c
2.02
3.65
3.53
2.05
4.11
4.35
4.08
6.36
10
8
6
4
2
0PPM
168.311
151.528
134.012
132.230
129.534
125.494
124.290
123.980
123.368
77.484
77.230
76.976
75.327
34.077
23.758
10.539
180
140
120
100
80
60
40
20
PPM

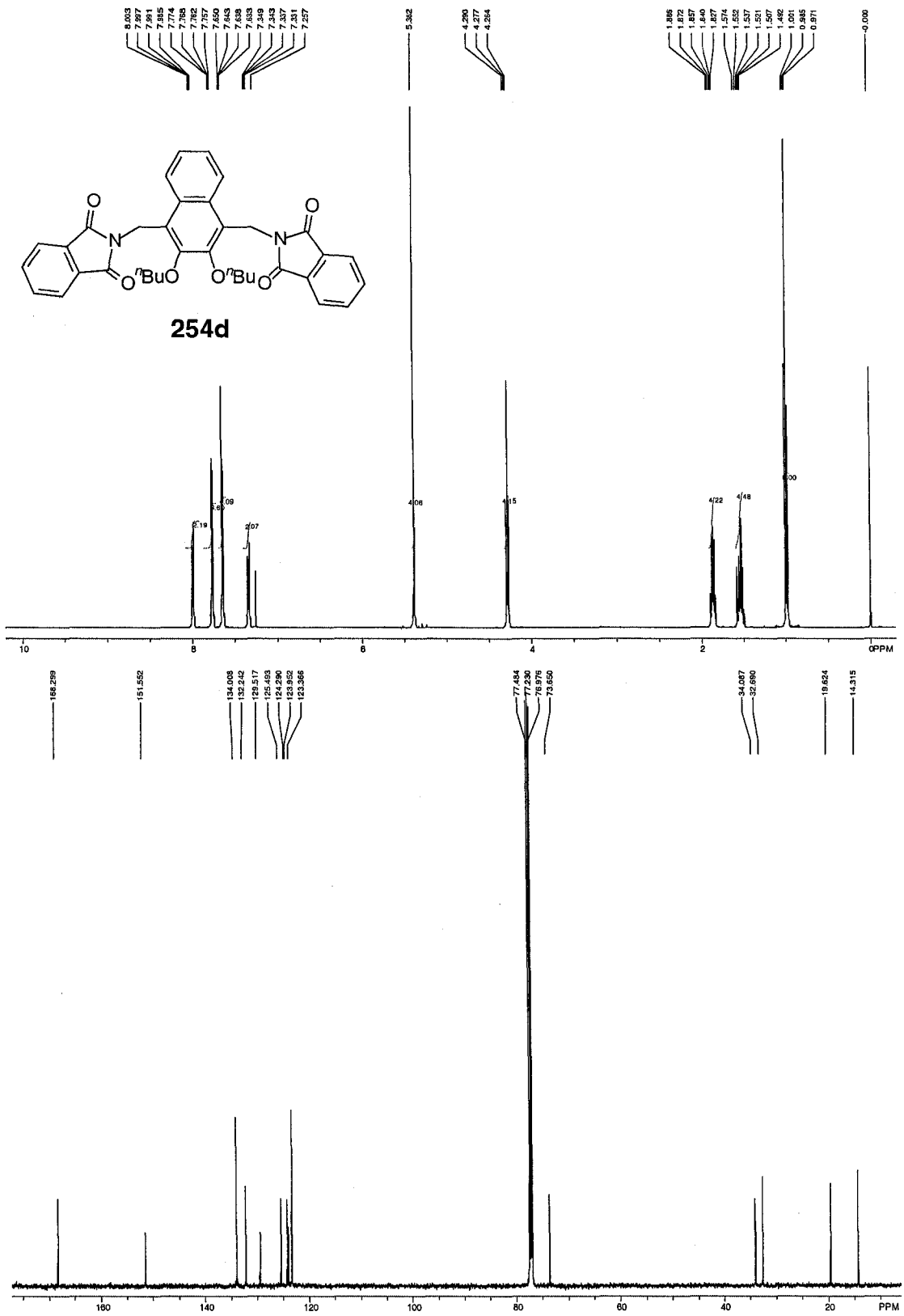
8.003
7.997
7.991
7.885
7.774
7.768
7.762
7.757
7.650
7.643
7.638
7.633
7.349
7.343
7.337
7.331
7.257
5.302
4.290
4.277
4.264
1.886
1.872
1.857
1.840
1.827
1.574
1.552
1.537
1.521
1.507
1.492
1.001
0.985
0.971
0.000
O
N
O
O
nBuO
OnBu
O
254d
5.19
5.09
4.07
4.06
4.15
4.22
4.48
10
8
6
4
2
0PPM
168.299
151.552
134.008
132.242
129.517
125.493
124.290
123.952
123.366
77.484
77.230
76.976
73.650
34.087
32.690
19.624
14.315
160
140
120
100
80
60
40
20
PPM


12.974
10.957
8.409
8.402
8.396
8.388
7.603
7.596
7.590
7.582
7.260
1.532
0.000
CHO
OH
OH
CHO
255
1.76
2.17
2.16
2.08
12
10
8
6
4
2
0 PPM
194.556
155.173
126.868
126.397
120.193
115.586
77.483
76.977
200
180
160
140
120
100
80
PPM

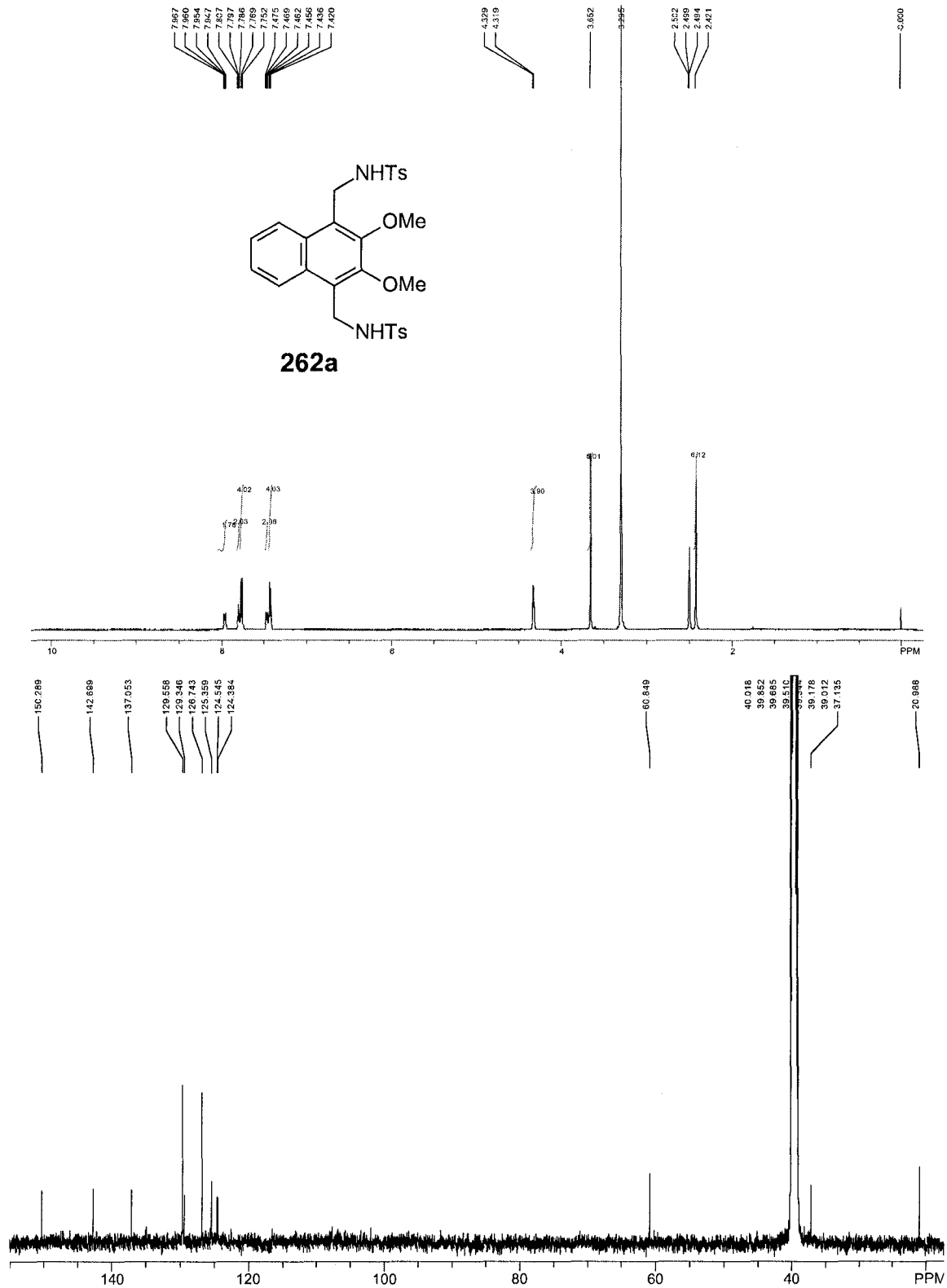
NHTs
OMe
OMe
NHTs
262a
PPM
140
120
100
80
60
40
PPM

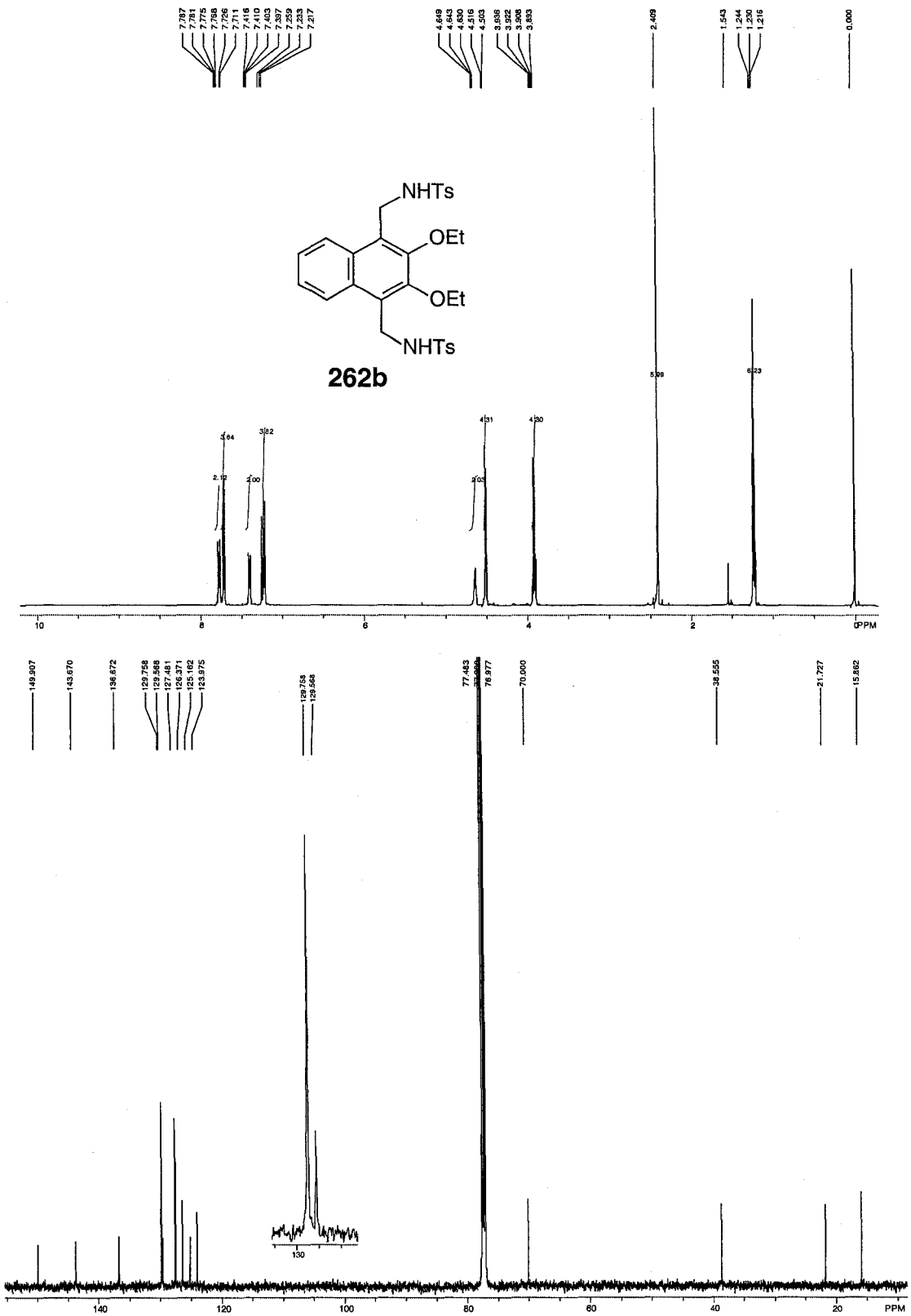
NHTs
OEt
OEt
NHTs
262b
PPM
PPM

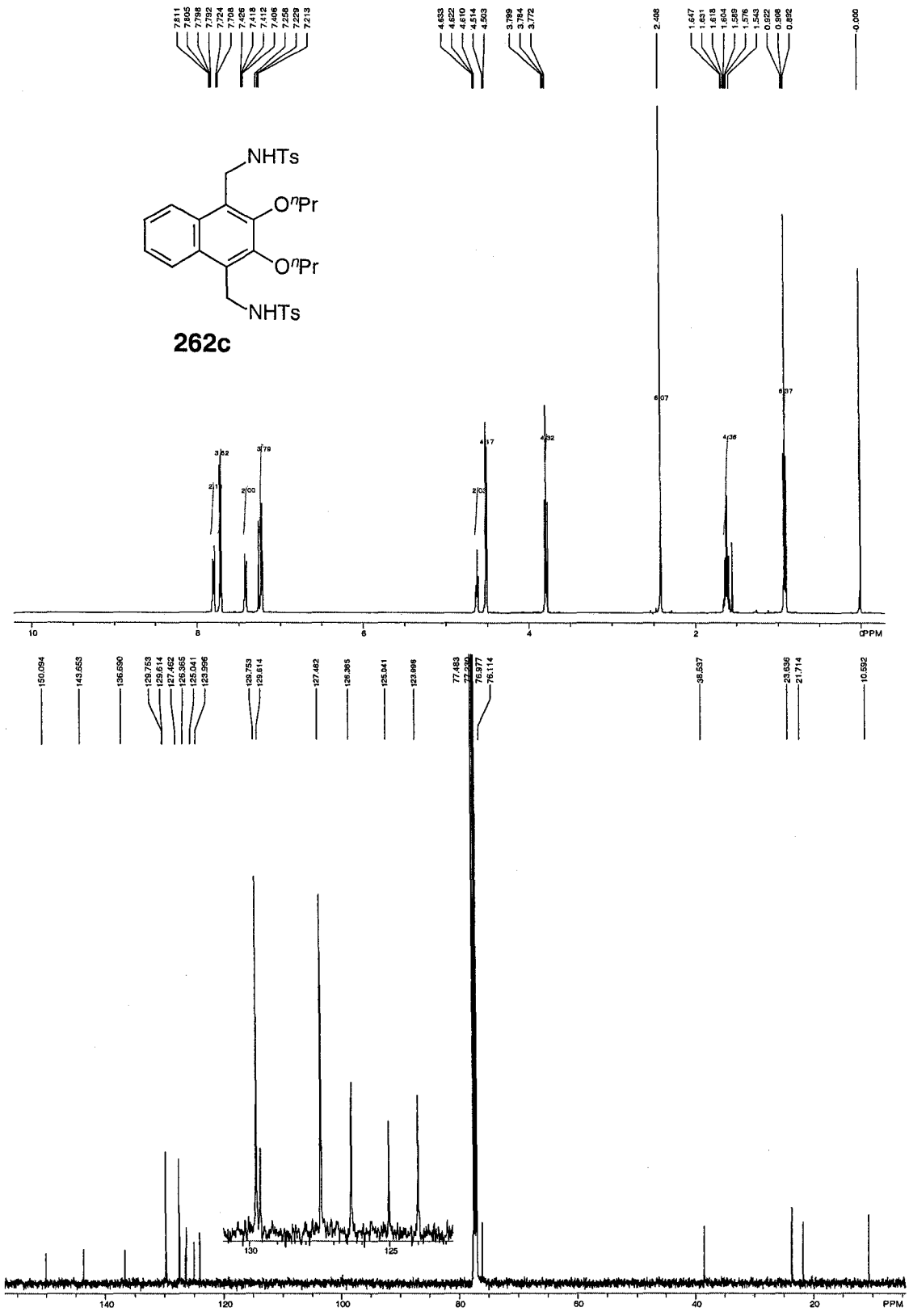
NHTs
O^{n}Pr
O^{n}Pr
NHTs
262c
PPM
PPM

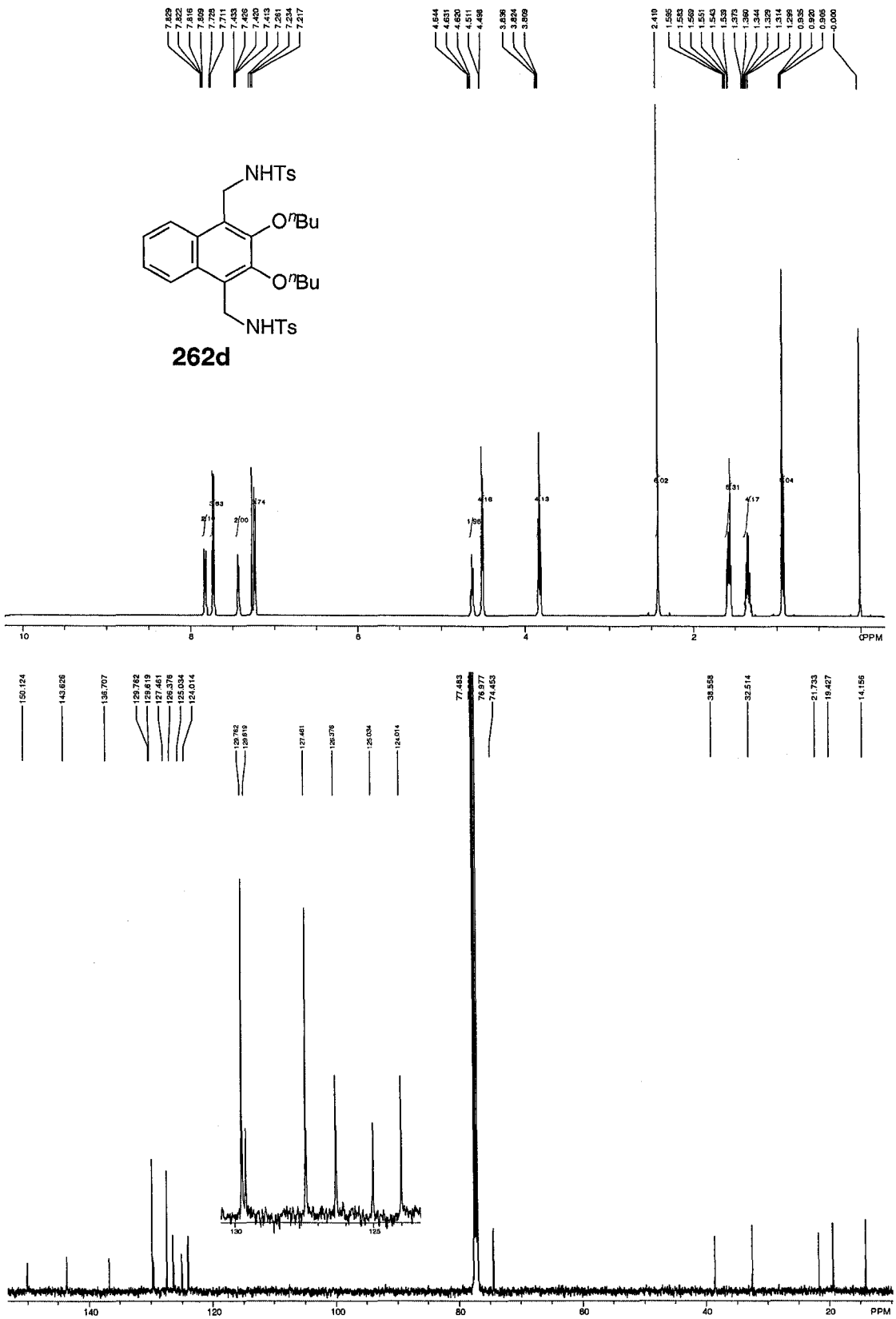
NHTs
O^{n}Bu
O^{n}Bu
NHTs
262d
PPM

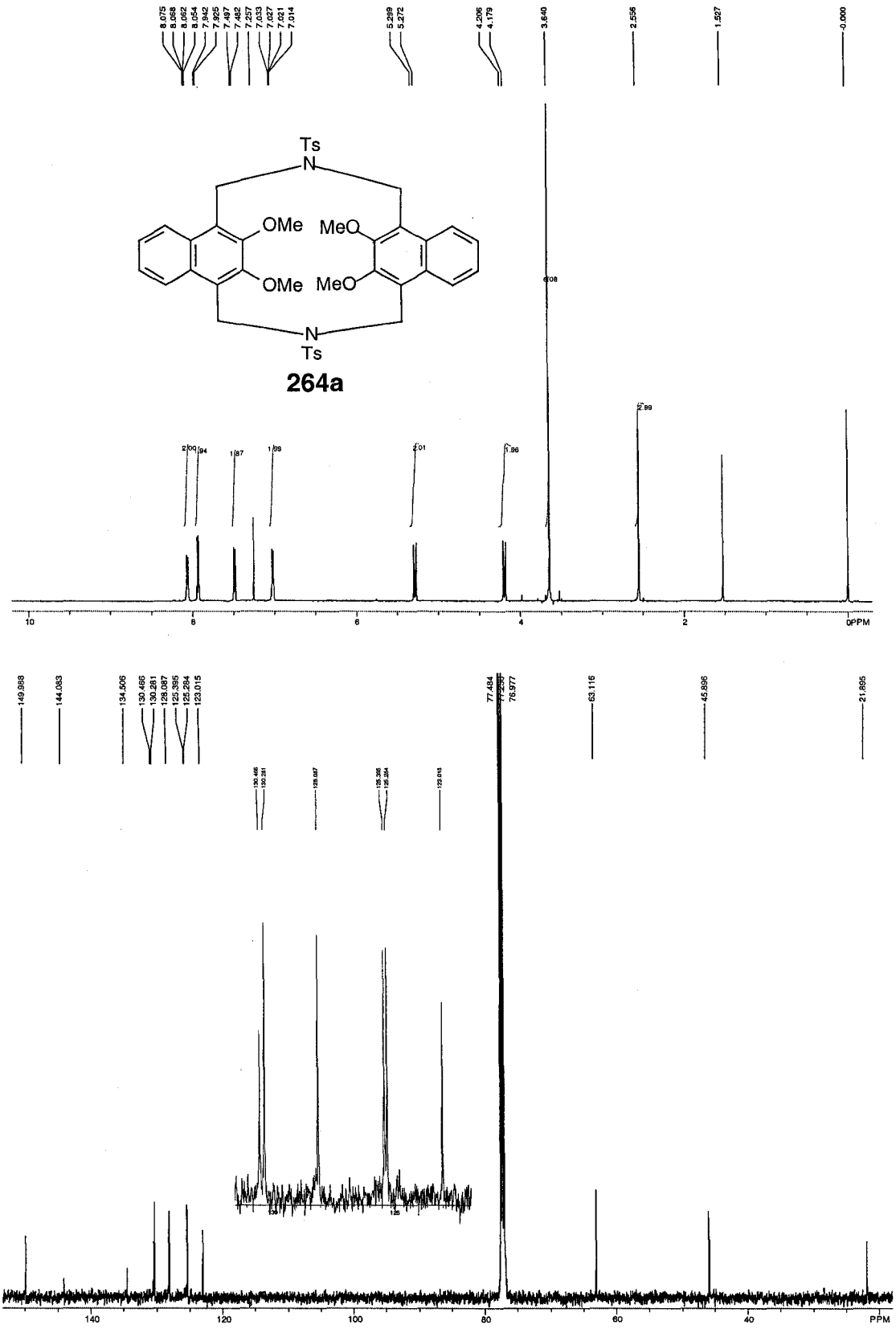
8.075
8.068
8.062
8.054
7.942
7.925
7.497
7.482
7.257
7.033
7.027
7.021
7.014
5.299
5.272
4.206
4.179
3.640
2.556
1.527
0.000
Ts
N
OMe
MeO
OMe
MeO
N
Ts
264a
6.08
2.00
2.04
1.87
1.89
2.01
1.96
2.89
10
8
6
4
2
0PPM
149.958
144.083
134.506
130.466
130.281
129.087
125.395
125.284
123.015
77.484
77.255
76.977
63.116
45.896
21.895
140
120
100
80
60
40
PPM

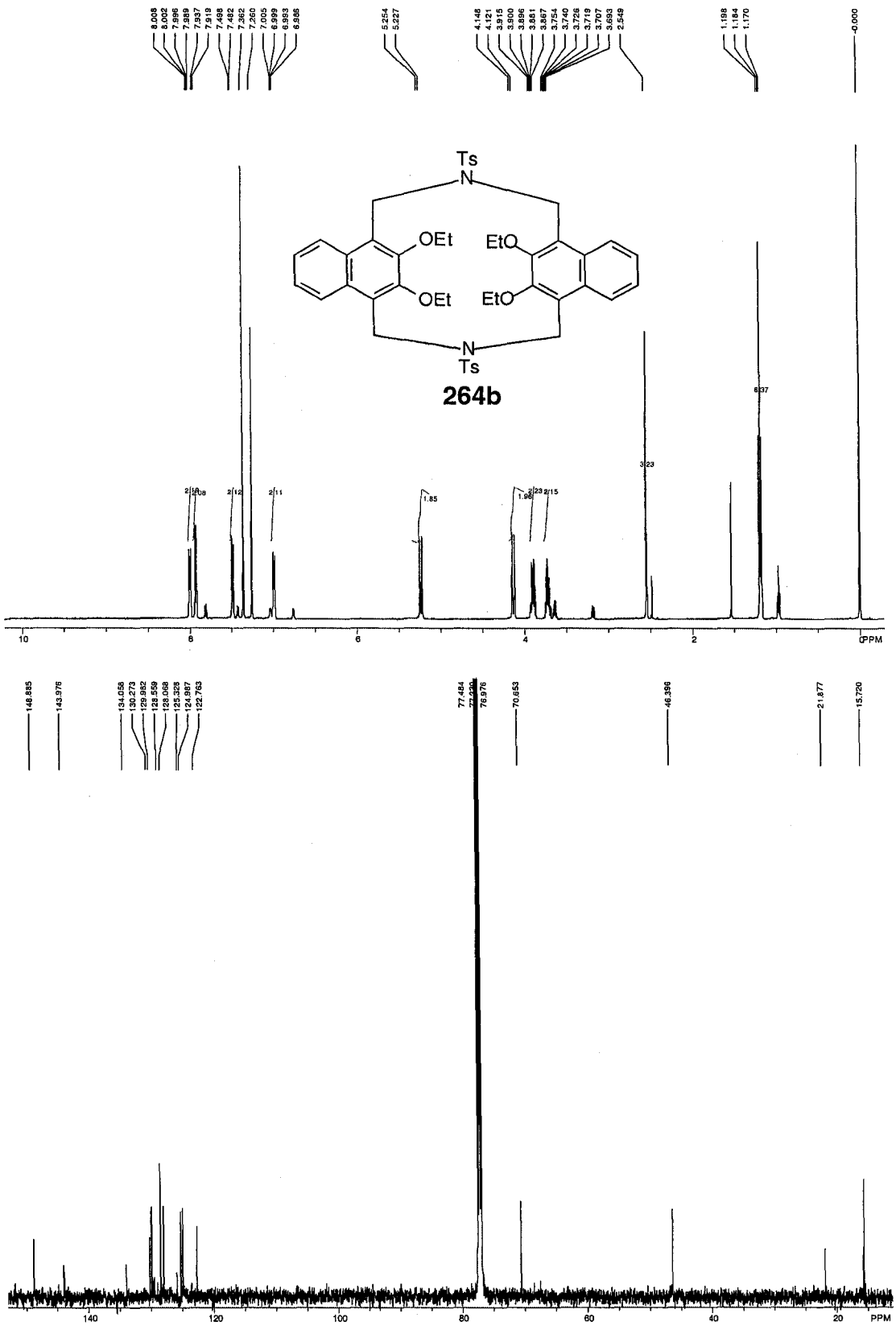
8.008
8.002
7.996
7.989
7.937
7.918
7.488
7.482
7.362
7.260
7.005
6.999
6.983
6.886
5.254
5.227
4.148
4.121
3.915
3.900
3.896
3.881
3.867
3.754
3.740
3.726
3.719
3.707
3.693
2.549
1.198
1.184
1.170
0.000
Ts
N
OEt
EtO
OEt
EtO
N
Ts
264b
2.08
2.12
2.11
1.85
1.98
2.23
2.15
3.23
6.37
10
8
6
4
2
PPM
148.885
143.976
134.058
130.273
129.982
128.559
128.068
125.328
124.987
122.763
77.484
77.268
76.976
70.653
46.396
21.877
15.720
140
120
100
80
60
40
20
PPM

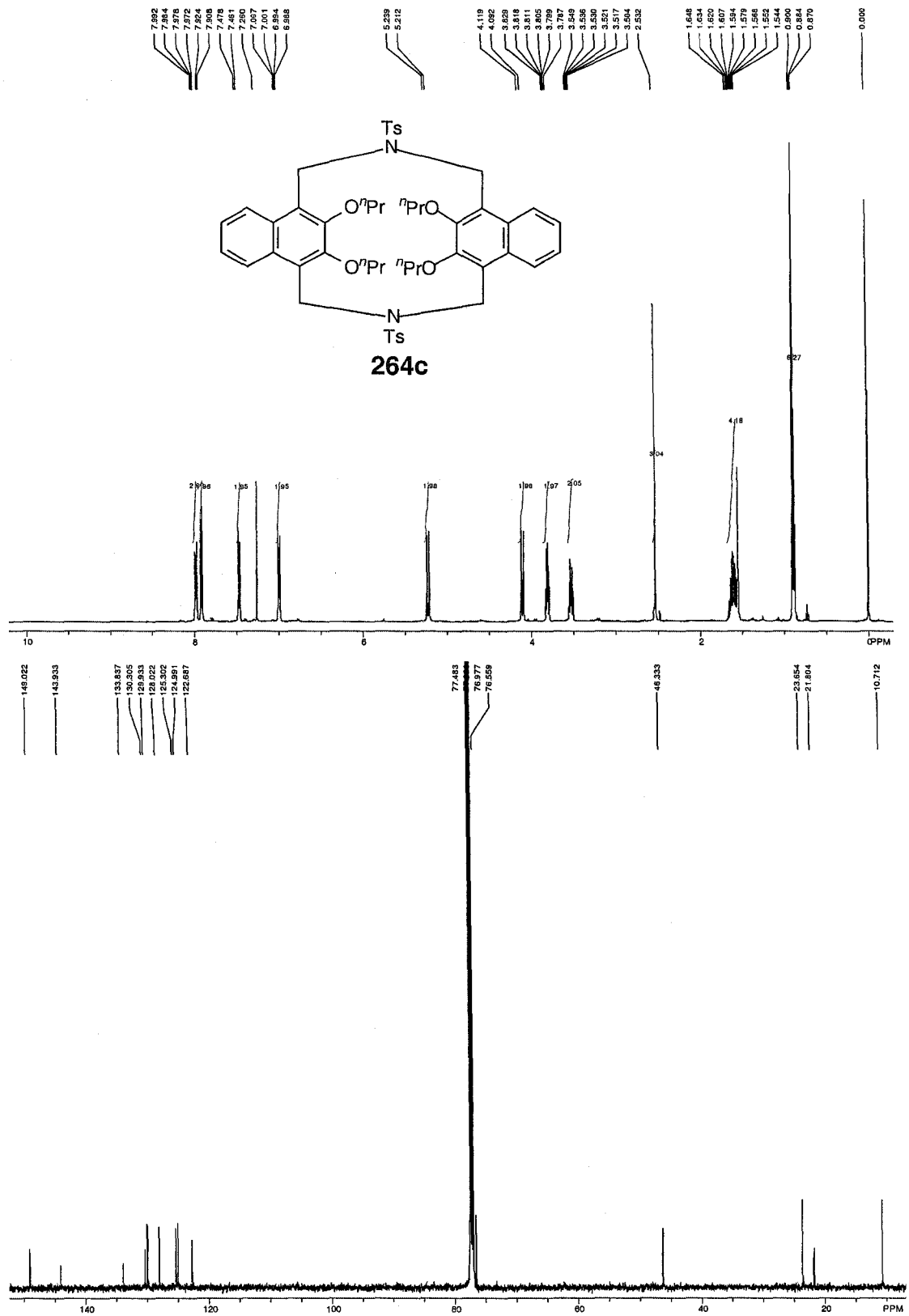
Ts
N
O^{n}Pr
^{n}PrO
O^{n}Pr
^{n}PrO
N
Ts
264c
PPM
PPM

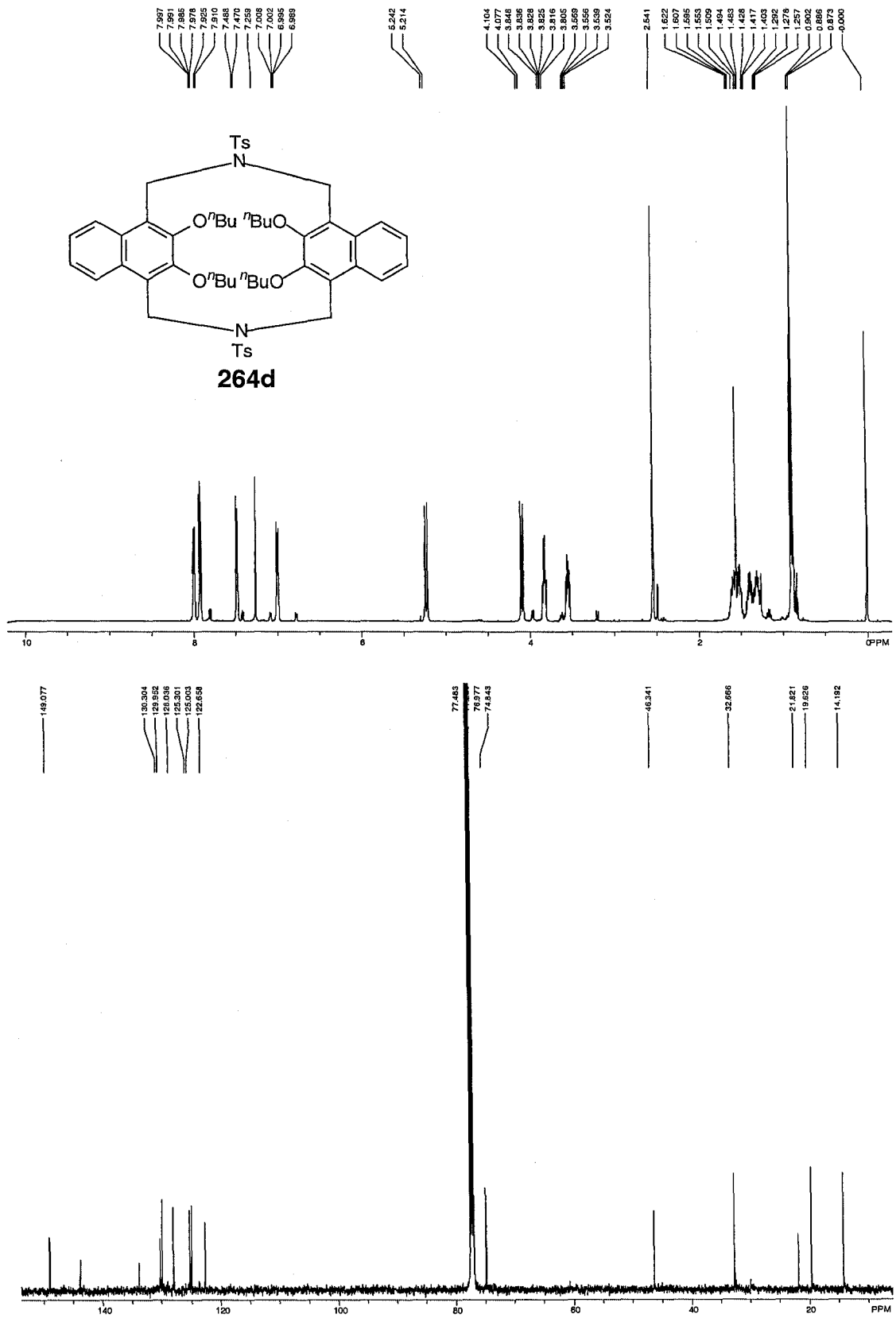
7.997
7.991
7.985
7.978
7.925
7.910
7.483
7.470
7.259
7.008
7.002
6.995
6.989
5.242
5.214
4.104
4.077
3.848
3.836
3.828
3.825
3.816
3.805
3.569
3.556
3.539
3.524
2.541
1.622
1.607
1.595
1.553
1.509
1.494
1.483
1.428
1.417
1.403
1.292
1.276
1.257
0.902
0.886
0.873
0.000
Ts
N
O^{n}Bu ^{n}BuO
O^{n}Bu ^{n}BuO
N
Ts
10
8
6
4
2
0PPM
149.077
130.304
129.952
128.036
125.301
125.003
122.658
77.483
76.377
74.843
46.341
32.666
21.821
19.626
14.192
140
120
100
80
60
40
20
PPM

264d